

\$49.95

EXPERIMENTAL METHODS in RF DESIGN



Wes Hayward, W7ZOI

Rick Campbell, KK7B

Bob Larkin, W7PUA



Published by: **ARRL** The national association for
AMATEUR RADIO

Basic Investigations in Electronics

Chapters on Amplifiers, Filters, Oscillators, and Mixers

Superheterodyne Transmitters and Receivers

Measurement Equipment

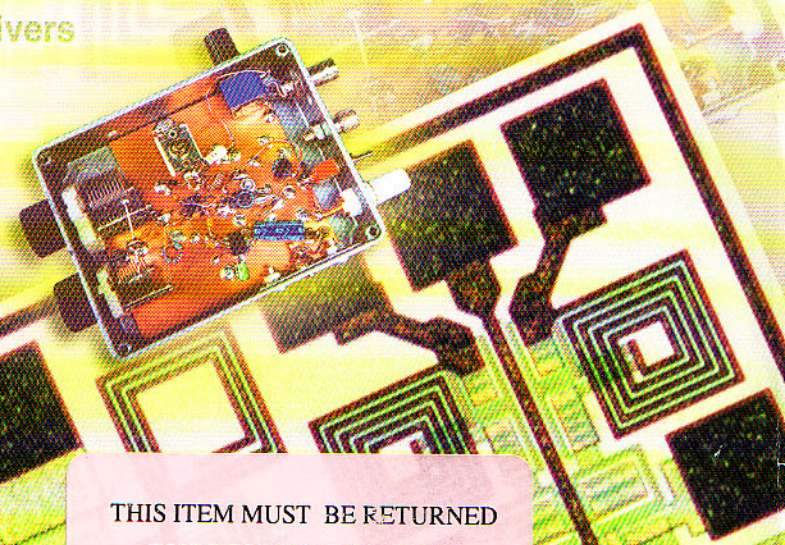
Direct Conversion Receivers

Phasing Receivers and Transmitters

DSP Components

DSP Applications in Communications

Field Operation, Portable Gear,
and Integrated Stations



THIS ITEM MUST BE RETURNED
BY RECORDED DELIVERY

CAGE

m03
V
wr...

Vm03/50387 d

EXPERIMENTAL METHODS in RF DESIGN



Wes Hayward, W7ZOI

Rick Campbell, KK7B

Bob Larkin, W7PUA

BRITISH LIBRARY
DOCUMENT SUPPLY CENTRE

12 NOV 2004

Editors:

Jan Carman, K5MA
Steve Ford, WB8IMY
Dana Reed, W1LC
Jim Talens, N3JT
Larry Wolfgang, WR1B

Proofreaders:

Kathy Ford
Jayne Pratt Lovelace

Production:

Michelle Bloom, WB1ENT
Paul Lappen
Jodi Morin, KA1JPA

Technical Illustration:

David Pingree, N1NAS

Cover Design:

Sue Fagan
Bob Inderbitzen, NQ1R

CD-ROM Development:

Dan Wolfgang



REG-27762906

Return Date

0005230 DEC 09

Request Ref. No.

VDXTL4432450 LOAN

If no other library indicated please return loan to:-
The British Library Document Supply Centre, Boston Spa,
Wetherby, West Yorkshire, United Kingdom LS23 7BQ

CONTENTS

Contents

Preface

1 Getting Started

- 1.1 Experimenting, "Homebrewing," and the Pursuit of the New
- 1.2 Getting Started – Routes for the Beginning Experimenter
- 1.3 Some Guidelines for the Experimenter
- 1.4 Block Diagrams
- 1.5 An IC Based Direct Conversion Receiver
- 1.6 A Regenerative Receiver
- 1.7 An Audio Amplifier with Discrete Transistors
- 1.8 A Direct Conversion Receiver Using a Discrete Component Product Detector
- 1.9 Power Supplies
- 1.10 RF Measurements
- 1.11 A First Transmitter
- 1.12 A Bipolar Transistor Power Amplifier
- 1.13 An Output Low Pass Filter
- 1.14 About the Schematics in this Book

2 Amplifier Design Basics

- 2.1 Modeling Simple Solid State Devices
- 2.2 Amplifier Design Basics
- 2.3 Large Signal Amplifiers
- 2.4 Gain, Power, DB and Impedance Matching
- 2.5 Differential Amplifiers and the Op-Amp
- 2.6 Undesired Amplifier Characteristics
- 2.7 Feedback Amplifiers
- 2.8 Bypassing and Decoupling
- 2.9 Power Amplifier Basics
- 2.10 Practical Power Amplifiers
- 2.11 A 30-W – 7-MHz Power Amplifier

3 Filters and Impedance Matching Circuits

- 3.1 Filter Basics
- 3.2 The Low Pass Filter, Design and Extension
- 3.3 LC Bandpass Filters
- 3.4 Crystal Filters
- 3.5 Active Filters
- 3.6 Impedance Matching Networks

4 Oscillators and Frequency Synthesis

- 4.1 LC-Oscillator Basics
- 4.2 Practical Hartley Circuits and Oscillator Drift Compensation
- 4.3 The Colpitts and Some Other oscillators
- 4.4 Noise in Oscillators
- 4.5 Crystal Oscillators and VXOs
- 4.6 Voltage Controlled Oscillators
- 4.7 Frequency Synthesis
- 4.8 The Ugly Weekender, MK-II, A 7-MHz VFO Transmitter
- 4.9 A General Purpose VXO-Extending Frequency Synthesizer



49961449

Return Date:

-8,DEC 04 0239

Request Ref. No.

OFZ11984 2543429 LOAN

for RMS
use only

If no other library indicated please return loan to:-

The British Library Document Supply Centre, Boston Spa,
Wetherby, West Yorkshire, LS23 7BQ

5 Mixers and Frequency Multipliers

- 5.1 Mixer Basics
- 5.2 Balanced Mixer Concepts
- 5.3 Some Practical Mixers
- 5.4 Frequency Multipliers
- 5.5 A VXO Transmitter Using a Digital Frequency Multiplier

6 Transmitters and Receivers

- 6.0 Signals and the Systems that Process Them
- 6.1 Receiver Fundamentals
- 6.2 IF Amplifiers and AGC
- 6.3 Large Signals in Receivers and Front End Design
- 6.4 Local Oscillator Systems
- 6.5 Receivers with Enhanced Dynamic Range
- 6.6 Transmitter and Transceiver Design
- 6.7 Frequency Shifts, Offsets and Incremental Tuning
- 6.8 Transmit-Receive Antenna Switching
- 6.9 The Lichen Transceiver: A Case Study
- 6.10 A Monoband SSB/CW Transceiver
- 6.11 A Portable DSB/CW 50 MHz Station

7 Measurement Equipment

- 7.0 Measurement Basics
- 7.1 DC Measurements
- 7.2 The Oscilloscope
- 7.3 RF Power Measurement
- 7.4 RF Power Measurement with an Oscilloscope
- 7.5 Measuring Frequency, Inductance, and Capacitance
- 7.6 Sources and Generators
- 7.7 Bridges and Impedance Measurement
- 7.8 Spectrum Analysis
- 7.9 Q Measurement of LC Resonators
- 7.10 Crystal Measurements
- 7.11 Noise and Noise Sources
- 7.12 Assorted Circuits

8 Direct Conversion Receivers

- 8.1 A Brief History
- 8.2 The Basic Direct Conversion Block Diagram
- 8.3 Peculiarities of Direct Conversion
- 8.4 Mixers For Direct Conversion Receivers
- 8.5 A Modular Direct Conversion Receiver
- 8.6 DC Receiver Advantages

9 Phasing Receivers and Transmitters

- 9.1 Block Diagrams
- 9.2 Introduction to the Math
- 9.3 From Mathematics to Practice
- 9.4 Sideband Suppression Design
- 9.5 Binaural Receivers
- 9.6 LO and RF Phase-Shift and In-Phase Splitter-Combiner Networks
- 9.7 Other Op-Amp Topologies, Polyphase Networks and DSP Phase Shifters
- 9.8 Intelligent Selectivity
- 9.9 A Next-Generation R2 Single-Signal Direct Conversion Receiver
- 9.10 A High Performance Phasing SSB Exciter
- 9.11 A Few Notes on Building Phasing Rigs
- 9.12 Conclusion

10 DSP Components

- 10.1 The EZ-Kit Lite
- 10.2 A Program Shell
- 10.3 DSP Components
- 10.4 Signal Generation
- 10.5 Random Noise Generation
- 10.6 Filtering Components
- 10.7 DSP IF
- 10.8 DSP Mixing
- 10.9 Other DSP Components
- 10.10 Discrete Fourier Transform
- 10.11 Automatic Noise Blankers
- 10.12 CW Signal Generation
- 10.13 SSB Signal Generation

11 DSP Applications in Communications

- 11.1 Program Structure
- 11.2 Using a DSP Device as a Controller
- 11.3 An Audio Generator Test Box
- 11.4 An 18-MHz Transceiver
- 11.5 DSP-10 2-Meter Transceiver

12 Field Operation, Portable Gear and Integrated Stations

- 12.1 Simple Equipment for Portable Operation
- 12.2 The "Unfinished," A 7-MHz CW Transceiver
- 12.3 The S7C, A Simple 7-MHz Super-Heterodyne Receiver
- 12.4 A Dual Band QRP CW Transceiver
- 12.5 Weak-Signal Communications Using the DSP-10
- 12.6 A 28-MHz QRP Module
- 12.7 A General Purpose Receiver Module
- 12.8 Direct Conversion Transceiver for 144-MHz SSB and CW
- 12.9 52-MHz Tunable IF for VHF and UHF Transceivers
- 12.10 Sleeping Bag Radio
- 12.11 14-MHz CW Receiver

Contents of CD-ROM

Index

PREFACE

The predecessor for this book, *Solid State Design for the Radio Amateur (SSD)*, was first published by ARRL in early 1977. The goal for that text was to present solid state circuit design methods to a community much more familiar with vacuum tube methods. But, another goal was integrated into the text, that of presenting the material in a way that would allow the reader to actually *design* his or her own circuits. Handbooks of the day presented only an encyclopedic overview of solid state devices with brief qualitative discussions about functionality. *SSD* described circuit elements in terms of models that could be used for analysis. Design consists of more than merely combining representative circuits from a catalog or handbook.

SSD succeeded with **design** becoming the key word in the title, especially in later years as the world became accustomed to all electronic equipment being predominantly solid state. What surprised many is that the book remained popular, even after many of the transistors used in the circuits were no longer available.

Experimental Methods in Radio Frequency Design (EMRFD) is the sequel to *SSD*, with **design** remaining as a central theme. Our goal is to present models and discussion that will allow the user to design equipment at both the circuit and the system level. Our own interests are dominated by radio frequencies, so the text discusses problems peculiar to radio communications equipment. A final emphasis in *EMRFD* is **experimentation**. A vital part of an experiment is measurement. We encourage the reader to not only build equipment, but to perform measurements on that gear as it is being built.

The word "experiment," often conjures memories of school exercises where a teacher has assembled equipment and we, as students, go through a prearranged set of steps to arrive at a conclusion, also predetermined. Although efficient, this is a poor representation of science. Rather, experimental science begins with a new idea. An experiment to test the idea is then generated, the experiment is built, measurements are made, and the results are pondered, which often results in new ideas to test. This can all be done by one person working alone. *EMRFD* encourages the participating reader to build equipment with an attitude of continually seeking to understand the equipment and to understand the primitive concepts that form the basis for the equipment and the circuits contained therein. Our greatest hope is that the text will illustrate the potential of amateur radio, and other personal science, as a training ground for the individual.

This text is aimed at a variety of readers: the radio amateur who designs and builds his own equipment; college students looking for design projects or wishing to garner practical experience with working hardware; young professionals wishing to apply their fresh engineering and physics coursework to kitchen table projects; non-engineers wanting to dabble in a technical field; engineering managers recapturing the fun of making things (instead of people) work; and technical explorers of all types.

The first chapter of *EMRFD* deals with the problems of getting started with experimentation. Numerous projects are presented, aimed at assisting the experimenter in beginning investigations in electronics. Chapters 2 through 5 then deal with specific circuit functions. Chapter 2 presents amplifiers while filters are discussed in Chapter 3. Oscillators emerge in Chapter 4, including

the natural extension of frequency synthesis. Mixers, including frequency multipliers, appear in the fifth chapter. These chapters are laced with projects that can be constructed, but they also emphasize important basic concepts. Chapter 6 moves on to present communications equipment, predominantly using super-heterodyne methods. System design considerations are included, especially with regard to distortion and dynamic range. The chapter contains several projects including a high performance receiver. Chapter 7 deals with measurement methods and includes considerable test equipment that the experimenter can build. Chapter 8 then moves on to a fundamental discussion of direct conversion. This is followed by a thorough treatment of the phasing method of SSB in Chapter 9. Chapters 10 and 11 present fundamental concepts of digital signal processing and illustrate them with projects. The book concludes with Chapter 12 featuring a variety of experimental activities of special interest to the authors.

A Compact Disc is included with the book. This CD contains some design software, extensive listings for DSP firmware related to Chapters 10 and 11, and a sizeable collection of journal articles relating to material presented in the text. The design software is written for a personal computer using the Microsoft Windows operating system, while the journal papers are presented in Adobe Acrobat (PDF) format.

This book is a personal one in that we have only written about those things we have actually experienced. We specifically avoided an encyclopedic discussion of material that we had not actually experienced through experiments. Equipment of interest to the three of us dominates. The amateur bands up to 2 meters are considered, and are illustrated with CW and SSB gear. The book uses some mathematics where appropriate. It is, however, kept at a basic level.

The book contains numerous projects that are suitable for duplication. Printed circuit boards are not generally available for these, although boards may become available at a later time. Readers should keep an eye on the world wide web for PCB information and other matters related to the book. See <http://www.arrl.org/notes/8799>. We generally prefer that builders use the projects as starting points for their own designs and experiments rather than duplicating the projects presented.

Acknowledgments

The following experimenters have contributed to this book through experiments, direct correspondence, encouragement, and by example. We gratefully acknowledge their contributions.

Bill Amidon (sk); Tom Apel, K5TRA; Leif Åsbrink, SM5BSZ; Kirk Bailey, N7CCB; Dave Benson, K1SWL; Byron Blanchard, N1EKV; Denton Bramwell, W7DB; Guy Brennert, K2EFB; Rod Brink, KQ6F; Kent Britain, WA5VJB; Wayne Burdick, N6KR; Russ Carpenter, AA7QU; Dennis Criss; Bob Culter, N7FKI; George Daughters, K6GT; John Davis, KF6EDB; Paul Decker, KG7HF; Rev. George Dobbs, G3RJV; Pete Eaton, WB9FLW; Gerry Edson, WA0KNW; Bill Evans, W3FB;

George Fare, G3OGQ; Johan Forrer, KC7WW; Dick Frey, K4XU;
 Barrie Gilbert; Jack Glandon, WB4RNO; Joe Glass, WB2PJS;
 Dr. Dave Gordon-Smith, G3UUR; Mike Grane, K3SRZ;
 Linley Gumm, K7HFD;
 Nick Hamilton, G4TXG; Mark Hansen, KI7N; Markus Hansen,
 VE7CA; Neil Heckt; Ward Helms, W7SMX; Don Hilliard,
 WØPW; Fred Holler, W2EKB; Robert Hughson;
 Pete Juliano, W6JFR;
 Bill Kelsey, N8ET; Ed Kessler, AA3SJ; Paul Kiciak, N2PK;
 Don Knotts, W7HJS; O. K. Krienke;
 Beb Larkin, W7SLB; John Lawson, K5IRK; Roy Lewallen,
 W7EL; John Liebenrood, K7RO; Larry Liljeqvist, W7SZ; B.
 F. Logan Jr., WB2NBD;
 Stephen Maas, W5VHJ; Chuck MacCluer, W8MQW; Jacob
 Makhinson, N6NWP; Ernie Manly, W7LHL; Dr. Skip Marsh,
 W6TFQ (sk); Mike Michael, W3TS; Jim Miles, K5CX;
 Dave Newkirk, W9VES;
 Gary Oliver, WA7SHI;
 Paul Pagel, N1FB;
 Dave Roberts, G8KBB; Mike Reed, KD7TS; Don Reynolds,
 K7DBA (sk); Dr. Ulrich Rohde, KA2WEU; Dr. Dave
 Rutledge, KN6EK; Tom Rousseau, K7PJT;
 Bill Sabin, WØIYH; Tom Scott, KD7DMH; Marty Singer,
 K7AYP; Derry Spittle, VE7QK;
 Fred Telewski, WA7TZY;
 Paul Wade, W1GHZ; Al Ward, W5LUA; Dr. Fred Weiss; Jim
 Wyckoff, K3BT;
 Bob Zavrel, W7SX; Bob Zulinski, WA8MAM;

We have certainly missed some folks in our list. Please accept our apologies for our oversight and our thanks for your help with

the book and related experiments.

Some folks have made special contributions and deserve special thanks. Colin Horrabin, G3SBI; Harold Johnson, W4ZCB; and Bill Carver, W7AAZ, collectively formed the "Triad," a group building the high performance transceiver partially described in Chapter 6. We sincerely appreciate their willingness to share their efforts and results with us. Thanks go to Roger Hayward, KA7EXM, for building some equipment described in the book as well as helping with field testing of numerous designs. Jeff Damm, WA7MLH, deserves special thanks for his efforts. He built equipment described in *SSD* and provided encouragement for this version. Special thanks to Merle Cox, W7YOZ, and Jim Davey, K8RZ, for several decades of bouncing around radio ideas, building the second prototypes, and manning the distant station for countless experiments. Very special thanks are extended to Terry White, K7TAU. Terry did high quality PC layouts for several of the designs presented in the text and in earlier *QST* articles. He also built some equipment shown in the book and provided measurement assistance on several occasions.

Special mention should be made of the efforts of the late Doug DeMaw, W1FB. As co-author of *SSD*, he provided interest and encouragement for this sequel. One of Doug's greatest qualities was his intense, sincere interest in radio communications. He designed and built radio equipment, used it on the air, and then clearly wrote about the efforts, establishing a standard for all to follow. We missed him often through the generation of this text.

Finally, we want to thank our families, and especially our wives: Charlene (Shon) Hayward, Sara Rankinen, and Janet Larkin. A book requires time and intense effort that often detracts from other activities. Our "better halves" have all tolerated these moments of distraction.

About the Cover Photograph

The cover photograph is an experimental 2.4 GHz IC direct conversion receiver front-end on a gallium arsenide die. The die is a little more than one millimeter wide, and less than one millimeter high. Gold-bond wires connect to the metal squares around the edge. The large spiral is a quadrature hybrid coupled inductor, and the matched inductors at the top are in a Wilkenssen

splitter. The passive circuitry is similar to Fig 9.39, and the photograph on page 9.43 shows this IC connected to baseband circuitry described in Chapter 9. Note the call signs on the die. "MAL," who was not licensed in 2001, is now K7MTL. Photograph by Dean Monthei.

About The Authors

All three of the authors share a similar early exposure to radio, obtaining an amateur license as a teen or earlier. They all started with the novice class license. Their early ham experiences expanded to become careers in science and electronics. All three are members of the IEEE Microwave Theory and Techniques Society and have published extensively in a wide variety of journals and books. All three writers contributed to all chapters of this text, but each author had a primary responsibility listed below.

Wes Hayward, W7ZOI

Wes received a BS in Physics from Washington State University in 1961 and an MSEE from Stanford University in 1966. He worked on electron device physics at Varian Associates, The Boeing Co., and Tektronix. He then did RF circuit design, first at Tektronix and then at TriQuint Semiconductor. Wes is now semi-retired, dividing his time between writing and consulting. Wes was the primary contributor to Chapters 1 through 7 and large parts of 12 and can be contacted at w7zoi@arrl.net.

Rick Campbell, KK7B

Rick received a BS in Physics from Seattle Pacific University in 1975, after two years active duty as a US Navy Radioman. He worked for 4 years in crystal physics basic research at Bell Labs in Murray Hill, NJ before returning to graduate school at the University of Washington. He completed the MSEE degree in 1981 and the PhD in EE in 1984. He served on the faculty at Michigan Tech University until 1996. Since 1996 he has been with the Advanced Development Group at TriQuint Semiconductor, designing microwave receiver circuitry. Rick had primary responsibility for chapters 8, 9, and large parts of 12. He can be contacted at kk7b@arrl.net.

Bob Larkin, W7PUA

Bob received a BS in EE from the University of Washington and a MS in EE from New York University. He worked for 12 years at Bell Labs in New Jersey in areas of circuit design and signal processing. In 1973 he and his wife Janet started Janel Labs where a variety of radio frequency products were manufactured. They moved the company to Corvallis Oregon in 1975 where it operated until being acquired by Celwave RF in 1991. He now works as a consultant specializing in microwave circuits. Bob was the primary contributor to Chapters 10 and 11 and wrote a section in Chapter 12. Readers can contact Bob at w7pua@arrl.net.

Getting Started

1.1 EXPERIMENTING, “HOMEBREWING,” AND THE PURSUIT OF THE NEW

Amateur Radio is a diverse and colorful avocation or hobby where the participants communicate with each other through the use of radio signals. The communications, which can encompass and extend beyond the planet, are often routine and predictable, but can at times be ethereal. The romance of communicating with the other side of the world blends with the joy of observing a complicated part of nature. For some of us, the wonder never disappears.

Although radio can be fun, our pragmatic society demands more than excitement when resources are used. The virtue that most often justifies our use of the radio spectrum is the growth of a proficient communications system that can be called upon in times of emergency. The examples of its use are numerous.

But, “ham” radio is more than this. It is a technical avocation of diverse educational potential. It has values that go well beyond that of a supplementary communications network.

Most radio amateurs have an interest in the technical details of the equipment they use. Historically, this was a requirement: The only way a radio amateur could assemble an operating station was to personally build his or her gear. Commercial equipment was rare, and was often prohibitively expensive. But today, high quality “ham” gear is readily available in most of the world, much of it at modest prices.

Although no longer necessary, it is still common for radio amateurs to build at least some of their own equipment. The reasons are varied and as numerous as the participants. A few purists consider building the equipment they use to be a non-optional, integral part of their hobby in the same way

that a fly fishing enthusiast would *never* consider fishing with a fly that he or she had not fabricated. The majority take an intermediate path, building parts of their radio stations while purchasing others. For some, building is an exercise in craftsmanship, an opportunity to generate equipment with an individual imprint and personality.

Common to all of these, amateur radio presents an opportunity that is rare among avocations, a chance for individual, unrestrained investigations in fundamental science and technology. This is a rarity in an age when most research and design is performed by teams of investigators within large organizations, be they universities or the engineering arms of corporations. There, the subjects chosen for investigation are often those of corporate or national interest. It is increasingly rare that a study is initiated out of simple curiosity. Fortunately, we are not so constrained within our personal investigations of radio science.

Consider an example. An experimentally inclined radio amateur envisions a new scheme for a receiver. It might be a better front end circuit, a new block diagram, or a way to realize some receiver functions with a computer. The experimenter can analyze the scheme, design an example, build a prototype, build and assemble needed test equipment, measure the receiver performance, compare it with predicted results, and use the receiver on the air. Each part of the investigation can interact with the others. All of the activity can be done without interference from other sources. The program will never be cancelled by the changing goals of an organization. Nor will it be rushed by the economic pressures of a corporate program.

The inspiration for experiment varies. In rare cases, the experimenter may feel that his or her work could lead to a new twist in the state-of-the-art, a better receiver. But more often it will just be a casual thought that “Hey, I’ve never built one of these before and I’ll learn something if I do.” The most common is an effort spurred by a need; a ham wants a rig to take along on a hiking trip when no such thing can be purchased. No matter what the origin, the experimenter can enjoy the knowledge that he or she is learning more about the subject and about the research process.

In this book we encourage all levels of what has become known as radio “homebrewing,” ranging from beginner projects to sophisticated multi-mode creations. We generally emphasize simple equipment described by primitive explanations. By *primitive*, we intend that the discussion relate to the most fundamental and basic circuit design concepts. The equipment and systems presented are themselves basic, often without the frills, bells, and whistles of commercial equipment. Some refinements will be discussed, allowing the experimenter to add those he or she needs.

This book emphasizes equipment design. Our interest is in basic circuit functions and the underlying concepts that allow them to be understood. This book is generally NOT a collection of projects for reproduction and construction. Although some of the equipment may be directly duplicated, we would prefer to have you adapt our results to fit your own needs.

This book is, in many ways, a sequel to an earlier effort, *Solid State Design for the Radio Amateur*.¹ That 1977 book, co-authored with the late Doug DeMaw,

W1FB, had goals similar to those outlined above, plus that of introducing solid-state methods to readers with experience limited to vacuum tube electronics. The later need has become arguable, for virtually all of our equipment is now based upon solid-state technology.

All of the circuits presented in this text have been constructed, tested, and used in practical, on-the-air situations. If there are exceptions where the authors have not

actually built an example of what is discussed, we will so state in the related text.

We emphasize the traditional communications modes of CW, the original digital mode, and SSB phone. Building little rigs and radiating and receiving continuous waves are to a radio experimenter much like playing scales and folk tunes are to a musician. They are the first things we learn, are important parts of the daily practice routine throughout life, and we

neglect them at our peril. The little rigs, and the concepts they represent, are at the core of wireless technology. It is not enough to play with them as a novice and then move on to other things; they need to be revisited over and over again at different stages of one's vocation, each time achieving a new level of mastery until finally one is probing the deepest mysteries of the art.

1.2 GETTING STARTED—ROUTES FOR THE BEGINNING EXPERIMENTER

What to build:

A frequent question asked by the prospective experimenter regards an initial project or subject for pursuit. A common choice for a first project comes from a desire to extend the capabilities of an existing station. The future experimenter already has experience with on-the-air activity and a working station. He or she then wants to extend that station to new bands, improved transceiver performance, or fabricate a rig offering portability. While these goals are all worthy, they can be difficult. They may be conceptually impossible for the beginner, and impractical for the seasoned experimenter with other life commitments. A better "first" experiment may well be something that is much simpler. Several simple projects are offered later in this chapter as suitable beginnings.

How to build it:

Another getting-started question regards the methods to use in building electronics. There are several options, all with their assets and weaknesses. A few are discussed below.

PRINTED CIRCUIT BOARDS

The primary construction scheme used in modern electronics is the printed circuit board (PCB). Here, pads or islands of metal are attached to an insulating material, usually epoxy-fiberglass. Wires on the parts are pushed through holes in the board and soldered to the pads, which are interconnected by printed metal runs, thus forming the circuit.

A PCB begins as a fiberglass sheet with copper laminated to one or both sides. The metal surfaces are then coated with a light sensitive "photo-resist" material. A pattern for the circuit is optically transferred to the surface and the unexposed material is washed away. The board is now placed in a solution that chemically etches some of

the copper away, leaving only those regions needed to form the desired circuit. After etching, the board is washed and drilled. Pure copper is easily corroded, so it is common to plate boards with a tin coating, forming a more stable and solderable surface. Refined boards include copper on both sides, and even plating on the inside of the holes. Industrial boards will often incorporate many layers.

Modern practice features *surface mount technology*, SMT, using small components without wire leads. The leads have been replaced with metallized regions on the parts that are then soldered directly to the board. The soldering provides physical mounting as well as electrical connection. The SMT boards are cheaper to build and usually much more dense. SMT parts can be so small that they are hard to handle without a good microscope. SMT is an interesting way to build if there is a need for really small equipment. The small size of SMT circuits often results in improved high frequency performance.

Growing SMT popularity in manufacturing means that surface mounted is the only available form for a component. Many parts don't exist in lead forms. In some cases they can be handled by the "Surfboards" by Capital Advanced Technologies which are found in DigiKey catalogs. These are small SMT boards with an interface that will adapt to other board forms.

Circuit boards have been built in a home environment by hams for generations. The reader should review the subject in *The ARRL Handbook* to find out more about the methods. A major problem with home etched boards is the disposal of the used etchant, usually a solution of ferric chloride. Disposal practices common in the past are now questioned in this era of enlightened recycling. Although some of the projects described in this text use etched boards, few of the boards were etched in our home labs.

BREADBOARDED CIRCUITS

Breadboard, as applied to electronics, is a term from a time when early radio experimenters built their equipment on slabs of wood, often procured from the kitchen. The term remains as an industry-wide description of a preliminary experimental circuit. There are numerous modern methods that can be used to generate a one-of-a-kind circuit.

UGLY CONSTRUCTION

A particularly simple method was outlined in an early *QST* paper and is now known as "Ugly Construction."² Although certainly not unique, the scheme works well and continues as a recommended method. The scheme consists of the following:

1. A ground plane is established using an un-etched scrap of copper clad circuit board material.
2. Following the schematic for a circuit being built, grounded components are soldered directly to the ground foil with short leads.
3. Some non-grounded parts are soldered to and supported by the grounded components.
4. Other non-grounded components are supported with suitable "tie down points" consisting of high value resistors.

5. Once finished and working, the board can be mounted in a suitable box, hidden from view if desired, where it becomes a permanent application of the idea. Ugly construction is illustrated in **Fig. 1.1**.

Casual circuit analysis allows the builder to pick the standoff resistor values. Any "high R" value resistors can be used. Usually, 1-MΩ resistors work well anywhere within RF circuits. The typical 1/4 W resistor of any value has a stray lead-to-lead parallel capacitance of about 0.3 to 0.4 pF, perhaps a little more with longer leads, and a series inductance of 3 to 5 nH.

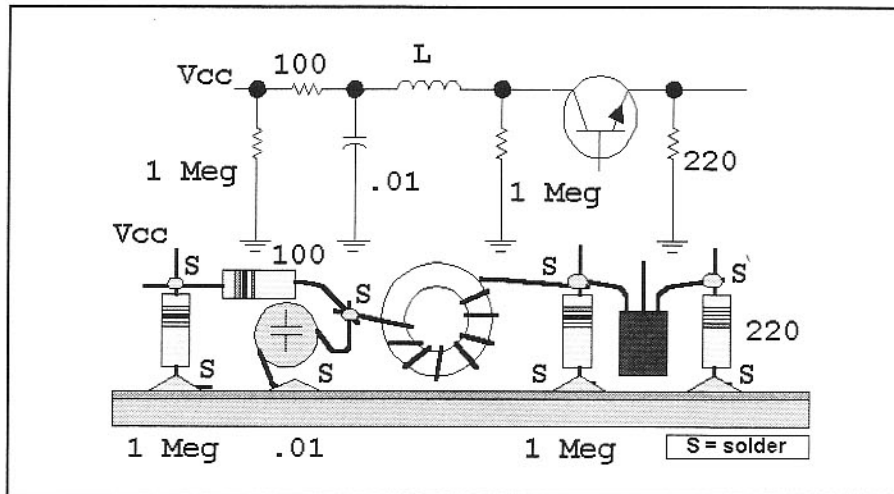


Fig 1.1—A partial circuit illustrating “ugly” construction.

Reactance is little consequence for work up through 150 MHz or so. High R means that resistance is high with respect to the reactance of the inductance. We sometimes use R values as low as $10\text{k}\Omega$. It is often surprising just how few standoff resistors are needed in an ugly breadboard.

The greatest virtue of the ugly method is low inductance grounding. Any construction scheme that preserves this grounding integrity will work as well. Picking a method is a choice that the builder has, a place where he or she can develop the methods that work best.

Integrated circuits can be placed on an ugly board with leads sticking up, “dead bug” style. There is little need to glue the chips down, for components and wires will eventually hold them in place. Grounded IC leads are bent and soldered directly to the foil.

Some builders prefer to maintain ICs with the IC label facing upward, allowing later inspection. They then bend all leads out in a “spread eagle” format.

We have never had a problem with ugly equipment being less than robust. Many of our ugly rigs have been hauled through the mountains of the Pacific Northwest in packs without incident. An outstanding example, the work of a friend, is the W7EL Optimized QRP Transceiver, a rig that has traveled around the world in suitcases and packs.³ Few if any standoff resistors were used in that rig.

MANHATTAN BREADBOARDING

Several other construction schemes offer similar grounding fidelity, including those where small pads of circuit board material are glued or soldered to the ground foil. These pads then have components soldered to them. We have found this

method to be especially useful for slightly massive components such as floating, non-grounded, trimmer capacitors. The specific glue type has little impact on circuit performance. Variations of this method have been called “Manhattan Construction,” and can be mixed with other breadboarding schemes. The reader can find numerous examples on the Web on sites dealing with QRP experiments, as well as in Fig 1.2.

The proponents of Manhattan Construction often use small round pads that are glued to a ground foil with epoxy or similar glue. The pads are placed so that all components are parallel to board edges and close to the ground foil. This produces an attractive board resembling a commercial, PC board. This does not seem to compromise performance.

With traditional ugly construction, parts can be moved about to make room for another stage. In the extreme, an entire circuit can be lifted and moved, a stage at a time, to another board.

A primary virtue of a bread-boarding scheme is *construction speed and flexibility*, especially important when the primary purpose of building gear is information about circuit behavior.

Some folks prefer to rebuild a circuit after a breadboarding phase, replacing an ugly prototype with a more permanent, production-like version. These efforts take additional time and rarely produce performance superior to the original breadboards. Even looks can be deceptive when one hides ugly breadboards behind more attractive front panels.

QUASI-PRINTED BOARDS

Some experimenters prefer to build equipment that looks like a PCB, even

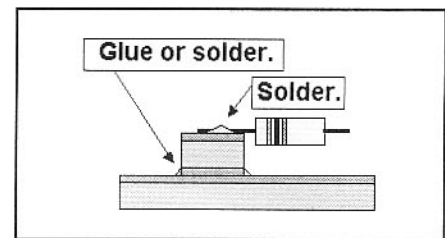


Fig 1.2—An example of “Manhattan” breadboarding.

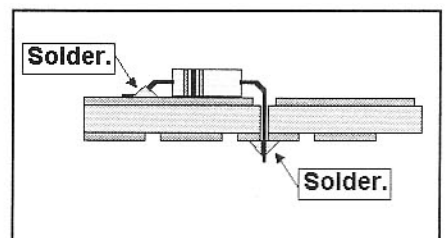


Fig 1.3—A “quasi-circuit board” scheme for breadboarding. The installed resistor here is soldered to ground and to a pad that connects to the rest of the circuitry.

when the board is not etched in a circuit-specific pattern. One method, called “checker-board,” uses double sided circuit board with one side functioning as a ground foil. The other side consists of a matrix of small islands of copper. These regions are created either by etching or manually with a hack saw. Patterns of squares on 0.1-inch centers accommodate traditional ICs. Holes are drilled in the islands where components must reside. A large drill bit then removes ground foil around the hole without enlarging it. No holes are required where a ground connection is needed. Components usually reside on the ground side of the board. See Fig 1.3.

The double sided checker-board can also serve for breadboarding with surface mounted components. Parts then reside on the pattern side with holes drilled to reach ground. Small leaded components can also be surface mounted.

The checkerboard scheme, “Manhattan” variants, and even double-sided printed boards have fairly high capacitance from pads to ground. These are often poor quality capacitors with low Q, under 100 for epoxy fiberglass board material, and are subject to water absorption. A single sided format is preferred for critical sections of a LC oscillator application.

1.3 SOME GUIDELINES FOR THE EXPERIMENTER

With *Solid-State Design for the Radio Amateur* came considerable interaction with the rest of the amateur radio community. A frequent question we heard was "How do I get started with experimenting?" Or, "I've read about and have even built some kits and published projects, but I want to go further. I want to do my own design. What is the next step?"

A set of guidelines is offered in an attempt to answer some of these questions. These are not firm, well established rules, but mere impressions and personal biases that we have generated, approaches that work for us. They are offered without guarantee.

• **KISS:** This British term is short for "Keep It Simple, Stupid." We often design equipment that is more complicated than needed. It is well worth some extra time during design to evaluate every part to see if it is really needed. The function of each part should be understood and justified. The circuit should function as intended. This does not imply that designs with the minimum number of parts are best. However, it is rarely justified to overdesign by adding extra components "because a problem might occur." For example, designs with a profusion of ferrite beads and "stability enhancing" resistors may be suspect.

• **Avoid lore:** Lore, in this case, refers to "knowledge" that is based upon experiences that are divorced from careful thought. A classic example in amateur radio regards the thermal stability of LC oscillators. Envision the amateur experimenter who built an oscillator using a toroid. The circuit drifted when he opened the window to the winter weather. The next evening he replaced the inductor with one wound on a ceramic coil form, noticing less drift when he opened the window. He concluded that ceramic forms are better than toroids, having never considered the specific coil forms that were used, the other components in the circuit, or the fact that the weather had improved. Poorly executed experiments like this often generate erroneous conclusions. The resulting lore, although interesting, should always be questioned. It is always better to do meaningful measurements.

• **Plan your projects with block diagrams:** Start with small diagrams where each block is a global element, perhaps containing several stages. Expand these to show greater detail. Block diagrams will be discussed further below.

• **Generate modular equipment:** A high performance receiver, for example, should

consist of several sections, each designed so that it can be built, tested, modified, and redesigned as needed, with minimal change to the rest of the system. Even the simplest little rig should be built a stage at a time, turned on sequentially, tested, and modified as needed. Single board transceiver designs are popular in the QRP arena. But realize that the ones that work well are probably the result of several rebuilds, and even then, some don't work very well; others are superb.

- Avoid excessive miniaturization: It takes much more time to build small things than those where the circuitry can expand without bound. Even when building small portable QRP transceivers, it's often worthwhile to establish the design with a larger breadboard.

- Base projects on your own goals: Our central personal goal is learning through experimentation. Hence, we base projects on questions that need investigation rather than what we need or want for on-the-air operation. But your goals may be different. It is worthwhile to review and define them as a means of picking the best projects for you. Isolate primary goals from those that are serendipity.

- Be wary of "Creeping Features." The term "*appliance*" often describes the transceivers that we purchase for on-the-air communications. Appliances, even ones that we build ourselves, are usually expected to have many features, but these *bells and whistles* can actually impede experimental progress. A single band, single mode transceiver can be as experimentally enlightening and informative as a multiple mode, general coverage transceiver.

- Use the literature. Peruse catalogs, data manuals, web sites, and even instruction manuals for circuit ideas. When a circuit method is not understood, it should be studied in texts appropriate to the technology. It is useful to build something with the part as a way to really understand that part.

- While planning is necessary, don't spend excessive time in the preliminary design phase of a project. Rather, outline preliminary ideas and goals, do initial calculations (on a computer only if they are really complicated), gather parts, and begin building. Enjoy the freedom that allows you to change your mind in the middle of an investigation. Refined calculations can occur during and after construction and are not just "design phase" activities.

- It's not about craftsmanship: A portion of the homebrewing community was schooled with the idea that "nice looking" circuit construction went along with good performance. But the two factors are generally isolated. This is illustrated in **Fig 1.4**. There is no relationship between having a nice looking, orderly circuit board and good performance from that board. Indeed, those saddled with the chore of designing a printed board to perform as well as an *ugly* breadboard may wonder if there might be an inverse relationship!

- Use breadboarding over a ground plane for communications circuits, especially when investigating new ideas. Use vector board or wire-wrap methods for slow digital circuits, but treat fast digital circuits as if they were RF functions. In general, build with those methods that will offer the best, low inductance, grounding while allowing circuits to be quickly designed, assembled, and tested. If you are concerned with aesthetic details, build a second version. Alternatively, an attractive panel can be used to hide ugly, but highly functional breadboards.

- Build what you use, and use what you build: Those of us in the homebrew end of amateur radio often kid our appliance operator friends, suggesting that a "real ham" should build instead of just operate. Some avid experimenters may take this too far; they build a rig, use it just long enough to confirm functionality, and go on to the next project, missing some exciting discoveries along the way. By using the equipment with tempered intensity, the experimenter will discover the strength and weakness of the rig, allowing the next project to be even more successful. The same arguments might be applied to software developments!

- Beware of the golden screwdriver: A good friend, WA7MLH, encountered a fellow on the air whose sole method for experimentation was to adjust all of his equipment for maximum output. He did this with a favorite screwdriver, which he treated as golden. After careful tweaking of all circuit elements that could be adjusted, he was almost always able to coax a 100-W transceiver into delivering 110 W of output. Unfortunately, what started as a good piece of equipment had become a distorted disaster. While we all tend to adjust circuits for "maximum smoke," linear circuitry should be confined to operate under linear conditions. It is important that the limits be recognized and adhered to. This is especially important when building SSB gear. Alignment means adjustment to the proper, measured level,

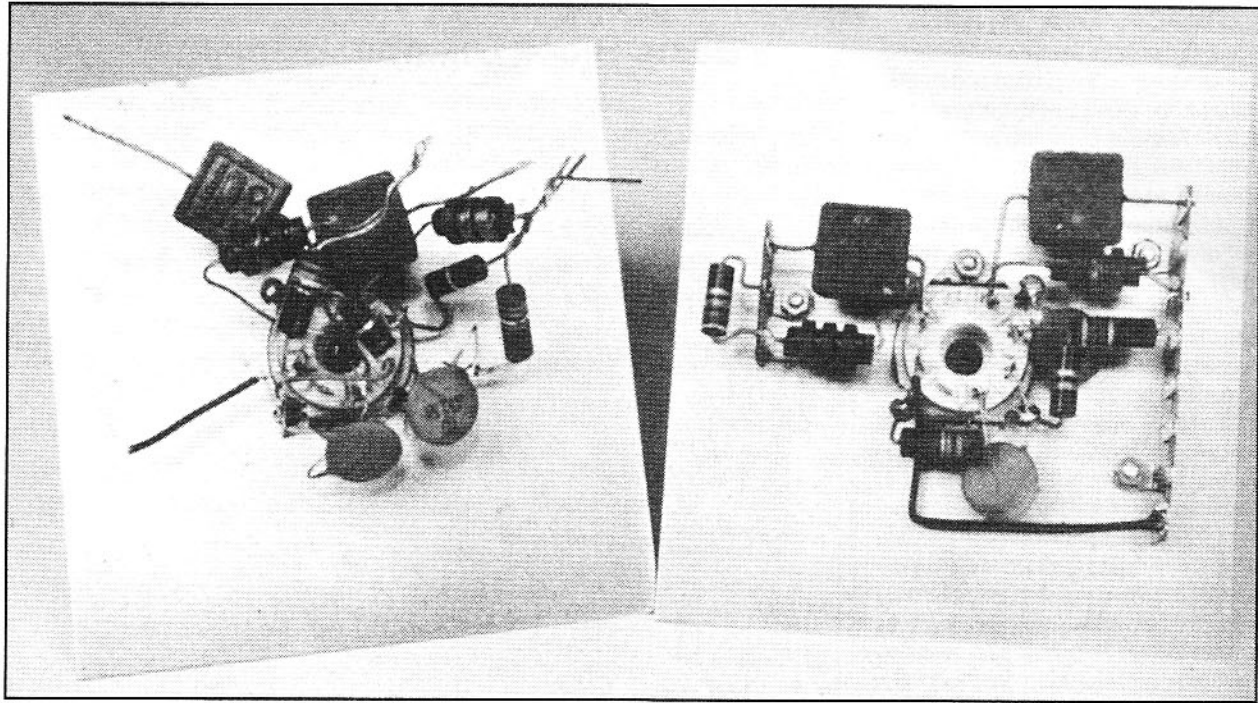


Fig 1.4—“Nice looking” circuit construction does not always equate to good circuit performance.

which may differ from maximum.

- Always keep notebooks for experiments: Record those wild circuit ideas that come up while you cut the lawn or watch TV; record important data during experiments, including the temperature when you open the window; take notes on the circuits that you build, including changes that are made during building and “turn on”. Date the notebook and place small dated labels inside the rigs so you can find the data when it’s needed. Use bound or spiral notebooks rather than loose-leaf documents, for they are more permanent. A long term computer based index of notebooks is very useful.

- Find others with the same passion for experimenting: Although this guideline is pretty obvious, it’s also easy for the experimenter to become isolated in his or her own world. Builder hams are rarely isolated. Finding the local ones will give you a place to communicate your ideas, hear about new thoughts, and to share junkbox parts as well as test equipment. Ask at

local clubs to find out who is building. Listen to the appropriate nets and attend the specialty clubs. Write to fellows who author articles of interest, especially if they live nearby. Watch the chat sessions on the Internet or the Web. Amateur radio is about communications, so don’t hesitate to communicate.

- Look toward the ordinary for explanations: When a design is not working as well as it should, we look for explanations that will explain the differences. All too often we consider the complicated answers, only to discover that the real answer is in the “obvious.” It is always worthwhile to return to fundamentals.

- Strive to build equipment that does not pollute the already abused radio spectrum: Make an effort to generate *clean* equipment, meaning that it does not emit signals at frequencies other than the intended ones. While most of this concern is with transmitters, the ideas should also be applied to receivers. The difficult question is “How clean is clean enough?” The

FCC has specifications for spurious emissions from US transmitters. These specifications depend upon transmitter output power. Even for equipment running full power, the specifications are generally easy to meet at HF. When power drops below 5-W output, they become even easier. Throughout this text we take the approach that even greater levels of cleanliness will be sought. This book includes a chapter on test equipment. One of the items featured there is a spectrum analyzer that will allow the builder to measure spectral purity.

A final “rule:” Don’t let any of these rules get in the way of experimenting and building! It’s OK if there are things that you don’t understand even if that includes the project you are about to build, for you will understand much more when you are finished. The real goal of this pursuit, and of this book is to *learn by doing*. The same can be said for other “rules” that may appear in the literature or on the web: Don’t let them keep you from experimenting.

1.4 BLOCK DIAGRAMS

Fig 1.5 shows a collection of elements that can be used in a detailed block diagram of a radio. This short list is generally extensive enough to describe the non-digital designs in this book.

Schematic and block diagrams serve a variety of purposes in electronics. The purpose of the block diagram is to present the functions and their interconnection used in a piece of equipment. Schematic diagrams present the details.

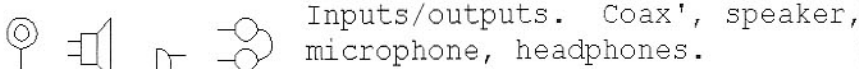
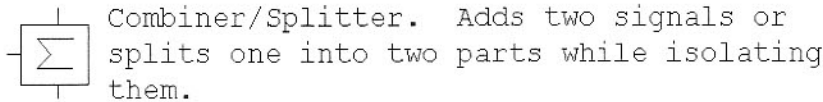
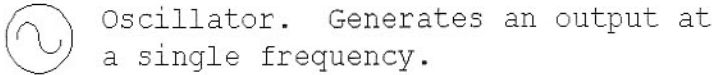
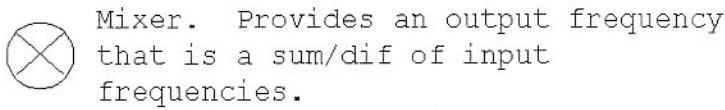
A block diagram is a useful way to plan and describe the equipment we wish to build. The block diagram will serve as the starting point for mathematical analysis that we may apply to the overall system. It can also emphasize the functions required to complete the design. This is illustrated with Fig 1.6 showing a direct conversion transceiver for the 40-meter band. Several filters are shown, illustrating the functions that are important for good performance. The low pass and the high pass between the mixer and audio amplifier are simple, consisting of one component each. There may be no components for the signal splitter, but the function remains.

Fig 1.7 shows a more elaborate circuit, a super-heterodyne SSB/CW transceiver for the 50-MHz band. The phasing method can also be used; such a 50-MHz transceiver is presented in Fig 1.8. Designing any of these systems begins by forming the block diagrams, which includes specifying each of the blocks. Once this is done, the individual circuits can be designed. Some elements are missing in the block diagram in the interests of clarity. It will be useful to add block detail during circuit design.

Some block details may differ from the final implementation, but functions remain. For example, the splitter and phase shifting functions are often combined in quadrature combiner circuits operating at RF. We sometimes show a 90-degree phase shift in one path with none in another where actual circuitry merely maintains a 90-degree difference.

These figures offer a glimpse of what the text will cover. The design of the block elements will each be discussed in individual chapters. Then, the blocks will be assembled in system chapters related to filter, phasing, and digital signal processing systems.

Basic Block Diagram Elements



Low Pass Filter



Resonator



High Pass Filter.



Bandpass Filter.



All Pass Filter
(Phase Shift network)

Fig 1.5—Common block diagram elements.

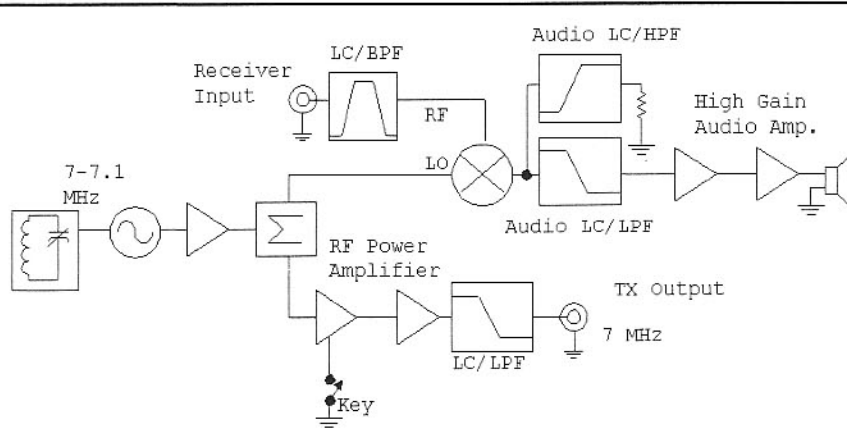


Fig 1.6—Block diagram of a direct conversion transceiver.

1.5 AN IC BASED DIRECT CONVERSION RECEIVER

This receiver design is one of the simplest possible that will allow CW and SSB signals to be received. It offers performance enough for on-the-air contacts while serving as an introductory construc-

tion effort.

The basis for this receiver is the NE602 (or NE612) integrated circuit. Originally introduced by Signetics in the late 1980s, the chip is easy to use and offers good per-

formance among very low current receiver components. The NE602 contains a mixer and an oscillator, two essential blocks needed for a receiver. The mixer in a direct conversion receiver serves to heterodyne the incoming antenna signal directly down to audio. The oscillator provides mixer LO (local oscillator) injection for this conversion. The oscillator within the NE602 is a single transistor followed by a buffer amplifier of undisclosed complexity. The NE602 mixer is a doubly balanced circuit of a type known as the Gilbert Cell with operation outlined in a later chapter.

The LM386N audio amplifier following the NE602 completes the receiver. The LM386N will drive a small speaker, or headphones of high or low impedance. The ideal set of "cans" to use with this receiver is a light weight pair of the sort used with jogging receivers or similar consumer gear.

The receiver is shown schematically in Fig 1.9. Our version is built using the "ugly" methods outlined earlier. If you use a pre-etched and drilled circuit board, take the time to study the board layout in detail, and trace the circuit while studying the schematic diagram. Merely stuffing parts and soldering will provide you with no more than soldering practice.

The signal from the antenna connector is applied to a pot that serves as a gain control with output routed to a single tuned circuit using L1, a toroid inductor. This circuit drives the mixer input at NE602 pins 1 and 2. The load within the IC looks like a pair of 1.5-k Ω resistors from the input pins to a virtual ground.

The NE602 oscillator has a collector tied to the positive power supply. The base of that transistor is available at pin 6 while pin 7 goes to the emitter. Internal bias resistors set the voltage and establish a current of about 0.3 mA in the Colpitts oscillator. Feedback capacitors in our circuit run between pins 6 and 7 and from pin 7 to ground. A 270-pF capacitor then ties the base to the rest of the tuned circuit.

A simplified version of the oscillator circuit is shown in Fig 1.10. This illustrates the way a simplified circuit is used to calculate the resonant frequency. Fig 1.10A shows the complete oscillator. But, the two 680-pF feedback capacitors have a series equivalent of 340 pF, as shown in part B of the figure. In going from Fig 1.10B to Fig 1.10C, we resolve the 50-pF variable and 10-pF fixed into 8.3 pF; the 270 and 340 pF become 150 pF. We evaluated both variable capacitors at their maximum value. Fig 1.10C has nothing but parallel capacitors which add directly to

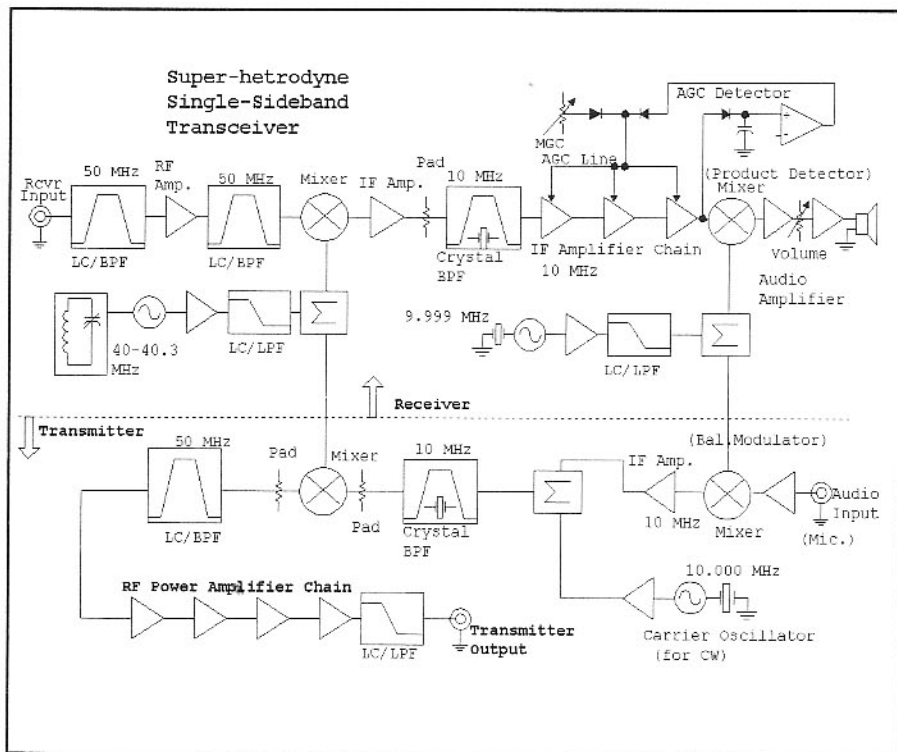


Fig 1.7—Block diagram of a super-heterodyne SSB transceiver.

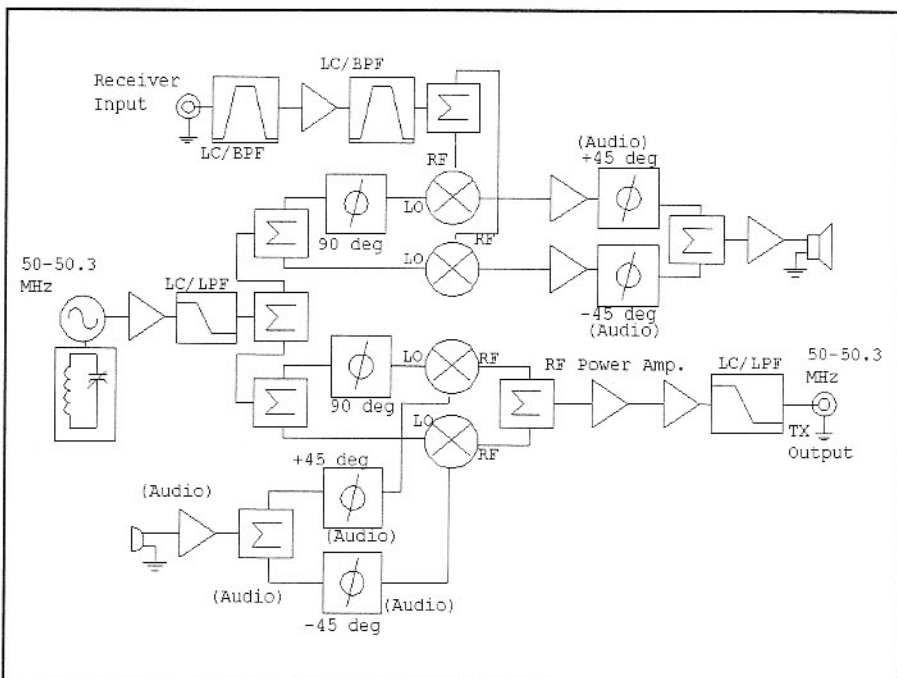


Fig 1.8—Block diagram of a phasing method SSB transceiver.

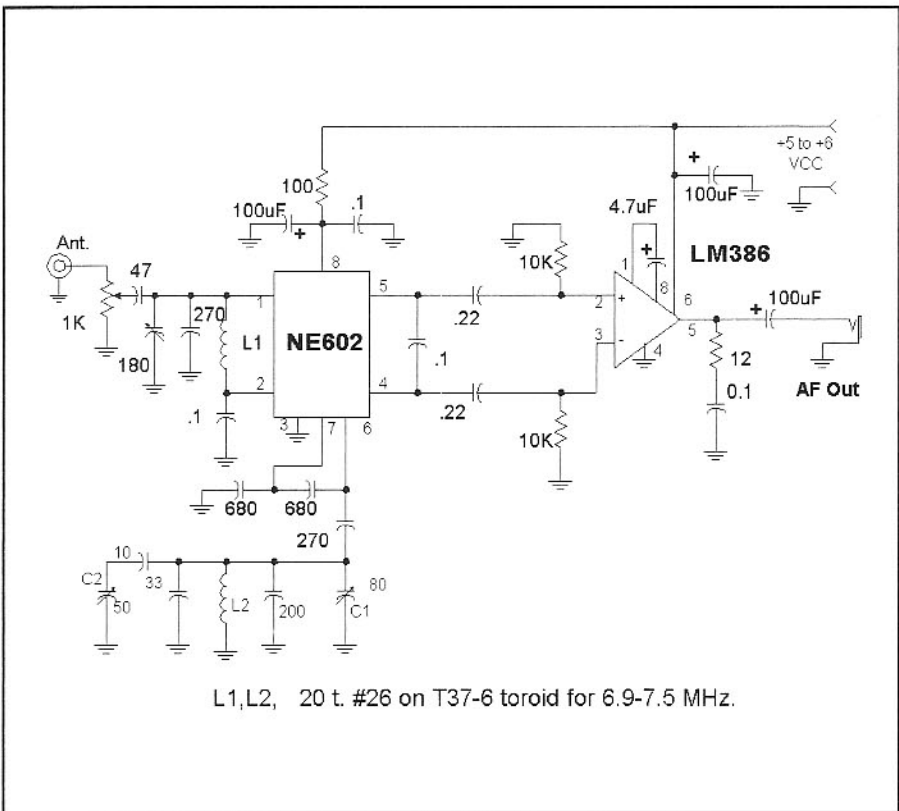


Fig 1.9—Direct conversion 7-MHz receiver using two integrated circuits.

form Fig 1.10D. A simple resonance calculation shows tuning to 6.9 MHz.

Two variable capacitor (C_1 and C_2) are used in our oscillator. They are nearly the same value. The larger, C_1 , directly parallels the inductor. A detailed analysis shows that it will tune over a wide range, the full 6.9 to 7.5-MHz span. C_2 is “padded down” with a 10-pF series capacitor. C_2 has a value ranging from 5 to 50 pF. The series capacitor then generates a composite C ranging from 3.3 to 8.3 pF, a 5-pF difference. Add capacitance in parallel with C_2 to create even greater bandspread (resolution or low tuning rate).

All fixed capacitors should ideally be NP0 ceramic types, readily available from major mail order sources. But, don't hesitate to try other caps if you have them in your junk box. The worst that will happen is that the receiver will drift more than desired. New parts are easily substituted later.

These capacitor variations are doubly significant. First, you can adapt a tuned circuit to work with whatever you have on hand. For example, common 365-pF AM broadcast capacitors can be used in both positions with appropriate padding. Second, the use of two capacitors is a very practical means for building simple receivers while avoiding the mechanical complexity of a dial mechanism. We have used double cap tuning for transceivers in other parts of the book. Adapt the circuit to what you have available.

The mixer input network at L1 that injects antenna signals into the NE602 uses an inductor identical to that in the oscillator, tuned with a mica compression trimmer capacitor. Any variable can be used here. If a 365-pF panel mounted cap is used, the 270-pF capacitor could be reduced in value. If the only available variable capacitor is much smaller than 180 pF, you may have to resize L1, or add or subtract net capacitance a bit to hit resonance. The inductance can be reduced by spreading or removing turns, or increased by compressing turns. Both circuits are very tolerant of such changes.

Once the mixer has been wired, most of the receiver is finished. The LM386 is a low power part with no heat sink required. This receiver draws only 7 mA when signals are low, with more current with louder signals. A simple 5-V power supply works well. A 6-V battery pack will run the receiver for extended periods.

The NE602 mixer features excellent *LO to RF isolation*. This means that there is little LO energy appearing at the mixer RF port, and hence, the receiver antenna terminal. The presence of such energy can lead to a common problem of “tunable hum” with

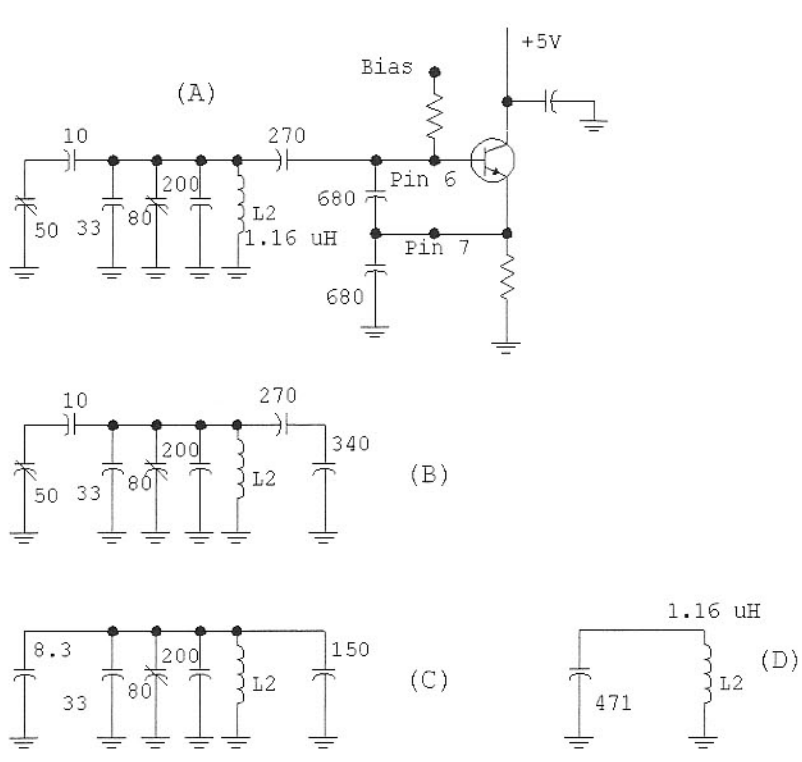


Fig 1.10—Simplified version of the oscillator in a NE602. See text for explanation.

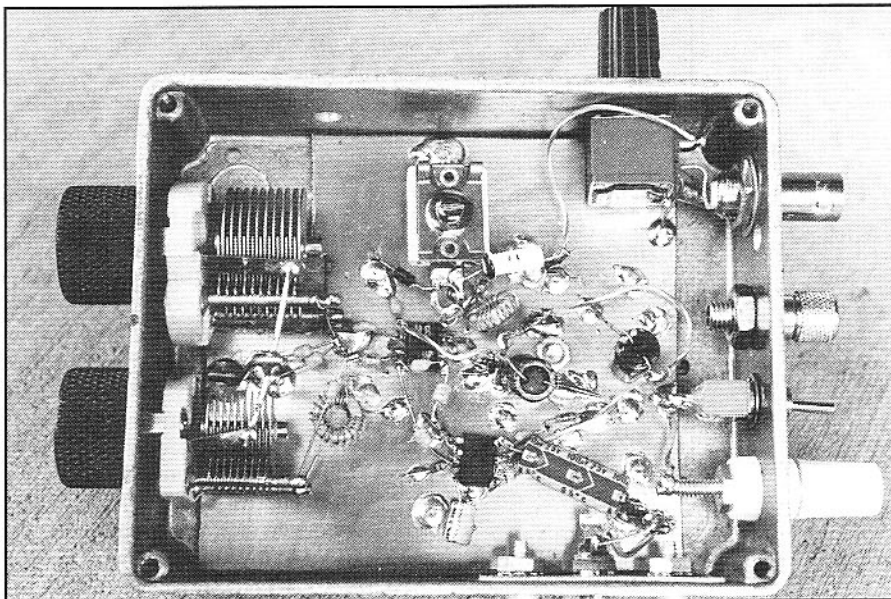


Fig 1.11—Direct conversion receiver assembly.

some direct conversion receivers.

The receiver also has problems. Some, the audio images, are intrinsic to all simple direct conversion receivers. This is the price, but also the thrill of such a design. The selectivity is lacking. This can be remedied with audio filters that can be placed in the receiver. Examples of audio filters are found elsewhere in this book. These filters would go between the mixer and the audio amplifier. It is easy to add such things to a breadboarded receiver, but more difficult with a printed board.

The greatest performance deficiency is the

poor strong signal handling capability of the receiver. Although helped a bit by placing the only gain control in the antenna lead, the problem is intrinsic to the NE602 mixer. The basic Gilbert Cell is capable of much more, but only when biased to draw considerably more current. The current is kept low in the NE602 by design, for it is intended for battery powered consumer equipment and not ham gear. Strong, high performance direct conversion receivers are described later in the book.

Initial turn-on and adjustment is straightforward. Apply power initially with a

100- Ω resistor in the power supply line. The resistor serves as a fuse if you have done something drastically wrong. Inserting the headphones when the output capacitor is uncharged will produce an audible pop. If the audio seems to be working, turn the receiver off, remove the extra resistor, and start again. Attach an antenna, advance the gain control and tune C1. Signals should be heard. Adjust the front-end tuned circuit for maximum signal. If you have a calibrated signal generator you can inject a signal and see if the operation is at the right frequency. If you have a general coverage receiver available, you can attach the antenna of this receiver to that of the general coverage receiver where you will be able to hear the LO signal. If an antenna is not available, you can throw 20 or 30 feet of wire out on the floor. While this is not going to compete with a good outdoor antenna, it will provide signals in abundance to listen to and confirm receiver operation.

The receiver in **Fig 1.11** was built for the 40-meter band. If you want to try a different band, all that is required is to change the two inductors. Increasing the 1.16- μ H inductor to 4.5 μ H will drop the receiver right into the 80 meter band. A band switching version would be practical.

The first popular receivers of this sort appeared in the USA in a *QST* paper by WA3RNC.⁴ Variations of a similar sort were generated and published in Europe by George Dobbs, G3RJV. George used a double tuned circuit in the front end to improve signal handling properties.

1.6 A REGENERATIVE RECEIVER

There was a time when simple vacuum tube regenerative circuits were the only receivers available to the radio amateur. Even when super-heterodynes became possible, the regenerative design remained as the entry level radio.

Regenerative receivers have become popular again, but they now generally use semiconductors. Much of this popularity has been fueled by the work of Charles Kitchin, NITEV.^{5,6} People now build regenerative receivers for the sheer joy of listening to a receiver that is extremely simple, yet is capable of receiving signals from all over the world. The radio offered here tunes from 5.5 to 16 MHz, covering three amateur bands, 7, 10.1, and 14 MHz, as well as international short-wave broadcasts at 6, 7, 9.5, 12, 13.5, and 15 MHz.

The core of a regenerative receiver is the detector. **Fig 1.12** shows a JFET version of a classic regenerative detector using a “tickler coil.” Signals from the antenna or a preceding radio frequency amplifier are applied to the tuned circuit, producing a voltage at the FET gate. This produces FET drain currents that vary at the RF rate. The RF drain current flows in the tickler coil which couples energy back to the original coil through inductive transformer action. If enough energy is coupled back, the circuit oscillates. Even when the coupling is weaker, insufficient for oscillation, the circuit can have very high gain. This makes the weakest signal large within the detector circuit. The presence of any large signal in a “square-law” device like a JFET will produce detection, which

means that audio also appears within the circuit. It need only be coupled out and applied to headphones or an audio amplifier to complete the receiver.

Our receiver uses some slightly unusual circuits that simplify the design. The detector is based upon a little appreciated variation of a traditional Hartley oscillator, a variant *without* transformer action. Instead, two series inductors, L1 and L2, serve as the traditional “tank,” or resonator. Toroids were used, although Q is not critical and traditional cylindrical coils will also work. Indeed, low Q radio frequency chokes offer opportunity to the experimenter.

The detector, Q2, uses a junction field effect transistor. While we used a 2N5454, the detector worked well with any N-chan-

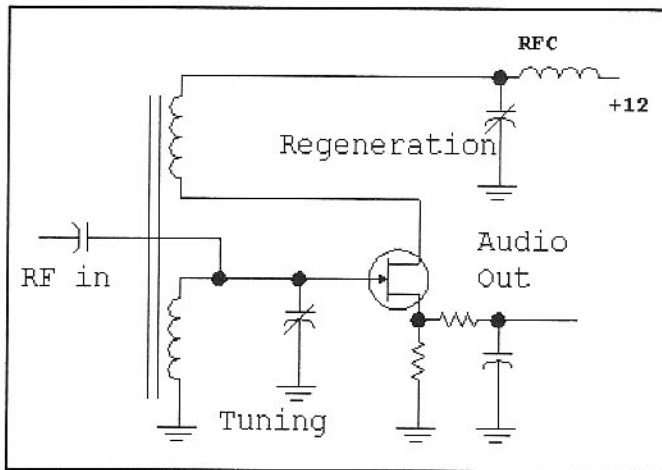


Fig 1.12—A classic regenerative detector.

C3, each with a large knob. C2 is a "band-set" while C3 is a higher resolution "band-spread" tuning, an action resulting from the series and parallel fixed capacitors around C3. Regeneration is controlled with another 365-pF variable capacitor. None of the variable capacitor values are terribly critical. If you find others at a flea market or hamfest, you can adapt the circuit to use them. That's part of the charm of a personalized regenerative receiver; it applies positive feedback to your imagination.

This circuit uses an RF amplifier, Q1. The gain is not really needed, or even desired. However, the amplifier provides a relatively stable driving impedance for the detector, and is a convenient way of varying the strength of the signals arriving at the detector. The RF amplifier is preceded by a 5th order low pass and 3rd order high pass filters. The high pass rejects signals from the AM broadcast band that could overload the receiver. The low pass attenuates FM and TV broadcast signals that could inter-modulate in the RF amplifier or detector, producing distortion within the receiver tuning range.

Audio gain is provided by Q3 driving

nel depletion mode FET we could find in our junk box. This included the U309, J310, 2N4416, 2N3819, and MPF-102, as well as some even more obscure parts. We couldn't find a FET that would not work. Use what you have! The complete receiver schematic is shown in **Fig 1.13**, and a front panel photograph appears in **Fig 1.14**.

We wound our own 1-mH choke for L3.

using a large ferrite bead. A 1-mH or 2.5 mH RFC will work well in this position. A 1-K resistor even functioned in place of L3, although the regeneration control was not as smooth as it was with an inductor.

The mechanical complications of a dial mechanism are avoided by tuning the receiver with two variable capacitors, C2 and

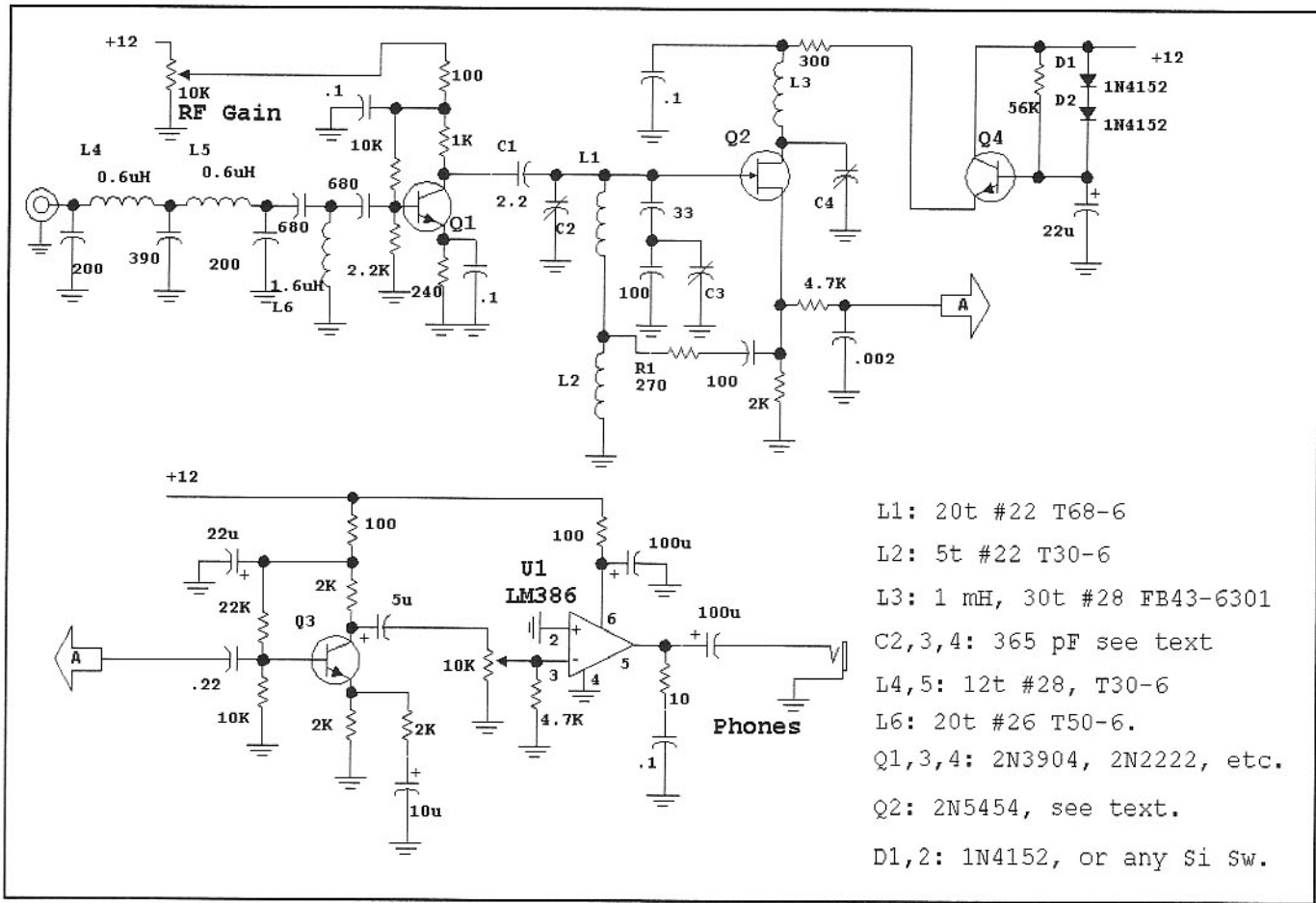


Fig 1.13—A regenerative receiver tuning from 5.5 to 16 MHz. See text for discussion of parts and construction.

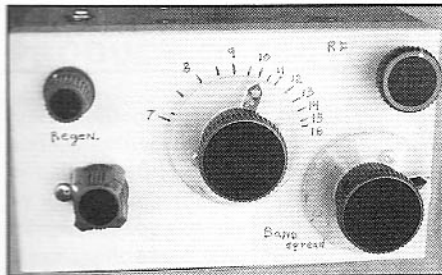


Fig 1.14—Front panel view of the regenerative receiver.

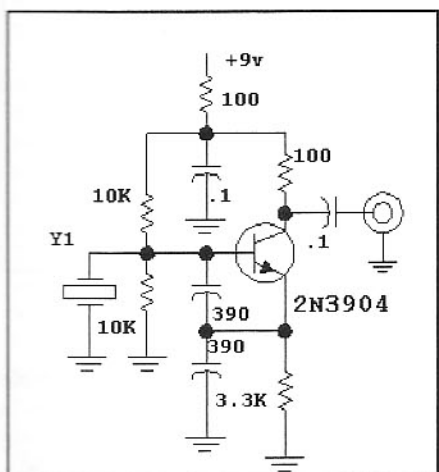


Fig 1.15—A simple crystal oscillator becomes a substitute for a signal generator.

U1, a common LM386N output amplifier. This will drive either low impedance "Walkman" type phones or a small speaker. Walkman is a Sony trademark. Q4 is an active decoupling filter that provides hum-free dc to the detector. Although the receiver of Fig 1.13 is shown with a 12-V power supply, it worked well with voltages as low as 6. Typical current is 20 mA at 12 V.

A signal generator with frequency counter is useful during initial experiments with the receiver. However, many builders may not have them available. **Fig 1.15** shows a suitable substitute, a crystal oscillator that will operate anywhere within the receiver range. Numerous inexpensive crystals are available from the popular mail order sources that will provide a starting point. For example, a 10-MHz crystal available for under \$1 will mark the 10.1-MHz amateur and the 9.5 to 10-MHz SW broadcast bands.

The receiver can be built in any of many forms. A metal front panel is a must, affording shielding between circuitry and

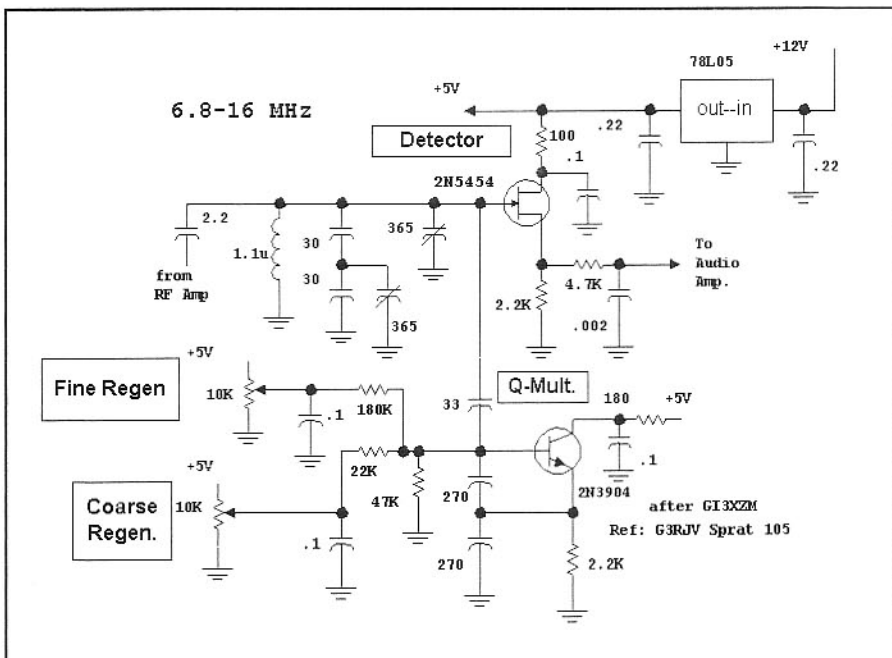


Fig 1.16—Alternative regenerative detector.

the operator's hands. However, the rest of the receiver could be as simple as a block of wood found in the garage. Our receiver was built "ugly" with scraps of circuit board material. One scrap will suffice, although our receiver used three, an indicator of earlier experiments. Other breadboards will work as well, but a printed circuit board should *never* be used for a regenerative receiver. Even if dozens are to be built, such as in a club effort, the project should emphasize open ended, flexible breadboarding to encourage experimentation.

Some experimentation may be required to set up the regeneration. Increasing L2 by a turn or decreasing R1 will both increase regeneration. However, too much inductance at L2 or too little resistance at R1 will produce such robust feedback that regeneration cannot be stopped or easily controlled.

Operation of this, or any regenerative receiver is a multiple control effort. Begin with the regeneration control, C4, at minimum capacitance, unmeshed, and set the two tuning controls at half. Set the RF gain for maximum gain, +12 V on the amplifier, with the audio gain in the middle and attach an antenna. Tuning C2 may produce a signal. Now slowly advance the regeneration, adding C at C4. It is normal for background noise to increase with a mild "plop" occurring in the headphones as the detector begins to oscillate. If the detector

becomes overloaded, reduce the RF gain control. Tune the receiver until an AM signal is found. Then reduce regeneration until the "squeals" subside. CW and SSB are best received with the regeneration well advanced. While the receiver works best with an outside antenna, it will function with as little as a few feet of wire tacked to the wall. The signal generator of Fig 1.15 requires no more than a two foot piece of wire on its output, somewhere in the same room as the receiver.

There are numerous interactions between controls, features that offer challenge and intrigue for the experimenter who takes the time to enjoy them. Numerous circuit refinements are available to the experimenter who wishes to continue the quest. The experimenter will discover a great deal from his or her efforts in operating this receiver. The availability of very high gain through positive feedback can be used to great advantage. But operation can be a greater challenge than found with a more advanced receiver.

A more recent experiment used a different regenerative detector, shown in **Fig 1.16**. This circuit eliminates one of the variable capacitors used in the other circuit, replacing it with a pair of potentiometers. This circuit was featured in a recent issue of *SPRAT* by George Dobbs, G3RJV, although the circuit seems to be the brain-child of G13XZM.⁷ Performance of the two circuits is similar.

1.7 AN AUDIO AMPLIFIER WITH DISCRETE TRANSISTORS

The amateur literature is rich with older designs using high impedance headphones. These designs are often very battery efficient, a vital performance virtue for portable or emergency equipment. But high impedance headphones that can be used with the more efficient designs have become rare. The answer to this dilemma is a simple audio amplifier that will drive low impedance headphones while maintaining reasonable efficiency.

One solution to the problem is one of many integrated circuits. Throughout the book we used the LM386 or op-amps to drive headphones of the Sony "Walkman" variety. An alternative circuit is shown in Fig 1.17. This amplifier uses commonly available discrete transistors. The version of the circuit that we built used leaded parts, but could just as well be built with SMT components. Q1 functions as a gain stage. The $2.2\text{-k}\Omega$ collector load (R8) with $100\text{-}\Omega$ degeneration (R4) produce Q1 bias current of 2 mA for an approximate voltage gain of 20. Q2 functions as a floating voltage source that establishes bias for complementary emitter-follower output transistors Q3 and Q4. Negative feedback through R3 reduces gain and establishes overall bias. This cir-

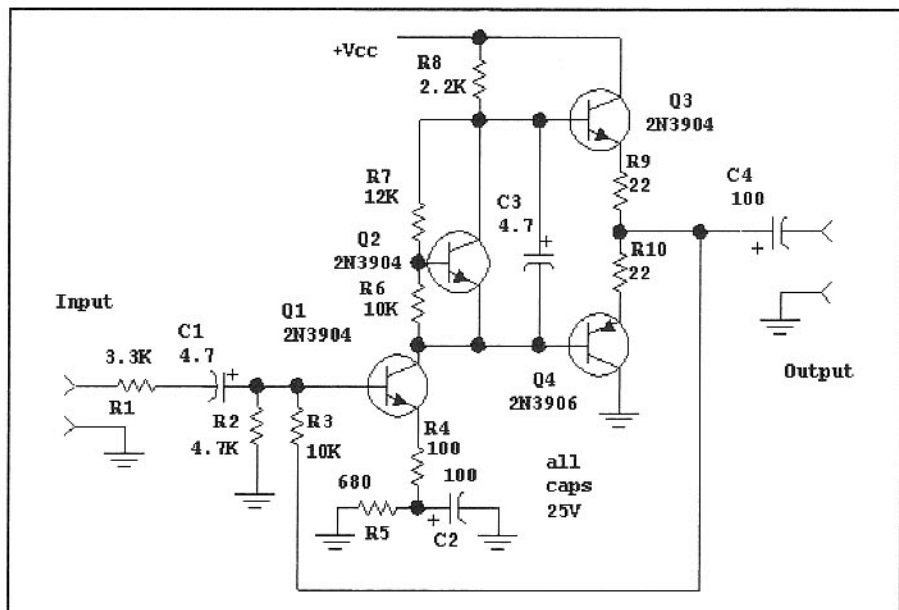


Fig 1.17—Simple audio amplifier using discrete components.

cuit is similar to many of the simpler integrated circuits. This circuit functions well with power supplies from 5 to 15 V.

An IC is usually the preferred solution.

However, the discrete solution is available when an IC is not. All of the transistors in this circuit are very inexpensive and usually found in the experimenter's junk-box.

1.8 A DIRECT CONVERSION RECEIVER USING A DISCRETE COMPONENT PRODUCT DETECTOR

The direct conversion receiver described earlier used a NE-602 integrated circuit to fulfill both the detection and the local oscillator functions. Discrete (non-integrated) components can also be used in these applications. The receiver shown in Fig 1.18 uses a differential amplifier as the product detector. This design, shown for operation in the 40-meter band, has been built with both traditional leaded components and with surface mounted technology (SMT) parts and appears in Fig 1.19.

Q1 functions as a local oscillator. Voltage control is used with any of several common tuning diodes. The Colpitts circuit uses small powder iron toroids for both leaded and SMT components. C1 is a combination of NP0 capacitors, selected during construction to resonate at the desired frequencies. With the parts shown, the receiver tunes over about a 50-kHz range in the 40-meter band. The range may be expanded by paralleling additional varactor diodes, increasing the value of the 82-pF blocking capacitor, decreasing the value of the 2.2-k Ω resistor in series with the tuning control, or combinations of these measures.

The oscillator is buffered with Q2, a common-emitter amplifier with emitter de-

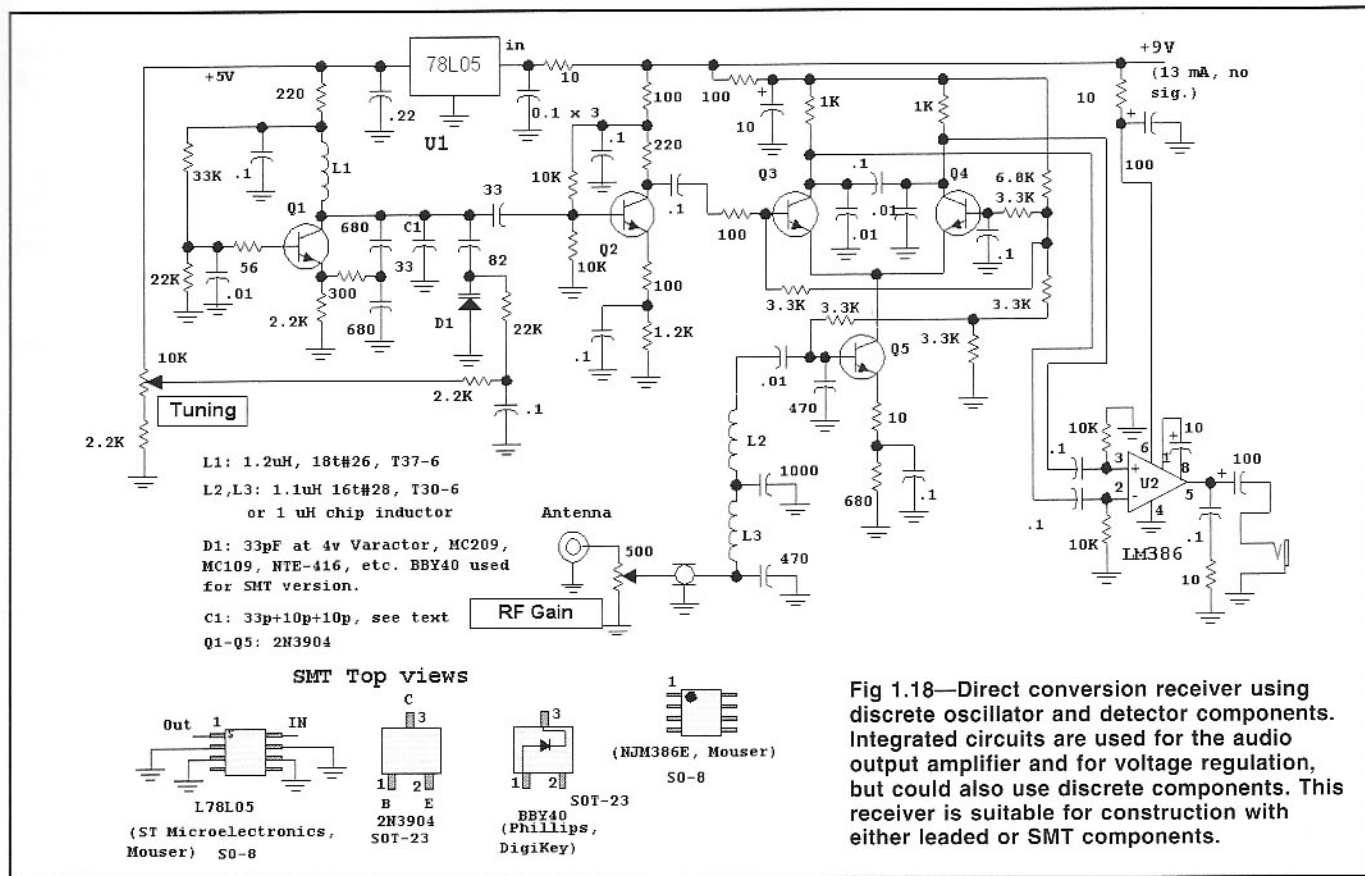
generation. This circuit, using negative feedback, uses a form found throughout the book, one where an added component reduces gain to improve performance. The output drives the mixing product detector consisting of Q3 and Q4. An RF signal is extracted from the antenna through a gain control, low pass filtered, and applied to the base of Q5 where it is amplified and converted to a current source

feeding Q3 and Q4. The mixer collectors are bypassed for RF.

The detector output feeds a differential signal to a LM386 audio amplifier. De-coupling became important with this stage, owing to the internal resistance found with a normal 9V battery. An uncomfortable "howling" oscillation disappeared with high decoupling capacitance for the audio amplifier.



Fig 1.19—Inside view of SMT direct conversion receiver.



1.9 POWER SUPPLIES

Among the many tools needed by the circuit experimenter, beginning or seasoned, is a power supply. Indeed, several are always useful. Batteries serve well for simple, low current applications. However, the more useful power supply extracts energy from the power mains. That ac voltage is applied to a transformer, is rectified, filtered with a large capacitor, and regulated with transistors and/or integrated circuits.

Two major design questions are presented to the beginner: What transformer should be selected and how large should the filter capacitor be? Fig 1.20 shows an example 12-V, 0.5-A design we use to address these questions.

Transformers are rated for RMS output voltage with a load. The peak voltage will be higher by a factor of 1.414, so a 12.6-V transformer will have a peak output of 17.8 V. The transformer current rating should equal or exceed the maximum desired dc current, so a 0.5-A transformer is adequate for this application. This is shown in part A of Fig 1.20. A switch and protective slow-blow fuse is added to the transformer primary.

A bridge rectifier using four diodes is added to the circuit to generate a dc output. The bridge is preferred over circuits with just two diodes, for a center tapped transformer is then not required. Bridge rectifier diodes should have an average current rating above the maximum power supply current. 1-A diodes would be fine for this application.

Some waveforms are shown in Fig 1.21. The “before filtering” voltage is the result of rectification for the circuit of Fig 1.20A. The “V-cap” trace shows the voltage across the capacitor when it is added to the circuit, Fig 1.20B. The significant detail is the *ripple*, or variation in unregulated output voltage occurring at the filter capacitor. Fig 1.22 shows ripple for two different capacitor values when the load current is 0.5 A.

A suitable regulator is the popular 7812. This three terminal regulator IC will provide the desired output with a *dropout* of about 2.5 V. Dropout is the minimum voltage difference between the regulated output and the higher unregulated input. With a 2.5-V dropout, the unregulated input must be 14.5 V or more over the entire cycle. Fig 1.22 shows that a 2000- μ F capacitor will be adequate, but 500 μ F will not. If we define ΔV as the difference between the peak rectified voltage and the minimum unregulated value, $17 - 14.5 = 2.5$, I as the output current, and Δt as the time for a half cycle (.0083 second for 60 Hz), the minimum capacitor value in

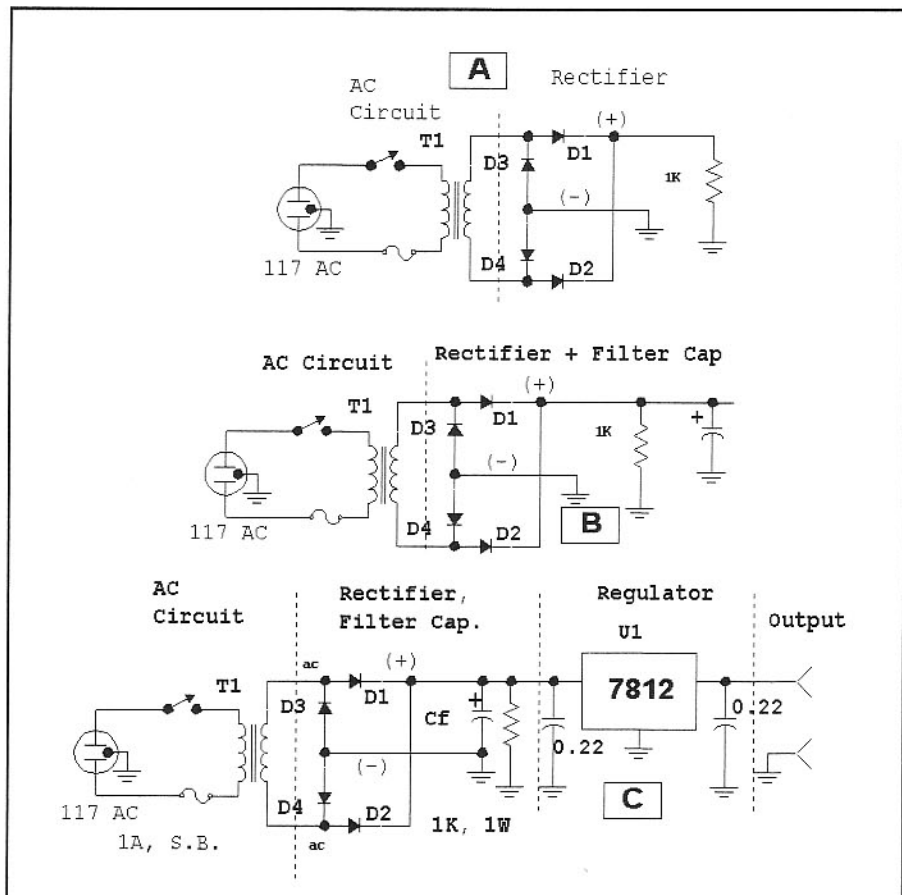


Fig 1.20—Fundamental power supply. Part A shows the transformer and rectifier, B adds the critical output filter capacitor, while C uses a 12-V regulator IC.

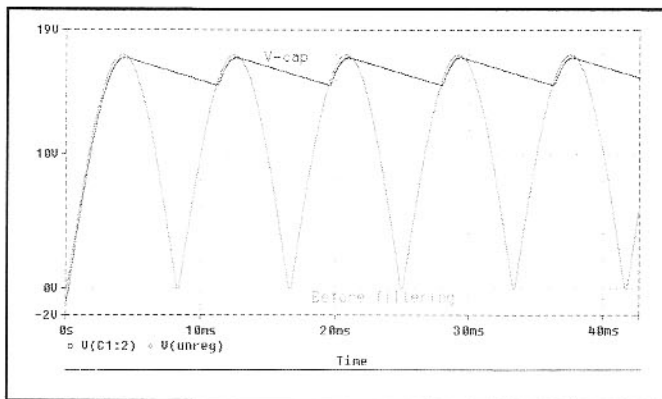


Fig 1.21—Waveforms for a simple power supply. The “before filtering” shows the raw rectified signal without any filter capacitor. The “V-cap” shows the voltage across the filter capacitor attached to the rectifier when loaded to a modest current.

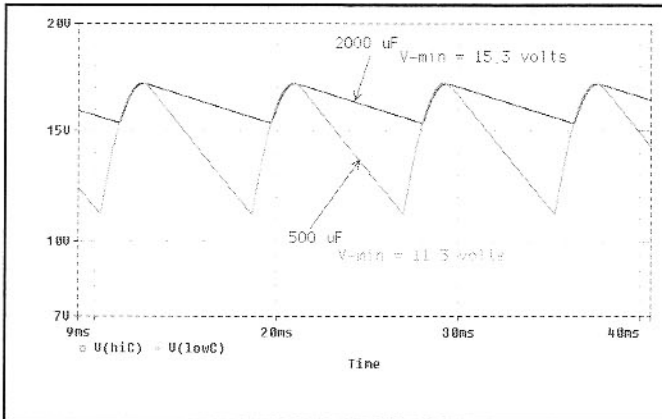


Fig 1.22—Waveforms showing the voltage across filter capacitors of two values when loaded with 0.5 A. See text discussion.

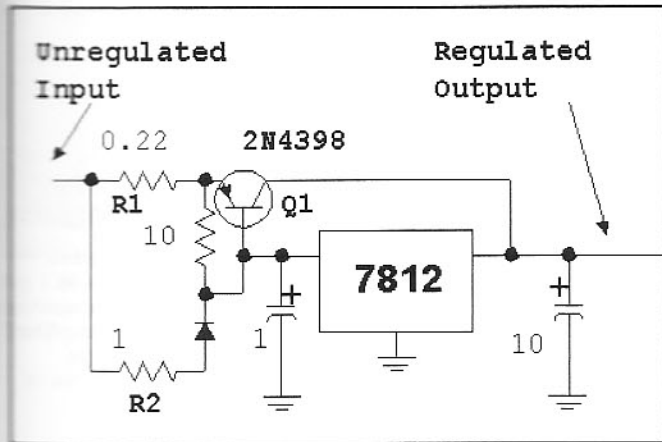


Fig 1.23—Extending the output current capability of a regulator with a “wrap-around” PNP transistor.

Farads is given by

$$C = \frac{I \cdot \Delta t}{\Delta V} \quad (\text{Eq 1.1})$$

For this example, Eq 1.1 predicts a minimum C of 1700 μF . A practical value of 2500 μF would be a good choice.

The complete circuit with the regulator is shown in Fig 1.20C. Extra capacitors, placed close to the regulator IC, serve to stabilize the IC. The user should check data sheets for the IC that he or she uses to evaluate stability. The 1-k Ω bleeder resistor consumes little current, but guarantees that the supply turns off soon after the switch is opened.

The 0.5-A rating of the 7812 becomes a problem when more current is needed. Fig 1.23 shows a circuit that will extend the output current rating by adding a power transistor. Q1 now carries most of the current with the split being determined by the ratio of R2/R1. The dropout for the total circuit is now that of the IC plus a little more than a volt for the diode/transistor and R1 and R2.

Fig 1.24 shows a supply using a LM317. This is a programmable voltage part that can supply outputs from 1.2 up to 37 V, set with two resistors, for an output current of 1.5 A. The power supply we built, used extensively for developing many of the circuits in this book, was variable voltage and also included a 12-V regulator as a second output. An 18-V transformer was used, for we wanted regulated outputs up to 20 V.

Many other regulators are found in vendor catalogs, many with considerably higher output currents and lower dropouts. The experimenter is encouraged to build his own circuits using them. Switching mode regulators offer interesting performance virtues with equally interesting challenges.

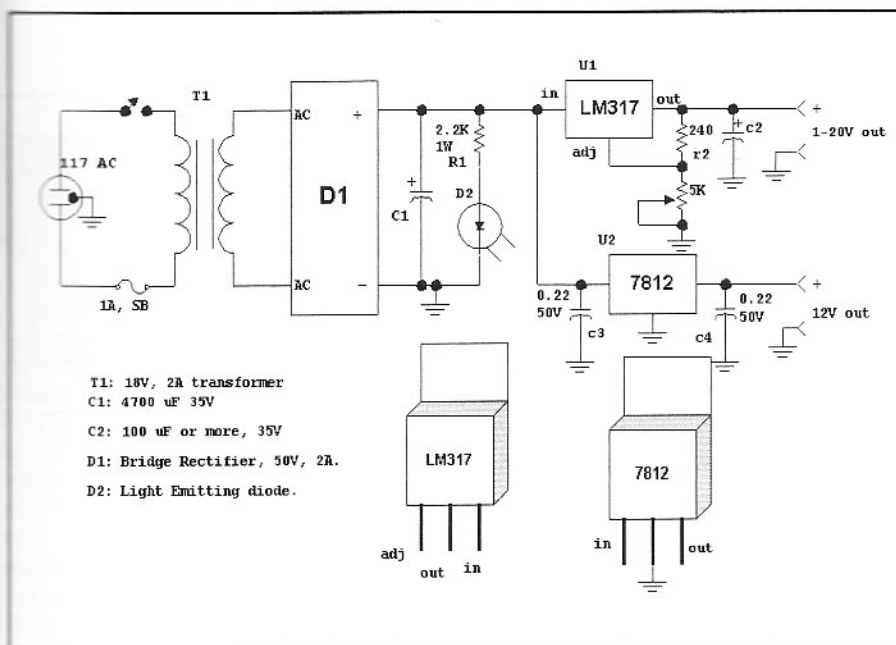


Fig 1.24—Practical dual output power supply featuring the LM-317 regulator.

1.10 RF POWER MEASUREMENTS

Before one can do any meaningful experiments with transmitters, you must be able to measure RF power. A basic scheme for doing this is shown in Fig 1.25. The RF is applied to the 50- Ω termination through a coaxial cable. It is necessary that a well defined impedance be available to absorb the transmitter power. The load must be capable of dissipating that power in the form of heat. So if the transmitter is capable of delivering, for example, 100 W, the 50- Ω load resistor must be capable of dissipating this power. The load must be a resistor that really appears as a resistor to

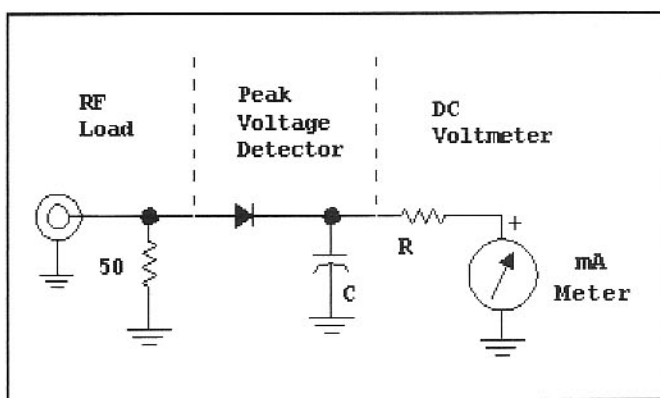


Fig 1.25—A basic RF power meter.

the radio frequency applied to it. This means that the usual power resistors sold by vendors, even if capable of dissipating 100 W, will not be suitable. They are usually built as a "wire wound" part, making them highly inductive for RF. It is sometimes possible to tune them, an interesting avenue for the advanced experimenter.

Suitable 50- Ω terminations, or "dummy loads" can be built with parallel combinations of 2-W carbon resistors, or similar 2 or 3-W metal oxide power resistors such as those manufactured by Yaego or Xicon. Some of these are used in power attenuators described in Chapter 7.

The RF power dissipated in the resistor will develop a corresponding RF voltage. That is rectified with a simple diode detector, providing a signal across the capacitor equaling the peak RF voltage, less 0.7 V for the diode turn-on voltage.

The power meter is completed with a suitable dc voltmeter. It can be as simple as a 0-1-mA current meter and a resistor, a FET voltmeter, or even a digital voltmeter.

Fig 1.26 shows a dual range power meter. Essentially it is a pair of power meters sharing a single meter movement. The higher power part of the circuit starts with a 4-W load built from two parallel 100- Ω , 2-W resistors. These can be carbon or metal film resistors. If 2-W resistors are not available, four parallel 200- Ω 1-W parts will work as well. The resulting RF voltage is rectified with a silicon switching diode. This should be a 100-V part such as the 1N4148, 1N4152, or similar diode. The voltmeter part of the circuit is a 20-k Ω resistor driving a 0-1 mA meter.

Assume a transmitter is attached and keyed on to produce an indication of 0.6 mA. This represents a peak of 12 V, for the meter multiplier is the 20-k Ω resistor. The resulting power is then calculated from the formula given with the figure, 1613 mW, or 1.6 W.

The 50-mW input to the power meter uses a single 51- Ω , 1/4-W, resistor with a more sensitive 1N34A rectifier diode. The meter multiplier is now just 1.5 k Ω . An approximate calibration curve is shown in **Fig 1.27**. The finished meter is shown in **Fig 1.28**.

Other schemes suitable for RF power measurement include terminated oscilloscopes, microwave power meters (usually using calorimeter measurement methods,) spectrum analyzers, and wideband logarithmic integrated circuits. Some of these will be covered in a later chapter.

Often we wish to examine an RF voltage to see if a circuit is "alive," and perhaps to adjust it. The classic method for doing this used an RF probe with a high impedance, usually vacuum tube or FET voltmeter. The method is still very useful, especially

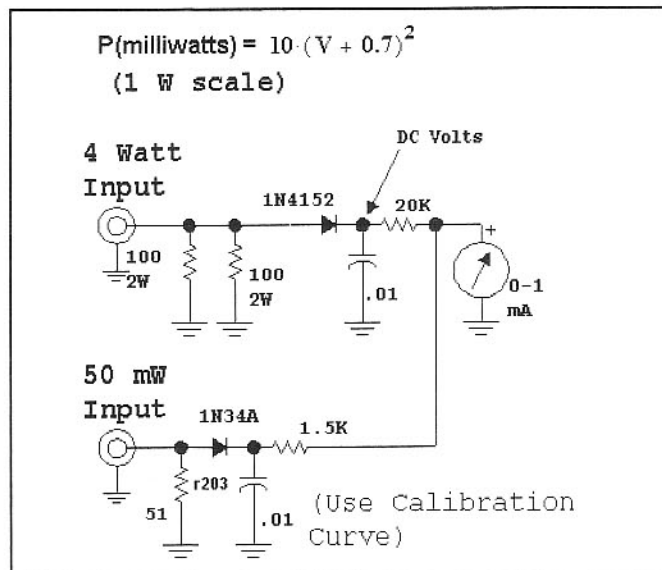


Fig 1.26—Dual range power meter. The 4-W input uses the formula to calculate power in milliwatts. The 50-mW range uses the curve of Fig 1.23.

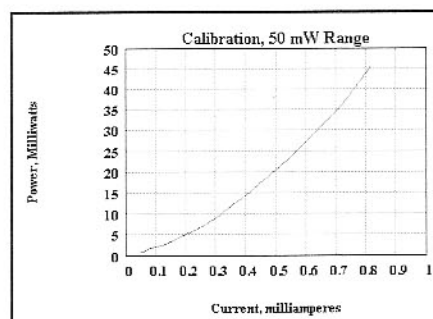


Fig 1.27—Calibration curve for the 50 mW range of the previous power meter.

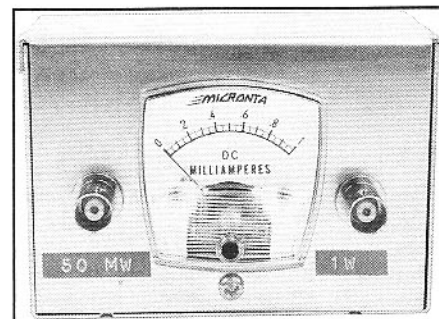


Fig 1.28—The front panel of the dual-range QRP power meter.

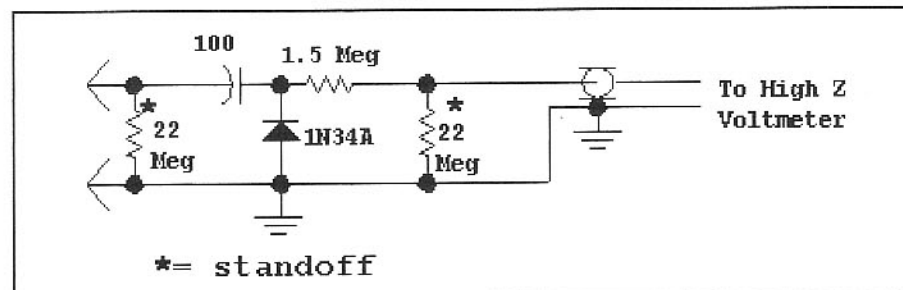


Fig 1.29—RF probe suitable for use with a VTVM, FET voltmeter, or even a DVM. Resistors marked with * are standoff resistors used for probe construction and have little impact on circuit operation.

when instrumentation is limited. **Fig 1.29** shows a very simple RF probe. The photo in **Fig 1.30** shows an open breadboard version; it's the sort of circuit that one builds when a measurement must be done immediately. A long lasting version of the same circuit might better be built inside a cylinder at the end of the coaxial cable.

The probe may require calibration. This is best done with one of the other power

meters and a small transmitter or similar RF source. The transmitter is attached to the power meter and the output is measured. The corresponding RF voltage is noted and the RF probe is attached to the power meter 50- Ω resistor, producing a result that can be compared.

Fig 1.31 shows a high impedance dc voltmeter suitable for use with this probe. It is also a good starting measurement tool for

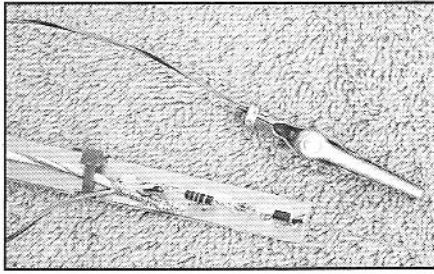
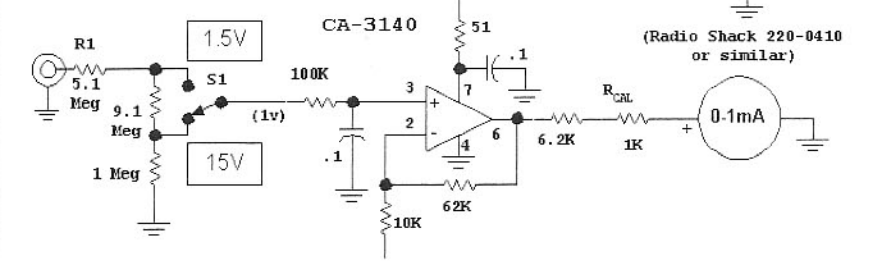


Fig 1.30—Close up view of an RF probe built on a strip of PC board material. The probe is a capacitor lead.

use in the lab. For general utility, it is useful to have the 5.1-MΩ resistor at the tip end of a probe that is inserted into a circuit for measurements. This allows the dc to be mea-

Fig 1.31—Simple high impedance voltmeter for measuring dc voltages in circuits. It can be used with the RF probe of Fig 1.29 and Fig 1.30.



sured without upsetting signals that may be present in the circuit. This circuit can be calibrated with a fresh 1.5-V battery; vary

the 6.2-kΩ resistor if needed.

We will have more to say about RF power measurement in Chapter 7.

1.11 A FIRST TRANSMITTER

This section describes the design of a simple transmitter suitable as a first rig, a project for someone who has never built a transmitter. It uses robust circuits with few adjustments required during construction. It can be built with nothing more than a voltmeter, a power meter, and power supply. We used an oscilloscope and a spectrum analyzer during the rig design phase and those results are presented. However, that equipment is not necessary for construction. The crystal controlled 2-W 40-meter transmitter is built with breadboard methods rather than with a printed circuit.

The circuit, shown in **Fig 1.32**, begins with Q1 functioning as a crystal controlled oscillator. Our crystal had a marked frequency of 7045 kHz. This was the specified frequency for operation with a 32-pF load capacitance. This Colpitts circuit uses a pair of series 390-pF feedback capacitors. The equivalent 195 pF parallels the crystal. Because this capacitance is much larger than the specified 32 pF, the operating frequency will be less than the marked 7045 kHz. If you want the frequency to be exact, a small trimmer capacitor can be placed in series with the crystal. We will eventually do this as a method of obtaining some slight tuning, but don't bother with this refinement in the beginning. The complexity of crystals is discussed in later chapters.

The oscillator is built on the end of a

scrap of circuit board material. The crystal was held on the board with a piece of double sided foam tape (Tesa, 67601). The oscillator worked right off with several V peak-to-peak observed at both the base and the emitter with an oscilloscope and 10X probe. The RF probe described earlier could also be used. The oscillator functioned well with supply voltages as low as 2.5 V. A quick check with a receiver confirmed the frequency.

The oscillator is followed by a buffer amplifier. A buffer is an amplifier that allows power to be extracted from an oscillator, or other stage, without adversely disturbing it. An ideal buffer often has a high input impedance so it can be attached without extracting any power. The best buffers have good reverse isolation, meaning that any signal present at the output is heavily attenuated at the input.

The first buffer tried was an emitter follower, a common choice to follow a crystal oscillator. Performance was poor. While the loading was light, the output was highly distorted. This problem behavior is discussed in detail in Chapter 2. The design was changed to the degenerated common emitter amplifier shown in **Fig 1.33**. We obtain the buffer input from the oscillator base instead of the more common emitter, for the waveform is cleaner, more sinewave-like, at that point.

The buffer is added to the crystal oscillator by soldering the required parts to the board or to other components. The board is not installed in a box at this time. Rather, it's loose where it is easiest to build and measure. We can tack solder small load resistors or coax connectors to the board to facilitate experimentation.

The buffer output transformer has a 4:1 turns ratio. The primary, the 12-turn winding on a FB43-2401 ferrite bead, or a FT37-43 toroid, which is virtually identical, has an inductance of about 50 uH. This

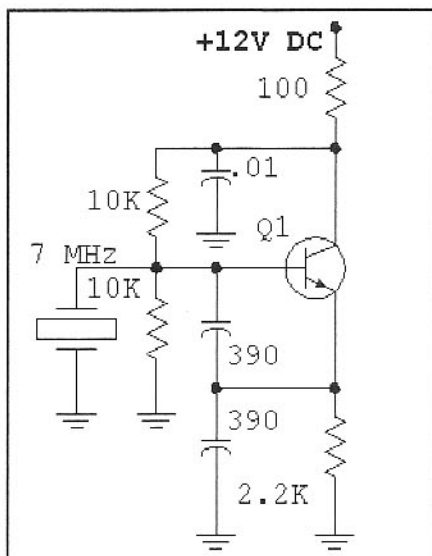


Fig 1.32—Crystal controlled oscillator that is the start of the beginner's transmitter.

has a 7-MHz reactance of $2.3\text{-k}\Omega$. The load on the output is transformed from $50\ \Omega$ up by the square of the turns ratio to $800\ \Omega$, the approximate impedance presented to the collector of Q2. The inductive reactance is much higher, so it does not impact the circuit operation. The output is not tuned, allowing it to function well over a wide frequency range.

We measured the power from the 3-turn output link on T1 by attaching a small length of coax cable that ran to the 50-mW input of the power meter described earlier. The output was +10 dBm, 10 mW, with $R1=270\ \Omega$, and was up to +15 dBm with $R1$ of $150\ \Omega$. Recall that the power meter has a $50\text{-}\Omega$ impedance.

We want more than 10 mW from our transmitter and will eventually add a power amplifier to reach an output of two W. That

amplifier will require modest drive of 200 to 300 mW. We could obtain more power by biasing the second stage for higher gain and output. A more conservative and stable, free from self-oscillation, approach adds a third stage.

The evolving design is shown in Fig 1.34 with a class C amplifier for Q3. We want this third stage to provide a power gain of 10 and pick another 2N3904. With an F_t more than ten times the operating frequency, gain will be good. The 2N3904 also has a beta that holds up well at high currents, a useful characteristic for a power amplifier. While we wanted class C operation in the 3rd stage, stability was deemed vital, so the circuit is degenerated with a $10\text{-}\Omega$ emitter resistor and a $100\text{-}\Omega$ load is placed at the base. Class C operation is assured. Q3 current disappears when RF

drive is removed from the amplifier.

The desired driver output power is $\frac{1}{3}$ W. This can be realized by properly loading the stage. We must present a resistive load to the collector given by

$$R_L = \frac{(V_{cc} - V_e)^2}{2 \cdot P_{out}} \quad (\text{Eq. 1.2})$$

where V_{cc} is the supply, V_e is the emitter voltage, and R_L is the load resistance in Ohms. $(V_{cc}-V_e)$ is about 11 V for this example, so the equation predicts a desired load of about $150\ \Omega$. An L-network, L1 and the 200-pF capacitor, is designed to transform a $50\text{-}\Omega$ load to "look like" $200\ \Omega$ at the collector. An RF choke provides collector bias for the transistor. While tunable components could have been used in the L-network to get the optimum output, we elected to use fixed values. We measured L1 and set the value to that desired. We then used a 5% value for the 200-pF capacitor. Variable elements are only needed in higher Q situations, or where it is not possible to find tight tolerance components.

Power output could be measured with the 4-W position of the watt meter. We used an alternative approach here. A $51\text{-}\Omega$ $\frac{1}{2}$ -W resistor was tack soldered into the circuit at the output point shown in Fig 1.34 and the output voltage was measured with an oscilloscope and 10X probe. The Q3 output was 123 mW, 7 V peak-to-peak at the load, with $R1=270\ \Omega$ in the buffer. Changing $R1$ to $150\ \Omega$ increased output to 314 mW. The DC current, 43 mA, was determined by measuring the voltage drop across the $10\text{-}\Omega$ decoupling resistor. The calculated efficiency is then 62%, good for an amplifier which contains resistors in both the emitter and collector. The 2N3904 at Q3 is operating well within ratings. Generally, a TO-92 plastic transistor like the 2N3904 can dissipate a quarter of a watt for extended times, or half a watt for the shorter intermittent periods encountered in a CW transmitter. This "rule of thumb" can be stretched with heat-sinking, or easily violated in thermally isolated settings. Owing to the good efficiency, the dissipation is only 200 mW in Q3.

Q3 power output varied smoothly from very low levels up to the maximum 314 mW as V_{cc} was adjusted from 5 to 12 V. This is generally a useful method for examining stability. We will eventually add a "drive control" to the circuit.

Before continuing we need to address the issue of spectral purity. Some observed waveforms have departed from a sinewave. This means that these waveforms are

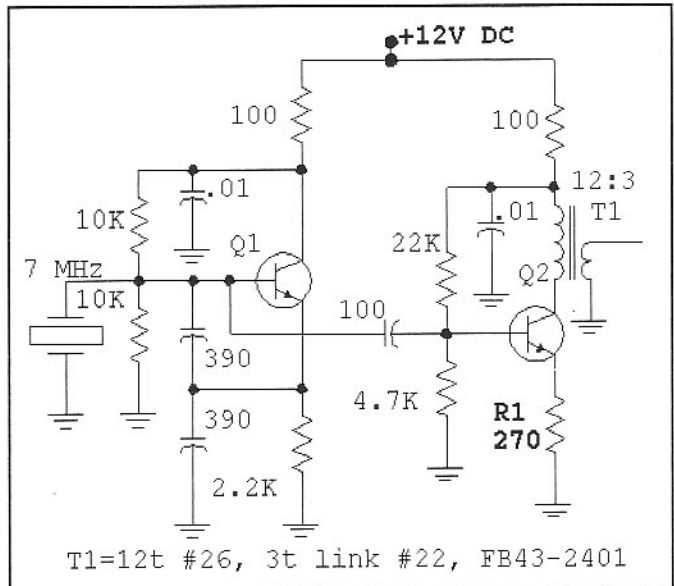


Fig 1.33—Evolving transmitter schematic showing the addition of a buffer amplifier, Q2.

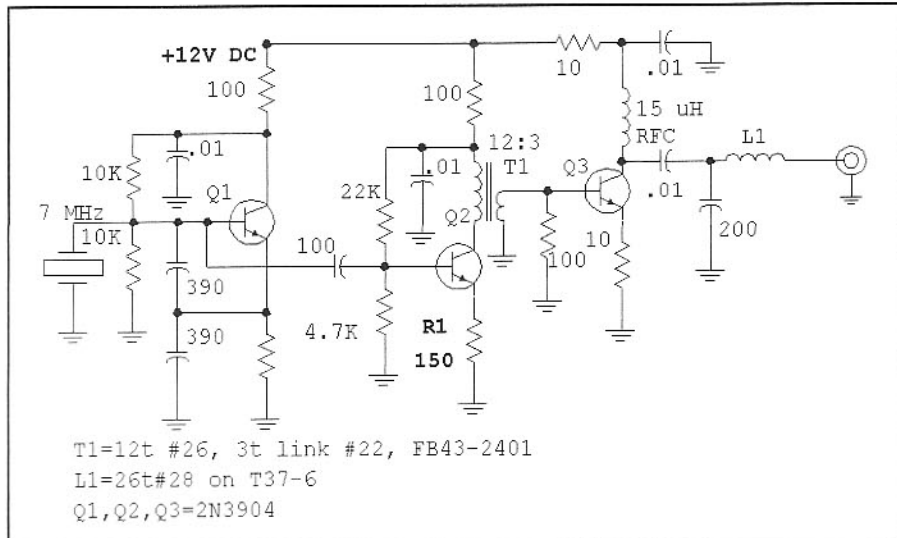


Fig 1.34—A Class C driver amplifier, Q3, is added to the transmitter.

harmonic-rich. This transmitter uses a crystal oscillator operating at the output frequency. The only signals that should be present anywhere within the transmitter are at 7 MHz or harmonics at 14, 21, 28, ... MHz. The only filtering needed is a low pass filter at the transmitter output. While the L-network that makes a 50- Ω load appear as 200 Ω at the Q3 collector

has a low pass characteristic, it has only two components and is not very effective as a filter. If the driver amplifier is going to be used by itself as a transmitter, another low pass filter should be added to the output. There is, however, little value in adding a better low pass filter after the driver if it is to be used only to drive another stage which will also be cre-

ating harmonic distortion. Spectrum analyzer measurements showed spurious driver outputs at -27, -30, -43, and -49 dBc for the second through fifth harmonics when the driver was delivering full output. The harmonic suppression was actually worse at lower output levels. The term dBc refers to dB down with respect to the carrier.

1.12 A BIPOLAR TRANSISTOR POWER AMPLIFIER

The project now starts to get exciting as we begin to experiment with higher output powers. The transistor we have selected for a 2-W power amplifier (PA) is a 2N5321. This is an NPN device in a TO-39 case with a collector dissipation of 10 W in an infinite head sink, or 1 W in free air, 50-V breakdowns, the ability to switch a current of 2 A, and a 50-MHz F_T , all for less than \$1. The low F_T restricts the device to the lower bands, but it also means that high frequency stability will not be an issue. The 2-W PA schematic is presented in Fig 1.35.

The first detail we must consider with the PA is a heat sink. Our intention was to increase power by about 10 dB to the 2 to 3-W level. If efficiency turns out to be 50%, we will have a collector dissipation that is the same as the RF output. The transistor can't support this power without a heat sink. We had a Thermalloy 2215A in the junk box which should be more than adequate. The transistor was mounted in the heat sink which was then bolted to a PC board scrap. Holes through the board made the leads available for soldering. Be careful to avoid any short circuits that are not intended. The transistor case is attached to

the collector terminal in most TO-39 packaged devices.

It's always difficult to estimate heat sink sizes. While one can do thermodynamic calculations, it's generally adequate with small transmitters to experimentally treat the problem. Touch the heat sink often during initial measurements. If it's too hot to touch, the heat sink is not large enough. We always seem to err in the conservative area with more heat sink than is needed.

The formula presented in Eq 1.2 shows that a 25- Ω load resistance presented to the collector will support the desired output. A simple pi-network was designed. The network Q was kept low, but was picked to generate a network with standard, and junk-box available, capacitors. A matching network design is presented in Chapter 3.

A 33-V Zener diode is attached from the collector to ground. The collector voltage will never reach these levels with normal Class-C operation, so the diode is transparent except for the sometimes substantial capacitance that it adds to the collector circuit. But, the diode conducts if the output load disappears, and prevents collector breakdown that might otherwise destroy the

transistor. Care was taken to keep the emitter lead short when the amplifier was built, for even small amounts of inductance can alter the performance. This is *not always* bad.

Transmitter testing *always* begins by attaching a 50- Ω load to the output. This can be a power meter or a resistor of the proper rating. The PA should never be run without a load.

The first PA we built for this project used the simplified circuit of Fig 1.36. This circuit suffered from instabilities which became clear as we varied the drive from the earlier part of the transmitter. At one point, the RF output and the collector current both changed abruptly. The oscilloscope showed frequencies well below the desired 7 MHz. Changing the collector RF choke from the original 15 μ H to a smaller 2.7- μ H molded choke moved the frequency up, but the instability was still present. However, changing the base circuit to one with a lower drive impedance completely solved the problem. The output power and collector current now vary smoothly as the drive is varied. The base transformer is a 2:1 turns ratio step-down that now drives the base from a

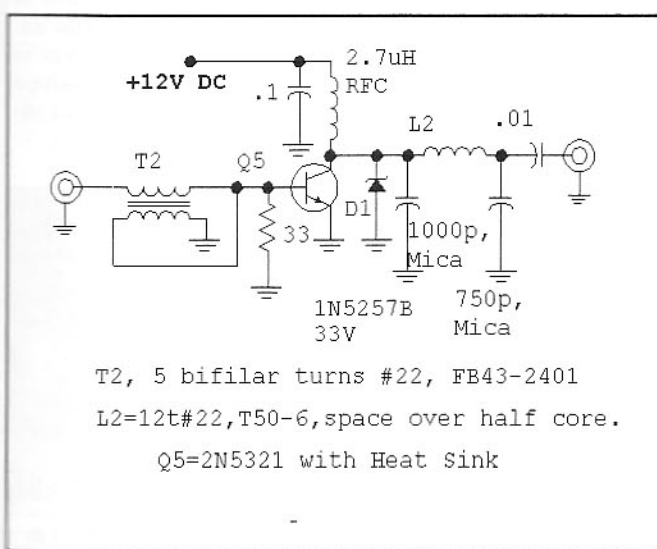


Fig 1.35—A 2 W power amplifier.

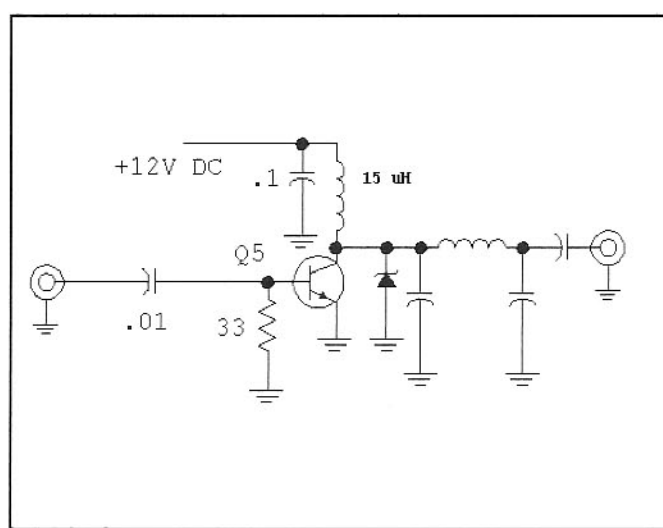


Fig 1.36—Earlier simplified PA design which suffered with stability problems. See text for discussion.

12.5- Ω source impedance. The 33- Ω base resistor absorbs some drive and tends to stabilize the amplifier. Changing this resistor is one of the experimental “hooks” available to the experimenter fighting instability.

The 2-W amplifier is installed in the transmitter. An output power of 2.25 W results from a drive of just over 100 mW. Increasing the drive produces higher out-

put. But once the output gets much beyond 3 W, Q5 begins to heat. Although a higher power was observed with the oscilloscope when the key was first pressed, the power decreases over a period of a few seconds before stabilizing. We investigated this by looking at the collector waveform at differing drive levels. When driven to 2.25-W output, the collector voltage varied between 3 and 23 V. As drive

increases, the bottom of the collector swing drops toward zero. But at this point the amplifier is fully loaded. Further excursions are not consistent with simple class C operation. More drive will cause higher current with little increases in output, allowing efficiency to decrease. This causes the heating. Changing both the matching network and drive power is needed for higher output.

1.13 AN OUTPUT LOW PASS FILTER

When the 2-W amplifier drive is adjusted for 2.25-W output, the measured efficiency was 47%. A spectrum analysis showed 2nd and 3rd harmonics at -36 dBc and -47 dBc. Addition of an outboard low pass filter removed all spurious responses to better than -75 dBc.

The outboard low pass filter is shown in Fig 1.37. This is a 7th-order Chebyshev design with a 7.5-MHz cutoff frequency and a ripple of .07 dB. The rather obscure ripple was picked to fit standard value capacitors that were on hand. The inner capacitors are parallel combinations of 680 and 180 pF. The measured insertion loss for the filter was 0.11 dB at 7 MHz. The filter was built into a small aluminum box, Fig 1.38, as an outboard appendage so it could be used for other projects. Also, the performance is superior when the shielding around the filter is absolute. If the same filter was built into the transmitter, there is a greater chance that ground currents and radiation could provide paths for signals to leak around the filter.

This extreme filtering is probably redundant. A much simpler filter could be built into the transmitter, near the output

coax connector, for adequate harmonic attenuation. Chapter 3 provides detail.

Practical Details

The modules built so far are mere scraps of circuit board material sitting on a bench with short pieces of wire to tie them together. They need to be refined and packaged to create a transmitter that we can put on the air. An almost complete schematic of the transmitter is shown in Fig 1.39.

The first refinement is a keying circuit. This function is performed by Q4, a PNP switching *integrator*. This is a favorite keying scheme of ours, allowing a grounded key to control the positive supply to a transmitter stage. Keying in the positive supply allows the grounded parts of the circuit to remain grounded without ever being disturbed by keying. Q4 serves the additional function of shaping the keying. When the key is pressed, current begins to flow in the 3.9-k Ω resistor. The current flows from Q4 base which “tries” to turn Q4 on. As the Q4 collector voltage begins to increase, the change is coupled back to the base through the capacitor. The

positive going signal opposes the current extracted by the 3.9-k Ω resistor. Hence, the collector does not switch immediately to a high state. Rather, it ramps upward at an approximately steady rate until Q4 becomes saturated. Forcing the stage to turn on smoothly over a couple of milliseconds restricts the bandwidth of the modulation related to turning the carrier on. That bandwidth will extend a few hundred Hz on either side of the carrier. Beyond that, no clicks will be heard in a good receiver.

A power output control is added to the emitter of Q2. Owing to the class C nature of the following amplifiers, the output control will allow the transmitter to run from the maximum output down to virtually nothing. The control is a screwdriver adjusted pot mounted on the board.

A variable capacitor, C1, is added to the crystal oscillator. The capacitor used in our transmitter tuned from 5 to 80 pF and provided a tuning range of 3 to 4 kHz. Use whatever is in your junkbox. While certainly not a substitute for a VFO, it allows the user to dodge some interference. A “spot” switch, S2, allows the oscillator to function without placing a signal on the air.

Finally, a transmit-receive system is added. This function is performed with a multi-pole toggle switch, a simple but ad-

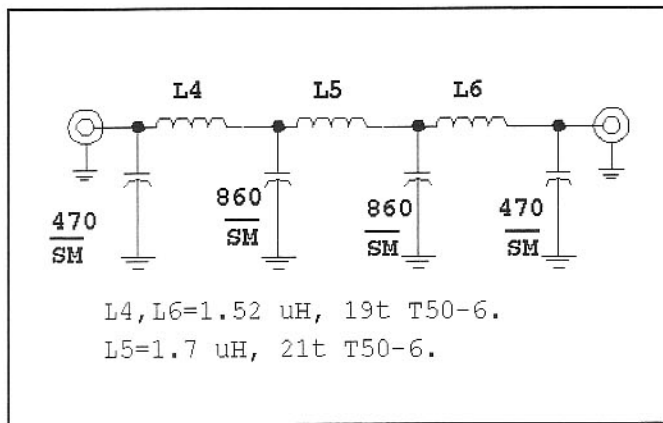


Fig 1.37—Low pass filter for use with the experimental transmitter.

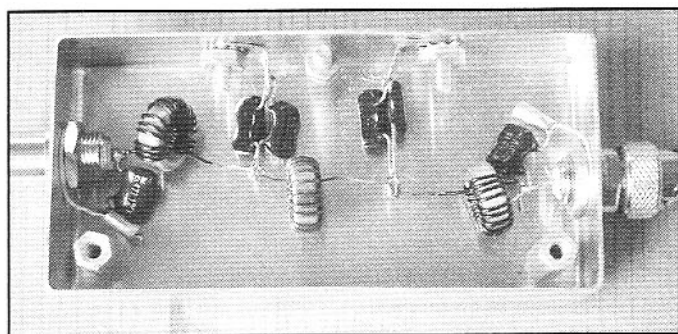


Fig 1.38—Inside view of the 7-element low pass filter built to go with the beginner's rig. The filter is also used with other equipment.

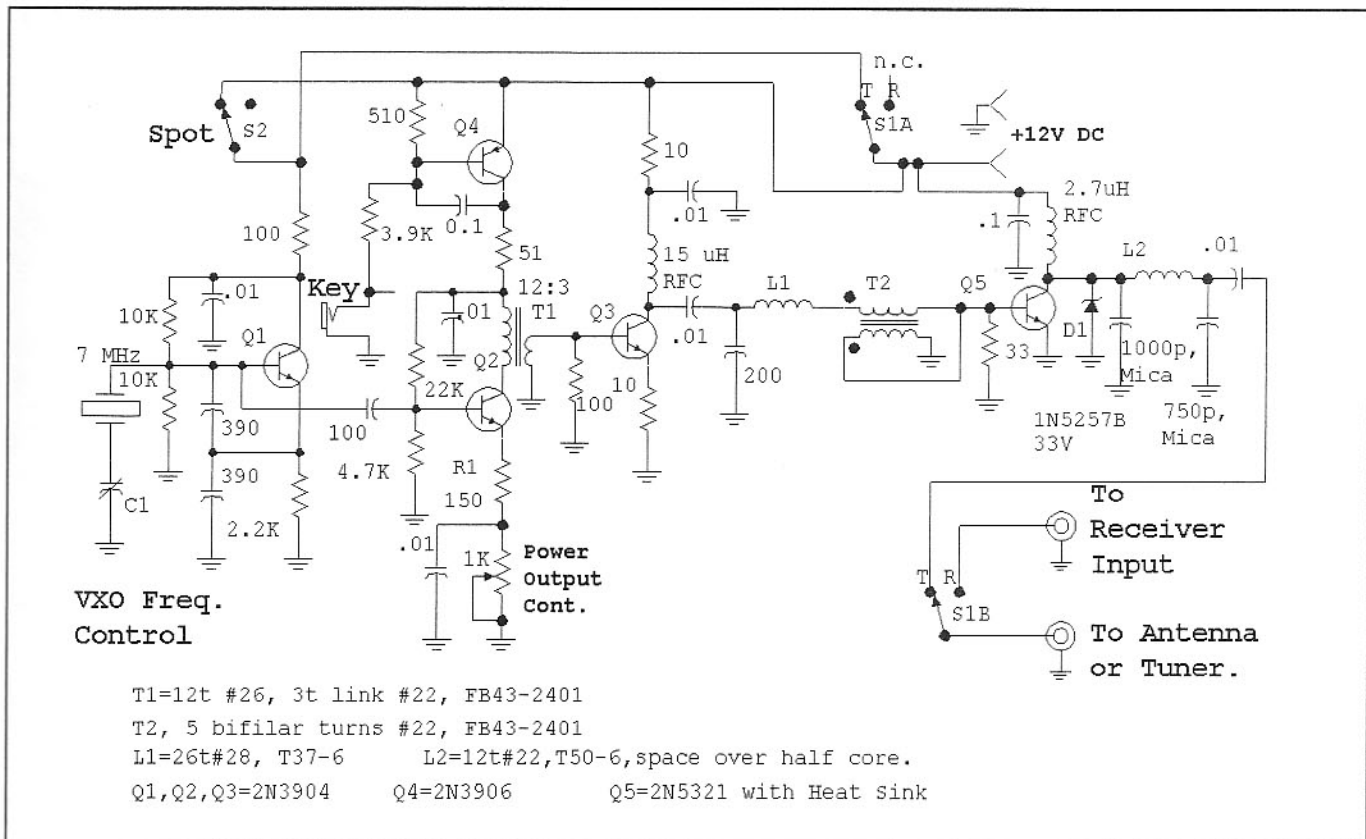


Fig 1.39—A nearly complete schematic of the transmitter. This version combines the PA with the earlier stages, adds shaped keyed, power output adjust, T/R switching, and VFO action.

equate solution. S1A applies the +12 V supply to the oscillator during transmit periods. The supply is always available to Q3 and Q5 and does not need to be switched. The keying circuit, Q4, controls

the supply reaching Q2. S1B switches the antenna from the receiver to the transmitter. The miniature toggle switch at S1 is suitable for powers up through a few watts. More refined T/R methods are presented

elsewhere in the book.

If this transmitter is to be used with a high quality modern receiver with a wide AGC range, a two pole switch is all that is needed at S1. The user can then listen to the transmitter in the receiver as the key is actuated. The more common scenario places this transmitter with a simple direct conversion receiver such as that described earlier in this chapter. It will then be impossible to turn the gain in that receiver down far enough to prevent overload. An answer to the problem is presented in Fig 1.40 where a sidetone oscillator is added to the system. A 555-timer integrated circuit functions as the square wave oscillator which is keyed on and off with Q5. Q5 base current routes through a 10-k Ω resistor attached to the key in Fig 1.39. R2 must be adjusted for the headphones used with the transmitter. The headphones are disconnected from the receiver during transmit intervals, attached only to the sidetone oscillator. Two phone jacks are included on the transmitter. A short cable then routes the receiver audio output from the receiver to the transmitter where it is switched. This scheme does not prevent the receiver from being overloaded, but guarantees that you don't have to listen when it happens. The receiver won't be damaged by

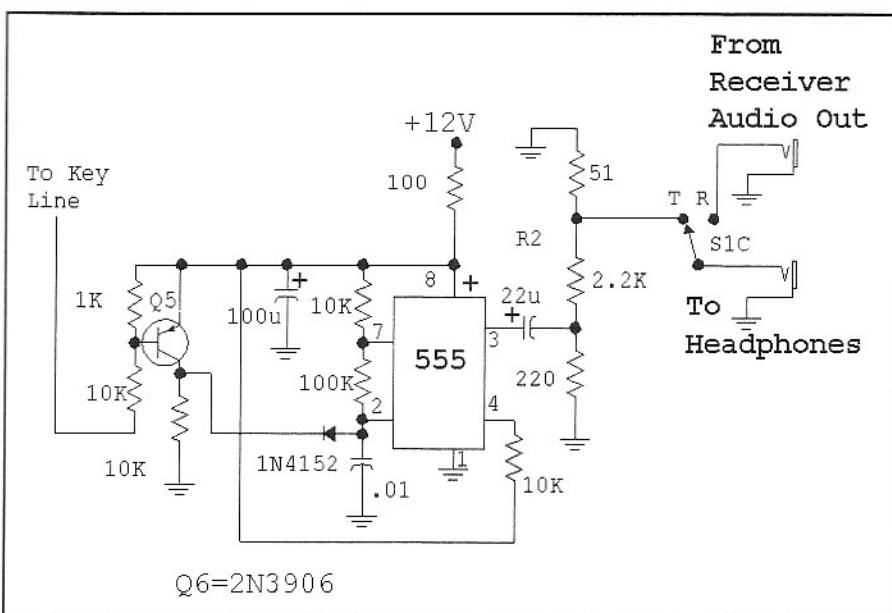


Fig 1.40—Sidetone oscillator for the transmitter. This circuit is also suitable as a code practice oscillator.

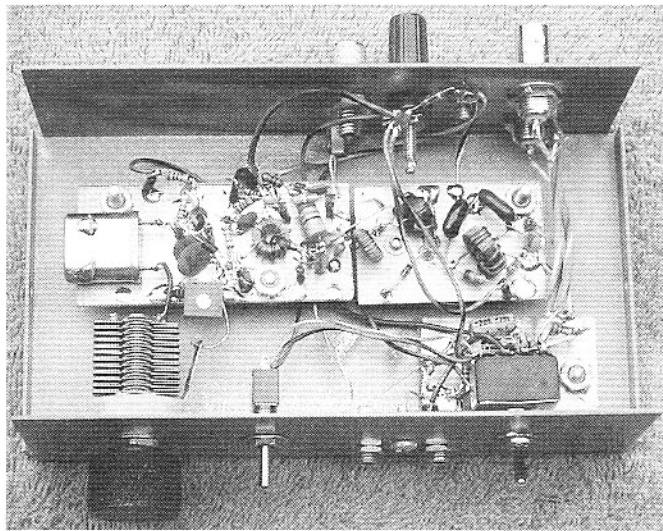


Fig 1.41—Overall view of the complete transmitter construction.

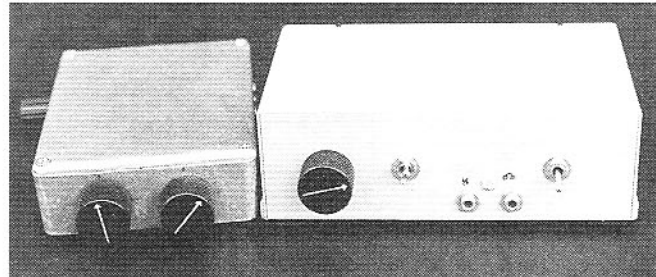


Fig 1.42—Outside view of the Beginner Station. At left is the beginner's direct conversion receiver with the transmitter at the right.

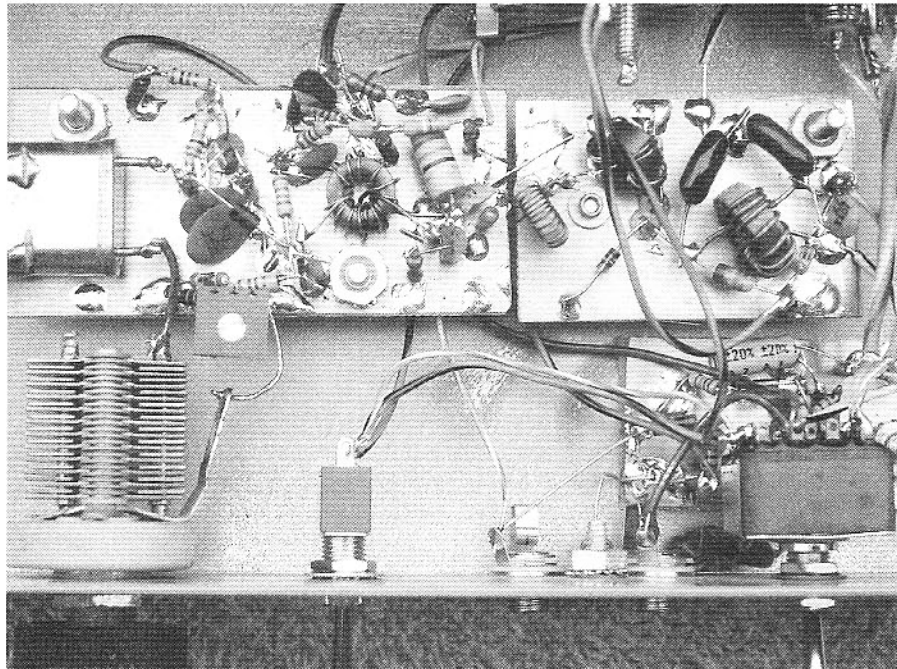


Fig 1.43—The inside view of the transmitter shows the capacitor and T/R switch mounted to the front panel with power and coaxial connectors on the rear. The left board contains the first three stages while the right board contains the 2-W power amplifier. A heat sink is under that board. A small board under the T/R switch contains the sidetone oscillator.

the overload. A third pole is needed on the switch for this refinement. Three pole double throw toggle switches are unusual, so we used one with four poles.

The complete transmitter is packaged in a standard box as shown in Fig 1.41. This one measured 2 x 3.5 x 6 inches, although whatever is available will work. Alternatively, you can build your own box. The outside of the box can be fixed to be as attractive as you would like it to be, consistent with personal tastes. The variable capacitor, C1, the spotting switch .S2, and the T/R switch are located on the front panel as shown on the right hand side of Fig 1.42. The key jack and a headphone jack are also located on the front. The rear panel contains power receptacles, a jack for the audio input from the receiver, and coaxial connectors for the antenna and a cable to the receiver input. The box we purchased for the transmitter had gray paint on it. Unfortunately, it had nearly as much paint on the inside as was on the outside. Inside paint was removed where components were grounded to the case. Details of the internal construction appear in Fig 1.43.

1.14 ABOUT THE SCHEMATICS IN THIS BOOK

The schematic diagrams used in this book differ slightly from other ARRL publications in that we use slightly different conventions. Not all details are presented in all schematics.

Capacitors are in microfarads if electrolytic or if they have decimal values less than 1. Values greater than unity are in picofarad if they are not electrolytic. Electrolytic caps always have a voltage rating greater than the V_{cc} or V_{dd} value used

in the circuit with 25 V being typical. In some applications we will use C values in nF, which stands for nanofarad. $1000\text{ pF} = 1\text{ nF}$.

RF transformers are specified by turns ratio rather than impedance ratio. Often this data is presented within the schematic diagram rather than as part of a caption. The same holds for inductance values. We strive to load the schematic with as much information as possible.

We generally label schematics with the parts that we used. But that does not mean that this is what you might want to use. An example is our frequent use the 1N4152 silicon switching diode. In all cases, virtually all of these can be replaced by the more common 1N4148 or 1N914. When there is a question about such details, look the part up and see if the parts you have on hand are similar. Then try the substitution.

REFERENCES

1. W. Hayward and D. DeMaw, *Solid State Design for the Radio Amateur*, ARRL, 1977.
2. R. Hayward and W. Hayward, "The Ugly Weekender," *QST*, Aug, 1981, pp 18-21. See also G. Grammer, *Understanding Amateur Radio*, ARRL, 2nd Edition, 1976, p 144.
3. R. Lewallen, "An Optimized QRP Transceiver," *QST*, Aug, 1980, pp 14-19.
4. J. Dillon, "The Neophyte Receiver," *QST*, Feb, 1988, p 14-18.
5. C. Kitchin, "A Simple Regenerative Radio for Beginners," *QST*, Sep, 2000, p 61.
6. C. Kitchin, "An Ultra-Simple VHF Receiver for 6 Meters," *QST*, Dec, 1997, p 39.
7. G. Dobbs, "A Stable Regenerative Receiver," *SPRAT*, Issue 105, Dec, 2000, p 21.

Amplifier Design Basics

2.1 MODELING SIMPLE SOLID STATE DEVICES

Small signal amplifiers are used in a receiver to bring weak signals up to the point that they can be heard in headphones. Large signal amplifiers in transmitters create even larger signals that, when applied to an antenna, propagate to be heard by the receivers. Clearly, the amplifier function is central to all that we do as radio experimenters.

Before we get into the details of the amplifier circuits, we examine devices that can amplify. A preliminary look at diodes soon evolves into a discussion of bipolar and field effect transistors. But, prior to that, we examine the modeling process.

Even the simplest electronic devices can be very complicated in their overall behavior, especially if all power levels and all frequencies are considered. Such a complete description can be overwhelming. Indeed, such a complete device picture would conceptually bury the salient behavior that the designer may seek when

he or she uses a device. What is needed is something simpler, a *model* with enough complication to be useful in practical applications, but with no extra frills.

We use models for even the simplest of parts. A resistor, for example, is modeled as an ideal element, a part that obeys Ohm's Law, with no other characteristics. The real resistor is more complicated: even the smallest surface mounted part has capacitance and inductance. Wire leads only make the effects larger. The L and C alter circuit behavior, but can be described by more elaborate models.

The Junction Diode

The first device we model in detail is the junction diode. The diode is a device that has polarity dependant properties. Specifically, if we insert an ideal diode in a functioning dc circuit that carries a current, the circuit will be unchanged by the presence of the diode if the polarity is for "forward bias." But, current flow will cease if the diode is reverse biased. The schematic diagram of Fig 2.1 illustrates a forward biased diode defined by this behavior. Reversing the diode leads eliminates current flow in the circuit.

The current in the circuit of Fig 2.1 is shown in Fig 2.2, a curve called an I-V characteristic. The current is that flowing through the diode and the voltage is that across the diode. Fig 2.2 plots a current that is completely determined by elements external to the diode. This particular part is called an "ideal" diode.

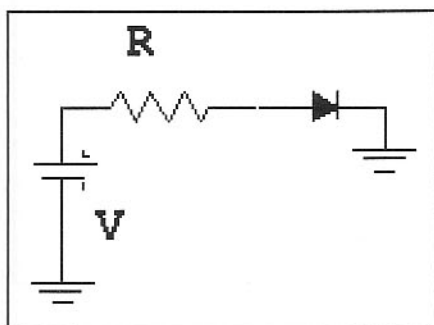


Fig 2.1—Forward biased junction diode.

A real world diode departs from the ideal. First, a slight voltage drop appears across the forward biased diode. Current remains very small until that level is exceeded. Second, the flow of diode current causes a slight additional voltage drop. A refined model with these characteristics is shown in Fig 2.3. The model becomes an ideal diode, a 0.6-V battery, and a diode resistor, R_D , that is the ratio of a small increase in applied voltage, ΔV , and the resulting small change in current, ΔI . We sometimes refer to the threshold (0.6 V in the figure) as a *diode offset voltage*. The offset will vary with diode type. Silicon junction switching and rectifier diodes usually have an offset of 0.6 to 0.7 V. Germanium and hot-carrier silicon diodes will have lower values, while some compound semiconductor parts have

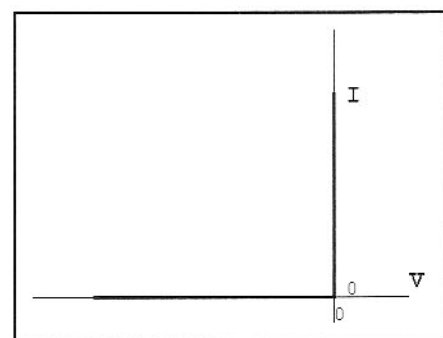


Fig 2.2—IV Characteristics for an ideal or perfect diode. The curve shows I for any possible V that might be applied to the ideal diode.

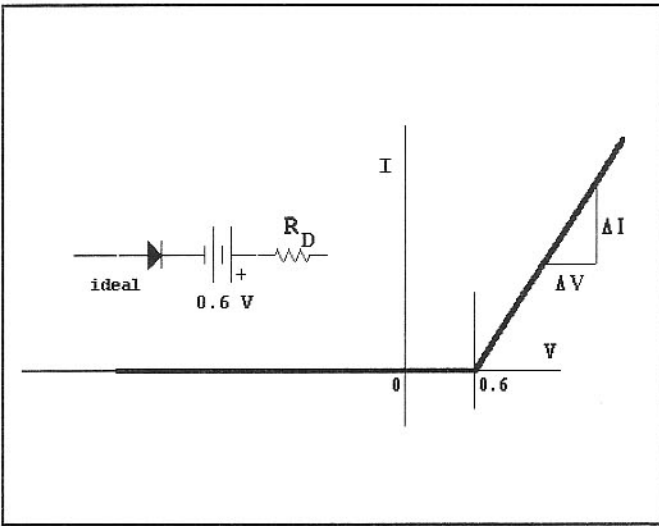


Fig 2.3—IV characteristic for a refined diode model.

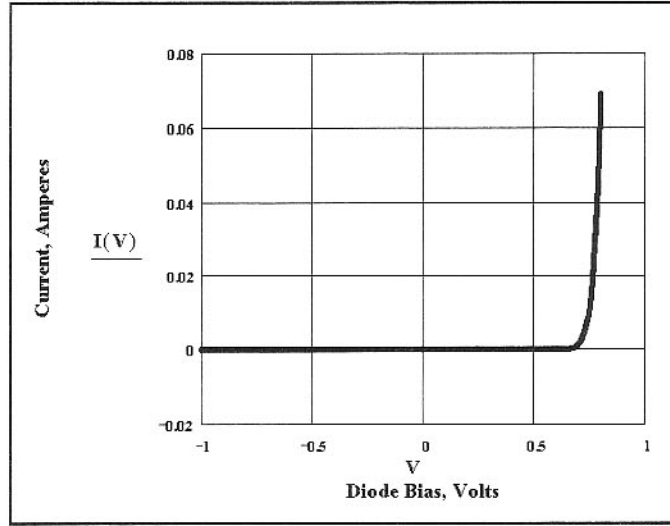


Fig 2.4—IV characteristic for a common junction diode. This follows the diode equation.

thresholds exceeding one volt.

The model of Fig 2.3 is more accurate than the ideal diode, but is still less than perfect in some situations. A much better diode representation is a mathematical model where current is given by an equation,

$$I = I_S \cdot (e^{qV/kT} - 1) \quad \text{Eq 2.1}$$

$$I \approx I_S e^{qV/kT}$$

where I_S is called the saturation current in amperes, q is the charge on an electron, k is Boltzman's constant, and T is the diode temperature in degrees Kelvin. The second, approximate form is common. This model, known merely as *the diode equation*, is illustrated in Fig 2.4 for the case of $T=300$ K (near room temperature) and $I_S = 3 \times 10^{-15}$ A, a value that we inferred from measurements for the popular 1N4148/1N4152 series of parts. Changing I_S generates new offset values. The diode equation is also significant because it originates as a description evolving from basic physics. Physics based models are generally preferred because they follow from fundamentals, even though they may not be as intuitive.

More refined diode models will include reverse breakdown, high frequency parameters (inductance and capacitance,) and even carrier lifetime. No matter what methods we use to analyze a circuit, the results of the analysis will only be as good as the models.

SMALL SIGNAL DIODE MODEL

The antenna signals that our receivers amplify are often in the microvolt region or less. We ask how the diode would

behave if one microvolt was applied to it. The current flowing in the diode, Eq 2.1, would be essentially zero if a microvolt was applied directly. But, the diode might have a much different response if the diode already had a bias current flowing.

Fig 2.5 shows part of a diode IV curve. The point corresponding to 5 mA DC current flow is marked with a tangent line. The slope of this line defines a resistance, a change in current for an applied change in voltage that occurs when a small signal is applied to the biased diode. The diode has a resistance of about 5Ω when the current is 5 mA, generally represented by

$$R_{IN} = \frac{26}{I(\text{mA})} \quad \text{Eq 2.2}$$

The factor 26 mV (or .026 V) comes from differentiation of Eq 2.1 and is a very common parameter in semiconductor electronics:

$$\frac{kT}{q} \approx .026 \quad \text{Eq 2.3}$$

A small signal diode model is no more than a simple resistor. We will make extensive use of small signal models as we move on.

The Bipolar Transistor

The bipolar transistor is a three terminal device. If we use the same equipment that we used to examine diodes, we might conclude that the bipolar transistor is just a pair of diodes in one package, attached as shown in Fig 2.6. This is an incomplete, yet useful model.

Let's place this model in a test circuit, shown in Fig 2.7. A variable voltage bias

source with a large base resistor is used, allowing us to control base current. A positive voltage is applied to the collector, *reverse* biasing the collector-base junction. The two-diode model would predict zero-collector current. But, collector current does flow in proportion to the current in the base. This is transistor action. The ratio of collector to base current is usually sig-

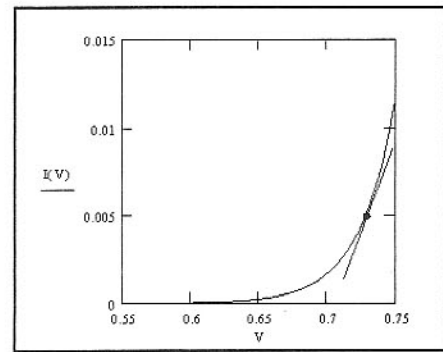


Fig 2.5—Small signal model for a junction diode represents it as a resistor with the slope shown. See text.

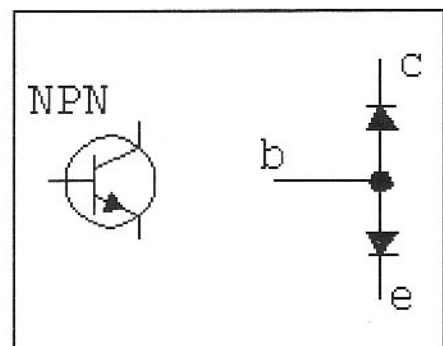


Fig 2.6—Apparent model of a bipolar transistor. This is what we would infer by examination with a VOM.

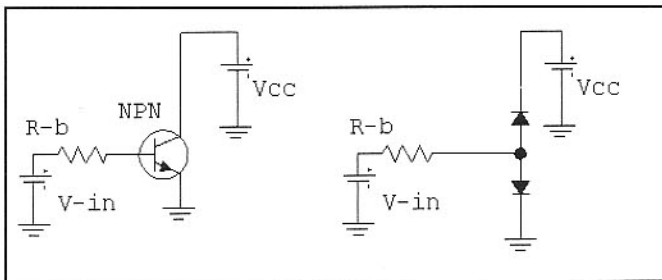


Fig 2.7—The circuit we used to bias a bipolar transistor for active operation. See text.

nified by the greek letter beta, β . A typical value might be 100.

The simplified model on the right side of Fig 2.7 is clearly in error. The “collector” diode is reverse biased by V_{cc} , yet considerable current flows against the diode arrow. A better model is shown in Fig 2.8A where the original diode pair is supplemented by a current source proportional to the current in the base-emitter diode. The model in Fig 2.8B is the model we use for evaluation of biasing circuits. It neglects the collector-base diode and refines the base-emitter diode.

SMALL SIGNAL BIPOLEAR TRANSISTOR MODEL

What happens with the bipolar transistor for small signals? How do we model it? The methods used with the diode are expanded to describe the transistor, as shown in Fig 2.9.

In Fig 2.9A, the input diode is replaced for small signals with a resistance. The resistance is exactly that used with the earlier diode, $26/I$ where I is now the DC current in milliamperes for the base-emitter diode. The current amplifying properties that we discovered earlier are preserved for small signals, so the small signal collector current remains at $\beta \times i_b$. We use a lower case “ i ” to emphasize the small signal levels.

An alternative small signal model is shown in Fig 2.9B. Here the resistance in series with the base has been replaced with one in the emitter. This resistance, termed r_e , is given by

$$r_e = \frac{26}{I_e} \quad \text{Eq 2.4}$$

where I_e is now the emitter current in milliamperes. The collector current exceeds that in the base by β , and the emitter current is the sum of the collector and base values, so the dc emitter current is greater than the base value by $(\beta+1)$. Accordingly, the emitter resistor of Fig 2.9B is smaller than the resistor of Fig 2.9A by $(\beta+1)$. Both models are equally valid, although that

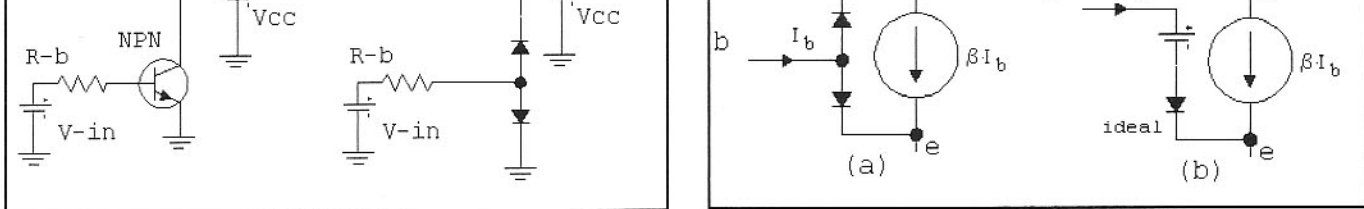


Fig 2.8—A current source is added to the diode pair to form a representative model. The diode is often ignored as in B.

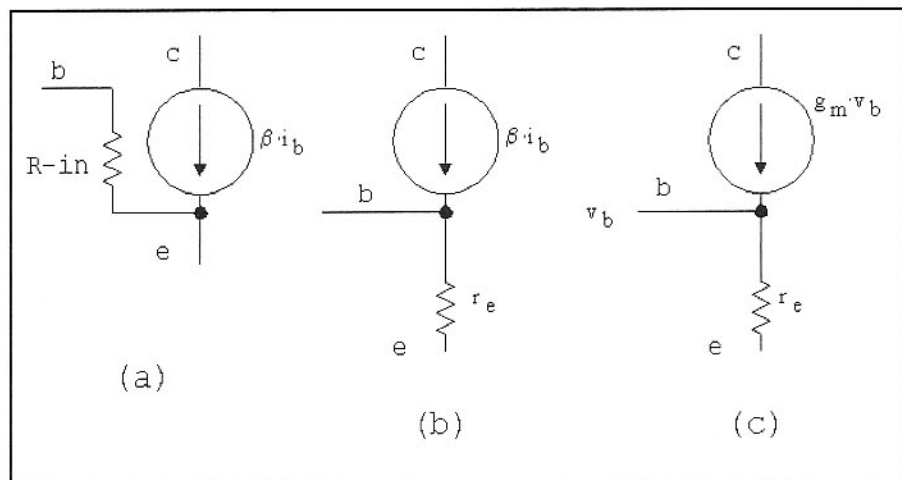


Fig 2.9 Evolution of a small signal transistor model.

using r_e is more common. Common emitter small signal amplifier input resistance is

$$R_{in} = (\beta + 1) \cdot r_e \quad \text{Eq 2.5}$$

A traditional viewpoint emphasizes the bipolar transistor as a *current controlled* device with β representing current gain. But beta can vary considerably for a given transistor type, suggesting that the amplifier gain may differ for different transistors, which is not true. A preferred small signal model is shown in Fig 2.9C, where the part is viewed as a *voltage driven* component. The output current source is now specified by a transconductance, g_m :

$$i_c = g_m \cdot v_b \quad \text{Eq 2.6}$$

The transconductance, g_m , is given by

$$g_m = \frac{I_E}{26} \quad \text{Eq 2.7}$$

While β may vary among transistors, g_m is well defined by emitter current.

Another feature of the model is illustrated by a simple amplifier design, shown in Fig 2.10A. An NPN transistor is biased with a base resistor attached to a positive supply. A load resistor, R_C , is placed in the collector. The base resistor is adjusted until the emitter current is 1 mA. The small signal model shown in Fig 2.10B is used for analysis.

With 1 mA emitter current, the transconductance is $g_m = 1/26$. Signal current is then $v_{in} \times g_m$. This current produces an output voltage because it flows in R_C , resulting in a voltage gain of $g_m \times R_C$, which is

$$G_v = R_C / r_e \quad \text{Eq 2.8}$$

Knowing biasing details, voltage gain can be predicted “by inspection” as a resistor ratio, independent of beta. Current gain, or β , is still of significance, for it will alter the signal current that flows when drive voltages are applied, which defines input impedance.

Note that we have said nothing about transistor type. Our discussion has considered the NPN, but has said little else of a specific nature. This is not an oversimplification. Much of the utility of the bipolar transistor results from properties that

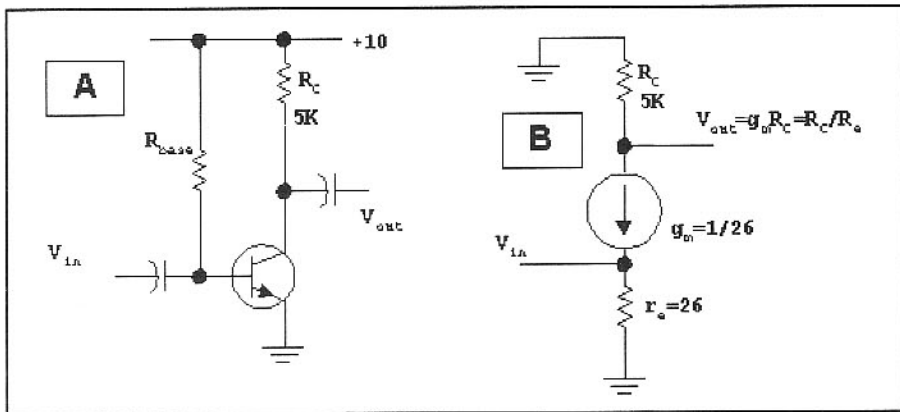


Fig 2.10—The simple amplifier at A is analyzed with the small signal model at B.

depend primarily upon the standing emitter current.

BIPOLAR TRANSISTOR BIASING

Accurate transistor current is vital to any design, because current determines small signal properties. The power dissipation, the power output capabilities, the distortion, and even frequency dependence are also determined by bias current and voltage. Biasing methods will be evaluated with the model of Fig 2.8B, where the base-emitter junction becomes an ideal diode with a 0.6-V battery. Collector current is then $\beta \times I_b$.

The first bias example we consider is that shown in Fig 2.11. A 1-kΩ load resistor appears in the collector, while the base is biased from the 12-V supply through a 100-kΩ resistor. The model assumes an offset of 0.6 V, so the base current is 11.4 V across 100 kΩ, or 114 μA. If transistor $\beta=100$, the collector current is 11.4 mA. But, the 1-kΩ collector resistor produces an IR drop of 11.4 V, leaving a collector voltage of only 0.6 V.

Repeating the calculation with slightly higher β predicts a negative collector voltage, impossible without a negative supply. Recall that earlier models included a collector-base diode that prevented the collector from being more than a diode drop below the base. Whenever the collector voltage equals or drops below that of the base, for an NPN, the transistor is said to be saturated.

The scheme of Fig 2.11 is, at best, a poor bias method. Slight changes in beta yield great uncertainty. Biasing is improved with negative feedback, with one form shown in Fig 2.12. The 100-kΩ resistor is biased from the collector rather than the 12-V supply. An intuitive examination shows that this is an improved method, even before we "crunch" any numbers. If the beta changes to drive the transistor toward saturation, the current through R1

will decrease from the reduced collector voltage. A lower than nominal beta will cause collector voltage to climb, forcing more base current to flow.

Application of the model and some algebra provides a general equation for Fig 2.12,

$$V_C = \frac{V_{cc} \cdot R_1 + V_{eb} \cdot \beta \cdot R_c}{\beta \cdot R_c + R_1} \quad \text{Eq 2.9}$$

An even better bias scheme is shown in Fig 2.13A, where the base is driven from

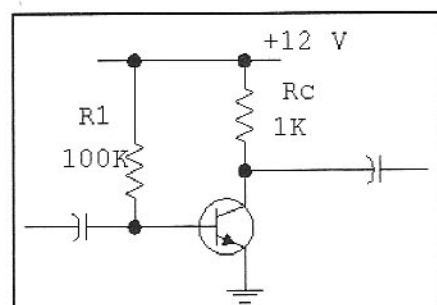


Fig 2.11—A simple amplifier used for bias analysis.

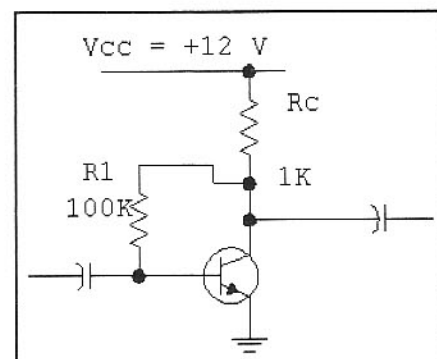


Fig 2.12—Improved bias is obtained from the collector.

the positive supply through a voltage divider, R_1 and R_2 . The equivalent circuit for the divider is shown in Fig 2.13B. The base voltage with the transistor temporarily removed is found from divider action as

$$V'_b = V_{cc} \cdot \frac{R_2}{R_1 + R_2} \quad \text{Eq 2.10}$$

where the prime indicates that the base is open circuited, and absent from the calculation. The emitter voltage is below the base by the 0.6-V offset, placing the emitter voltage at 1.45 V. The emitter current is then determined by the 330-Ω emitter resistor as 4.39 mA. The collector current is almost the same as that in the emitter, and the drop across the collector load puts V_c at 7.61 V.

This analysis, although close, is in error. Base current flow produces an IR drop in the biasing resistor chain. This decreases the base voltage below the value shown in Fig 2.13 by about 0.25 V. There are two solutions to this problem. One would replace R_1 and R_2 with a "stiffer" voltage divider. Values of 3.3 kΩ and 680 Ω would work well, but at the price of greater power consumption. The other alternative is a more careful analysis. If this is performed, the emitter current is given by

$$I_e = \frac{(V_{cc} \cdot R_2 - V_{eb} \cdot (R_1 + R_2)) \cdot (\beta + 1)}{(R_2 + R_1) \cdot R_3 \cdot (\beta + 1) + R_1 \cdot R_2} \quad \text{Eq 2.11}$$

The I_e value for the components in Fig 2.13 is 3.759 mA.

PNP biasing is identical to that of the NPN, except that the voltages are measured with regard to the positive power supply, which may or may not be "ground." See Fig 2.14.

Fig 2.15 shows a natural refinement to the biasing scheme. Here another resistor is added, a normal part of a decoupling scheme. The added resistor provides negative feedback like that used earlier in Fig 2.12. This, in combination with the feedback from R_3 of Fig 2.13 further stabilizes bias.

A scheme useful for biasing an NPN transistor with a directly grounded emitter is shown in Fig 2.16. A PNP transistor emitter senses the dc collector voltage and compares it with the PNP base at a reference, V_r , established with voltage divider R_1 and R_2 . The reference divider is usually designed to put most of the power supply on the NPN collector. The 0.1-μF capacitor stabilizes the negative feedback bias loop. With the values shown, the bias is defined by

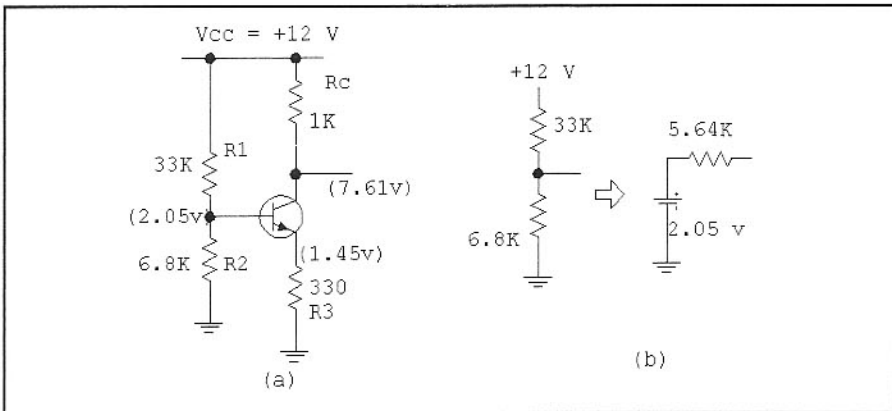


Fig 2.13—Evolution of base bias from a voltage divider.

$$V_R = \frac{V_{CC} \cdot R_2}{R_1 + R_2}$$

$$I_C = \frac{V_{CC} - V_R - 0.6}{R_A} \quad \text{Eq 2.12}$$

The Field-Effect Transistor

Although the bipolar transistor is our work horse, various forms of *field effect transistor*, or FET, are close in popularity. Among FETs, one of the most common is the junction variant, the JFET. A JFET is much like vacuum tube triodes of the past and is easily biased and used in amplifier applications. FETs, including the JFET, generally lack the uniformity and predictability of a bipolar transistor. JFETs tend to be low noise devices. Not only is the noise figure low, but the low frequency flicker, or "1/F" noise is small. This combination makes the JFET especially useful for low noise oscillators.

Fig 2.17 presents the test setup that allows us to measure, and then model the JFET. The example is an N-channel Depletion mode JFET. A drain power supply, $+V_{dd}$, is applied. The gate voltage is then varied while examining the current that flows. **Fig 2.18** is a resulting plot of drain current vs gate-to-source voltage with constant drain voltage. The gate voltage is negative for most of the curve. The gate can be no more than 0.6 V positive, for the gate of a JFET is actually a diode junction. The metal oxide silicon field effect transistor, MOSFET, has similar properties, but uses an insulating gate. There is then no diode clamping action.

Once gate-to-source voltage drops to an adequate level, drain current goes to zero and the FET is said to be in "pinch-off." The pinch-off voltage, the gate-source V_g where current drops to (or nearly to) zero,

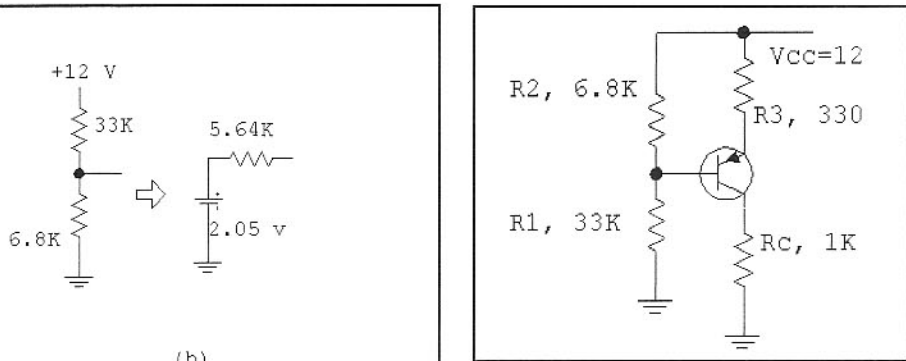


Fig 2.14—PNP biased to the same conditions as we established with the NPN example.

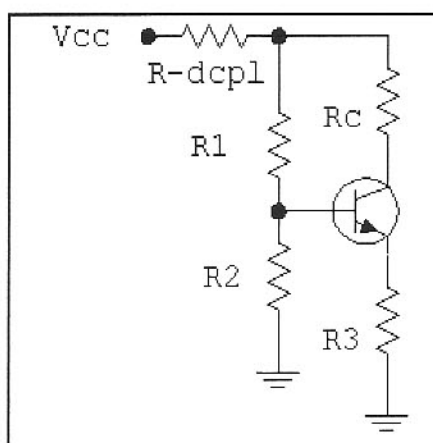


Fig 2.15—Decoupling resistor adds negative feedback to the biasing with an emitter resistor.

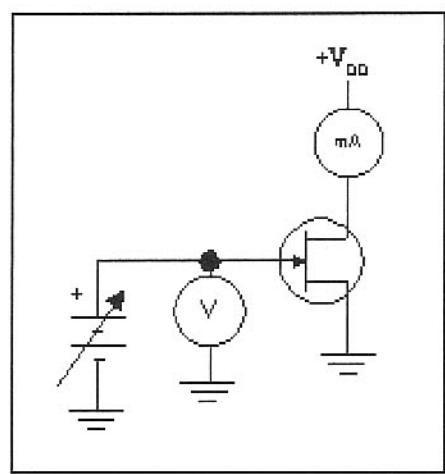


Fig 2.17—Test setup used to evaluate a JFET.

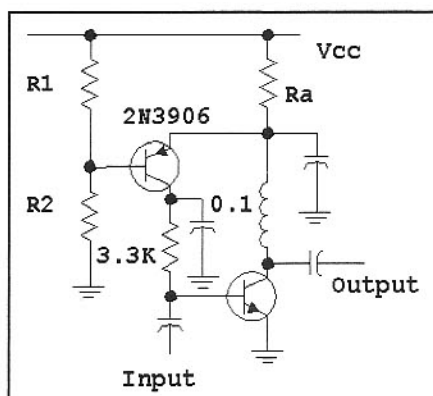


Fig 2.16—A "wrap-around" PNP biases an NPN with grounded emitter. The 0.1- μF capacitor stabilizes bias and is the dominant element in the bias loop.

is at -3 V for the example of Fig 2.18. These data are typical for the popular J310 JFET. A drain voltage higher than the magnitude of the pinch-off is usually required to ensure linear operation. This is

often called operation in the *saturation* region. *Saturation* is just the opposite condition in a FET from *saturation* in a bipolar transistor.

Fig 2.19 shows the usual source resistor method used for biasing an N-Channel JFET at a current below I_{dss} . The current flowing through the resistor establishes a positive source voltage. As current increases, the source voltage increases, causing the gate-to-source voltage difference to become more negative. This is the action needed to decrease current, eventually stabilizing the bias. The action of an external source R is a form of negative feedback, just as we used with an emitter resistor in the case of a bipolar transistor. Fig 2.19 includes some JFET equations.

SMALL SIGNAL JFET MODEL

Fig 2.18 showed a complete curve, describing large and small signal behavior as well as JFET biasing. The simplified small signal model is shown in **Fig 2.20**. Here an open gate terminal accepts an input voltage. That signal then controls an

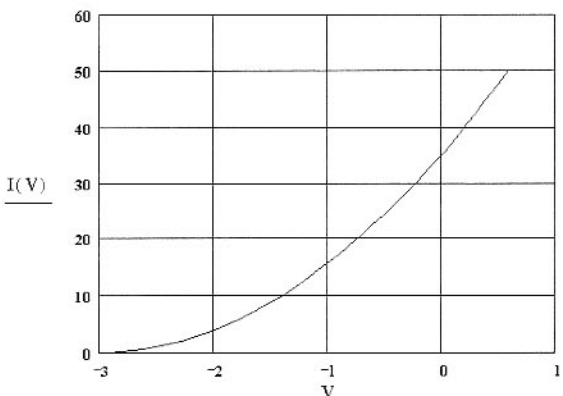
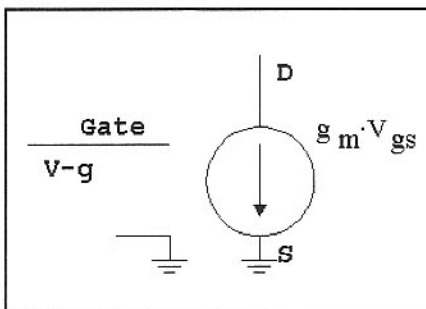


Fig 2.18—Drain Current vs Source-to-Gate Voltage for J310 type Junction Field Effect Transistor. $I_{dss}=35\text{ mA}$ and $V_p=-3\text{ V}$. V_p is the voltage where drain current goes to zero. I_{dss} is the drain current when the gate and source are both at the same potential.

output current source related to the input by a transconductance, g_m , with

$$g_m = 2 \cdot \frac{I_{dss}}{V_p} \cdot \left(1 + \frac{V_{sg}}{V_p} \right) \quad \text{Eq 2.13}$$

For example, if we biased the FET for a gate voltage equaling half of the pinch-off value, with $I_{dss}=35\text{ mA}$ and $V_p=-3\text{ V}$, the small signal transconductance is 0.0117 S ,



2.2 AMPLIFIER DESIGN BASICS

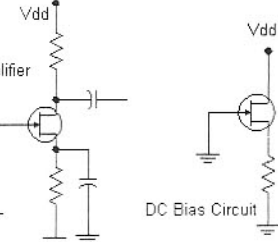
Having examined basic device models and biasing, we now evaluate some basic amplifier designs, first with the bipolar junction transistor (BJT) and then the junction field effect transistor (JFET).

We begin with a single stage audio design, Fig 2.21. The circuit that we might build is presented in Fig 2.21a, while a biasing related part is shown in Fig 2.21b. The voltage divider, $10\text{ k}\Omega$ and $3.3\text{ k}\Omega$, creates an equivalent source of 2.481 V at the base. This decreases by 0.6 V in moving through the transistor to produce an emitter voltage of 1.881 V . The emitter current is then 1.881 mA . With $\beta=100$, base current is $19\text{ }\mu\text{A}$, well below the $752\text{ }\mu\text{A}$ in the voltage divider. The collector voltage is then

$10-1.881=8.119\text{ V}$. The collector-to-emitter voltage, V_{ce} , is 6.238 and power dissipation is the product of this voltage with the standing current, 11.73 mW .

Small signal transistor characteristics are established by emitter current. The resulting small signal model is that in Fig 2.21c. The $1\text{-k}\Omega$ emitter resistor has disappeared from the circuit for it is well bypassed by the $100\text{-}\mu\text{F}$ capacitor. The small signal r_e is $26/I_e(\text{mA})=13.82\text{ }\Omega$. The input resistance looking into the base is almost $1.4\text{ k}\Omega=r_e\times(\beta+1)$.

The input source is a 1-mV voltage generator in series with a resistance of $1\text{ k}\Omega$, which might represent a previous stage. The source is AC coupled to the base



$$\text{Basic FET equation: } I_D = I_{dss} \left(1 + \frac{V_{sg}}{V_p} \right)^2 \quad \text{Pinchoff voltage is negative for an N-channel FET}$$

$$\text{Source Bias Resistor } R_s = R_s I_D \quad \text{so, } R_s = \frac{-V_p}{I_D} \left(1 - \sqrt{\frac{I_D}{I_{dss}}} \right)$$

$$\text{Current with set source } R_s: \quad I_D = \frac{V_p}{(2R_s^2 I_{dss})} \left(V_p + \sqrt{V_p^2 - 4R_s I_{dss} V_p} \right) - \frac{V_p}{R_s}$$

Fig 2.19—JFET bias circuit and equations. The left circuit is a practical amplifier, while that on the right is the bias equivalent. Pick a desired drain current, I_D (must be less than I_{dss}), and use the middle equation to find the required source resistor. The resulting source voltage is given by Ohm's Law.

Fig 2.20—Simplified small signal JFET model.

or “amps per volt.” From the equations in Fig 2.19, we see that the DC drain current is then 8.75 mA , which is realized with a source R of $171\text{ }\Omega$. The low frequency input resistance is essentially infinite.

through a $10\text{-}\mu\text{F}$ capacitor which has a 1-kHz reactance of $16\text{ }\Omega$. Being very small compared with the amplifier input or the source, it may be neglected for a 1-kHz analysis. The same argument may be made for the output capacitor. The result is the small signal circuit of Fig 2.21d. The power supply is missing in the small signal models where V_{cc} is replaced by ground; the supply is fixed and does not change with audio signal current, so it is effectively a signal ground.

We characterized the BJT by a transconductance, $g_m=0.0724\text{ amp/volt}$. Also, we neglect any effect related to the base bias divider on the small signal model.

The 1-mV input signal is voltage

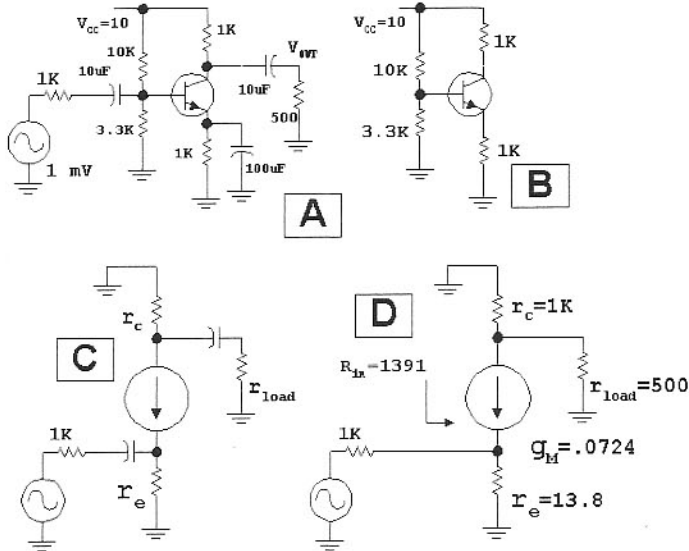


Fig 2.21—Single transistor audio amplifier design. See text for details.

divided between the $1\text{-k}\Omega$ source resistance and the $1.39\text{-k}\Omega$ input resistance. The base input voltage becomes 0.582 mV to produce a collector signal current of $i_c = g_m \times v_{bc} = 0.0421\text{ mA}$. This current flows through a resistance of $333\text{ }\Omega$, the parallel equivalent of the $500\text{-}\Omega$ load and the $1\text{-k}\Omega$ collector resistance. The output voltage is then $0.0421\text{ mA} \times 333$, or 14.02 mV for a circuit voltage gain of 24.1 . Note that this is also exactly the ratio

$$G_V = \frac{R_L}{r_c} \quad \text{Eq 2.14}$$

where the load is the total impedance *seen* by the collector.

The form of this equation is especially intuitive, emphasizing the role of r_c as a degeneration resistance. If we placed a $10\text{-}\Omega$ resistor in series with the $100\text{-}\mu\text{F}$ emitter bypass capacitor, the net emitter resistance would be $10 + 13.8 = 23.8\text{ }\Omega$ and the voltage gain would become 14 . The role of emitter current is clear; Increasing standing emitter current causes r_e to decrease, increasing voltage gain. Emitter degeneration is a common feedback scheme.

We have treated the bipolar transistor as a voltage controlled device. Beta was indirectly used in the calculation, but only to set transistor input resistance. This, in turn, established the fraction of the 1-mV input voltage that appeared at the base.

There is a counter intuitive nature to the modeling presented in Fig 2.21D. The

schematic shows the input is tied to ground through r_e , the $13.8\text{-}\Omega$ resistor, which would severely attenuate the signal. However, the current source representing the transistor is also attached to the input node, and that current moves in unison with the input voltage. This yields the results outlined.

We calculated a voltage gain. The gains of greater interest are power ratios. One of interest to the RF designer is, simply, *power gain*, the output power divided by input power. The output power is calculated (for Fig 2.21) as V^2/R where R is the $500\text{-}\Omega$ load and V is the 14.02-mV output. Output power is then $3.93 \times 10^{-7}\text{ W}$. The input power is the base voltage (0.582 mV) across the transistor input R of $1.4\text{ k}\Omega$, or $2.435 \times 10^{-10}\text{ W}$. The power gain is the ratio of the two powers, 1614 . Using a dB relationship, this becomes 32.1 dB . This is high but reasonable for a single transistor, for this amplifier operates at low frequencies. Such gain from a single transistor at radio frequencies is more difficult.

Power gain is fundamental but is not always the gain we measure. We usually measure *transducer power gain*, especially when working with RF circuits. Transducer gain is output power delivered to a load vs the maximum power *available* from the input generator. We have already calculated output power. The available power from the source is the power that would be delivered to a termination that was impedance matched to the generator. The generator was a 1-mV

open circuit source behind a $1\text{-k}\Omega$ resistor, so the load that would allow the maximum available power to be extracted would be a $1\text{-k}\Omega$ resistor. The available input becomes 0.5 mV across $1\text{k}\Omega$, or $2.5 \times 10^{-10}\text{ watts}$, leaving a transducer gain of 1572 , or 32.0 dB . This is nearly as high as the power gain. The gain difference is a consequence of the input impedance mismatch. We will have more to say about gains and dB later in this chapter.

A common practice converts a voltage gain to decibel form with the familiar $20 * \log(G_V)$, 27.6 dB for this example. This is *not* a correct result, for the source impedance is not the same as the load impedance. The decibel construct is one that should only be applied to power ratios. It works with voltage ratios only when the related resistances are equal.

In the amplifier we analyzed, the input was applied to the base while the emitter was grounded through a large bypass capacitor. Hence, the input was applied between the base and the emitter. The output was extracted from the collector-emitter port. This is a common-emitter (CE) configuration, for the emitter is common to input and output. A common-collector (CC) amplifier is shown in Fig 2.22.

The complete amplifier circuit is shown in Fig 2.22A, while the small signal version is in Fig 2.22B. The open circuit dc base voltage is 5 V , so the emitter bias current is 4.4 mA , leading to $r_e = 5.91\text{ }\Omega$.

The follower of Fig 2.22B is driven from a $1\text{-k}\Omega$ source impedance. It is terminated in a pair of $1\text{-k}\Omega$ resistors in parallel. The input resistance of a follower is given by

$$R_{IN} = (\beta + 1) \cdot (r_e + R_L) \quad \text{Eq 2.15}$$

while the output impedance is

$$R_{OUT} = \frac{R_S}{(\beta + 1)} + r_e \quad \text{Eq 2.16}$$

The voltage gain for the emitter follower is

$$G_V = \frac{R_L}{R_{IN} + r_e} \quad \text{Eq 2.17}$$

Substituting r_e into these equations shows that the follower has a gain of 0.988 , essentially 1 , accounting for the circuit name. Setting β to 100 , the input resistance is $51\text{ k}\Omega$ while the output resistance is $15.8\text{ }\Omega$. The input resistance and the voltage gain both grow if the follower is lightly loaded. The output resistance decreases as the source impedance drops.

It is very common to dc-couple a follower to a preceding amplifier; this is illustrated in Fig 2.23.

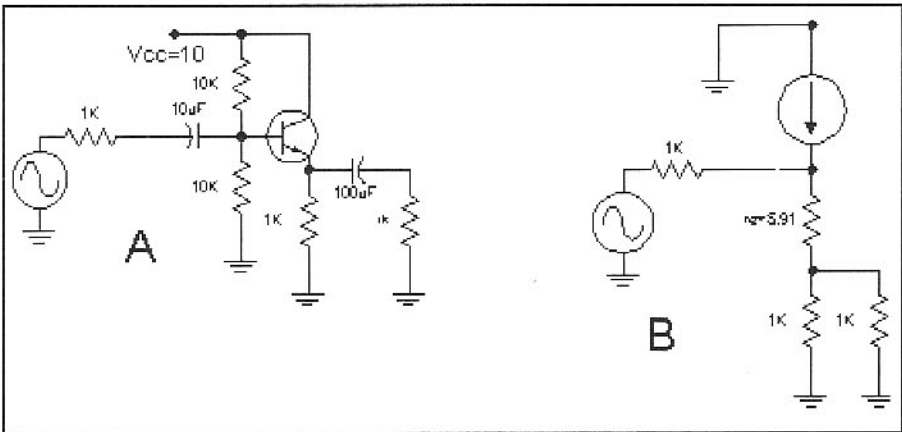


Fig 2.22—Common collector amplifier, also known as an emitter follower.

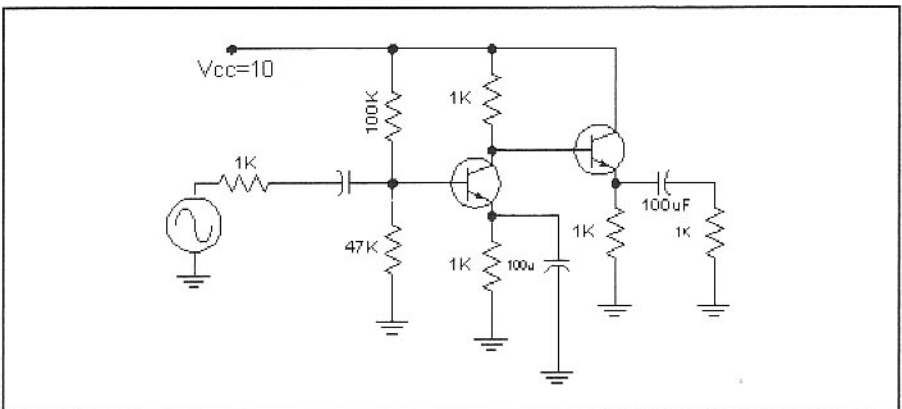


Fig 2.23—Voltage Amplifier with a DC coupled emitter follower.

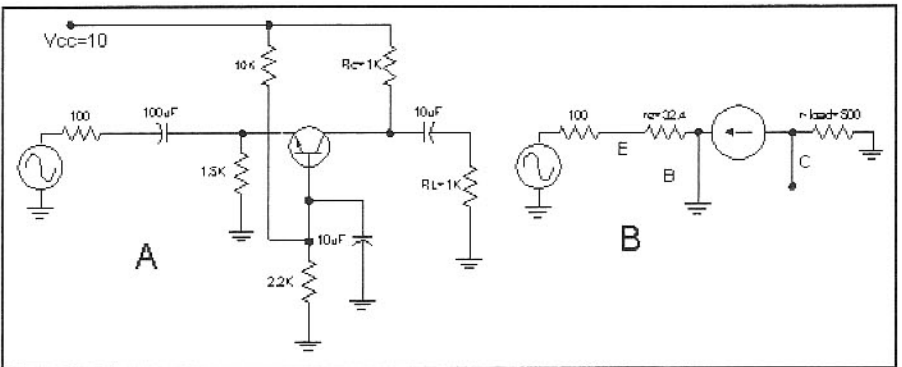


Fig 2.24—Common Base Amplifier with small-signal equivalent.

The third basic amplifier configuration is the common base (CB) amplifier of **Fig 2.24**.

The input resistance for the common base (CB) amplifier is

$$R_{IN} = r_e = \frac{1}{g_m} \quad \text{Eq 2.18}$$

The current gain for the CB amplifier is given by the parameter α ,

$$\alpha = \frac{\beta}{\beta + 1} \quad \text{Eq 2.19}$$

which is normally very close to unity. We essentially assume that the current injected into the CB amplifier appears at the output. The voltage gain is then

$$G_V = \alpha \cdot R_L \quad \text{Eq 2.20}$$

The voltage gain for the CB amplifier

can be very large. However, this is somewhat synthetic, for the input impedance is usually very low, making the amplifier difficult to drive. The common applications use a current source to drive the CB amplifier, realized by placing an extra resistance in series with the input.

The CB amplifier has the useful property that it offers excellent reverse isolation. That is, the input impedance of a CB amplifier is not affected by anything that happens to the output circuit. The example shown in Fig 2.24 is biased to a current of about 0.8 mA, producing an input resistance of 32Ω .

The equations for the small signal properties of the various amplifiers are derived in *Introduction to RF Design*¹ and are discussed in *The Art of Electronics*.²

The CC amplifier had a low output impedance. Nothing was said about the common emitter and common base amplifier output resistance. Both are essentially infinite for the simple models considered where the BJT is modeled as an “ideal current source.”

Most of the amplifier analysis we have done is based upon simple models, ones that have but one or two parameters. Beta has only minor impact on circuit performance. The dominant element in all of the models is r_e , the emitter resistance. This parameter is directly related to current, a parameter under the control of the circuit designer. This would suggest that *all* bipolar transistors are more alike than they are different and that the only major differences are in the frequency capability and size. This is generally an accurate view of the small-signal bipolar transistor.

Small-Signal FET Amplifiers

The field effect transistor families are similar to the BJT; as three terminal devices, they can be configured into three different forms. **Fig 2.25** shows the common source, common gate, and common drain (or source follower) configurations for an N Channel JFET.

There are many similarities between BJT and JFET circuits. The common gate FET amplifier (CG) has a low input impedance with a high output impedance. The topology offers excellent reverse isolation. The follower (CD) has a low output impedance with a very high input impedance.

JFET bias current is controlled by the designer, just as it was with the BJT. Resistor values may, however, have to be device specific, picked for a given FET to establish performance. Within a given JFET type, for example, a 3:1 variation in

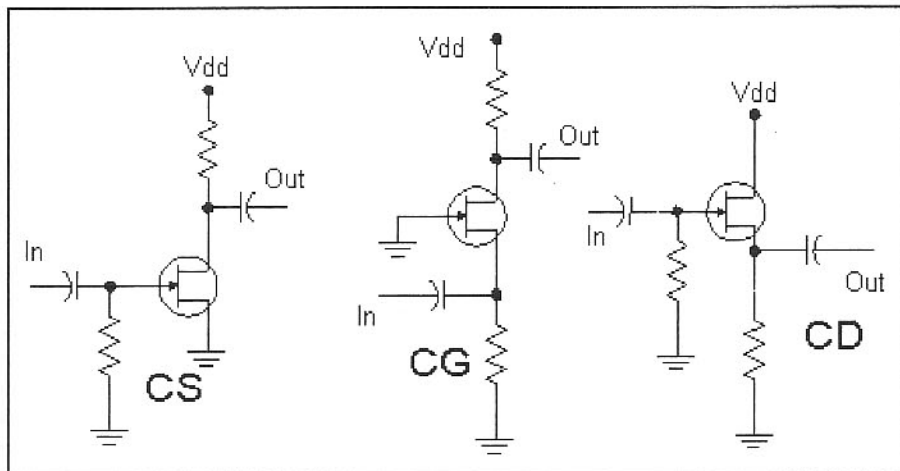


Fig 2.25—Common Source, Common Gate, and Common Drain JFET Amplifiers.

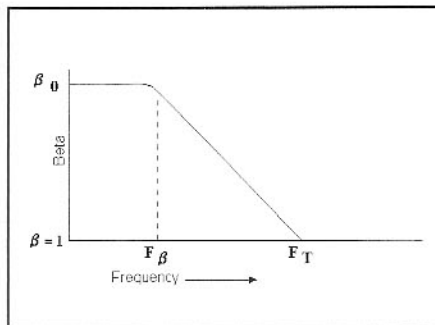


Fig 2.27—Current gain vs Frequency for a BJT.

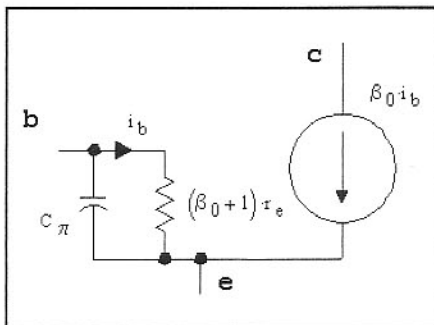


Fig 2.28—The hybrid-pi transistor model.

I_{dss} is common. A similar variation exists with pinchoff voltage. The combination of these two variables might lead one to feel that it would be nearly impossible to design with FETs. Fortunately, it's not that bad, for the variations are related to each other. That is, a given JFET in a family with a high I_{dss} will also tend to have a pinchoff with a more negative value, producing less variation in g_m , the dominant small signal characteristic.

There is good reason for the similarities between FET and BJT amplifiers. Many of the properties result from feedback that is added to a circuit by the configuration. For example, the follower has the load in series with the current source. The voltage developed across the load then generates a signal that contributes to the control of the current generator.

The JFET has an additional property not predicted by the preceding model, the switch action illustrated in Fig 2.26. The JFET functions here as a series SPST switch. An input ac signal is applied to the

FET channel (the source-drain path) and is routed to the output when the control voltage is positive with regard to the channel. The channel is the current path between source and drain. The channel is biased above ground by the voltage divider. The switch is open circuited if the control voltage is more negative with regard to the channel than the FET pinchoff voltage. The switching FET may be modeled as a voltage controlled variable resistor in this application. Lowest R occurs when the control voltage is at or above the channel. The gate resistor is usually large, allowing the control to be several volts higher than the channel. Although the gate diode is then forward biased, current is small and of little consequence.

Virtually all FET types function well as switches. Enhancement mode MOSFETs offer the advantage of no gate diode to complicate the circuit. GaAs MOSFETs are useful in very high speed switching applications where they may be used for microwave signal control. JFETs and

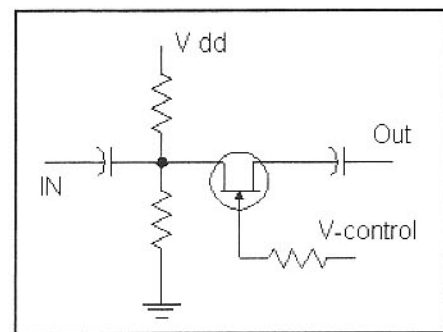


Fig 2.26—A JFET operating as a series switch.

MOSFETs are useful audio switches in many applications.

The FETs may be used as voltage variable resistors. As such, they can function in gain control circuits.

High Frequency Effects

Little has been said about the effects of high frequency. Yet, much of our interest as radio experimenters is in the performance of transistor circuits at frequencies well beyond the range of our simple models.

The first thing that happens to the BJT as frequency increases is that β decreases over the dc and audio values. This is shown in the curve of Fig 2.27 of β vs frequency. The low frequency β is shown as β_0 . The frequency where β drops to a value of unity is called the current gain bandwidth product, or more often, just as F_t . Dropping to a frequency of $F_t/2$ will produce $\beta=2$. The frequency where β begins to depart from β_0 is called the "beta cutoff."

The role off of current gain with frequency is modeled with an added base capacitor, Fig 2.28. The other elements are generally unchanged, so the complete roll off may be attributed to the capacitor across the input. The circuit shown in Fig 2.28 is called the hybrid- π model.

At low frequencies an output signal from a transistor is either in phase (0 degrees) or out of phase (180 degrees) with the input signal. These simple phase relationships no longer hold above the β cutoff where the mathematics change, taking on a (formally) complex character.

A typical BJT is the 2N3904. This NPN transistor has a typical F_t of about 300 MHz and a low frequency β_0 of 100. This places the β cutoff at about 3 MHz. This device will have some phase shift effects at all frequencies within the HF spectra and higher.

2.3 LARGE SIGNAL AMPLIFIERS

Our previous small signal viewpoint is now expanded. We will examine overdriven receiver circuits only intended for small signals. A more common large signal amplifier is a transmitter stage, a circuit intended to function at high levels.

Distortion is a consequence of large signal operation. Distortion in an amplifier merely means that the output is something different than a replica of the input. A distorting circuit driven by a sinewave will have non-sinewave outputs when viewed in the time domain, experimentally with an oscilloscope. In the frequency domain, the distortion appears as harmonics. A distorting circuit driven by two or more signals may contain outputs that are the result of intermodulation, frequencies that are sums and differences of input frequency multiples.

The BJT model of greatest popularity is an extension of the diode equation,

$$I_E = I_{ES} \cdot e^{\frac{q \cdot V}{k \cdot T}} \quad \text{Eq 2.21}$$

where I_{ES} is called the emitter saturation current. V is the voltage on the base-emitter diode. The other parameters are the same as appeared with the diode equation in Section 2.1. This is part of the model known collectively as the Ebers-Moll equations. The non-linear exponential behavior is intrinsic to the bipolar transistor. Detailed use of this model takes us well outside the realm of this text, but is highly recommended for those with such interests.³

Many large signal properties of amplifiers are extensions of simple circuit analysis. Although the details are always buried within refined models, much can be discerned from careful analysis without analytic complexity. Some examples will be used to illustrate this.

Fig 2.29 shows a simple audio amplifier driven with a 1 kHz signal behind a

1-kΩ impedance. We observe an output voltage at the collector. The dc base voltage is approximately ¼ the power supply, so the emitter is at about 1.8 V. The emitter current is then 1.8 mA, producing a dc collector bias voltage of 8.2 V. The emitter current leads to a small signal r_e value of about 14 Ω. Voltage gain is 70 with the 1-kΩ collector load. The input resistance will be a little over 1 kΩ if β is 100. This means that the base signal voltage is just over half the generator value.

From the bias and small signal analysis, we predict that an input of 20 mV peak at the generator will produce a bit over 10 mV at the base. The voltage gain of 70 applied to this will give a peak collector signal of 0.7 V, or a peak-to-peak value of 1.4 V. The 8.2-V zero signal collector value will then move between 7.5 V and 8.9 V. This is still a long way from the +10-V supply or the 2.5-V base where saturation would be approached. We would expect a sinewave input to generate a sinewave output.

Fig 2.30 shows waveforms for three drive levels: .02 V, 0.1 V, and 0.5 V peak. The sinusoidal output is very close to the values we estimated. However, the other two cases are severely distorted. The 0.1-V drive case, five times stronger than the initial 20-mV input, is enough to cause the output to reach the 10-V positive power supply, causing collector current to drop to zero. The other part of the cycle is still well behaved with approximately sinusoidal outputs.

The most severely distorted output results from the largest input signal, 0.5 V peak, also shown in Fig 2.30. At the posi-

tive extreme, the transistor is cutoff with current having vanished. At the other end, the transistor current is well beyond the bias value. The collector has dropped below the base voltage and the transistor is saturated for the bottom, voltage-flat parts of the curve.

Simple models predict much of the nonlinear behavior, without formal analysis. The base-collector diode prevents collector voltages more than a diode-drop below the base. But, the collector current generator is capable of increasing “as needed” to supply larger currents, but only of the prescribed polarity. The larger drive examples would sound very distorted if this audio amplifier was part of a receiver.

The next example is a familiar emitter follower that might be on the output of an oscillator. A follower has a low output impedance, and should, we reason, be capable of delivering power to a low impedance such as a mixer. But this

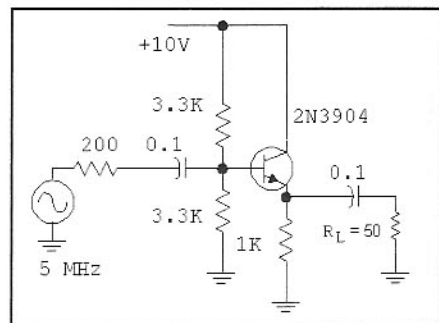


Fig 2.31—Emitter follower to drive a 50-Ω load. This circuit is not biased to deliver the needed output power.

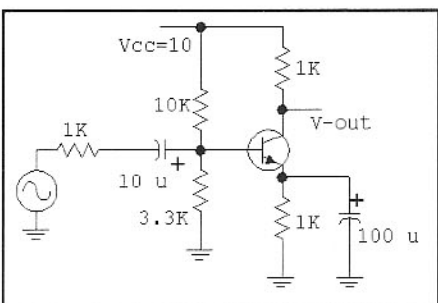


Fig 2.29—A simple audio amplifier examined for large signal performance.

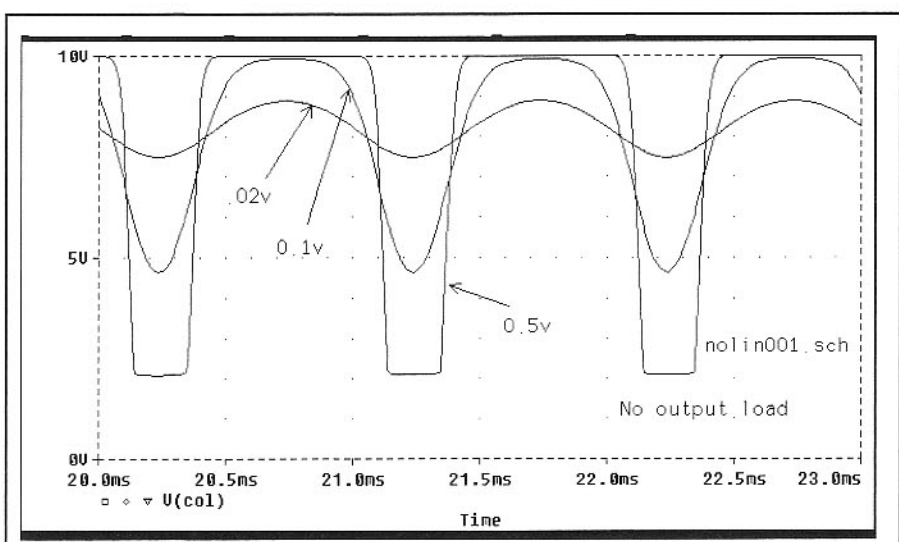


Fig 2.30—Output waveforms for the simple amplifier at several drive levels.

reasoning is flawed.

The emitter follower circuit is shown in Fig 2.31. A pair of 3.3-k Ω resistors bias the base at half the 10-V power supply, and the emitter is biased with a 1-k Ω resistor. $I_e=4.4$ mA, setting r_e to 5.9 Ω . The follower is driven from a 200- Ω source resistance for an output resistance of 7.9 Ω . If this circuit was going to be used to drive a 50- Ω filter, the 50- Ω resistance would be realized by adding a series 43- Ω resistor to the output.

This follower circuit is being driven by a signal source with a peak amplitude of 0.5 V. The input impedance is well above the 200- Ω driving source, so virtually all of the available generator signal is present at the base.

The modeling process is applied to capacitors with the same importance that it is to transistors. A capacitor accumulates charge through current flow, never allow-

ing the voltage across the capacitor to instantaneously change. The capacitor could conceptually be replaced by a battery. In no-signal conditions the 4.4-mA transistor current flows in the 1-k Ω bias resistor with zero current in the 50- Ω load.

Applying a positive going signal to the base merely turns the transistor on harder. As the base voltage increases from the 5-V no-signal level to 5.5 V, the emitter will follow from 4.4 V to 4.9 V. We now have +0.5 V on the output load, forcing an output current of 10 mA to flow. The current in the 1-k Ω bias resistor has increased to 4.9 mA, so the total transistor current is 14.9 mA.

A negative-going base signal produces complications. A small negative base drive of 0.1 V to 4.9 V would drop the emitter to 4.3 V, which drops the output to -0.1 V. The current in the 50- Ω load becomes -2 mA.

With the emitter voltage at 4.3 V, we still have 4.3 mA flowing in the 1-k Ω resistor. The transistor current has now dropped to 2.3 mA. Because it is still positive, the transistor is still controlling the output and the follower continues to follow.

But what happens when the drive reaches the full negative value of -0.5 V? If the linear, small signal model applied, the base would drop to 4.5 V, leaving the emitter at 3.9 V with the output at -0.5 V, producing a current in the load of -10 mA. But the current flowing in the bias resistor would still be 3.9 mA, implying that the transistor current would be -6.1 mA. This is not possible! The transistor can supply current via the model current generator, but that current cannot be negative.

Fig 2.32 presents the waveforms. The negative going excursion is clipped at the point when the transistor emitter current drops to zero, leaving all output current to flow in the 1-k Ω resistor.

This simple circuit has illustrated the difference between small signal and large signal models. Currents of either polarity are allowed in a small signal model. The large signal behavior is restricted to that dictated by the model, in this case limited to the positive current flow predicted by the Ebers-Moll equation.

The low small signal output impedance of a follower was a consequence of negative feedback. The load in series with the output creates a voltage that is applied to the transistor in opposition to the signal driving it. If we allow the follower to "run out of current," the transistor is cut off with zero current flow. The low output impedance is no longer present during that part of the cycle when transistor current flow has ceased.

Fig 2.33 shows the output after the design was modified. The emitter bias resistor was changed from 1 k Ω to 330 Ω , increasing the emitter bias current to 12.6 mA. This is larger than the needed 10 mA, so the output remains clean. But, even a slight increase in drive could allow the distortion to return. The ultimate refinement might be a complementary output such as is found with many audio amplifiers.

The next example considered is a 10-MHz Class A amplifier intended to develop a few milliwatts of output power. The circuit is in Fig 2.34. The base is biased from a 10-V supply through a voltage divider of 10 k Ω and 3.3 k Ω , producing a DC emitter voltage of 1.64 V. The 200- Ω emitter resistor sets an emitter current of 8.2 mA, yielding a small signal r_e of 3.2 Ω . The 50- Ω output load sets the small signal voltage gain at 16.

A common approximation sets high

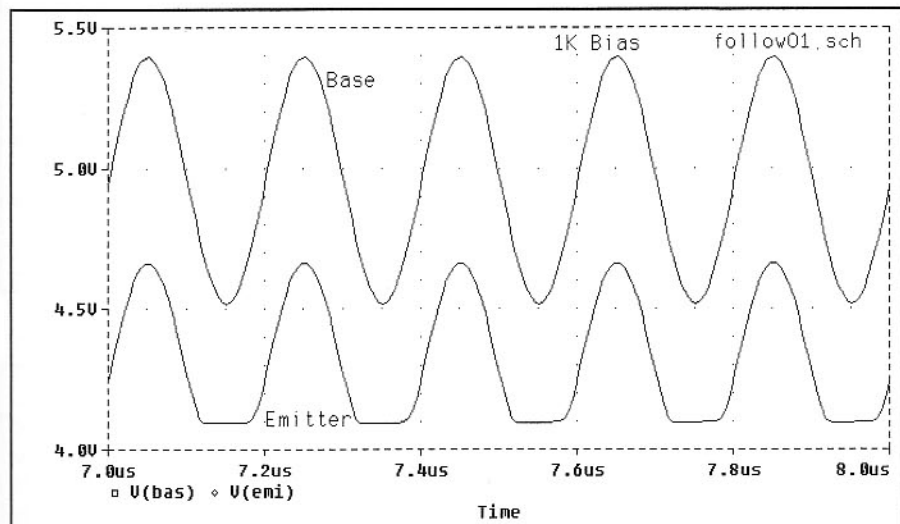


Fig 2.32—Follower waveforms.

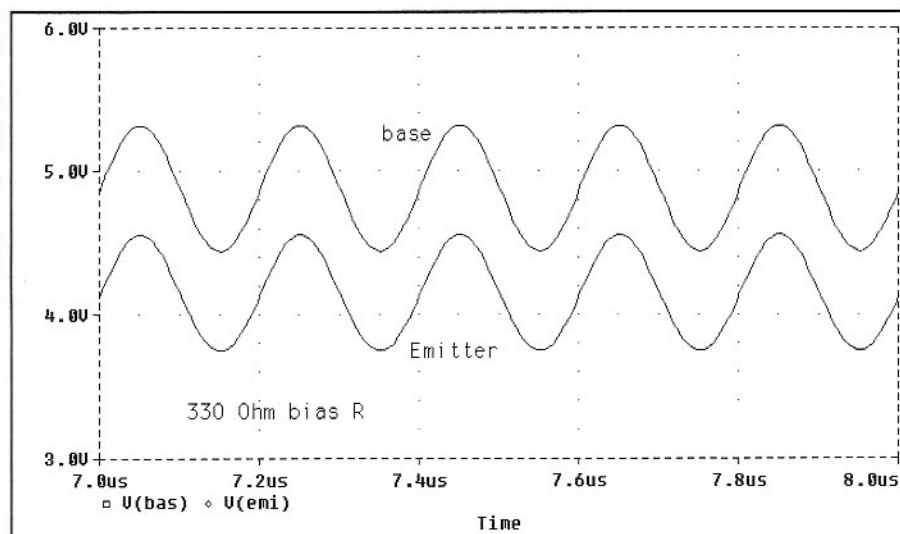


Fig 2.33—Follower output waveforms after increasing the standing bias current.

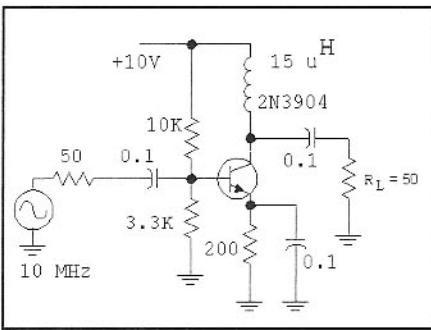


Fig 2.34—A class A amplifier.

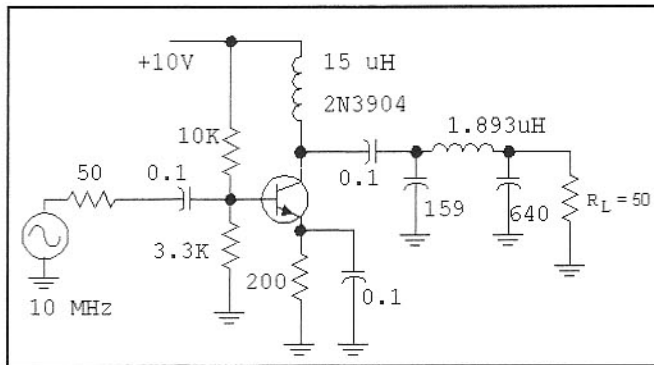


Fig 2.35—The class A amplifier is modified with output impedance transformation for higher output power.

frequency β at F_i/F , placing β at 30. This sets input resistance of about $100\ \Omega$, which predicts that about 2/3 of the open circuit input voltage will appear at the base. An input signal of 10 mV peak produces about 6.7 mV on the base. Applying the small signal voltage gain, the output will be 105 mV peak. Perhaps of greater interest, the load current for this output is 2 mA peak. The transistor collector current varies from the quiescent (no-signal) value of 8.2 mA up to 10.2 mA and down to 6.2 mA. While small signal characteristics are preserved, the output current is already becoming a sizable fraction of the DC bias current.

A characteristic found with the present circuit that we did not see in earlier amplifiers results from the use of a collector RF choke. The inductor has the properties of a constant current source. As a dc current is established in the inductor, the action of the inductor "tries" to maintain that value. This allows the collector voltage to exceed V_{ce} , which never occurred when a collector resistor supplied bias current. This is shown in plots which follow.

We now increase the input drive to 50-mV peak. This is a five times increase over the 10-mV case, so we expect a similar increase in both the output voltage and current if small signal conditions are preserved. Measurements and computer simulations both confirm this general behavior, although the output signals depart considerably from sinusoids. Output voltage across the load is about 0.5 V peak. Collector current drops almost to zero at one point in the cycle but reaches a maximum of about 19 mA, about twice the bias value. Distortion is severe.

The amplifier with 0.5-V drive is current limited, for the current drops to zero at one point in the drive cycle. However, the voltage excursions are still small. The output power with a 50- Ω load is about 2.5 mW.

Consider changes in load resistance seen by the collector. If we maintain drive at 0.5 V peak, the collector signal current

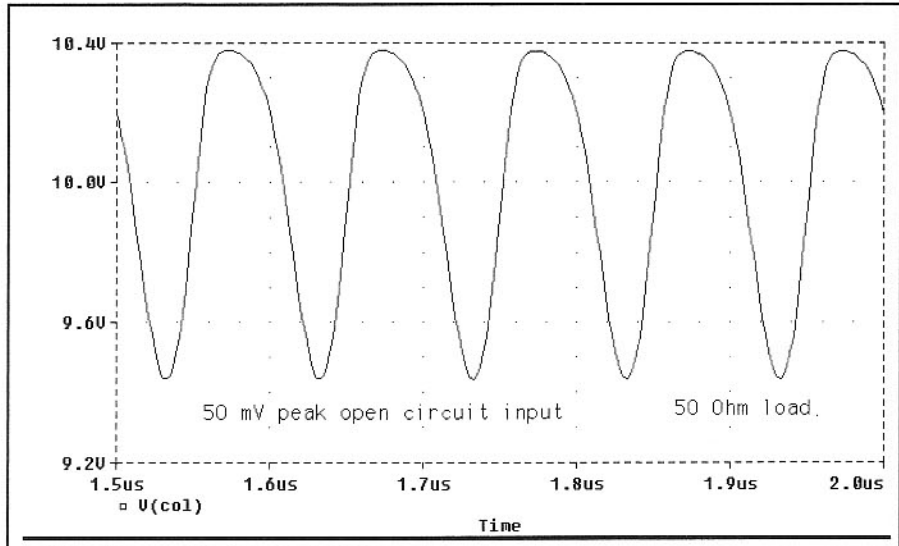


Fig 2.36—50- Ω termination on the class A amplifier.

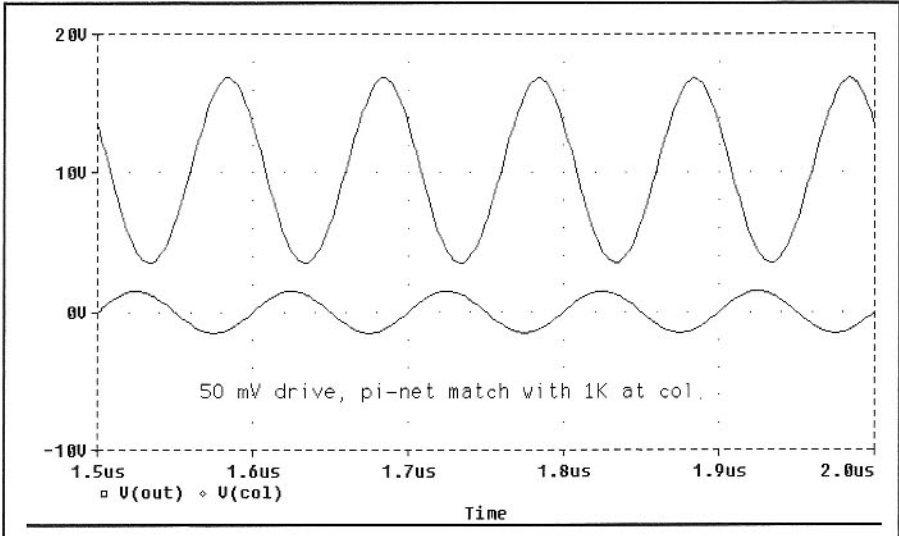


Fig 2.37—Collector (upper) and output load (lower) voltages with the pi network output circuitry.

will be the same. Output voltage can, however, increase as R_L grows. To obtain the maximum power output, we wish to pick a load that allows the collector voltage to drop nearly to the base value (saturation)

while going an equal distance above V_{ce} at the opposite part of the cycle. This voltage excursion should occur as the current varies from twice the bias value down to zero. The load resistance that allows this is

$$R_L = \frac{(V_{CC} - V_B)}{I_E} \quad \text{Eq 2.22}$$

where I_E is the dc bias value. A more familiar form expresses the load in terms of a desired output power,

$$R_L = \frac{(V_{CC} - V_B)^2}{2 P_{out}} \quad \text{Eq 2.23}$$

where R_L is the load resistance in Ohms, V_{cc} is the power supply, V_B is the DC base

voltage, and P_{out} is the output in Watts. This form applies to Class B and C amplifiers as well as the class A amplifier under discussion.

Application of Eq 2.22 predicts a load resistance of just over 1000 Ω for maximum output. Changing the load to 1 k Ω in the circuit produces a 10-MHz output of 11 V peak-to-peak corresponding to a power of about 16 mW. Even larger resistance would have produced voltage limiting, so this is close to optimum.

More often than not, 1000 Ω is not the impedance that the designer wishes to use as a termination for the amplifier just

designed. Rather, he or she wishes to measure the amplifier output with 50- Ω instrumentation and perhaps drive other circuits with a 50- Ω impedance. The solution is found in Fig 2.35 where an impedance transforming π -network is inserted between the 50- Ω load and the collector. This network makes the termination "look like" 1000 Ω at 10 MHz. It also has low pass filtering characteristics, attenuating energy at 20 MHz, 30 MHz, and higher harmonic frequencies. Fig 2.36 shows the collector waveform when the 50- Ω load is connected directly to the collector. The waveforms after matching are shown in Fig 2.37.

2.4 GAIN, POWER, DB AND IMPEDANCE MATCHING

Audio and other low frequency amplifiers are easily analyzed with the low frequency models used for biasing. But most of our interest is in higher frequencies where measurement difficulties persist. These encourage us to consider power instead of the voltages and currents that dominate the view of the circuit theorist. This emphasis is an integral part of RF design and forms the basis for this section.

The emphasis on power measurement goes back to early methods. Power at radio, microwave, and even optical frequencies was measured using a Bolometer. The Bolometer is based upon temperature measurements. A resistive load is embedded in a thermally well-insulated chamber. The application of RF power causes a temperature increase, which can be detected with a thermometer. But, the same increase in temperature can be produced with application of direct current. Measurement of the direct current and related voltage then provide a very fundamental

determination of the RF power.

The other reason we are concerned with power is that it is power and not voltage or current that is more fundamental. Power is the rate that energy is transferred, whether it be a rate of dissipation, such as the power that becomes heat in a resistor, or the rate that energy may pass through a surface, such as the rate that a radio or light wave passes through a plane. That plane could well be the capture area of an antenna. The unit for power is the Watt (W), or Joules per second. We are more familiar with it being the product of current and voltage.

An amplifier application is presented in Fig 2.38 consisting of a voltage source with related source resistance, the amplifier, and an output load. While 50 Ω is common for both the source and load, this is certainly not necessary. But, if power is to be measured, we must have some resistance, for a voltage across an open circuit provides no power.

Consider the simple circuit of Fig 2.39 consisting of a voltage source, V , and a source resistance, R_S . We will terminate this in a load R . Ohms Law provides the net current, while voltage divider action gives the voltage across the load, yielding the power

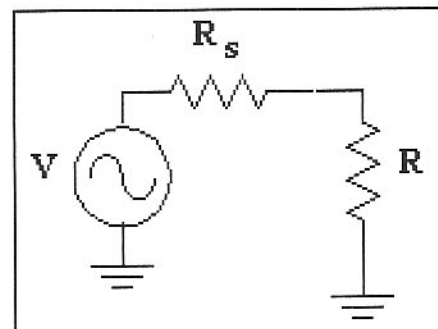


Fig 2.39—A voltage with a source resistance R_S delivers power to a load R .

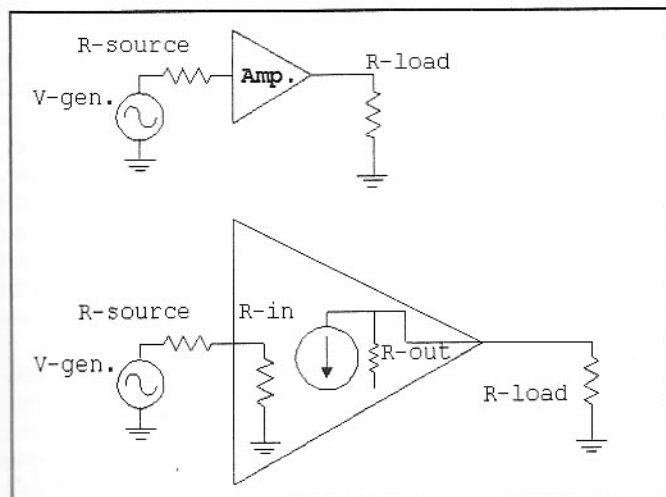


Fig 2.38—Basic amplifier with resistive input and output impedances.

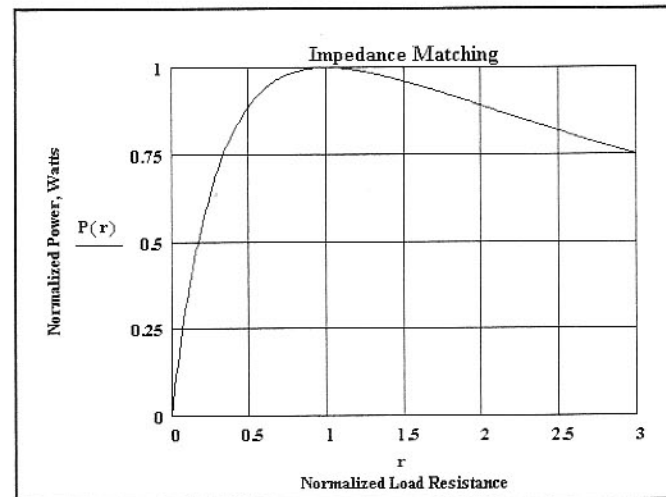


Fig 2.40—Power delivered to the load is maximum when the load resistance equals that of the source.

$$P = \frac{V^2 \cdot R}{(R_s + R)^2} \quad \text{Eq 2.24}$$

A plot of power vs R is given in **Fig 2.40** where we have normalized the curve. The maximum power is shown as 1 and the normalized resistance, defined as $r = R/R_s$, is 1 when power is maximum. This is the familiar result that the maximum power transfer occurs when the load resistance, R , equals that of the source, R_s . We then say that the source is *matched* to the load. In the general case, the source impedance can have a reactive part. Then, maximum power transfer occurs when the load is a complex impedance with the same resistance as that in the source impedance.

When a generator voltage and the related source resistance are specified, the power extracted when the generator is terminated in a matched load is called the *available power*, for it is the maximum power that is available from that generator.

The amplifier of Fig 2.38 has an input resistance, R_{in} , and an output resistance, R_{out} . The rest of the amplifier is modeled with a controlled current generator. The amplifier will be matched at the input when $R_s = R_{in}$. The output is matched with a load $R_L = R_{out}$. Picking these source and load resistances will produce this perfectly matched amplifier. While it sounds easy enough, it can be very complicated in a practical RF application. In a practical amplifier R_{in} will depend upon the load, R_L , while R_{out} will depend on R_s . Eventually stability becomes a dominating issue. Circuits that are unconditionally stable can eventually be matched perfectly at both input and output.

Source and load resistances are not changed directly as a means of achieving matched conditions. Rather, a 50- Ω generator might be applied to an impedance transforming network that presents a different impedance to the amplifier input. These networks are discussed in greater detail in Chapter 3.

We always are interested in the "gain" of an amplifier. This usually means *power gain*, which is the ratio of two power levels. With a known source voltage, V , and source resistance, R_s , and the modeled input resistance R_{IN} (from Fig 2.38), we can calculate the input power. Output power can also be calculated when the amplifier is well modeled. Knowing the powers, the *power gain* is:

$$G_P = \frac{P_{OUT}}{P_{IN}} \quad \text{Eq 2.25}$$

The maximum possible gain is that

occurring when both input and output are matched.

The power gain of Eq 2.25 is rarely measured directly. Instead, we more often measure or calculate *transducer gain*, first mentioned in Section 2.2. Transducer gain is:

$$G_T = \frac{P_{OUT}}{P_{AV}} \quad \text{Eq 2.26}$$

where P_{out} is the power delivered to the load and P_{AV} is the power *available* from the source. Power gain and transducer gain are equal in a perfectly matched amplifier. A variant of transducer gain is the *insertion power gain* obtained when a transmission line is broken, and an amplifier is inserted. This occurs when both R_s and R_L are identical, usually 50 Ω .

The Decibel, or dB.

Gain can be expressed as a numeric ratio, but is more often specified in decibels, given by

$$dB = 10 \cdot \log \left(\frac{P_1}{P_2} \right) \quad \text{Eq 2.27}$$

where P_1 and P_2 are two different powers. If an amplifier has a 5 mW output and is being driven by a generator with an available power of 1 mW, the power ratio P_{out}/P_{AV} is 5, for a transducer power gain of 7 dB.

The dB construct was not invented to confuse the prospective designer. Rather, it is a natural consequence of the mathematics. Output power is calculated from an input power and a numeric gain by using multiplication. It is also calculated from a dB ratio, but now simpler addition is used.

The dB construct is useful for other comparisons. For example, we might examine the harmonic distortion in an amplifier and find that for a 3-mW drive at 7 MHz, output appears not only at 7 but at 14, 21 and 28 MHz. If the 14-MHz output is less than the 7-MHz output by a factor of 500, we say that the 2nd harmonic is 27 dB below the fundamental. The 7-MHz component is often regarded as a carrier and the 14-MHz component is then said to be at -27 dBc where the "c" indicates dB with regard to a *carrier* or reference power.

Another often used variation of the dB ideal occurs when a power is referenced against a standard of *one milliwatt*. We then say that the power is in dBm, meaning power referenced to *one mW*. This does *NOT* depend upon impedance. The dBm values will be positive or negative depending on their relationship to 1 mW. A one watt QRP transmitter has an output of 1000

mW or +30 dBm. But a strong received signal from the terminals of an antenna might be at one microwatt, 30 dB below the 1 mW, or at -30 dBm.

Many instruments are calibrated in dBm. The dBm output of a signal generator is a measure of the *available* output power of the generator. *Available power*, discussed above, was the power actually transferred for the single case when the load matched the source. It is common for the output to be specified in a 50- Ω system, a common RF standard. A signal generator set up for an output of +10 dBm will deliver that power to a 50- Ω load attached directly. It will also deliver that power to a 200- Ω load if an appropriate 2:1 turns ratio transformer is placed between the load and the generator.

RF detection instruments, such as RF power meters or spectrum analyzers, are also calibrated in dBm. These instruments usually have a 50- Ω input impedance. They behave like a 50- Ω resistive load when attached to a generator. A 50- Ω signal generator set for an output of -40 dBm should produce an indication of -40 dBm when attached to a spectrum analyzer.

Wideband instruments used for general purpose electronic measurements include wideband voltmeters and oscilloscopes. They usually have high input impedance, typically 1 M Ω . When used with a 10X probe, the input resistance becomes 10 M Ω . The measurement philosophy behind the design of these instruments is to present such a small load to a circuit being measured that the instrument can be ignored. The oscilloscope is usually used in an *in situ*, or in-place measurement. This contrasts with the measurement philosophy of many RF measurements, which use *substitution*. For example, we *substitute* a power meter for the antenna when we wish to measure transmitter output power.

The wideband oscilloscope can be used for measurements in a 50- Ω system, but it becomes vital to establish a well defined input impedance. This is done with a 50- Ω resistive termination. A form that can be built for the home lab is shown in **Fig 2.41**, while a photo in **Fig 2.42** shows a home-built version and a couple of commercial terminators. The commercial models are built with low inductance disk resistors that offer higher bandwidth than can be easily achieved with leaded parts in a homebuilt box.

Gain measurements in a 50- Ω environment are straightforward with the terminated oscilloscope and a signal generator. The generator is first attached directly to the terminated oscilloscope with a length of coaxial cable. The 'scope response is noted, and power is calculated to be sure

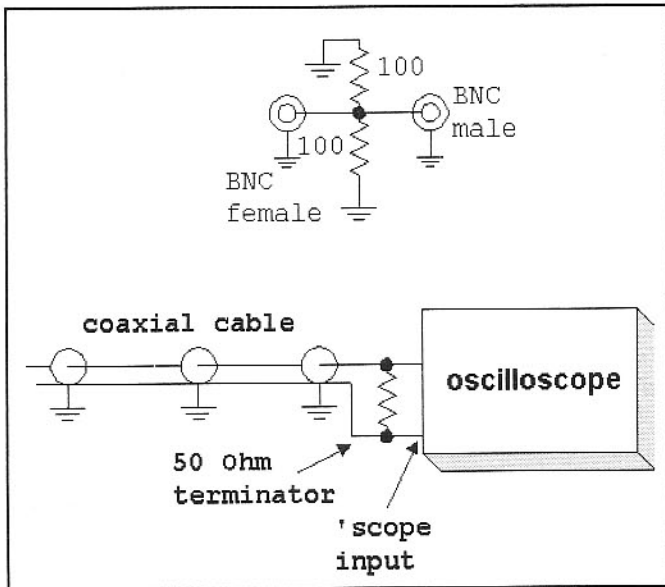


Fig 2.41—Terminators for oscilloscope input loading. See Chapter 7 for additional detail on power measurements.

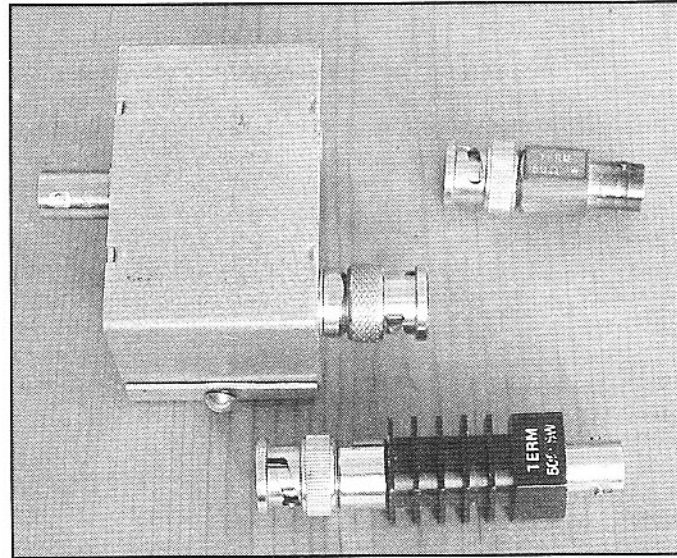


Fig 2.42—Homebrew and surplus terminators.

that this is not too large for the amplifier. The cable is then disconnected, the amplifier is attached, another section of cable is inserted to connect to the instrumentation, the amplifier is powered, and the new response is noted. The response will (hopefully) be larger than it was without the amplifier in place.

Several approaches can be used to determine gain. The first would be to measure the new voltage with the terminated oscilloscope and then calculate a new output power. The transducer gain then becomes $10 \log (P_{out}/P_{AV})$. This scheme works well with a calibrated oscilloscope operating within its bandwidth.

The alternative method removes all need for oscilloscope calibration and accurate response at the test frequency, but places a greater burden on the signal generator. The reference is first established with the signal generator attached directly to the oscilloscope. The response is noted, as is the output setting for the generator. The amplifier is then inserted in line, and the signal generator output is reduced until the 'scope response is exactly the same as noted earlier. The new generator output is examined and found to be lower than the original. The difference in generator settings in dB is then the transducer gain.

Gain can still be determined, even if the signal generator is not calibrated. A step attenuator is inserted in the generator output. Attenuation is increased when the amplifier is placed in the system until a reference 'scope response is duplicated. The attenuator difference is then the gain.

The oscilloscope can, of course, be used

with a 10X probe to study the amplifier. Output power can be measured from a voltage determination at a load on the amplifier output. But amplifier input power is not defined when the input impedance is unknown. Although common, it is rarely valid to merely measure a voltage ratio to calculate a power or transducer gain.

Measures of impedance match and mismatch

In Fig 2.40 we saw that the power transferred from a source to a load depends upon the match between the two. This curve has a symmetry that is not immediately obvious. Although the power transferred from the source to the load is 100% only when the match is perfect, the degree of match depends only on the ratio of one resistor to the other without regard to which is larger. That is, if the source is 50Ω , we see that power transfer is 88.9% effective for loads of either 25Ω or 100Ω . Similarly, 12.5Ω or 200Ω loads produce 64% power transfer and so forth. The ratio of these resistances to 50Ω (always with the larger number taken) is called the *voltage standing wave ratio*, or VSWR.

The term VSWR arises from transmission line behavior and it relates to voltages measured along a transmission line that is not matched. While we can do this measurement with RF voltmeters and suitable transmission lines, this is not the way we usually measure the degree of impedance match. (Actually, some microwave experimenters still do just this measurement.) Rather, we perform bridge measurements

of a related term called *voltage reflection coefficient*, often signified by the Greek letter Gamma, Γ . Gamma is given for resistive loads,

$$\Gamma = \frac{R - R_0}{R + R_0} \quad \text{Eq 2.28}$$

where R_0 is the reference resistance. In the examples we have discussed, R_0 would be the source resistance while R is the load. Gamma is related to VSWR through

$$\text{VSWR} = \frac{1 + |\Gamma|}{1 - |\Gamma|} \quad \text{Eq 2.29}$$

where the bars around Γ indicate that only the magnitude of Γ is used. In the general case, Γ has both magnitude and angle, corresponding to complex impedance with both resistive and reactive parts. Also, the more general form of Eq 2.28 uses complex impedance to define Gamma, $\Gamma = (Z - Z_0)/(Z + Z_0)$.

Fig 2.40 showed power transfer effi-

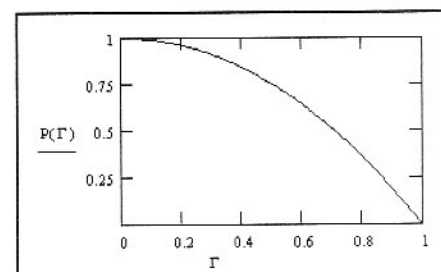


Fig 2.43—Power transfer related to reflection coefficient.

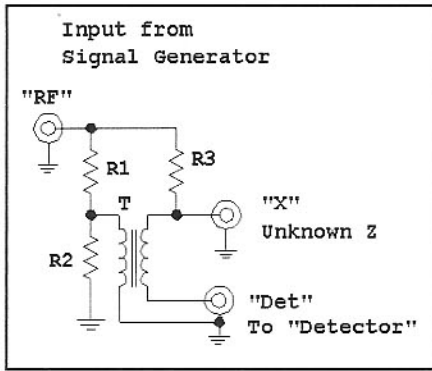


Fig 2.44—Return Loss Bridge. All resistors are normally 50 Ω.

ciency as a function of the terminating resistance. A similar plot is given in Fig 2.43 where power is now plotted against reflection coefficient, Γ .

Although reflection coefficient, Γ , may seem like an esoteric impractical parameter, it is easily measured (in magnitude) using a simple apparatus that can be built in the home lab. This circuit, shown in Fig 2.44, is called a *return loss bridge*, or RLB. The three resistors in the bridge are 50 Ω when building a bridge for use in a 50-Ω system. The signal generator is assumed to then have a 50-Ω impedance as well. The transformer is a *common mode choke* (see Chapter 3.) Construction is discussed in Chapter 7.

The bridge action occurs because all resistors are 50 Ω. Assume that the "X" port, the unknown, is terminated in 50 Ω. Then half of the voltage applied at the "RF" port appears at the junction of R1 and R2. But half also appears at the "X" port. The voltages are equal on either side of the common mode transformer, so no signal appears at the detector. In contrast, a larger signal appears when the unknown "X" port is either open or short circuited.

Use of the return loss bridge is presented in Fig 2.45, where an amplifier input will

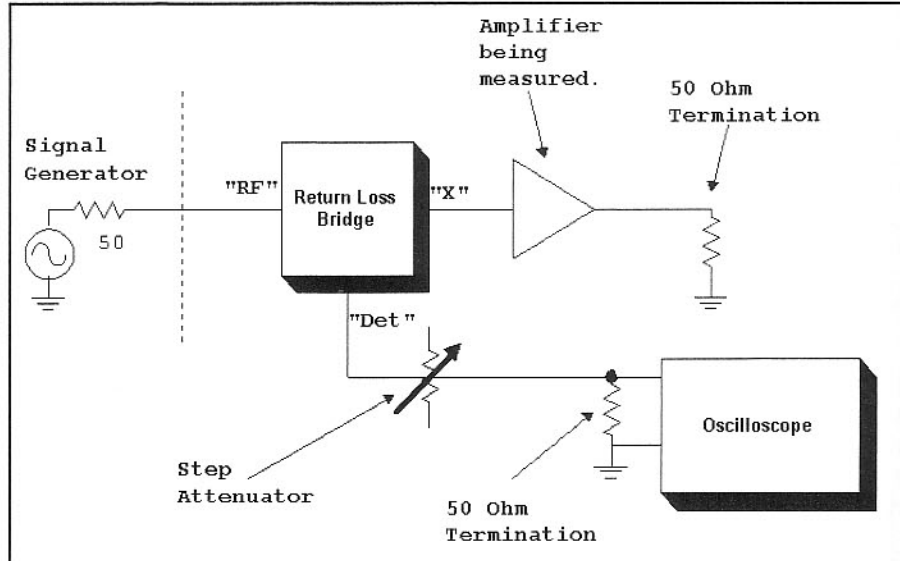


Fig 2.45—Using a return loss bridge with an amplifier.

be measured. The bridge is first open circuited at the "X" port, and the detector response is noted. Then, a 50-Ω terminator is placed on the "X" port. A large decrease in detector response should be noticed. This response is a measure of how well the RLB is functioning and is called the bridge *directivity*. An amplifier (power on) is now attached to the "X" port through a coaxial cable, and a terminator is attached to the amplifier output. The detector response will be lower than the level present with the "X" port open circuited by a ratio called the *return loss*, a dB value. The step attenuator in the detector can be adjusted to attenuate the reference to better measure return loss.

Return loss is related to Γ through

$$R.L. = -20 \cdot \log \Gamma \quad Eq\ 2.30$$

The inverse form is

$$\Gamma = 10^{\frac{-R.L.}{20}} \quad Eq\ 2.31$$

While we have illustrated the RLB with oscilloscope detection, a 50-Ω power meter or spectrum analyzer is preferred. Both are described in Chapter 7. These are 50-Ω instruments, so they do not require the external terminator so vital to the oscilloscope. The 'scope suffers from two problems that compromise this application. First, it is a wideband instrument, so noise limits the sensitivity, making it difficult to see the weak signals that are readily seen in a spectrum analyzer. Second, many of the terminations that we might measure are narrow bandwidth loads. As such, they will produce high return loss at one frequency, but not at the harmonics. The usual signal generator is harmonic rich. The harmonics are resolved and, hence, ignored in a spectrum analyzer measurement.

2.5 DIFFERENTIAL AMPLIFIERS AND THE OP-AMP

The differential amplifier, or *diff-amp*, is the foundation for most silicon analog integrated circuits in use today, making it a very important topology. Here we investigate differential amplifier fundamentals and examine a major derivative of it, the operational amplifier, or *op-amp*.

Following the name, the differential amplifier is a circuit intended to amplify a difference. The differential amplifier has two input terminals. The output, which can be between two collectors or from just one,

is then proportional to the voltage (or current) difference between the inputs. The basic differential amplifier using NPN bipolar transistors is presented in Fig 2.46.

We start with two identical transistors biased at the same dc base voltage. The two emitters are attached and returned to ground through a common resistance, as in Fig 2.46A. Two identical collector resistors are attached, biased from a common supply. This circuit can have signals applied in two ways. If the two bases are

driven together, the composite circuit would behave as one transistor. The two collector signals would then be identical. This operation is called *common-mode* drive or excitation. The large emitter resistor becomes a degeneration element, causing the common-mode gain to be low.

The other diff-amp drive is the *differential-mode*, where one base is driven in one direction while the other is driven by an opposite polarity. Assume that Q1 and Q2 are biased with a dc base voltage of 5. The

voltage at the common emitter is then 4.4. Total current will be 4.4 mA for an emitter resistor of $1\text{ k}\Omega$. If the two transistors are identical, each will be biased to an emitter current of 2.2 mA. We now apply a differential signal causing V_{b1} to increase by 10 mV while V_{b2} drops by an equal 10 mV. The emitter voltage remains essentially constant. V_{c1} decreases while V_{c2} increases by an amount related to the gain. A useful property of this circuit is that total current does not change with differential drive.

Fig 2.46, part B shows the circuit varia-

tion found most often in integrated circuits where the emitter resistor is replaced by a third transistor. Set V_{b3} to 2 volts and pick the Q3 emitter resistor for the same 4.4 mA. This leaves bias conditions for Q1 and Q2 as they were, although the common mode gain is even lower.

Q3 is a constant current source, a circuit that acts as if the bias for Q1 and Q2 came from a very large negative power supply with an equally large resistor. The effect of this topology is to force the sum of the currents in Q1 and Q2 to remain constant. This has two important consequences.

First, a differential amplifier is very easy to decouple. With constant total current, signals are not injected onto the V_{cc} power supply, very important when the diff-amp is one of many such circuits within an IC.

The other consequence of the constant current source is that drive applied to just one input will result in differential output signals. This is shown in the amplifier of Fig 2.47. The two collector voltages have equal amplitudes and are out of phase with each other.

Although differential amplifiers are abundant in integrated circuits, they are also useful and practical in discrete form. Fig 2.48 shows a diff-amp with readily available parts that might be used to provide balanced local oscillator drive to a mixer without transformers. This circuit is

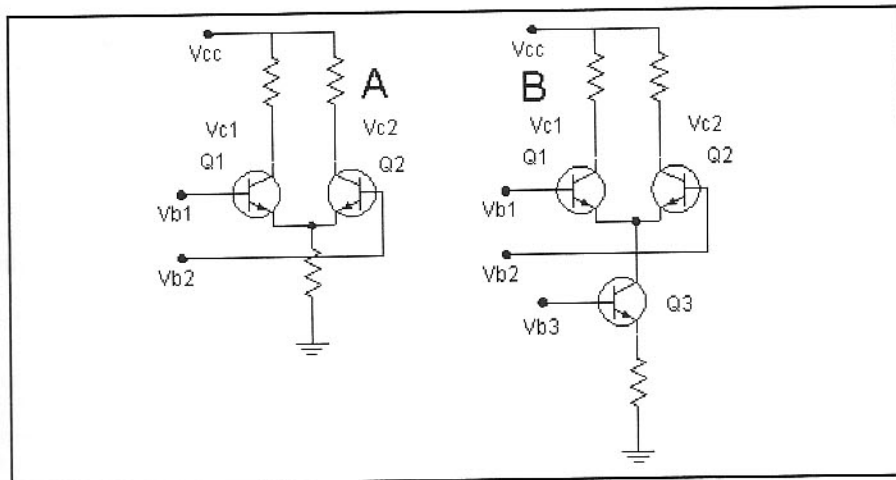


Fig 2.46—Differential Amplifiers.

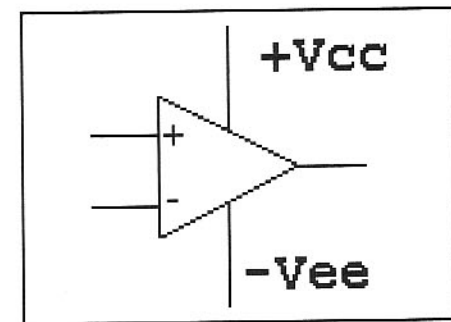


Fig 2.49—Schematic diagram for an operational amplifier.

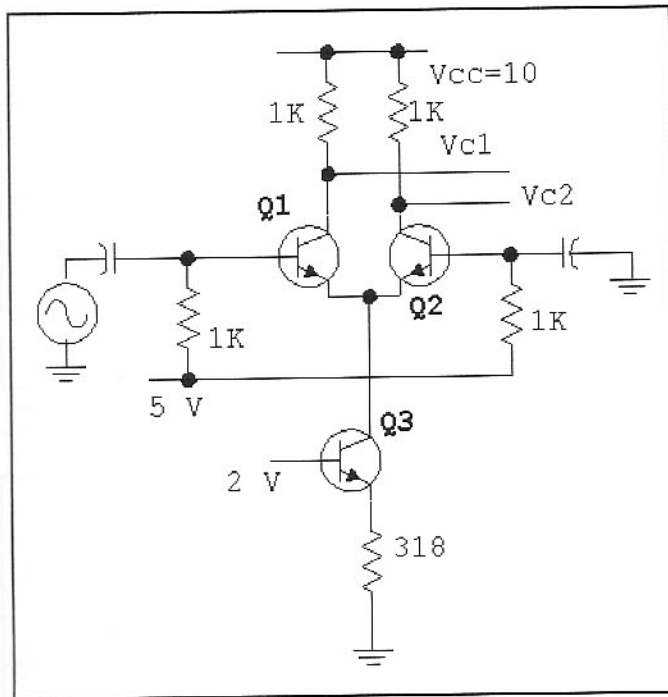


Fig 2.47—Differential Amplifier that converts a single ended signal into a differential one having two outputs with a differential relationship. The 2 and 5-V points are fixed voltage, usually generated within the IC containing this differential pair.

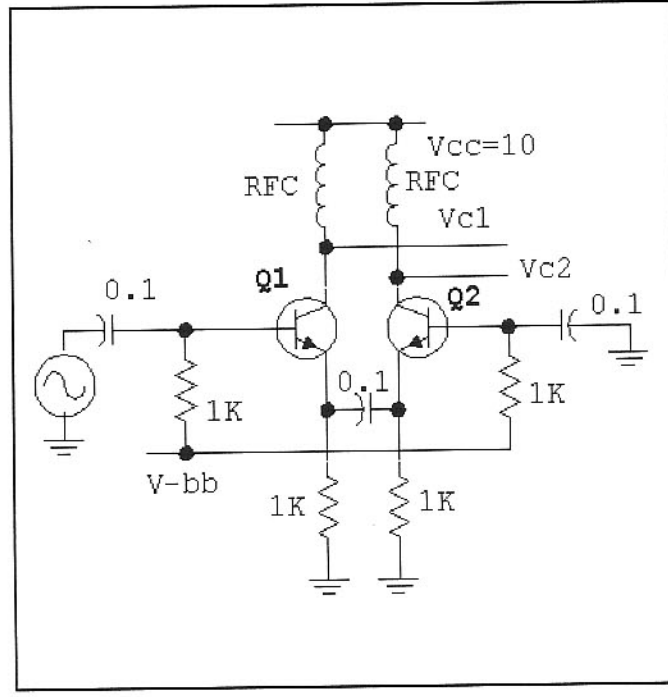


Fig 2.48—Differential Amplifier built with discrete components. The emitter resistors are adjusted for equal current in the two transistors. V_{bb} represents a base bias power supply, which could be a simple voltage divider from the higher supply.

useful because it provides a balanced output with reduced even order harmonics as well as power gain. The use of two emitter resistors eases the need to have identical transistors.

Having examined properties of the diff-amp, we will now look at the “ultimate” diff-amp example, the operational amplifier. An op-amp is shown schematically in Fig 2.49. The internal circuitry can be rather complicated; familiar examples such as the 741 or 358, will include a dozen or more transistors while high performance variants will have many more.

The operational amplifier (Fig 2.49) is shown with two power supplies, although virtually all can be used with a single supply. The basic operation is, in some ways, exactly like the simple diff-amps discussed above. The op-amp has two inputs just as the diff-amp has two base inputs that effect their outputs. The usual op-amp, however, has just one, single ended output. Moreover, the output voltage can be either above or below the input voltages.

The usual op-amp has several gain stages, all cascaded with the output of one feeding the input of the next. As such, the low frequency voltage gain is often very high with values ranging from 50,000 up to over one million. While op-amp gains are often expressed in dB (using the familiar $20 \log(V_{out}/V_{in})$ formula), this is often incorrect. **The dB form only pertains to power ratios.** The equation relating voltage ratio is valid only when terminating impedances are equal.

A typical op-amp can provide output voltages from near the negative power supply up to within a volt or two of the positive supply. The inputs can also occur at a wide variety of voltages. A 741 op-amp will work with inputs that are from about $V_{cc} + 2$ to $V_{cc} - 2$. This span is called the *common mode input range*. Op-amps using PNP bipolar input transistors can have a common mode input range that extends all the way to the negative supply. Examples include the LM-324 and LM-358, which are especially useful with single power supplies.

Assume that the “-” input in Fig 2.49 is constant at ground with power supplies of +15 and -15 volts. Set the “+” input several volts negative. The output will then be very negative, as low as it can go. As the “+” input is increased, the output remains negative until the input gets close to ground. Then, the output will start to increase very quickly. The output goes above ground as the “+” input becomes just a few millivolts positive. The voltage gain may be evaluated from a curve of the output vs the input. With even modest inputs, the output reaches the positive

power supply, or “rail.” The “+” input is called the *non-inverting input* for the output polarity follows it in direction.

Circuit operation is similar if the non-inverting (“+”) input is grounded and the positive going signal is applied to the “-” or inverting input, except that now the output moves in the opposite direction. That is, the output makes a transition from the positive power supply to the negative one. Repeating these experiments at reference voltages other than ground shows that the output depends only upon the **voltage difference** between inputs.

The input transistors for most op-amps are biased for low current operation, causing the input impedance to be quite high. We usually neglect R_{in} during the analysis of op-amp circuits.

Op-amps are rarely operated “open loop,” as described above. Instead, they are used with negative feedback. This is illustrated in Fig 2.50. Power supplies are omitted in the op-amp circuits that follow, but are assumed to be + and - 15 volts.

Assume initially that the “+” input for Fig 2.50 is at ground. If the output was at a different voltage, the inverting input would then be at a level other than ground. This would then produce a difference voltage at the inverting input that forces the input toward ground.

Increase the non-inverting input to +1 volt. Similar arguments show that the output increases until the inverting input is also at +1 volt. The circuit of Fig 2.50 is a

voltage follower with a gain of +1. The value of the feedback resistor is of no consequence for this circuit, for the input current is very small. (A practical unity gain follower normally has the output shorted to the inverting input.)

The modification in Fig 2.51 adds an equal valued resistor from the inverting input to ground. Setting V_{in} to 0 forces the output to ground. However, when we set the input to +1 volt, we find that the output moves to +2 volts. Our circuit now has a non-inverting gain of 2. This is confirmed through voltage divider action. The voltage at the “-” input must be half of that at the output; a voltage other than +1 at the “-” input would produce an input difference that would move the output.

Fig 2.52 shows an inverting amplifier. The “+” input is grounded with an input applied to a resistor attached to the inverting input. We start with the amplifier input at ground. The output must then be at ground. Increasing the excitation to +1 volt causes the inverting input to “try” to go positive, an action that is inverted with gain in the op-amp. The system is in equilibrium when the output is -1 volt. The amplifier then has an inverting gain of 1.

A general behavior has emerged from this discussion, easing further analysis: *Negative feedback around an op-amp always has the effect of forcing the two inputs to have the same voltage.* This can be used to derive the usual formulas for gain of closed loop amplifiers. The char-

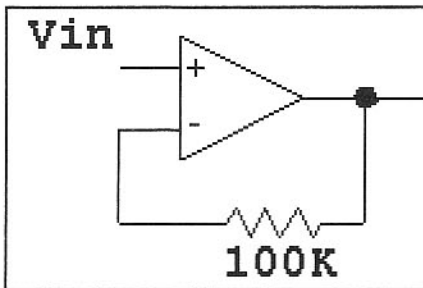


Fig 2.50—A unity gain follower.

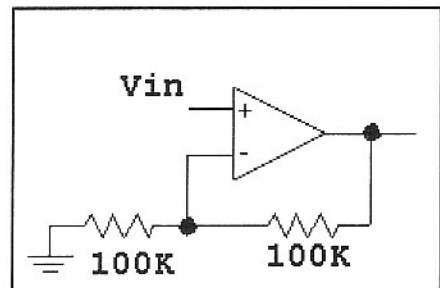


Fig 2.51—A follower with a gain greater than unity.

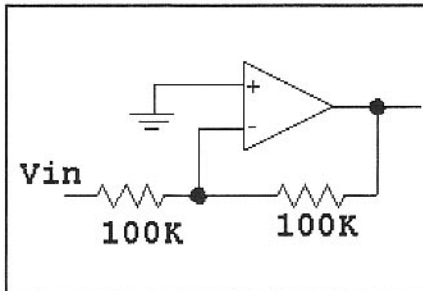


Fig 2.52—An inverting amplifier with unity gain.

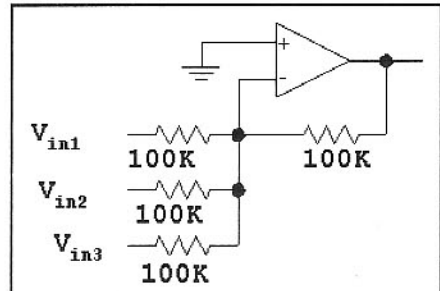


Fig 2.53—A summing amplifier with three inputs.

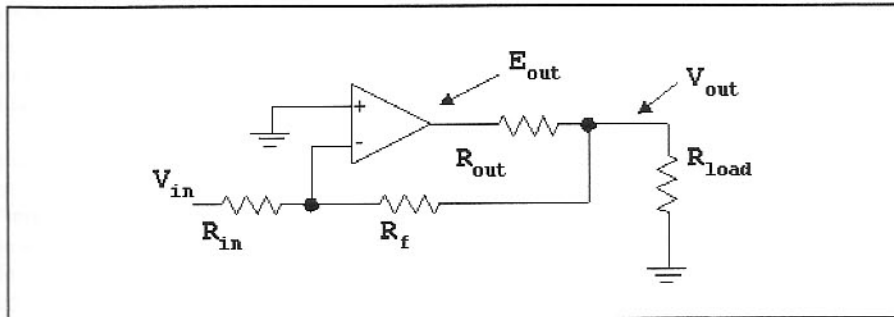


Fig 2.54—Feedback reduces an output resistance.

acteristic is maintained so long as all inputs and outputs are maintained within the allowed ranges.

The inverting input of a closed loop amplifier is often described as a “summing node,” illustrated in Fig 2.53 with three inputs. All three have the same input resistor values, so the gain for each input is the same at -1 . This circuit is sometimes referred to as a “mixer” in audio circles, although the term *mixer* has a much different meaning for the RF experimenter. Analysis is direct. The feedback resistor maintains the two op-amp inputs at the same voltage, which is ground in this example. Any single input will change the output accordingly while feedback keeps the summing node at ground. We calculate the current entering the summing node for each input and note that the total current into the summing node, including that from the output via the feedback resistor, must be zero. This defines the output response.

A highly useful effect of negative feedback is that of altered impedance. The zero voltage difference at the inverting amplifier of Fig 2.52 tells us that the voltage at the “-” input is essentially zero. There is, however, signal current flowing into the node. The effect of the feedback is to reduce the impedance at that node to near zero.

Feedback also decreases output resistance. Fig 2.54 shows an ideal op-amp with an added output resistance, R_{out} . Feedback is extracted from the output end of this resistor. Because V_{out} drives the feedback resistor, it is this point (V_{out}) that is controlled by the feedback element, R_f . Changing the load (R_{load}) may have impact on E_{out} , the op amp direct output, but it has little effect on V_{out} ; the output impedance at V_{out} is very low, a result of the feedback.

The effects of feedback from a parallel resistor are most dramatic with op-amps where the open loop gain (that gain

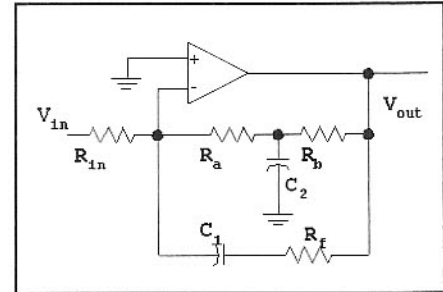


Fig 2.55—The R_a - R_b - C_2 network establishes DC bias with little impact on AC gain. C_1 and the related resistor then set AC gain. If C_1 has a small reactance compared with its series resistor, the gain will grow with increasing frequency.

without feedback) is very high. Negative feedback is also useful in single stage amplifiers using but one transistor. The effects are similar; parallel negative feedback reduces gain, making it depend primarily on resistor values, and reduces both input and output impedance. Not all forms of negative feedback reduce impedance. Emitter degeneration in a transistor amplifier increased amplifier input R as it reduces gain.

Placing capacitors (or inductors) in a feedback path will force the amplifier gain to depend upon frequency. An example is presented in Fig 2.55 where C_1 causes gain to be lower at high frequencies. C_2 has the effect of allowing R_A and R_B to set DC conditions with little effect on gain for AC signals. But, this must done with care to avoid stability problems.

2.6 UNDESIRED AMPLIFIER CHARACTERISTICS

The ideal amplifier is linear with an output that is an exact replica of the input with the only difference being greater amplitude and a phase difference. There should be no other output frequencies. If two inputs are applied to an ideal linear amplifier, the result will be two outputs, each being just what would be seen if each input was applied alone, with nothing else added. Several phenomena compromise amplifiers from this ideal. They include noise, gain compression, harmonic distortion, and intermodulation distortion.

Noise in Amplifiers

Noise is a familiar corruption in an amplifier. The noise of concern is not what we most often hear coming from our HF receivers; that noise generally arises from thunder storms somewhere in the world, or power

lines somewhere in our community. Rather, we are concerned with the noise that is generated within the circuitry. The dominant component of this noise, so called thermal noise, originates from random motion of the electrons within a conductor. This noise shows up as a voltage that appears between the two conductor ends. The available power present is $kT\Delta B$ (in watts) where k is Boltzman's constant, T is absolute temperature in Kelvin, and ΔB is the bandwidth we use to observe the noise. Although a power $kT\Delta B$ is available from any conductor, the related voltage is very small if the conductor is a good one. A resistor, a conductor with larger resistance, allows a larger voltage to appear, but with the same available power. (Available power was discussed in an earlier section.)

Fig 2.56 shows a simple amplifier terminated in 50Ω at both input and output.

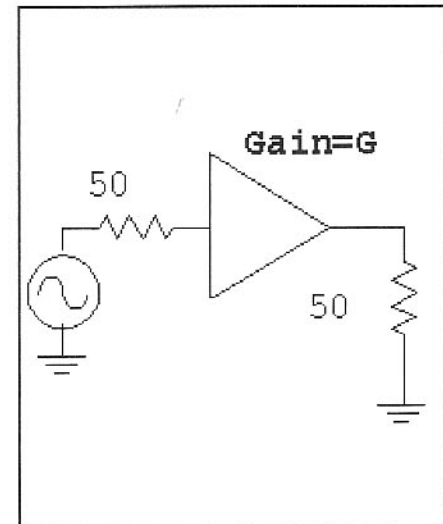


Fig 2.56—A terminated amplifier used for noise analysis.

The source and load resistances generate noise. The noise generated by the output load is normally ignored during a noise analysis of the amplifier, for the circuit designer is primarily concerned with the *available* noise from the amplifier. The noise from the input source is increased by the amplifier gain, just as any signal would be increased. There is nothing that can be done to avoid this noise. If the amplifier available power gain is G and the available noise power from the input source is N_i , the output noise will be $G \cdot N_i$, even when the amplifier is perfect and noiseless.

A real world amplifier will have a noise output that is even higher than the amplified input noise. The output noise is greater by a ratio that we call the *noise factor* or *noise figure*, designated by F . The logarithmic form of *noise Figure* is $NF(dB) = 10 \cdot \log(F)$. The two forms, algebraic ratio or dB, are used interchangeably, although the algebraic ratio is used in all of the equations that follow. The extra noise is that generated within the active device and circuit components.

A formal treatment of noise⁴ deals with noise power ratios. Noise factor is given by,

$$F = \frac{N_{out}}{G \cdot N_{in}} \quad \text{Eq 2.32}$$

where N_{out} is the output noise power delivered to the load, N_{in} is the noise power available from the input resistance, and G is the available power gain of the circuit. N_{in} is the noise power available from the source resistance when it has a temperature of 290 K. NF is the ratio of two noise powers. The larger number (numerator) is the noise actually coming from the amplifier while the smaller (denominator = $G \cdot N_{in}$) is the noise that would be coming from the amplifier if it generated no noise of its own. A perfect, noiseless amplifier would have $F=1$ from the equation, or converting to dB, $NF=0$ dB.

Gain, G , is the power gain we normally associate with an amplifier: output signal power delivered to the load, S_{out} , divided by S_i , an input signal power. If we insert this gain ratio into the noise figure defining equation, and rearrange the terms, we obtain

$$F = \frac{S_i / N_i}{S_{out} / N_{out}} \quad \text{Eq 2.33}$$

This describes a combination of signal and noise. Essentially, noise figure can be interpreted to be a degradation in signal to noise ratio as we progress through the amplifier. This equation can be rearranged to

$$F = \frac{S_{in} \cdot N_{out}}{S_{out} \cdot N_{in}} = \frac{G_{NOISE}}{G_{SIGNAL}} \quad \text{Eq 2.34}$$

where G_{NOISE} is the *noise gain*, the output noise power divided by the available input noise power. G_{SIGNAL} is the familiar signal gain used above. All forms of these equations are used in deriving some of the results we use with noise figure.

Typical NF values range from 1 to 10 dB for the amplifiers that we frequently use in RF systems. Mixers tend to have higher noise figures. Modern FET amplifiers are capable of NF as low as 0.1 to 0.2 dB at UHF with values under 1 dB even possible at 10 GHz.

We frequently ask for the noise factor of a cascade of two amplifiers. This result is

$$F_{NET} = F_1 + \frac{F_2 - 1}{G_1} \quad \text{Eq 2.35}$$

where F_1 and F_2 are noise factors for stage 1 and 2, respectively, and G_1 is the available power gain for the first stage. While the noise from both stages contributes to the net noise factor, the 2nd stage noise contribution is reduced by the gain of the first stage. Clearly, if we can calculate NF for two stages, we can perform the calculations several times and obtain the result for any number of stages.

Noise figure is a vital amplifier and receiver characteristic at VHF where external noise (thunder storms, etc) is low. While a low noise figure is rarely needed at lower frequencies, it becomes more important when small antennas are used.

Noise figure is also a vital parameter within a receiver, for careful control of noise will allow the designer to use low gain, which keeps distortion low. Details are discussed in later chapters.

Recall that the noise power available from a resistor is kTB . A useful number to remember is that $kT = -174$ dBm at "room" temperature of 290 K. If the noise was observed in a receiver with a bandwidth of 3 kHz (a voice "channel"), B would be 3000 Hz and $10 \times \log B$ is 34.8 dB. The noise power available from the resistor would then be -174 dBm + 34.8 dB = -139.2 dBm. A receiver can be thought of as a large amplifier. If the receiver had a 10 dB noise figure, the output noise would be the same as would appear if an input noise of -139.2 dBm + 10 dB = -129.2 dBm was applied to the input of a perfect, noiseless receiver.

The related noise voltage from a resistor is

$$V_N = \sqrt{4 \cdot k \cdot T \cdot B \cdot R} \quad \text{Eq 2.36}$$

where k is again Boltzmann's constant (1.38×10^{-23}), T is the resistor temperature in K, B is bandwidth in Hz and R is the resistance in Ω . The available power, kT , is called a *spectral power density*, usually in W/Hz. The resulting voltage, V_n , is a *spectral voltage density* in volts-per-root-Hz. Op-amps often have noise specified in terms of an equivalent input *spectral voltage density* of noise. The same method is sometimes used for transistors, although noise figure is the more common parameter used to specify an RF design.

Amplifier noise figure is not always a

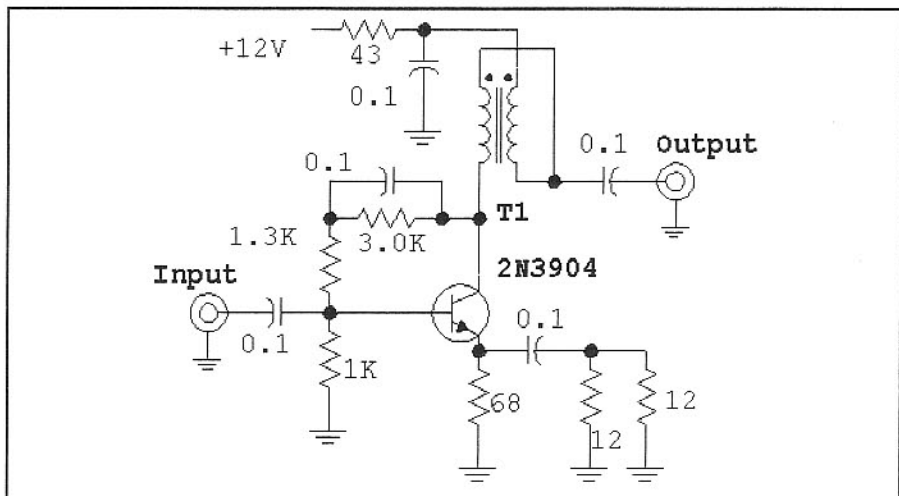


Fig 2.57—Feedback amplifier illustrating gain compression and distortion. This circuit has 20-mA I_c . T_1 consists of 10 bifilar turns on a FT-37-43 ferrite toroid core, although the specific core type is not critical. This circuit features a small signal gain of 20.5 dB and a good impedance match to 50Ω at both input and output. See text for noise Figure, gain compression, and intercept results.

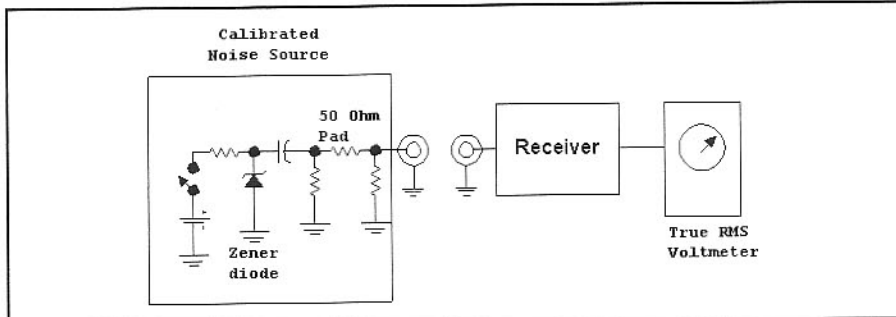


Fig 2.58—Scheme used to measure receiver noise figure. Audio voltmeter examples are the HP3400A or the Fluke Model 89.

simple constant that may be extracted from a data sheet and applied to a design. Rather, data sheet noise figure is specific to a "typical" amplifier, or more often, is the best NF one can achieve. The noise figure of a specific design then depends upon device biasing and the impedance presented to the device input.

An example amplifier is shown in Fig 2.57 in connection with our discussion of distortion. This amplifier was measured with an HP-8970 Noise Figure test set as 6 dB at 10 and 20 MHz. The circuit is discussed further as we investigate feedback amplifiers.

The most common method for noise-figure measurement is shown in Fig 2.58. This drawing deals with a receiver. However, the same source is used to measure an amplifier by following it with a receiver (or spectrum analyzer). After a measurement of the cascade is obtained, the earlier equation is used to obtain the NF of the amplifier alone. The critical part of the measurement system is the noise source. The one used here is a Zener diode. When the switch is open, the diode is off. The pad attenuation, if large, forces the output impedance to be close to $50\ \Omega$. When the diode is turned on by closing the switch, the noise increases by a large amount. The noise increase is called the *excess noise ratio*, ENR, and is about 22.5 dB for our noise source, which is described in Chapter 7.

With a 22.5 dB ENR, the noise output of a perfect, noiseless receiver would increase by 22.5 dB when the source is turned on. But the receiver is contributing noise of its own, so the noise *increase* will be less than 22.5 dB. The output increase is called the "Y-factor." Noise factor (a power ratio rather than dB) is related to the ENR and Y by

$$F = \frac{\text{ENR}}{Y - 1} \quad \text{Eq 2.37}$$

where both ENR and Y are power ratios rather than dB values. Consider an example:

A 22.5 dB ENR corresponds to ENR=178 as a power ratio. If we measure Y of 19 dB for a receiver, the corresponding power ratio is 79.4. F is then 2.27, or NF=3.6 dB.

Gain Compression

Most non-ideal amplifier behavior occurs at higher powers with a simple example being gain compression. Fig 2.57 showed a typical amplifier that illustrates gain compression and other problems. The circuit is a feedback amplifier with a 20 mA collector current. This circuit, which was built and measured, has migrated into numerous receiver and transmitter applications. No heat sink is needed in normal applications.

Small signal amplifier gain was 20.5 dB. Repeating the measurement at several input powers allows one to plot a graph of gain Vs power. Eventually a point is reached where the gain begins to drop. The output power where the gain is 1 dB below the small signal value is called the 1-dB compression point and occurred at an output of +16.5 dBm.

Harmonic Distortion

A familiar amplifier distortion appears in the form of harmonics. If an amplifier is driven at one frequency, amplifier non-linearity generates a distorted output. That output will contain the original input plus harmonic components. A harmonic is an integer multiple of the input frequency. The amplifier of Fig 2.57 was measured with a spectrum analyzer. The input was from a crystal controlled 14-MHz source

followed by a 15-MHz low-pass filter, guaranteeing a drive free of harmonics. The measurement results are shown in Table 2.1.

The drive power was varied from -20 to +5 dBm with a step attenuator. The 14-MHz output, although increasing with drive, still showed gain compression, severe at the highest drive. At lower levels the harmonics (also shown in dBm) grow at a level proportional to the harmonic number. Hence a 10 dB drive change causes a change of about 20 dB in 2nd harmonic and about 30 dB in 3rd harmonic. This simple behavior disappears as the amplifier enters gain compression. Most linear circuits display harmonic amplitudes proportional to order with increasing drive.

It is common to specify harmonic (and other) distortions in terms of "dBc," which is dB with regard to the desired *carrier*. Hence, with a drive of -10 dBm, the desired output was +11 dBm, and the 2nd harmonic was -30 dBm, or -41 dBc.

Intermodulation Distortion, IMD

We next consider intermodulation distortion, IMD. Intermodulation describes the behavior of an amplifier when it is driven with two signals ("tones") that are generally close to each other in frequency. Second order IMD then creates undesired outputs at the sum and the difference frequencies. The *desired* output of a mixer is often a 2nd order IMD product between the RF and LO. Third order IMD from two tones at f_1 and f_2 generates products at $(2f_2-f_1)$ and $(2f_1-f_2)$. The *order* relates to the number of frequencies participating in a distortion process where $(2f_1-f_2)$ can be thought of as f_1 , f_1 , and f_2 . Order is also ambiguously related to the underlying mathematical description of the distortion.

Consider an example where two equal strength, -15 dBm tones at 14.0 and 14.2 MHz are applied to the amplifier of Fig 2.57. The desired outputs occur at the original frequencies at a level of +5 dBm, 20 dB above the drives. Also present are the third order IMD terms at 13.8 and 14.4 MHz. A sketch of the spectrum analyzer response is shown in Fig 2.59 with the analyzer set for a +10 dBm reference level at the top of the display. The distortion

Table 2.1 All powers are in dBm, dB with regard to one mW.

Drive Power	14 MHz	28 MHz	42 MHz	56 MHz
-20 dBm	+1 dBm	-51 dBm	-72 dBm	—
-10	+11	-30	-46	—
0	+18	+3	-7	-35 dBm
+5	+21	+11	0	-1

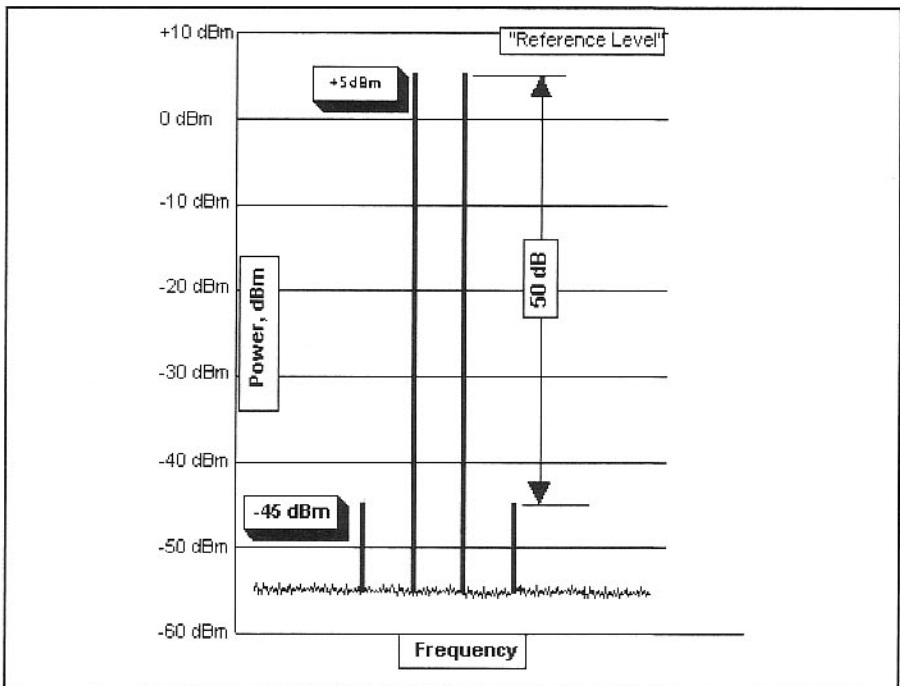


Fig 2.59—Spectrum from the feedback amplifier when driven with two tones. The smaller signals are third order intermodulation distortion. If this was the input to a receiver, all of these signals could be heard.

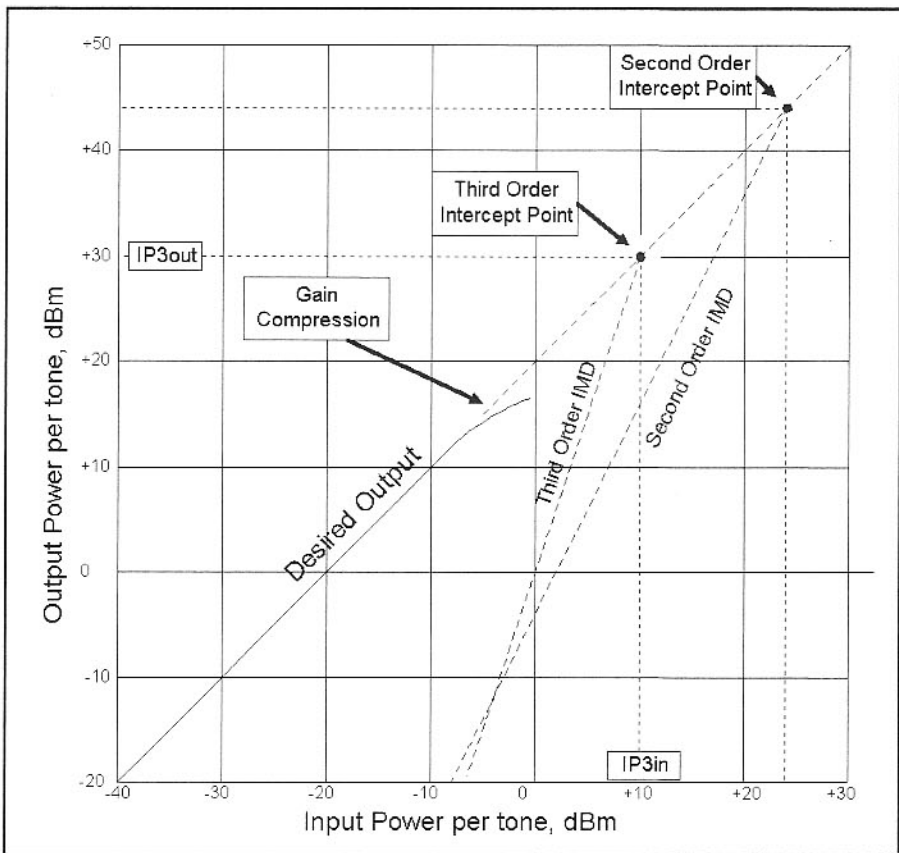


Fig 2.60—Plot of amplifier output vs input when two equal input tones are varied together. Both the desired output amplitude and the distortion product amplitudes are plotted, although only extrapolation distortion is shown. Gain compression is evident. The distortion products intersect the desired output at the intercept points.

outputs have a power of -45 dBm. The IMD products are said to be 50 dB below one of two equal desired output tones.

Transmitters are sometimes described by an IMD that is below the desired output by a specified amount. But, implicit in such a specification is transmitter operation at rated output power. There is rarely a “rated output” for amplifiers like this one.

Amplifier intermodulation distortion generally depends upon drive level. Increasing drive by 1 dB will cause third order IMD powers to increase by 3 dB. This was readily confirmed during the tests to obtain the data of Fig 2.59. Continuing this procedure allows us to plot both desired output power for each tone and distortion power for each IMD product. This plot is shown in Fig 2.60. The curves are “log-log” form, with both x and y axis in dBm. The “desired output” plot is a linear straight line (slope=1) until gain compression is encountered. The third order distortion plot is a straight line following a steeper path.

It is useful to extend the two curves, each being straight lines on the log-log plot, until they intersect. The point where the desired and the third order curves cross is called the *third-order intercept point* or sometimes just the *intercept point*. There are two power values (input and output) associated with this point, with the values differing by the small signal amplifier gain. These values are very useful as a Figure-of-merit for the amplifier. The higher the *third order output intercept*, IP_{3out} , the more immune that amplifier is to distortion problems. We sometimes see this called OIP₃, with the “O” indicating that the number relates to the output. IIP₃ is also popular to indicate *third order input intercept*. OIP₃ and IIP₃ differ by the stage gain.

Note that the intercept is mathematical; it is usually impossible to operate an amplifier with an output power as high as the output intercept. The amplifier intercept, IP_{3out} or OIP₃, is more than a mere figure of merit. If the operating output powers are known and if IP_{3out} is specified, the distortion can then be calculated with

$$IMDR = 2 \cdot (IP_{3out} - P_{out}) \quad \text{Eq 2.38}$$

where IMDR is the *IMD Ratio* in dB, the difference between the desired signal and the distortion; IP_{3out} is the output intercept in dBm; and P_{out} is the output power in dBm. Both powers are “per tone,” one of two identical values. For example, our test amplifier has $IP_{3out} = +30$ dBm. If we drive the amplifier with two tones to an output of -7 dBm per tone, the IMD ratio is

74 dB, leaving the output distortion products at -81 dBm.

It is not necessary to actually draw the plot of Fig 2.60 to obtain the intercept. Rather, it can be inferred from a single distortion measurement with Eq 2.38; this is the usual practice.

Intercepts have another very important use. If the output intercepts of all stages in a cascade are known, a composite intercept can be calculated for the cascade. Consider the two-stage amplifier of Fig 2.61. Each stage has a gain of 12 dB, but the second stage has lower IMD than the first. The intercepts of each stage can be *normalized* to any desired point in the cascade. Picking the overall amplifier input as that point, the first stage ($IP_3out = +15$ dBm) has $IP_{3in} = +3$ dBm, while the second stage has an intercept at the cascade input of $IP_{3cin} = -4$ dBm, 24 dB below that stage's output intercept. The second stage will dominate distortion, which becomes clear when they are compared at a single normalized plane within the chain. We can calculate the input intercept of the cascade with

$$IP_3(mW) = \left(\frac{1}{IP_{3A}(mW)} + \frac{1}{IP_{3B}(mW)} \right)^{-1}$$

Eq 2.39

where all powers are now mW rather than

dBm. (See section 2.5 for the conversion.) Once we have the cascade input intercept, it can be moved to the output by adding the gain of the cascade. Eq 2.39, derived in *Introduction To Radio Frequency Design*,⁵ describes coherent voltage addition of third order distortion products, so it represents a worst case. We have experimentally observed that this worst-case behavior is usually realistic.

Fig 2.60 also includes second order IMD. A second order intercept point, and values for IP_{2in} and IP_{2out} are defined in the same way as those of the third order ones. If inputs occur at f_1 and f_2 , second order IMD occurs at frequencies

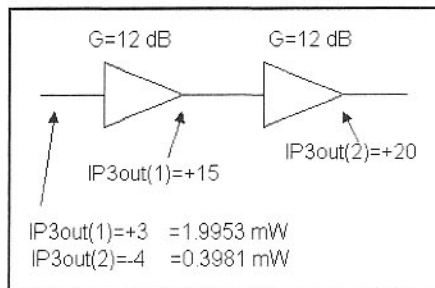


Fig 2.61—A cascade of two amplifiers, each well specified for gain and output intercept. The composite intercept is easily calculated. An extension of this allows an entire system to be analyzed for IMD.

(f_1+f_2) and (f_1-f_2) . These distortion frequencies are usually far removed from the inputs. Hence, they can be removed with a filter following the amplifier. This is not possible with third order products very close to the frequencies causing the distortion.

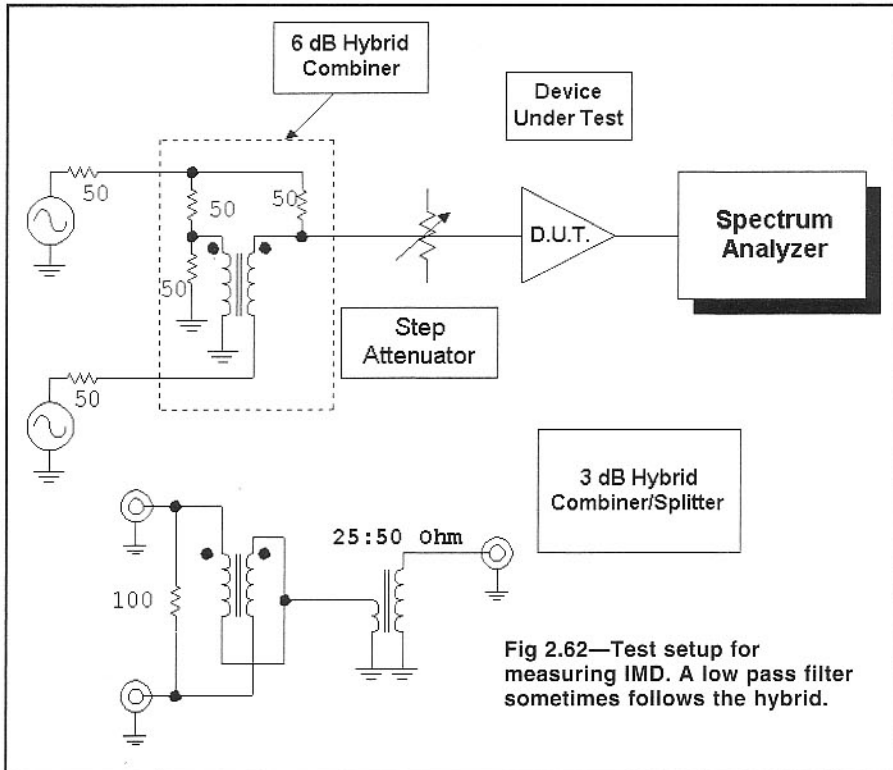
The test amplifier was found to have a second order output intercept of +44 dBm. Second order intercepts are generally numerically higher than the third order ones, although the second order distortion does not drop as quickly. Second order IMD can be a major difficulty in wide band designs, such as general coverage receivers or spectrum analyzers.

It is interesting to compare the 1 dB compression power with output intercepts. Our test amplifier had $P_{out}(-1\text{ dB})=+16.5$ dBm and $IP_{3out}=+30$ dBm, a difference of 13.5 dB. Differences of 13 to 16 dB are common for amplifiers with bipolar transistors. Smaller values (7 to 10 dB) are more common with silicon JFETs and with GaAsFETs. The difference is *not* intended to be a Figure-of-merit. Indeed, *smaller* numbers indicate that a device can be operated closer to its intercept. Typically any of the devices we commonly use for amplifiers cannot operate at powers as high as their output intercepts.

A test set used to measure 2nd and 3rd order intercepts is shown in Fig 2.62. The key to the scheme is the hybrid combiner that adds the output of two signal generators while preserving impedance match and isolating the two generators. A 6-dB hybrid is the preferred scheme owing to the excellent isolation afforded. But a 3-dB hybrid can be substituted if good quality signal generators are used. A 6-dB hybrid is a network with an output that is 6 dB lower per tone than each input. Note that the 6-dB hybrid has the same schematic as a return loss bridge. Hence, one instrument can be used to measure impedance match and to isolate signal sources. Every home lab needs at least one hybrid combiner.

The intercept formalization is generally restricted to circuits with constant, or nearly constant, bias current. A Class AB or B amplifier where current grows with applied drive is not generally described by an intercept. Rather, it is characterized with a simple IMD ratio, usually at full power output.

Further information on distortion and noise is found in *Introduction to Radio Frequency Design*.⁶ The reader is also referred to Bill Sabin's presentation in the 1995 (and later) *ARRL Handbook*⁷ concerning distortion, including that of 2nd order IMD.



2.7 FEEDBACK AMPLIFIERS

A circuit form appearing often in this book is the feedback amplifier. This is a circuit with two forms of negative feedback with (usually) a single transistor to obtain wide bandwidth, well controlled gain, and well controlled, stable input and output resistances. Several of these amplifiers can be cascaded to form a high gain circuit that is both stable and predictable.

The small-signal schematic for the feedback amplifier is shown in Fig 2.63 without bias components or power supply details. The design begins with a NPN transistor biased to a stable dc current. Gain is reduced with emitter degeneration, increasing input resistance while decreasing gain. Additional feedback is then added with a parallel feedback resistor, R_f , between the

collector and base. This is much like the resistor between an op-amp output and the inverting input which reduces gain and *decreases* input resistance.

Several additional circuits are presented showing practical forms of the feedback amplifier. That in Fig 2.64 shows a complete circuit. The base is biased with a resistive divider from the collector. However, much of the resistor is bypassed, leaving only R_f active for actual signal feedback. Emitter degeneration is ac coupled to the emitter. The resistor R_E dominates the degeneration since R_E is normally much smaller than the emitter

bias resistor. Components that are predominantly used for biasing are marked with "B." This amplifier would normally be terminated in $50\ \Omega$ at both the input and output. The transformer has the effect of making the $50\ \Omega$ load "look like" a larger load value, $R_L=200\ \Omega$ to the collector. This is a common and useful value for many HF applications.

Fig 2.65 differs from Fig 2.64 in two places. First, the collector is biased through an RFC instead of a transformer. The collector circuit then "sees" $50\ \Omega$ when that load is connected. Second, the emitter degeneration is in series with the bias, instead of the earlier parallel connection. Either scheme works well, although the parallel configuration affords experimental flexibility with isolation between setting degeneration and biasing. Amplifiers without an output transformer are not constrained by degraded transformer performance and often offer flat gain to several GHz.

The variation of Fig 2.66 may well be the most general. It uses an arbitrary transformer to match the collector. Biasing is traditional and does not interact with the feedback.

Feedback is obtained directly from the output tap in the circuit of Fig 2.67. While this scheme is common, it is less desirable than the others, for the transformer is part of the feedback loop. This could lead to instabilities. Normally, the parallel feedback tends to stabilize the amplifiers. The equations and curves presented below pertain to circuits with feedback taken directly from the collector.

The circuit of Fig 2.68 has several fea-

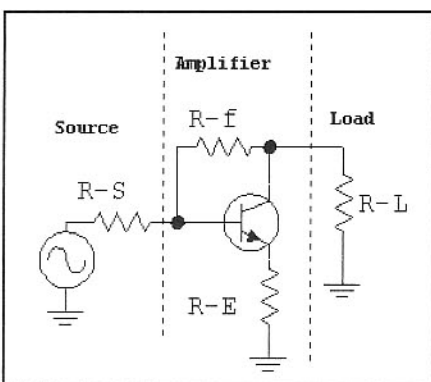


Fig 2.63—Small signal circuit for a feedback amplifier.

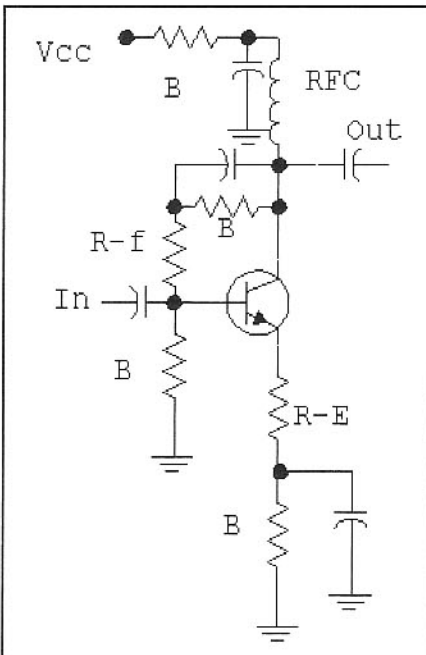


Fig 2.65—A variation of the feedback amplifier with a $50\ \Omega$ output termination at the collector.

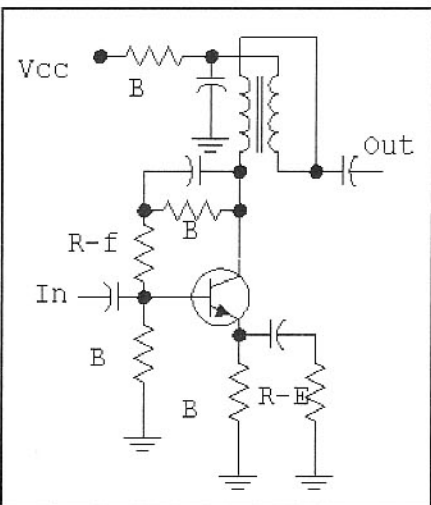


Fig 2.64—A practical feedback amplifier. Components marked with "B" are predominantly for biasing. The $50\ \Omega$ output termination is transformed to $200\ \Omega$ at the collector. A typical transformer is 10 bifilar turns of #28 on a FT-37-43 ferrite toroid. The inductance of one of the two windings should have a reactance of around $250\ \Omega$ at the lowest frequency of operation.

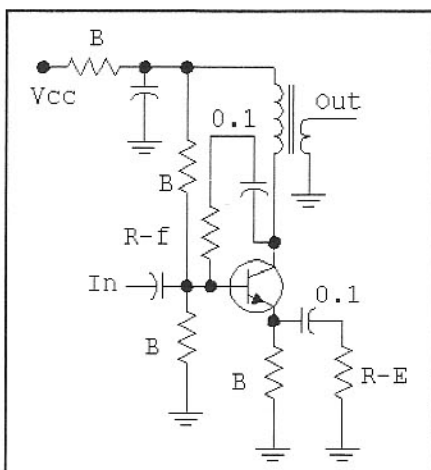


Fig 2.66—This form uses an arbitrary transformer. Feedback is isolated from bias components.

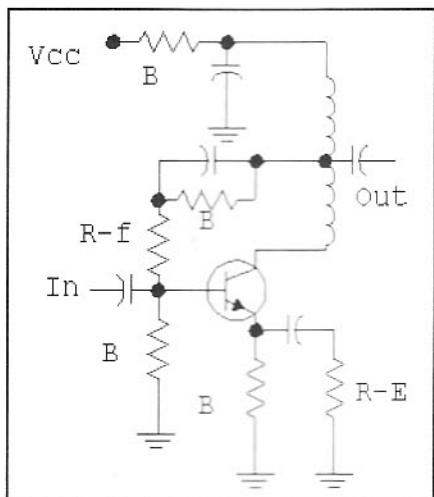


Fig 2.67—A feedback amplifier with feedback from the output transformer tap. This is common, but can produce unstable results.

tures. Two transistors are used, each with a separate emitter biasing resistor. However, ac coupling causes the pair to operate as a single device with degeneration set by R_E . The parallel feedback resistor, R_f , is both a signal feedback element and part of the bias divider. This constrains the values slightly. Finally, an arbitrary output load can be presented to the composite collector through a π -type matching network. This provides some low pass filtering, but constrains the amplifier bandwidth.

Design Procedure

Design begins by picking a bias current, usually dictated by output power and IMD requirements. Next the output load impedance presented to the collector (or drain) is chosen. A value of $200\ \Omega$ is probably the most common, for it affords good gain with reasonable current. With that load, the output power will be restricted to around 200 mW in 12-volt systems. Progressively lower impedances will allow higher output power. Most feedback amplifiers end up being designed for $50\ \Omega$ input resistance.

The emitter degeneration and feedback

resistors are chosen next. A reasonable input and output impedance match occurs with

$$R_f \cdot R_e = R_s \cdot R_L \quad \text{Eq 2.40}$$

where R_f is the parallel feedback and R_e is the net degeneration resistance, $r_e + R_E$. Here R_E is the external degeneration, and r_e is the current dependant value, $26/I_e(\text{mA})$. For example, an amplifier driven by $50\ \Omega$ and terminated in $200\ \Omega$ might use $10\ \Omega$ external degeneration and 10-mA current for $R_e = 12.7\ \Omega$. $R_f = 787\ \Omega$ would produce $R_{in} \approx R_s$ and $R_o \approx R_L$, with R_{in} and R_o being the input and output resistances for source and load R_s and R_L . A practical choice would be $R_f = 820\ \Omega$, a standard value.

There is still a wide range of values that can be used for degeneration and feedback. The final choice is made on the basis of desired gain, which can be determined by the equations presented in Fig 2.69. The choice is eased by example data in Table 2.2. While the data in the table is for one current, 20 mA, it will provide an initial estimate.

The equations of Fig 2.69 appear long and messy, but are easily programmed for a calculator or computer.

Fig 2.70 shows the gain obtained when

Table 2.2

Simulated Gain vs Degeneration and Feedback Resistors for a 2N3904 biased with $I_e=20\ \text{mA}$ where $r_e=1.3\ \Omega$. Gain was calculated at 14 MHz, so $\beta=300/14=21$. Resistors were picked as standard values and to provide an input return loss better than 10 dB. The first example is the amplifier described in the previous section.

Load	R-degen	R-feedback	Gain
200 Ω	6 Ω	1.3 k Ω	20.3 dB
	3.9 Ω	3 k Ω	24.8 dB
	4.7 Ω	2.7 k Ω	23.9 dB
	5.6 Ω	2 k Ω	22.3 dB
	6.8 Ω	1.6 k Ω	20.7 dB
	10 Ω	910 Ω	16.8 dB
	12 Ω	750 Ω	15.1 dB
	15 Ω	560 Ω	12.6 dB
	18 Ω	430 Ω	10.3 dB
	22 Ω	330 Ω	7.7 dB
50 Ω	2.7 Ω	820 Ω	20.0 dB
	3.9 Ω	680 Ω	18.2 dB
	4.7 Ω	560 Ω	16.9 dB
	5.6 Ω	470 Ω	15.6 dB
	6.8 Ω	390 Ω	14.1 dB
	10 Ω	270 Ω	10.7 dB
	12 Ω	220 Ω	8.8 dB
	15 Ω	150 Ω	5.4 dB

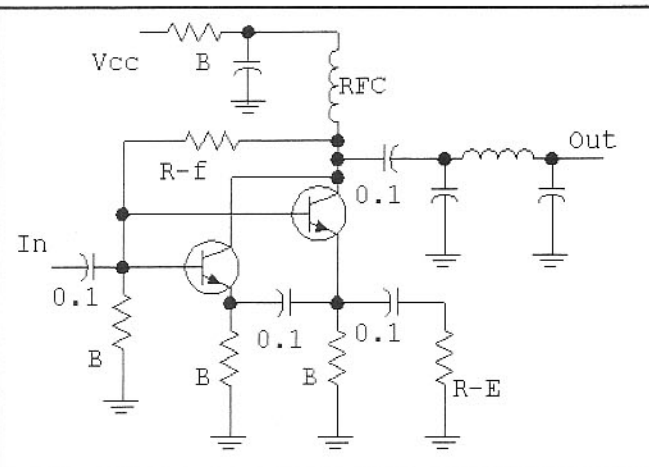


Fig 2.68—Feedback amplifier with two parallel transistors.

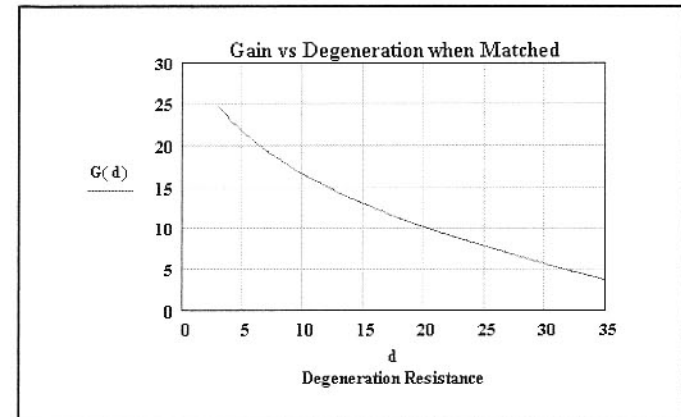


Fig 2.70—Gain Vs net degeneration resistance when the amplifier is matched. This evaluation occurred at 14 MHz with a 2N3904 biased to 20 mA with a 50- Ω source and 200- Ω load.

$$G := 10 \log \left[4 \cdot R_L \cdot R_s \cdot \frac{\left[(\beta + 1)^2 R_e^2 - 2\beta R_f (\beta + 1) \cdot R_e \right] + \beta^2 R_f^2}{\left[[(1 + \beta) \cdot R_e + R_s] \cdot R_f + (R_L + R_s + \beta \cdot R_s + \beta \cdot R_L) \cdot R_e + \beta \cdot R_s \cdot R_L + R_L \cdot R_s \right]^2} \right]$$

$$R_{in} := (1 + \beta) \cdot (R_f + R_L) \cdot \frac{R_e}{(1 + \beta) R_e + \beta \cdot R_L + R_L + R_f} \quad R_o := \frac{\left[[(1 + \beta) \cdot (R_f + R_s)] \cdot R_e + R_s \cdot R_f \right]}{(1 + \beta) R_e + R_s + \beta \cdot R_s}$$

Fig 2.69—Transducer Gain G in dB, Input resistance, R_{in} , and Output resistance, R_o , both in Ohms for a feedback amplifier. The analysis is restricted to the case where parallel feedback is obtained from the collector. R_f is the parallel feedback and R_e is the total emitter degeneration (see text.) R_s and R_L are the source and load resistances, and are arbitrary for this analysis. β is the current gain and is approximated as a scalar value, $\beta=F_t/F$ where F_t is the current gain-bandwidth product and F is the operating frequency, both in MHz.

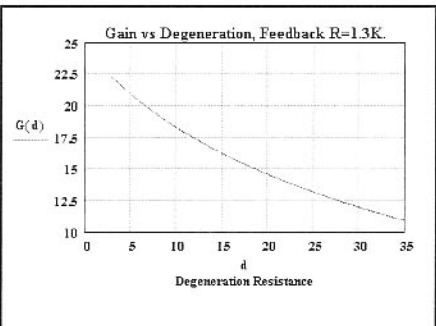


Fig 2.71—Gain Vs degeneration for fixed feedback R of 1.3 k Ω .

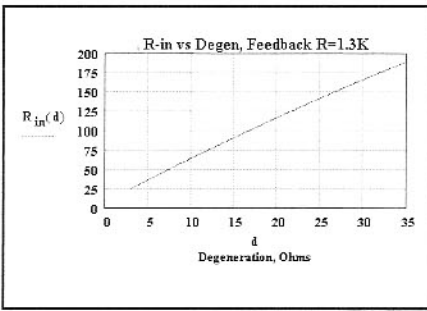


Fig 2.72—Input resistance Vs degeneration for fixed feedback resistance.

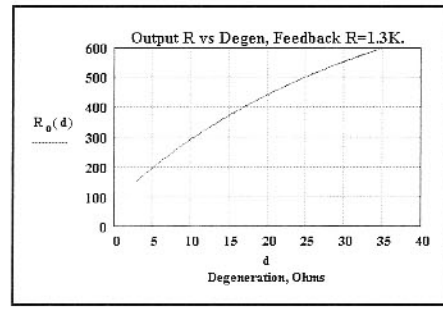


Fig 2.73—Output resistance Vs degeneration for a fixed 1.3-k Ω feedback resistance.

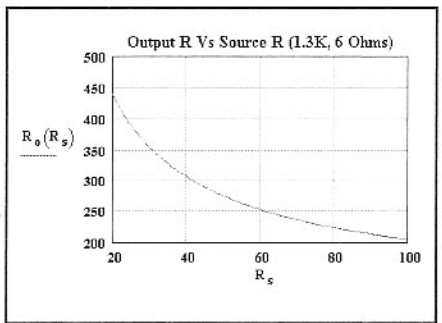


Fig 2.74—Output resistance depends on the source resistance.

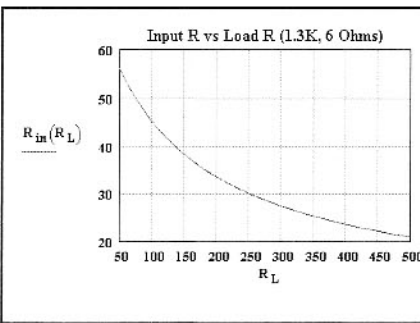


Fig 2.75—Input resistance as a function of load resistance.

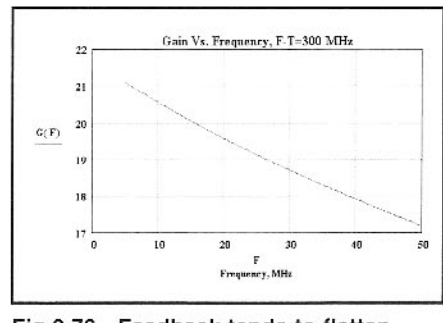


Fig 2.76—Feedback tends to flatten frequency response. This is even more dramatic with lower gain amplifiers.

Eq 2.40 is applied, forcing a reasonable input and output impedance match.

It is common to build an amplifier only to then find that the gain must be changed a little. The effect of changing the emitter resistor is presented in Fig 2.71 for a fixed $R_f=1.3$ k Ω . The same 14-MHz, 20-mA bias case is assumed. Fig 2.72 and Fig 2.73 show the related effect on terminal resistances.

A characteristic of feedback amplifiers (sometimes useful, sometimes frustrating) is that they are partially *transparent*. The input resistance becomes a strong function of the load while the output resistance depends upon the source. This is illustrated in Fig 2.74 and Fig 2.75. Again, a 1.3-k Ω feedback R and 6- Ω external degeneration are used. The amplifier transparency is partially “fixed” with the addition of an attenuator at the amplifier output, especially useful when the amplifier must interface with filters and switching-mode mixers. Pads must be added with care, for they will decrease overall gain, available output power and output intercept.

Feedback extends the bandwidth of transformer terminated amplifiers. Fig 2.76 shows gain vs F for the example amplifier with a 2N3904 at 20 mA, 6- Ω degeneration and 1.3-k Ω R_f , 50- Ω source and 200- Ω load. There is less than a 3-dB variation over the HF spectrum, and the amp is usable up to 50 MHz, even with a modest 2N3904. Higher F_t transistors can produce much greater bandwidth, especially when configured for low or modest gain without any transformers that might compromise frequency response.

While we usually think in terms of building feedback amplifiers with bipolar transistors, they are just as tenable with FETs. Fig 2.77 shows a JFET version of the amplifier. This circuit uses no degeneration resistor. The FET is self-biased with a bypassed source resistor, and the biased FET transconductance is calculated using equations presented earlier. Having this value, we can then ask “what current (r_e) in a bipolar transistor would produce the same transconductance?” Finding that value, we then use the same equations for analysis that were applied to the bipolar, Fig 2.69.

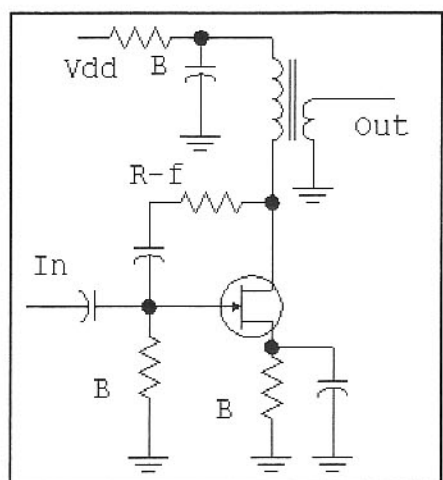


Fig 2.77—A feedback amplifier using a FET. See text for design details.

Feedback amplifier noise figure is usually greater than that from the same transistor without feedback. Noise available from the feedback resistors is injected into the circuit. A feedback amplifier was built

using a 2SC1252 transistor ($F_t \approx 2$ GHz) with degeneration and feedback resistors of $5.1\ \Omega$ and $1.8\ k\Omega$. Noise figure was measured with an HP8970B test set for differing standing currents. The noise figure was 1.8 dB in the HF spectrum for $I_c=10\text{ mA}$, increasing to 3.3 dB with 63 mA . Noise figure for the 2N3904 example amplifier featured in this section (20 mA , $6\ \Omega$ and $1.3\ k\Omega$, $200\text{-}\Omega$ load) was measured at 6 dB.

Fig 2.78 shows a feedback amplifier with two transistors in a Darlington configuration. This circuit is typical of several popular silicon monolithic integrated circuit amplifiers that are presently available. Those components within the dotted line are part of the IC. Q1 and Q2 usually have F_t above 5 GHz, so the amplifiers offer useful performance to 2 GHz and beyond with gain from 10 to nearly 20 dB.

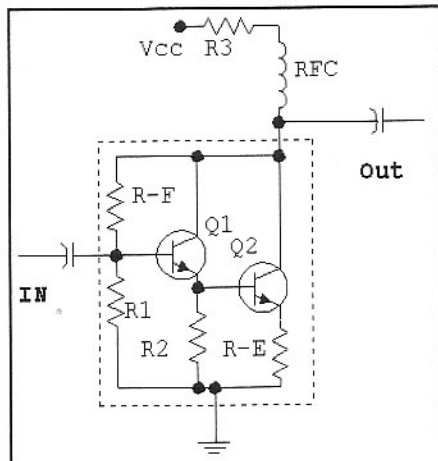


Fig 2.78—Feedback amplifier with a Darlington connection of transistors.

These amplifiers are specified by their distributor for a voltage on the output pin with a specified current allowing the user to pick R_3 for an available V_{cc} . For example, the Minicircuits MAR-2 is specified for 25 mA at 5 V. Hence, for a 12-V power supply, $280\ \Omega$ would be needed for R_3 . This IC should not be used without a dropping resistor. The power dissipation in the resistor should be checked. It's only 175 mW in this example, so a $\frac{1}{4}\text{-W}$ resistor would suffice.

Fig 2.79 presents another two discrete transistor feedback amplifier. This is a buffer amplifier designed by W7EL. This circuit is similar to MAR circuits parts, but uses transformer output coupling for even

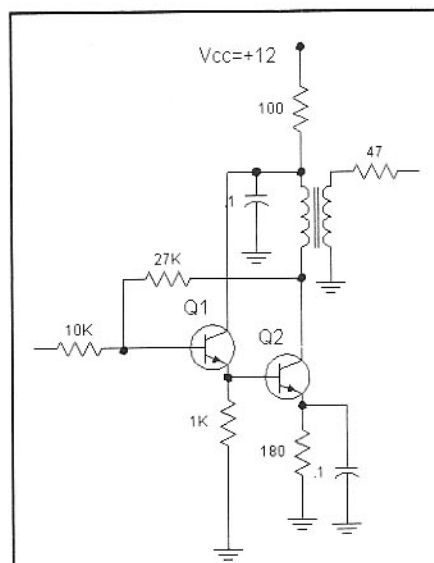


Fig 2.79—Feedback amplifier, the design of W7EL, often used as an oscillator buffer.

greater available gain. The input resistor should be driven from a source at DC ground. Bandwidth depends on the output transformer with severe distortion possible at low frequencies if it does not have adequate reactance. A typical 7-MHz application uses a 20-turn primary on a FT-37-43 toroid with a 5-turn output link.

A common base amplifier with transformer output coupling is shown in **Fig 2.80**. This circuit uses no feedback other than the $47\text{-}\Omega$ degeneration. This is presented as an evolutionary step toward a feedback amplifier, but it is very useful as shown. The common base topology features excellent reverse isolation, and, as such, it is an excellent VFO buffer. The amplifier is biased to about 4 mA collector current, so has an input resistance at the emitter of $6.5\ \Omega$. Adding a series $47\text{-}\Omega$ resistor creates a reasonable input match to a $50\text{-}\Omega$ source. The power gain will be determined by the ratio of turns on the output auto-transformer.

An interesting variation of this circuit is presented in **Fig 2.81**. The $47\text{-}\Omega$ input resistor has been replaced by a single turn link through the transformer core. The operation is easily understood if we think of driving the input with a current source. The low input impedance at the emitter has no impact on the current flowing. Essentially the same current flows in the collector (recall that the current gain of a common base amplifier is unity), but it now flows in the high impedance multiple turn transformer windings. This allows the circuit to provide power gain. We now "sample" the collector current with a winding, creating a voltage across the winding. The new "voltage" is placed in series with the low emitter input imped-

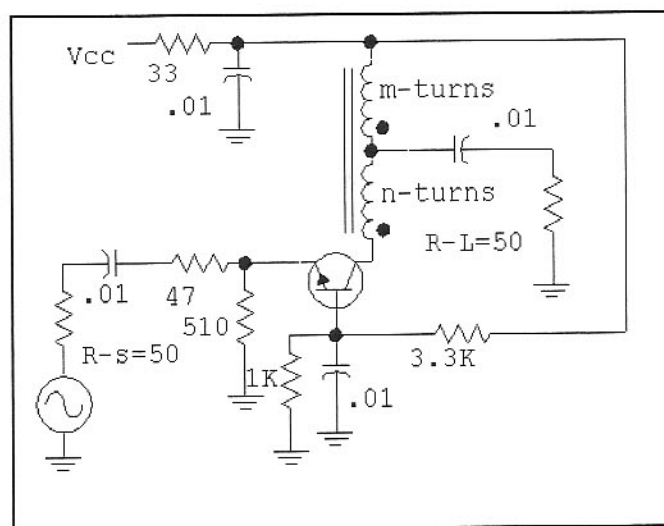


Fig 2.80—Common base amplifier with an input resistance. See text.

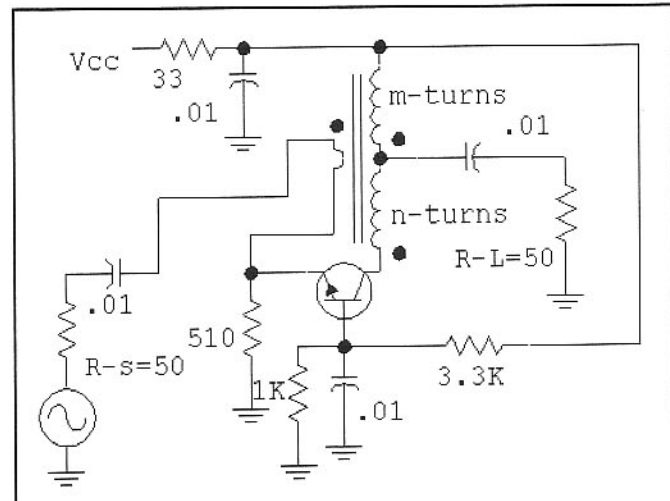


Fig 2.81—A transformer feedback amplifier designed by D. Norton of Anzac.

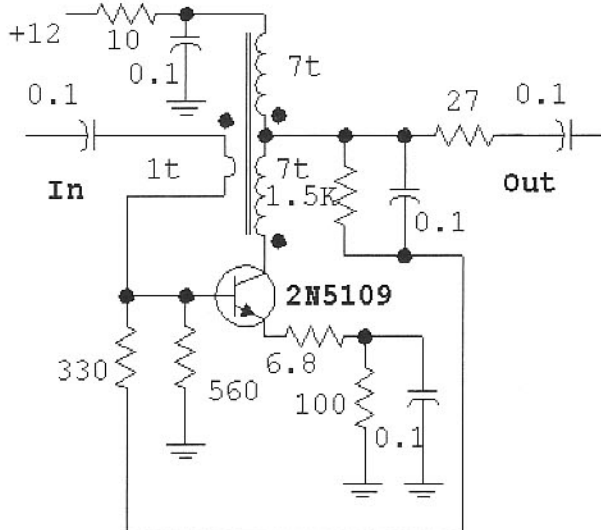


Fig 2.82—A modified feedback amplifier where transformer feedback increases input impedance.

ance to create a 50- Ω input termination. However, this is done without any resistors, so the noise figure is not compromised. This amplifier is the brainchild of David Norton of Anzac.⁸

The Fig 2.81 amplifier will be matched if

$$n = m^2 - m - 1 \quad \text{Eq 2.41}$$

to produce a transducer power gain of $20\log(m)$ dB. For example, if $m=3$, n is then 5, and the power gain is 9.5 dB. The transformers for these amplifiers are often wound on a binocular-type balun core. A turn through such a ferrite core is counted as a single pass of wire through *both* holes. Polarity is vital to construction of the transformer. If wound wrong, the input impedance will be negative, almost guaranteed to create oscillation. In amplifiers of this kind that we have built, we measured excellent input impedance match

(25-dB return loss) over a 5 to 100 MHz range with noise figure under 2 dB. This amplifier, however, suffers from a major problem; the terminal impedances depend strongly on the termination at the other port. The circuit is worse than resistive feedback amplifiers in this regard.

Transformers can be further applied to extend performance of amplifiers. Fig 2.82 shows a generally traditional feedback amplifier that is modified by passing the input lead through the transformer core to alter input impedance. This topology is early work of Rohde.⁹

Fig 2.83 shows a FET amplifier (small signal circuit only) using an input transformer. A tapped transformer feeds signal to both the FET source and the gate. The winding driving the source sees a low impedance, so adjustment of turns ratio can ensure a perfect match. The gate winding, even though there is no signal current flow-

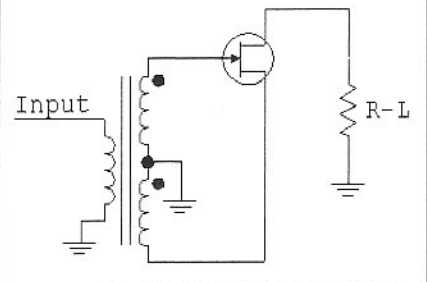


Fig 2.83—Small signal circuit of a transformer type feedback amplifier using a JFET.

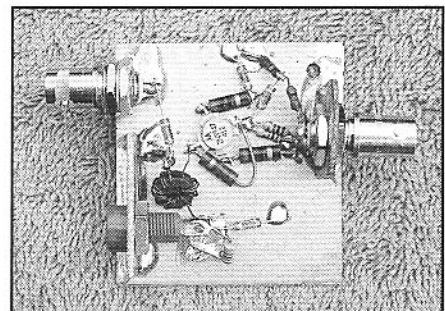


Fig 2.84—A feedback amplifier example. This circuit supplements test equipment. With $V_{cc}=12$, $I_c=65$ mA and $OIP3=+42$ dBm, Gain=16 dB, and bandwidth exceeds 50 MHz.

ing, provides the gate voltage needed for gain and low noise performance. Design details are given in *Introduction to Radio Frequency Design*, p 216.¹⁰ Bill Carver, W7AAZ, has built practical versions of this amplifier. See *QST*, May, 1996,¹¹ with further discussion in Chapter 6.

Transformer feedback amplifier design is a subject that continues to produce design activity. The reader can find more information starting with papers by Trask^{12,13} and Koren.¹⁴

Fig 2.84 shows an example of a feedback amplifier.

2.8 BYPASSING AND DECOUPLING

Our amplifier designs have included grounded points that were not really at ground. Rather, those points are “signal grounded” through bypass capacitors. Obtaining an effective bypass can be difficult and is often the route to design difficulty.

The problem is parasitic inductance. Although we label and model parts as “capacitors,” a more complete model is needed. The better model is a series LRC, shown in Fig 2.85. Capacitance is close to

the marked value while inductance is a small value that grows with component lead length. Resistance is a loss term, usually controlled by the Q of the parasitic inductor. All components show some inductance, including a wire. Even a leadless SMT component will display inductance commensurate with the dimensions. A wire has an inductance of about 1 nH per mm of length.

Bypass capacitor characteristics can be measured in the home lab with the test

setup of Fig 2.86. Fig 2.87 shows a test fixture with an installed 470-pF leaded capacitor. The fixture is used with a signal generator and spectrum analyzer to evaluate capacitors. Relatively long capacitor leads were required to interface to the BNC connectors, even though the capacitor itself was small. The signal generator was tuned over its range while examining the spectrum analyzer response, which was minimum at the series resonant frequency. Parasitic inductance is calculated from this

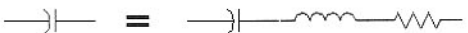


Fig 2.85—Model for a bypass capacitor.

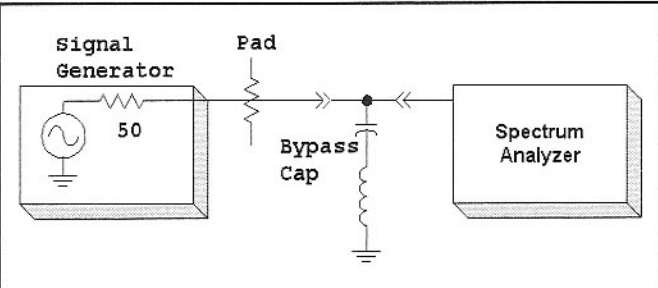


Fig 2.86—Test set for home lab measurement of a bypass capacitor.

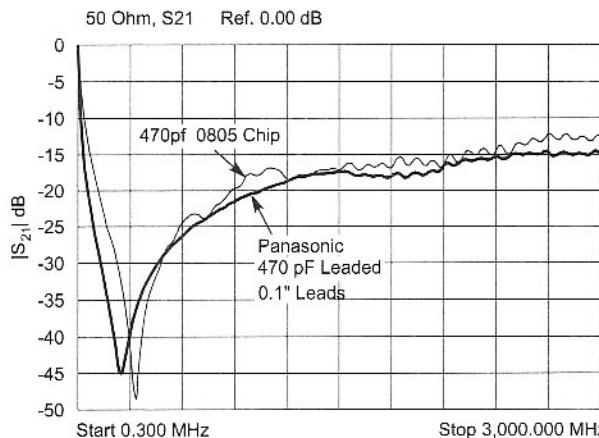


Fig 2.88—Network analyzer measurement of 470-pF shunt capacitors. Both SMT and leaded parts are studied.

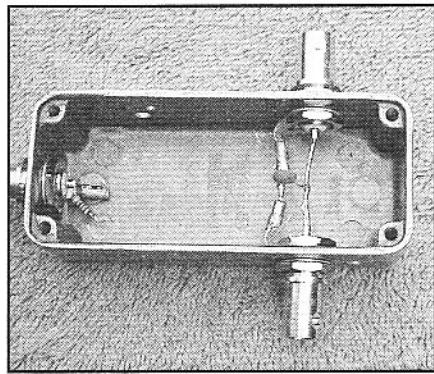


Fig 2.87—Test fixture for measuring self resonant frequency of capacitors.

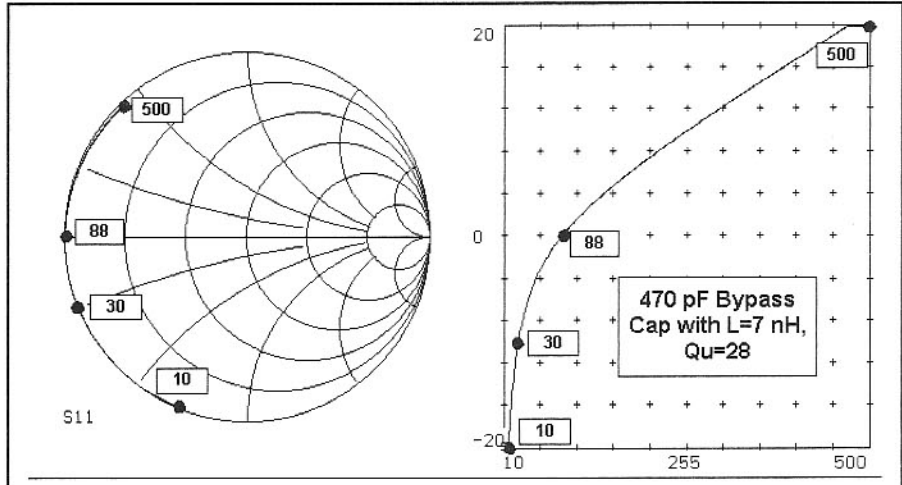


Fig 2.89—Impedance of a 470-pF bypass capacitor.

frequency. The C value was measured with a low frequency LC meter. Measurement gear is discussed in Chapter 7.

The measured 470-pF capacitor is modeled as 485 pF in series with an inductance of 7.7 nH. The L is larger than we would see with shorter leads. A 0.25-inch 470-pF ceramic disk capacitor with zero lead length will show a typical inductance closer to 3 nH. The measured capacitor Q was 28 at self-resonance of 82 MHz but is higher at lower frequency.

Data from a similar measurement, but with a network analyzer is shown in Fig 2.88. Two 470-pF capacitors are measured, one surface mounted and the other a lead part with 0.1-inch leads.

Fig 2.89 shows two calculated plots for the 470-pF capacitor. The one on the left is a Smith Chart showing the behavior vs. frequency, while that on the right is a plot of component reactance vs. frequency. Reac-

tance dominates, keeping the data on the edge of the Smith Chart, for the Q is moderate at 28. Bypassing is “perfect” at only one frequency, that of series resonance. An ideal (no inductance) capacitor would have a capacitive reactance of about 2Ω at 150 MHz. The actual 150-MHz value is inductive with a magnitude of about 5Ω .

Traditional lore tells us that the bandwidth for bypassing can be extended by paralleling a capacitor that works well at one frequency with another to accommodate a different part of the spectrum. Hence, paralleling the 470 pF with a $.01\text{-}\mu\text{F}$ capacitor should extend the bypassing to lower frequencies. The calculations are shown in the plots of Fig 2.90. The results are terrible! While the low frequency bypassing is indeed improved, a high impedance response is created at 63 MHz. This complicated behavior is again the result of inductance.

Each capacitor was assumed to have a series inductance of 7 nH. A parallel resonance is approximately formed between the L of the larger capacitor and the C of the smaller. The Smith Chart plot shows us that the impedance is nearly 50 Ω at 63 MHz. Impedance would be even higher with greater capacitor Q. This behavior is a dramatic example of lore that is generally wrong!

Bypassing can be improved by paralleling. However, the capacitors should be approximately identical. Fig 2.91 shows the result of paralleling two capacitors of about the same value. They differ slightly at 390 and 560 pF, creating a hint of resonance. This appears as a small “bubble” in the reactance plot and a tiny loop on the Smith Chart. These anomalies disappear as the C values become equal. Generally, paralleling is the scheme that produces the best bypassing. The ideal solution is to

place a chip cap on each side of a printed circuit run or wire at a point that is to be bypassed.

Additional capacitors were measured. A .01- μF disk (leaded, 50-V, 0.2-inch diameter) was resonant at 20 MHz in the test fixture shown, indicating an inductance of 6.5 nH. The Q was 5.7. Two different 0.1- μF leaded capacitors were investigated. Both had identical capacitance even though one was larger than the other. The inductance was about 4.5 nH with Q=5 for both.

Matched capacitor pairs form an effective bypass over a reasonable frequency range. Two of the .01- μF disks have a reactance magnitude less than 5 Ω from 2 to 265 MHz. A pair of the 0.1- μF capacitors was even better, producing the same bypassing impedance from 0.2 to 318 MHz. The 0.1- μF capacitors are chip components with attached wire leads. Even better results can be obtained with multi-layer ceramic chip capacitors. Construction with multiple layers creates an integrated paralleling. We have measured some 0.2- μF parts with an inductance of 2 nH. The multi-layer components are more expensive than the monolithic 0.1- μF parts investigated.

Some applications (e.g., IF amplifiers) require effective bypassing at even lower frequencies. Modern tantalum electrolytic capacitors are surprisingly effective through the RF spectrum while offering high enough C to be useful at audio. The parts should be evaluated for critical applications.

We have discussed the problem of bypassing, but have neglected the related problem of decoupling. The bypass capacitor usually serves a dual role, first creating the low impedance needed to generate a "signal" ground. It also becomes part of a decoupling low pass filter that passes dc while attenuating signals. The attenuation must function in both directions, suppressing information in the power supply that might reach an amplifier while keeping amplifier signals from reaching the power supply.

A low pass filter is formed with alternating series and parallel component connections. A parallel bypass is followed by a series impedance, ideally a resistor. Additional shunt elements can then be added, although this must be done with care. An inductor between shunt capacitors should have high inductance. It will resonate with the shunt capacitors to create high impedances just like those that came from parasitic L in the bypasses. This makes it desirable to have an inductance that is high enough that any resonance is below the band of interest. But series inductors have their own problems; they

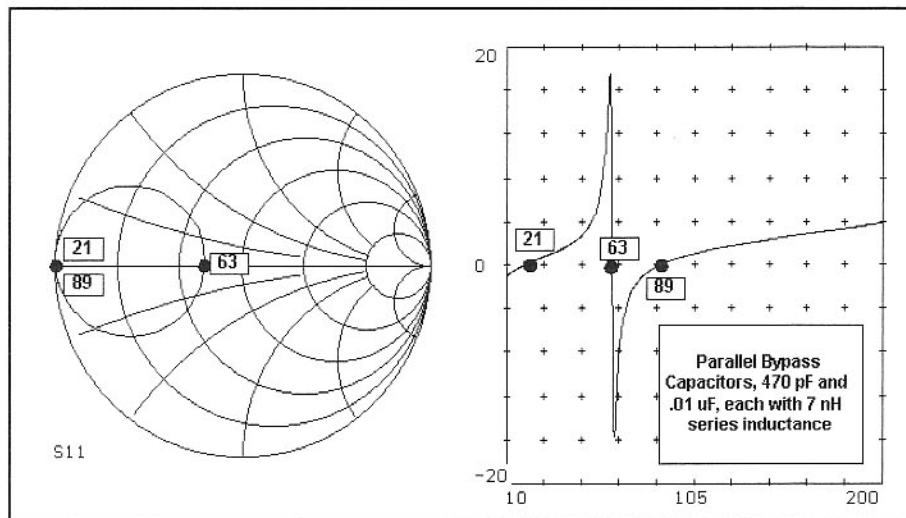


Fig 2.90—The classic technique of paralleling bypass capacitors of two values, here 470 pF and .01 μF . This is a terrible bypass! See text.

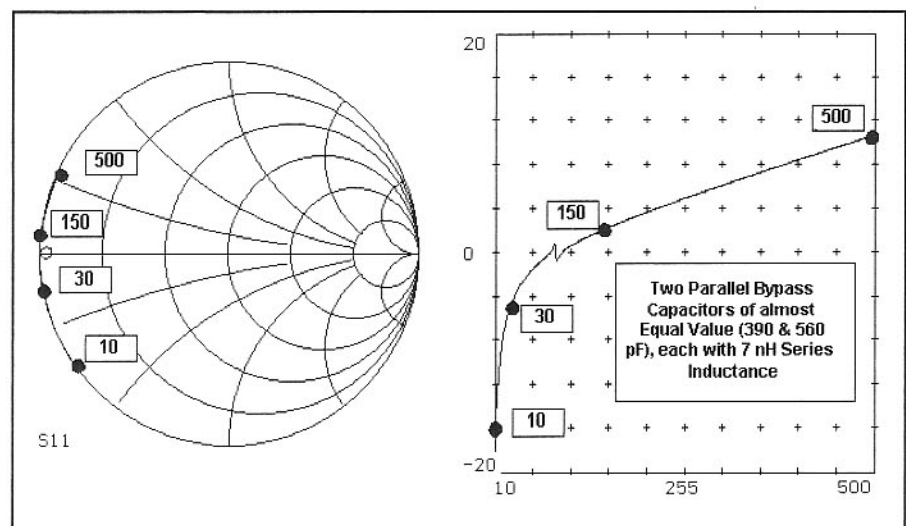


Fig 2.91—Paralleling bypass capacitors of nearly the same value. This results in improved bypassing without complicating resonances.

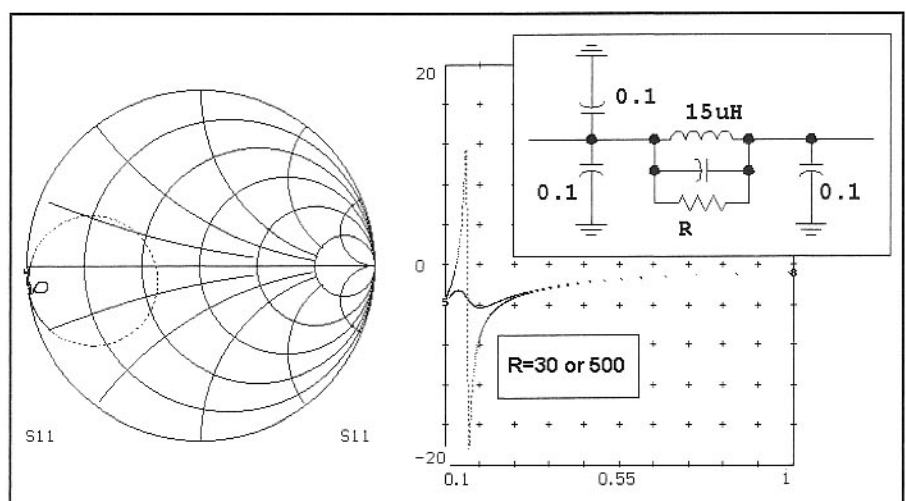


Fig 2.92—Two different resistor values parallel a decoupling choke. The lower, 30- Ω value is more effective. See text.

have parasitic capacitance that create their own self-resonance.

A couple of available RF chokes were measured (now as series elements) with the equipment described earlier. A 2.7- μ H molded choke was parallel resonant at 200 MHz, indicating a parallel capacitance of 0.24 pF. The Q at 20 MHz was 52. A 15- μ H molded choke was parallel resonant at 47 MHz, yielding a parallel C of 0.79 pF. This part had a Q of 44 at 8 MHz.

Large inductors can be fabricated from series connections of smaller ones. The best wideband performance will result only when all inductors in a chain have about the same value. The reasons for this (and the mathematics that describe the behavior) are identical with those for paralleling identical capacitors.

Low inductor Q is often useful, which encourages us to use inductors with ferrite cores. Inductors using the Fair-Rite

(Amidon) -43 material have Q in the 4 to 10 region in the HF spectrum. One can also create low Q circuits by paralleling a series L of modest Q with a resistor.

Fig 2.92 shows a decoupling network and the resulting impedance when viewed from the "bypass" end. The 15- μ H RFC resonates with a 0.1- μ F capacitor to destroy the bypass effect just above 0.1 MHz. A low value parallel resistor fixes the problem.

A major reason for careful wideband bypassing and decoupling is the potential for amplifier oscillation. Instability that allows oscillations is usually suppressed by low impedance terminations. The base and collector (or gate and drain) should both "see" low impedances to ensure stability. But that must be true at all frequencies where the device can produce gain. It is never enough to merely consider the operating frequency for the amplifier. A par-

allel resonance can be a disaster. When the ultimate bypassing is not possible, negative feedback that enhances wideband stability is often used.

Capacitors also appear in circuits as blocking elements. A blocking capacitor, for example, appears between stages, creating a near short circuit for signals while accommodating different dc voltages on the two sides. A blocking capacitor is not as critical as a bypass, for the impedances on either side will usually be higher than that of the block.

Emitter bypassing is often a critical application. As we have seen, a few Ohms of emitter degeneration can drastically alter amplifier performance. A parallel resonant emitter bypass could be a profound difficulty while a series resonant one can be especially effective. Clearly, detailed modeling is the answer to component selection.

2.9 POWER AMPLIFIER BASICS

The remainder of this chapter deals with power amplifiers, a subject dear to the radio experimenter. The earliest tinker among us cut our teeth on attempts to extract more power from the already stressed amplifier devices of the day. We all recall stories of 6L6 receiving vacuum tubes being coaxed into providing high output power by immersion in an oil bath. The rest of us have tried to extract power from transistors, only to see the device disappear "in smoke." Experience of this sort is a "right of passage" for all RF experimenters; don't miss it!

Classes of Amplifier Operation

Many of the amplifiers considered so far have been "Class A." The class of operation of an amplifier is determined by the fraction of a drive cycle, or duty cycle where conduction occurs. The Class A amplifier conducts for 100% of the cycle. It is characterized by constant supply current, regardless of the strength of the driving signal. Most of the amplifiers we use for RF applications and many audio circuits in receivers operate in Class A.

A Class B amplifier conducts for 50 % of the cycle, which is 180 degrees if we examine the circuit with regard to a driving sinewave. A Class B amplifier draws no DC current when no input signal is applied. But current begins to flow with any input, growing with the input strength.

A Class B amplifier can display good envelope linearity, meaning that the output amplitude at the drive frequency changes linearly with the input signal. The total absence of current flow for half of the drive cycle will create harmonics of the signal drive.

A Class C amplifier is one that conducts for less than half of a cycle. No current flows without drive. Application of a small drive produces no output and no current flow. Only after a threshold is reached does the device begin to conduct and provide output. A bipolar transistor with no source of bias for the base typically operates in Class C.

The large-signal models discussed earlier are suitable for the analysis of all amplifier classes. Small-signal models are generally reserved for Class A amplifiers.

The most common power amplifier class is a cross between Class A and B, the Class AB amplifier that conducts for more than half of each cycle. A Class AB amplifier at low drive levels is indistinguishable from a Class A design. However, increasing drive produces greater collector (or drain) current and greater output.

Amplifier class letter designators were augmented with a numeric subscript. A vacuum tube Class AB1 amplifier was one operating in AB, but with no grid current flowing. In the absence of grids, the numbers have disappeared.

While wide bandwidth Class A and Class B amplifiers are common, most cir-

cuits operating in Class C and higher are tuned at the output. The tuning accomplishes two things. First, it allows different terminations to exist for different frequencies. For example, a resistive load could be presented at the drive frequency while presenting a short circuit at some or all harmonics. The second consequence of tuning is that reactive loads can be created and presented to the amplifier collector or drain. This then provides independent control of current and voltage waveforms.

While not as common as A, B, and C, Class D and E amplifiers are of increasing interest. The Class D circuit is a balanced (two transistor) switching format where the input is driven hard enough to produce square wave collector waveforms. Class E amplifiers usually use a single device with output tuning that allows high current to flow in the device only when the impressed voltage is low.

Class A and AB amplifiers are capable of good envelope linearity, so they are the most common formats used in the output of SSB amplifiers. Class B and, predominantly, Class C amplifiers are used for CW and FM applications, but lack the envelope linearity needed for SSB. Recent work with a 4th method of SSB may change that, allowing distorting amplifiers to be used in SSB service.¹⁵

Efficiency varies considerably between amplifier class. The Class A amplifier can reach a collector efficiency of 50%, but no higher, with much lower values being

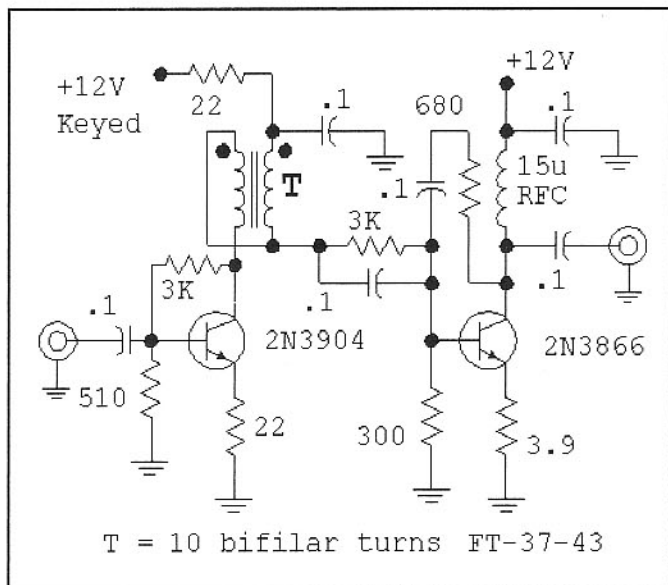


Fig 2.93—Class AB amplifier chain.

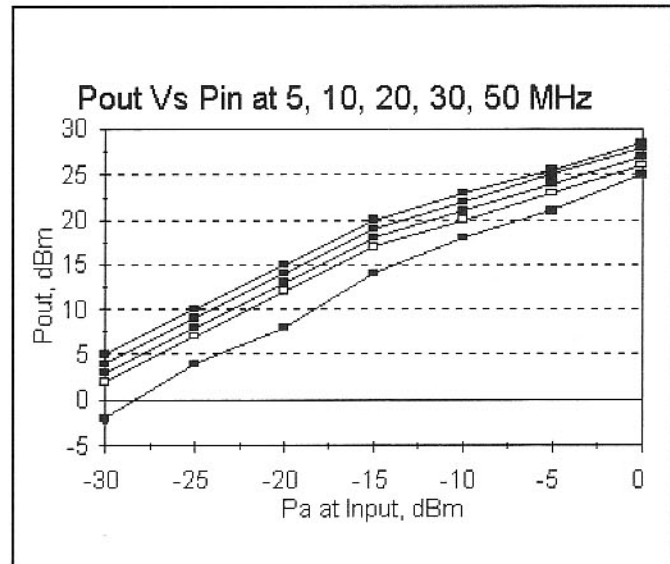


Fig 2.94—Gain compression characteristics for the simple power chain.

typical. Class AB amplifiers are capable of higher efficiency, although the wideband circuits popular in HF transceivers typically offer only 30% at full power. A Class C amplifier is capable of efficiencies approaching 100% as the conduction cycle becomes small, with common values of 50 to 75%. Both Class D and E are capable of 90% and higher efficiency.

An engineering text treating power amplifier details is Krauss, Bostian, and Raab's *Solid State Radio Engineering*.¹⁶ A landmark paper targeted to the home experimenter was that presented by a group from Cal Tech in *QST* for May and June, 1997.¹⁷

A Two-Stage General Purpose Class AB Amplifier

The circuit of Fig 2.93 operates in Class AB with an output of half a watt in the HF spectrum. This circuit was originally built

as a general purpose gain block for CW transmitters. Total current is about 80 mA with no RF drive, reaching 200 mA or more when drive is increased with most of the increase occurring in the second stage. Fig 2.94 shows P_{out} Vs. P_{in} at 5, 10, 20, 30, and 50 MHz for this amplifier when operating with a 12-V supply. The measurements were done with a signal generator and a spectrum analyzer. Low frequency gain is high at 35 dB, dropping to 28 dB at 50 MHz. Low frequency output power is over half a watt, with over a quarter of a watt available at 50 MHz. However, gain is severely compressed at this level. Higher output power is available with impedance matching.

A heat sink is used on the output transistor, for dissipation becomes high with large drive. The dissipation in the 2N3904 is 350 mW, safe for keyed (low duty cycle) CW applications, but marginal for SSB or digital modes.

The third order intermodulation distortion was measured at 14 MHz. With an

output of +10 dBm per tone, the output intercept was +32 dBm. Increasing drive for +20 dBm per tone output (100 mW/tone or 400 mW PEP) yielded a higher value of $IP3_{out}=+35$ dBm. This is expected, for total current is now higher at 180 mA.

The power supply for the input stage is normally keyed when used for CW transmission. The bias for the output stage is derived from the same supply resulting in a typical backwave 70 dB below full output. "Backwave" is the residual signal present from a CW transmitter during key-up periods.

This design, although lacking in efficiency, is otherwise very useful and has been used in over a dozen transmitters or transceivers in our stations. It can be driven by a crystal oscillator on any HF band to form an effective QRP transmitter. Preceding it with a feedback amplifier produces a DSB or SSB chain suitable for QRP use, or as a driver for a five watt PA.

2.10 PRACTICAL POWER AMPLIFIERS

This section presents several design examples for power amplifiers. A two watt bipolar power amplifier was presented in Chapter 1 with the "Beginner's Transmitter." Some simple power meter circuits were also included.

A CW-QRP Rig Amplifier

A familiar RF power amplifier encountered by the experimenter is that used with a low power (QRP) transmitter. The popular design provides about 1.5-W output from a 12-V supply. The load resistance the collector would "like to see" is then

$$R_L = \frac{V_{CC}^2}{2 \cdot P_{OUT}} \quad \text{Eq. 2.42}$$

Evaluation yields $R_L=48$, so close to 50Ω that no impedance matching network is required at the output. Only a low pass filter is required to attenuate the strong harmonics that are often created by the circuit. The amplifier circuit is shown in Fig 2.95. The 7-MHz design illustrates the design ideas, which are frequency invariant.

The amplifier input is to be driven from a 50Ω source. While not required, it promotes convenient measurement. The builder can then test and adjust the driver stages alone, with the earlier transmitter stages, and without the complications of the output amplifier. This amplifier will usually require a drive power of 20 to 100 mW, depending upon the transistor type used in the amplifier. The 50Ω drive is transformed downward to "look like" a 12.5Ω source at the base. This transformation provides the high base current required for efficient operation. The 18Ω base resistor serves as a wideband load for the input driver, even during the part of

the drive cycle when the base is reverse biased. Decreasing this resistance can improve stability at the price of gain.

Base matching occurs with T1, a simple transmission line transformer consisting of a bifilar winding on a ferrite core. These transformers are discussed in the filter chapter. Other impedance transformation circuits can also be used, including tuned L, π , or Tee networks. The stage that must drive this will probably be loaded with a higher impedance, perhaps 200Ω . Another bifilar transformer could be used, or a single ferrite transformer with a 4:1 turns ratio could make the transition from 200 to 12.5Ω in one step.

It is important that the base drive be provided by a low impedance source. A higher source resistance might supply the needed base current, but then develop high voltage during the negative part of the drive cycle. This could lead to emitter base breakdown, a phenomenon that creates transmitted noise and a slow performance degradation in the output transistor. Emitter-base breakdown is easily observed with a wideband oscilloscope. A low driving impedance also helps stability.

A small heat sink is needed for a TO-39 transistor such as the 2N3866 or 2N3553. A clip-on heat-sink will suffice. The transistor can even be soldered into a hole in a circuit board. If the latter method is used, the hole must be isolated from circuit ground with extra capacitance absorbed into the design.

The amplifier includes extra components that are not always needed. One is the familiar Zener diode at the collector. This should have a breakdown value of about 3 times V_{cc} but less than the transistor breakdown. The diode's purpose is to load the amplifier if it loses an output termination. The diode conducts only if the collector voltage becomes too high, thus

saving the more expensive output transistor from damage. The typical Zener diode will have a relatively high capacitance, even before breakdown, requiring that the input C in the low pass filter be reduced in value.

The virtue of this diode is open to debate. It is often seen in amateur applications, especially with transistors not intended for Class C RF applications. It is not so common in commercial applications using transistors intended for RF. The protection function is easily studied with a high-speed oscilloscope.

An RF choke routes bias to the collector. An extra inductor is placed in series with the supply, providing a series impedance for decoupling. A resistor then parallels the decoupling choke, as discussed in an earlier section. An optimum decoupling RFC uses large lossy ferrite beads.

A 7-MHz series tuned circuit is formed by the 50-pF, 10- μ H combination. The back-to-back diodes provide a short circuit for large RF signals, generating a convenient electronic T/R system. This scheme, and similar T/R methods are discussed in Chapter 6.

A low ripple Chebyshev low pass filter with a cutoff frequency of about 7.5 MHz is recommended. Details appear in Chapter 3. The capacitance at the transistor end of the filter should be reduced to account for Zener diode capacitance and the 50 pF related to the T/R. No component values are shown for this example.

The ideal transmitter design will include variable RF drive. Besides being useful for communications, it is a very useful experimental tool.

Amplifier adjustment consists of nothing more than varying the drive power while watching the output to a 50Ω load. Amplifier operation without a load should be avoided. The output power should change smoothly with drive, with any jumps suggesting instability.

It is interesting to monitor efficiency while drive is varied. Drive is adjusted, output power is measured, power supply current is noted, input power is calculated, and the resulting efficiency is calculated. Efficiency is usually low when the output is considerably less than the design level, but increases with drive. It will often be possible to drive the amplifier to an output greater than 1.5 W, usually at the price of efficiency. If you are interested in higher output, the output network should be re-designed accordingly.

It is useful to examine amplifier performance with a variety of loads. This is easily done with a transmatch. The dummy

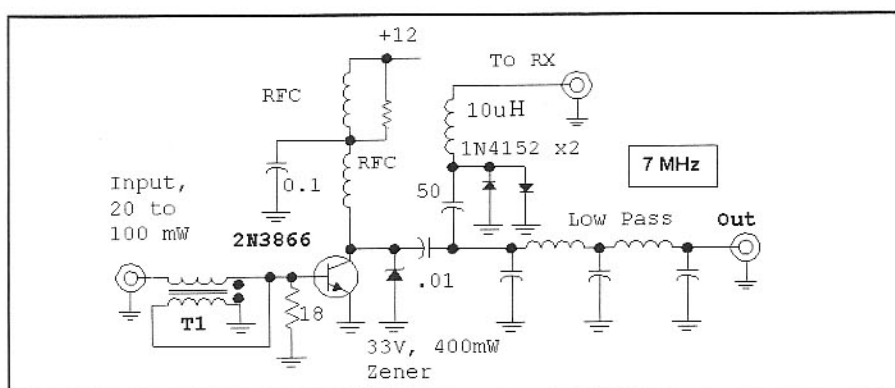
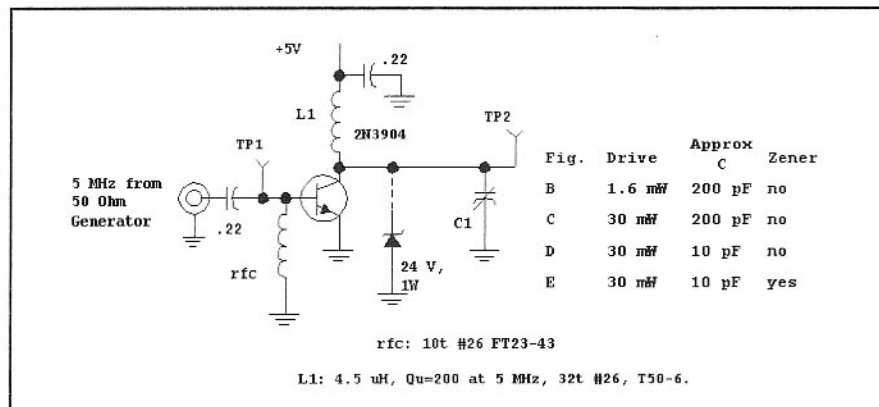


Fig 2.95—Typical output amplifier in a QRP transmitter.

Waveforms of a Class-C Amplifier

In an effort to garner intuition about the voltages in Class-C amplifiers, a low power experiment was performed with the circuit of **Fig A**. A signal generator provided base drive to the 2N3904 amplifier. The collector was biased at 5 V through a $4.5\text{-}\mu\text{H}$ high Q inductor. A variable capacitor allowed the inductor to be tuned to the drive frequency, or be detuned for an inductive collector termination. A Zener diode could be added to the circuit.



Test points are available at the transistor base and collector, allowing the voltages to be monitored with a high speed oscilloscope, a Tektronix 7704A in this case.

The first case examined was the reference for the experiment with results shown in **Fig B**. The low RF drive barely excites the base, but turns the transistor on at the peaks. The resulting current is a short spike, but still produces a very clean collector waveform, just reaching

Fig A—RF Drive is applied to the base of a BJT while the un-terminated collector is biased through a tuned circuit. The data table relates results to operating conditions.

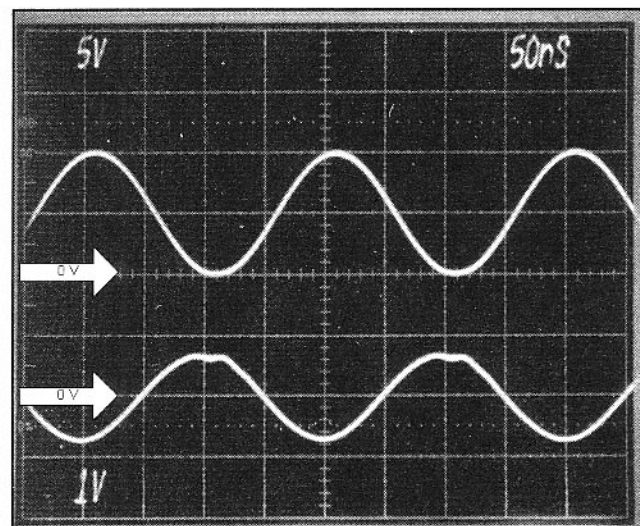


Fig B—Low drive produces a clean collector waveform in the upper trace. The lower trace shows the base voltage. In all cases, the vertical sensitivity is shown for each trace, and the 0-V line is marked at the left of the trace.

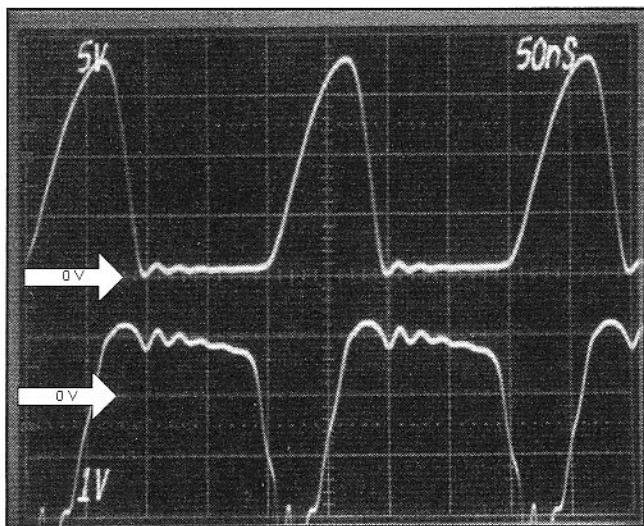


Fig C—Increased drive produces severe clipping in the base voltage and an 18-V peak collector signal.

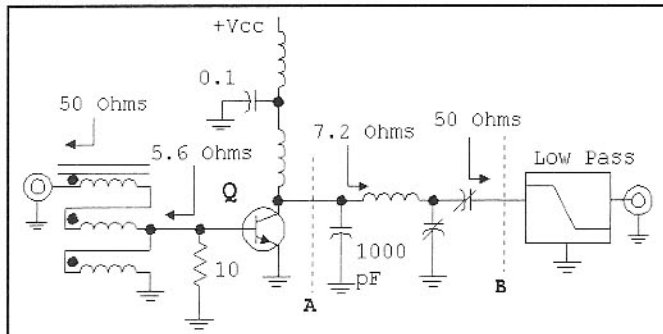


Fig 2.96—Schematic for a 10-W output Class C amplifier. The input auto-transformer might consist of 3 turns through a binocular type balun transformer core. A Thomson 2SC1969 would be a good transistor choice, but try other parts as well. See text.

load is placed at the transmatch output, and the collector voltage is observed with an oscilloscope and 10X, 10-MΩ probe. The output power will be 1.5 W when the transmatch is properly adjusted. However, output power will drop considerably as the transmatch is “tweaked.” The collector voltage will undergo major changes during this adjustment, with voltages sometimes going well beyond the expected 24-V value observed when operating in the usual class C mode with a

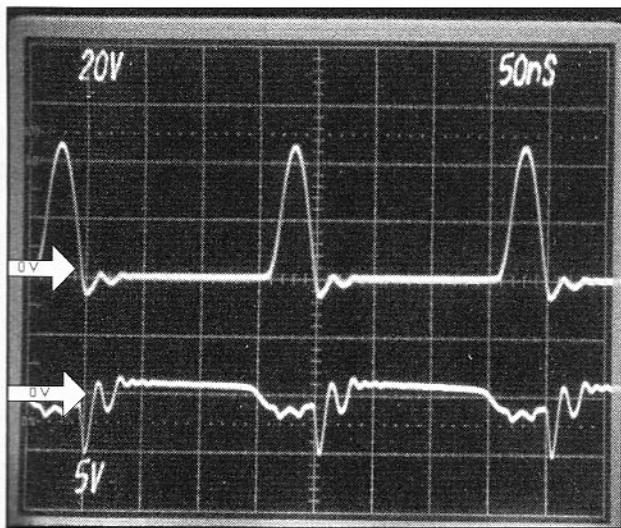


Fig D—Operation with an inductive load allows the collector voltage to ring up to over 40 V on positive peaks.

zero at the bottom of the oscillation. The positive collector peak easily reaches twice the supply value. Just a hint of base conduction can be seen at the peak of the base waveform. The conduction must be occurring only over a small fraction of the applied waveform, for the base spends most of the cycle below 0.6 V. The Zener diode is disconnected for the first experiments.

The RF drive is now increased to 30 mW, more than we would normally use with this small transistor. The base voltage exceeds 1-V peak, which causes the collector voltage to drop to zero. The base voltage "tries" to stay on for more than half of the cycle, evidence of charge storage, a phenomenon intrinsic to the BJT. But when the base does stop conducting, the collector voltage "rings up" to 18 V, well beyond the 5-V supply. These results are in **Fig C**. Base voltage ringing at higher frequency is evident.

The collector resonance of the last example is eliminated by detuning the capacitor to a low value. The collector now sees a predominantly inductive impedance, resulting in the over 40-V peak signal of **Fig D**.

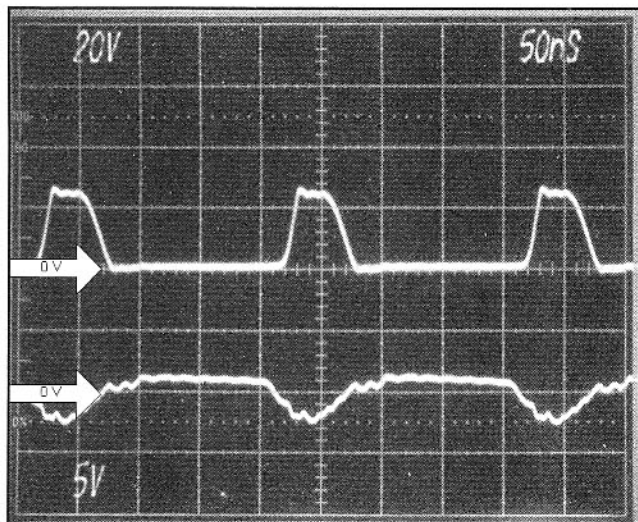


Fig E—The Zener diode is attached, effectively protecting the transistor from excess voltage.

Note the change in vertical scale. The transistor is probably on the verge of damage at this point. Note also that the base voltage has changed, having been altered by the stressed collector.

The amplifier has no resistive load other than that represented by the unloaded resonator Q and provides no output power. The collector could be loaded by adding a resistor across the inductor, which would reduce the collector voltage. Even with loading, an inductive component in the collector impedance will allow high voltages to be generated.

The final experiment connects the Zener diode, producing the waveforms shown in **Fig E**. The collector voltage is now clipped at the 24-V breakdown of the Zener diode. The base conduction duty cycle is still high, a result of the high drive and charge storage. But the transistor is now saved from damage.

These experiments illustrate the effects of an inductive collector termination, Zener diode protection, and variable drive. The experiments could be extended with other devices, more aggressive applied stress, and loading that would allow DC collector current to increase.

"proper" termination. It is not unusual to see the amplifier go into oscillations during the severe mismatch that happens with this transmatch experiment. The oscillations should not be destructive at this power level, so long as the transistor has a modest heat sink and is protected against excessive collector voltage. It is a good idea to monitor the heat sink temperature (by touch is good enough) during these experiments. A current limited power sup-

ply is always useful, if not vital, during experiments of this sort.

Consider placing a pad between the transmitter and the transmatch. If we used, for example, a 1-dB pad, the worst-case return loss would be twice the attenuation, or 2 dB. The corresponding worst-case VSWR is 8.7:1 (see Eq 4.6.) If the amplifier can now withstand all possible adjustments of the transmatch, we say that the amplifier can withstand an 8.7:1 VSWR at

all angles. The pad is, of course, removed after the test.

A 10-W CW Amplifier

While the 1.5-W amplifier is ideal for the seasoned QRP operator, others may want a bit more power. Outputs of 10 to 20 W are interesting. A few dB gain can make a big difference in results while still sporting and practical for portable operation.

There are numerous inexpensive bipolar transistors that will provide this power including many not normally used for RF. One should look for devices specified for a peak current that exceeds twice the anticipated level (1.5 to 2 A for this case), collector breakdown voltages well above the expected level (24 V here), and an f_T at least 3 to 5 times the expected operating frequency. Power dissipation should equal or exceed the planned output. A suggested 10-W amplifier is shown in Fig 2.96.

The input resistance is expected to be lower than for the 1-W amplifier, so we drive the circuit from a lower impedance source. This can be an auto-transformer, as shown in Fig 2.96, or a 3:1 or 4:1 turns ratio classic transformer. Binocular type ferrite balun cores are excellent in this application, noting that each turn now consists of one full pass through both holes in the core. Other wideband transformer configurations are listed in the transformer discussion in the Filter chapter. The input can also be driven from a low Q L-C-C Tee network like that used in the output, designed for an impedance of a few Ohms.

A 10-W output calls for a resistance of 7.2Ω presented to the collector when $V_{cc}=12$. (See Eq 2.42) This amplifier uses tuned circuitry in the form an L-C-C type Tee network. This particular topology is excellent in that component values are usually practical, network Q can be kept low for low loss, and once designed, the network is easily "tweaked" for slightly different impedances. A good design value for Q is 2 to 3. The network between the dotted lines in Fig 2.96 is used for impedance transformation while the filter attenuates harmonics.

The normal Tee network is modified slightly; a fixed capacitor with a reactance magnitude near the load resistance value is placed at the collector. This kills high frequency gain, helping to ensure VHF stability. Silver mica capacitors are a good choice for network capacitors with ceramics for bypass and blocking elements.

A suitable test load is six paralleled 300Ω , 2-W resistors. The drive is increased slowly while monitoring the RF output and collector current. The output Tee network capacitors are tuned for maximum output at each power level. An oscilloscope is especially useful during such experiments, allowing easy observation of oscillations, should they occur. More often than not, oscillations will occur at low frequencies, so a wideband 'scope is not mandatory. This amplifier will probably use no more than $\frac{1}{4}$ -W of drive, so the builder may wish to add a pad if the driving transmitter delivers more than this.

The amplifier is set up for Class-C

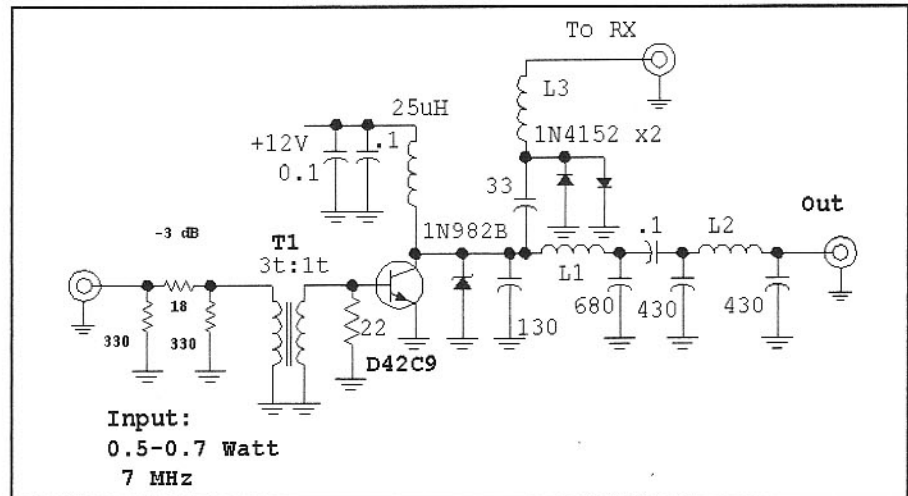


Fig 2.97—High efficiency amplifier after W7EL. T1=3-turn primary, 1-turn secondary, #30 wire, on Fair-Rite 2843002402 Balun core. Count one turn on a balun core as a pass through *both* holes. L1=0.71 μ H= 13 t. on T44-6; L2= 1.05 μ H = 19 t on T37-6, L3=15 mH molded RFC. Q is a GE D42C9 plastic power transistor.

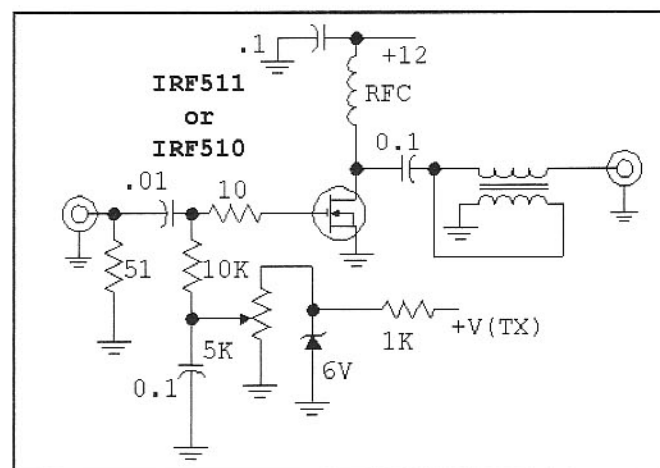


Fig 2.98—Simple HEXFET linear amplifier for QRP rigs.

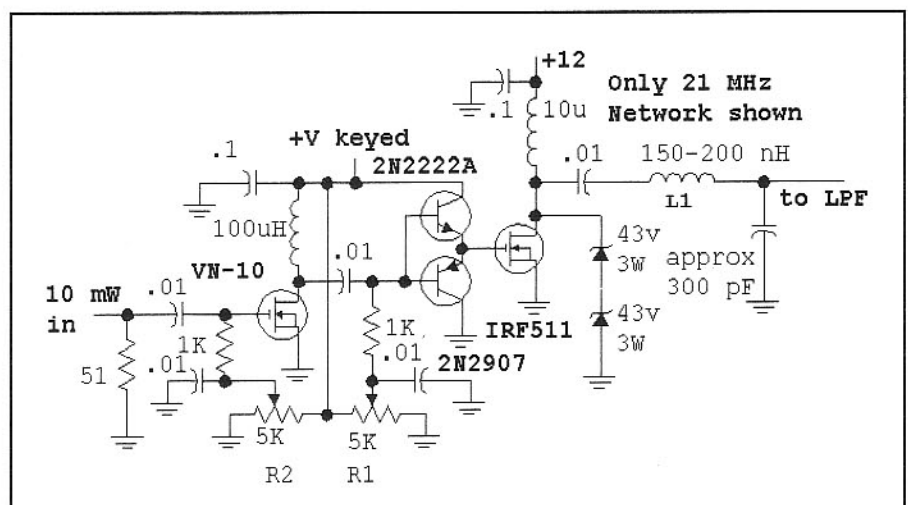


Fig 2.99—Dual band Direct Coupled HEXFET Amplifier after W7EL. This circuit operates at 14 and 21 MHz. L1 is 7 turns on a T37-6 and is the inductor for an L-Network at 21 MHz. The 1N5367 Zener diodes protecting the FET drain add about 140 pF to the circuit and are a vital part of the network. The band-switch adds more series inductance for a 14-MHz L-Network. Both impedance transforming networks are followed by low pass filters. R1, 5 k Ω , is adjusted for about 20-mA quiescent current in the IRF511, while R2, 5 k Ω , sets the quiescent current in the VN10 at 40 mA. The keyed driver power supply is less than +12 and is varied to establish output power.

operation, although it could be modified for class AB linear operation with little other change required. Linear biasing is discussed below.

An Enhanced Efficiency Amplifier

An interesting and subtle amplifier from Roy Lewallen, W7EL, is presented in Fig 2.97. Dubbed the "Brickette," it was intended to follow a 1.5-W output, 7 MHz QRP transceiver.

This amplifier used an unusual transistor, a GE D42C9. The available drive is attenuated with a 3-dB pad, which was needed for stability. The original W7EL application used a 6-dB pad. The amplifier contains the usual Zener protection diode, but now with a 75-V breakdown. A peak collector voltage of 65 was measured with this circuit, even with $V_{cc}=12.0$ V. The circuit transforming the 50- Ω load to a lower value at the collector is a simple L-network. The resistance presented to the collector is higher than expected, and is inductive, allowing the high RF voltages. The net result is a collector efficiency of 85% or greater with an output of 7 to 9 W. What began as a Class C design probably now operates in Class E. The measurements have been repeated and confirmed with several versions of the circuit, all showing high efficiency.

The adjustment procedure was similar to that presented for the 10-W design. However, Roy kept increasing drive while adjusting the output network for increased power and efficiency.

The T/R series-tuned circuit is attached to the collector. Although the networks present an impedance less than 50 Ω to the receiver, the mismatch is not a problem at 7 MHz.

HEXFET Amplifiers

Power FETs became popular in the late 1970s. While some manufacturers introduced devices specified for RF, the market was dominated by switching applications. A major supplier is International Rectifier with a line of devices called HEXFETs.

The HEXFETs are available as both N and P channel enhancement mode parts with a gate threshold around 4 V. The transconductance of the typical N-channel device is very high, often rivaling that of a bipolar power transistor at comparable currents. While the input gate is a very high impedance at DC, high capacitance at all three terminals limits high frequency gain. HEXFETs are often high voltage devices, allowing a wide variety of supply voltages.

Fig 2.98 shows an RF amplifier using an IRF511 or the IRF510, preferred for higher breakdown. Either part has a low "on" resistance of 0.6 Ω , important for efficiency. This circuit is set up for an output of about 6 W from a 12-V supply. A 2:1 turns ratio transformer generates a 12- Ω drain load. This class AB circuit will function in either CW or linear SSB applications. The bias should be adjusted for a quiescent current of 100 mA or more for SSB while lower levels are suitable for CW. The output transformer is a bifilar winding on a ferrite core and is suitable for any of the HF bands. We have used this circuit up through 14 MHz. The FET should reside on a modest heat sink.

The HEXFET amplifier uses a 10- Ω gate resistor to preserve HF stability. A ferrite bead should **not** be substituted for the resistor.¹⁸

An interesting direct-coupled amplifier appears in Fig 2.99. This circuit, another creation of W7EL, uses a dc coupled IRF511 to generate an output of 5 W at either 14 or 21 MHz with a measured efficiency of about 75%.

Higher Powers

HEXFETs offer an inexpensive and interesting route to higher power. We have built single band CW amplifiers for output powers from 10 to 50 W on many of the HF bands. The inexpensive IRF530 HEXFET is an excellent choice for the bands up through 14 MHz. A 30-W 7-MHz CW amplifier is described later.

The IRFP440 and IRFP450 have been used in high efficiency CW amplifiers discussed later. These parts should also offer

interesting opportunities for the experimenter. Although more expensive than HEXFETs, some vendors build parts especially for RF power applications. A search of the web can yield numerous data with suggested experiments. See, for example, an interesting paper by K4XU and the related Web site of Advanced Power Technology at www.advancedpower.com.¹⁹

SSB Amplifiers

The bipolar and FET amplifiers presented can be adapted for linear operation as shown in Fig 2.100. Bipolar transistor base bias should come from a voltage source. If the more typical current source is used, the DC current cannot easily increase with RF drive as is needed for Class AB operation. A voltage source bias uses a diode as a shunt "regulator," Fig 2.100A. The diode is biased with a resistor from the same supply that powers the amplifier. The silicon diode is in intimate thermal communications with the output transistor. Some designs use a stud-mounted diode bolted to the PA transistor heat sink. Others attach the diode to the transistor with epoxy.

The BJT amplifier is usually biased at the quiescent level recommended by the transistor manufacturer. A 10-W part might use an idling collector current of 20 to 30 mA. A larger current should flow through R-bias with the diode serving as a shunt regulator. Increasing the resistor current increases the standing current in the amplifier, one of the handles available to the experimenter for improved IMD performance from the amplifier.

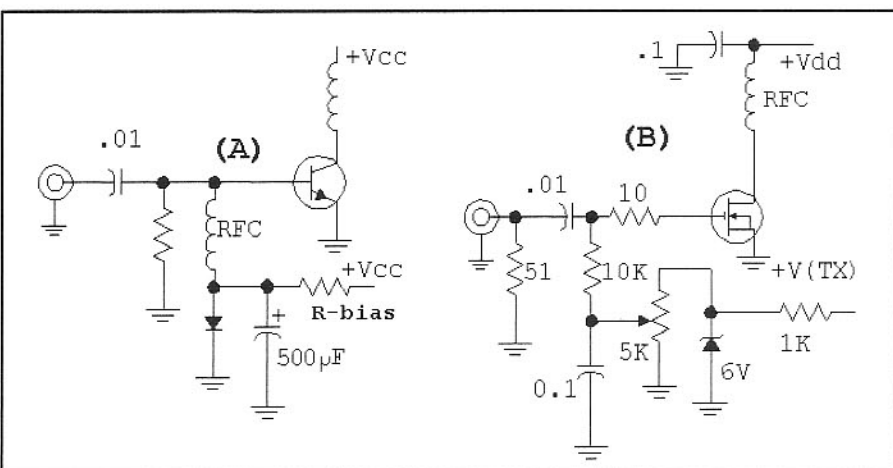


Fig 2.100—Biasing schemes for linear amplifier operation of (A) bipolar transistors and (B) power FETs. The base RFC used with the BJT can have small reactance, for the input impedance is low. The diode is bypassed with a 500- μ F electrolytic capacitor. The base resistor may or may not be needed. R-bias in (A) should have moderate dissipation, for the current may be high.

Fig 2.100B shows FET biasing for SSB. This is generally simpler than with a BJT, for bias current is low. The FET bias is easily controlled with small transistors, easing T/R switching problems. As with bipolar transistor amplifiers, the FET circuits present a compromise between efficiency and linearity. Amplifier IMD can be reduced with higher standing currents, although the heat sink requirements grow.

Amplifier biasing methods are discussed in more detail in the text by Dye and Granberg.²⁰ Included are schemes for temperature compensation.

Push-pull operation is common with both FET and bipolar linear amplifiers. There are several advantages to this. First, two devices are used instead of one, spreading the thermal load over a larger

region. Second, transformer coupling between device inputs will prevent large reverse voltages on bipolar base-emitter junctions. One forward biased junction serves to clamp the reverse voltage on the other device. Finally, the balanced operation will reduce even order harmonic and intermodulation distortion.

Negative feedback is often used with Class AB amplifiers, usually in the form of an ac coupled resistor between base and collector, or gate and drain. Feedback stabilizes gain over frequency. The negative feedback is applied individually to each device in a push-pull pair. Negative feedback is sometimes extracted from a winding in an output transformer or bias element in a push pull pair.

Push pull bipolar transistors are essen-

tially in parallel for biasing. For this reason, and to help maintain RF balance, RF power bipolar transistors are often sold in matched pairs. This has become so common that the price penalty is minimal.

The ease of FET biasing includes push pull amplifiers, which is illustrated in the practical circuit shown in Fig 2.101. This SSB linear amplifier, the work of AA3X (now K3BT), uses a pair of IRF511s in a push pull circuit to develop an output of 30 W PEP. The circuit uses a solid ferrite block for the output transformer, T3. Fig 2.102 shows a sketch for the output transformer, T3.

Separate bias lines set up a quiescent current for each FET. A DVM measuring total current during bias adjustment allows the two currents to be set equal to each other. While matched transistors might be

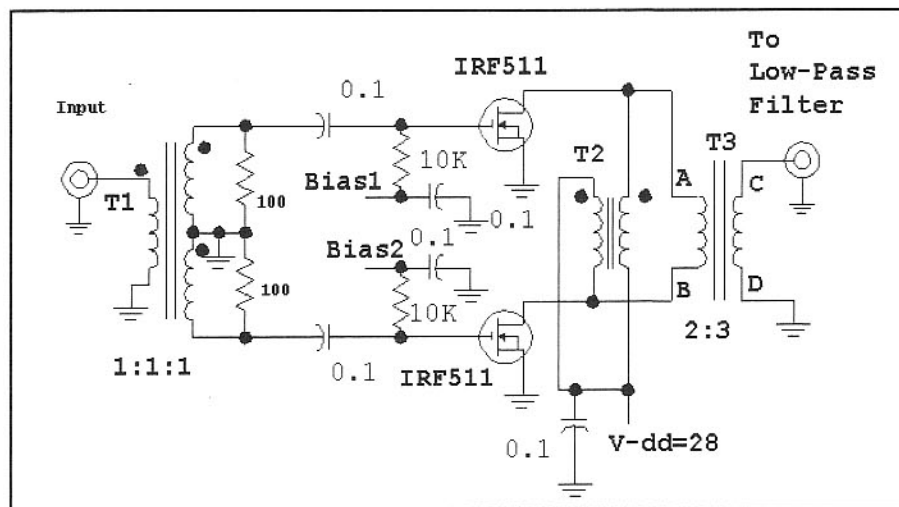


Fig 2.101—An amplifier using a push-pull pair of IRF511s. This circuit, the creation of AA3X, is capable of up to 30-W output with $V_{dd}=28$ V on the lower HF bands. Reduced output and gain are available at 14 and even 21 MHz. Input transformer T1 is 12 trifilar turns #26 on a FT50-43 ferrite toroid. T2 is 12 bifilar turns of #22 on a stack of two FT37-50 toroids. This amplifier was originally in *QST*, Hints and Kinks, for January, 1993, page 50.²¹ See reference and text for practical details.

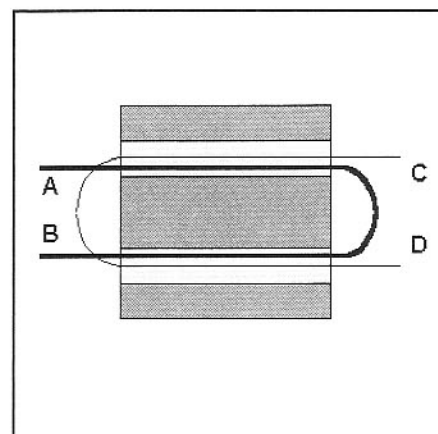


Fig 2.102—Transformer detail for T3 of the AA3X amplifier. The primary, A-B, shown here as a single turn, but actually uses two turns, two complete passes through the core. The secondary (also just shown as one turn) is 3 turns, three complete passes through the core. The windings end on opposite sides of the ferrite block, a BN-43-7051.

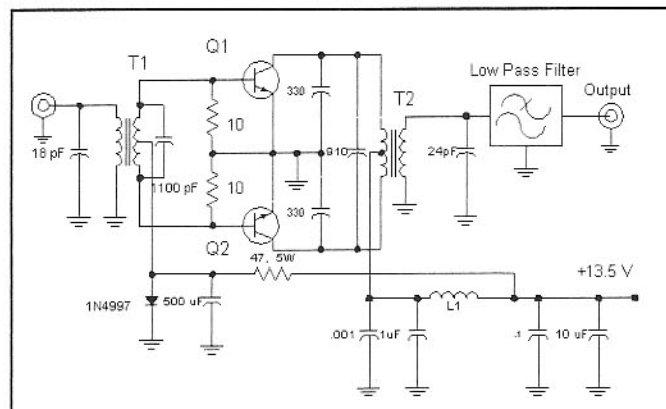


Fig 2.103—100-W BJT Amplifier. This circuit, originally described in *Motorola Engineering Bulletin*, EB63,²² is capable of an output power of over 100 W from 3 to 30 MHz. Q1 and Q2 are matched MRF454s mounted to a large heat sink. L1 is a piece of #18 wire loaded with 9 ferrite beads. Both transformers have a 4:1 turns ratio with the winding, consisting of ferrite loaded brass pipe, attached to the transistors. The one-turn windings are center tapped. The 4-turn input and output windings are plastic covered wire wound through the center of the tubes. Similar transformers could be built with 3/16-inch diameter brass tubing (available at hobby stores) loaded with FB-77-63 Ferrite beads. T1 would use 4 while T2 would use 10 beads. A larger bead and tubing size would be better for T2. The transformers used in our amplifier were supplied with the kit from Communication Concepts, Inc. of Beavercreek, Ohio. See *QST* advertisements for a current address. CCI has several other kits for power amplifiers.

desirable, K3BT reports that he has had good results with devices with severely mismatched thresholds. Equal currents of about 20 mA per transistor are recommended. This amplifier has been used on the amateur bands from 3.5 to 21 MHz, although the available output power is less at the higher end.

The output transformer (3:2 turns ratio) presents a load of $22\ \Omega$ between the two drains. The resulting load is lower than might be desired for high efficiency, a common tradeoff with linear amplifiers favoring lower distortion. The K3BT amplifier should be built with a large heat sink, especially if experiments are planned with variable bias currents.

Careful low impedance termination of the HEXFET inputs provides stability. The power gain is still high enough to make the parts very useful, even with the reduced gain related to the low source impedance. The stability problem is largely the result of internal feedback within the FETs. While extremely difficult with bipolar transistors, it becomes possible with FETs to neutralize the circuits, canceling the destabilizing effects of internal feedback. These methods were common place with vacuum tubes, but have largely been ignored with semiconductors. A neutralized push-pull 18-MHz linear power amplifier using IRF-511s is included in Chapter 11.

A high power bipolar transistor amplifier is shown in Fig 2.103. This circuit was originally described in a Motorola engineering bulletin, EB63 (ref 22), and was offered in kit form from CCI. (www.communication-concepts.com) The amplifier is capable of over 100 W of output over the entire HF spectrum. A matched pair of MRF454s is used with a 13.5-V power supply.

This circuit is a classic, similar to many of the output amplifiers in typical transceivers. Brass pipe transformers are used at both the input and the output. Some negative feedback is used, along with capacitive loading to improve gain flatness. This version of the amplifier has been tested over the 2 to 30-MHz band and found to operate as described in the applications note, although we did not measure IMD. The circuit has been used extensively on the 40-M band. It performed well as a SSB amplifier, being easily driven by a 1.5-W QRP SSB transceiver. It has seen more service following a 1-W CW transmitter.

The original version of this amplifier included an RF actuated circuit to control a built-in T/R relay. The RF actuated scheme was found to be completely unsuitable for either CW or SSB use. When RF drive was

initially applied, the relay was activated. But amplifier current started to grow before the output was properly terminated, causing the amplifier to draw excessive current. The power supply was current limited at 25 A. As the supply went into limiting, the voltage dropped to 7 V before starting to recover. The relay then dropped out and the cycle repeated. The relay chattered for about half a second before stabilizing. The RF actuated circuitry was eventually replaced with an electronic T/R system with diode switching.

T2, the output transformer, has a single turn between collectors with a 4-turn secondary. The 4:1 turns ratio transforms the $50\ \Omega$ load to appear as a $3.1\ \Omega$ load, collector-to-collector. The load applied to each collector is then $1.56\ \Omega$. Rearrangement of Eq 2.42 shows that an output of 58 W should be available from each device at $V_{cc}=13.5\text{ V}$ for a net output of 117 W.

In spite of the T/R problems, the amplifier is a recommended circuit. The MRF454 is very robust, and has provided us with classic power amplifier experience. We recommend modified bypassing to use parallel capacitors of equal value.

A Look at some High Efficiency Amplifiers

All of the power amplifiers presented are conceptually simple, many using the same or similar schematic diagrams, even

though intended for differing applications. Class-C amplifiers are designed by picking a load resistance using Eq 2.42 and designing an output network to achieve that load at the operating frequency. The device is then biased for zero current without drive. With the usual threshold, application of an input sine wave produces Class-C operation.

Linear amplifier design is similar. An output network is designed for the peak envelope output, again with Eq 2.42. Moving toward even lower load resistance may enhance linearity at the price of efficiency. The linear amplifier is biased for class AB operation. This begins with class A bias, but usually allows device current to increase with applied RF drive. While efficiency at the peak envelope power is poor, the normal voice has an average power well below the peak, providing a useful compromise.

An amplifier discussed earlier (the Fig 2.97 circuit by W7EL) featured improved efficiency. It is interesting to examine the networks that produced this result.

Fig 2.104 shows a schematic and a Smith Chart impedance plot for the output matching network the Beginner's Transmitter of Chapter 1. Frequency sweeps from 3.5 to 21 MHz for this 7-MHz design. The impedance at 7 MHz is nearly real at about $25\ \Omega$, providing the needed load for Class-C operation. The impedance is capacitive for all other frequencies. This

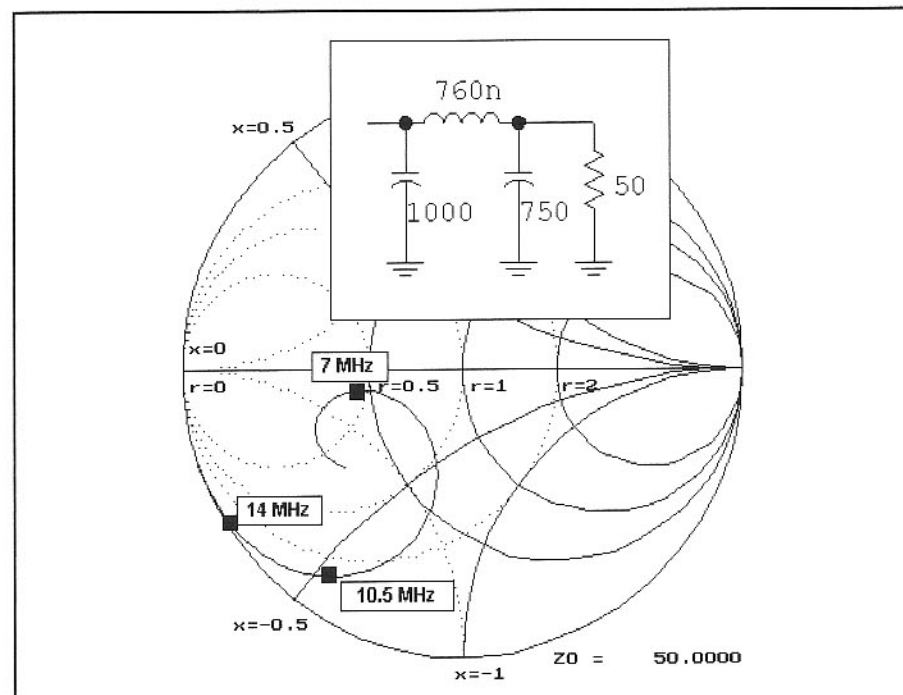


Fig 2.104—Smith chart plot of the impedance “seen” by the collector of the 2N5321 2-W “Beginner’s Transmitter” from Chapter 1.

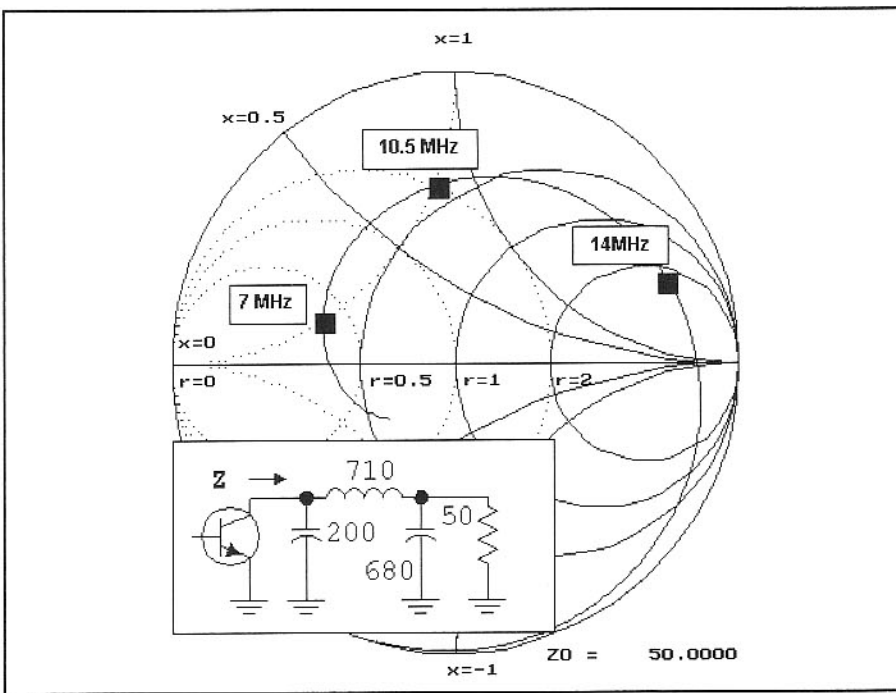


Fig 2.105—Smith Chart plot for the Brickette of W7EL, shown in Fig 2.97. The impedance is inductive until reaching the second harmonic. There is a slight change in the plot when additional C is added at the collector to account for the Zener diode.

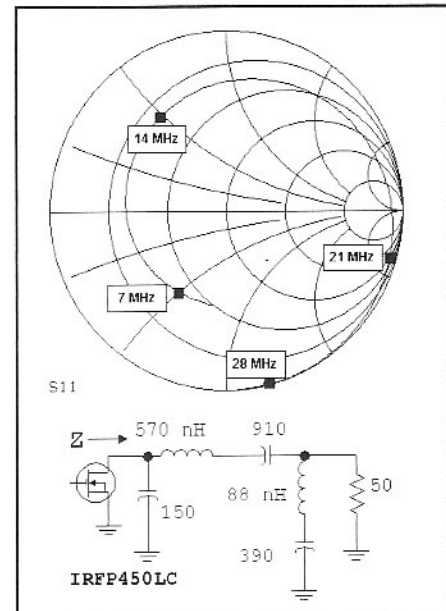


Fig 2.106—50- Ω Smith chart display of impedance for a 400-W amplifier operating at 13.5 MHz. See text.

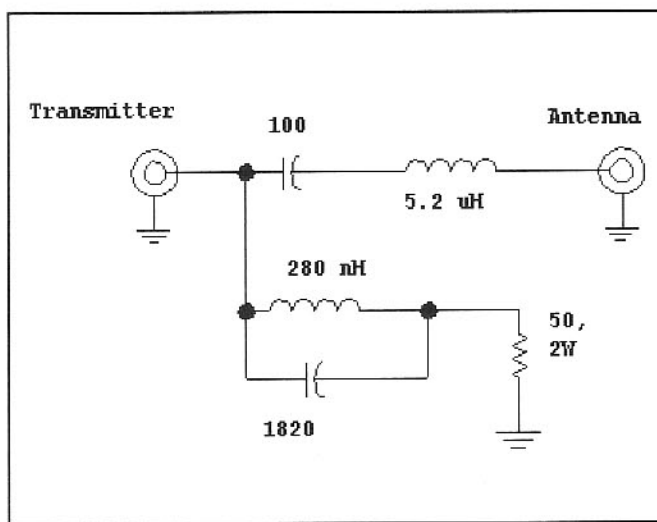


Fig 2.107—Diplexer, bandpass-bandstop type, used for harmonic attenuation from a 7-MHz transmitter. The reader should consult the original QST article²³ for details.

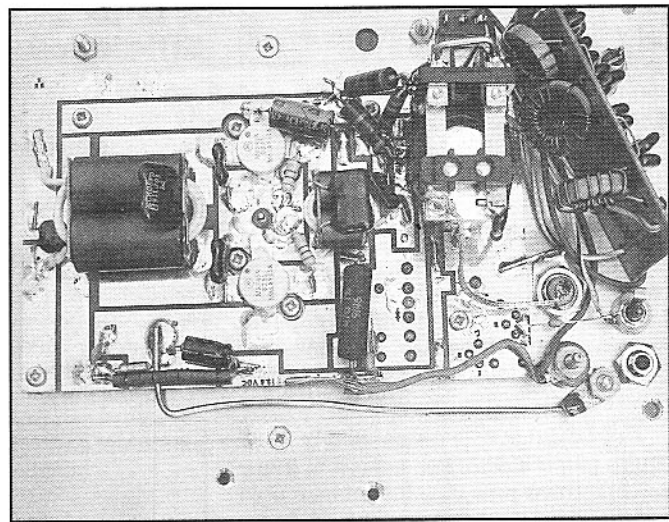


Fig 2.108—Top view of 100-W bipolar amplifier. The board is bolted to a large heat sink that is also the top of the module.

amplifier (7 MHz, 2.2-W output, 12-volt supply) was stable and reproducible, but had only 50% efficiency.

The contrasting amplifier was W7EL's "Brickette" of Fig 2.97. The output network is also a π -network, and the resulting impedance plot is shown in Fig 2.105. The plot differs from the simple Class-C circuit. The impedance has a real part of about 17 Ω near the design frequency, but is inductive for much of the sweep. R_L is about twice that we would use for a

Class-C design. Z becomes capacitive only above the 2nd harmonic. This amplifier has excellent efficiency (85 to 90%) at 7 to 9-W output (7 MHz, 12-V supply) and has been stable.

Class-E amplifiers have become of increasing interest in the past few years. Recent HEXFET offerings from International Rectifier provide very high power capability at modest price. While the amplifiers are now used only for digital applications (including CW), recent work

has paved the way for SSB with non-linear high efficiency amplifiers.²⁴ The recent work of greatest interest to the experimenter evolves from the EE department at California Institute of Technology.²⁵

Fig 2.106 shows an example of a high efficiency Class-E amplifier.²⁶ The partial schematic shows two modifications to the simple pi-network used in the other two circuits. First, the normal inductor is replaced by a series LC. This provides the same inductive reactance at the 13.5-MHz

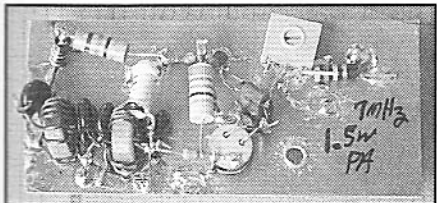


Fig 2.109—A 1.5-W 7-MHz amplifier using a 2N3866.

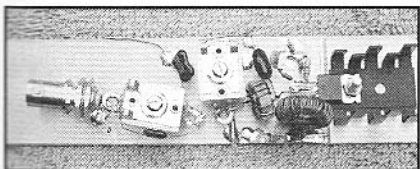


Fig 2.110—An RF power amplifier using an IRF510 HEXFET. The output network is an LCC type Tee-network. Up to 10 W was obtained from this circuit.

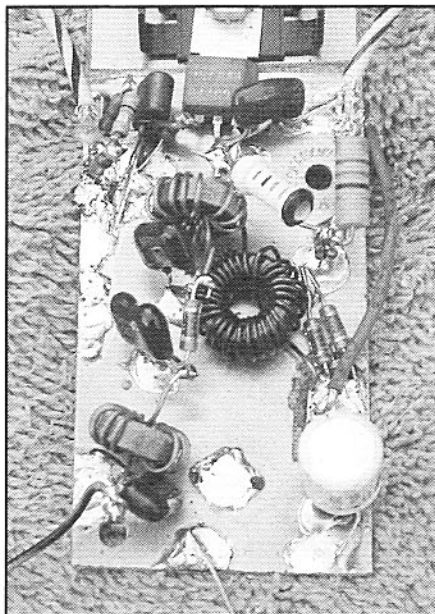


Fig 2.111—A high efficiency 7-MHz amplifier (circuit of Fig 2.97).

design frequency, but greater inductive reactance at higher frequencies. This presents the needed load to the FET drain needed to allow the voltage to grow ("ring up") to values much larger than the supply and offer the phase control needed for efficiency. A Class-E amplifier is characterized by high current flowing only when the

voltage across the device is close to zero.

The other modification is at the load end of the network. The usual parallel capacitor is replaced with a parallel-connected series tuned circuit (88 nH and 390 pF). This circuit is resonant at the 2nd harmonic

of the 13.5-MHz drive frequency of this example. This amplifier provides an output of 400 W with a drain efficiency of 86%. This circuit, which uses a 120-V supply, could be adapted to the 20-meter amateur band. The load impedance is $13.5+j19 \Omega$ at the 13.5-MHz operating frequency, but is purely capacitive by the time the 2nd harmonic is reached. Eq 2.42 would predict an 18- Ω load for this output and V_{dd} . This circuit is very similar to the 7-MHz design presented in *QST* for May 1997.²⁷

Spectral purity is an issue with these amplifiers. The resonant trap at twice the operating frequency included in the designs helps. One would normally insert additional low pass filters to attenuate harmonics. However, this normal low pass filter has an input impedance that is real and 50 Ω at the operating frequency, but is almost a short circuit at the harmonics. An improved harmonic reduction filter form is shown in Fig 2.107. This circuit is called a diplexer and has the characteristic that the input impedance is 50 Ω at all frequencies. Other dippers are used elsewhere in the book.

Fig 2.108 through Fig 2.111 show some of the design implementations described in this section.

2.11 A 30-W, 7-MHz POWER AMPLIFIER

While QRP can be great fun, especially in a portable application, there are times when more power can make a large difference in station effectiveness. The amplifier shown in Fig 2.112 is intended to boost the output of a QRP rig to the 30 to 40-W level with an inexpensive HEXFET. A moderate heat sink is used, allowing extended testing and operation.

The amplifier requires about 1 W of drive for full output. If more drive is available, it may be dissipated in an input attenuator. A 3.3-dB pad is shown in the figure. This is followed by T1, a bifilar wound ferrite transformer providing gate drive for the FET. The low impedance drive is needed to accommodate the high

input C of the IRF530. A 10- Ω , 1-W resistor provides a wide band termination.

The drain circuit is supplied with a +25-V source through an RFC (L1) made with a large powdered iron toroid. The exact value is not critical. The RF resistance that should be presented to the drain for a 30-W output is 10 Ω . This is realized with T2, a bifilar wound ferrite transformer. This part of the circuit is open to considerable experimentation for those so inclined. T2 is followed by a low pass filter for harmonic attenuation. Inductor L5 is tuned for parallel resonance at 7 MHz. An attached resistor then provides a termination for the amplifier transistor at frequencies other than 7 MHz when a

trans-match with a peaked high pass characteristic is used. The combination emulates the diplexer described earlier.

A T/R system is included to supply a signal to the receiver input. As shown, this system has a measured insertion loss of about 3 dB, the result of the low Q RF choke at L7 and the shunting effect of C1. This loss of no consequence at 7 MHz.

An adjustable bias is available for this amplifier, provided by a PNP switch circuit keyed with a signal from the driving transmitter. A grounding signal is applied at J1 to turn on the PNP switch. FET bias is adjusted at R1 (S1 open) for a few milliamperes of drain current with no RF drive during key-down periods. The switching

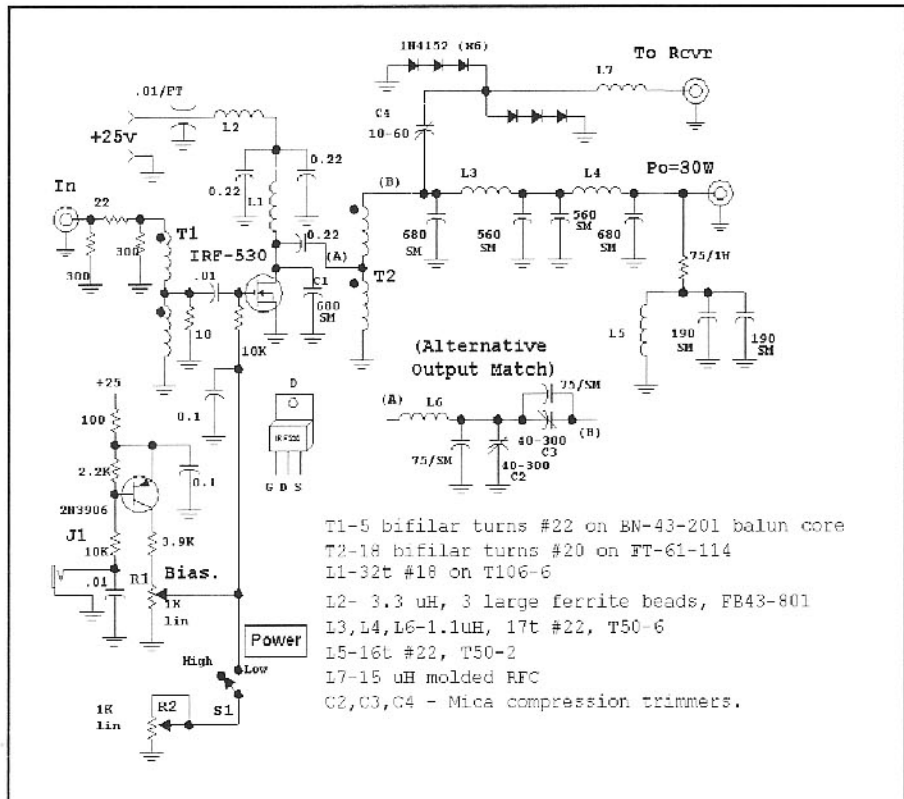


Fig 2.112—Schematic for the 30-W, 7-MHz power amplifier. See text for details.

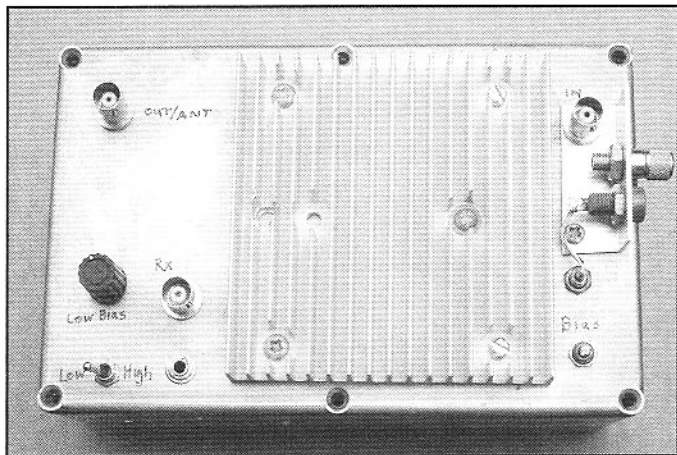


Fig 2.113 —The 30-W amplifier.

action removes bias during receive, preventing amplifier noise from overwhelming the receiver. The standing current for SSB operation can be adjusted to larger values, up to 1 A. Monitor heat sink temperature to be sure that it never becomes too hot during transmit periods.

Throwing switch S1 to the low power position allows the power output to be dropped to levels from well below a watt up to 5 W, controlled by a knob on R2. This scheme works well even with an output less

than the input drive.

Initial turn-on begins by terminating the amplifier in a 50Ω load with at least 30 W of dissipation capability. A current limited power supply is attached. RF drive well below the required level is applied while the output is monitored with an oscilloscope or RF detector. Drive is slowly increased while examining the output waveforms. Clean signals with smoothly varying levels should be seen with changes in drive. Any sudden change sug-

gests stability problems. We saw no such problems with this amplifier.

Monitoring drain voltage with an oscilloscope (60-MHz bandwidth) revealed some disturbing characteristics. When C1 is absent, the drain voltage contained extensive harmonic current, evident from the fine structure around the positive peaks. While these harmonics are blocked from the outside world by the low pass filter, they should be controlled or reduced at the FET where they can compromise efficiency. The low pass filter was temporarily removed from the system, allowing the wideband output load to appear at point "B" in the circuit. This immediately cleansed the signal at the drain, removing the high frequency spikes. The low pass filter appears as a large shunt capacitance at plane B in the figure. This load is reflected through T2, allowing the transformer leakage inductance to appear at the FET drain. This is the load that will allow the higher frequency currents to flow.

The ideal solution for this situation is a diplexed low pass output filter, mentioned above. Sabin studied diplexer filters and presented his work in *QEX* for July/August, 1999.²⁷ The amplifier used with these filters was described in the Nov/Dec 1999 *QEX*;²⁸ both papers are excellent and are included on the book CD.

We elected not to use a diplexer filter in this amplifier. Rather, C1 is included at the drain. With C1 in place, the drain voltage goes up to about 60 V, well within the FET ratings. Although there is still distortion in the drain waveform, harmonic currents are not excessive.

Several transformer structures were tried at T2. The most interesting variation replaced the wideband transformer with a narrow band LCC type Tee-network, also shown in the figure. This circuit was adjusted for maximum output while slowly advancing drive power. Over 45 W of output was available with this circuit. The drain waveform was very clean, reaching a peak of 75 V. C1 was still present at the FET drain during this experiment. The T-network was designed to provide 10Ω to the drain with a Q of 5. Experiments with other networks will allow you to move over the ill-defined border between class B or C operation toward class E. FETs with higher voltage ratings should be considered for these experiments.

This circuit has been used in several variations for years and on several bands up through 14 MHz. Higher bands should also be possible with experimentation. We have always been impressed with the robust character of the devices. The typical power supply used is a surplus open-frame linear regulated type with 4-A

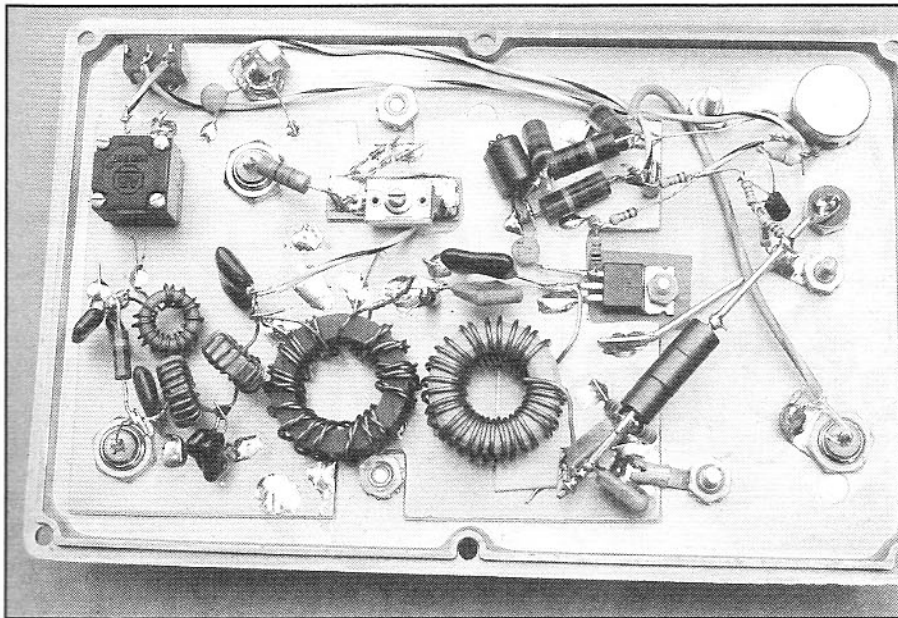


Fig 2.114—Inside the 30-W amplifier.

current limiting. Typical current is 2.5 A. The use of slight forward bias helps to guarantee stability.

The present interest in QRP operation is generally applauded as both fun and worthwhile. However, many folks miss some exciting experimental rewards by an overly strong adherence to a synthetic 5-W limit. This amplifier is a chance to examine the other side of the power switch. See **Fig 2.113** and **Fig 2.114** for two views of the 30-W amplifier.

REFERENCES

1. W. Hayward, *Introduction to Radio Frequency Design*, Prentice-Hall, 1982, and ARRL, 1994.
2. P. Horowitz and W. Hill, *The Art of Electronics*, Second Edition, Cambridge University Press, 1989.
3. P. Gray and R. Meyer, *Analysis and Design of Analog Integrated Circuits*, Second Edition, Wiley, 1984.
4. *IEEE Standard Dictionary of Electrical and Electronics Terms*, ANSI/IEEE Std 100/1984, Published by IEEE and Distributed by John Wiley, 1984.
5. See Reference 1.
6. See Reference 1.
7. *The ARRL Handbook for Radio Amateurs*, ARRL, 1995, pp 17.5-8, 17.10, 17.22-25.
8. D. Norton, "High Dynamic Range Transistor Amplifiers Using Lossless Feedback," *Microwave Journal*, May, 1976, pp 53-57.
9. U. Rohde, "Eight Ways to Better Radio Receiver Design", *Electronics*, Feb 20, 1975, p 87.
10. See Reference 1, p 216.
11. W. Carver, "A High-Performance AGC/IF Subsystem", *QST*, May, 1996, pp 39-44.
12. C. Trask, "Common Base Amplifier Linearization Using Augmentation," *RF Design*, Oct, 1999, pp 30-34.
13. C. Trask, "Distortion Improvement of Lossless Feedback Amplifiers Using Augmentation," *Proceedings of the 1999 IEEE Midwest Symposium on Circuits and Systems*, Las Cruces, NM, Aug. 1999, Vol 2, pp 951-954.
14. V. Koren, "A New Negative Feedback Amplifier," *RF Design*, Feb, 1989, pp 54-60.
15. R. Campbell, "A Novel High Frequency Single-Sideband Transmitter Using Constant-Envelope Modulation", *1998 IEEE MTT-S International Microwave Symposium Digest*, 98.2, (1998 Vol II [MWSYM]) pp 1121-1124.
16. H. Krauss, C. Bostian, and F. Raab, *Solid State Radio Engineering*, Wiley, 1980.
17. E. Lau, K. Chiu, J. Qin, J. Davis, K. Potter, and D. Rutledge, "High Efficiency Class-E Power Amplifiers" *QST*, May, 1997, pp 39-42 and Jun, 1997, pp 39-42.
18. Technical Correspondence, *QST*, Nov, 1989, p 61.
19. R. Frey, "A 300-W MOSFET Linear Amplifier for 50 MHz," *QEX*, May, 1999, pp 50-54 and "Letters to the Editor," *QEX*, Jul, 1999, p 63.
20. N. Dye and H. Granberg, *Radio Frequency Transistors: Principles and Practical Applications*, Butterworth-Heinemann, 1993.
21. J. Wyckoff, "Hints and Kinks", *QST*, Jan, 1993, p 50-51.
22. T. Bishop, "140W (PEP) Amateur Radio Linear Amplifier 2-30 MHz", *Communications Engineering Bulletin*, EB63, Motorola Semiconductor Products, Inc, Phoenix, AZ, Jul, 1978.
23. See Reference 17.
24. R. Campbell, "A Novel High Frequency Single-sideband Transmitter Using Constant-Envelope Modulation," *1998 MTT-S International Microwave Symposium*, Digest 98.2, (1998 Vol. II, [MWSYM]): pp 1121-1124.
25. See Reference 17.
26. J.F. Davis and D.B. Rutledge, "A Low-Cost Class-E Power Amplifier with Sine Wave Drive," *1998 MTT-S International Microwave Symposium*, Digest 98.2, (1998 Vol. II, [MWSYM]): pp 1113-1116.
27. W. Sabin, "Diplexer Filters for an HF MOSFET Power Amplifier," *QEX*, Jul/Aug, 1999, pp 20-26.
28. W. Sabin, "A 100-W MOSFET HF Amplifier", *QEX*, Nov/Dec, 1999, pp 31-40.

Filters and Impedance Matching Circuits

Filters constitute one of the major blocks in a communications system and are especially important to the radio experimenter. The performance offered by a filter may well define the performance and/or cost of a project. The experimenter who can design and build his or her own filters has control over that

performance and equipment cost.

There are several ways of segmenting filters into groups. The usual scheme segments filters according to frequency response, such as low pass vs high pass. Others methods segment by the kind of components used. In that regard, this chapter deals first with LC filters, and later with

RC active and crystal filters. Filters can also be classified by the way they deal with impulses of energy. The filters presented in this chapter are generally “infinite impulse response” filters, or *IIR*. Finite impulse response filters (*FIR*) are detailed in a later chapter emphasizing digital signal processing (DSP).

3.1 FILTER BASICS

A filter is, in the most general sense, a circuit block that linearly modifies the nature of the signals applied to it. When we say linear, we mean that the output is a replica of the input, changed in amplitude and/or phase. However, no additional frequencies appear.

The term *domain* refers to our emphasis when describing and measuring a phenomenon. When a filter is examined in the frequency domain, we characterize the filter by the way it behaves with different frequencies. We may then change focus and examine the time domain response. For example, we may investigate the time delay imposed upon a signal as it passes through a filter. The DSP filter designer has the ability to simultaneously examine and often control both the time and frequency domain responses.

The response of a filter is measured by examining the transfer properties of the circuit. The voltage transfer function is the output voltage (usually across a termination) divided by the input voltage that caused the output. This is just the familiar voltage gain that we used with amplifiers. In the case of a filter, that “gain” is usually a loss, a number less than one, with a corresponding negative dB value.

Simple filters are built from mathemati-

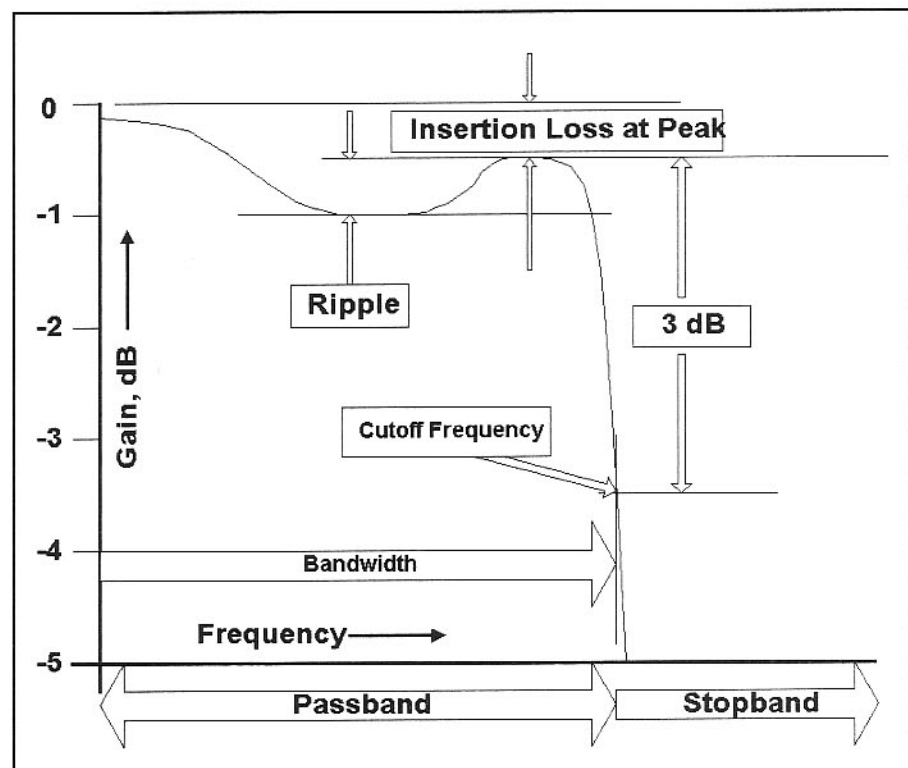


Fig 3.1—Low pass filter characteristics showing the passband and stopband, bandwidth, 3-dB cutoff, passband ripple, and insertion loss. This filter has approximately 0.5 dB IL at the frequency of peak response while passband ripple is also 0.5 dB. The vertical axis is the gain through the filter, output power Vs available input power when the filter is properly terminated. (Formally, the usual gain used is the forward scattering parameter, S₂₁). Horizontal axis is frequency.

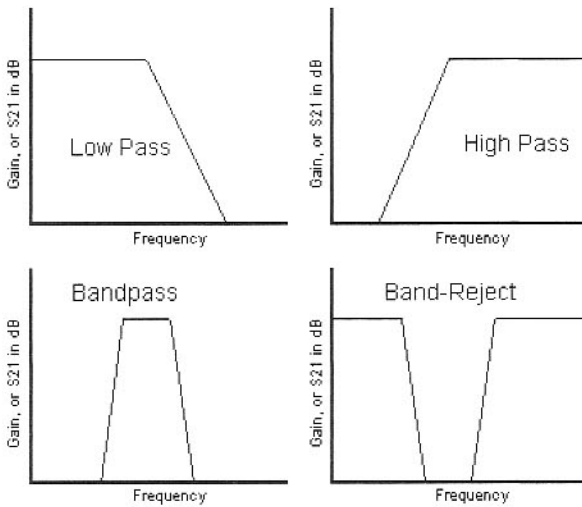


Fig 3.2—The frequency responses of various filter forms.

cally ideal inductors and capacitors. Such a filter, one without resistors, is called *lossless*. All of the power applied to a lossless filter is available at the output. Real filters containing resistive elements, desired or otherwise, will suffer from some loss. Loss in dB is a positive number, and loss as a power ratio is greater than 1.

The traditional filters we use are classified with regard to frequency domain response, illustrated with a low pass filter in Fig 3.1. This figure is a plot of filter gain vs frequency. We encountered several different kinds of power gain in Chapter 2. The one usually used with radio frequency

filters is transducer gain.

A low-pass filter is one that transfers all input frequencies below a specified cutoff frequency. The spectrum below the cutoff is called the passband while the region of higher attenuation above the cutoff is called the stopband. A filter dissipates some of the available power applied, called insertion loss. The filter of Fig 3.1 has an insertion loss (IL) of about half a dB at the highest frequency peak. IL is about 0.1 dB at very low frequency. The cutoff frequency is usually defined as that frequency where the response is 3 dB less than the peak passband response. Addi-

tional variations in gain within the passband occur with some filters; these variations are termed passband ripple.

A high-pass filter is similar to the low pass except that the regions are interchanged; the passband, the region containing desired signals, is now above the stopband.

A bandpass filter is one that passes a given region, often narrow, while rejecting most frequencies. The bandwidth of a bandpass filter is the difference between two points 3 dB below a peak. A band-reject filter is the opposite, a filter that passes most of the spectrum while rejecting a specified region. Finally, an all-pass filter is one that passes all frequencies applied to its input. The all-pass filter is useful because it can alter the phase of signals passing through it without altering signal amplitude. The various types (except for the all-pass) are summarized with regard to frequency response in Fig 3.2.

Passive filters conserve energy; power flowing into the input must go somewhere. If input energy is at a frequency within the filter passband, that energy emerges at the filter output where it can be used. (A fraction of the energy is lost in any real, passive filter, being dissipated in the losses of the inductors and capacitors that form the circuit.) In contrast, energy in the filter stopband is reflected. That is, an impedance mismatch is created by the filter elements such that power is not efficiently delivered from the source, through the filter and to the output. Most LC filters display this property, allowing us to use input impedance match as another way to examine filter performance. The primary performance indicator remains the transfer function.

3.2 THE LOW-PASS FILTER—DESIGN AND EXTENSION

A low pass is a filter that passes frequencies below a specified cutoff frequency while attenuating those above. It is a vital component of almost any communications system. The low pass is also the basis for other filter forms. Once we have a low-pass filter designed, cataloged, and understood, the properties and the component values can be extended to generate any of the other basic filter types. One extension changes the low pass into a high-pass circuit. Another modification changes the low pass to a bandpass. A band-reject filter is a direct result of transforming a high-pass circuit, itself derived from a low-pass prototype. The practical application details of these methods will be presented, although many mathematical details will be ignored in this treatment. Analytic de-

tail can be found in *Introduction to Radio Frequency Design*¹ or numerous other texts.

A simple three-element low-pass filter is given in Fig 3.3. This circuit consists of a series inductor and a pair of shunt capacitors. The filter is driven with a generator with a source resistance R_s , and is terminated in a load of R_L . The source and load are a vital part of the circuit; the transfer function depends upon having both ends of the filter properly terminated. A filter that is terminated in resistive loads at each end, input and output, is called a doubly-terminated filter. Most of the LC filters that are interesting to us will be doubly terminated.

Figure 3.3B shows another three-element filter. This one uses two series in-

ductors with one shunt capacitor. With proper design, this filter will have exactly the same transfer function as that of Fig 3.3A. This is a common detail of filters; they often have dual forms.

We can tell by inspection that both filters of Fig 3.3 are low-pass circuits. The series inductor is a short circuit at dc and has reactive impedance that grows with frequency. Hence, it will inhibit the flow of energy through the circuit more as frequency increases. The same argument can be made about the capacitors. They behave as an open circuit at dc. However, as frequency increases, they show lower and lower impedance, more effectively shunting the energy flowing in the circuit.

A low-pass filter will have a number of elements equaling the order. The filters of

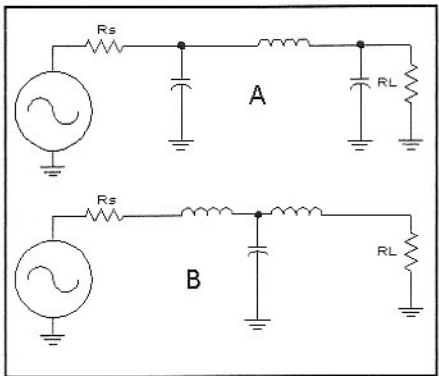


Fig 3.3—Three element, or 3rd-order low-pass filters.

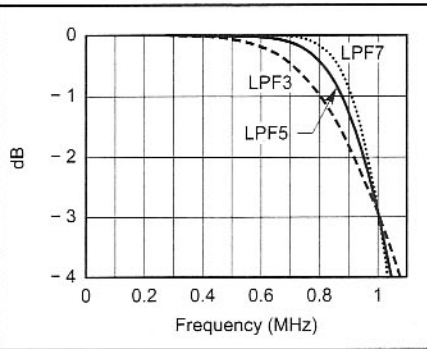


Fig 3.5—Butterworth filter transfer functions showing the passband details.

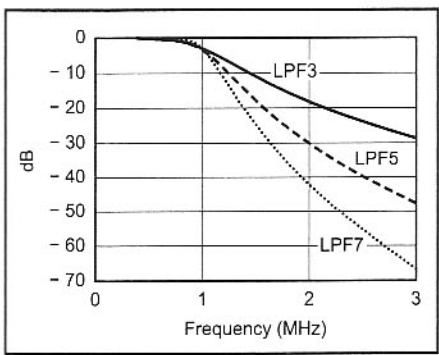


Fig 3.4—Transfer function for low-pass filters with order 3, 5 and 7. Adding sections will increase stopband attenuation.

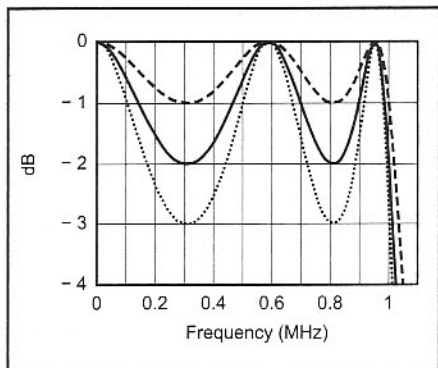


Fig 3.6—Chebyshev 5th-order low-pass filter transfer functions showing passband ripples of 1, 2, and 3 dB. These extreme ripple values are rarely used, but illustrate the concepts. Note that there is a half cycle of ripple for each filter element.

Fig 3.3 are 3rd-order filters. A low pass with 5 elements is a 5th-order circuit and offers greater attenuation in the stopband. The component type must alternate as we progress down the low-pass filter, going from series inductor to shunt capacitor and so forth. If there were, for example, two series inductors next to each other, they would behave as one single inductor. (The term “order” comes from the mathematics. A 5th-order low-pass filter has a transfer function where the denominator is a 5th-order polynomial, meaning that the frequency appears raised to the 5th power.)

Fig 3.4 shows response plots for three different low-pass filters. These circuits all have a 3-dB cutoff frequency of 1MHz, but differ in the number of components. These filters have order 3, 5 and 7. Odd-order pi filters are popular, offering maximum performance vs the number of inductors used.

Filter Shapes

All three of the filters analyzed in Fig 3.4 used a Butterworth design. This refers to the mathematical details that describe the filter; this one has a transfer function

described as a Butterworth polynomial. Another popular shape is the Chebyshev. There are many more. The ideal is a brick wall low pass filter, an unattainable goal with an absolutely flat response throughout its passband, and infinite attenuation in the stopband. The responses of Fig 3.4 suggest that achieving the ideal is going to be difficult. Wanting to do as well as we can with minimum difficulty, we accept some compromise. By picking different compromises, we will end up with different filter shapes.

The Butterworth filter is one that is designed to be maximally flat within the passband. (The slope of the transfer function is to be zero at zero frequency.) This is illustrated in greater detail with Fig 3.5, a repeat of Fig 3.4 showing only passband details. All of the filters are flat at zero frequency. Although the curves are smooth throughout the passband, attenuation grows as we approach cutoff.

The Chebyshev filter allows a different

kind of error. This filter type allows ripples of equal amplitude to occur within the passband. Three transfer functions for Chebyshev low-pass filters are shown in Fig 3.6. The three circuits are all 5-pole, or 5th-order low-pass filters, now using a 1 MHz ripple cutoff frequency. The circuits have passband ripples of 1, 2 and 3 dB. Even though the three filters show large ripples, they all show 0 dB loss at points through the passband. The frequencies are not a function of ripple value. These filters were designed for ripple cutoff frequency. That is, a filter with 1-dB passband ripple will have the last point of -1 dB response at the ripple cutoff frequency. Chebyshev filters can be designed for either a desired 3-dB cutoff, or a ripple cutoff. Odd ordered Chebyshev filters have zero attenuation at zero frequency while even ordered versions will have a dc attenuation equal to the ripple. Stopband attenuation is a strong function of passband ripple. The more ripple allowed within the passband, the greater the stopband is attenuated.

There are numerous other polynomial types that form useful and interesting low-pass filters. Some are of direct interest for low-pass filters while others are of greater utility as the beginnings of other filter types. For example, the Bessel filter, also known as the max flat delay filter, is often used as a starting point for bandpass filters with minimum ringing. This will be discussed later with LC and quartz crystal bandpass filter design.

Low-Pass Filter Design

The design of practical low-pass filters begins with tables of normalized values. These component values, $g(n)$, are either capacitor or inductor values for the n -th part in a low-pass filter with a 1Ω termination and a cutoff frequency of $1/(2\pi)$ Hz. While this is rarely a filter that anyone would wish to build directly, it is a convenient form for scaling to practical filters. It's also a mathematical simplification.

Table 3.1 shows some $g(n)$ values for a few representative low-pass filters. The Butterworth part of the table gives data in terms of a 3 dB cutoff frequency, while the Chebyshev filter data are calculated on the basis of a ripple cutoff.

A practical low-pass filter is easily designed with data from Table 3.1. Design begins by picking a cutoff frequency in Hz and a resistive termination, in Ω , for each end of the filter. The filters that are designed from the table are doubly terminated in equal values. Having picked the critical parameters, a low-pass filter has inductor and capacitor values given by

$$L(n) = \frac{g(n) \cdot R_0}{2 \cdot \pi \cdot f} \quad \text{Eq 3.1}$$

$$C(n) = \frac{g(n)}{R_0 \cdot 2 \cdot \pi \cdot f} \quad \text{Eq 3.2}$$

where $g(n)$ is the n -th normalized value from the table, R_0 is the terminating resistance in Ω , f is frequency in Hz, $L(n)$ is the n -th inductor in Henries, and $C(n)$ is the n -th capacitor in Farads.

The first part can be an L or C. If the first part is an inductor, the second one will be a capacitor, the third another inductor, and so forth. Both forms generate the same resulting transfer function.

Consider an example, a 4-th order Butterworth low-pass filter. The normalized values from the table are $g(1)=0.7654$, $g(2)=1.85$, $g(3)=1.85$, and $g(4)=0.7654$. Let's design this filter for a 3-dB cutoff of 10 MHz with a termination of 50Ω at each end. The filter will begin with an inductor. Hence,

$$L(1) = \frac{0.7654 \cdot 50}{2 \cdot \pi \cdot 10 \cdot 10^6} = 0.609 \cdot 10^{-6}$$

$$C(2) = \frac{1.85}{50 \cdot 2 \cdot \pi \cdot 10 \cdot 10^6} = 5.889 \cdot 10^{-10}$$

$$L(3) = 1.472 \cdot 10^{-6}$$

$$C(4) = 2.436 \cdot 10^{-10}$$

The resulting filter is shown in Fig 3.7A while the dual form, the variation beginning with a shunt capacitor, is presented in Fig 3.7B.

The filter example picked for Fig 3.7 was a special case, an even ordered design. As such, the dual filter, which is the one starting with the alternative component type, is really the same filter, but with the input and output exchanged. If we had picked an odd order filter to illustrate the two filter types, we would have filter (A) with more capacitors than inductors while (B) would be dominated by inductors.

The denormalization equations are simple and easily programmed in a spreadsheet, a programmable calculator, or in any popular computer language.

What might be the obvious route to a filter design may not be the most practical. The logical sequence calculates the values, purchases and or builds the components, and then assembles the circuit. Inductors are not a problem, for the user

can pick a number and position of turns as needed to realize a required value. But capacitors tend to come only in standard values. The non-standard values can be synthesized with parallel combinations of capacitors, although this often leads to bulkier and more expensive circuitry than desired, and parallel capacitors lead to additional resonances. An alternative route is:

- Design an initial low-pass filter.
- Analyze the filter to confirm that the desired response is realized. Computer programs such as *GPLA* or *ARRL Radio Designer*² work well. Other analysis programs are often found on the Web.
- Substitute available capacitors for those calculated in the design phase and analyze the results.
- Adjust inductor values to "fix" variations that might have occurred as a result of using practical capacitors.

Most low-pass filters, especially the simple Butterworth and Chebyshev designs, are insensitive to small component value changes. Slight adjustments toward practical values will often have so little impact that there will be no need for additional adjustments. If a refined program is used for design, it is easy to vary the filter order and ripple to obtain a desired response, especially in a low-pass filter.

The radio experimenter will often use a low-pass filter at a transmitter output, for a low pass will attenuate harmonics, the predominant distortions created in the output stages. An ideal low-pass filter, however, is not required. Rather, the need is for a filter that will attenuate harmonics and will pass a relatively narrow band of

frequencies. The required passband is often no more than 10 or 20% in width. It is not necessary to do a good job at very low frequencies. Chebyshev or Butterworth filters may not be the best choices.

An interesting, and often practical filter type is the almost unknown ultra-spherical low-pass filter.^{3,4} An ultra-spherical filter is like the Chebyshev to the extent that it has passband ripples. However, the

Half-Wave Filter

The popular half-wave filter is a very tolerant low-pass filter form. L and C have a reactance equal to the terminating resistance. The middle capacitor is twice that at the ends. This filter, a low pass, is designed at the operating frequency rather than a cutoff. This filter will have a 3-dB cutoff that is about 40% above the design frequency and only offers about 25-dB attenuation at the second harmonic. A 7-MHz half-wave filter will use $L=1.1 \mu\text{H}$ and $C=450 \text{ pF}$ when designed for $R=50 \Omega$. This filter will have a phase shift of 180 degrees at the operating frequency; hence, the circuit name.

$$R_S = R_{\text{Load}}$$

$$X_L = X_C = R_S$$

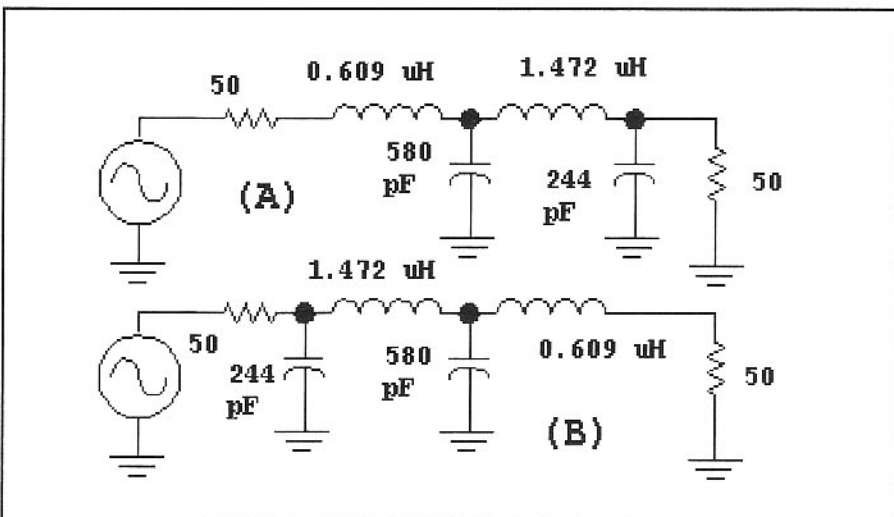
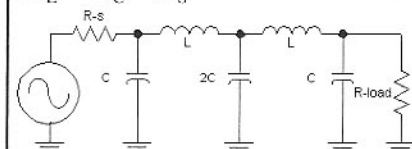
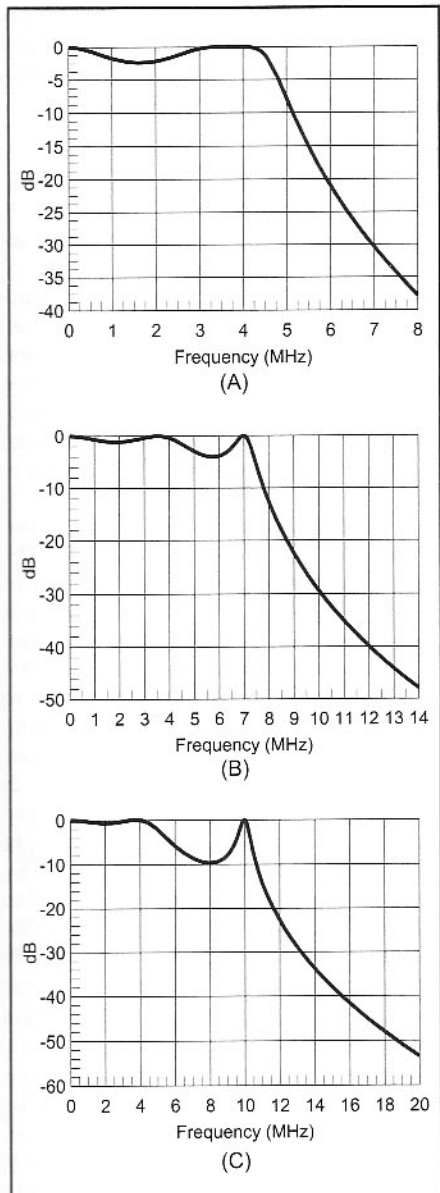


Fig 3.7—Two forms of a 4th-order, 50- Ω , doubly-terminated, 10-MHz cutoff Butterworth low-pass filter.

Table 3.1

Normalized Values for Butterworth and Chebyshev Low-Pass Filters. These are used with the Low Pass and High-Pass de-normalization equations. All of the data presented are for doubly terminated filters. Butterworth filters are designed on the basis of a 3-dB cutoff while a ripple cutoff is used for the Chebyshev filters.

Type	N	g(1)	g(2)	g(3)	g(4)	g(5)	g(6)	g(7)
Butterworth	2	1.414	1.414					
	3	1	2	1				
	4	0.7654	1.85	1.85	0.7654			
	5	0.618	1.618	2	1.618	0.618		
	6	0.5176	1.414	1.932	1.932	0.5176		
	7	0.445	1.247	1.802	2	1.247	0.445	
	8	0.39	1.11	1.66	1.66	0.39	1.11	
.01 dB Chebyshev	3	0.6292	0.9703	0.6292				
	5	0.7563	1.305	1.577	1.305	0.7563		
	7	0.797	1.392	1.748	1.633	1.748	1.392	0.797
0.1 dB Chebyshev	3	1.032	1.147	1.032				
	5	1.147	1.371	1.975	1.371	1.147		
	7	1.18	1.423	2.097	1.573	2.097	1.423	1.18



ripples are not necessarily of equal magnitude. The Chebyshev filter is a special case of the ultra-spherical. The transfer function for three variations of the ultra-spherical filter is shown in Fig 3.8. All of these 5th-order filters are designed at the highest peak frequency rather than at a cutoff frequency. Eq 3.1 and Eq 3.2 still apply. The $g(n)$ values are shown in Table 3.2.

Fig 3.8A shows what we might call a wide ultra-spherical filter, a circuit with about a 20% bandwidth for 0.2-dB variation, yet having stopband characteristics like those of a very high ripple Chebyshev low pass. This example circuit was configured for complete coverage of the 3.5-4 MHz band.

Fig 3.8B shows a medium width ultra-spherical filter. The main virtue of this circuit is the extreme flexibility offered with regard to component value. The price of this is the need for an adjustable element in the middle of the filter. This is especially suited to junk box driven projects. The example is a filter for a 7-MHz transmitter. The end capacitors might, in practice, be 1200-pF silver mica while the middle capacitor could be a 1000-pF part paralleled with a 200-pF mica trimmer.

with a 200-pF mica trimmer.

Fig 3.8C presents the result of a narrow ultra-spherical filter. This circuit has a peak 3-dB bandwidth of about 200 kHz at 10 MHz while offering 54-dB attenuation at the 2nd harmonic of the peak.

While the ultra-spherical filters offer band-pass filter like performance with low-pass stopband characteristics, they can also suffer from high loss with low-Q components. They should be analyzed or measured when applied to narrow band applications.

High Pass Filters

The low-pass filter is the basis for this section; it is the cornerstone that supports all other passive LC filters. Occasionally, a high-pass filter is required in a piece of equipment. A high pass has a passband that extends upward from a cutoff frequency. The stopband of a high pass is below the cutoff.

Once we have a set of normalized low pass tables, designing a high-pass filter is an easy extension. The conceptually easy approach is a two-step process: Having picked a cutoff frequency, a low pass of

Fig 3.8—(A)We might call this a wide ultra-spherical filter, a circuit with about a 20% bandwidth for 0.2-dB variation, yet having stopband characteristics like those of a very high-ripple Chebyshev low pass. This example circuit was configured for complete coverage of the 3.5-4 MHz band. (B) A medium width ultra-spherical filter. The main virtue of this circuit is the extreme flexibility offered with regard to component value. The price of this is the need for an adjustable element in the middle of the filter. This is especially suited to junk box driven projects. The example is a filter for a 7-MHz transmitter. The end capacitors might, in practice, be 1200-pF silver mica while the middle capacitor could be a 1000-pF part paralleled with a 200-pF mica trimmer. (C) The result of a narrow ultra-spherical filter. This circuit has a peak 3-dB bandwidth of about 200 kHz at 10 MHz while offering 54-dB attenuation at the 2nd harmonic of the peak.

Table 3.2

Normalized Ultra-spherical low-pass filter data.

Case	$g(1)$	$g(2)$	$g(3)$	$g(4)$	$g(5)$
Wide U.Sp.	1.759	0.704	2.352	0.704	1.759
Medium U.Sp.	2.717	1.087	2.56	1.087	2.717
Narrow U.Sp.	3.456	1.382	1.787	1.382	3.456

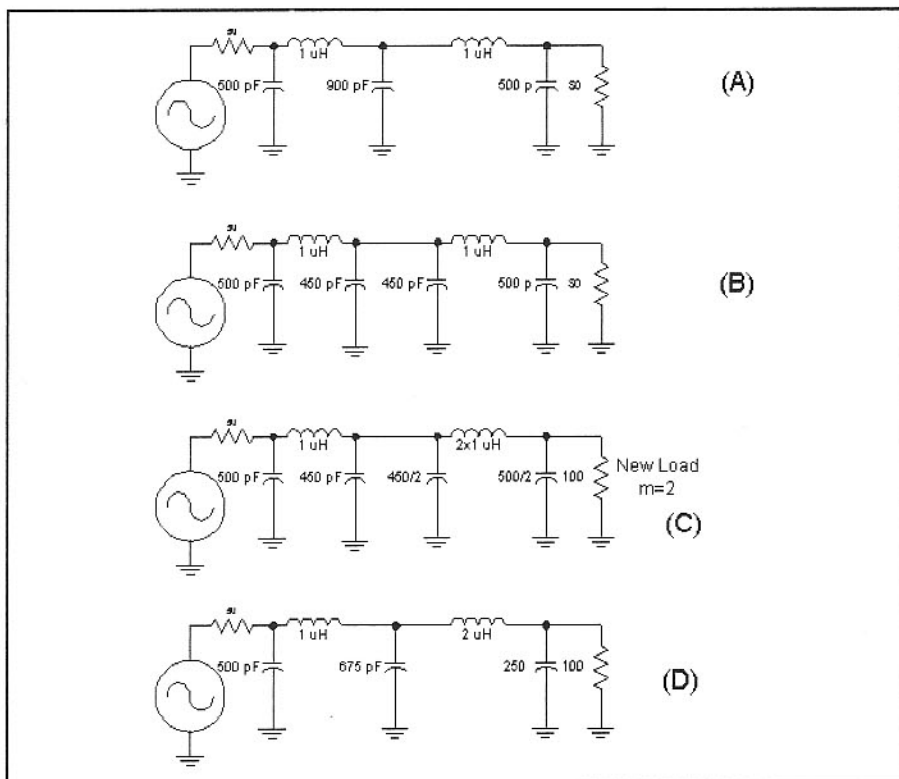
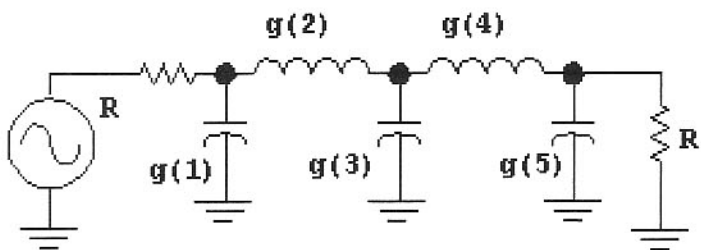


Fig 3.9—Low-pass filter illustrating Bartlett's Bisection Theorem that allows a termination to be changed to a new value.

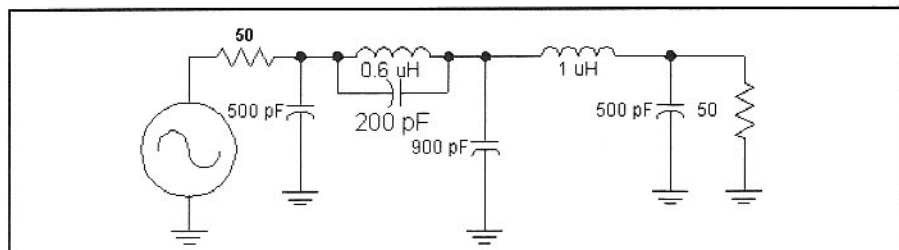


Fig 3.10—Changing an inductor to a "trap" creates a frequency of very high attenuation in the stopband.

the desired order and shape is designed. Then, each low-pass element is replaced with a high-pass one that has the same reactance at the cutoff. Series inductors are replaced with series capacitors; shunt capacitors become shunt inductors.

Alternatively, the tables of $g(n)$ values may be used directly for high-pass filter design. The viable equations are then

$$C(n) = \frac{1}{g(n) \cdot R_0 \cdot 2 \cdot \pi \cdot f} \quad \text{Eq 3.3}$$

$$L(n) = \frac{R_0}{2 \cdot \pi \cdot f \cdot g(n)} \quad \text{Eq 3.4}$$

where $g(n)$ are the normalized low-pass elements from Table 3.1, R_0 is the terminating resistance and f is frequency in Hz. The inductance value, $L(n)$, is in Henrys and capacitance, $C(n)$, is in Farads.

As with the low-pass filters, once a high-pass filter is designed, it should be confirmed with some appropriate calculations and, later, measured after construction.

Some Simple Transformations

There are several circuits that can be designed with relative ease once a low pass or high-pass filter is in place. Some will be discussed here, for they offer considerable flexibility and opportunity to the experimenter.

We often need different terminations at filter ends. A method for doing this is provided by the Bartlett's Bisection Theorem, illustrated in the low-pass filter shown in Fig 3.9.

The first filter, shown in Fig 3.9A, is a symmetric 50-Ω 5th-order low pass. The filter is a low pass with a 3-dB cutoff of about 10 MHz. This filter is redrawn in part B with the filter split in the mid point. The two half sections are identical. We wish to change the output termination to 100 Ω while preserving the same filtering characteristics. The ratio of the new termination, 100 Ω, to the original 50 Ω is 2. The filter is transformed by increasing series elements (the L) by $m=2$ in the right side. The shunt elements are decreased by the same factor of m . This is illustrated in Fig 3.9C with the final filter in Fig 3.9D. The multiplier m can be any value greater than 0.5. This method is used later in the book in the design of some filters for a SSB transceiver.

The next filter modification that we consider adds capacitors or inductors to a filter. This scheme is used in the design of elliptic, or Cauer-Chebyshev low-pass filters where adding components that create

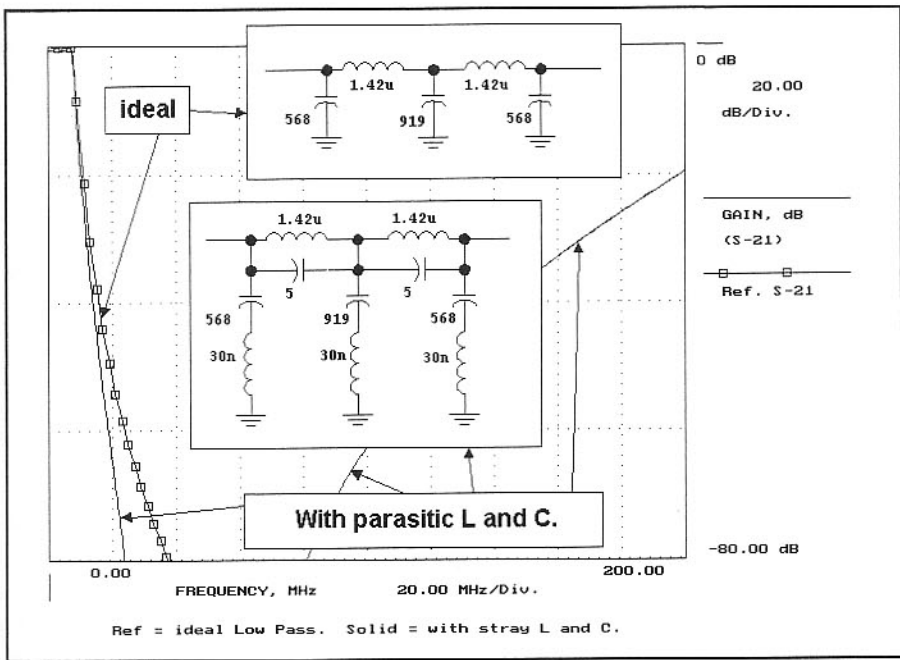


Fig 3.11—The VHF performance of HF low-pass filters is significantly altered by parasitic inductance and capacitance. The parasitic elements are modeled as being larger than normal to illustrate the effects.

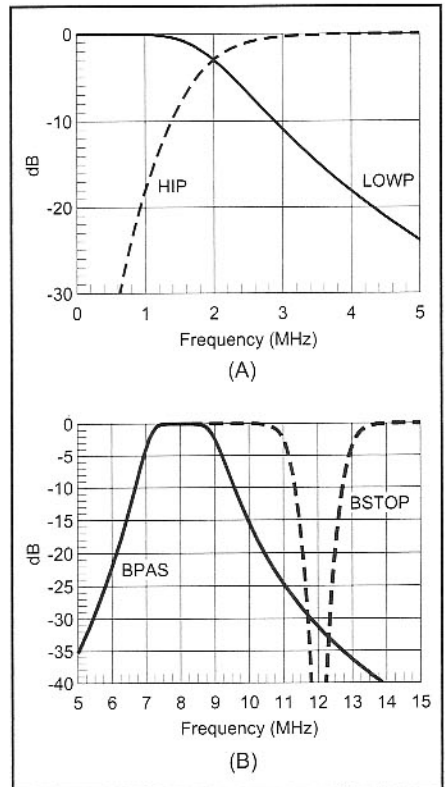


Fig 3.13—Transfer functions for the low pass and high pass (A) and the bandpass and bandstop filters (B).

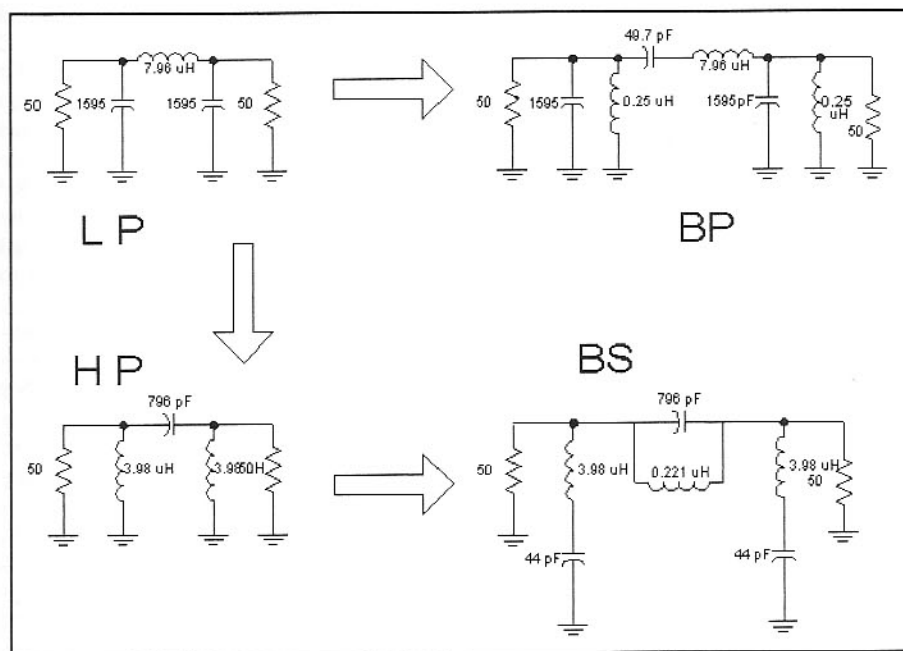


Fig 3.12—A low-pass filter (LP) is the prototype for the high pass (HP). The components in the low pass may be resonated to produce a bandpass (BP) filter with a bandwidth equaling the original low pass. Similarly, the high-pass elements are tuned to produce a bandstop filter (BS) with a 3-dB notch width equaling the bandwidth of the high pass.

“trap” frequencies alters the stopband of a filter. This is illustrated in Fig 3.10 where a low-pass filter is modified. The first inductor, originally a 1- μ H unit, is paralleled with a 200-pF capacitor. The inductor is reduced to 0.6 μ H so the LC combination will have approximately the same reac-

tance at the filter cutoff frequency.

This “elliptic” modification can be extended by converting both inductors to traps and by adding series inductance with any or all of the shunt capacitors. The modification shown leaves the passband almost unchanged, but increases the

attenuation at 14 MHz. Unfortunately, the attenuation at the higher end of the stopband, above 20 MHz, is not as good as it was with the original low-pass filter; this is typical of elliptic filters. Another disadvantage of the method is that component losses have much greater impact than they did without the traps, especially near the cutoff frequency. All of these changes are easily modeled with computer analysis. Design tables are found in numerous standard filter texts.⁶

The trap characteristics we describe are always present to one extent or another, even when they are not featured. Assume we needed a low-pass filter to follow a 7-MHz transmitter. A 5th-order circuit was designed for a 0.2-dB ripple Chebyshev shape with a 7.5-MHz ripple cutoff frequency. The designed filter is the “ideal” circuit in Fig 3.11 with response shown as the “reference.” The analysis is extended out to 200 MHz. The other circuit in the figure includes the “accidental” effects of parallel capacitance across the inductors and inductance in series with the capacitors. Both improve the steepness of the rolloff. But they both contribute to a severely degraded VHF stopband attenuation.

The next transformation we consider resonates the elements of low pass and high-pass filters. We begin by designing a

3rd-order low pass with a cutoff of 2 MHz. A similar 2-MHz high pass is designed; the filters are shown in Fig 3.12. Once the low and high-pass circuits are in place, each element is resonated. The three-element low pass maps into a 6-component bandpass filter. The new filter is centered at the resonance frequency, here 8 MHz,

with the 2-MHz bandwidth of the parent low pass. This method is generally limited to wide bandwidths, perhaps 20% or more. Impractical component values are sometimes avoided by terminating the filter in resistances greater than 50 Ω.

A similar transformation is applied to the high-pass filter, resulting in a bandstop

filter. A frequency of 12 MHz was picked for this example. The same restrictions that accompanied the wide bandpass filter apply to this design.

The transfer function for the low pass and high pass are given in Fig 3.13 along with the response for the bandpass and band stop.

3.3 LC BANDPASS FILTERS

The LC bandpass filter is a critical function in determining the performance of a typical RF system such as a receiver. An input filter, usually a bandpass, restricts the frequency range that the receiver must process. A later IF filter determines the overall receiver bandwidth. This filter often uses crystals, although LC filters were popular in older receivers. Audio filters often use LC elements, although RC active circuits, or the computational abilities of digital signal processing add further selectivity and confine the noise to a desired spectrum.

The LC filters we discuss in this section are narrow with a bandwidth from 1 to 20 % of the center frequency. Even narrower filters are built with resonators with higher Q; the quartz crystal is an example that will be discussed later where bandwidths of less than a part per thousand are possible. The basic concepts that we examine with LC circuits will transfer to the crystal filter.

Losses in Filters and Q

The key elements in narrow filters are tuned circuits made from inductor-capacitor pairs, quartz crystals, or transmission line sections. These resonators share the properties that they store energy, but they have losses. A chime is an example. Striking the chime with a hammer produces the waveform of Fig 3.14. A parameter called Q, for quality factor, describes the rate that the amplitude decreases with time after the hammer strike. The higher the Q, the longer it takes for the sound to disappear. The oscillator amplitude would not decrease if it were not for the losses that expend energy stored in the resonator. The mere act of observing the oscillation will cause some energy to be dissipated.

The chime was an acoustic resonator, but the same behavior occurs in electric resonators. A pulse to an LC causes it to ring; losses cause the amplitude to diminish. The most obvious loss in an LC

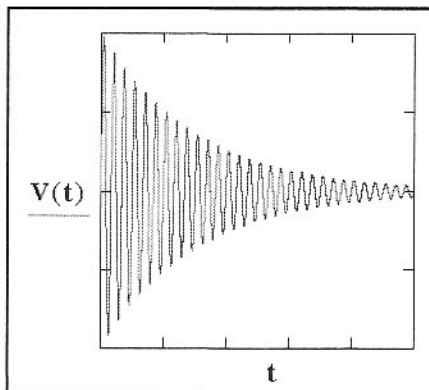


Fig 3.14—The amplitude of a chime's ring after being struck by a hammer. Units are arbitrary.

circuit is conductor resistance, including that in the inductor wire. This resistance is higher than the dc value owing to the skin effect, which forces high frequency current toward the conductor surface. Other losses might result from the motion of magnetic regions in an inductor core or the movement of dielectric parts of a capacitor.

An inductor is modeled as an ideal part with a series or a parallel resistance. The resistance will depend on the Q if the inductor was part of a resonator with that quality. The two resistances are shown in Fig 3.15.

$$R_{\text{Series}} = \frac{\omega \cdot L}{Q} \quad \text{Eq 3.5}$$

$$R_{\text{Parallel}} = Q \cdot \omega \cdot L$$

The higher the inductor Q, the smaller the series resistance, or the larger the parallel resistance is needed to model that Q. It really does not matter which component is used.

The Q of a resonator is related to the bandwidth of the tuned circuit by

$$\text{BW} = \frac{f_C}{Q} \quad \text{Eq 3.6}$$

where f_C is the tuned circuit center frequency. This Q is also that of the inductor in a tuned circuit if the capacitor is lossless.

The single tuned circuit is presented in two different forms in Fig 3.16. In the top, a parallel tuned circuit consisting of L and C has loss modeled by three resistors. The one labeled by R_p is the parallel loss resistance representing the non-ideal nature of the inductor. (Another might be included to represent capacitor losses.) But the LC is here paralleled by three resistors: the source, the load, and the loss element. R_p would disappear if the tuned circuit was built from perfect components. The source and load remain; they represent the RF world where a source resistance must be present if power is available and a load resistance must be included if power is to be extracted.

Eq 3.5 and **Eq 3.6** can be applied in several ways. If the resonator is evaluated with only the intrinsic loss resistance (in either series or parallel form) the resulting Q is called the unloaded Q, or Q_u . If, however, the net resistance is used, which is the parallel combination of the load, the source, and the loss in the parallel tuned circuit, the resulting Q is called the loaded value, Q_L . If we were working with the series tuned circuit form, the loaded Q would be related to the total series R.

Consider an example, a parallel tuned circuit (Fig 3.16 top) with a 2-μH inductor tuned to 5 MHz with a 507-pF capacitor. Assume the parallel loss resistor was 12.57 kΩ. The unloaded Q calculated from Equation 3.5 is 200. The unloaded bandwidth would be $5 \text{ MHz} / 200 = 25 \text{ kHz}$.

Assume that the source and load resistors were equal, each 2 kΩ. The net resistance paralleling the LC would then be the combination of the three resistors, 926 Ω. The loaded Q becomes 14.7 with a loaded bandwidth of 339 kHz. The loaded Q is

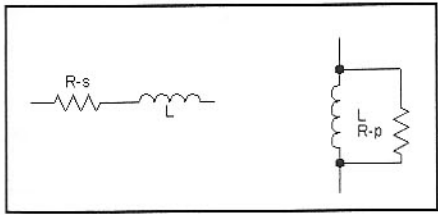


Fig 3.15—Inductor Q may be modeled with either a series or a parallel resistance.

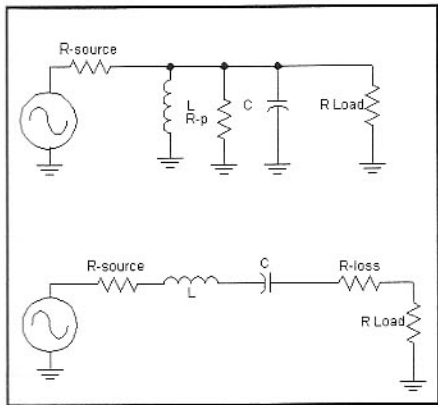


Fig 3.16—Two simple forms of the single tuned circuit.

also called the filter Q, for it describes the bandwidth of the single tuned circuit, the simplest of bandpass filters.

This filter has an insertion loss. This is illustrated in Fig 3.17, which shows the filter without the L and C, effects that cancel at resonance. We use an arbitrary open circuit source voltage of 2. The available power to a load is then 1 V across a resistance equaling the 2-kΩ source. If the resonator had no internal losses, this available power would be delivered to the 2-kΩ load. However, the loss R parallels the load, causing the output voltage to be 0.926 V, a bit less than the ideal 1 V. Calculation of the output power into the 2-kΩ load resistance and the available power shows that the insertion loss is 0.67 dB.

This exercise illustrates two vital points that are general for all bandpass filters. First, the bandwidth of any filter must always be larger than the unloaded bandwidth of the resonators used to build the filter. Second, any filter built from real world components will have an insertion loss. The closer the Q of the filter approaches the unloaded resonator Q, the greater the insertion loss becomes.

A parallel tuned circuit illustrated these ideas; the series tuned filter would have produced identical results. Generally, the insertion loss of a single tuned circuit relates to loaded and unloaded Q by

$$IL (\text{dB}) = -20 \cdot \log \left(1 - \frac{Q_L}{Q_U} \right) \quad \text{Eq 3.7}$$

The Q of a tuned LC circuit is easily measured with a signal generator of known output impedance, R_0 , and a sensitive detector, again with a known impedance level, often equaling the generator R_0 at 50 Ω. The test-set is shown in Fig 3.18. The test setup of Fig 3.18 uses equal loads of value R_0 and equal capacitors to couple from the terminations to the resonator. Equal capacitors, C_1 and C_2 guarantees that each termination contributes equally to the resonator parallel load resistance. The voltmeter across the load is calibrated in dB.

To begin measurement we remove the tuned circuit and replace it with a direct connection from generator to load. The available power delivered to R_0 is calculated after the voltage is measured. The resonator is then inserted between the generator and load, and the generator is tuned for a peak. The measured power is less than that available from the source, with the difference being the insertion loss for the simple filter. Capacitors C_1 and C_2 are adjusted until the loss is 30 dB or more. With loss this high, the intrinsic loss resistance of the resonator will dominate the loss.

The generator is now tuned first to one side of the peak, and then to the other, noting the frequencies where the response is down from the peak by 3 dB. The unloaded bandwidth, Δf , is the difference between the two 3 dB frequencies. The unloaded Q is calculated as

$$Q_U = \frac{f_c}{\Delta f} \quad \text{Eq 3.8}$$

This method for Q measurement is quite universal, being effective for audio tuned circuits, simple LC RF circuits, VHF helical resonators, or microwave resonators. The form of the variable capacitors, C_1 and C_2 , may be different for the various parts of the spectrum, but the concepts are general. Indeed, it is not even important how the coupling occurs. The Q measurement normally determines an unloaded value, but loaded values are also of interest when testing filters.

Coupling

Coupling refers to the sharing of energy between resonators. Two resonators in a filter are generally tuned to exactly the same frequency. However, when an element (L or a C) is attached to cause energy in one to be shared with the other, two re-

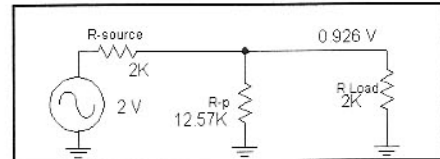


Fig 3.17—Simplified parallel tuned circuit at resonance. The effect of loss is illustrated.

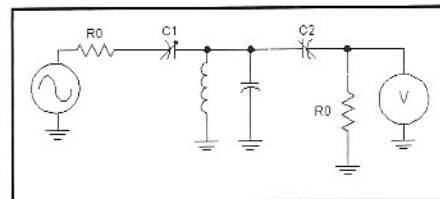


Fig 3.18—Test setup for measuring the Q of a resonator. The source and load are assumed identical. The two coupling capacitors are adjusted to be equal to each other. The output signal is measured with an appropriate ac voltmeter, a high impedance oscilloscope, or a spectrum analyzer.

sponse peaks often appear with frequency separation becoming a measure of the coupling. This is illustrated with the circuit of Fig 3.19, which results in the curves of Fig 3.20.

The frequency separation between peaks is a measure of the coupling between the resonators. The utility of this parameter is in the measurements that become possible. The filter designer needs only to generate a method for coupling to produce a desired frequency difference in order to realize a given filter. Such measurements (or calculations) are a vital part of building filters with unusual tuned circuits, such as UHF helical resonators. A natural extension of this measurement is a collection known as the Dishal Method.⁷ The Dishal method is extremely useful in the adjustment of multiple resonator filters. The method is discussed further in *Introduction to Radio Frequency Design* and in Chapter 9 of Zverev's text.

Multiple Resonator Bandpass Filters

Bandpass filters with several tuned circuit are designed with relative ease with careful application of some basic steps:

The resonators must have an unloaded Q that is higher, usually by a factor of 3 or more, than the desired filter Q, which is $f_c/\Delta f$ where f_c is center frequency and Δf is bandwidth.

A filter shape (e.g., Butterworth or

0.2- dB Chebyshev, etc) is defined by the loaded Q of end resonators and by coupling between resonators.

These end Q values and coupling values between resonators are obtained from normalized tables of k and q . Some values for double and triple tuned filters are given in **Table 3.3**.

Bandpass filter design with normalized coupling and loading uses k and q tables. These are directly related to the normalized g_K values used for low-pass filter design. The g_K data is useful for quickly estimating the insertion loss of virtually any bandpass filter we might design. The loss in dB is

$$\text{Loss (dB)} = 4.34 \cdot \frac{F}{Q_U \cdot B} \cdot \left(\sum_k g_k \right)$$

where F , B , and Q_U were defined above. The g_K values are the normalized low-pass elements for the shape in question. Assume that we wish to build a 4th order bandpass filter with a 0.1-dB Chebyshev shape. The low pass parameters are $g1=1.109$, $g2=1.306$, $g3=1.77$, and $g4=0.818$. The sum of the elements is then 5.003. If we were going to build this filter at 144 MHz with a bandwidth of 5 MHz and we had managed to build resonators with $Q_U=500$, we would then expect an insertion loss of 1.25 dB. This formula is attributed to Cohn.^{8,9}

The sidebar equations may be used to write a computer or calculator program for designing these circuits. This can then be combined with inductance calculations (for the number of turns on solenoid or toroids, for example) to generate tables of filter designs. This has been done to form **Table 3A** (see sidebar on page 3.14). The inductors used are all wound on toroid cores; the inductance values shown are very close to actual values when the toroids are wound with a single, evenly spaced winding. The Q_U values are approximate, although they are typical of measured data. Larger wire size will increase Q slightly. The data in the table are calculated values, but are typical of those we have built and confirmed on numerous occasions.

Double-Tuned Circuits

The double tuned circuit (DTC) can take on many forms, all showing the same basic shape around the passband so long as they develop the same end section Q values and the same coupling between resonators. A familiar "top coupled" DTC uses a series capacitor to couple terminations to parallel

tuned circuits to set end section Q. Coupling between resonators is established with a small valued capacitor between the "hot" ends of the tuned circuits. The DTC in this form is presented, with design equations, in the sidebar on page 3.14.

Filter shape options are available in the sidebar DTC procedure. The Butterworth is generally a good starting point, for it is easily realized with practical components.

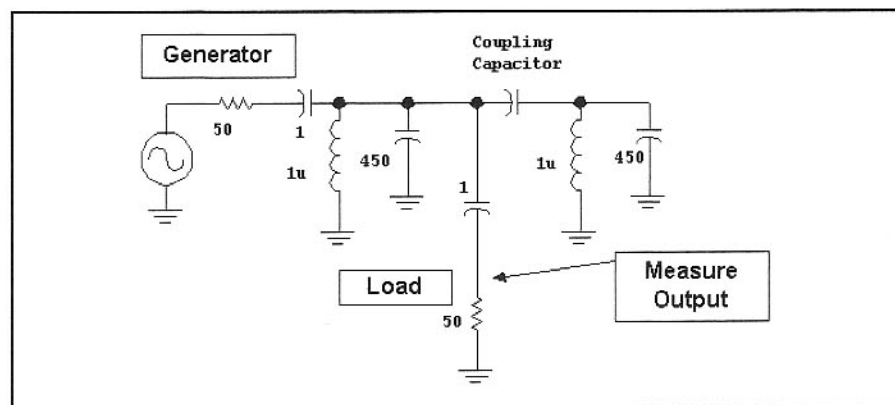


Fig 3.19—Scheme for measuring and defining coupling between two tuned circuits. C12 is either 10 or 20 pF while the resonators are both 1μH paralleled with 450 pF. "Probe" capacitors are 1 pF.

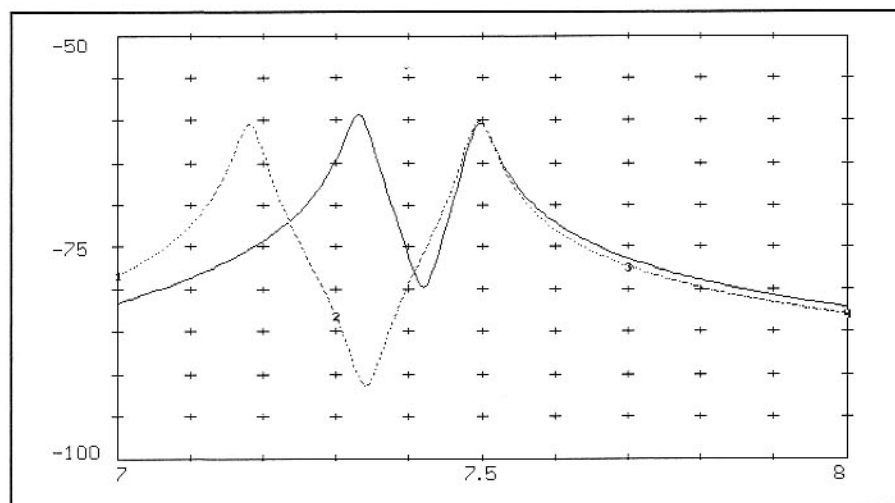


Fig 3.20—Separation of response peaks indicating coupling between two resonators. The solid line uses a 10-pF coupling capacitor while the dotted line uses 20 pF.

Table 3.3

***k* and *q* Values for Two- and Three-Pole Filters**

Passband Ripple, dB	<i>n</i>	<i>k</i>	<i>q</i>
Butterworth	2	0.7071	1.414
0.1 dB	2	0.7107	1.638
0.25	2	0.7154	1.779
0.5	2	0.7225	1.9497
0.75	2	0.7290	2.091
1.0	2	0.7351	2.3167
1.5	2	0.7466	2.452
Butterworth	3	0.7071	1.000
0.1	3	0.6617	1.4328
0.25	3	0.6530	1.6330
0.5	3	0.6474	1.8640
0.75	3	0.6450	2.0498
1.0	3	0.6439	2.2156
1.5	3	0.6437	2.5169

The Triple-Tuned Filter

While the ever-popular double-tuned circuit is often adequate, there are many cases where more performance is needed. The third-order bandpass is a special case, easily designed with the same equation (and hence, software) used for a double-tuned circuit. This possibility emerges if you compare a double-tuned circuit with the example triple-tuned circuit shown in **Fig 3.21**. This particular filter is centered at 16.2 MHz with a design bandwidth of 0.5 MHz. **Fig 3.22** shows the response of the triple-tuned filter, along with that of a double-tuned circuit built with the same inductors.

The triple-tuned filter is designed with different k and q values than used for a double-tuned circuit. Set $q=1$ and $k=0.707$ for a triple tuned Butterworth filter. Then, the coupling capacitors and the end matching capacitors are the values provided by the sidebar equations. The last equation in that series provides the tuning capacitor values for the end sections. The middle tuning capacitor is given by

$$C_M = C_0 - 2 \cdot C_{12} \quad \text{Eq 3.9}$$

Building a triple-tuned filter is no more difficult than one with two resonators. If it is designed for a slightly wider bandwidth than might be used with a 2-pole design, the filter is often easier to align, has similar insertion loss, and offers improved stopband attenuation, the usual primary goal of bandpass filtering.

The design of higher order ($N > 3$) bandpass filters is similar to the DTC. Coupling between resonators (numbered m and n) is described by a normalized coupling coefficient, k_{mn} . The values will generally differ for each pair of resonators. End loading, perhaps different for the two ends, is described by normalized end section q values, q_1 and q_n for a filter with n resonators. Denormalization establishes loaded end Q values that are then established as with the DTC. The individual parallel-tuned circuits are individually tuned to the filter center frequency with all other parallel resonators short-circuited. A calculator or computer program written for the design of double-tuned circuits may often be used, without modification, for the design of higher-order filters.

The bandpass filters examined so far used parallel tuned circuits. Series resonators may also be used. This variation is shown in **Fig 3.23** with the design procedure given in the literature.

With either form, values for normalized k and q are obtained from a table of values such as those published in the classic book

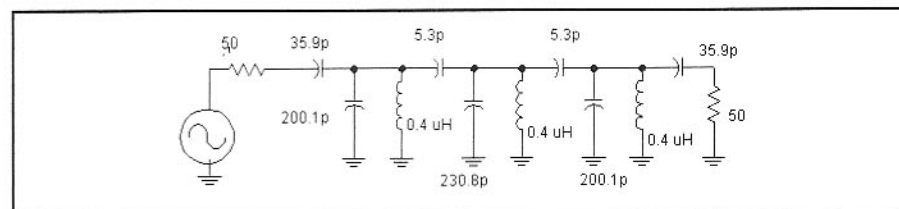


Fig 3.21—A triple-tuned circuit centered at 16.2 MHz with a bandwidth of 0.5 MHz.

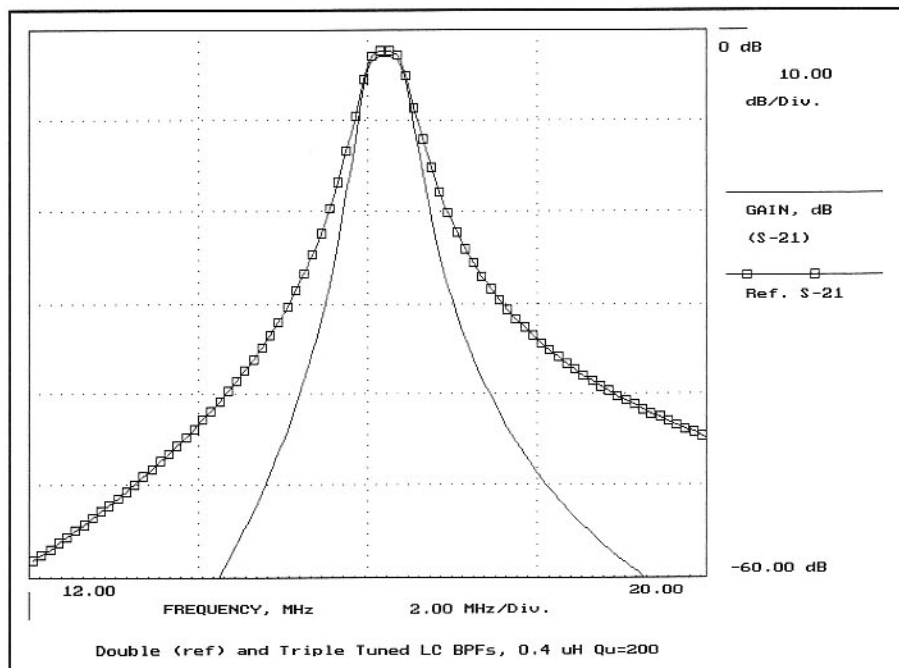


Fig 3.22—Response of triple and double-tuned circuits built with 0.4 mH inductors with $Q_U=200$.

by Zverev. The values may also be calculated in computer programs. Sometimes one encounters tables of predistorted k and q values. Predistortion is a process to retain a desired filter shape, even with losses present.^{10,11,12}

Some filters are mixtures between the forms presented. An example is presented in **Fig 3.24** where the familiar small coupling capacitor is replaced with a shunt capacitor, usually large in value. A small value shunt inductor could also be used.

Filters at VHF and Higher

Bandpass filters are sometimes easier to realize at VHF and above than at lower frequency, the result of higher available resonator Q_U at VHF. Building an air-core coil with a Q of even 200 at 2 MHz requires a considerable volume. However, one with such a Q at 200 MHz can be very small. This results from skin effect changing with frequency.

The book CD includes a tutorial paper on the DTC.¹³ That article outlines methods for experimentally realizing simple bandpass filters at any frequency. The methods outlined there are easily applied to VHF and microwave filters, including those using transmission-line resonators.

Resonators can take on much different forms at higher frequency. One common and popular form is the quarter-wavelength long resonator. This is built by forming a section of transmission line that is just slightly less than 0.25 wavelength. One end is then short circuited while the other is open circuited. The resonator Q will depend upon frequency, geometry, and dielectric material. Air (or vacuum) dielectrics offer highest Q . The conductivity of the surface metal will significantly affect Q . Copper surfaces are excellent, with silver being even better.

Fig 3.25 shows a method for evaluating a transmission line resonator. This is a schematic, yet practical scheme for building filter elements with, for example,

Stopband Attenuation of Bandpass Filters

A 9-MHz bandpass filter required for a mixer experiment was built with available components. A triple-tuned circuit was fabricated from top-coupled parallel tuned circuits. The filter was examined in greater detail after the experiment was finished. While the filter satisfied the immediate need, the performance was far from ideal. A deep notch appeared in the stopband at about 11 MHz. Then what should have been an ideal filter became a disaster with a stopband attenuation of only 40 dB at 40 MHz.

This behavior had been observed earlier in a 7-MHz bandpass filter, shown in **Fig 3A**. The circuit was built on a scrap of circuit board material that was then bolted into an aluminum box. The BNC connectors at each end were "grounded" to the board with short wires from solder lugs under the connector nut. The filter was excited with a signal generator while examining the other end with a spectrum analyzer. We observed that the stopband attenuation improved slightly when a screw driver blade short circuited various spots on the circuit board edge to the aluminum box. This pointed toward grounding as a major problem with this filter.

A new 9-MHz bandpass filter was then built. The components used in the original, which was built like the 7-MHz filter "bad filter," were lifted and used in the new one. But the new circuit was fabricated in a box built from circuit board material (**Fig 3B**). The walls were soldered to the box floor, creating a cleaner ground. One of the long walls was initially left off, easing the filter construction. Filter performance was improved even before the 4th wall was added. The wall was added and the circuit was measured, revealing a stopband null at 43 MHz. The depth was at -110 dBc, near the limits of our measurement capability. The response at 70 MHz, the top of the spectrum analyzer range, was -83 dBc.

A single shield was added to the filter that removed the null and dropped the 70-MHz response to -96 dBc. The filter is shown in the photo "good filter."

The behavior observed is easily modeled with the circuit of **Fig 3C**. The stray coupling, related to ground currents, is modeled by lifting all ground connections in the filter and

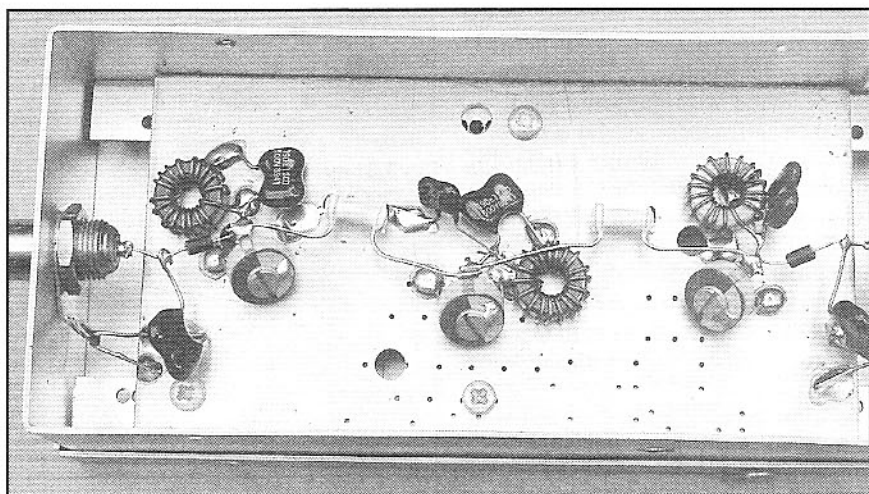


Fig A—Bad filter—This bandpass filter performed well around the 7-MHz passband but had poor stopband attenuation. A very deep attenuation notch appeared at about 15 MHz.

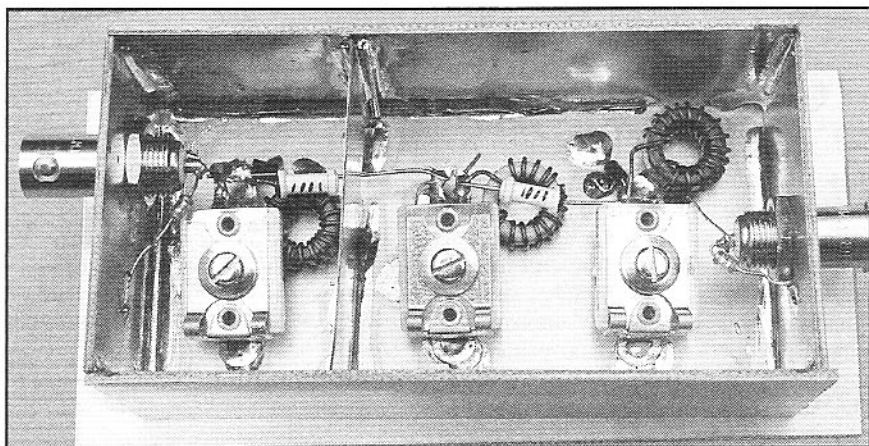


Fig B—Good filter—A box built from scraps of circuit board material produced a response with good stopband attenuation.

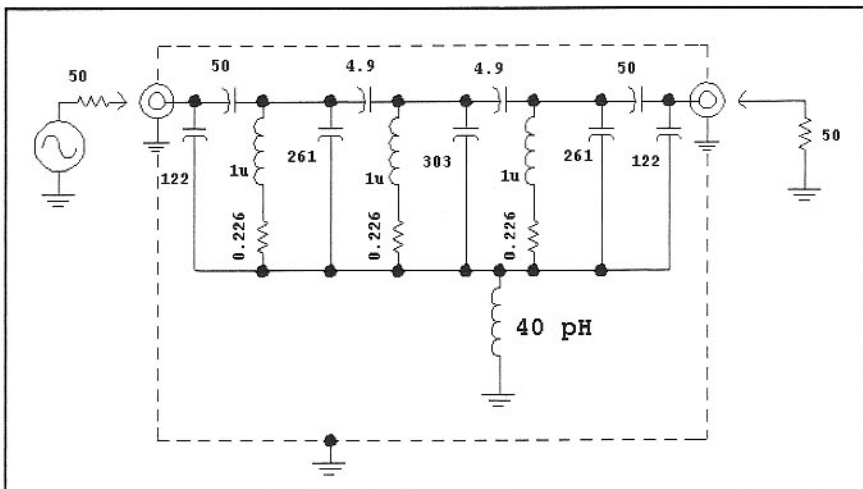


Fig 3C—The traditional bandpass filter is modified with a mutual inductor, raising the bandpass filter above ground. The resistance in series with the 1- μ H inductors represents Qu of 250 at 9 MHz.

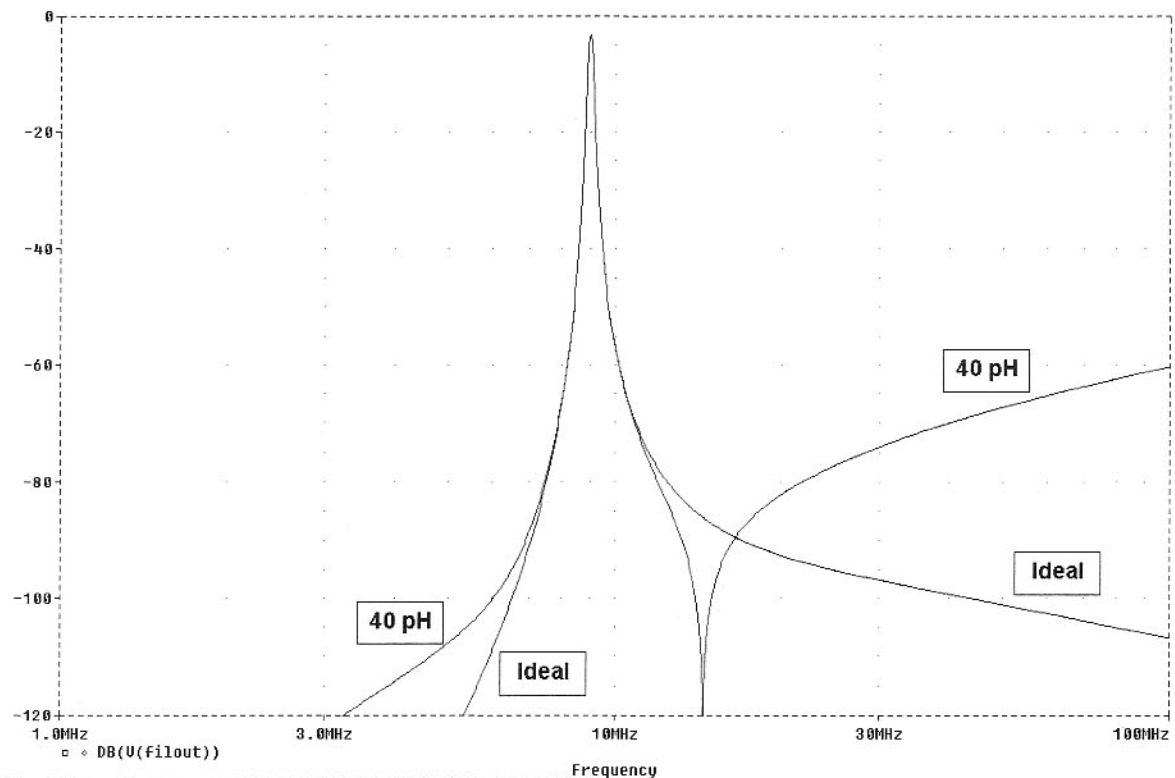


Fig 3D—The response of the ideal filter and that of the mutual coupling inductor are compared. The ideal response was realized in measurement when one shield was added to the filter.

attaching them to a common inductor. An inductance of only 40 pico Henry (yes; pH and not even nH) produced coupling that matched the measured performance. The "before and after" transfer responses are shown in Fig 3D.

Clearly, ground integrity is a vital part of an RF circuit, especially a bandpass filter using high Q resonators. Enclosures fabricated from soldered scraps of circuit board material or similar solid conductor

are ideal, often far superior to aluminum boxes, especially following oxidation. Painted aluminum boxes are even worse. Clearly, measurements should always be performed.

0.141-inch outside diameter semi-rigid coaxial cable like that used in microwave systems. The center conductor is made available at both ends. It is shorted with as little inductance as possible at one end. Then, a 50Ω generator and a 50Ω load with detector are loosely coupled to the "hot" end of the resonator. The coupling capacitors may be nothing more than small pieces of wire spaced a small distance from the high impedance end of the resonator. The couplings from the generator and to the detector should be on opposite sides of the line to reduce direct interaction. The coupling is adjusted for a high insertion loss and the frequency is swept until the center frequency is found. The unloaded

Q is measured by determining the 3-dB bandwidth. Center frequency may be adjusted by adjusting line length.

If a bandpass filter is to be built with the lines, the end section loading may be realized with the scheme shown in Fig 3.26. The "grounded" end of the resonator is attached to a coaxial connector in a ground plane. The center wire is attached to the connector and a short is created with a small inductor consisting of nothing more than a very short wire. The wire length is adjusted to set end section Q . The line shield should be carefully grounded very close to the coaxial connector.

Once proper end section Q is established and resonators are tuned to the proper cen-

ter frequency, a working filter can be built by placing the two close enough to each other that the "hot" ends are in close proximity. This scheme works well for filters for the 432 and 1296-MHz bands. The line sections may be bent to fit available space.

The transmission-line double-tuned circuit just described used semi-rigid coaxial cable. Another common transmission line filter uses so-called hairpin circuits. Micro-strip transmission lines are printed on circuit board material in this filter. The lines are each a half wavelength long and are bent into a "U", or hairpin shape. An example of a hairpin filter with three resonators is shown in Fig 3.27.

The design of these filters is a straight-

DTC Design

Pick a center frequency, F, and a bandwidth, B, both in Hz. Pick an inductor; it can be of essentially arbitrary value, although a good "starting value" would be $L=10/F$ where L is in Henry and F is still in Hz. The unloaded inductor Qu should be approximately known. One must also pick normalized k and q values. For a Butterworth shape, $k=0.707$ and $q=1.414$. For a filter with some passband ripple, but steeper skirts, use 0.25 dB Chebyshev values of $k=0.7154$ and $q=1.779$. The design equations are:

$$\omega = 2 \cdot \pi \cdot F$$

$$C_0 = 1 / (\omega^2 \cdot L)$$

$$C_{12} = C_0 \cdot \frac{k \cdot B}{F}$$

$$Q_E = \frac{q \cdot F \cdot Q_U}{B \cdot Q_U - q \cdot F}$$

$$C_E = \frac{1}{\omega} \cdot \frac{1}{\sqrt{R_0 \cdot Q_E \cdot \omega \cdot L - R_0^2}}$$

$$C_T = C_0 - C_E - C_{12}$$

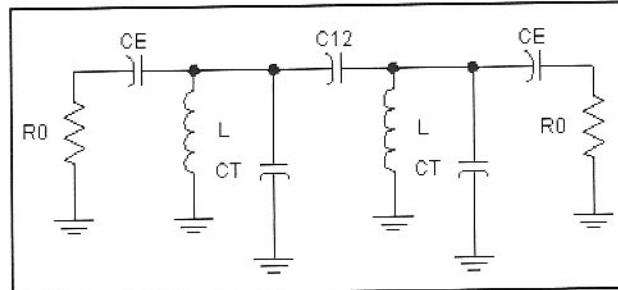


Table 3A

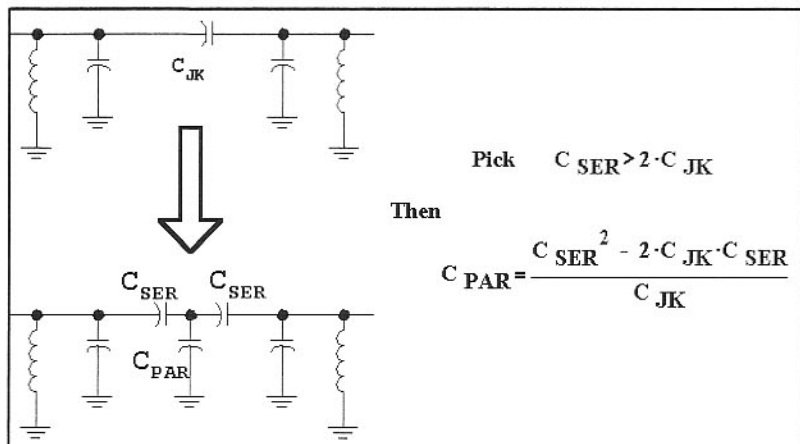
Double Tuned Circuits using the sidebar circuit. All filters are doubly terminated in 50Ω at each end.
The core designators use the copyrighted numbering scheme of Micrometals, Inc.

F-MHz	BW-MHz	Core	Turns	L- μ H	Q-u	C-end	C-12	C-tune
1.85	0.1	T68-2	35	6.98	200	250 pF	41 pF	775 pF
3.55	0.1	T68-2	35	6.98	200	62	5.7	220
3.6	0.2	T68-2	35	6.98	200	93	11	177
3.9	0.2	T68-2	35	6.98	200	79	8.7	152
7.1	0.2	T50-6	17	1.156	250	56	8.7	371
7.05	0.1	T50-6	17	1.156	250	35	4.4	402
7.05	0.1	T50-6	20	1.6	250	30	3.2	286
10.1	0.1	T50-6	17	1.156	250	14	1.5	199
10.1	0.1	T50-6	10	0.4	250	20	4.4	597
14.1	0.2	T50-6	10	0.4	250	21	3.2	295
14.2	0.2	T50-6	10	0.4	250	34	6.3	271
18.1	0.2	T50-6	10	0.4	200	10	1.5	182
21.1	0.2	T50-6	10	0.4	200	6.1	1.0	135
21.25	0.5	T50-6	10	0.4	200	16	2.3	122
25	0.2	T50-6	10	0.4	200	2.9	0.57	98
28.2	0.4	T50-6	10	0.4	150	5.6	0.8	73
28.35	0.7	T50-6	10	0.4	150	9.8	1.4	68
50.2	1.0	T50-6	10	0.4	150	3.5	0.4	21
14.1	0.2	T50-6	5	0.1	200	38.7	12.8	1224
14.1	0.2	T50-6	7	0.196	200	27	6.5	617
14.1	0.2	T50-6	10	0.4	200	19	3.2	296
14.1	0.2	T50-6	15	0.9	200	13	1.4	127
14.1	0.2	T50-6	20	1.6	200	9.5	0.8	69
14.1	0.2	T50-6	25	2.5	200	7.6	0.5	43
14.1	0.2	T50-6	30	3.6	200	6.4	0.36	28.7
14.1	0.2	T50-6	35	4.9	200	5.4	0.26	20.3

Note: Only a couple of core types are needed to cover the entire spectrum from 1.8 to 50 MHz. The last eight table entries describe the same filter, a 14.1-MHz circuit with a 200-kHz bandwidth. The number of turns is allowed to vary, illustrating the freedom available to the filter designer. The builder with a computer program set up for design can vary inductance and bandwidth to realize a desired filter with standard (and junk-box available) component values.

Small Numeric Value Capacitors

Top coupled LC bandpass filters often use capacitors with small numeric value. These are becoming increasingly difficult to obtain. However, a simple substitution will provide the same coupling, but with larger more convenient values, picked with the equations shown. For example, assume a filter design calls for a capacitor with $C_{JK}=1.2\text{ pF}$. The substitute network can use any value of C_{SER} that is greater than 2.4 pF . Assume we use series capacitors of 10-pF value. The parallel capacitor is then $C_{PAR}=63.3\text{ pF}$. A practical value would be either 56 or 68 pF . The new network will have an equivalent parallel component at each end; you must reduce the capacitance that tunes the resonators accordingly.



forward chore with a modern computer, although it's a job for professional-level microwave simulation software.

The total length of each section is 0.5 wavelength for proper tuning. The two end sections are usually identical. The lengths of the end sections are $2(X4) + X5$ while that for the middle section is $2(X4) + X3$. End section loading is determined by $X2$, essentially the spacing from the center of the end resonators, a virtual ground point. Coupling between resonators is established across the "gap" shown in Fig 3-27, analyzed by considering the overlapping sections as directional couplers. It is important for the computer analysis to include the junctions to the $50\text{-}\Omega$ lines (Tee junctions) and a proper model for the open line ends. The designer must also have good information about the board material including loss, dielectric constant, and thickness between the pattern layer and the ground foil below.

The hairpin filter is generally a lossy structure when built on conventional circuit board materials used by amateurs. This material generally has a loss tangent of $.02$, producing resonator Q of 50 . As such, narrow filters are not possible. Hairpin filters generally have 10 to 20% bandwidth unless built on some of the more exotic materials.

Hairpin filters have responses at harmonics frequencies. A half wave resona-

tor is resonant at frequencies where the line is $1, 2, 3$, etc wavelengths long.

Another popular structure for higher frequencies is the helical resonator. These were very popular for UHF FM mobile radios of just a few years ago. A helical resonator is a section (usually one quarter wavelength) of line using a helical transmission line. A helical line is a solenoid coil-like structure placed inside a shielded enclosure. We can think of a wave as propagating along the wire at the speed of light. Hence, the propagation velocity parallel to the axis is much less than that of light. This is a slow wave structure. Cutting a quarter wavelength section, grounding one end with the other open circuited, forms a resonator. The usual helical resonator is just under a quarter-wavelength long. The extra length required for resonance is compensated by adding a small adjustable capacitor to the end, often nothing more than a grounded metal screw close to the "hot" end of the center conductor.

Numerous review articles have appeared describing the helical resonator and filters using them. Equations are often given for resonator dimensions, an implication that they must conform to a well-defined structure. Generally, there is much greater freedom available to the builder. A helical filter may still work well if built in a volume that is "too small."

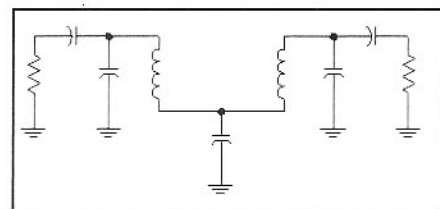


Fig 3.24—Double-tuned circuit with a shunt capacitor for coupling between resonators. This illustrates one of numerous bandpass filter topologies that are mixtures of the two methods presented.

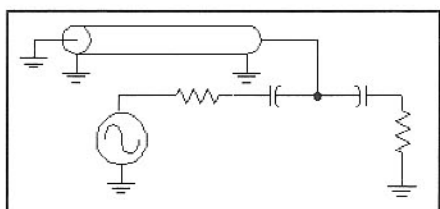


Fig 3.25—A quarter wavelength of transmission line forms a resonant tuned circuit.

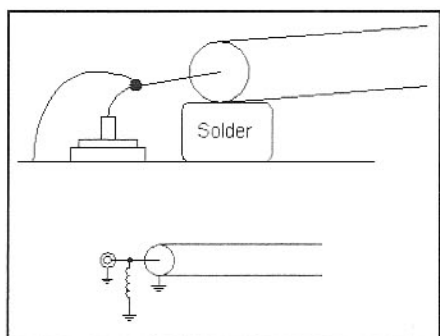


Fig 3.26—Loading (coupling to the "outside world") can be controlled with small wire inductors.

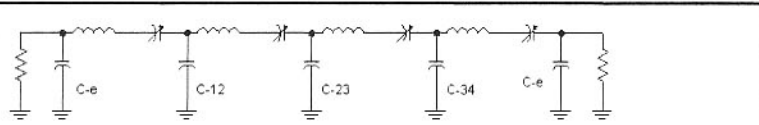
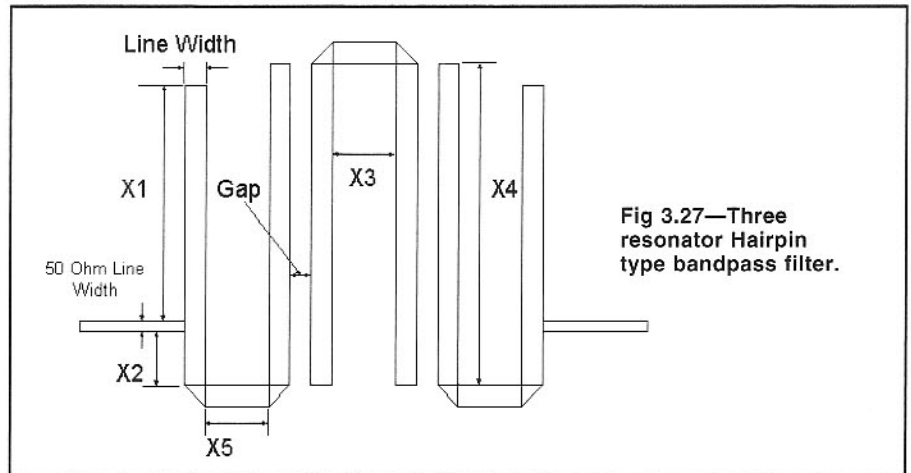


Fig 3.23—Bandpass filter using series tuned circuits. In this example, $N=4$.

A casual glance may not reveal a true identity. That is, a helical resonator with a tuning capacitor looks like a shielded LC resonator. However, the difference becomes clear if wideband measurements are done with loosely coupled probes like the ones that have been described for Q measurement. Such measurements will show a high Q at the fundamental frequency and additional responses (also having high Q) at 3, 5, and other odd harmonics of the fundamental. In contrast, a pure LC resonator will not show these departures. If capacitance is added to a helical resonator to decrease fundamental frequency, the higher frequencies will not move as fast. Slight capacitive loading might move the first "spurious response" to 4 F0 with greater departure as loading grows. Q remains high and excellent filters can still be built.

Helical resonators are coupled to each other with a variety of methods, although the most popular is through apertures, or holes in the walls between adjacent resonators. As with other filter types, the coupling can be related to the frequency spread between peaks when the resonators are unloaded. End section loading is realized in a variety of ways with helical resonators. A small line from a coaxial connector can be tapped onto the helix. The



usual tap point is very close to the grounded end, often a small fraction of one turn. Again, the loading may be adjusted to establish an end section loaded Q.

We have only scratched the surface with some filter types we have built. A detailed review of the literature will reveal numerous other filter topologies of interest. The bandpass filters presented here are transformed from simple low-pass filters, the so-called all-pole low-pass circuits with nothing more than series inductors and shunt capacitors. Other low-pass filters

such as the Elliptic can be transformed to bandpass form to generate bandpass circuits with transmission zeros next to the passband.

Another variation injects a transmission zero in a passband with no additional inductors. This is realized by an additional coupling capacitor that couples energy between non-adjacent resonators. This method was used in a 144 MHz transceiver discussed later in the book.¹⁴ There is a great deal of work available to be done by the curious experimenter.

3.4 CRYSTAL FILTERS

No element is more intimately related to radio receivers than the quartz crystals used in filters. The early super-heterodynes of the 1930s obtained single-signal selectivity with a crystal filter using but one crystal, a practice that continued through the 1970s. The use of high quality filters using a multiplicity of crystals became popular in the 1950s as SSB replaced classic AM as the radiotelephone method of choice.

Crystal Fundamentals

A modern quartz crystal is usually a round disc of single crystalline quartz with metalization on each side. The metal films serve to create (and sense) an electric field within the quartz. The basic structure is shown in Fig 3.28.

The basis for the interesting circuit properties of a quartz crystal is the piezoelectric effect. This effect is a material characteristic where an electric field causes a mechanical displacement. The mechanical motion is at right angles to the electric field in the quartz crystal. An electric field occurs when a voltage is placed between the two metalization layers attached to the crystal. The opposite effect also occurs; a mechanical motion generates an electric field.

The action of a quartz crystal when subjected to an electrical impulse is analogous to striking a bell or chime with a hammer: the energy of the impulse causes an oscillation to occur, a ringing that dies out in time. The resonant frequency of the chime is related to mechanical dimensions. In the

same way, the resonant frequency of a quartz crystal is related to the crystal thickness. The Q of a quartz crystal can be very high, from 10,000 to over one million. The motions of a quartz crystal are transverse with the crystal vibrating parallel to the surface. This allows the Q and resonant frequency to be altered by surface effects. The reader with an interest in the physics of quartz crystals is referred to the classic text by Virgil Bottom.¹⁵

The quartz crystal is modeled as the LC tuned circuit shown in Fig 3.29. L_m and C_m are termed "motional" parameters for they relate to the mechanical motion of the crystal. The equivalent series resistance, ESR, is an element representing losses; it is related to the crystal Q. The final element, C_0 , is the parallel, or holder capacitance. This C is a simple consequence of the crystal construction as a parallel-plate capacitor. This value is the sum of the parallel plate C (the dominant element) and some stray C related to the package housing the crystal. The parallel and the motional capacitance are related in the usual AT cut crystal. (AT cut refers to the crystallographic orientation of the crystal. Many of the crystals we deal with in radio are AT cut.) The relation between capacitors is approximately

$$C_0 = 220 \cdot C_m$$

Table 3.4 shows some measured representative values for some junk-box crystals. A crystal placed between a 50- Ω signal generator and 50- Ω load shows a response like that of Fig 3.30. If the crystal was a simple series tuned circuit without the parallel capacitor, C_0 , the response would be a simple peak.

A crystal filter can be built with a single crystal with the scheme of Fig 3.31. L-networks at each end transform 50 Ω to present 500 Ω at the crystal. Transformer T1 provides an out-of-phase voltage to drive a phasing capacitor. This signal combines with the energy flowing through the crystal parallel capacitance to control the position of the notch. The 10-pF capacitor increases the effective parallel C of the crystal, moving the notch closer to the peak while the 25-pF capacitor resonates the ferrite transformer. Fig 3.32 and 3.33 show the result of tuning the phasing capacitor.

Changing the terminating L-networks can alter the filter response. The bandwidth will decrease if the terminating impedance is dropped. A link could be used on T1 to replace the input L network while an output could be terminated with another wideband transformer. The modified circuit would then function well with a wide variety of crystals. Bandwidth will, of course, vary considerably as the com-

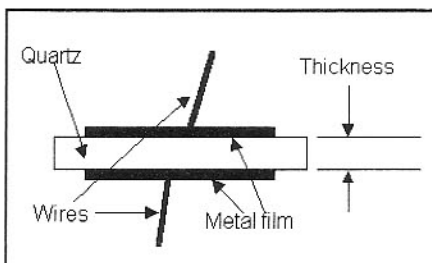


Fig 3.28—Cross section of a quartz crystal.

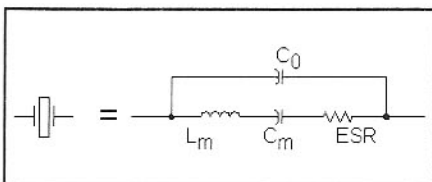


Fig 3.29—Symbol and circuit model for a quartz crystal.

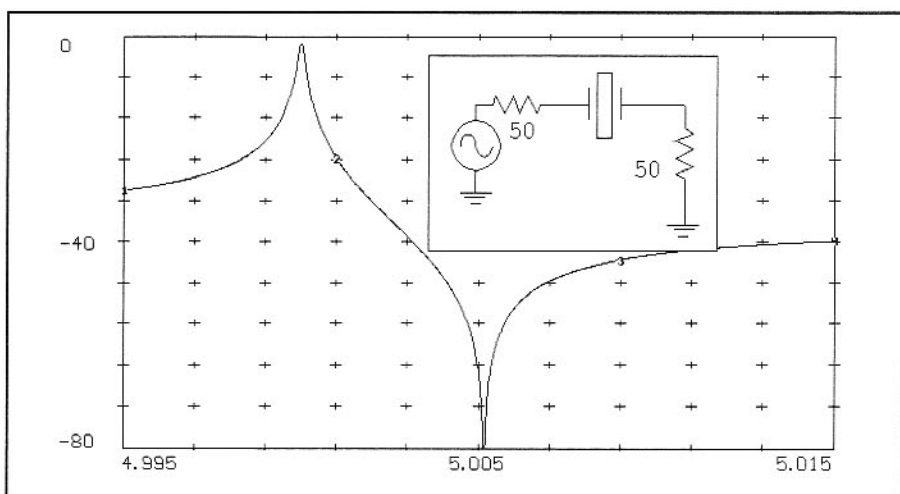


Fig 3.30—Crystal in a 50- Ω system with response. This crystal has a 5-MHz series resonant frequency, $L_m=0.098$ H, $Q=240,000$, and $C_0=5$ pF.

Table 3.4

Freq. MHz	L_m , H	C_m , pF	C_0 , pF	Q	ESR, Ω
3.58	0.13	.0152	3.35	50,000	58
5.0	.098	.0134	2.275	240,000	12.8
10.0	.020	.01267	2.8	200,000	6.3

ponents are changed. This filter type could even be used ahead of a receiver.

Crystal Measurement and Characterization

Earlier we swept an LC tuned circuit that was loosely coupled to a generator and a detector. A bandwidth measurement produced a Q_u . Loose coupling to a parallel tuned circuit occurred with a high impedance source and load. The crystal is a series tuned circuit and needs a low impedance environment for the loose coupling required for measurements. We can measure a crystal in the 50- Ω system shown in Fig 3.34.

The signal generator should be well buffered and extremely stable. The input of the circuit shown begins with a 20-dB pad, compensating for mismatch. The load can be a 50- Ω terminated oscilloscope, a spectrum analyzer, or a sensitive power meter. (See Chapter 7 or *QST*, June, 2001.) A 50- Ω , switched, 3-dB step attenuator is

a useful aid in determining bandwidth.

A crystal is inserted in the test set (Fig 3.34) and the generator is tuned for a peak output. Note the peak response amplitude and the frequency F_0 where it occurs.

Having measured peak response, remove 3-dB attenuation from the system, increasing the response. Tune the generator upward until the response drops to the level of the previous peak and record the frequency. This is one of the -3 dB frequencies. Repeat this step by finding the lower -3 dB point. The frequency difference, ΔF , is the 3 dB-loaded bandwidth in Hz for this test setup, which will be greater than the unloaded crystal bandwidth.

Knowing ΔF , return the generator to the frequency of peak response. Remove the crystal and plug the 100- Ω pot into the test set. Adjust the pot for the same meter reading; remove the pot from the test setup and measure its resistance with a digital voltmeter. This is approximately the ESR of the crystal.

Some experimenters have mounted the pot in a panel and switched it into the circuit as needed. This may give inaccurate results owing to stray inductance. The pot should be mounted to a suitable "dummy crystal" with short leads.

A detailed analysis of the method reveals errors. These can be reduced substantially by shifting to lower measurement impedance.

The test set of Fig 3.34 is complete, providing both motional parameters and Q information. However, measurements with this apparatus become tedious. A simple crystal oscillator can provide the motional parameters. This circuit, Fig 3.35, includes a series capacitor that may be switched into the circuit to produce a frequency shift. Related equations are included with the figure.

The required Q_u for filter applications will depend upon the filter bandwidth and center frequency as well as on the filter shape and the number of resonators. A reasonable rule of thumb for most filters (LC and crystal) is that the "normalized Q" must exceed twice the number of resonators. Normalized q , q_0 , is defined as Q_u

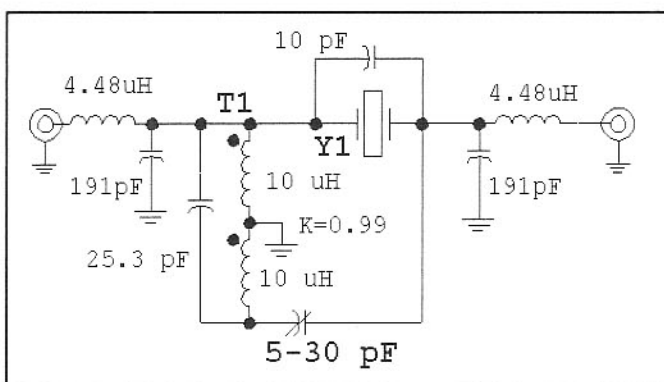


Fig 3.31—A single crystal filter using the crystal of Fig 3.30. T1 is 12 bifilar turns #26 on a FT-50-61 ferrite toroid. This filter has a 3-dB bandwidth of 1.4 kHz.

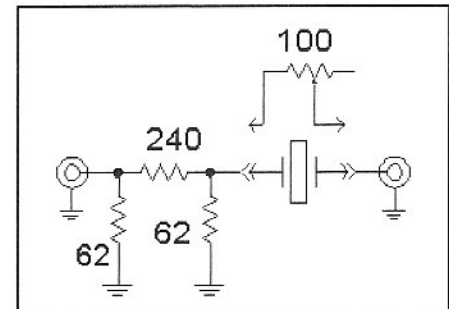


Fig 3.34—Simple test set for crystal measurement. The pad is a 20-dB, 50- Ω circuit. The output should be terminated in 50 Ω . A maximum input power from the generator would be about -10 dBm, resulting in a maximum to the crystal of -30 dBm. The 100- Ω pot is substituted for the crystal for ESR measurement. See text. Approximate equations for motional parameters are:

$$Q_u = \frac{1.2 \cdot 10^8 \cdot F}{\Delta F \cdot R_s}$$

$$C_M = 1.326 \cdot 10^{-15} \cdot \frac{\Delta F}{F_0^2}$$

$$L_M = \frac{19.1}{\Delta F}$$

F = Crystal Freq in MHz, ΔF = BW in test fixture in Hz, R_s = ESR, equivalent series resistance.

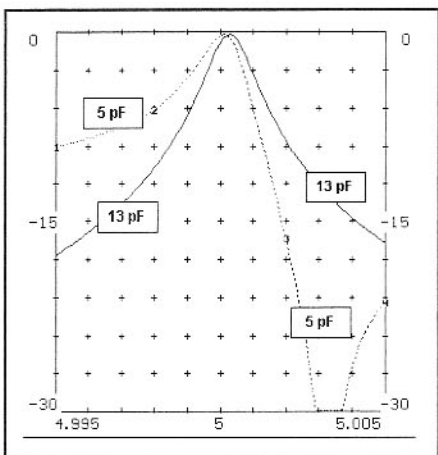


Fig 3.32—Response of the single crystal filter of Fig 3.31 when the phasing capacitor is at minimum value of 5 pF. The solid line represents the case of exact balance when the phasing capacitor equals the crystal C_0 .

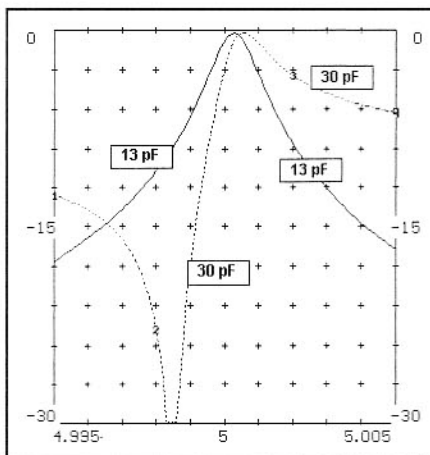


Fig 3.33—Response of the single crystal filter of Fig 3.31 when the phasing capacitor is at maximum value of 30 pF. The solid line represents the case of exact balance when the phasing capacitor equals the crystal C_0 .

divided by the filter Q, or

$$q_0 = \frac{Q_U \cdot B}{F} \quad \text{Eq 3.10}$$

A 500 Hz bandwidth filter at 5 MHz would have filter Q of 10,000. If crystal $Q_U=100,000$, $q_0=10$ and the filter would be practical with 5 crystals.

Generally, the most practical way to build crystal filters in the home lab begins with a large number of essentially identical crystals. These can sometimes be found at local surplus houses, often for very low prices. Equally good sources are mail order catalogs selling microprocessor crystals. Measurements (by W7AAZ) confirmed that many crystal brands offer good Q_U with a minimal frequency spread. But this is changing, even at this writing. The experimenter might consider ordering a

small lot (perhaps 10) of a given crystal type. He or she can then measure them for Q and frequency distribution. If results are suitable, another order can be placed for a larger number. Typical cost for these crystals is around \$1 each, so a batch of 10 crystals is still much less expensive than ordering even one special crystal.

Crystals should be matched to within 5 to 10% of the filter bandwidth to build effective filters. Hence, crystals for a 500-Hz wide CW filter should be matched within 25 to 50 Hz of a nominal frequency.

The recommended measurement procedure begins by numbering and marking all crystals in a set with stick-on labels. The crystals are measured for oscillation frequency in the same oscillator. If the "G3UUR" oscillator is used, be sure you specify which switch position is used, and record it in the notes. Measure motional

parameters for several crystals to guarantee that there is small spread between crystals. It is also worthwhile to measure a few crystals for Q_U . The data is then entered into a computer spreadsheet where it is sorted according to frequency, making it easy to select matched crystals for a filter.

How many crystals should be purchased to make one filter? The answer is difficult, for it could vary a great deal with the crystal manufacturer. Generally, the purchase of 2 or 3 times as many crystals as the number of filter resonators is a good start. More is always useful. A larger lot, perhaps 100, almost guarantees a large selection of filters using most of the crystals. Left over crystals will be used in oscillators. It is rarely practical to build homebrew filters for already existing equipment.

Designing Simple Crystal Filters

Having characterized a set of crystals, we can now consider a filter design. The procedure will depend on the quality of the filter to be built. Some filters are easy, while others may require extensive and very careful measurement as well as computer simulation. Both extremes will be discussed.

Most of the filters we will discuss use the lower sideband ladder topology. An example is presented in Fig 3.36. The crystals are series elements in a ladder. Shunt capacitors couple energy between adjacent crystals. A mesh is one loop of a ladder, one crystal and the two shunt coupling capacitors on either side of it. A mesh could also be a load, a matching capacitor, a crystal, and one coupling capacitor. Some meshes include a series capacitor to tune the mesh to the same frequency as the other meshes in the filter.

The first method presented ignores the parallel crystal capacitance, treating the crystal as a simple series LC circuit. This scheme is suitable for simple CW filters. (Although we think of narrow filters as being more exotic than wide ones, it is generally easier to build narrow crystal filters.) This will be illustrated with an example, a 4th-order filter at 5 MHz with a 400 Hz bandwidth and a Butterworth shape. The $n=4$ Butterworth is a symmetrical filter with $q_1=q_4=0.7654$, $k_{12}=0.8409$, $k_{23}=0.4512$, and $k_{34}=0.8409$. The crystals have a 5-MHz center frequency, a motional inductance of 0.098 H, parallel C of 3 pF, and Q_U of 240,000. Normalized Q is $q_0=19.2$, so this is a realizable filter. Calculating the motional C from resonance at 5 MHz, we find $C_m=0.010339$ pF. We calculate the cou-

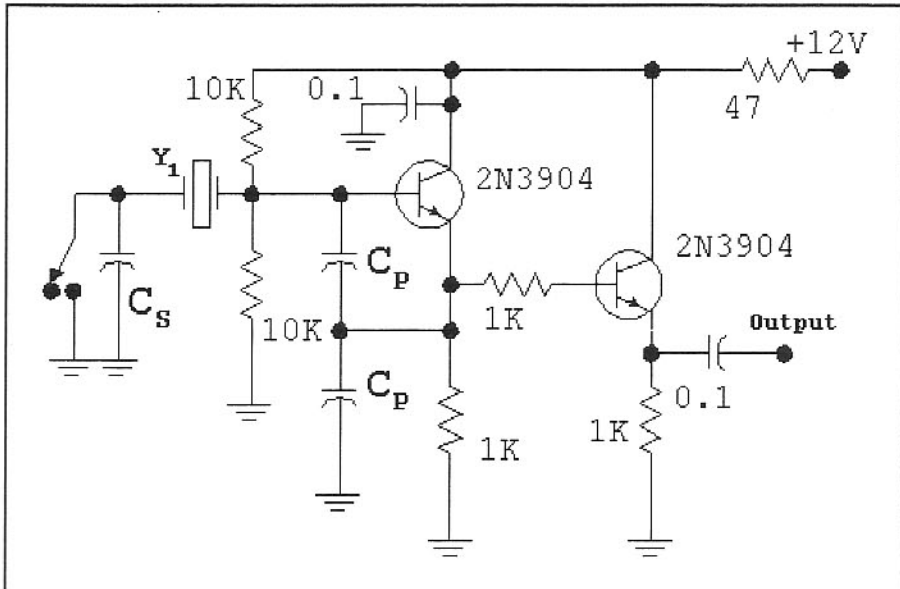


Fig 3.35—The G3UUR method for measuring quartz crystal motional parameters A simple circuit to measure the motional parameters of fundamental mode quartz crystals. A crystal to be evaluated is placed in the circuit at Y_1 and oscillation is confirmed. The frequency is measured. Then the switch is thrown and the frequency is measured again. Typical values are $C_p=470$ pF and $C_s=33$ pF. C_m will have same units as C_s . Be sure that C_s includes the stray capacitance of the switch as well as the circuit part. Then:

If

$$C_s \ll C_p$$

then

$$C_M \approx 2 \cdot C_s \cdot \frac{\Delta F}{F}$$

and

$$L_M = \frac{1}{\omega^2 \cdot C_M}$$

where $\omega=2\pi F$ with F now in Hz. ΔF is the F difference observed when the switch is activated. Example: Use capacitors mentioned above, 10 MHz crystal; $F=1 \times 10^7$, $\Delta F=1609$ Hz, to yield $L_m=.0239$ H and $C_m=10.6$ fF. (1000 fF = 1 pF.)

pling capacitors with

$$C_{jk} = \frac{C_m \cdot F}{k_{jk} \cdot B} = \frac{1}{4 \cdot k_{jk} \cdot B \cdot \pi^2 \cdot F \cdot L_m}$$

Eq 3.11

where B is the bandwidth; F and B are both in Hz. Substituting, we find $C_{12}=C_{34}=154$ pF and $C_{23}=286$ pF. The end terminating resistance is given by

$$R_E = \omega \cdot L \cdot \left[\frac{B}{q \cdot F} - \frac{1}{Q_U} \right] \approx \frac{2 \cdot \pi \cdot B \cdot L_m}{q}$$

Eq 3.12

The end resistance is 309Ω , yielding the preliminary filter as shown in

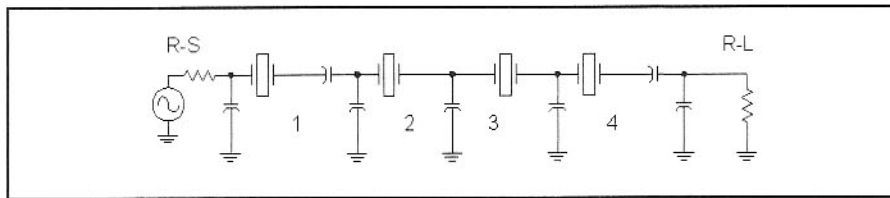


Fig 3.36—Lower sideband ladder filter with four crystals. The four meshes are labeled for reference in the discussion.

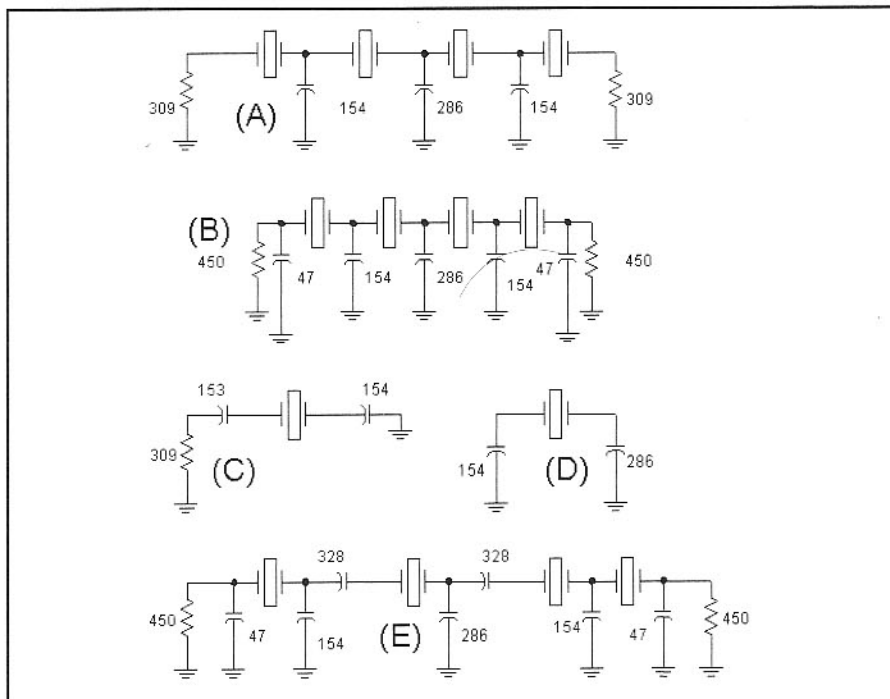


Fig 3.37—Evolution of a bandpass filter showing the steps in the design. See text for details.

Fig 3.37A. The filter has yet to be tuned. The filter would, otherwise, be finished if we wanted to terminate in this resistance. To illustrate the general case, we will terminate in a larger value, 450Ω .

A termination R_0 will “look like” a smaller value R_E if it is shunted with a parallel capacitance, C_E where

$$C_E = \sqrt{\frac{(R_0 - R_E)}{R_E \cdot \omega^2 \cdot R_0}}$$

Eq 3.13

Using the values from above, we obtain an end capacitor of 47 pF, producing the next version of the filter as shown in Fig 3.37B. Only filter tuning remains.

The end meshes, 1 and 4, are terminated in a parallel RC circuit. The equivalent series RC consists of the original end resistance, R_E , and a capacitance C' where

$$C' = \frac{C_E^2 \cdot \omega^2 \cdot R_0^2 + 1}{C_E \cdot \omega^2 \cdot R_0^2}$$

Eq 3.14

C' is 153 pF, R_0 is 450Ω , and R_E is 309Ω for this example.

The end meshes are shown, isolated from the other meshes, in Fig 3.37C while the interior meshes are shown in isolation in Fig 3.37D. The end meshes have a net series C of 76.7 pF while the interior ones have a net series C of 100.1 pF. Both will be detuned from the nominal crystal 5 MHz, but the meshes with the smallest capacitance will be detuned by the largest amount. The lower meshes can be properly tuned by added series C so that they have the same net series C as the highest frequency one. This will occur with a tuning C of

$$C_T = \frac{C_{\text{High}} \cdot C_{\text{Mesh}}}{C_{\text{Mesh}} - C_{\text{High}}}$$

Eq 3.15

Using $C_{\text{Mesh}}=100.1$ pF and $C_{\text{High}}=76.7$ pF, a proper tuning capacitor is 328 pF. The final filter circuit is shown in Fig 3.37E.

The computer generated response for this filter is shown in Fig 3.38.

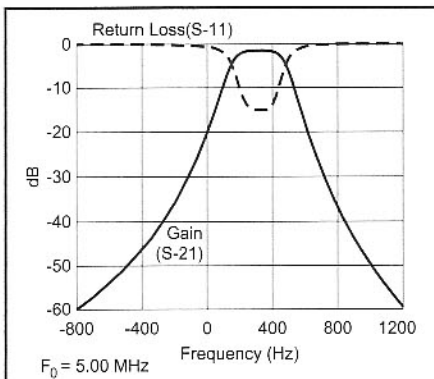


Fig 3.38—Response for the crystal filter designed in Fig 3.37.

Accounting for Parallel Crystal Capacitance

The quartz crystal model of Fig 3.29 is generally an accurate one. C_0 has little effect in filters that are sufficiently narrow, so was ignored in the previous design. The 5-MHz CW filter just presented was designed for a 400-Hz bandwidth with a Butterworth shape. The shape is very close to an ideal Butterworth.

Problems increase as the filter bandwidths grow. This is illustrated with Fig 3.39 which shows the response of two different 3-kHz bandwidth filters using 3.58-MHz TV color burst crystals. The

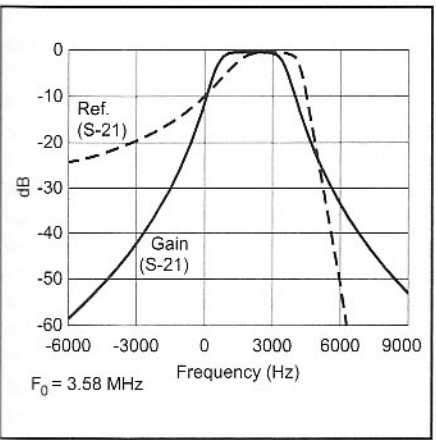


Fig 3.39—The response of two crystal filters built from 3.58-MHz color burst crystals. One uses ideal crystals with zero C_0 to produce a symmetrical shape. The other (with dashed line) uses $C_0=4\text{ pF}$ crystals.

solid curve is the response we would like, designed with ideal crystals with zero parallel capacitance. $C_0=4\text{ pF}$ produces the other response. The filter bandwidth is too narrow and the attenuation is markedly increased. It is for this reason that this circuit is named the lower sideband ladder filter.

Response distortion results because the parallel C_0 makes the series resonators behave as if they had a larger motional L than is measured. This effect is plotted in Fig 3.40 for the 5-MHz crystals used in the earlier CW filter design. The lower curve shows the effect of a 2-pF parallel capacitance while the upper curve is for $C_0 = 5\text{ pF}$. Here, X is the ratio of L_{eff} to L_m . The horizontal axis in the curve is δf , the offset from the series resonant frequency. These effects were discussed in greater detail in *QEX* for June, 1995, where

detailed design equations are given. The corrections related to the effective inductance are included in the program *XLAD.exe*. Both the program and the 1995 *QEX* paper are included on the book CD.

The effective inductance is larger than the normal motional L by a factor of 2 or more. This reduces the effective motional capacitance by the same factor. Accordingly, the coupling capacitors must be reduced by the same factor. The change also alters the calculation of end resistance. The new terminations and reduced coupling capacitors will then alter the filter tuning.

One can build symmetric filters if the effect of parallel capacitance is eliminated. One way to do this parallels each crystal with a large inductance. The value required is one that resonates with C_0 , forming a parallel trap that is then bridged by the series resonant portion of the crystal. An experimental filter was built to examine this idea. The inductance used was smaller than required for resonance, so small trimmer capacitors were added. The filter, built with 3.58-MHz color burst crystals for a 3.5-kHz bandwidth, is shown in Fig 3.41. The measured response is presented in Fig 3.42.

Crystal filters built with paralleled inductors suffer from degraded stopband response. Although the performance around the filter center is as designed, it degrades a few hundred kHz away from center, necessitating the crystal filter be supplemented with an LC bandpass.

The Min-Loss Filter of Cohn and other Simplified Forms

A simplified non-mathematical scheme for building crystal filters uses the Min-Loss circuit. This circuit is the result of fundamental work by S. B. Cohn where he described a family of coupled resonator filters that achieved very low insertion loss while maintaining good stopband attenuation.¹⁶ A really interesting property of these filters was the fact that they used identical resonators that were coupled to each other with equal values of coupling. This means that all shunt coupling capacitors in a Min-Loss crystal filter are equal. If the filters are designed without shunt end loading capacitors, tuning is greatly simplified. A Min-Loss type crystal filter is properly tuned if

- all crystals have the same frequency,
- all coupling capacitors are of the same value, C ,
- series capacitors having the same capacitance as the coupling C are placed in series

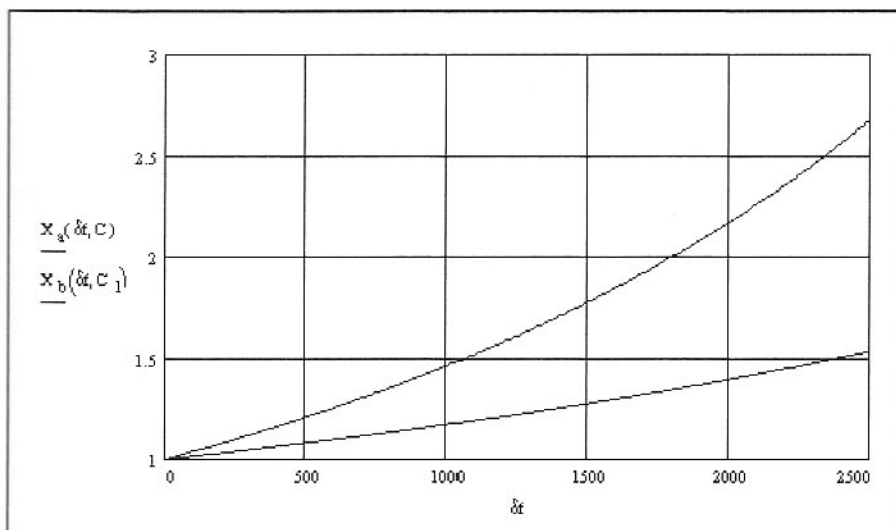


Fig 3.40— X , defined as L_{eff}/L_m , is plotted for frequency offset, δf , above crystal series resonance in Hz. These 5-MHz crystals had parallel C of 2 and 5 pF.

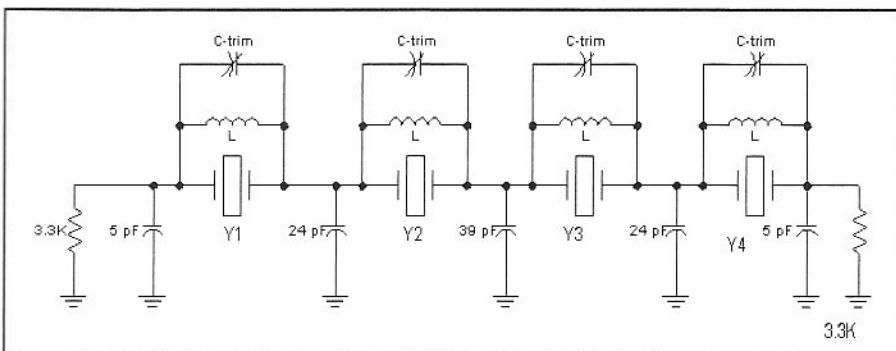


Fig 3.41—Experimental crystal filter.
 $Y1,2,3,4 = 3.58\text{-MHz surplus color burst crystals. } (L_m=0.117\text{H}, C_0=4\text{ pF})$
 $L = 151\text{ }\mu\text{H, 48 turns #30 on FT-50-61 Ferrite toroid.(Amidon)}$
 $C\text{-trim} = 3\text{--}12\text{ pF ceramic trimmer. See the referenced QEX paper for adjustment procedure.}$

Butterworth Crystal Filter, 3.58 MHz

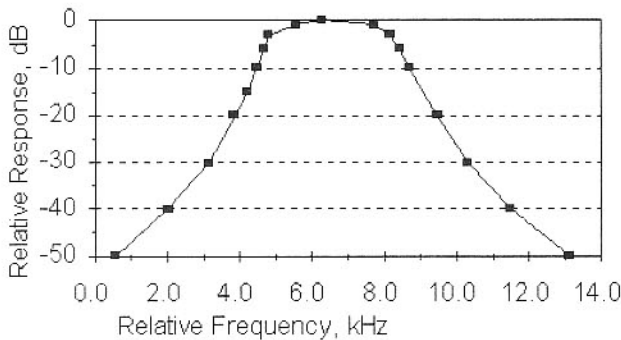


Fig. 3.42—Measured response for the filter shown in Fig. 3.41.

with both end crystals

- both terminations are equal and properly related to coupling.

A crystal filter of this type, with five resonators, is shown in Fig. 3.43.¹⁷

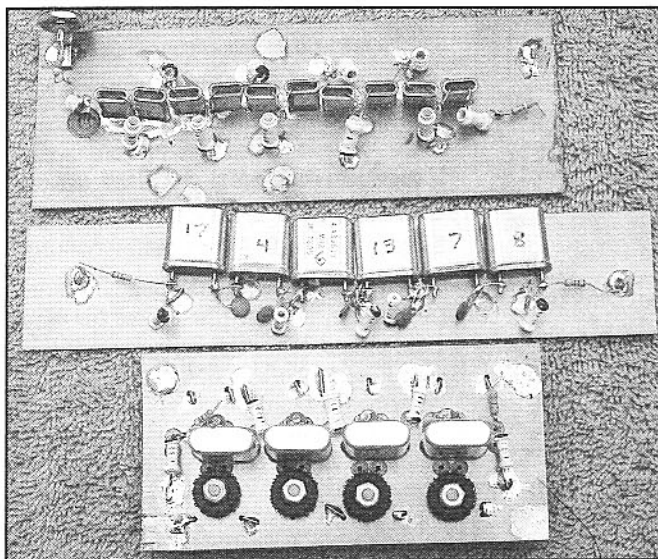
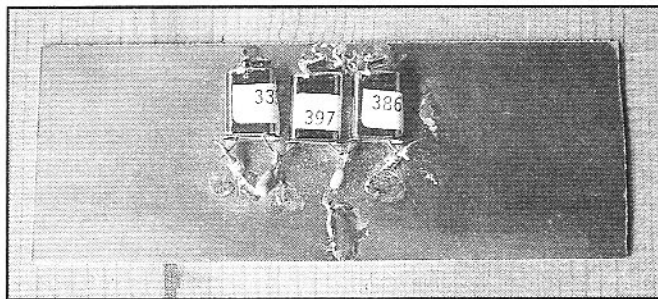
This filter topology often appears with the name “Cohn Filter,” titled for the original circuit theorist who contributed so extensively to our design methods. Other filters have also appeared with the Cohn name. Here we have divorced the name from this simple crystal filter, for it is but one example from Cohn’s body of work, a collection that is much richer and more extensive than has been presented in the amateur literature.

While most of the Min-Loss crystal filters we build are fabricated without design (i.e., without any mathematical analysis), they may certainly be studied and designed on the computer. The normalized coupling coefficients and end section Q for this filter type are approximately given by

$$k_{jk} = \frac{1}{2} \cdot \exp\left(\frac{\ln(2)}{N}\right) \quad \text{Eq. 3.16}$$

$$q = \frac{1}{k_{jk}} \quad \text{Eq. 3.17}$$

A three element crystal filter at 10 MHz. The metal can crystals have small wires soldered to them that are then grounded to the foil.



Three experimental crystal filters. The top circuit uses 10 crystals in a circuit with equal coupling between resonators (Cohn). The bottom filter is that from Fig. 3.41.

where n is the number of resonators. These values are tabulated for n from 2 to 10 in Table 3.5. (The first few points appeared in the original Cohn paper, while k and q for $N > 5$ are extrapolations via our above equations.)

Shown in Fig. 3.44A are transfer function plots for two different filters of this type. The wider, lower loss one has 3 resonators while the other has 8 crystals. Both circuits were designed for 5 MHz with a 500-Hz bandwidth using high Q crystals with $L_m = 0.098$ H. Part A of the figure shows close-in details while Fig. 3.44B shows the response to the -80 dB level. Part C of the figure shows the group delay for the filter with 8 resonators. (More will be said about group delay shortly.) All three plots are computer generated re-

Table 3.5

N	k	q
2	0.707	1.414
3	0.63	1.587
4	0.595	1.683
5	0.574	1.741
6	0.561	1.782
7	0.552	1.811
8	0.545	1.834
9	0.54	1.852
10	0.536	1.866

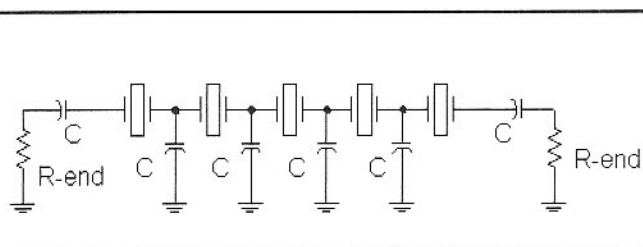


Fig. 3.43—Min-Loss type crystal filter with equal coupling and simplified tuning.

sponses, although they are in good agreement with measurements on similar filters. We have built Min-Loss crystal filters up to 10th order.

The data of Fig 3.44 illustrate the salient properties of the Cohn filter. The passband shape is smooth with minimal ripple for the low order filters ($N=3$), but becomes distorted as the number of resonator grows beyond five. The ripples on the passband edges near the skirts become extreme with wider bandwidth filters. The $N=8$ data of Fig 3.44B illustrate the excellent shape afforded by the Min-Loss filter. However, the time domain performance as depicted in the group delay plot suggests

that this filter may have severe ringing if built for narrow (CW) bandwidths.

Although the two filters ($N=3$ and $N=8$) described in Fig 3.44 have different responses, they are remarkably similar in component values. The $N=3$ filter used 146-pF capacitors and 181Ω terminations while the $N=8$ filter used 168 pF and 155Ω . A filter designed with two or three crystals can be extended with the same capacitor values and terminations. This becomes extremely useful for the experimenter.

The Min-Loss crystal filter has virtues of low insertion loss and good skirts, but at the price of poor passband shape with higher orders. Some other filters offer similar non-mathematical simplicity and better passband performance, with a group of crystals all at the same frequency. Fig 3.45 shows such a filter. This design is a Butterworth design at 10 MHz with normalized parameters of $q=0.765$, $k_{12}=k_{34}=0.841$, and $k_{23}=0.541$. This filter is designed with a pure resistive termination at the ends (no shunt end capacitors.) The equations predict the end resistance and the shunt capacitors. The series tuning capacitors are yet to be established. However, the values are clear from inspection. If the end capacitors are set to the value of the center capacitor (85 pF,) each mesh has the same capacitors in the related loop.

Design with the equations does not take the parallel crystal capacitance effects into account. This is done with curves like those of Fig 3.40 that establish an increased effective inductance value that can then be applied with the equations. Approximate designs without the curves will still result in practical filters at the higher frequencies (8 MHz and up) although the bandwidth will be a bit narrower than the design values.

from the ordinary. There are numerous phenomenon that tend to degraded performance and remove "crispness." One that can ruin an otherwise excellent receiver is an IF filter with excessive group delay. All filters have time delay, a truth that cannot be avoided. The filters that "sound" the best are those that have small delay for a given bandwidth and, of greater import, behave like a transmission line with little variation in group delay over the passband.

The group delay of an eighth order Min-Loss filter was presented in Fig 3.44C. The delay was high, exceeding 10 milliseconds in part of the passband. The group delay variation over the passband was also severe. This filter, although very selective, would probably not sound good, especially with noise pulses.

Two 5-MHz filters were designed for a bandwidth of 500 Hz, each with five crystals. One filter used a 0.1-dB ripple Chebyshev response while the other used a linear phase response. The Chebyshev results are shown in Fig 3.46 while the linear phase response is given in Fig 3.47. Both plots overlay group delay and gain. The "ears" of the Chebyshev group delay plot line up with the 3-dB edges of the passband, so all delay variations are heard. In contrast, the region of low group delay in the linear phase filter extends well beyond the filter bandwidth edges. Both of these filters have been built and tried in an experimental CW receiver. The linear phase filter was more difficult to build, but sounded much better. The skirts were steep in the Chebyshev, so it presented adequate selectivity. We found the linear phase filter in need of more skirt selectivity. Although not shown in the figures, the Chebyshev filter group delay was 2.5 times as large as the linear phase filter delay.

We have also had good results with an intermediate filter shape, the Gaussian-to-6 dB response. This is a filter with a rounded peak shape for the top 6 dB, but with steep Chebyshev-like skirts. Transitional filters (Gaussian-to-6 dB, Gaussian-to-12 dB, linear phase, and maximum flat delay) are slightly more difficult to build than the Min-Loss, Butterworth, or Chebyshev filters, for they lack the sym-

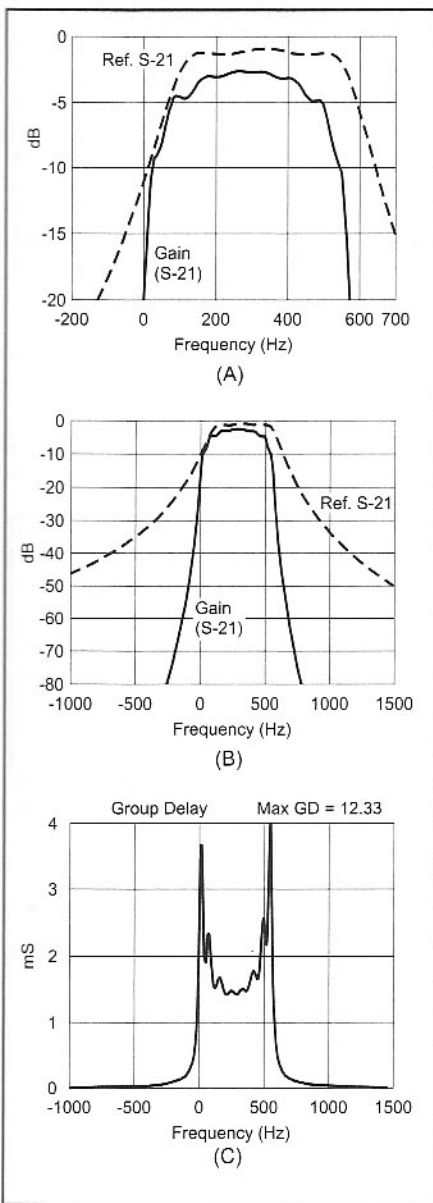


Fig 3.44—Min-Loss crystal filter responses. A and B compare 3rd and 8th order filters in responses to -20 and -80 dB. C shows the group delay for the 8th order filter.

Ringing, Group Delay and Filter Passband Shape

All serious receiver experimenters have their favorite efforts, receivers with specifications differing little from others, but with a "crisp sound" that sets them apart

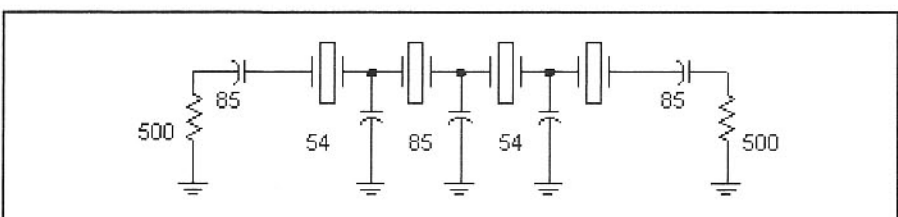


Fig 3.45—10-MHz SSB bandwidth filter using crystals with identical frequencies and "easy" tuning. This filter has a Butterworth shape; the simplified tuning method often works well with N=4 Chebyshev filters.

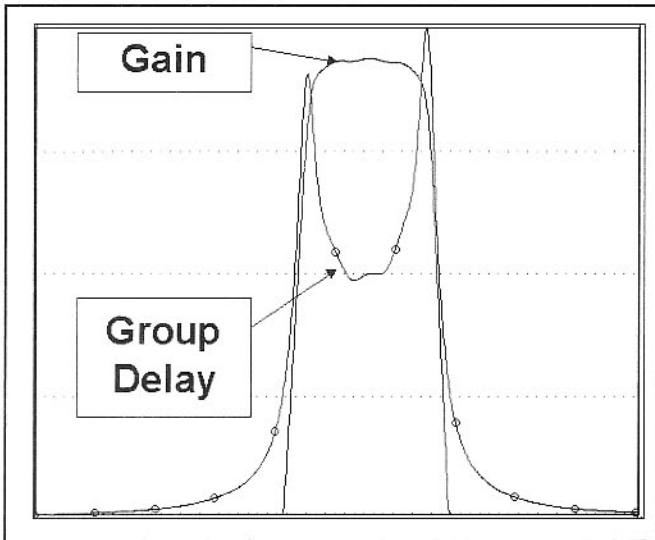


Fig 3.46—Group delay and gain for a Chebyshev crystal filter. The gain is plotted over a 20-dB range.

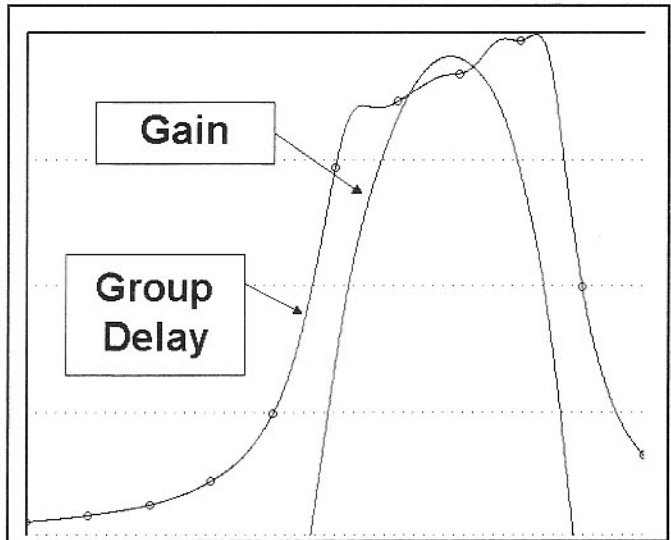


Fig 3.47—Group delay and gain for a linear phase crystal filter. The gain is plotted over a 20-dB range.

metry of the traditional types. If the transitional filters were commercially available, they would probably be very expensive. On the other hand, they offer a challenge that is well worth the effort for the advanced experimenter. The reader should

review the work of Carver¹⁸.

Intuition would suggest that a FIR (finite impulse response) filter, usually realized with DSP, would have significantly reduced ringing. Some do, but some others still show significant ringing.

Extreme selectivity always seems to bring some ringing. Generally, it is the less selective schemes with smooth peak shapes that always sound the best, without regard to the method used to achieve it, traditional hardware or digital signal processing.

3.5. ACTIVE FILTERS

While most receivers are super-heterodyne designs with an IF, some simple superhets as well as virtually all direct conversion receivers obtain much of their selectivity from audio filtering. Audio frequency inductors have become available in recent years, making traditional LC designs viable at low frequencies. Even prior to the arrival of those parts, some builders had built audio filters with surplus telephone toroids. Still, the most common method for audio filtering uses RC active circuits. An RC active filter combines gain with resistors and capacitors to synthesize inductor behavior.

The Low Pass Filter

Figure 3.48 shows an active low pass filter form known as the voltage controlled voltage source (VCVS). It uses an operational amplifier configured as a non-inverting amplifier, usually with a gain of one. Two resistors and two capacitors complete the circuit. Fig 3.48 shows part values for the two resistors, here assumed equal, and one capacitor. The other capacitor is a multiple of the first. A representative set of responses is shown in Fig 3.49 where A has

a value of 1, 2, 5, and 10. A peak appears in the response as A exceeds 2. The circuit provides a voltage gain of 1.7 when A=10.

The filter has a two-pole Butterworth response when A=2. For A ≤ 2 and for equal R, the 3 dB cutoff frequency is given by

$$F_{C.O.} = \frac{\sqrt{A - 2 + \sqrt{2 \cdot A^2 - 4 \cdot A + 4}}}{2 \cdot \pi \cdot R \cdot C_1 \cdot A} \quad Eq\ 3.18$$

where A is the capacitor ratio, C₂/C₁. For example, with R=10 kΩ, C₁=.01 μF (.01 μF = 10 nF), and A=1 (equal capacitors), the cutoff is 1024 Hz. Eq 3.18 can be solved for R for an arbitrary cutoff frequency.

If A exceeds 2 the filter takes on a peaked response. It is then more convenient to work with the peak frequency as a function of R, C, and A, the capacitor ratio. If A>2, the peak frequency is given by

$$F_{PEAK} = \frac{\sqrt{A - 2}}{2 \cdot \pi \cdot A \cdot C \cdot R} \quad Eq\ 3.19$$

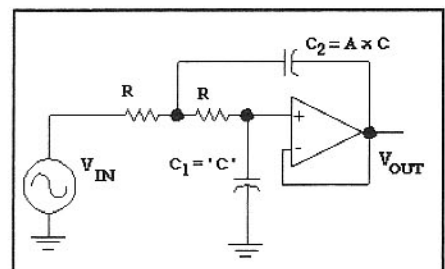


Fig 3.48—RC active low-pass filter. The op-amp is assumed to be powered from dual supplies around ground. Other biasing schemes are presented later. The operational amplifier is configured for a non-inverting gain of 1. C₂, the feedback capacitor, is A × C₁ where A is a value greater than 1.

Table 3.6

A	Voltage Gain	A	Voltage Gain
2.2	1.004	6.8	1.41
2.4	1.014	10	1.67
3.3	1.088	22	2.4
3.6	1.12	33	2.9
3.9	1.14	47	3.46
4.7	1.22		

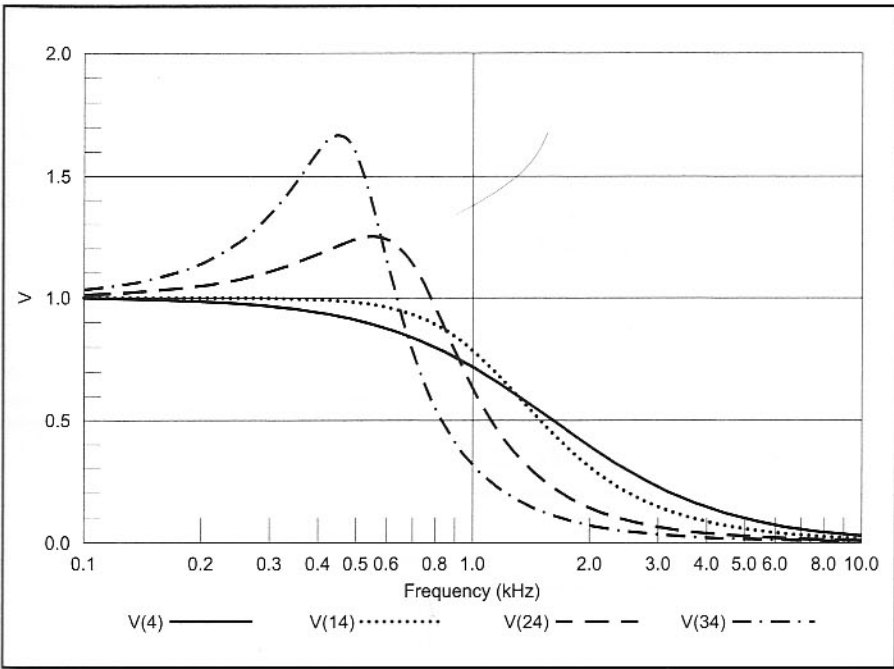


Fig 3.49—Response of the filter shown in Fig 3-48 with $A=1, 2, 5$, and 10 . These curves, and several others in this section, were generated with *Super Spice* from Compact Software. The solid line corresponds to $A=1$ while the highest peak is for $A=10$.

Some values of low pass voltage gain at the response peak are tabulated vs A , the capacitor ratio, in **Table 3.6**.

There are numerous ways to design practical low-pass filters with the equations. A cascade of sections like those in Fig 3.48 would form Butterworth or Chebyshev filters of high order. Each capacitor corresponds to one pole in the response, one L or C in the traditional filter. Generally, each two-pole low-pass section will differ from the others in higher order Butterworth or Chebyshev filters. For details, see the text by Johnson, et al.¹⁹

Alternatively, several identical low-pass sections can be cascaded to form a useful circuit. These filters are easy to analyze and design, and offer excellent performance, especially with simple direct conversion receivers. An example of a filter of

this type is shown in **Fig 3.50**. Three two-pole sections with $A=2$ are cascaded to form a 6-pole filter suitable for SSB reception. The response for this filter is shown in **Fig 3.51**. The dip at low frequency results from the $1\text{-}\mu\text{F}$ input coupling capacitor.

Cascades of peaked low-pass filters ($A>2$) can be very useful. The gain can be considerable when several stages are cascaded. These filters take on a bandpass like shape, offering an attractive response for direct conversion receivers intended for CW use.

The filter shown in **Fig 3.50** is biased for single power supply operation. This scheme is especially attractive with the low-pass filter, for an entire chain of filter sections may be biased with only one divider. If LM-358 or LM-324 op-amps are used, a pull down resistor should be

connected from the amplifier output to ground. The resistor should pass a standing current of about 1 mA . Severe cross-over distortion will result without this loading.

High-Pass Filters

Figure 3.52 shows a VCVS type high-pass filter. This circuit is the dual of the low pass just discussed. It is designed with equal valued capacitors. The resistors now differ by a factor “ A ”. The usual filters have the grounded resistor as the one with larger value. **Fig 3.53** shows the response

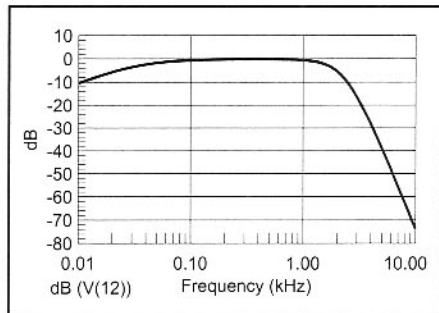


Fig 3.51—Response for the cascade of identical low-pass sections presented in **Fig 3.50**. This is a calculated result, although we have built several similar designs.

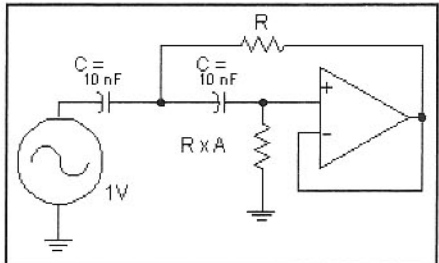


Fig 3.52—Voltage controlled voltage source high-pass filter. The operational amplifier is again set for a closed loop gain of +1.

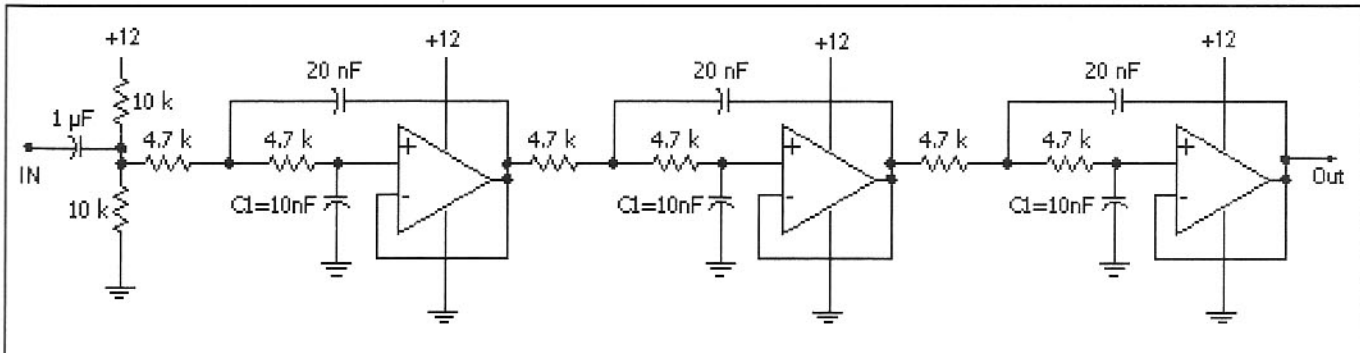


Fig 3.50—Practical low-pass filter that can be built with common op-amps, such as the 741, 1458, 358, 324, 5532.

The VCVS low-pass filter with equal resistors has a transfer function of

$$H(s) = \frac{1}{1 + 2 \cdot s \cdot C \cdot R + s^2 \cdot C^2 \cdot R^2 \cdot A} \quad \text{Eq 3.20}$$

where s is now the complex (LaPlace) frequency, $s=j\omega$ in the frequency domain. C is the shunt capacitor while $A \times C$ is the feedback capacitor. The corresponding frequency domain response is

$$\left| \frac{V_{out}}{V_{in}} \right| = \sqrt{\frac{1}{(1 - 8 \cdot \pi^2 \cdot f^2 \cdot R^2 \cdot C^2 \cdot A + 16 \cdot \pi^4 \cdot f^4 \cdot R^4 \cdot C^4 \cdot A^2 + 16 \cdot \pi^2 \cdot f^2 \cdot R^2 \cdot C^2)}} \quad \text{Eq 3.21}$$

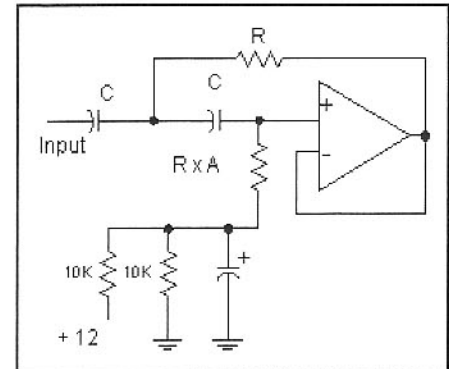


Fig 3.54—Biasing method for high-pass filter sections. A voltage divider creates a synthetic ground at half of the single supply.

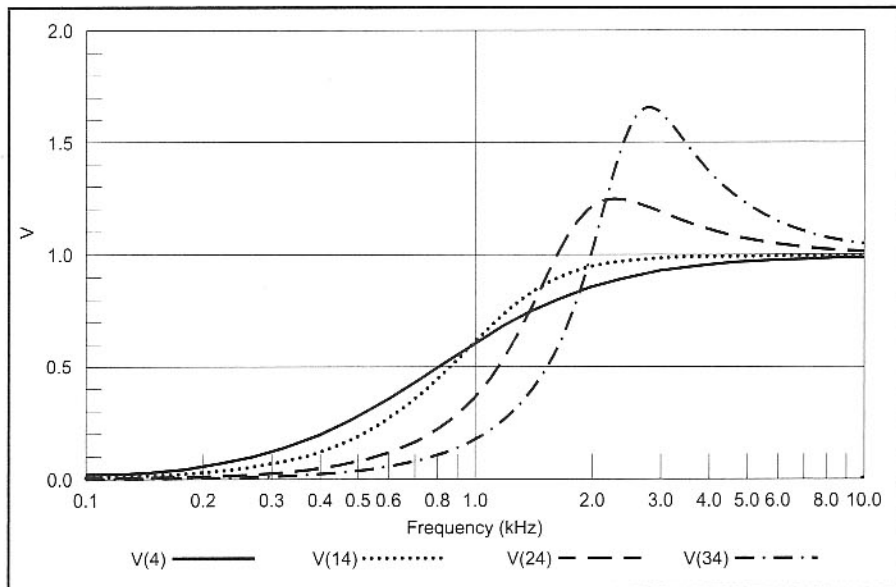


Fig 3.53—Transfer functions for four versions of the high pass section of Fig 3.52. The resistor ratio varies, taking on values of $A=1, 2, 5$, and 10 . The solid line corresponds to $A=1$ while the highest peak is for $A=10$.

for four different filters, all with 10-nF capacitors and a 20-kΩ ungrounded resistor. The grounded resistor varies to set gain and peaking. The values used are 20 kΩ, 10 kΩ, 4 kΩ, and 2 kΩ.

The characteristics of the high-pass section are much like those of the low pass. The circuit begins to take on a peaked response when A exceeds 2. A peaked high pass will have a peak frequency given by

$$f_{PEAK} = \frac{1}{2 \cdot \pi \cdot C \cdot R \cdot \sqrt{A - 2}} \quad \text{Eq 3.22}$$

There is no peak if $A < 2$. The pure high pass then has a 3 dB cutoff frequency given by

$$f_{-3dB} = \frac{\sqrt{(2 - A) + \sqrt{2 \cdot A^2 - 4 \cdot A + 4}}}{2 \cdot \pi \cdot C \cdot R \cdot A} \quad \text{Eq 3.23}$$

The VCVS high-pass sections do not have a dc path through them that allows the easy biasing afforded by the low pass. A high-pass section may be biased with the methods shown in Fig 3.54 when dual power supplies are not available.

The high pass and low-pass forms may be combined in a cascade to form bandpass filters with excellent stopband attenuation. An example response is shown in Fig 3.55 where four peaked low-pass sections are

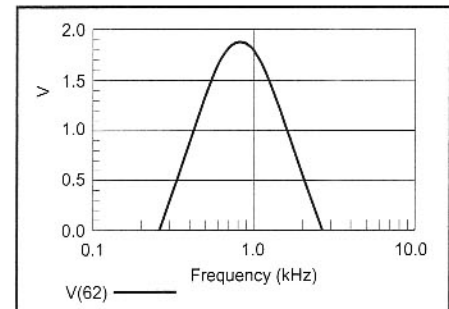


Fig 3.55—The 4x4 filter, a cascade of four peaked low-pass sections (6.8 kΩ, 10 nF, and 50 nF) followed by four peaked high-pass sections (20 nF, 27 kΩ, and 5.6 kΩ)

cascaded with four peaked high-pass sections.

Active Bandpass Filters

A bandpass-filter section is shown in Fig 3.56 using an operational amplifier in an infinite gain multiple feedback circuit. The IGMFB circuit is practical with common op-amps such as the 741, 1458, and 5532. The topology is represented with two equal valued capacitors and three resistors. One of the resistors allows the user to specify circuit gain as well as center frequency and Q or bandwidth. The design begins by picking these values for voltage gain K (a dimensionless ratio), Q , f_0 in Hz, and C in Farads. The required resistors are then

$$R_1 = \frac{Q}{K \cdot \omega_0 \cdot C} \quad \text{Eq 3.24}$$

$$R_2 = \frac{Q}{(2 \cdot Q^2 - K) \cdot \omega_0 \cdot C} \quad \text{Eq 3.25}$$

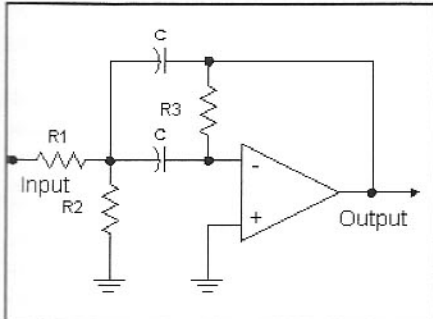


Fig 3.56—Infinite gain, multiple-feedback (IGMFB) bandpass filter. This topology is capable of moderately high Q and gain with practical components.

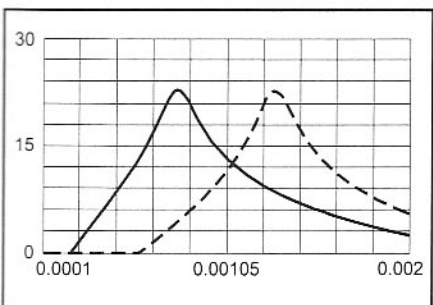


Fig 3.57—Calculated gain in dB for the IGMFB bandpass filter shown in Fig 3-56. This version used the resistor and capacitor values calculated in the text for Q=5 at 800 Hz with a gain at resonance of 2. The solid curve represents the nominal response while the dashed curve shows the result of tuning R2 to a lower value. Changing R2 to a 1 kΩ-variable in series with a 560-Ω fixed resistor would produce a tunable bandpass characteristic with essentially constant gain and bandwidth. This tuning scheme works well only when R1>R2. This sweep was generated with Super-Star Professional from Eagle Software.

$$R_3 = \frac{2 \cdot Q}{\omega_0 \cdot C} \quad \text{Eq 3.26}$$

where $\omega_0=2\pi\times f_0$. We see from Equation 3.25 that the gain should be less than $2Q^2$. For example, a filter using 22-nF capacitors with a center frequency of 800 Hz, a Q of 5, and a gain at resonance of 2 is built with $R1=22,600 \Omega$, $R2=942 \Omega$, and $R3=90.4 \text{ k}\Omega$. The transfer function for this filter is shown in Fig 3.57.

The IGMFB bandpass filter must be biased with the method shown earlier for a high pass filter if a single power supply is to be used. This filter form is ideal if

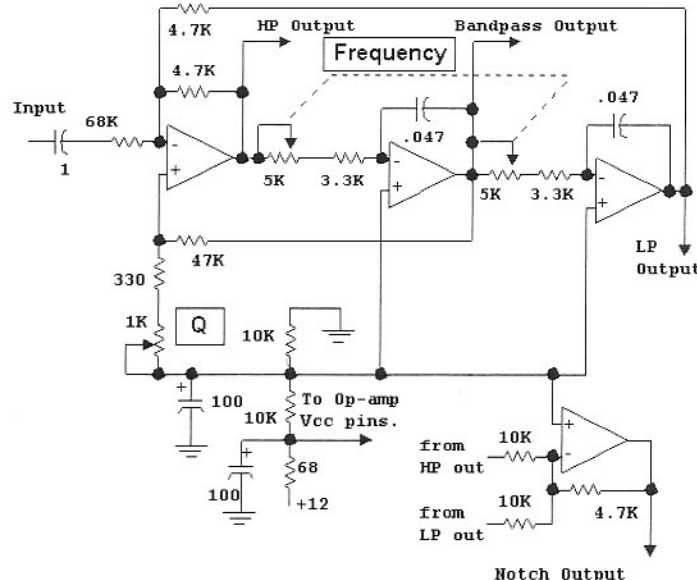


Fig 3.58—State-variable audio filter for CW receiver applications. All op-amps are 741 or 1458. The op-amp pin numbers are not shown. The builder must also connect the power supply line to the V_{cc} point on the op-amps. This circuit was inserted between the audio gain control and the output amplifier in a high performance CW receiver.

several sections are to be cascaded. It is sometimes useful to provide a rotary switch allowing the user the ability to select one of several outputs in a cascade. Each section of a IGMFB filter can have a Q as high as 10 or 20.

Other bandpass circuit forms are also suitable. An especially interesting one is the so called state-variable filter, which uses three operational amplifiers. The one circuit will simultaneously provide low pass, high pass, and bandpass outputs. Adding one more op-amp will even allow a notch filter function. An example is shown in Fig 3.58. This circuit is tunable over the normal range used for CW notes and has variable Q. The notch is not included in the version that was built, but could be added with the circuitry shown.

The reader interested in more information on the state-variable filter should examine the article by Howard Berlin.²⁰ The state-variable filter is an especially interesting circuit for those with a mathematical inclination, for the circuitry is an exact replication of the equations.

The All-Pass Filter

An especially interesting, but very simple RC active filter circuit is the all-pass of Fig 3.59. This circuit uses an op-amp, a single section RC low pass filter, and a pair of resistors. Although we

analyze the circuit with mathematics, much of the behavior is clear from inspection. At very low frequency, the capacitor is an open circuit. The op-amp input impedance is very high, so the input voltage is also that appearing at the point marked "E." The negative feedback action forces the inverting op-amp input to also be E. The only way for this to happen is for the output to also equal E. At low frequency the output is in phase with the input and has the same magnitude for unity gain. In contrast, at very high frequency, the capacitor is a short circuit. The op-amp

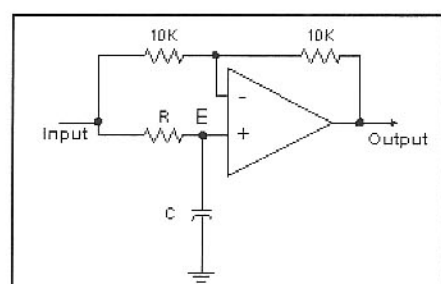


Fig 3.59—Basic, single section all-pass filter. This circuit has unity gain at all frequencies, but has a continually changing phase response. It is useful for phase shift networks such as those used for the phasing method of single sideband.

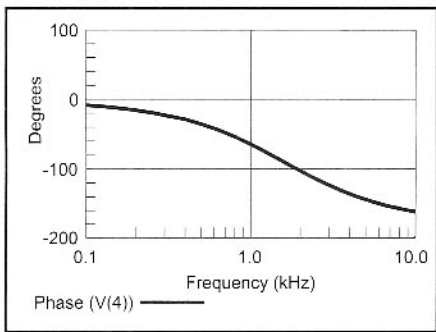


Fig 3.60—Phase response for an all-pass filter.

then behaves as the familiar inverting amplifier (180 degrees of phase shift) with unity gain.

The transfer function for this circuit is

$$H(j\omega) = \frac{1 - j \cdot \omega \cdot R \cdot C}{1 + j \cdot \omega \cdot R \cdot C} \quad \text{Eq 3.27}$$

where $\omega = 2\pi f$ with f in Hz. This circuit has an amplitude response of unity at all frequencies and a phase shift given by

$$\theta = \cos^{-1} \left[\frac{1 - \Omega^2}{1 + \Omega^2} \right] \quad \text{Eq 3.28}$$

where $\Omega = f/f_0$ with f_0 being the frequency where the network has a 90 degree phase. f_0 is given by

$$f_0 = \frac{1}{2 \cdot \pi \cdot R \cdot C} \quad \text{Eq 3.29}$$

The phase response of the network is presented in **Fig 3.60** for the case of $R=10\text{ k}\Omega$ and $C=10\text{ nF}$.

A common application for the all-pass network is to generate the audio phase shift needed in a phasing type SSB receiver or transmitter. Examples are found in Chapters 8 and 9.

A FIR Bandpass Filter

The all-pass filter serves as a frequency dependent delay element for a variety of

applications. An unusual one is in a special bandpass filter, one with a finite impulse response. The basic, repeated element in this filter is a delay element, shown in **Fig 3.61**. The delay arises from a cascade of two all-pass networks. The RC in the all-pass is picked for 90 degrees of phase shift at 800 Hz. Hence, the cascade of two has 180° shift at 800 Hz. The shift is less at lower frequency, but more at higher frequency. The circuit of Fig 3-61 behaves like a transmission line with length of one half-wave at 800 Hz.

The halfwave lines are repeated and cascaded to form a line that is, in this example, 4.5 wavelengths long at 800 Hz, shown in **Fig 3.62**. The line is tapped at each half wave point. Because the line is built from several operational amplifiers, the tap points are low impedance and can be loaded without interaction or other adverse consequence, difficult with a real transmission line.

A sinusoidal audio signal at 800 Hz is applied to the input. The signal looks the same at all points along the line except for changes in phase. If we extract two signals from two taps on the line that are separated by one full wavelength, the two signals will be in phase. If the two signals are added, they will produce a signal that is twice the original. If, however, the two taps are one (or three, or five,...) half wavelengths apart, the result is complete cancellation, for the two components are then equal in magnitude, but out of phase. The cancellation can be turned into positive reinforcement if we add 180 degrees of phase shift to one before addition; this results from an inverter.

Fig 3.62 shows a complete filter. All taps with even numbers are summed together in a summing amplifier U1. U2 serves a similar role for signals from odd numbered taps. U3 inverts one resultant signal with the final output extracted from U4 as the sum of the two. An output response is presented in **Fig 3.63**.

This filter has a characteristic that differs from the typical audio filter, the finite nature of the impulse response. The usual bandpass audio filter, such as described

earlier, will ring virtually forever when subjected to a noise impulse. The long ringing is evident from the mathematics; it is also evident from listening to such a filter. In contrast, the FIR filter has a impulse response that is limited to the total delay of the all pass structure. A filter like this one will still “color” noise, but that noise will not bring about the sometimes terrible ringing that would occur with a cascade of high Q resonators. Note the rounded peak shape; it’s similar to that found with filters with the better time domain responses.

The filter circuit shown in **Fig. 3.62** is not completely impractical, although it is not recommended as a construction project. One of the authors built several FIR audio bandpass filters in the late 1970s. In some, the signals from the taps had unequal weighting, accomplished by changing the summing resistors from each tap. The number of taps grew to impractical extremes. (Don’t ask!) Taps can be added as the delay length grows. The results were mixed with the eventual conclusion that a filter of this type was not practical in simple analog form. The experiments were, nonetheless, among the most enlightening that we have ever experienced!

A large number of taps is possible and completely practical today in FIR filters based upon digital signal processing. It is informative to continue the analogy.

- A DSP audio filter begins by sampling the incoming signal. The incoming signal is merely a voltage that changes with time. Sampling means that the signal is captured at one instant in time. This must occur quickly and often, at least twice for every cycle for the highest frequency that our audio system will process.
- Each sample is applied to an analog-to-digital converter. The A to D provides a stream of data that can be processed. It can be done in a high speed general purpose computer or in special circuitry designed specifically for this task. The digitized data is stored in computer memory.
- Computer memory also contains data that was stored from earlier moments. Remember that we are sampling the signal at least twice per cycle for the incoming data we wish to process. The memory has the data just sampled, that from one sample period back, from two periods back, and so forth, extending into the past by a number of “taps” commensurate with our ability to store and process.
- At each interval in the process, we will multiply each of the stored numbers by a constant, weighting the samples in the same way that they are weighted by the summing resistors in the analog filter. They are then added together to obtain a

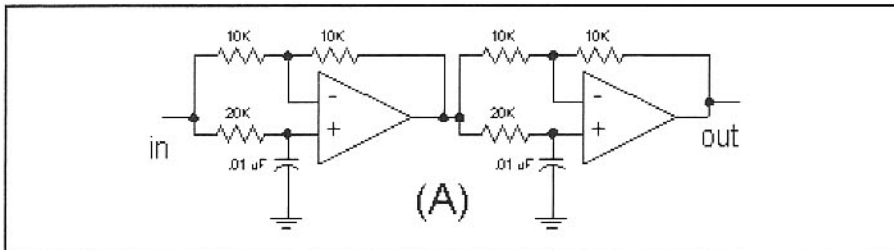


Fig 3.61—Half wave transmission line emulator.

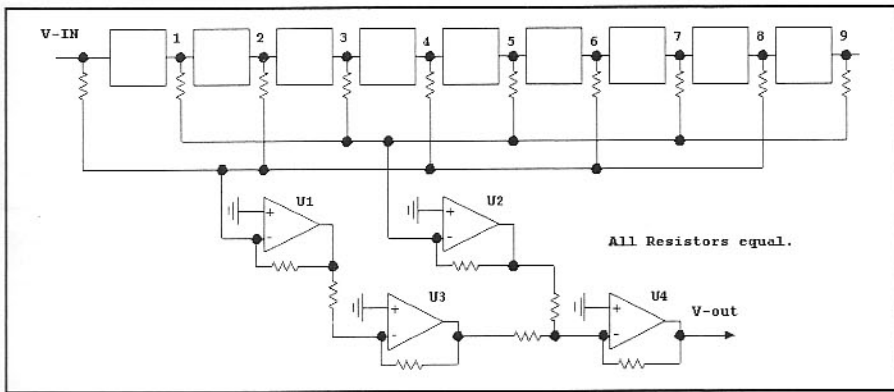


Fig 3.62—A Finite Impulse Response, or FIR bandpass filter built from a cascade of all-pass filters. This filter has 9 taps. Op-amps U1 through U4 serve to add signals from the various taps.

final result.

- The digital output “word” is applied to a DAC, a digital-to-analog converter that provides a signal that can be injected into an audio amplifier and, eventually, headphones.

- Data is eliminated from memory at each step in the process. We only go as far back in time as our computing power will allow.

Among the significant lessons that emerge from a study of FIR filters is the

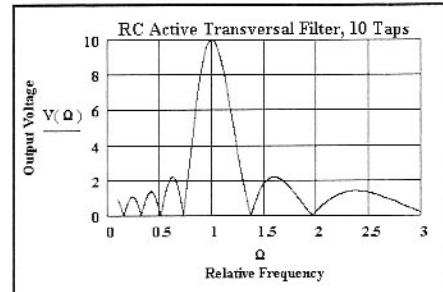


Fig 3.63—Transfer function of a 10-tap FIR filter.

realization that filtering is a comparative process; a signal is compared with a replica from an earlier point in time. The nature of the comparison is direct and clear in the FIR filter. It is present in the simpler filters, be it a single LC resonator or crystal, or an active version with an identical function. The signal components from earlier times vanish from the resonator as they dissipate in the tuned circuit losses.

3.6 IMPEDANCE MATCHING NETWORKS

Most filters built from inductors and capacitors were designed to achieve a desired frequency domain result: They accepted an input consisting of many frequencies, but allowed only a few to emerge at the output. Other LC circuits are designed for impedance transformation. An impedance transforming or matching network is one that accepts power from a generator with one characteristic impedance, the source, and delivers virtually all of that power to a different impedance, the load. Both source and load may be complex with both real and imaginary (reactive) parts. Simple designs are performed at only one frequency. More refined methods can encompass a wide band of frequencies.

Impedance transforming networks generally have filtering properties, even if they are not designed for that characteristic. We found earlier, for example, that a modified low-pass filter could be terminated in an impedance that differed from the original design value, serving a wideband matching role.

Directional Impedances

Consider point A in the circuit of Fig 3.64. A frequent question we hear is, “What is the impedance at point A?” This

question does not have a good answer, for we did not ask the right question. Impedances are directional. A better question would have been, “What is the impedance looking into the amplifier from the plane marked by A.”

The circuit in the figure is a simple amplifier operating at, for example, 50 MHz. The input impedance looking into the base is $20 - j10 \Omega$. This value would be reasonable for an RF transistor biased to a few mA and operating at $F_T/10$. Wishing

to transfer as much power into this amplifier from the source as possible, we will strive for a conjugate input match by designing a suitable input network. One of many possible networks that will realize such a transformation is the L-network shown, transforming from 50Ω down to 20Ω . If we then add an inductance with 10Ω reactance in series with the inductor of the L-network, we will have transformed the 50Ω source to look like the desired $20 + j10$ needed by the amplifier.

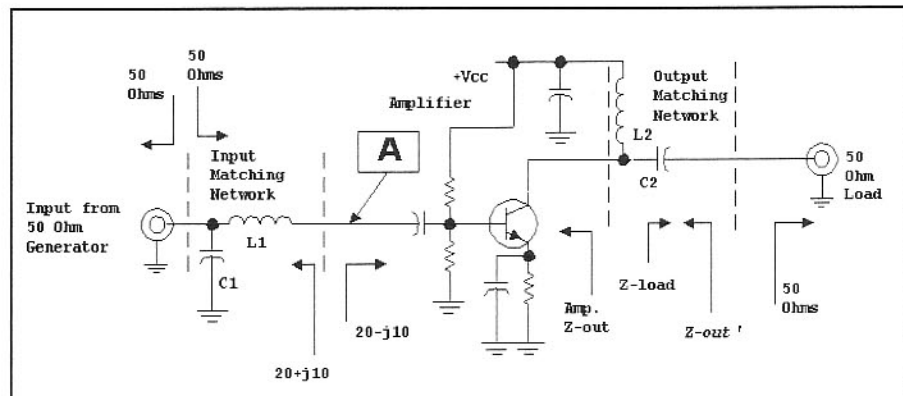


Fig 3.64—An amplifier with matching networks at input and output illustrating directional impedances. See text.

We were careful to match the input, but will not seek a conjugate match at the output. This often occurs with, for example, power amplifiers where we present a specific load, Z_{LOAD} , to the collector in order to realize a well defined output power. But this load will generally be different than a conjugate match to the amplifier output impedance, Z_{OUT} . Although a conjugate output match may well provide the highest gain and the maximum output power for small signal conditions, that output load could produce limiting that constrains large signal output power.

Input matching resulted from a low-pass type L-network. An input blocking capacitor is an integral part of the amplifier. Output matching is performed with a high-pass type L-network, which serves double duty by providing a route for V_{cc} to reach the transistor. There is no "perfect" match anywhere through the output. Recall also that changing the load presented to the amplifier will probably alter the input impedance.

We often build transforming networks that will present impedances for reasons other than matching. Output loading for power was mentioned. We sometimes present impedances at the input of low noise amplifiers that will optimize noise figure, usually different than those that provide best gain. We must be clear in defining our goals when designing matching circuits, and exercise similar clarity when talking about such circuits.

The L, π and Tee-Networks

Perhaps the most common LC impedance transforming network is the L, so named because it uses two elements, one as a series element with the other as a parallel one, resembling the capital L on its side. Both L-network forms are shown in Fig 3.65. The lower value resistor, R_1 , is transformed by adding a series reactance. The higher value, reactive impedance, is resonated at one frequency with a parallel reactance, yielding a load that looks like a real impedance of value R_2 .

The same equations apply if we wish to transform a higher resistance, R_2 , to "look

like" a lower one, R_1 . This bilateral nature is a general characteristic of all lossless networks. The derivation of these equations is outlined in Chapter 4 of *Introduction to RF Design*.²¹

We can define a network Q as the ratio of the parallel resistance, R_2 in this example, to the reactance of the parallel element. That is, we treat the network as if it was a parallel tuned circuit. Network Q is related to the voltage transformation of the network, but is not always a good indicator of network bandwidth.

$$X_S = \sqrt{R_1 \cdot R_2 - R_1^2} \quad \text{Eq 3.30}$$

$$X_P = \frac{R_1^2 + X_S^2}{X_S} \quad \text{Eq 3.31}$$

$$Q = \sqrt{\frac{R_2}{R_1}} - 1 \quad \text{Eq 3.32}$$

Consider an example: We wish to transform a 10- Ω resistance to look like 50 Ω at 7 MHz. The series reactance, from the equations, is 20 Ω and the parallel one is 25 Ω . The low-pass form, the L-network with a series inductor, would use $L = 0.455 \mu\text{H}$ and 909 pF. The high-pass form would use 0.568 μH and 1137 pF. Both networks offer essentially identical performance at the design frequency, but differ in their filtering properties. The Q of this L-network is 2. Q is a characteristic of the L-network that is established by the transformed impedances.

Another popular network is the pi, named because its three elements resemble the Greek π . This network is shown in low pass form in Fig 3.66. Again, R_1 is restricted.

Q is now a network parameter that the designer must pick. It can take on a wide variety of values, although they are bounded. The lowest Q allowed is defined by Eq 3.32, presented above for the L-network. If you used this value, the

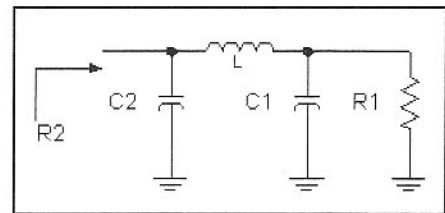


Fig 3.66—Schematic and corresponding design equations for the popular π -network.

pi-network equations collapse to those for the L. Low Q values are generally preferred with the low impedances usually found with solid-state circuits, offering more practical component values and lower network loss. Higher Q tends to restrict bandwidth, just as it would in a simple tuned circuit. It also exacerbates the effects of loss in the network L and C parts.

As an example, we examine the same 10- Ω load that must be transformed to 50 Ω ; we pick a network Q of 5. The results are $X_{C2}=10 \mu\text{F}$, $X_{C1}=4.88 \mu\text{F}$, and $X_L=13.56 \mu\text{H}$. At 7 MHz, the respective component values are 2274 pF, 4660 pF, and 0.308 μH .

A high-pass variant of the pi network is also possible. The pi-network component values may not be as practical as those in some other circuits, especially when Q is high.

$$R_2 \geq R_1$$

$$X_{C_2} = \frac{R_2}{Q} \quad \text{Eq 3.33}$$

$$X_{C_1} = R_1 \cdot \sqrt{\frac{R_2 / R_1}{Q^2 + 1 - R_2 / R_1}} \quad \text{Eq 3.34}$$

$$X_L = \frac{Q \cdot R_2 + R_1 \cdot R_2 / X_{C_1}}{Q^2 + 1} \quad \text{Eq 3.35}$$

Although less common, a very practical and useful network is the Tee using two capacitors and one inductor. Component values are practical and loss is low, especially for the low impedances found with solid state circuits. The design begins by picking a network Q.

The T-network has the same minimum Q as the pi network, which is the Q of the L-network given by Eq 3.32. The Tee circuit is shown in Fig 3.67. Intermediate variables, A and B, are used in these calculations.

We pick the same example used before

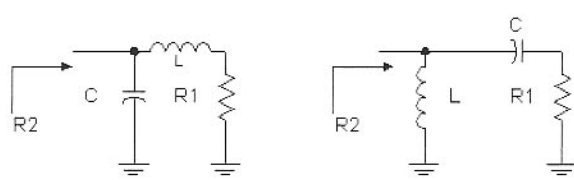


Fig 3.65—L-Network with design equations when $R_1 < R_2$.

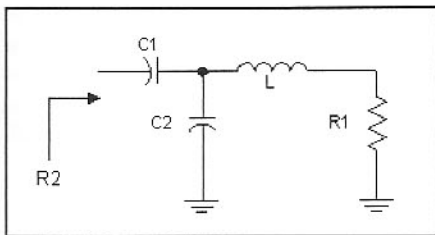


Fig 3.67—LCC type Tee-network and design equations.

with $R_1=10$, $R_2=50$, and $Q=5$.

The resulting reactance values become $X_{C_1}=88.12$, $X_{C_2}=102.5$, and $X_L=50$, all in Ω . At 7 MHz, these values correspond to 258 pF, 222 pF, and 1.137 μH , respectively. These components are especially practical for both input and output networks of RF power amplifiers if mica compression variable capacitors are used.

$$R_2 > R_1 \\ B = R_1 \cdot (Q^2 + 1) \quad \text{Eq 3.36}$$

$$A = \sqrt{\frac{B}{R_2} - 1} \quad \text{Eq 3.37}$$

$$X_L = Q \cdot R_1 \quad \text{Eq 3.38}$$

$$X_{C_1} = \frac{B}{Q - A} \quad \text{Eq 3.39}$$

$$X_{C_2} = A \cdot R_2 \quad \text{Eq 3.40}$$

Increasing the inductor, then adding a series capacitor that cancels the added inductive reactance, may modify all the networks described. The modified networks are more easily adjusted and can provide narrower bandwidth.

We often view π or T-networks as back to back L-networks, transforming from a nominal impedance to another, and then back. This has the effect of increasing overall circuit Q or selectivity. Cascaded L-networks can have the opposite effect of decreasing selectivity, an extremely powerful tool when building circuits to function over wide bandwidth.²²

The Transmission Line as a Transformer

Transmission lines have well known impedance transforming properties. A termination of value R_1 is transformed to a new value, R_2 , by a transmission line that

is a quarter of a wavelength long with a characteristic impedance Z_0 given by

$$Z_0 = \sqrt{R_1 \cdot R_2} \quad \text{Eq 3.41}$$

If, for example, we wished to transform a 10- Ω load to appear as 50 Ω at 7 MHz, we would use a line with a characteristic impedance of 22.4 Ω . The length would be $\lambda/4$ at 7 MHz, about 25 ft in cable with a velocity factor of about 0.7. This characteristic impedance is impractical, but could be approximated with parallel sections of higher impedance lines. (Line with $Z_0=25 \Omega$ can be purchased.) Transmission line transformers are sometimes practical at this low frequency, especially in antenna systems where the lines are needed anyway. Coaxial transmission lines can be coiled with virtually no impact on their behavior so far as the fields within the line. The quarter wavelength lines are often called "Q-Sections." A transmission line need not have a $\lambda/4$ to serve as a transformer. A Smith Chart is often used for the design of these elements.

Transmission lines become more practical circuit elements at higher frequencies. One printed line form is microstrip, shown in Fig 3.68. The lower conductor is a ground plane on the back of a circuit board while the upper conductor is a printed run. Electric field lines between the conductors are found in the dielectric as well as in air. Hence, these transmission lines have a velocity factor part way between that of air and that of the higher dielectric constant insulator.

Microstrip is versatile, for it can be designed for about any characteristic impedance in the 10 to 100- Ω region, or more. The wider lines have lower Z_0 . Robert Wilson, KL7ISA and Hal Silverman, W3HWC, in "Wire Line—A New and Easy Method of Microwave Circuit Construction," described a wonderful

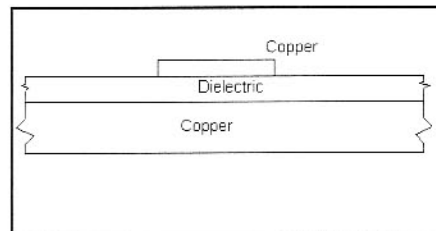


Fig 3.68—Microstrip transmission line shown in cross section. The dielectric material is the insulated portion of a printed circuit board. The lower conductor is usually a solid ground plane. The drawing is not to scale.

variation that the experimenter can build without etching in the July 1981 *QST*.²³

Another practical transmission line form is a simple twisted pair of insulated wires. Wire insulated with plastic often produces lines with a characteristic impedance around 100 Ω . Enamelled #24 wire will produce line with an impedance near 50 Ω when tightly twisted.

A variation on the quarter-wave line matching uses synthetic transmission lines. Here, a transmission line is replaced by a pi-network using inductors and capacitors. A sidebar earlier in this chapter discussed the half-wave filter, a variation of this circuit. Fig 3.69 shows a synthetic quarter-wave example, the same case considered earlier at 7 MHz. Transforming from 10 to 50 Ω occurs with a 22.4- Ω line.

Powdered Iron Toroid Inductors and Transformers

Inductors are realized with many structures, ranging from straight wire pieces to solenoid and toroid coils. The solenoid is easy to wind and can exhibit high Q, especially at VHF. However, the magnetic field of a solenoid extends well outside the coil

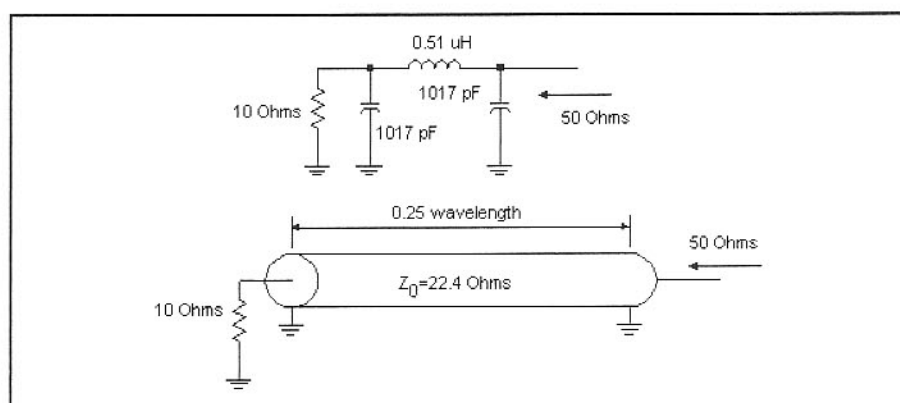


Fig 3.69—A synthetic quarter wavelength line is formed at 7 MHz with three equal reactance values of Z_0 of a Q section.

dimensions, leaving it free to couple to other circuit elements in close proximity, including conductive walls that can alter Q. In contrast, the toroid inductor has most (but not quite all) of its magnetic field confined to the core interior, allowing a toroid to be mounted directly against a ground plane with minimal change in inductance or Q. The Q available for low volume coils is generally much higher for toroids up through 30 MHz.

Toroids are more difficult than solenoids to wind, creating apprehension among beginning experimenters. It is, however, straight forward, even if time consuming.

Toroid inductance is almost exactly proportional to the square of the number of turns,

$$L = K \cdot n^2$$

Eq 3.42

A common core is the T30-6 from Micrometals with inductance constant, K , of $3.6 \text{ nH}/t^2$ (nano-henry per turn squared.) Various manufacturers use other units that can be related directly to the K we find convenient for RF parts. A coil with 15 turns evenly wound around most of this core has a predicted inductance of 810 nH , or $0.81 \mu\text{H}$. Generally, the highest Q will result when the cores use the largest wire that will fit in one layer. It is important for Q, and especially for temperature stability, that the wire be tightly wound against the core. A more temperature-stable coil can often be built with a wire size smaller than that producing the highest Q.

Micrometals, Inc copyrights the usual toroid numbering scheme, illustrated here with T30-6. The -6 indicates a specific core material or "mix," while the 30 indicates an outside diameter of 0.30 inch. A manufacturer or vendor catalog might list the inductance constant for the T30-6 as $36 \mu\text{H}$ per 100 turns. The user can convert these constants to whatever form he or she prefers.

A toroid is wound by counting the number of passes through the center hole. While solenoids can have a fractional number of turns, this does not happen with toroids. A single turn on a toroid consists of the wire passing through the hole just one time.

We built the inductor mentioned by winding 15 turns of #28 wire over about 90% of a T30-6 core. Using an Almost All Digital Electronics L/C Meter IIB, the inductance was measured as 872 nH , 8% above the prediction. Part of the difference was probably the result of slight bunching of some of the turns. The permeability tolerance normally associated with these

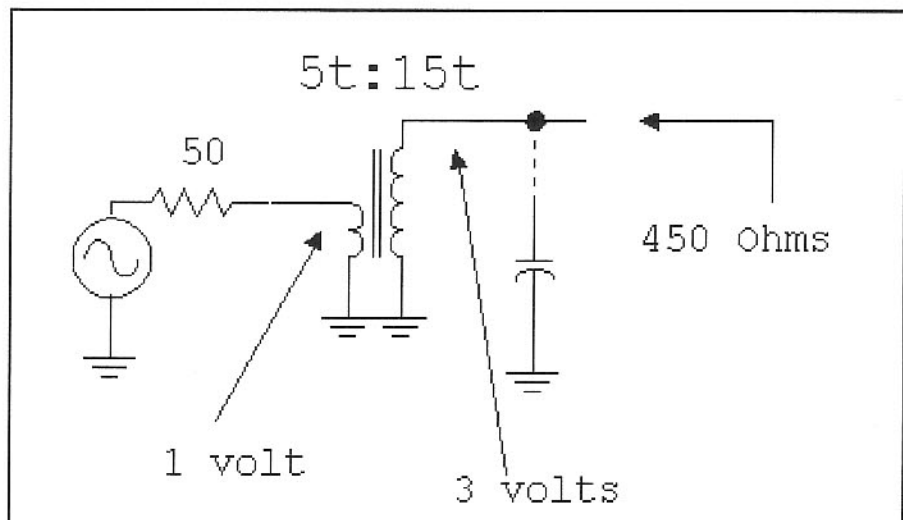


Fig 3.70—Circuit illustrating the transfer characteristics of an ideal transformer.

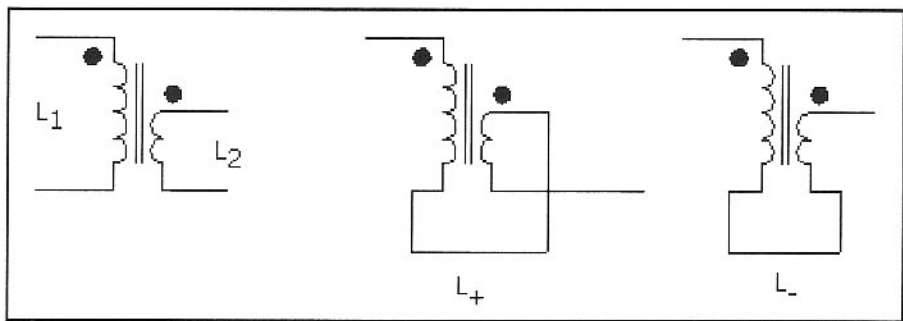


Fig 3.71—Method for connecting windings that allows coupling coefficient to be calculated. This method is general and can be applied with powdered iron or ferrite core transformers. The results become less accurate when coupling is strong, and it is not unusual to calculate $k > 1$. This is usually an indication of capacitance.

cores is $\pm 5\%$. The accuracy is usually better as inductance and core size grow.

The windings were then compressed to cover only 60% of the core, increasing inductance to $1.039 \mu\text{H}$. This 15 to 20% increase is typical and offers a convenient means for adjustment.

This inductor can be used directly in impedance matching networks, or as part of a L/C filter. The reader should consult the extensive data available from Amidon Inc. This is found at an excellent Web site, www.amidon-inductive.com/.

A common impedance matching network uses a powdered iron inductor with a second winding, forming a transformer. The inductor we just described was modified by adding a 5 turn link of #26 wire on the remaining bare portion of the core. The measured inductance was 206 nH . This is much higher than the 90 nH the formula would predict, but the coil is severely compressed. (Even with the 5 turns spread over the complete core, $L=121 \text{ nH}$.) The 15 turn winding L was unchanged at 1039 nH .

We expect RF voltage to increase in pro-

portion to the turns ratio and impedance to transform with the square of the turns ratio in an ideal transformer. Hence, a $50\text{-}\Omega$ generator attached to the 5-turn link should provide three times the voltage across the 15-turn winding with the combination looking like a $450\text{-}\Omega$ source to the following circuitry, as shown in Fig 3.70. If it was terminated in a $450\text{-}\Omega$ load, the impedance match looking into the link should be perfect. This transformer might be used to match between a $50\text{-}\Omega$ amplifier and a $450\text{-}\Omega$, 10-MHz crystal filter.

But, these ideals are not realized. First, the impedances are highly reactive. This is remedied by tuning the secondary with a parallel capacitor, 244 pF at 10 MHz. This brings the voltage gain nearly up to the predicted 3 when the output is terminated, but impedance match is still poor. This is a result of less than ideal coupling.

The coupling coefficient is easily measured with the same instruments used to measure inductance. This is shown in Fig 3.71. L_1 and L_2 are the 5 and 15 turn windings and are measured with the other

winding open circuited. The two windings are then connected as shown in Fig 3.71 and the composite inductance values are measured as L_+ and L_- . The coupling coefficient is then given:

$$k = \frac{(L_+ - L_-)}{4 \cdot \sqrt{L_1 \cdot L_2}} \quad \text{Eq 3.43}$$

This method was presented by Bill Carver, W7AAZ, in the January, 1998 issue of the *QRP Quarterly*.²⁴ When the method was applied to the test transformer, we measured $L_+ = 1533$ nH and $L_- = 872$ nH, leading to a coupling coefficient of $k=0.357$. The input VSWR exceeds 2:1 for this transformer, even when tuned and properly terminated.

Ideally, all inductors should be measured after they are wound. While the traditional tuned transformer is still a practical component, it may require more design effort than an impedance transforming network built from discrete elements.

The Ferrite Transformer

The powdered iron core transformer discussed above had to be resonated to function as desired. Even after tuning, it suffered for a lack of coupling. Both problems are overcome with higher inductance, which occurs with the much higher permeability found in ferrite cores. The toroid is the most common form, but balun cores, with their binocular shape, are also popular. Most of the powdered iron cores we use have initial permeability under 10 while typical ferrites show μ values between 40 and 5000.

Recall the classic inductor, a component that “tries” to maintain whatever current is flowing at any instant. It is the dual of the capacitor, which does not allow voltage to change instantly. Consider a switch that connects a battery to an inductor. The inductor current is zero before the switch closed, so it must be zero immediately afterward. There is no restriction on the voltage. The voltage impressed on L changes quickly, soon reaching the battery value. The current conserving characteristic of the inductor is a result of the magnetic field. When the switch is closed, current begins to flow. But as soon as the field starts to build up, the changing magnetic field generates an electric field (hence, a voltage) that opposes the electric effect that caused the current in the first place. This is a non-rigorous statement of Faraday’s Law, one of Maxwell’s equations. The inductor is shown with curves illustrating

the behavior in **Fig 3.72**.

Inductor current increases without bound in the ideal, lossless case. Losses, resistance within the wire and the battery, would limit the current to a finite, but large level in a practical circuit.

Consider now a modified structure. The single winding inductor is replaced with a pair of windings, shown in **Fig 3.73**, that are very close together. The wires, although isolated from each other, occupy virtually the same space and see essentially the same magnetic field. If we left the second winding (BB') open circuited, voltage from A to A' builds up in the same way that it did with the simple inductor. Measurement across either winding will show the same voltage profile. But, no current flows in BB' when it is open circuited.

The behavior changes when we repeat the experiment with a load at BB' . As the voltage builds, load current will begin to flow. Transformer action begins. The current in the second winding will generate a magnetic field, just as that in the primary winding did. But the field from the secondary is in a direction opposite to that from the first winding. Because the net magnetic field has been reduced (nearly) to zero, current flow is determined by R , the external load.

The transformer described (Fig 3.72), with the two wires in close proximity, is said to be bifilar. Bifilar windings are often twisted. One manufacturer supplies Multifilar® wire with strands of differing

colors, simplifying transformer construction. (Multifilar® parallel banded magnet wire from MWS Wire Industries.)

The dots on the transformer schematic are useful. An increasing voltage at one dot produces an increasing voltage at the other. Current entering the A dot equals that leaving the B dot. This behavior arises because the magnetic field vanishes within the core. If the primary (AA') had N_p turns while the secondary (BB') had N_s turns, the currents would obey the more general boundary condition that

$$N_p \cdot I_p = N_s \cdot I_s \quad \text{Eq 3.44}$$

Bifilar winding and the use of a high permeability magnetic material produce tight coupling, approaching $k=1$. Coupling is measured for a ferrite transformer with the same method outlined for a powdered iron design, Fig 3.71. Strong coupling means that all of the magnetic field lines created by the primary also couple into the secondary. In a practical transformer, some of the primary field loops out from the core, only to return without communicating with the secondary.

The transformer is often modeled as an ideal one with added components, shown in **Fig 3.74**. The ideal transformer has a voltage ratio proportional to the turns ratio and a current ratio defined by **Eq 3.44**. L_p is the primary inductance, the value we would measure if the primary was examined without a secondary termina-

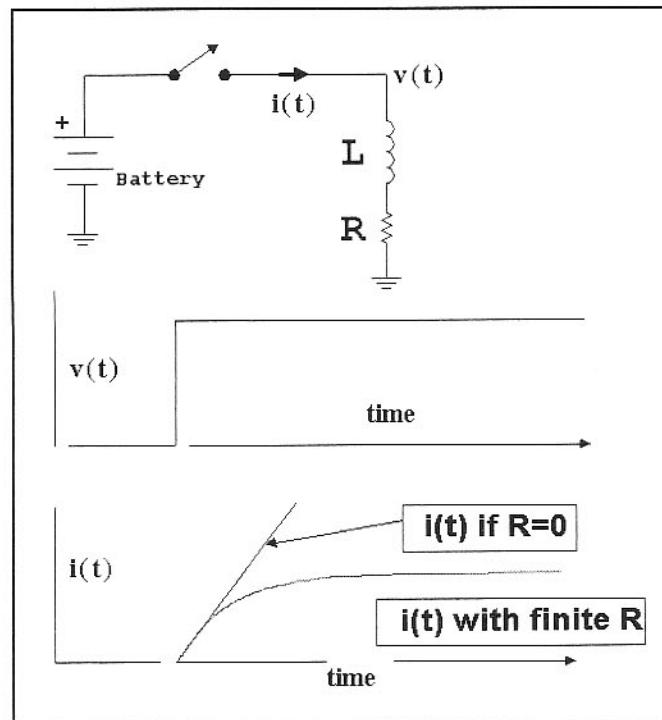


Fig 3.72—Principles of an ideal inductor, with waveforms. The current would grow linearly forever in an ideal component. Resistance establishes an ultimate value.

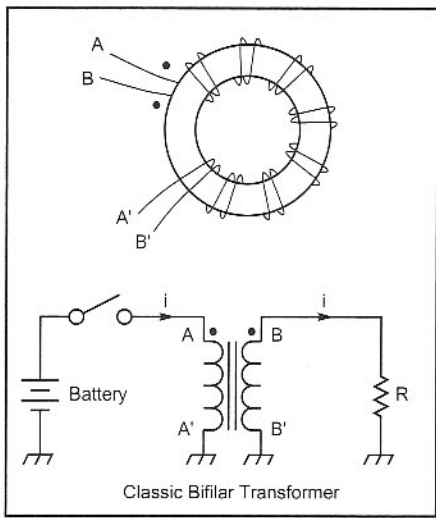
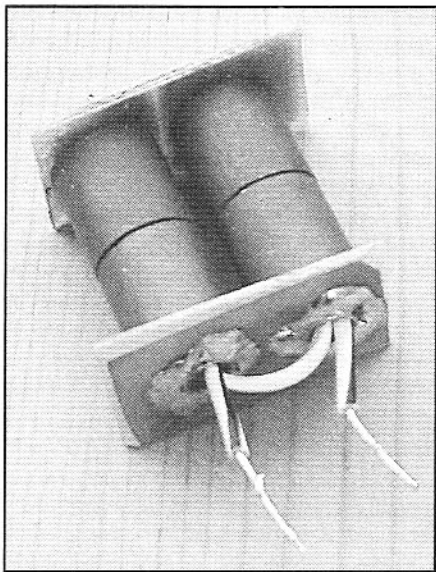


Fig 3.73—Current flow in a bifilar wound transformer.



RF transformers can be built by placing ferrite beads over brass tubing that forms a single turn winding. Circuit board material connects the tubing ends with a short at one end. A multiple wire winding is then threaded through the middle of the tubing, guaranteeing tight coupling.

tion. The L-leakage is the inductance accounting for the magnetic flux that does not pass through both windings. R1 and R2 account for losses. The transformer is a bandpass circuit with L_p presenting a short at dc and very low frequency; L-leakage, a series element, presents a high impedance at high frequency.

A practical transformer will have a primary inductance with a reactance at least 5 times the terminating resistance at the low frequency limit and a leakage inductance reactance less than 1/5 the resistance at the

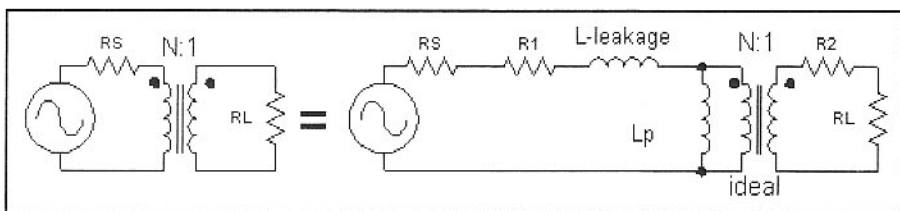


Fig 3.74—A transformer model.

highest frequency, and loss resistances small with respect to the source and load. Inductance of windings on ferrite cores is proportional to the square of the turns, although the higher permeability of ferrite produces dramatically higher “ k ” constants for use with Eq 3.42. For example, the popular FT37-43 ferrite toroid has k of about 360 nHt^2 . Core loss can be modeled as a parallel resistance, which is also proportional to the square of n , although this formulation is not in general use.

Examples of practical transformers are found throughout the text. A wonderful treatment of the modeling of this “simple” component is presented by Clarke and Hess.²⁵ A more complete review of transformer modeling is presented by Chris Trask.²⁶ We generally use powdered iron toroid cores for high-Q inductors with good temperature characteristics while ferrites are relegated to low-Q wideband transformer application. However, this distinction is not required. Some powdered iron cores are suitable for wideband transformers while some ferrites have excellent Q at HF. A good example of the later is –63 material from Fair-Rite Products Corp (www.fair-rite.com), often producing Q values of several hundred at HF.

Ferrite Transmission Line Transformers

The example presented above to illustrate basic transformer action used a bifilar

winding, with one wire as primary and the other as a secondary. A pair of wires also forms a transmission line. As such, it can operate as a transmission line transformer such as a Q-section according to Eq 3.41. Even if it is not a proper $\lambda/4$ length, it will still transform the impedance seen at one end from that presented at the other. The transmission line properties persist if the line is wound in the shape of a coil, including a toroid. But the structure then assumes a different extended behavior, summarized in a classic paper by Ruthroff.²⁷

The simplest ferrite transmission line transformer is that shown in Fig 3.75. This structure, formed with a bifilar winding on a toroid was at one time called a balun. A balun is a structure that generates a balanced voltage from one that is single ended. This connection does not force such balance and is, hence, not strictly a balun, even though it does perform some of the isolation chores that we might ask of a balun. Perhaps a better name is *isolation transformer*. Transformer action, described above, does force equal currents in the two windings, so this circuit is sometimes also called a *current balun*.

The isolation transformer is labeled AB at one end of the winding while the other end is A'B'. Wires A and B are not attached to each other, a useful detail to keep in mind when winding such transformers without wires of differing color. Viewing this structure as a transmission line, cur-

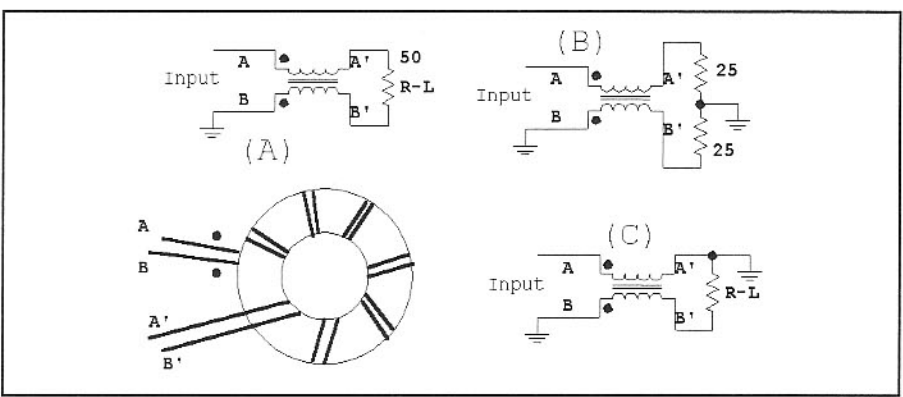


Fig 3.75—Part A: Basic isolation transformer using a transmission line on a ferrite toroid. This structure has some balun like properties. Part B shows a balanced load connected to a single-ended drive while C shows polarity inversion.

rent at point A' is delayed from that at A. However, the ferrite core and traditional transformer behavior would force equal current through a winding, and indeed, in the other winding.

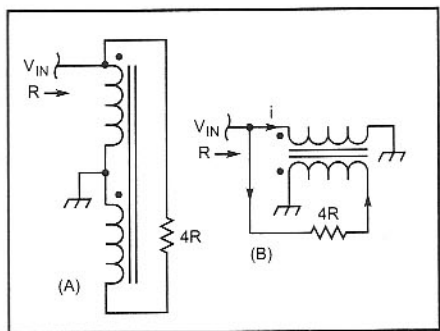


Fig 3.76—A 4:1 step-up balun transformer.

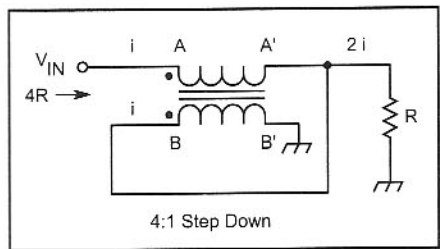


Fig 3.77—A single ended impedance step down transformer.

The isolation transformer of Fig 3.75 has a single ended input. The single ended drive will appear as a balanced output on a balanced load such as that in part B. In this sense, it is a balun structure. However, if the load becomes unbalanced, as in Fig 3.75C, the input may still be applied to the termination.

It is instructive to mentally connect the two wires at one end (A and B) together, doing the same thing at the other (A' and B') end. The result is an inductor. Several turns on a high permeability ferrite would produce considerable inductance. This is termed a common mode inductance. Separating the wires, a load placed across one end, A'B', is then seen differentially (between A and B) at the other end. This structure is often called a common mode choke for common mode signals at one end are isolated from the other by the large inductance, while differential signals are not impeded.

The isolation properties of this structure allow us to drive one end while treating the other end as if it were a separate generator. An isolation transformer (Fig 3.75C) can produce a polarity reversal.

It is useful to connect the output of an isolation transformer in series or parallel with the input. An interesting example is shown in Fig 3.76 where a load is connected between the input and the inverted output. The composite input will carry

twice the current that one transformer winding carries, resulting in a true balun, for it forces equal, but out of phase voltages to appear between the ends. This is a 4:1 impedance transforming balun.

The same structure is reapplyed in Fig 3.77. The transformer forces twice the current to flow in the output as at the input. The isolation properties of the transmission line transformer are used to parallel an output with a "direct connection" to the input. This circuit now serves an unbalanced-to-unbalanced role. This circuit is used for transforming from $50\ \Omega$ down to the $12.5\ \Omega$ input on a RF power amplifier. We also saw it used extensively to cause a $50\text{-}\Omega$ load to look like $200\ \Omega$ at the collector of a feedback amplifier.

These wideband transformers may be viewed as either transmission line circuits or as conventional transformers. Their operation is consistent with either set of boundary conditions. The transformers are designed with about $\lambda/8$ to $\lambda/4$ of transmission line at the upper frequency of the circuit. The characteristic impedance of the line is consistent with line behavior for the terminations considered. If, for example, we built a 4:1 step down from 50 to $12\ \Omega$ using Fig 3.76, Z_0 should be $25\ \Omega$. This could be realized by paralleling two $50\text{-}\Omega$ windings on the core. A $50\text{-}\Omega$ winding consists of a tightly twisted pair of #24 enamel wires.

The transformer of Fig 3.78 is a true 1:1 balun. The termination impedance is that seen at the input, but the circuit creates two voltages that are equal in magnitude, but out of phase.

A useful step down circuit for high power single ended amplifiers is the 9:1 circuit of Fig 3.79. This transformer uses two cores to drop from $50\ \Omega$ down to about $6\ \Omega$. Series connections at the input side drive parallel ones at the output. A similar series/parallel circuit is presented in Fig 3.80 where two cores form a balanced to balanced 1:4 impedance ratio step up transformer.

Numerous other kinds of transmission line transformer can be built, some almost diabolic in their cleverness. The reader is referred to Motorola Applications Note AN-593²⁸ for further interesting examples.

Some Multiple Port Networks

All of the networks presented in this section have used but two ports, an input and an output. There are, however, several multiport networks that are of special interest to the radio amateur. The first is the so called "Splitter/Combiner" shown

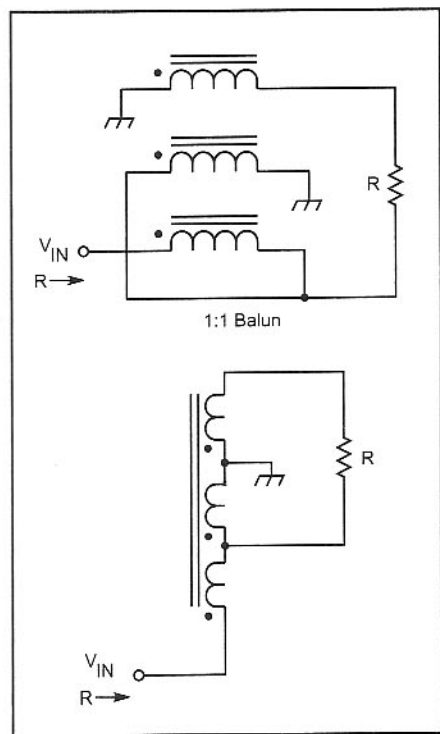


Fig 3.78—A 1:1 impedance ratio true balun transformer.

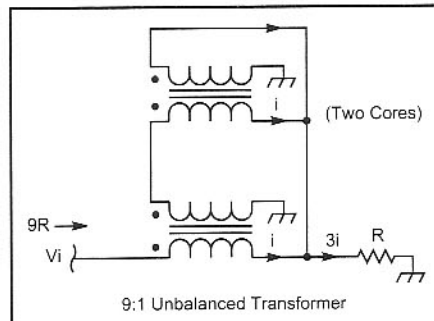


Fig 3.79—Illustration of a 9:1 unbalanced transformer.

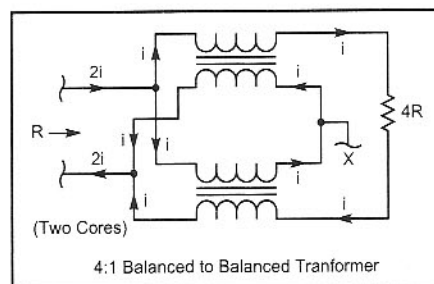


Fig 3.80—A 4:1 balanced-to-balanced transformer.

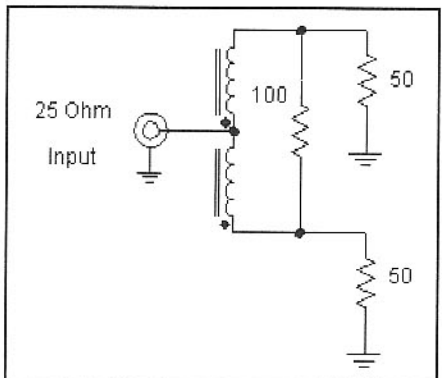


Fig 3.81—An in-phase splitter/combiner network. Use 10 bifilar turns on a FT-37-43 ferrite toroid for the HF spectrum.

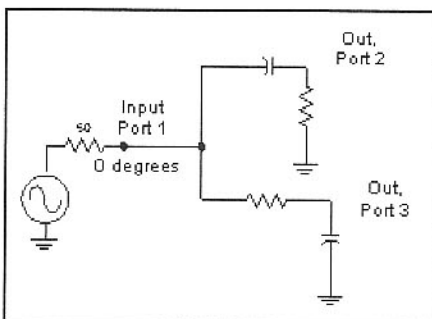


Fig 3.83—Phase shift network for RF phasing in simple SSB equipment.

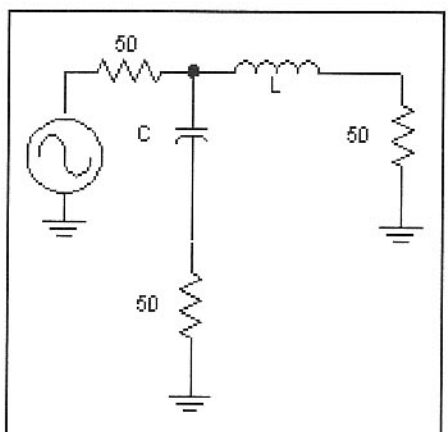


Fig 3.82—First-order low-pass/high-pass diplexer.

In **Fig 3.81**, This circuit, using nothing more than a bifilar winding on a ferrite toroid, accepts energy from a single generator with a $25\ \Omega$ characteristic impedance and supplies that energy to two outputs, each with a $50\ \Omega$ impedance. A $50\ \Omega$ input can be transformed down to $25\ \Omega$ with any of the matching schemes presented above. Variations of this network use transmission lines or L-Networks. The $100\ \Omega$ resistor absorbs excess power that becomes available when one of the two output ports is miss-terminated. A common application splits the output of a local oscillator chain to drive two mixers. The circuit isolates the two outputs. This circuit is called a 3-dB hybrid transformer, for the power in each output, neglecting losses, is 3 dB below the input, while Hybrid refers to transformer-like circuits that provide isolation between two of three ports. Hybrids were used in early telephones to isolate the microphone from the earphone.

Fig 3.82 shows a three port circuit where

two outputs receive drive from a single input. This circuit, a diplexer, is similar to a crossover network used in audio systems. Frequencies below a cutoff pass through the inductor and are dissipated in the related termination. Signals above cutoff pass through the capacitor to the related resistor. The L and C are picked with regard to the source impedance such that there is always a perfect impedance match presented to the generator. If the cutoff frequency is f , then the related angular frequency is $\omega_c = 2\pi f$. Then, the L and C for a perfect match are

$$L = \frac{R}{\omega_c} \quad C = \frac{1}{\omega_c \cdot R} \quad \text{Eq 3.45}$$

The diplexer is applied where mixers (e.g., diode rings) must be terminated in a wideband $50\ \Omega$ to minimize distortion. The diplexer shown is an especially simple one where each arm is a one pole low pass or high pass filter. Nic Hamilton, G4TXG, has described high order low pass high pass dippers.²⁹ A third-order example of this design is shown in the diplexer sidebar. Dippers can also be built with combinations of band-pass and bandstop networks, also summarized in the sidebar.

An interesting, yet simple phase shift network is shown in **Fig 3.83**. A generator drives two one pole filters that are terminated at their output in open circuits. The two capacitors, equal in value, are picked to have a reactance at one frequency equal to R , the resistor value used in each arm. The phase difference for this network is 90 degrees at all frequencies. However, the two output amplitudes are equal only at the design frequency.

An especially interesting four-port circuit form is the directional coupler. The coupler has an input and output, usually with low loss between them. A third is called the “forward” coupled port, for the

energy available is proportional to the energy flowing from the “input” to the “output.” A fourth is the “reflected” coupled port with energy proportional to that flowing from the “output” to the “input.” **Fig 3.85** shows a schematic representation of a directional coupler, which is also a practical topology in microstrip form. Part B of Fig 3.85 shows a wideband variation using ferrite transformers.³⁰ A practical version of the wideband coupler using three transformers was designed by Roy Lewallen³¹ and is included on the book CD.

The directional coupler is extremely useful for a variety of applications. When used with a power meter or spectrum analyzer, reflected energy is a measure of the impedance at the output port, leading to popular in-line power meters such as the W7EL design. But the coupler can also be used to inject signals on a line. The coupling value is the power ratio between the output and the coupled ports and is $1/N^2$ for the ferrite version. Most directional couplers have coupled energy that is in phase with the output. The microwave literature abounds with interesting couplers.

A coupler is also characterized by directivity. Assume that the thru path is terminated in an open (or short) circuit and a power P_1 is measured in the reflected port. If the main path is now loaded with a perfect match, the reflected power will drop to P_2 . The ratio of P_1 to P_2 is called the directivity. We consider directivity with a number of bridge circuits in Chapter 7.

Directional couplers can be built with lumped components, even at VHF. A lumped element example with -28 dB coupling with 20-dB directivity at 144 MHz is included in a design discussed later in the book and included on the book CD. That design is a quadrature coupler, discussed below.³² There are numerous references in the literature to directional couplers. See, for example, Andre Boulouard.³³

The twisted-wire quadrature hybrid directional coupler is a very useful variation. This circuit was described by Reed Fisher, W2CQH.^{34,35} Fisher's *QST* article is included on the book CD-ROM. Also see.^{36,37} For information on distributed couplers, see.^{38,39} This is a 3-dB coupler, for the coupled output is below the input by 3 dB, producing two outputs of equal strength. The circuit is called a quadrature coupler because there is a 90-degree phase difference between the two output ports. A HF variation, built for the 7-MHz band, is shown in **Fig 3.84**.

The design equations for the coupler are identical to those presented for the diplexer, **Eq 3.45**. However, in this case, the capacitance is the total C in the circuit.

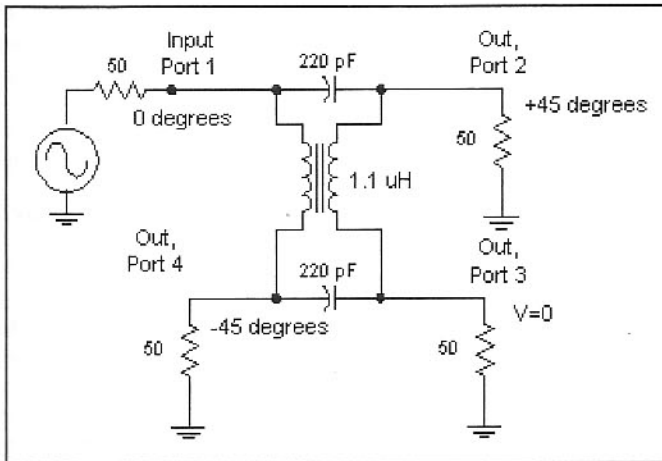


Fig 3.84—Quadrature coupler for 7 MHz.

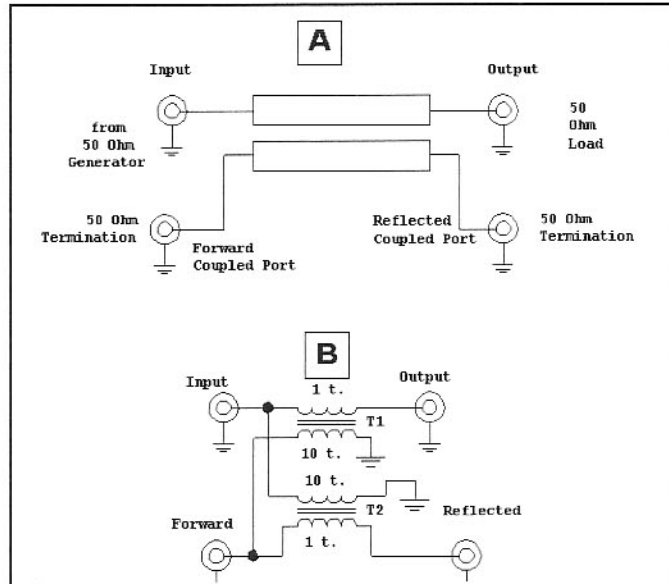


Fig 3.85—Part A shows a general schematic for a directional coupler while B presents a wideband version using ferrite core transformers. The coupling on B is 20 dB owing to the 10:1 turns ratio used. This is a practical circuit if wound with FT37-43 or FT37-75 cores. A single binocular core can be used for both transformers.

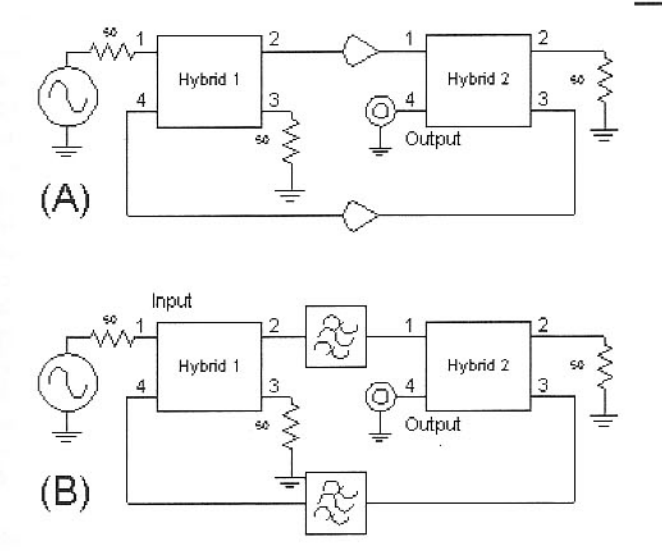


Fig 3.86—Some applications for quadrature hybrids. Identical amplifiers (A) or filters (B) are combined to form termination insensitive linear circuits. The extra terminations required are shown in the circuits.

This must be halved to build the circuit. As Fisher points out, the capacitance of the tightly wound bifilar pair (12 pF in his example) is measured and removed from the calculated C before construction. The inductance is that of the two windings in parallel, essentially the same as that of a single winding on the core of interest. Fisher used a low-permeability ferrite core, while we have generally used powdered iron cores, owing primarily to availability. Small powder iron cores such as the T25 in the -6, -12, or -17 materials are suitable through 150 MHz.

At the design frequency, the circuit is a 3-dB coupler, providing equal power at port 2 and 4. However, the coupling is different at other frequencies. The very interesting properties of the quadrature hybrid are summarized:

1. There is power transfer from port 1 to 2.

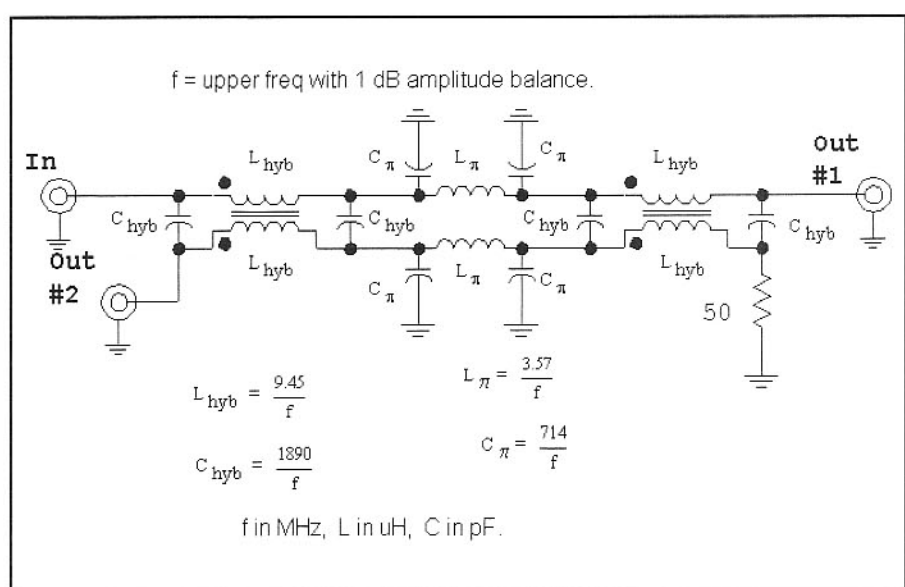
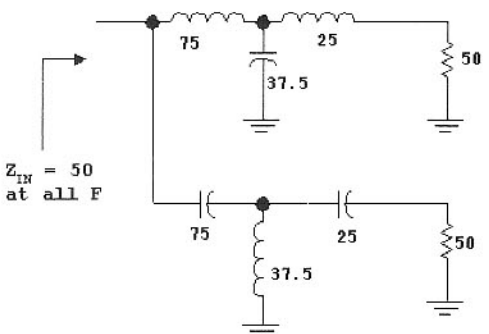


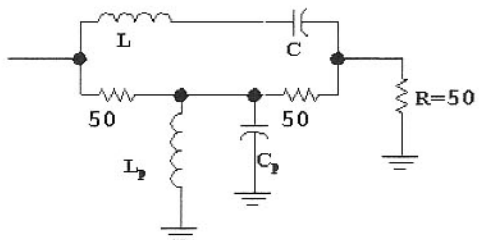
Fig 3.87—Extended bandwidth quadrature hybrid network.

Third order Low Pass High Pass Diplexer



L and C values shown are reactance at the cutoff frequency.

Bandpass-Bandstop Diplexer



1. Pick cutoff frequency F and Q (from 1 to 10)

2. $\omega = 2\pi \cdot F$

$$3. L = \frac{50 \cdot Q}{\omega}$$

$$4. C = \frac{1}{\omega^2 \cdot L}$$

$$5. C_p = \frac{L}{R^2}$$

$$6. L_p = \frac{1}{\omega^2 \cdot C_p}$$

Typical diplexer configurations and equations.

2. Power is transferred from port 1 to 4.
3. There is no power transfer from port 1 to 3 when all ports are properly terminated.
4. There is no reflected power back out of port 1, again with proper terminations.
5. The phase difference between ports 2 and 4 is 90 degrees.

The characteristic of greatest interest will depend upon the application. The phase difference is important in the construction of phasing-method SSB equipment. However, it is the isolation from reflection problems, item 4, that leads to some of the more subtle applications. Two examples, each using a pair of couplers, are shown in Fig 3.86. In part A, two amplifiers are combined, while in B, two filters are combined. In both cases, the two elements must be identical. However, the networks to be combined need not be impedance matched for a good match to exist at the input. For example, the two amplifiers could be FET circuits that have an L network at the input. Such a circuit produces a very poor input impedance match, but an excellent noise figure. Alternatively, two conditionally-stable amplifiers can become an unconditionally stable circuit when imbedded in quadrature hybrids. This balanced scheme is attributed to Engelbrecht and Kurokawa.^{40,41,42} A termination insensitive crystal filter is described in Chapter 6 where quadrature couplers are applied.

The circuit of Fig 3.86 is narrow bandwidth with identical output amplitudes at only one frequency. However, the bandwidth can be extended to an octave by cascading two identical quadrature hybrids with a pair of pi-networks between. This topology, with related design equations, is shown in Fig 3.87.

REFERENCES

1. W. Hayward, *Introduction to Radio Frequency Design*, Prentice-Hall, 1982; ARRL, 1984. Also see *The ARRL Handbook*, 1995 or later editions.
2. *GPLA* accompanies *Introduction to Radio Frequency Design* (see Ref. 1) as a DOS program. *GPLA 2002* is a Windows version included on the book CD. *ARRL Radio Designer* was formerly available from ARRL.
3. W. Hayward, *Ham Radio Magazine*, Jun, 1984, p. 96.
4. D. Johnson and J. Johnson, "Low Pass Filters Using Ultraspherical Polynomials," *IEEE Transactions on Circuit Theory*, Vol CT-13, No. 4, Dec, 1966, pp 364-369.
5. Tortorella, *RF Design*, Mar/Apr, 1983.
6. Zverev, *Handbook of Filter Synthesis*, Wiley, 1967.
7. M. Dishal, "Alignment and Adjustment of Synchronously Tuned Multiple-Resonant-Circuit Filters," *Elect. Commun.*, Jun, 1952, pp 154-164.
8. S. B. Cohn, "Dissipation Loss in Multiple-Coupled-Resonant Filters," *Proc. IRE*, Aug, 1959, pp 1342-1348.
9. G. Matthaei, L. Young, E. M. T. Jones, *Microwave Filters, Impedance-Matching Networks and Coupling Structures*, McGraw-Hill, 1964.
10. See Reference 6.
11. A. B. Williams, *Electronic Filter Design Handbook*, McGraw-Hill, 1981.
12. W. Hayward, *Introduction to Radio Frequency Design*, ARRL, 1994, Ch 3.
13. W. Hayward, "The Double-Tuned Circuit: An Experimenters Tutorial," *QST*, Dec, 1991, pp 29-34.
14. R. Larkin, "The DSP-10: An All-Mode

- 2-Meter Transceiver Using a DSP IF and PC-Controlled Front Panel, Part 1," *QST*, Sep, 1999, pp 33-41.
15. V. Bottom, *Introduction to Quartz Crystal Unit Design*, Van Nostrand Reinhold, 1982.
16. S. B. Cohn, "Dissipation Loss in Multiple Coupled Resonators", *Proc IRE*, Aug, 1959.
17. W. Hayward, "Designing and Building Simple Crystal Filters", *QST*, Jul, 1987, pp 24-29.
18. Carver, K6OLG, "High-Performance Crystal Filter Design," *Communications Quarterly*, Winter, 1993.
19. D. E. Johnson, J. R. Johnson, and H. P. Moore, *A Handbook of Active Filters*, Prentice-Hall, 1980.
20. H. Berlin, "The State-Variable Filter," *QST*, Apr, 1978, pp 14-16.
21. W. Hayward, *Introduction to Radio Frequency Design*, ARRL, 1994, Ch 4.
22. G. L. Matthaei, "Tables of Chebyshev Impedance-Transforming Networks of Low-pass Filter Form," *Proc IEEE*, Aug, 1964, pp 939-961.
23. R. Wilson and H. Silverman, "Wire Line - A New and Easy Method of Microwave Circuit Construction," *QST*, Jul, 1981, pp 21-23.
24. W. Carver, "Measuring Capacitors and Inductors," *QRP Quarterly*, Jan, 1998, p 37.
25. Clarke and Hess, *Communications Circuits: Analysis and Design*, Addison-Wesley, 1971.
26. C. Trask, "Wideband Transformers: An Intuitive Approach to Models, Characterization and Design," *Applied Microwave and Wireless*, Nov, 2001.
27. Ruthroff, "Some Broad-Band Transformers", *Proc. IRE*, Aug, 1959.
28. N. Dye and H. Granberg, *Radio Frequency Transistors: Principles and Practical Applications*, Butterworth-Heinemann, 1993, Ch 10.
29. Hamilton, "Improved Direct Conversion Receiver Design", *Radio Communications*, Apr, 1991, Appendix.
30. W. Hayward, *Introduction to Radio Frequency Design*, ARRL, 1994, Ch 4.
31. R. Lewallen, "A Simple and Accurate QRP Directional Wattmeter," *QST*, Feb, 1990, pp 19-23, 36.
32. R. Larkin, "An 8-Watt, 2-Meter 'Brickette'," *QST*, Jun, 2000, pp 43-47.
33. A. Bouloard, "Lumped-Element Quadrature Couplers," *RF Design*, Jul, 1989.
34. R. Fisher, "Broadband Twisted-Wire Quadrature Hybrids," *IEEE Transactions on Microwave Theory and Techniques*, Vol. MTT-21, No. 5, May, 1973, pp 355-357.
35. R. Fisher, "Twisted-Wire Quadrature Hybrid Directional Couplers," *QST*, Jan, 1978, pp 21-23.
36. J. D. Cappucci and H. Seidel, US Patent 3,452,300, *Four Port Directive Coupler Having Electrical Symmetry with respect to Both Axes*, issued Jun 24, 1969.
37. J. D. Cappucci and H. Seidel, US Patent 3,452,301, *Lumped Parameter Directional Coupler*, issued Jun 24, 1969.
38. B. M. Oliver, "Directive Electro-Magnetic Couplers," *Proc. IRE*, Oct, 1954.
39. S. B. Cohn, "Shielded Coupled Strip Transmission Line," *MTT*, Oct, 1955.
40. K. Kurokawa, "Design Theory of Balanced Transistor Amplifiers," *Bell System Technical Journal*, Vol. 44, No. 10, Oct, 1965, pp 1675-1698.
41. R. S. Engelbrecht and K. Kurokawa, "A Wideband, Low Noise, L-band Balanced Transistor Amplifier," *Proc. IEEE*, Vol 53, Mar, 1963, pp 237-246.
42. R. S. Engelbrecht, US Patent 3,371,284, *High Frequency Balanced Amplifier*, Feb 27, 1968.

Oscillators and Frequency Synthesis

Almost all of the Amateur Radio equipment we build will contain at least one oscillator. It may be a simple crystal controlled circuit, a tuned LC variable frequency oscillator, or even a direct-digital synthesizer, a circuit that provides an output similar to what we might expect from a simpler circuit. A basic oscillator might be a simple one tuned by a mechanical variable capacitor. Alternatively, it might be voltage controlled. Combinations of all of these are possible and are common in modern communications equipment.

The *local oscillator* (LO) is a critical part of any communications system. Modern transceiver performance is often com-

promised by LO systems that suffer from excess phase noise, effectively limiting the receiver dynamic range. While *quiet* oscillators, those with low phase noise, can be built using traditional methods, these circuits often lack the thermal stability of a synthesizer.

Beyond their practical importance, oscillators are extremely interesting circuits. An effective oscillator can be built with a single transistor. Yet, this simple, primitive circuit will include both positive feedback, causing oscillation to start at the desired frequency, and negative feedback that maintains operating amplitude constant with time.

A frequency synthesizer offers outstanding thermal stability and frequency accuracy. A synthesizer using a handful of integrated circuits, each containing hundreds of transistors, is less expensive to manufacture than a high quality mechanically tuned LO system. It is more reliable, owing to a reduced number of moving parts. Frequency synthesis is not, however, the answer to all of the LO problems presented to the experimenter. Some PLL synthesizers are burdened by excessive phase noise. Those using DDS, while quieter, emit spurious outputs, often in profusion. Both use an excess of digital circuitry that can often corrupt a receiver environment.

4.1 LC-OSCILLATOR BASICS

Oscillators may be classified in a number of ways. One categorizes the circuit by the devices used for the active element and the resonator, such as the *bipolar transistor*, *crystal controlled oscillator* and the *JFET LC oscillator*. One can also classify oscillators according to a historic circuit form, such as the Colpitts or Hartley. An oscillator can be classified by the active device configuration, such as *common-emitter*. Finally, it can be classified according to the method used during design, such as a *negative resistance* oscillator.

The first question we ask (or should ask) is if an oscillator will indeed oscillate when power is applied.

Fig 4.1 shows a block diagram of an oscillator. The circuit is segmented into two elements: a resonator or tuned circuit, and an amplifier. The tuned circuit output

is applied to the amplifier input. But, the amplifier output is routed back to the input of the tuned circuit.

Assume that the circuit has a power supply attached, but through some means or another the resonator is short-circuited

with a switch or otherwise altered so that the circuit is not oscillating. The switch is then opened, restoring resonator functionality. The amplifier is operational with normal operating bias applied; hence, it generates noise. The noise present at the

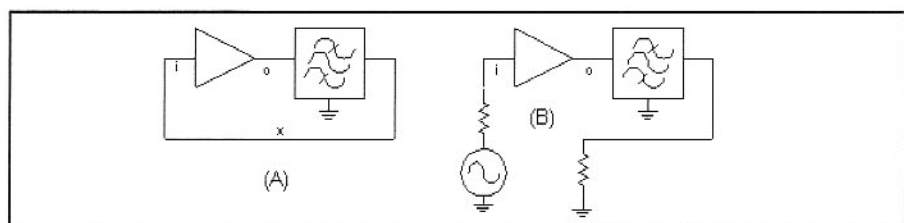


Fig 4.1—Block diagram of an oscillator. Part A shows the basic oscillator while part B illustrates the method used for analysis. This analysis can be applied to either LC or crystal oscillators, or even circuits using RC filters to replace the resonator. Amplifier input and output is labeled with "i" and "o."

input is amplified to appear at the output with greater amplitude. This noise is spread more or less evenly over a wide bandwidth. The amplifier output is applied to the tuned circuit where it is filtered and phase shifted. The resulting signal emerges where it is again applied to the amplifier input. For each frequency, the signal that has traversed the amplifier-resonator loop emerges with a new amplitude and new phase. If the amplifier has a net gain at the resonator center frequency, the signal at that frequency is larger after having traversed around the circuit. It will continue to grow with each round trip.

There will be one unique frequency where there is no net phase shift as energy at that frequency traverses the loop. This eventually establishes the oscillator operating frequency. Energy at frequencies above and below the center *carrier* frequency will be shifted further in phase with each trip around the loop, eventually emerging 90 degrees away where it no longer contributes to the power.

We have just described oscillator *starting*. Oscillation will begin if the signal grows in amplitude with each pass around the loop and if the phase is the same as it was in the beginning. These are the so-called Barkhausen criterion. They are measured or analyzed with the system in the Figure. The loop has been broken at "X" in part "a" of the Figure. A signal source and a load are inserted that allow the gain to be measured, shown in part "b."¹

The amplitude cannot continue to grow without bound. Something must occur within the circuit that will reduce the overall gain to the level just needed to maintain a stable amplitude. This usually occurs through current or voltage limiting, with current limiting generally preferred. (Automatic gain control can also be used.) Biasing details usually establish limiting and set oscillator operating level. A high operating level is generally desired.

We rarely analyze starting in an HF oscillator we wish to built for a project. Rather, we merely build and examine the oscillator to see if there is an output.

The Colpitts and Hartley Circuits

While there are numerous named LC oscillators, they can generally be categorized as Colpitts or a Hartley variations with both circuits named for their inventors, early radio pioneers from the Bell Labs of the 1920s and 1930s era. The basic forms are shown in Fig 4.2, A and B. The only difference between the two is in the means for feedback. The Hartley (B) uses a tapped inductor while the Colpitts (A)

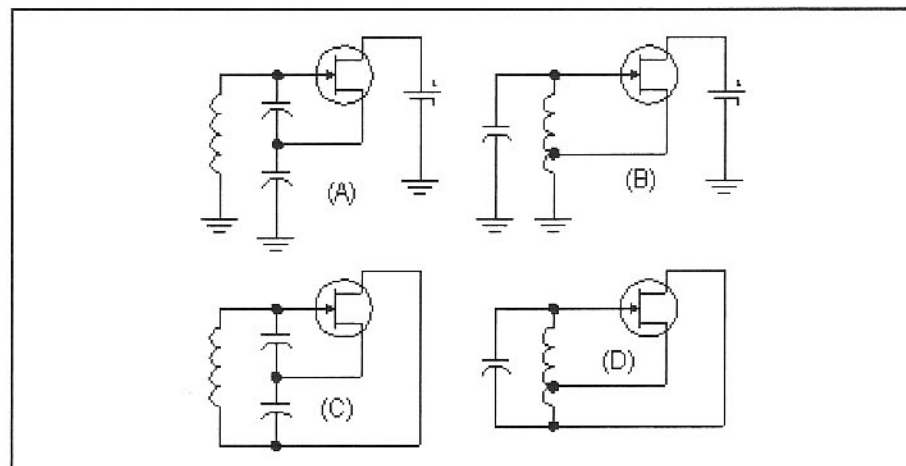


Fig 4.2—Colpitts (A) and Hartley (B) oscillators. The versions at (C) and (D) have the ground removed, allowing any of the three FET terminals to be grounded. The bias is eliminated from the last two circuits. Although illustrated with FETs, bipolar transistors are often used.

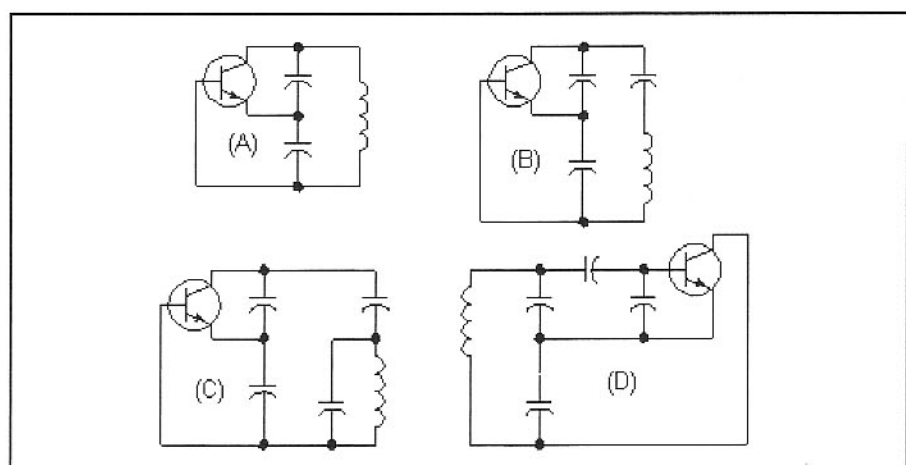


Fig 4.3—The Colpitts (A) evolves into the Clapp (B) and then the Seiler (C). The Vackar oscillator at (D) is yet another variation on the Colpitts where the base is driven from a lower impedance, achieved with a capacitor tap across one of the usual "Colpitts Capacitors." These oscillators can be designed with either FETs or bipolar transistors.

uses capacitors.

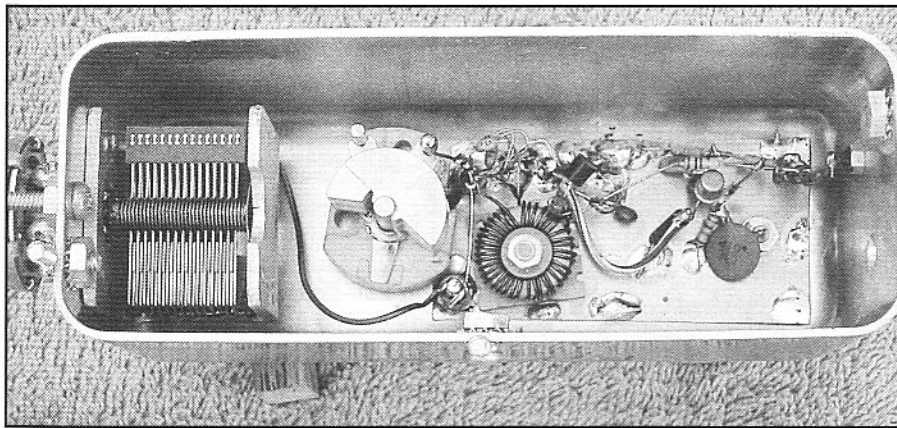
The Hartley and the Colpitts oscillators of Fig 4.2 A and B use a source follower amplifier. This distinction is an arbitrary one, as is illustrated with the two variations of Fig 4.2 C and D, which are drawn without a ground. The ground and biasing can then be inserted as needed by the designer.

The operation of the Hartley is often explained with transformer action. The source follower of Fig 4.2B has a high input and relatively low output impedance, and a voltage gain close to 1. The amplifier output signal is applied to the tap on the tuned circuit. Transformer action then increases the voltage that appears at the gate. Breaking the loop at either the FET gate or source will show the required

greater-than-unity, zero phase shift starting gain.

The Colpitts circuit (Fig 4.2A) may not be as intuitive. Detailed circuit analysis will show that driving the capacitive tap with a low impedance source will produce the required voltage step up in the composite tuned circuit. Indeed, a similar analysis shows that the same action occurs in the Hartley oscillator even if there is no magnetic coupling between the two inductor sections. Transformer action is not required! A Hartley is easily built with two separate coils, an occasionally useful variation.

The Hartley oscillator with positive feedback resulting from inductors can have an advantage over the Colpitts: If it is tuned with a variable capacitor with mini-



This Hartley Oscillator is mounted in a stamped box. A vernier drive is attached to the capacitor shaft and is fixed to the box with a single bolt that prevents rotation. Spade lugs allow a lid to be attached to the box.

mal fixed capacitance, it will produce a wider tuning range than is easily realized with a Colpitts. There is no other fundamental advantage of one over the other.

The Colpitts oscillator has several popular variations shown in Fig 4.3. The first circuit (A) is the basic Colpitts, now shown with a bipolar transistor. Part B shows the

Clapp oscillator, also called a *series tuned* Colpitts. The Clapp starts with a Colpitts circuit, but replaces the usual inductor with a larger one. Then, the extra inductive reactance is removed with a series capacitive reactance. Part C shows yet another variation, the Seiler, where a Clapp is modified. The Clapp inductor is replaced by a smaller one paralleled with a capacitor. The Clapp is capable of greater energy storage than a similar Colpitts while the Seiler allows the active device to be well decoupled from the resonator. These three are analyzed in greater detail in *Introduction to Radio Frequency Design*, Chapter 7.

A final variation shown in Fig 4.3D is the Vackar. In this circuit, the Colpitts capacitor attached to the base is expanded, allowing the base to be driven from a lower source impedance. This would provide excellent decoupling between the active transistor and the resonator. The Vackar is discussed later in greater detail.

4.2 PRACTICAL HARTLEY CIRCUITS AND OSCILLATOR DRIFT COMPENSATION

A good oscillator is thermally and mechanically stable in frequency and has low noise. We'll look at the stability issues in this section, leaving noise for later, and will illustrate the ideas with practical circuits suitable for duplication.

The first circuit we examine is a simple LC Hartley oscillator suitable as a LO in the HF spectrum. We have used this circuit in applications from 1 to 50 MHz, and have breadboard variations that extend from audio to 3 GHz. The 7-MHz circuit presented in Fig 4.4 uses a JFET.

Generally, an inductor with reactance of around 100Ω offers a good starting point in design, although this is very non-critical. The tap position is similarly uncritical; start with a tap up from ground by about 20% of the number of turns.

If this oscillator is built with no fixed capacitance other than stray values, a frequency range approaching 4:1 can be expected. Much of the capacitance in the tank is fixed for narrow tuning ranges. All fixed capacitors should be NPO types. NPO is an abbreviation for *negative positive zero*, a capacitor type with a capacitance that does not change with temperature. The capacitor between the hot end of the resonator and the FET gate should have a small C value. The input C of the FET is typically

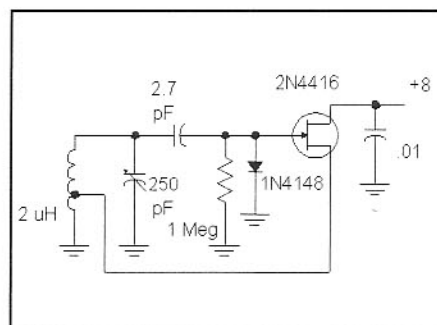


Fig 4.4—Practical 7-MHz Hartley oscillator.

around 1 pF, so any series capacitor with a similar or slightly larger size will do.

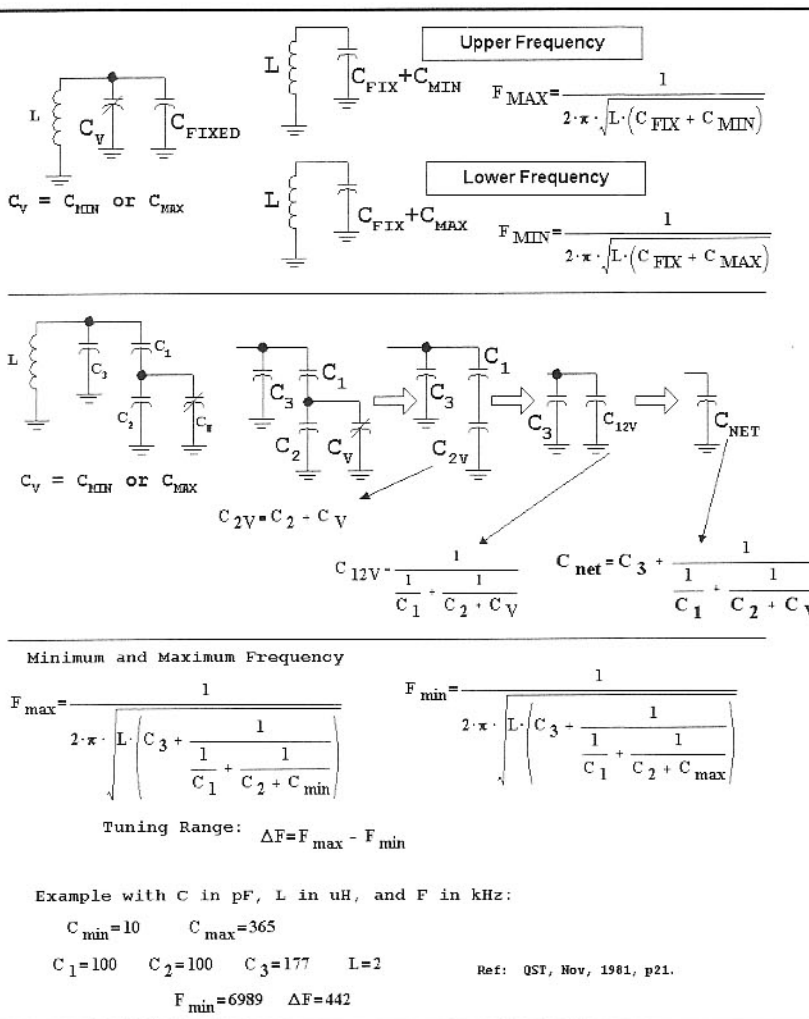
The oscillator of Fig 4.4 uses one large variable capacitor for tuning. A typical circuit will use combinations of fixed and variable capacitors, configured to tune a narrow range with the variable element. The equations are shown in a sidebar.

The gate diode is often described as a "clamping element," for it does not allow the gate to become more positive than about 0.6 V. However, the primary function is a detector to supply the FET with negative bias. A signal voltage present on the tank circuit causes diode current when the anode is positive by 0.6 V. The current

through the 2.7-pF blocking capacitor charges it. The average dc voltage on the tank side of the capacitor must be zero, for the coil is at dc ground. Hence, the charged capacitor causes an average negative voltage to appear at the FET gate. This negative bias builds toward FET pinchoff as oscillator amplitude increases. If the oscillator operating level changes during tuning, the negative bias will change, allowing FET gain to change as needed to maintain a nearly constant output. This automatic gain control (AGC) action is much like the limiting that also occurs in the Hartley. Limiting will occur on a cycle-to-cycle basis while the AGC responds to an average level. The AGC offers a coarse control, leaving the limiting to set the final level.

The voltages described are easily observed with a high-speed oscilloscope with a 10X probe. Even a high quality probe will load the HF oscillator tank, compromising accuracy, but qualitative details can still be seen.

This oscillator normally operates with a 5 to 20-V peak-to-peak signal on the tank. It can be even higher if an extra shunt capacitor is used at the gate, mimicking that design feature in the Vackar oscillator. The phase noise capabilities of the Hartley oscillator of Fig 4.4 are good,



A simple resonant circuit is tuned with parallel capacitors as shown in the top section. The tuning range is controlled by the ratio of the variable capacitance to the fixed one.

Often an available variable capacitor has greater capacitance than required for a desired frequency range. While plates can sometimes be removed, a better solution embeds the variable capacitor in a network of fixed capacitors. The evolution of this network is shown in the middle section. The variable, \$C_v\$ and \$C_2\$ are paralleled to form the equivalent \$C_{2V}\$. This is then placed in series with \$C_1\$ for the equivalent \$C_{12V}\$. This is paralleled by \$C_3\$ to form the total capacitor, \$C_{NET}\$. The overall frequency is calculated from the usual resonance relationship. The equations are shown, with capacitors in Farads, inductance in Henrys and frequency in Hz.

There is considerable flexibility available to the designer, afforded by picking \$C_1\$ and \$C_2\$ values. Some combinations with \$C_1\$ much smaller than the variable capacitor can produce highly nonlinear tuning.

although not the ultimate. (Phase noise is discussed later in this chapter.)

The 1-M\$\Omega\$ resistor represents a load on the tank. It also discharges the series blocking capacitor. If a smaller resistance is used, the blocking capacitor will discharge more quickly. The energy to maintain bias comes from the RF envelope, further loading the resonator. Resistor values around 1 M\$\Omega\$ are generally optimum.

Experiments were performed to examine the effect of resistor and blocking capacitor values, and unloaded resonator Q. If extreme values (long time constant) were used with degraded tank Q, the oscillator could become amplitude unstable, producing a phenomenon called *squegging*. A sketch of the observed gate voltage is shown in **Fig 4.5** for an oscillator using a 2N4416 FET. This unusual behavior was observed

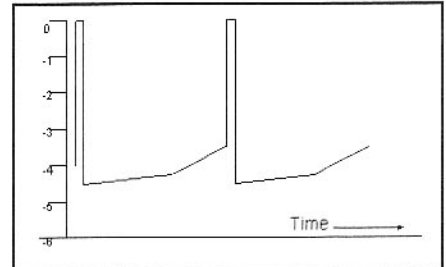


Fig 4.5—Squegging in a Hartley oscillator, an on-and-off mode where the oscillator is not functioning except during short periods. The vertical scale shows the gate voltage. Extreme values of blocking capacitor and bias resistor are required to produce this behavior in the FET Hartley oscillators.

when tank \$Q_U = 30\$, the gate resistor was increased to values much larger than 1 M\$\Omega\$, and blocking capacitors of 200 pF or more were used.²

The supply voltage used with this oscillator should be larger than the magnitude of the FET pinchoff. A supply of +5 is high enough for a 2N4416 with pinchoff of -3 V. The supply should be regulated and come from a moderately low dc impedance. In one experiment, we built this oscillator with a 6-V Zener diode with a 3.9-k\$\Omega\$ resistor fed from a 12-V supply. The high resistance value was picked for overall efficiency. The oscillator would not start. DC voltmeter measurements showed that the FET only had 1 V on the drain. The FET was trying to draw a current of \$I_{ds}\$, leading to excessive drop across the 3.9-k\$\Omega\$ resistor. A smaller (470-\$\Omega\$) dropping resistor solved the problem, but at the cost of higher power consumption. A better solution is a 100-\$\Omega\$ drain-decoupling resistor supplied by a dc emitter follower with the base referenced to a Zener diode paralleled by a large electrolytic capacitor. A small charging current can then be used, maintaining efficiency. Three terminal regulator ICs also work well in this application. This is one of many examples where *extra circuitry improves efficiency*.

Temperature Compensation

Generally, the most important characteristic of oscillators built for radio application is frequency stability. Stability relates to a change in frequency other than the desired ones that occur with tuning. This change, or *drift*, occurs in two forms. One is the warm up drift occurring when an oscillator is first turned on and allowed to operate at constant temperature. The sec-

JFET Hartley Oscillator

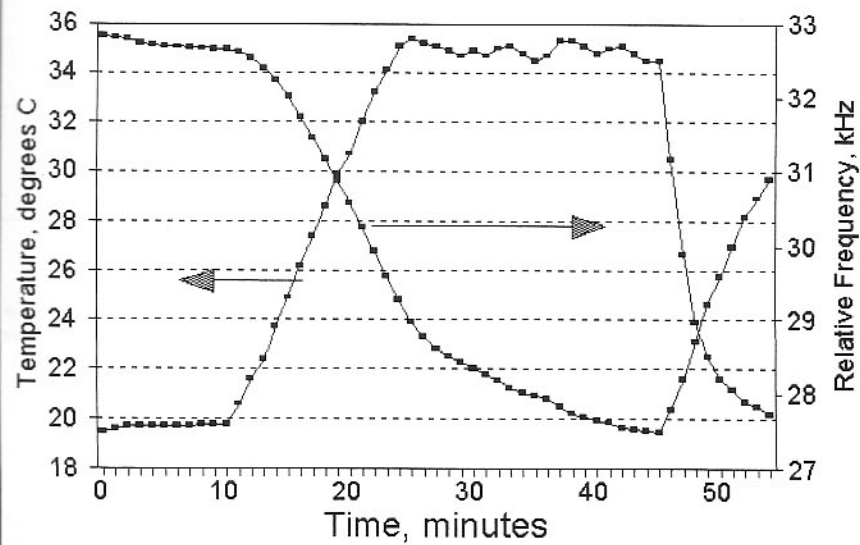


Fig 4.6—Temperature and frequency vs. time for a Hartley oscillator operating in a simple environmental chamber. The heat was turned on at 10 minutes. It was cycled off and on after 25 minutes to maintain an approximately constant temperature. The chamber lid was removed and a cooling fan was turned on at 46 minutes.

ond is the drift with changing temperature. Both effects are thermal in origin, but the warm up drift is caused by temperature changes in individual components resulting from heating by the circulating currents within the circuit. Warm up drift is normally small compared with the drifts that occur when an oscillator is subjected to even a modest temperature change.

Thermal drift may be of little consequence when equipment is built and used in a typical home environment where room temperatures are stable. But the oscillator that was "rock solid" during home operation may become a very poor performer when subjected to portable environments. The most extreme examples we have encountered occurred when we took equipment on mountaineering trips. The temperature at the summit of a glacier clad, cloud covered mountain can be below freezing, even in mid summer. But the temperature can quickly shoot up when the clouds blow away for a few minutes, only to plummet downward as soon as the clouds return. It's important to design for these extremes if they might be encountered. While not as severe, drift problems are common even when we are on the flatlands.

Oscillator temperature compensation is surprisingly easy, requiring little equipment beyond the simple frequency counter and DVM that most experimenters already

possess. All that is needed is a simple environmental chamber with a thermometer. The chamber is built from an inexpensive Styrofoam box. A light bulb is placed inside the box along with the circuit being tested. A small fan stirs the inside air to complete the chamber. Temperature is measured with an integrated circuit intended for this purpose. Leads supply power to the IC and route a dc signal out of the chamber for measurement with a DVM. An oscillator to be tested is placed in the chamber with cables routed to the outside for power and for frequency measurement. The oscillator is turned on for a while before the heat source is applied, providing a measure of warm-up drift. Heat is then applied, causing the temperature to increase.

Data for a 7-MHz Hartley oscillator is shown in Fig 4.6 where frequency and chamber temperature are plotted vs time. The oscillator was operated for 10 minutes before applying the 60-W heat source, producing a typical 150-Hz warm-up drift. Chamber temperature immediately started to increase when the heat source was turned on. The frequency did not respond immediately, for the oscillator was housed in a moderately tight container. When frequency began to drop, it moved about 5 kHz for a 15°C temperature increase. The external heating induced drift was over 30 times the warm up

drift! The heat source was only operated intermittently after the 25-minute mark to maintain chamber temperature. Oscillator drift continued as the internal components came up to temperature.

Measurements are simpler when the tested oscillator is only a small board with low thermal mass, capable of quicker temperature changes.

Thermal frequency stability depends on the resonator coil and all related capacitors. Most oscillators we built use toroid inductors wound on SF (-6) material. A newer material with a -7 designation is reported to be slightly more stable. The -6 material has a permeability of about 10 and a temperature coefficient of inductance (*TCL*) of +35 parts per million per degree Celsius (C). This means that an inductor of 1 micro-henry will increase by 35 pH (i.e., 0.000035 μH) when the temperature increases by 1 degree C. Temperature coefficients are generally specified in normalized, dimensionless form, (parts per million) allowing convenient scaling. The normalized rate of change of frequency, *TCF*, is related to all of the components in the oscillator resonator. If, for example, a tank consisted of two parallel capacitors and an inductor, the temperature coefficient of frequency is related to that of the components by

$$\text{TCF} = \frac{\Delta F}{F} = -\frac{1}{2} \left[\frac{\text{TCL} + \text{TC}_{C1} \cdot \frac{C_1}{C_{\text{TOT}}} + \text{TC}_{C2} \cdot \frac{C_2}{C_{\text{TOT}}}}{C_{\text{TOT}}} \right] \quad \text{Eq 4.1}$$

where C_1 and C_2 are the capacitors with temperature coefficients TC_{C1} and TC_{C2} , TCL is the temperature coefficient of the inductor, and TCF is the temperature coefficient of frequency of the oscillator in normalized parts. C_{TOT} is the total capacitance, C_1+C_2 . The negative sign arises because an increase in L or C leads to decreasing frequency. The factor of one half comes from the square root relationship of frequency to L and C.

Consider a 7-MHz example, using a 2- μH inductor carefully wound on a T50-6 toroid. Assume TCL is +50 ppm/ $^{\circ}\text{C}$, slightly worse than the quoted material performance, which will be explained later. Initially assume that the inductor is paralleled with 250 pF of perfectly non-drifting NP0 capacitors. The only part that will drift will be the inductor. From Eq 4.1, the 50 ppm/ $^{\circ}\text{C}$ will produce a TCF of -25 ppm/ $^{\circ}\text{C}$, or -25 Hz per MHz. The 15-degree shift of Fig 4.6 would then produce a frequency change of -2.6 kHz.

We now replace the single capacitor with two, a 150-pF NPO ceramic and a 100-pF polystyrene. The nominal frequency remains 7.118 MHz. Assume that the NPO capacitor is not perfect, having a TC of +5 ppm/ $^{\circ}\text{C}$. The poly cap has TC = -150 ppm/ $^{\circ}\text{C}$. The TCF for the circuit is

$$\text{TCF} = -\frac{1}{2} \cdot \left[50 + 5 \cdot \frac{150}{250} - 150 \cdot \frac{100}{250} \right]$$

Eq 4.2

This oscillator has a much improved TCF of +3.5 ppm per degree C. This is 3.5 Hz drift per MHz of observed frequency per $^{\circ}\text{C}$. A 10-degree C temperature rise would produce a 245-Hz frequency increase, a very stable VFO. The stability results from the use of a combination of parts with temperature coefficients that cancel each other.

The temperature coefficient of frequency, TCF, is reduced from that of the compensating capacitor to half the ratio of the compensating capacitor to the total resonator C. Capacitors with a temperature coefficient of -750 ppm/ $^{\circ}\text{C}$ are readily available. They can be placed directly across a resonator or in series with a NPO capacitor for compensation. If capacitor C1 has a known TC, but is placed in series with an NPO capacitor, C2, the resulting TC of capacitance is given by

$$\text{TC}_{\text{net}} = \frac{C_2}{(C_1 + C_2)} \cdot \text{TC}_{C_1} \quad \text{Eq 4.3}$$

For example, if we place a 47-pF capacitor with TC of -750 ppm/ $^{\circ}\text{C}$ in series with a 10-pF NPO capacitor, the result is 8.2 pF with a TC of -132 ppm/ $^{\circ}\text{C}$.

Although polystyrene capacitors can be used for compensation, they are not ideal. The TC of -150 ppm/ $^{\circ}\text{C}$ is not a precise number. The TC itself has a tolerance of +/- 50 ppm/ $^{\circ}\text{C}$, allowing a polystyrene capacitor to have a TC ranging from -100 to -200 ppm/ $^{\circ}\text{C}$. This variability is common, even among NPO capacitors. For example, one of the best commonly available NPO capacitor types is one with a so-called C0G characteristic, where the G designates a TC tolerance of +/- 30 ppm/ $^{\circ}\text{C}$.

Our example used an inductor TC that differed from the published value for the powdered iron core. The difference relates to the way the core is wound. If a large wire is hand wound on a toroid, with the wire size picked to fill the core to produce highest possible Q, there is a good chance that the wire will gap away from the core for part of each turn. This leaves unsupported loops that can expand or contract with heat, producing ill-defined character-

istics. A more temperature stable coil is produced with a wire size that is smaller than that producing maximum Q. The Q degradation is usually not large.

Temperature coefficients are themselves temperature dependent. An oscillator that has been compensated at one temperature may not be as stable at temperature extremes.

Another subtle problem has to do with stress built into the wire during the winding process. We first observed this while temperature testing bandpass filters built from toroids. The filter frequency would change as temperature increased, but would not come back to the original frequency when the circuit returned to room temperature. However, a second excursion to high temperature and back would produce the expected return. Evidently, the first excursion to high temperature (85 $^{\circ}\text{C}$) and back relieves the stresses left in the metal during winding. W7EL has dropped coils into boiling water after winding; subsequent cooling produces a more stable inductor.

None of the temperature stability and compensation arguments relate to oscillator topology. There is nothing that will make one type more stable than another so long as the circuit does not degrade tank Q from improper limiting. The compensation methods described here for the Hartley apply equally to other circuits presented later. Capacitor variability makes it difficult to predict and control stability, encouraging the serious builder to measure his or her VFO.

Powdered iron toroid cores (-6 and -7 material from Micro-Metals) produce stable and reproducible inductors if carefully wound. Some other coil forms may produce stable coils, although the reader should not trust poorly documented testimonials (lore) regarding slug tuned forms or other schemes that are not easily duplicated and quantified.

The most stable oscillators are built from collections of components that all have low drift. A really bad component can be compensated, but only over a narrow temperature range.

Drift measurements in a measured, variable temperature environment are much more meaningful than mere warm up drift measurements. A suitable chamber can be built at very low cost in an evening. The chamber is described in a paper included on the book CD.³

Variations on the Simple Hartley

The oscillator described has been a long time favorite among QRP experimenters.

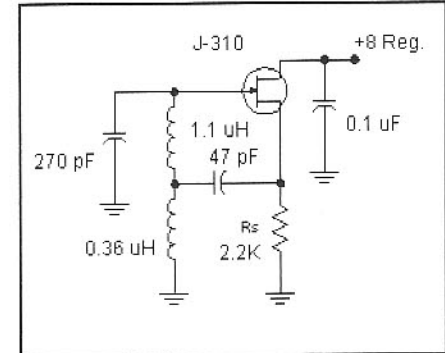


Fig 4.7—A Hartley oscillator using source bias and two inductors. The larger inductor is 17 turns on a T50-6 toroid. The smaller one is 10 turns on a T30-6. Output can be extracted from the resonator with a capacitive tap and appropriate buffering.

There are, however, some variations that should also be considered. Fig 4.7 shows an oscillator without ac coupling into the gate, removing the AGC action of earlier oscillators. The amplitude is determined by more traditional current limiting. The FET in the example has a pinchoff voltage of -3 V. The source resistor places the source at a positive potential, even before oscillation has started. As oscillation builds, follower action causes the source voltage to reach large positive values. The gate also reaches positive values, but is always offset below the source. During part of the cycle, the gate-source voltage drops to or below pinchoff; the greater the fraction of each cycle spent in this condition, the greater will be the gain reduction, which establishes the final operating level. With a 2.2-kΩ source resistor, the gate signal was 11 V peak-to-peak. This dropped significantly when the source R was increased to 10 kΩ.

The oscillator of Fig 4.7 has an additional unusual feature: The usual tapped coil is replaced with two isolated coils. This has the advantage that the circuit is easily band-switched, a sometimes-messy problem with tapped inductors.

The “Huff ‘n Puff”

Frequency counter circuitry can be used to stabilize a moderately good oscillator, achieving nearly the stability of a synthesized oscillator.⁴

This scheme uses normal frequency counter circuitry such as that in Fig 4.8. A stable crystal oscillator is the foundation. The result is divided with a large counter, a straightforward operation with CMOS circuits such as the 4060 or similar industrial timer parts. The division is extended

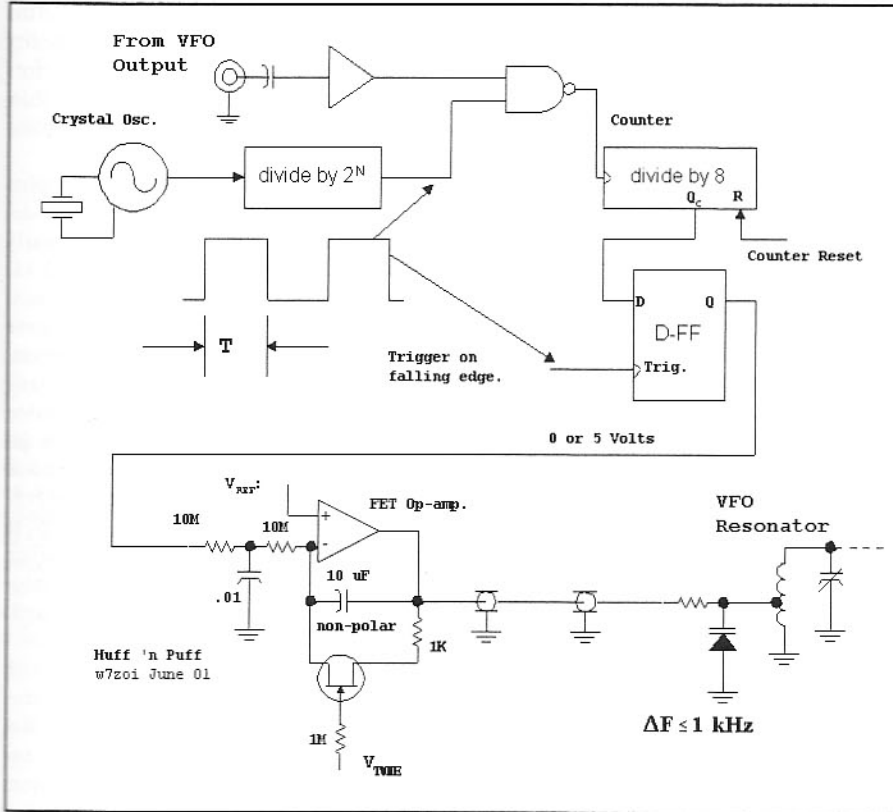


Fig 4.8—This scheme uses normal frequency counter circuitry. A stable crystal oscillator is the foundation.

to produce a square wave with a positive half period of length T . Assume $T=0.1$ second. A well-buffered sample of the VFO is applied to a conditioning amplifier followed by a gate controlled by the timing signal T . This allows timing data to reach a counter for 0.1 second. Let's assume the oscillator to be stabilized has a

frequency 300 Hz above 5.0 MHz, and is thermally stable with no drift of its own. In a 0.1 second period the 8 bit counter input will see 500,030 transitions, so it will overflow again and again. When the gate signal terminates at the end of the period T , the 8 bit counter will have overflowed a total of 62,503 times and will end the period with a logic 1 in the output digit, indicating a count of 4, 5, 6, or 7. The negative edge of T is detected and used to trigger a D-Flip-flop that memorizes the result. The saved digital 1 causes Q of the FF to be at 5 V. This signal is applied to the input of an op-amp integrator circuit which generates an output that ramps downward, but at a very low rate. This slowly changing voltage causes the VFO frequency to decrease.

The frequency goes down slightly as a result of the applied signal. Finally, after a few cycles of counting, it will have dropped enough that the signal held in memory becomes a logical zero, resulting in an integrator input of 0 V. This now causes the op-amp output to again ramp upward, slowly increasing the frequency. The overall effect of the added circuit elements is to force the oscillator to never be at a fixed, exact frequency, but to move (huffing and puffing) between two frequencies. These two references are 40-Hz apart for our example, so changes are not noticed in normal applications. Greater resolution is available with a shorter count or longer sample period.

We now allow a slow thermal drift to occur. This has the effect of altering the time when we reach one of the transition frequencies. However, the drift will be cancelled so long as it is well under 40 Hz in a 0.2-second window.

A FET switch is placed across the integrator timing capacitor. This FET is turned on when the oscillator is tuned.

The Huff 'n Puff scheme can be extremely useful for adding stability to a circuit that is already reasonably solid. It is a wonderful tool for the experimenter, for it can be added to an already existing design. Several experimenters have expanded the basic system in recent times.⁵

4.3 THE COLPITTS AND OTHER OSCILLATORS

One of the most popular oscillator circuits among radio experimenters has been Colpitts in one of its many forms. The basic circuit, along with several of its derivative forms, was presented at the beginning of the chapter. Some practical variations are presented here.

Fig 4.9 shows a simple Colpitts oscillator using a junction FET. Although very simple, this circuit is capable of excellent performance. The variation shown operates at approximately 7.5 MHz with a common drain JFET. Addition of a variable capacitor and trimmer to this circuit

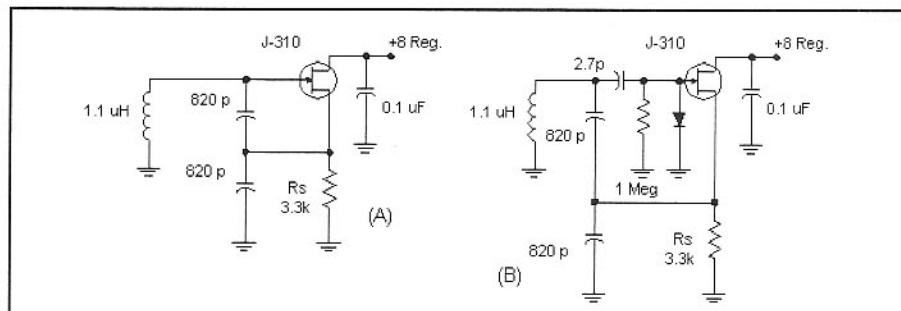


Fig 4.9—Two versions of a Colpitts oscillator. The variation at B is more tolerant of FET variations. The lower noise versions of this oscillator have larger C with reduced L values.

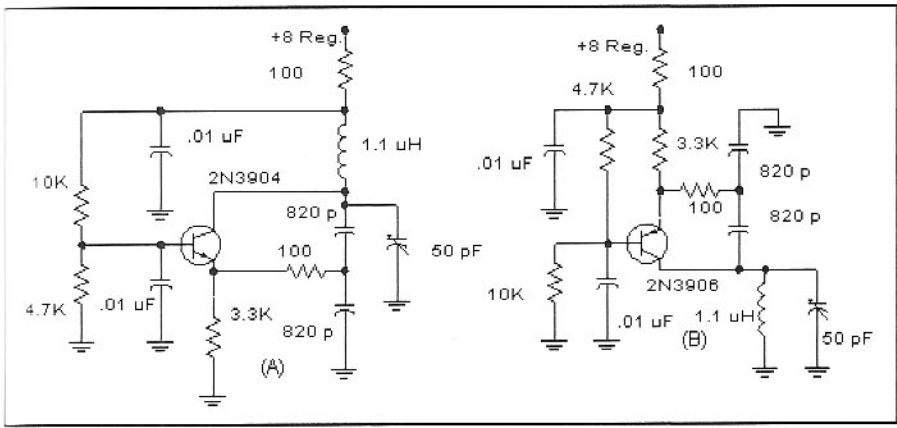


Fig 4.10—Colpitts oscillators using bipolar transistors. Although these circuits were designed around the 2N3904 (NPN) and 2N3906 (PNP), transistor type is not critical for general-purpose applications. The 2N5179 is a good general-purpose choice for VHF applications. The PNP has the advantage that the tank is at ground, removing the bypass capacitor of the NPN tank from the frequency-determining loop. The PNP is also handy when varactor diode tuning is planned.

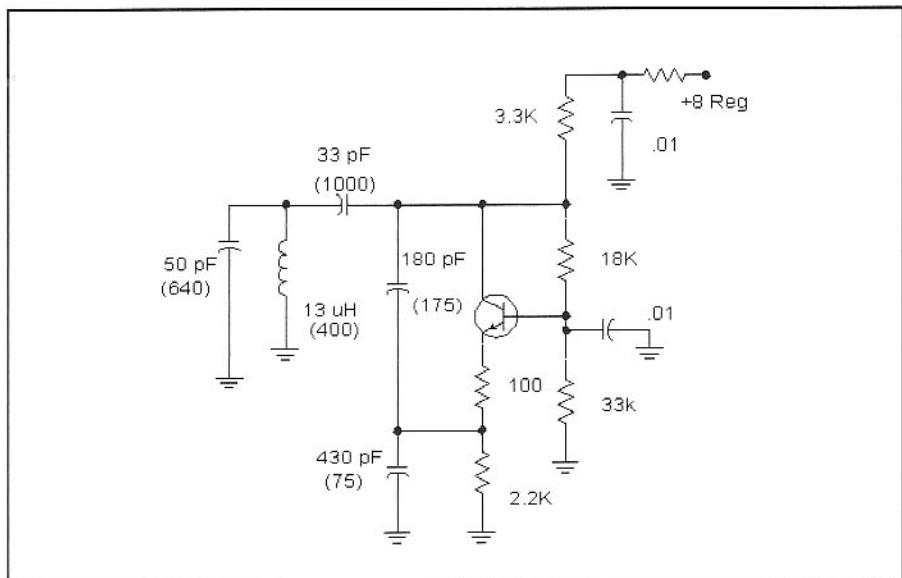


Fig 4.11—A Seiler oscillator for 5-MHz operation. The values shown in parentheses are reactances, allowing the circuit to be scaled to other frequencies. Transistor type is not critical, although the circuit works well with a 2N3904.

will drop it down into the 40-meter band. The circuit uses a source resistor to set operating level. In the variant with diode clamping, the source resistor may be replaced with a choke, although the negative feedback at low frequency from the resistor is believed to improve phase noise close to the carrier. While shown with a J-310 FET, FET type is not critical. The J310 used for the measurements on this oscillator had a pinchoff voltage of -3.1 V and I_{dss} of 37.5 mA . The circuit draws just over 1 mA during operation. The R_s value may require adjustment if built with a low gain JFET.

While the preferred device for HF

Colpitts oscillators and variations is usually the JFET (owing to reduced low frequency noise), bipolar versions are still popular and effective. Bipolar Colpitts oscillators are shown in Fig 4.10. The familiar form is that in A using an NPN transistor. The PNP version (Fig 4.10B) is convenient, for the dc grounded collector removes the need for a good bypass capacitor that becomes part of the frequency-determining resonator.

The two oscillators presented in Fig 4.10 are designed for operation near 7 MHz. Like any of the circuits presented, they can be scaled to any frequency within the HF and low VHF spectrum, and even down to audio.

The frequency stability will depend upon the criterion outlined earlier. That is, if quality NPO capacitors and -6 or -7 toroid inductors are used, reasonable stability is predictable. Temperature compensation can be applied to further improve the performance.

A subtlety haunts the bipolar Colpitts circuits of Fig 4.10 in the form of ill-defined limiting. The circuit will nearly always oscillate. However, if the $3.3\text{-k}\Omega$ emitter bias resistor is reduced, the transistor will go into saturation at the negative extreme of the collector voltage waveform. This action extracts energy from the tank and dissipates it in the transistor saturation resistance. This can severely degrade the loaded tank Q, compromising phase noise and thermal stability. The emitter degeneration decreases starting gain and helps to establish current limiting as the mechanism determining operating level. Transistor saturation is easily detected with a high-speed oscilloscope.

A simple Colpitts should be built with high capacitance and low inductance, storing the greatest energy in the resonator. But there is a practical limit to this trend. Eventually, stray inductance of the capacitors and the wiring in the tank, including bypass capacitors, will all contribute to the overall L in greater proportion. The stray inductance generally has a considerably lower Q and poorer stability than that of a powdered iron toroid inductor.

Fig 4.11 shows a Seiler oscillator using a bipolar transistor. The values shown are for 5-MHz operation, with reactance at the operating frequency shown in parentheses, allowing scaling. As mentioned earlier, the Seiler can be analyzed as a variation of the Clapp, which is the familiar “series tuned” version of the Colpitts. This circuit has some very useful characteristics. First, the *Colpitts capacitors* (the 180 and 430-pF capacitors providing the in-phase feedback from collector to emitter) are large compared with the 33-pF coupling capacitor to the inductor. This decouples the active device, including parasitic capacitance, from the rest of the tank. Second, current limiting is well established with this circuit. (Computer analysis shows that the transistor stays well away from saturation when the $100\text{-}\Omega$ degeneration is used.) Even though the current is small in this circuit, about 1 mA , the signal voltages can be quite high. We measured over 10 V pk-pk across the inductor. The collector signal is much smaller at $2.5\text{ V peak-to-peak}$. Output can be obtained from the junction of the Colpitts capacitors.

The Colpitts oscillators presented have all operated at the lower end of the HF spectrum. The Colpitts and Hartley can

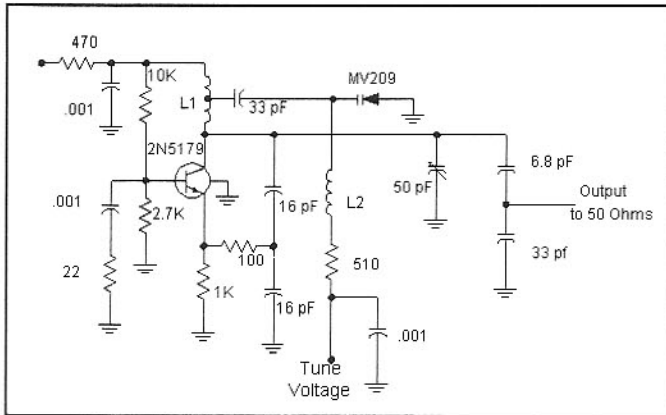


Fig 4.12—A Colpitts VHF oscillator. L1 is 50 nH, 3 turns of #22 bare wire. It is initially wound on a 1/4-20 machine screw as a former. The bolt is then removed. The varactor diode is attached to a tap (approximately center) on the coil in order to reduce the tuning sensitivity. The diode tunes the oscillator by 4 MHz around 134 MHz with a voltage from 5 to 12. L2 is a 2.7 μ H RFC. The trimmer capacitor allows the circuit to tune from 71 to 153 MHz. Power output is -2 dBm to a 50- Ω termination.

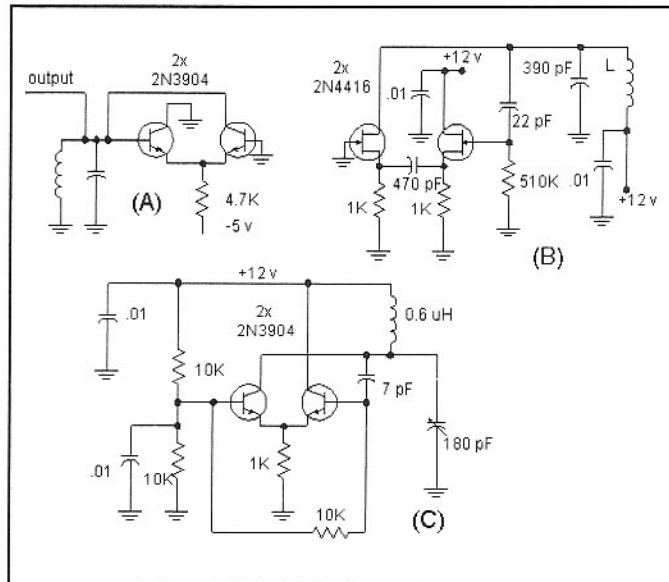


Fig 4.13—Negative resistance one-port oscillators for application at HF and VHF. See text for discussion.

both be scaled for operation at much higher frequencies. Shown in **Fig 4.12** is a VHF Colpitts oscillator. This circuit was originally set up as a voltage controlled local oscillator in a SSB transceiver at 144 MHz. It can, however, be set up for a wide frequency range by spreading or compressing the turns on the coil, which uses an air dielectric.

Numerous other oscillator forms are available for wide frequency range applications. Three are shown in **Fig 4.13**. The first bipolar circuit (**Fig 4.13A**) is a primitive variation of the scheme used in the Motorola MC-1648. The version shown uses NPN transistors with a negative supply. The same circuit will work with a single positive power supply with PNP transistors such as the 2N3906. The oscillator is a one-port type where two non-inverting amplifiers, an emitter follower and a common-base, are cascaded. The output is returned to the input with a shunt-tuned circuit attached at the common point. This scheme can be built on the bench and made to function over an extremely wide frequency range. Low Q tank circuits are favored. This circuit suffers from very low stored tank energy, the result of voltage clipping by the transistors.

The second circuit uses J-FETs in a variation of the same topology. This circuit, similar to one used in the HP-8662 synthesized generator⁶, does not suffer from the voltage limiting found with the simple bipolar version. The circuit shown in **Fig 4.13B** is one that was breadboarded from available com-

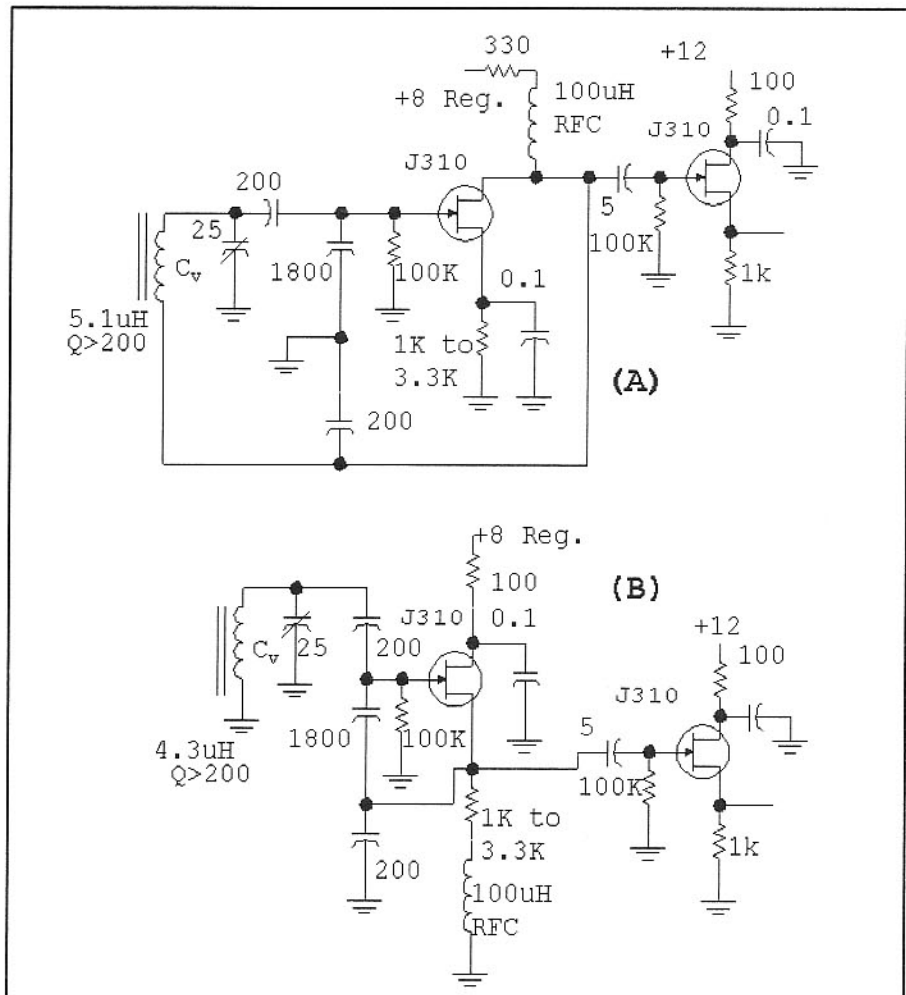


Fig 4.14—The Vackar circuit shown is identical to the Seiler circuit presented earlier except for the choice of component values.

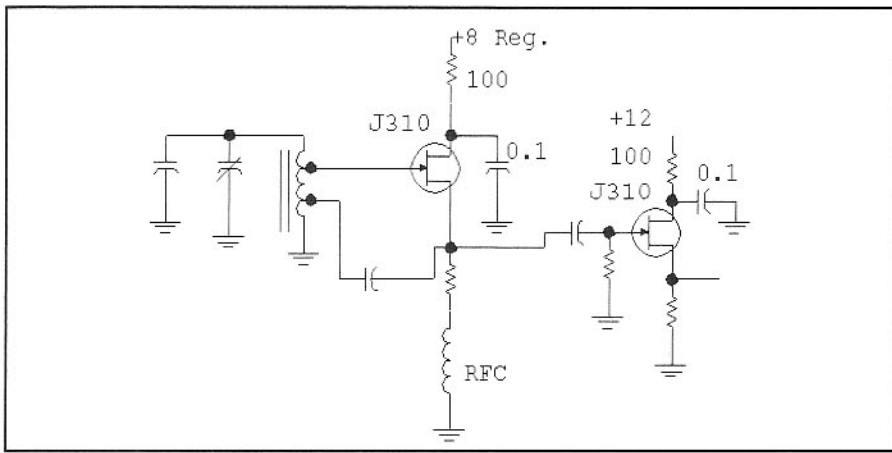


Fig 4.15—This figure shows a variant of the Vackar oscillator with a Hartley theme. The source and gate are both tapped down on the resonator as a means of isolating the tank from the resonator.

ponents. With an inductor consisting of 20 turns on a T50-2 toroid, the circuit operated at 5.34 MHz with 20-V peak-to-peak on the tank. Changing the resonator allowed operation up to 200 MHz.

Figure 4.13C shows a third version of this oscillator that was built, this time using 2N3904 bipolar transistors. Again, the signal was 20-V peak-to-peak across

the resonator.

Fig 4.14 shows the Vackar oscillator. Part A is a JFET adaptation of a vacuum tube design appearing in the 5th edition of the *RSGB Radio Communications Handbook* with components chosen for 7-MHz operation.⁷ Output is extracted with a high input impedance buffer attached to the oscillator drain. Part B of the Figure is

essentially the same circuit with the ground point shifted from the source to the drain. The inductance value is slightly lower in B than in A, for variable capacitor C_V connects to ground in B. If the capacitor had been returned to the FET source in B, the L value would be the same as at A for 7-MHz resonance.

The Vackar circuit in Fig 4.14B is identical to the Seiler circuit presented earlier except for the choice of component values. The unique component in the Vackar is the large capacitor across the FET gate-source. This component is critical; increasing the value will drop the starting gain to the point that oscillation will not commence. A decrease in inductor Q will have a similar effect. The decoupling between resonator and FET is near optimum in the Vackar. Passive component temperature coefficients will still dominate thermal stability.

Fig 4.15 shows a variant of the Vackar oscillator with a Hartley theme. The source and gate are both tapped down on the resonator as a means of isolating the tank from the resonator. This circuit is a direct transformation of that of Fig 4.14B and is often used at VHF for low noise oscillators.⁸

4.4 NOISE IN OSCILLATORS

Some mention has already been made regarding oscillator noise. We don't traditionally think of noise when discussing oscillators. However, noise is present in any practical electronic circuit; the oscillator is certainly no exception. Indeed, excess LO noise is typically the dominant phenomenon limiting the performance of most transceivers in the late 1990s time frame.

Before discussing oscillator noise, we should consider some RF measurements. A spectrum analyzer (SA) is the instrument normally used to examine radio frequency signals. The SA is essentially a calibrated, swept receiver, usually without audio output. Signal strengths are displayed on a CRT or similar screen. When a sinusoidal carrier is applied to a spectrum analyzer, a response is noted at the frequency of that carrier. Changing the analyzer bandwidth will have little impact as we observe the carrier. The amplitude is unchanged. It is specified as a power in dBm. (See Chapter 2 for a discussion of dBm.)

Noise is different. If strong, wideband noise is applied to a spectrum analyzer, it will cause the baseline to rise. If we increase the spectrum analyzer bandwidth

by a factor of 10, the baseline will further increase by 10 dB. We cannot describe the noise with a simple "dBm level." Rather, noise is specified as a power density, the power that would appear in a 1-Hz bandwidth. If we apply a wide band noise source to a spectrum analyzer set to a resolution bandwidth of 10 kHz and the response comes up to the -60 dBm line, we say that the spectral density of noise is -100 dBm/Hz; the 10-kHz bandwidth is "40 dB wider" than a 1-Hz wide filter. Recall that $10 \cdot \log(10,000) = 40$.

If a carrier was also present in the noisy display described, we might make reference to a *carrier to noise ratio* (CNR). (We use the term "ratio," for we are examining the ratio of power. However, we calculate this with a simple subtraction, for the power values are already in a dBm format.) If the carrier was -15 dBm with the noise at -60 dBm with a 10-kHz bandwidth, which corresponded to -100 dBm/Hz, we would say the CNR was 85 dBc/Hz, with dBc standing for dB with respect to a *carrier*. (We usually talk of CNR, carrier to noise ratio, rather than NCR, noise to carrier ratio, for the carrier is much stronger than the noise and is the louder.

There is often a sign discrepancy in these discussions, requiring care on the part of the reader.)

Recall the earlier discussion of oscillator starting. (Fig 4.1) Wideband noise at the amplifier input port was amplified, but was then filtered in a resonator. The "signal" within the bandwidth of the resonator is transferred with little attenuation and is again applied to the amplifier input. With a few "trips" around the loop, the signal has grown to the point that limiting begins. As limiting occurs, the net gain around the loop diminishes, eventually stabilizing at unity, the level needed to sustain amplitude-stable oscillation, but no more. Unity gain occurs at the resonator center frequency (or very close to it) where the net phase shift is zero degrees.

Consider the gain characteristics at frequencies close to but slightly removed from the carrier. For example, suppose we build an LC oscillator operating in the amateur 20-meter band with a *loaded* tank Q of 100. The 3-dB bandwidth will then be 1% of 14 MHz, or 140 kHz. Signals 70 kHz on either side of the carrier are attenuated by 3 dB and shifted in phase by + or - 45 degrees. Signals closer to the

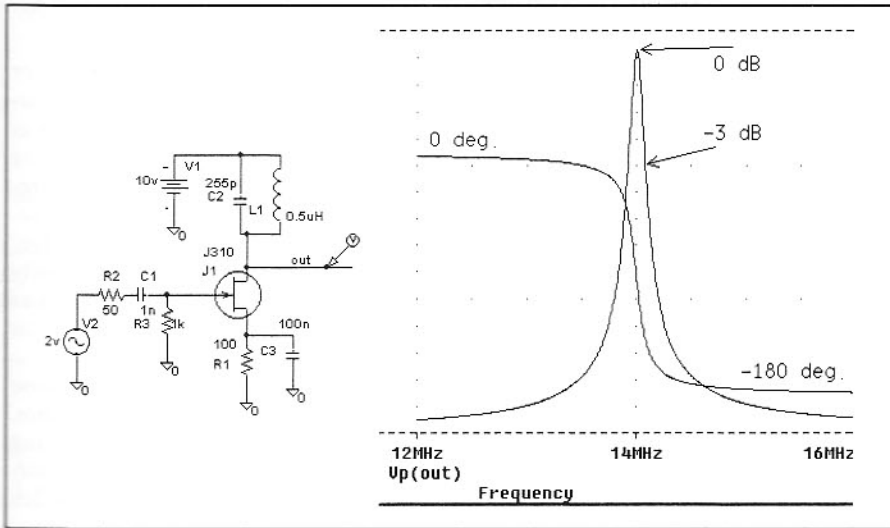


Fig 4.16—An example circuit of an amplifier followed by a resonator. The amplitude and phase responses are shown vs frequency.

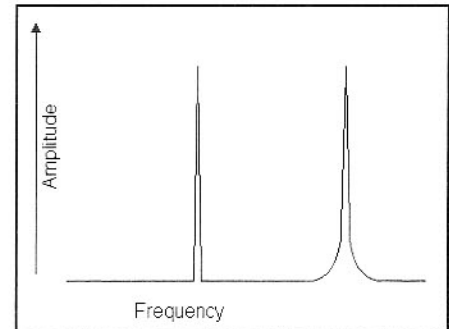


Fig 4.17—A spectrum analyzer output showing two signals with identical amplitude. The peak at the left is “perfect,” having a vertical spike shape. The width represents the spectrum analyzer bandwidth. The right hand signal has noise, which appears as a modulation on either side of the carrier. The flat horizontal line is the background noise level of the spectrum analyzer.

carrier have less phase shift and less than 3-dB attenuation. This behavior is illustrated with the amplifier and resonator of Fig 4.16.

Although amplifier gain in an oscillator is limited, noise is still present. That noise will still be amplified and filtered in the resonator. Each time a burst of noise energy passes through the resonator, it is shifted in phase and attenuated. Noise very close to the center must travel around the loop several times before it is phase shifted and attenuated enough to disappear. Signals further from the carrier will disappear with fewer passes around the loop.

The noise arises from two sources. One is the wideband noise of the transistor. The other noise starts at a lower frequency. This *baseband* signal modulates the carrier to generate sidebands in the same way that a low frequency sine wave might modulate a carrier to generate discrete sidebands. The modulation happens within the circuit *nonlinear* amplifier, a nonlinearity that is always present in a self limited oscillator.

Noise associated with an oscillator is usually *phase noise*, a variation in frequency or phase. Amplitude noise is also present, but it is usually much less than the phase variation, a result of limiting. Also, oscillators are often used with mixers with limiting characteristics with regard to LO power, further reducing the impact of amplitude noise.

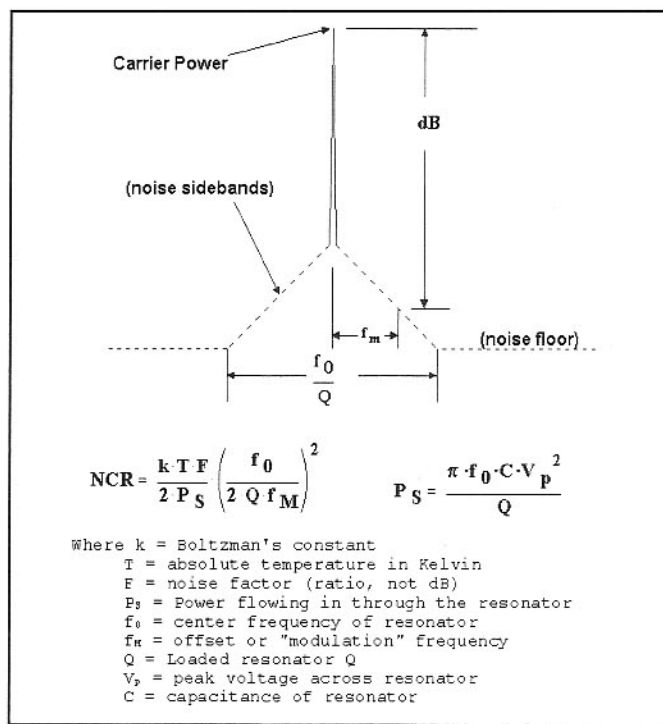
A sketched spectra of an oscillator observed in a spectrum analyzer is shown in Fig 4.17. The left peak represents a perfect signal, one without noise. The right peak contains excess noise sidebands typical of that found in a noisy oscillator or synthe-

sizer. If the SA bandwidth is increased, the noise will increase. The response to the carrier peak, however, will not change. A photographed spectral display is also shown.

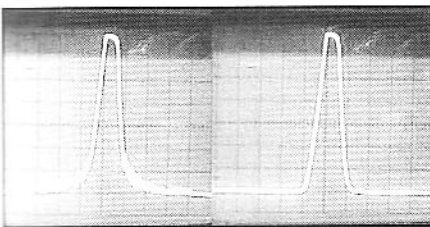
The spectrum of an oscillator with noise is shown in greater detail in a sidebar figure. A wideband noise floor exists within the oscillator feedback path. The noise then grows at frequencies within the loaded bandwidth of the oscillator resonator.

The phase noise of an oscillator can be predicted with the equations given in the sidebar.⁹

Consider a typical example, an average 14-MHz oscillator. It uses a loaded resonator *Q* of 100, tank capacitance of 100 pF, transistor noise figure of 10 dB, and a peak tank voltage of 4 V. Analysis with the sidebar equations shows a wideband phase noise floor of -162 dBc/Hz and, at 10 kHz, noise of -146 dBc/Hz.



Noise spectrum of an oscillator based upon the work of D.B. Leeson.



Spectrum analyzer plots from two oscillators. The left is especially noisy, producing noise sidebands where the signal merges into the noise floor. The quiet oscillator (right) lacks these excess sidebands, allowing the signal to go all the way down to the noise floor set by the spectrum analyzer. The left trace was produced with an Epson SG-8002 Programmable Oscillator (4.26 MHz) while the right trace came from a 7-MHz crystal controlled oscillator.

The Effects of Phase Noise

At first glance, phase noise sounds like an esoteric detail that probably has little impact on practical communications. This is generally true. Few oscillators are so noisy that they hamper normal communications in a band occupied with weak to average signals. But things change dramatically when a local station shows up on a band or when a contest starts with attendant stronger signals.

Assume that a receiver uses an ideal filter (perfect skirts) with a bandwidth of 500 Hz. The receiver uses noiseless oscillators. Even if a very strong noiseless carrier is applied to the receiver, a listener will hear a strong response when the receiver is tuned to it, but nothing as soon as the receiver is tuned away.

Consider now a carrier with noise, perhaps keyed with "CQ" so we can recognize it. As the receiver tunes toward the keyed carrier, we first hear some keyed noise. The noise grows in strength as we get closer to it, until finally the carrier is within the receiver passband, producing a clean, crisp note. The noise reappears on the other side, symmetrical with the first side.

We can't always put the blame on "the other guy." Assume that the keyed carrier applied to the receiver is noiseless, but that we now use a noisy oscillator as the LO in our receiver. The perceived result is exactly the same as we heard before with the noisy CW signal. The effect that we hear is called "reciprocal mixing."

This result is expected. The IF response is the difference (or sum) frequency of the LO and the RF signal. Any frequency change in either one will cause the IF to

contain the same change, the same phase or frequency noise. The phase noise is just an instantaneous change in frequency of one of the oscillators.

While our illustrations have presented oscillator noise as viewed in a spectrum analyzer, few analyzers are good enough to actually do this measurement for the local oscillators we need in our HF and VHF transceivers. Like receivers, spectrum analyzers have limited dynamic range. Consider the oscillator mentioned earlier with a phase noise density of -146 dBc/Hz at 10 kHz from the carrier. 146 dB is the difference between the carrier and the noise if analyzer bandwidth is 1 Hz. If we used a more practical bandwidth of 1 kHz, the carrier to noise ratio is still 116 dB. An analyzer capable of looking at this carrier and the noise at the same time would need a dynamic range greater than 116 dB. This is close to the present state of the art. Oscillator noise measurements for typical oscillators (at HF) must use modified methods. An example will be given later.

Designing Quiet Oscillators

Many of the methods used to design good LO systems are implicit in the Leeson design equations presented in the earlier sidebar. Some rules are:

- Use moderately low noise transistors in low noise circuits.
- Use a high Q resonator so that the noise sideband width is low. It is *loaded* Q that is important. A high unloaded Q that is degraded by the circuit does little good. If an oscillator is built with a loaded Q close to the unloaded Q, the insertion loss through the resonator will be high, which increases operating gain and increases noise. (This effect was treated in the filter chapter.) This degrades the wideband noise floor.
- The goal is a high carrier-to-noise ratio, which is enhanced with a high carrier. Hence, the best oscillators are those operating with high stored energy in the resonator. This means high power. Even with 8 or 10-V power supplies, it is not unusual to find oscillators with over 50-V peak-to-peak across resonator components. High energy also results from high capacitance in simple resonators.

- Limiting characteristics are critical in an oscillator, with current limiting being preferred. The circuit should operate in a way that allows the transistor current to drop to zero over part of the cycle to limit gain. Less desirable voltage limiting occurs when a low impedance is created over part of an operating cycle; that low

impedance then loads the resonator, degrading Q.

- The transistors used in an oscillator should have low noise at both the operating frequency and at baseband. This is important because low frequency noise is heterodyned up to the operating frequency in a working oscillator to modulate the carrier. For this reason, MOSFETs and GaAsFETs, normally perceived as low noise parts, are not as desirable in oscillators as quiet bipolar transistors or JFETs.
- The better oscillators are often those without excessively large starting gain. This places less demand on limiting within the oscillator. The operating circuit is closer to a linear amplifier which has less tendency to mix low frequency noise up to modulate the carrier. Emitter or source degeneration is often a useful modification.

An excellent example of a low noise oscillator is shown in Fig 4.18. This oscillator was originally designed by Linley Gumm, K7HFD, and is a good example of a simple circuit that functions well. It features excellent phase noise performance and high output power.

The circuit was designed specifically for high stored resonator energy and high power. Total emitter current is 28 mA, or 14 mA per transistor. The emitter RF choke converts the 47- Ω emitter R into an constant current source.

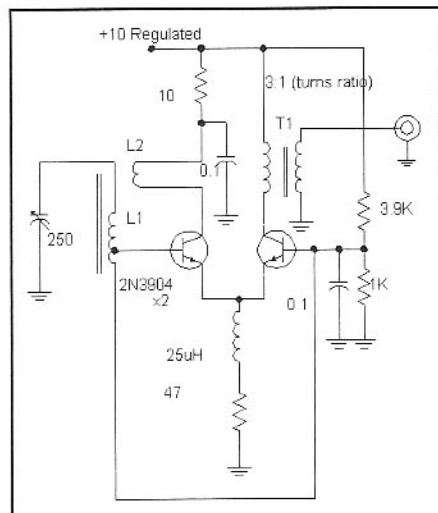


Fig 4.18—Low Noise 10-MHz Oscillator designed by K7HFD. L1 is 1.2 μH , consisting of 17 turns on a T68-6 toroid core. The tap is at 1 turn from the grounded end while the link is 2 turns wound over L1. The link must be properly phased for oscillation. Although not shown, ferrite beads were used on both bases and collectors.

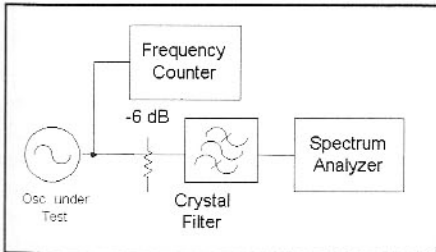


Fig 4.19—System used to measure phase noise in the K7HFD oscillator.

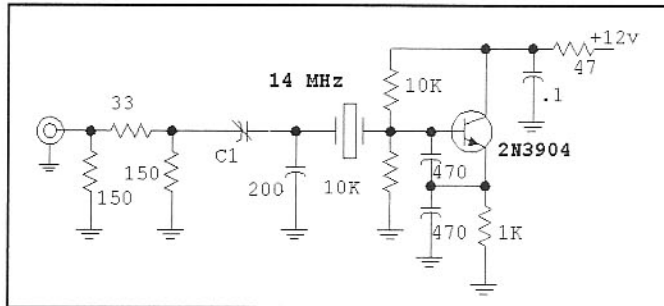


Fig 4.20—Crystal oscillator used for receiver reciprocal mixing measurements. C1 is adjusted for a power output of -10 to -20 dBm.

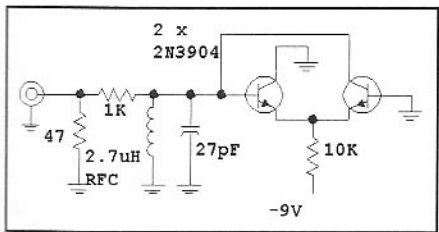
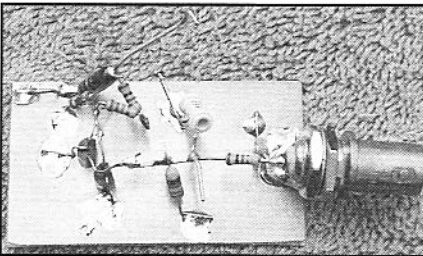


Fig 4.21—Easily built example of a noisy oscillator that the reader can construct to observe phase noise. It is instructive to evaluate this circuit with the design guidelines offered earlier to see just why this is such a poor oscillator.



The circuit of Fig 4.21 is especially bad for phase noise. This can be built as a simple experiment that will allow you to hear the results in a station receiver.

A differential amplifier with heavy base drive will behave as a limiting switch. The total current will oscillate between the two transistors with one collector, and then the other conducting the total current. The high standing current is further increased with an output autotransformer, yielding a measured 10-MHz output power of +17 dBm.

The peak current in the T1 primary also appears in L2, the 2-turn “tickler” link coil over L1. The load presented to the transistor by the link comes from the transistor base and the intrinsic loss of L1. Neglecting the transistor for the moment, the unloaded resonator Q is about 250 for a T68-6 core wound with heavy wire. At 10 MHz, the effective parallel resistance across L1 is about 18 k Ω . This value is diminished by the square of the turns ratio to present a 250- Ω load to the collector. The signal current through this load pro-

duces a peak collector signal of 3.3 V. This transforms to a base signal of 1.6 peak V; the signal across L1 is similarly calculated as 56 V peak-to-peak. These values are all significant. The low collector impedance establishes current limiting with no chance of voltage limiting. The restricted base drive guarantees that emitter-base breakdown will not occur.

A crystal filter, shown in the system of Fig 4.19, was used to evaluate the oscillator noise. The outboard filter had a 3-kHz bandwidth and skirts that were steep enough to provide over 50-dB rejection to signals 10 kHz away from the filter center. The oscillator was tuned to the filter center and the power reaching the analyzer was measured. The LO was then tuned 10 kHz away. The attenuation in the analyzer could then be reduced enough to measure the noise response. The K7HFD circuit produced phase noise that was below the

carrier by 156 dBc/Hz. Even though this circuit was originally built and tested in the early 1970s timeframe, it still holds its own with modern equivalents.

Other oscillator circuits, many of them relatively simple, also offer good phase noise performance. For example, the simple Hartley circuit of Fig 4.1, has been measured several times. Versions operating at 5 MHz often indicate phase noise of -150 dBc/Hz at 10 kHz spacing. Rohde reports that computer simulations suggest this Hartley topology will have degraded performance closer to the carrier.¹⁰

The Hartley oscillator results were measured indirectly by measuring a crystal oscillator with a receiver using the Hartley. A typical circuit used for the testing is shown in Fig 4.20. This circuit can be used with a crystal filter 10 kHz away from the oscillator, or with a crystal notch filter at the oscillator frequency. Assuming the crystal oscillator to be *perfect*, all phase noise observed is attributed to the receiver LO. Even without the assumption, observed results will bound the LO performance. The crystal filter is required because of the limited dynamic range of the typical receiver. The loaded Q of a crystal, the “tank” in a crystal oscillator, can be a thousand times higher than that of a typical LC tank. The resulting phase noise is often quite low, in line with Leeson’s equation.

Fig 4.21 shows an oscillator at the other extreme. This 15-MHz circuit is rich in phase noise. It is well worth building and applying to a general coverage receiver to observe first hand just what a noisy oscillator will sound like in a receiver.

4.5 CRYSTAL OSCILLATORS AND VXOS

One of the most common oscillator forms is that using a quartz crystal as the resonator. They may be ordered from a number of sources for modest cost with only a short manufacturing delay. A crystal cross-section, symbol, and an equivalent circuit are shown in Fig 4.22. Crystals were also discussed in the filter chapter.

A typical crystal oscillator circuit is the Colpitts shown in Fig 4.23. It is the series LC of the crystal model, Fig 4.22, which now serves as the "inductor" in this circuit. Owing to the series motional C, this

circuit is actually a Clapp oscillator variant. With the components shown, the circuit will function with fundamental mode crystals from about 2 to 20 MHz or more. Transistor type is not critical with the ubiquitous 2N3904 being a good choice. If the crystal is specified for a "load capacitance" of 32 pF, the oscillator can be adjusted to the exact frequency with C1. This will occur when the total loop capacitance is 32 pF, which is approximately the series equivalent of the two 470-pF capacitors and C1. In many applications C1 can

merely be eliminated.

Output can be extracted with an emitter follower driven by Q1's emitter. The signal on the base of Q1 is often about the same magnitude, but is spectrally cleaner. It is also possible to insert a small resistor (100 Ω or so) in the Q1 collector and to use the developed signal voltage as an output. While well isolated from the resonator, the collector signal is usually very rich in harmonics.

Fig 4.24 shows another scheme for extracting an output signal. Here, C1 becomes a selected, fixed capacitor in series with the crystal. It is no longer convenient to adjust the frequency with C1, for the capacitance will vary both F and output voltage. However, an output obtained in this manner can be extremely clean with all harmonics being over 50 dB below the desired output. Phase noise is also low with this topology.

A popular and especially simple crystal oscillator is the Pierce circuit shown in Fig 4.25. If the circuit is redrawn with the ground shifted to either the base or the collector, we see that this is yet another version of the Colpitts. This circuit functions well with a wide variety of crystals from 2 to 20 MHz or even higher. The circuit generally operates at the crystal fundamental. Output is easily obtained with a follower from either the collector or base. If C1 is lifted from ground, a direct output of a few milliwatts is available.

Another Colpitts variation is presented in Fig 4.26. This oscillator is capable of 10 to 25-milliwatts output and can function at either fundamental or overtone frequencies (explained below). The circuit uses the relatively high base-emitter capacitance of the transistor as part of the capacitive feedback needed for oscillation, again as a Colpitts variation. External C3 vanishes except for the 1.8 and 3.5-MHz bands where values of 330 and 200 pF can be used, respectively. C2 varies from 100 pF at 3.5 and 7 MHz to 22 pF at 28 MHz and 10 pF at 50 MHz. L1 uses a toroid with a reactance of about 250 Ω . The output link is 10 to 20% the number of turns on L1. This is a very robust oscillator that takes little experimentation to get going.

A crystal overtone is a different operating mode for an AT-cut quartz crystal. Any crystal will display a fundamental resonance as well as overtone responses. Sometimes the crystals are manufactured in a way that will substantially enhance one mode over another. A general model for a quartz crystal including overtones is shown in Fig 4.27. The model presented so far included only the fundamental mode, related to N=1 in the figure. But

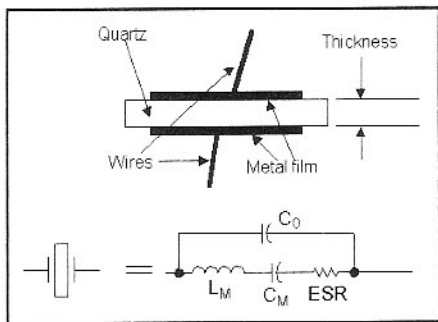


Fig 4.22—Cross-section, symbol and model for a quartz crystal.

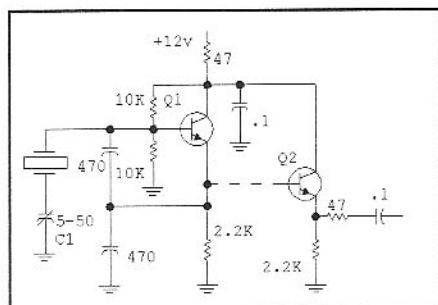


Fig 4.23—Typical Colpitts crystal oscillator. Power output is low. Extra amplifiers are usually used to increase power to the level needed to drive a ring mixer or function in simple transmitters.

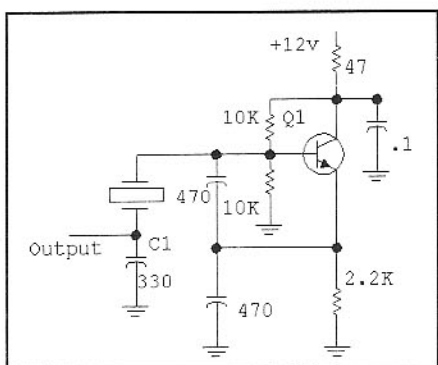


Fig 4.24—Method for extracting low noise, low distortion output from a crystal oscillator.

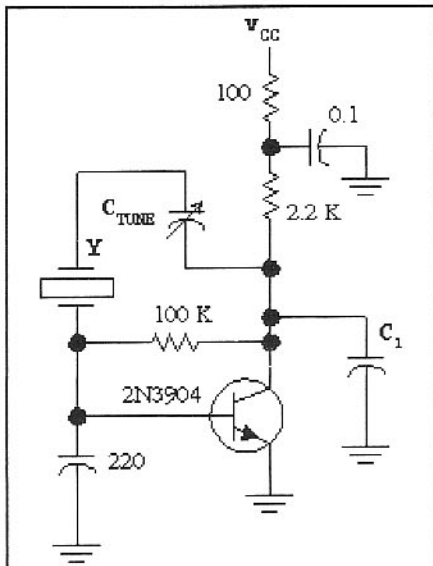


Fig 4.25—Pierce type crystal oscillator. C1 can be as little as 10 to 20 pF. Vcc can be from about 3 up to 15 V. C_{TUNE}, often omitted, is a trimmer with a maximum of 50 or 100 pF.

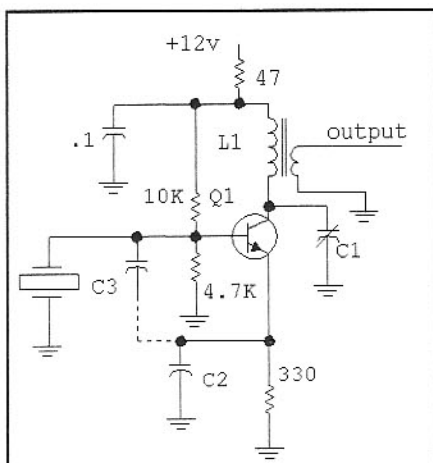


Fig 4.26—General purpose power oscillator for use from 2 to 70 MHz. Q1 is a 2N3904 or similar medium F_T device. See text for component value discussion.

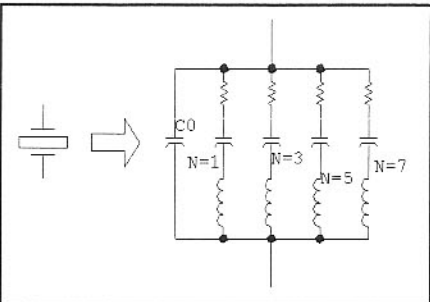


Fig 4.27—More detailed model for a quartz crystal. All motional inductance values are identical, with motional capacitance scaling with frequency. See text.

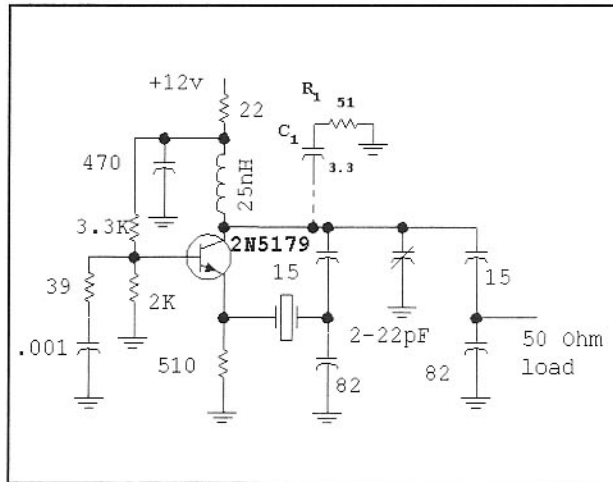


Fig 4.28—Butler oscillator for 100 MHz. L=25 nH. This is formed with a 1.7 inch piece of #22 enameled wire wound in the threads of a 6-32 machine screw.(3.3 mm dia, 12.6 turns/cm) The wire ends are stripped and 3 turns are wound on the screw, which is then removed. C1 and R1 form a network to suppress UHF oscillations at 500 to 1000 MHz. The suppression circuit generates a UHF load that is largely absent at the operating frequency.

other *odd* harmonic modes are also possible. (Even order harmonics are not consistent with the mechanical boundary conditions needed so support oscillation.)

An oscillator operating at an overtone must include additional frequency dependent circuits that will select the desired overtone. Simple fundamental mode circuits, such as those presented, will emphasize the lower frequencies where starting gain is higher. The circuit of Fig 4.26 included a tuned circuit peaked at the operating frequency.

Fig 4.28 shows a popular and effective overtone circuit, the Butler oscillator. This circuit is essentially an LC Colpitts oscillator with a quartz crystal inserted in the feedback path. The LC tank should have a loaded Q from 10 to 20. A Q that is too low could allow oscillation at the wrong overtone, while a Q too high will make tuning difficult. An excellent method to align this circuit replaces the crystal with a resistor equaling the equivalent series resistance (ESR) of the crystal. If ESR is unknown, use a 33- Ω resistor in place of third overtone crystals and a 56- Ω for 5th overtone crystals. The oscillator is adjusted for the proper operating frequency with the resistor in place. The resistor is then replaced with the crystal with no additional adjustment needed. Most overtone circuits, including the Butler, can be used for fundamental mode operation by proper adjustment of the tuned circuit.

This circuit is sometimes “neutralized” by placing an inductance in parallel with the crystal. The value resonates with C0, the crystal parallel capacitance. If C0=3 pF for the 100-MHz crystal of Fig 4.28, the inductance would be 0.84 mH. Be sure that the inductor used has a self-resonance well above 100 MHz. We have generally found that this inductor can be eliminated from the circuit.

The Butler oscillator shown in Fig 4.28

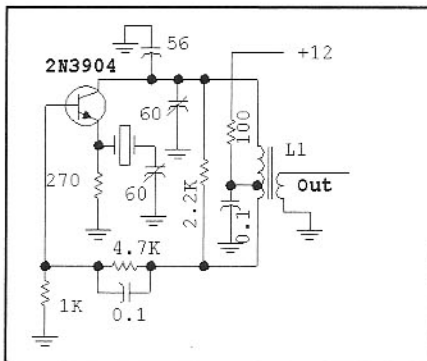
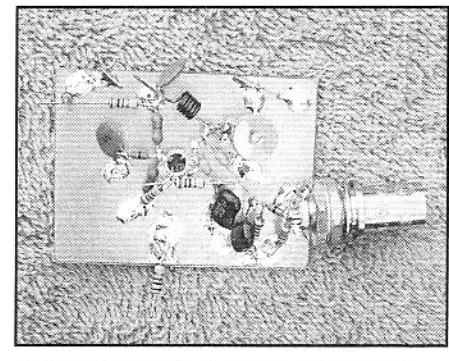


Fig 4.29—An oscillator designed by inserting a crystal in series with the feedback path of a Hartley LC oscillator. The ground point is then shifted to the tap on the coil. The version shown is set up for 10 MHz operation, but tuning can be shifted to other frequencies. Eliminating the tuning capacitors and replacing the transformer with one using a ferrite core also works well. Y1=10 MHz fundamental; L1=30t T 50-6, tapped at 7 turns and 6 turns for the link.

will provide an output of 10 mW to 50 Ω . The load is part of the design; if the load is ill defined, use a 50- Ω pad at the oscillator output. Never try to adjust the oscillator without the load in place. The Butler oscillator generally exhibits excellent phase noise. Although a trimmer capacitor in series with the crystal will allow some frequency adjustment, it is much less effective with overtone crystals than with fundamental mode parts. Never try to adjust oscillator frequency with the crystal by changing collector tuning, for that could cause the circuit not to start when power is first applied.

The Butler used a Colpitts as the basis. **Fig 4.29** presents a useful variation of this circuit that begins as a Hartley with the crystal in the feedback path from the coil tap to the emitter. The ground point is then



A Butler oscillator. The circuit of Fig 4.28 is breadboarded here without the crystal. Instead, a 51- Ω resistor is placed in the crystal position. This is a useful way to test the oscillator.

shifted, placing ground at the coil tap. This puts one end of the crystal at ground, or connected to a trimmer. This circuit functions well as either an overtone or fundamental mode oscillator with low phase noise and moderate output. The circuit functions well (fundamental mode only) if the tuned output transformer is replaced with a ferrite transformer.¹¹

The Vxo

The crystal oscillators shown so far have often included a trimmer capacitor for fine frequency adjustment. If the tuning range can be made larger, the circuit can be used as a high stability substitute for a variable frequency LC oscillator, taking on the descriptor *VXO*. A typical VXO circuit is shown in **Fig 4.30**.

The circuit of Fig 4.30 was built and tested with numerous crystals from our junk box. Crystals at and above 14 MHz could typically be tuned by 0.1% of the marked frequency when L=0, with the bottom frequency being close to the marked crystal frequency. For example, a crystal

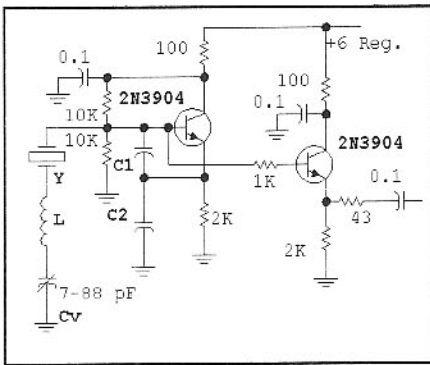


Fig 4.30—Basic VCO circuit. C_2 is typically twice C_1 , which is 100 pF at 10 MHz and higher, doubling for 7 MHz. L is determined by experiment. C_V can be about any variable capacitor, but should be one with small minimum capacitance. L may = 0, 2.7 μH or 5.4 μH .

marked 14060 kHz tuned from 14059.0 to 14070.4 kHz (11.4-kHz shift) with C_1 and C_2 of 100 and 200 pF. Adding inductance moved the bottom of the range downward with a much smaller change in the upper edge. $L=5.4 \mu\text{H}$ produced 14053.0 to 14068.4 kHz (15.4-kHz shift.) In another example, an 18-MHz crystal shifted 13.3 kHz with no inductance, but shifted over 25 kHz when 3.7 μH was added. 5.4 μH in that circuit produced unstable operation, emphasizing the need for experimentation.

In some cases a variety of crystals were available from different manufacturers, all at approximately the same frequency. Results varied only slightly. Larger values for C_1 and C_2 were required for oscillation at 7 MHz and lower.

With even greater added inductance, the lower frequency drops further and the range expands. However, stability also degrades. Eventually, if oscillation is maintained, it may not be crystal controlled. Experimentation and careful analysis can both pay large dividends. With zero or only modest added inductance, the frequency stability of a VCO is nearly as good as the original oscillator. This makes the circuit especially attractive for narrow tuning range equipment such as VHF/UHF CW and SSB rigs.

Extreme tuning nonlinearity is common with most VCO circuits. Most of the frequency shift tends to be compressed at the high frequency (low C) end of the range. This effect is so extreme that it is very difficult to implement a predictable shift for use in, for example, a direct conversion transceiver.

The typical VCO suffers from considerable variation (unflatness) in output power with tuning. The VCO of Fig 4.30 can vary by nearly 10 dB. This is relieved with the circuit shown in Fig 4.31 where a

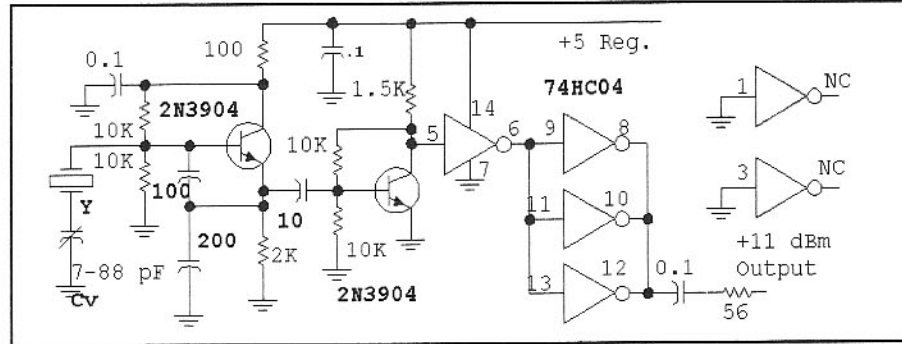


Fig 4.31—Adding HCMOS inverters can substantially flatten the output of a VCO. Output filtering will be required.

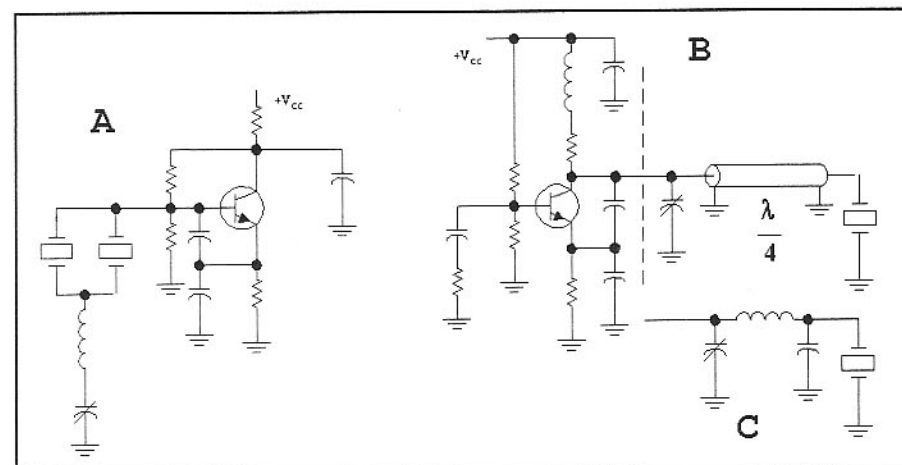


Fig 4.32—Two VCO circuits of interest to the experimenter. That at A is known in Japan as the Super VCO, and is the creation of JA0AS and JH1FCZ. The circuit at B uses a quarter wavelength of transmission line while that at C is the lumped element equivalent.

CMOS inverter is added as an output buffer. The circuit shown provides an output of +11 to +12 dBm for a total current of around 35 mA. The output is very rich in harmonics, so low pass filtering will often be required. Different numbers of parallel inverters may be used to control output power. The square waveform at the inverter output can also be useful for frequency multiplication.

Two VCO circuits are shown in Fig 4.32 that are of special interest to the experimenter. One adds a second crystal, producing almost double the tuning range of the same circuit with one. The crystals should be close in frequency, but need not be an exact match. We encountered this circuit in the worldwide web where it is known as the "super VCO."¹² The two elements in parallel behave like one crystal, but with twice the motional and fixed capacitances and half the motional inductance. This is the direction needed for greater "tunability."

The second VCO of Fig 4.32 uses a quar-

ter wavelength of transmission line to convert a crystal series resonance to appear at the collector as a parallel resonance. The alternative version of this circuit uses a lumped element equivalent for the transmission line. The real virtue of this scheme is that the troublesome crystal parallel capacitance is absorbed into the "line." The performance of this circuit can be truly outstanding, although the circuit can be difficult to adjust. In one experiment we were able to tune a 7-MHz crystal by a range of over 100 kHz. The circuit has problems that present challenge to the designer/builder. The Q of the equivalent parallel resonator varies dramatically over the tuning range, making it difficult to maintain clean limiting in the transistor or to obtain an output with a stable amplitude.¹³

The Hartley theme circuit presented earlier (Fig 4.29) is especially well suited to VCO applications, especially when built with ferrite transformers. This topology is used in a 28-MHz VCO transmitter presented in Chapter 12.

4.6 VOLTAGE CONTROLLED OSCILLATORS

The oscillators presented so far have used mechanical variable capacitors for tuning. The other traditional tuning scheme is inductive, the *permeability-tuned oscillators* of Collins fame. Both depend on well-engineered mechanical designs, a desirable, but disappearing characteristic. The voltage-controlled oscillator is replacing the "simple" mechanically tuned oscillator of the past. That oscillator is then used as part of a frequency synthesizer. In a few cases, the VCO is used "open loop," without synthesis.

The dominant component used for voltage control of oscillators of concern in this text is the varactor diode. Any diode will exhibit a capacitance. When the diode is reverse biased, the capacitance will vary inversely with the applied voltage. The reverse biased diode is inserted in a VCO circuit to become the tuning element in that oscillator.

Figure 4.33 shows a 7-MHz voltage tuned oscillator. This circuit was designed to serve as the main control for a direct conversion transceiver. (Described later as the *Western Mountaineer*.) Q1 functions as a high C Colpitts oscillator. Inductor L1 is resonated with the 470-pF Colpitts capacitors and C1, a fixed capacitor of over 600 pF. The value was hand picked for resonance, with only a small, 10-pF trimmer for final adjustment.

Earlier measurements with a small environmental chamber had established the tuning diode temperature coefficient at 5 V as +442 ppm/ $^{\circ}\text{C}$. This is generally quite severe, over ten times worse than NPO oscillator components.

This oscillator was initially built without the diode, stable operation was confirmed, the diode was added, and environmental chamber measurements were done. The tuning diode D1, a Motorola MV209, was temperature compensated with a second diode, D2. The sense diode is placed in the same thermal environment as the tuning diode. The complete oscillator and its buffer are shielded from the rest of the circuitry, for the oscillator runs at the same frequency as the transmitter PA in this rig. The diode standing current is adjusted by picking R1, generating the needed voltage change with temperature. R1=10 k Ω worked well in our circuit, but should be picked with the environmental chamber for individual applications. This compensation scheme was suggested to us by WA7TZY.

The oscillator supply is regulated with U1, a 78L05 three-terminal regulator. The original Zener regulation was unstable with temperature, adding extra complication. The regulated voltage also provides

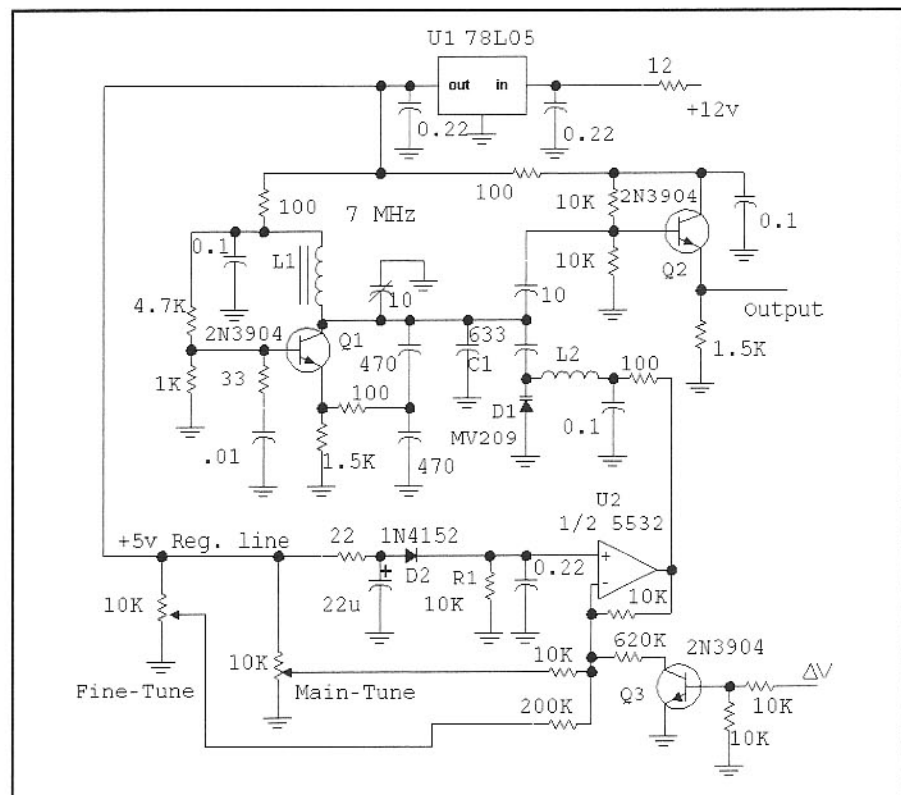
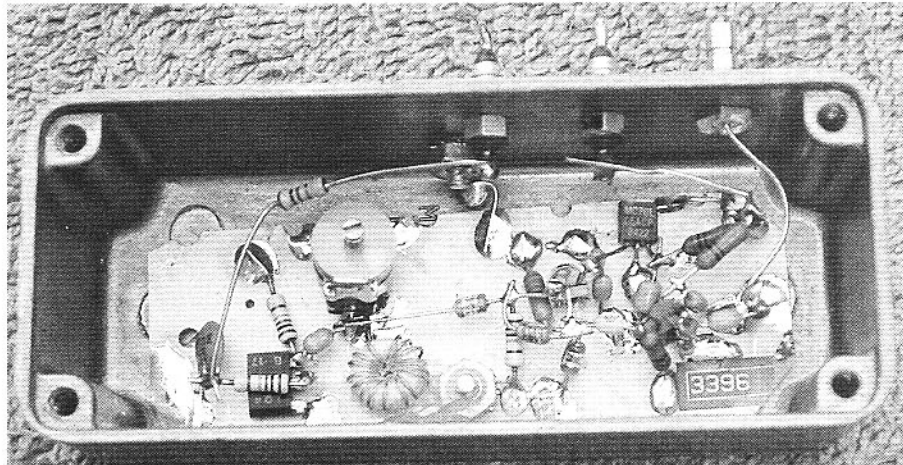


Fig 4.33—A varactor tuned 7-MHz oscillator with a restricted tuning range of about 60 kHz. Temperature compensation is provided with D2, a sense diode. L1=12 turns #26 on a T30-6 toroid. L2 is a 15- μH RF choke.



Inside view of the 14-MHz VCO.

sense-diode biasing and serves as the supply for the tuning controls.

The op-amp, U2, combines two tuning controls and an offset voltage while providing a regulated tuning voltage. The circuit is configured to maintain at least 4.3 V on the tuning diode. In many varactor-tuned oscillators, RF voltage will be rectified by the diode, allowing conduction during part of the cycle, degrading stabil-

ity, phase noise, and tuning linearity. This occurs with low tuning voltage and is usually detected as a decrease in VCO output.

The final temperature coefficient realized with this oscillator was about 2 ppm/ $^{\circ}\text{C}$. The transceiver has appeared to be "rock solid" during field operation, including winter snowshoeing treks.

A 14-MHz VCO is shown in **Fig 4.34**.

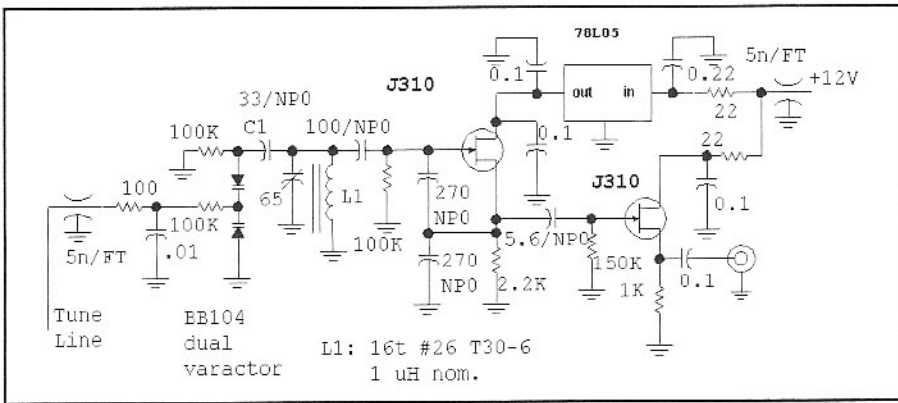


Fig 4.34—14-MHz VCO for use in synthesizer experiments. L=16 turns on a T30-6 toroid coated with Q-dope to reduce micro-phonic effects.

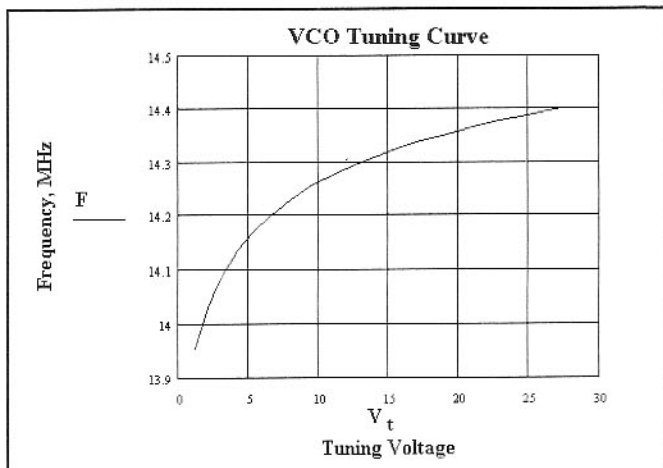


Fig 4.35—
Frequency vs
control voltage for
14-MHz VCO. An
average sensitivity
for this circuit
over the 2 to 10 V
range is 30 kHz/V.

A J310 FET was used with source resistor biasing. The varactor diode was a surplus BB104, similar to the Motorola MV104. The Toshiba 1SV103, used in some imported equipment, might be a suitable substitute. Two individual varactor diodes can also be used. This oscillator can be set up for a wider frequency range by picking C1. Over 1 MHz of tuning was available with C1=100 pF. C1 was dropped to 33 pF for a reduced range. The

tuning characteristics for this oscillator are shown in Fig 4.35. The circuit is built in a Hammond 1590A enclosure with coaxial output and feedthrough capacitors for power and tuning. A 65-pF plastic trimmer provides coarse tuning.

The use of back-to-back varactor diodes is common in VCOs, for it reduces the effects of rectification of the oscillator signal. It is also common to see many diodes operated in parallel. This topology shows

lower noise than a smaller number of higher-capacitance diodes.

The phase noise of this oscillator was measured using a 14-MHz single conversion superhet receiver with extensive crystal filtering. The VCO was battery powered with the battery also biasing the varactor, which was filtered further with a 100- μ F capacitor. The signal was attenuated to -31 dBm and applied to the receiver input through a step attenuator. Audio output was monitored with an HP3400A true-RMS voltmeter with receiver AGC set off. The audio noise output in the meter was noted 5 kHz away from the carrier. The receiver was then tuned to the carrier and the step attenuator was increased until the response was the same as observed with the noise. Additional attenuation of 110 dB was required to reach this response. The noise bandwidth was 500 Hz, producing a measured CNR of -137 dBc/Hz. It is not clear if this noise comes from the VCO or from the receiver VFO, but this value is a useful "worst case" limit. No phase noise could be detected at 10 kHz offset. No outboard crystal filter was used for this measurement, placing us at the limit of what we can measure with this setup.

Voltage tuning with diodes tends to compromise noise and stability performance. However, reasonable results are available if the tuning range is kept small. An attractive scheme uses varactor tuning over a small range with PIN diode switching in larger frequency steps. PIN diode capacitor switching is illustrated in a transceiver (*The Lichen*) offered in Chapter 6.

The reader working on a synthesizer for a high performance (wide dynamic range) receiver should review the extensive literature on voltage controlled oscillators. Numerous methods are available to design these circuits. It is often the varactor diodes that ultimately limit noise performance. Noise supplied to the diode on tuning lines can also compromise performance.¹⁴

4.7 FREQUENCY SYNTHESIS

Virtually all of the local oscillator systems used in modern communications equipment now use frequency synthesis in one form or another. Two circuit types dominate synthesis: the phase-locked loop (PLL) and direct-digital synthesis (DDS). The two schemes are often used together. The Huff 'n Puff scheme described earlier is a frequency lock method and is not usually the basis for synthesis. The reason is that frequency lock allows frequency errors, which are absent in PLL or DDS synthesizers.

A PLL for frequency synthesis in its simplest form is shown in Fig 4.36. The first component is a voltage-controlled oscillator characterized by a tuning sensitivity in Hz/V. This sensitivity usually varies over the tuning range. The next component is the phase, or phase difference detector, a circuit that provides a dc output proportional to the phase difference between two RF inputs. The third element is a "loop filter." In its simplest form, this is (for a second order loop) a single pole RC filter with a couple of resistors and one

capacitor. More often it's an operational amplifier offering low frequency gain as well as filtering properties. The low pass filtering is needed to remove signal components coming from the phase detector. The dc from the detector and loop filter must be of the proper magnitude to drive the VCO tuning line. Because this is a negative feedback system (a type of *servo loop*), the phase of the feedback signal as it moves through the loop to eventually reach the VCO must be tailored for loop response.

A PLL that is “locked” forces the VCO to be at exactly the same frequency as the reference. If the reference is tuned, the VCO will follow, maintaining not only the same frequency but a phase relationship that depends on the characteristics of the detector. If the loop dynamics are “wrong,” the VCO may not respond smoothly to a change in the reference frequency. In the extreme, the loop can oscillate.

We begin our discussion of the PLL with an experiment to evaluate a Mini-Circuits SBL-1 mixer operating as a phase detector. Most of us have no easy way to accurately measure phase, but we can do things to infer it. In this vein, we first characterize a piece of coaxial cable, a 25-foot length available in a home lab. A “half wave” balun was fabricated from the cable, shown in Fig 4.37A. The two balanced output points were attached to 100- Ω resistors with the junction attached to an RF spectrum analyzer. The signal generator was tuned until a null was found at 12.88 MHz. This occurs when the cable is a half wavelength long, producing 180 degrees of phase shift between the two ends. A half wavelength in free space at this frequency is 38.2 feet, so the velocity factor of our coax is 0.65, which is about what we would expect. The phase delay in the coaxial cable will be directly proportional to cable length and to frequency. We know the length and frequency that yield a phase shift of 180 degrees, so we can calculate the phase for any arbitrary frequency.

The characterized coaxial cable is now used in the test set of Fig 4.37B. The signal generator output is divided in a power splitter consisting of three 51- Ω resistors. This preserves a 50- Ω environment while equally splitting the input power. One signal is applied directly to the SBL-1 LO port. The other is attenuated by 10 dB, phase shifted with the cable, and applied to the mixer RF port. The output was low pass filtered with a simple RC filter and measured with a digital voltmeter. The signal generator amplitude was adjusted to produce the specified +7 dBm LO drive level. This overall circuit is familiar as a delay-line discriminator.

A quick tuning of the signal generator showed that the output was zero at 6.4 MHz where coax phase shift is 90 degrees. Data was taken over the 3 to 10-MHz spectrum to generate a plot (Fig 4.38) showing output voltage as a function of phase. This is close to a straight line over a wide phase range, with the departure at low angles resulting from a signal generator output decrease near 3 MHz. (We used a modest drive at the mixer RF port; the mixer is approximately linear to RF drive at this level.) Examination of the data in Fig

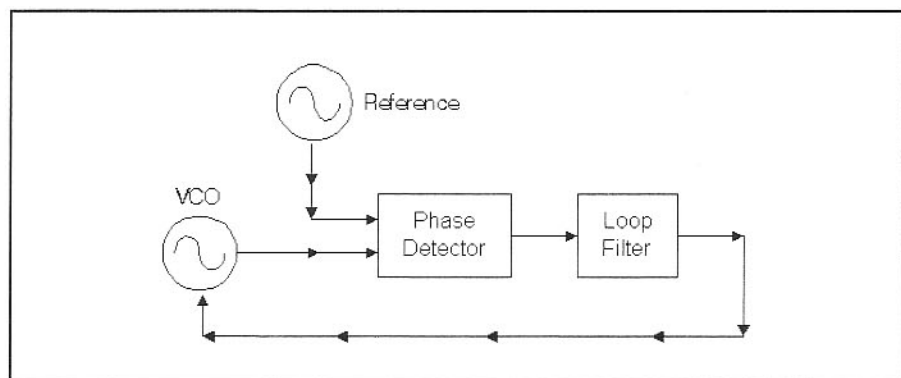


Fig 4.36—Basic Phase Locked Loop.

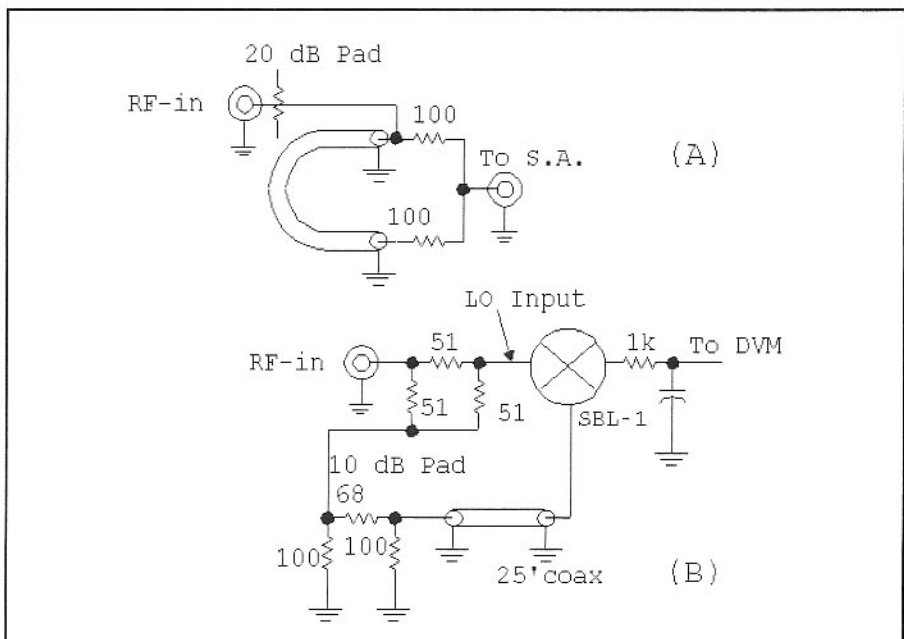


Fig 4.37—Part A characterizes the phase shift in a section of coax cable that is then used in part B to evaluate a SBL-1 as a phase detector.

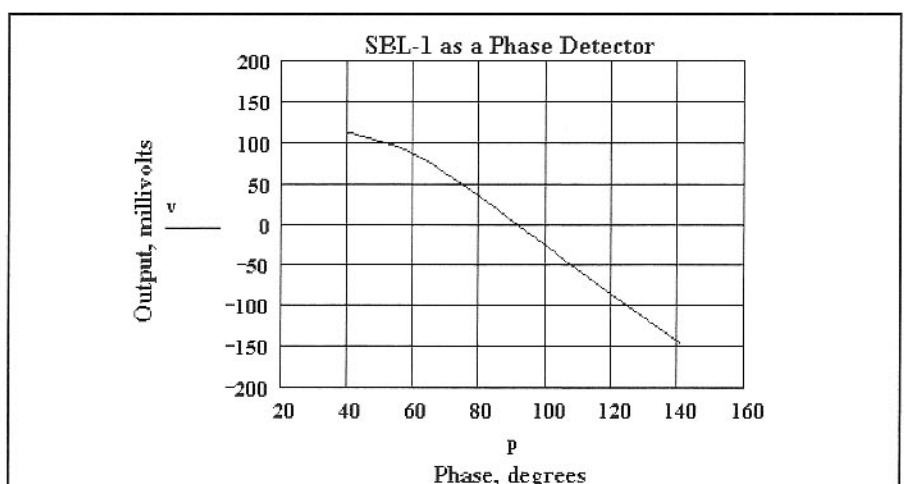


Fig 4.38—Dc output vs phase for a SBL-1 operated as a phase detector.

4-38 shows that the slope (phase gain) is -2.96 millivolt per degree, or -0.17 V/radian. Repeating these experiments with other cable lengths show that this circuit responds to phase rather than frequency.

Having characterized the phase detector, we can now build a phase locked loop. We will use the 14-MHz VCO described earlier (Fig 4.34), an oscillator with an average tuning sensitivity of 30 kHz/V with the available voltages when we use a 12-V bench supply. A general-purpose signal generator is the “reference” in the loop shown in Fig 4.39. The SBL-1 details are shown to emphasize the dc isolation properties of the ring and transformer windings. An operational amplifier increases the relatively low output of the detector to drive the VCO tune port. The LM358 used was available for the experiment; a better choice would be an OP-27 or similar low noise part.

The loop was originally tested while running the phase detector at the low RF port level used for measurements. Although phase lock was possible, performance was poor. Increasing the levels to $+7$ dBm at both mixer ports produced more robust behavior. The circuit is initially turned on without seeing any indication of “lock.” An oscilloscope was used to monitor the op-amp output, which came up to about 4 V, the level set by the $3.9\text{-k}\Omega/2.2\text{-k}\Omega$ voltage divider. The signal generator was then tuned. Lock was achieved when it passed through the VCO resting frequency. The VCO will then track the reference over the full op-amp output range.

Intuition suggests that achieving lock would be difficult, that both signals would have to be at the same frequency before phase lock can ever be realized. But lock

does occur, even with a slight frequency difference. Consider two input signals, a reference and a VCO, separated by 1 kHz and applied to the *phase detector*, which is the same topology as a mixer. The mixer will produce 1-kHz currents. This low frequency component will generate sidebands about both the reference and the VCO. These components appear in the mixer output. One of the VCO sidebands is now directly on top of the reference, producing a dc component that will pass through the loop filter where it can be amplified and move the VCO toward a locked condition. A similar sideband is on top of the VCO frequency.

Analysis like this offers some explanation, albeit sketchy, of a related phenomenon called *injection locking*. This occurs when an external signal is applied to an operating oscillator. If the signal is strong enough, it can cause the oscillator to move frequency until it becomes locked to the injected frequency. The same modulation sidebands are created within the oscillator and operate in much the same way.

Although these modulation processes are powerful, they are restricted. A simple PLL will have a well-defined *pull-in range* where capture is possible.¹⁵

This experimental loop was designed for a closed loop bandwidth (open loop unity gain frequency) of 2 kHz with a damping factor of 5, parameters determined by the choice of the resistor and capacitor values of the loop filter. Although we pick *loopfilter* components, the parameters describe the overall PLL and not just the op-amp and related parts.

This seemingly simple circuit is useful, not only as an illustration of the concept, but as a way to obtain two signals that have a well-defined phase relationship to each

other. With a diode ring phase detector, the locked oscillator will differ from the reference by 90 degrees. A sidebar shows a practical PLL with a diode ring phase detector.

Other mixers, including the popular Gilbert cell, work well as a phase detector. The most popular phase detectors use digital circuits. Fig 4.40 shows a common circuit, a so-called phase-frequency detector. This digital circuit is fed with digital voltages to the clock inputs of two *data flip-flops*. The D-FF is a topology that transfers the level on the Data input to the Q output when a clock transition occurs. The data, in this circuit, is just a logic 1, for the D input is tied to the positive power supply. A NAND gate resets both D-FFs when both have a high Q output. If the two inputs are signals at the same frequency and are in phase, the output will be a very narrow spike, defined by the logic speed. If, however, there is a phase difference, the Q related to the first FF triggered will stay positive for a short period, producing an output with a net dc component.

This circuit will also compare frequencies. If one frequency is higher than the other, the dc average of the two outputs will, after filtering, cause the VCO to sweep toward equal frequencies. Even if this detector is not the primary phase detector in a PLL, it can still serve to compare two frequencies, a handy feature in some applications.

The digital phase frequency detector uses digital logic. However, the simple loops discussed so far have dealt with analog signals. An analog signal is easily converted to digital form with the circuit shown in Fig 4.41. The $10\text{-k}\Omega$ and $4.3\text{-k}\Omega$ resistors form a voltage divider with a voltage gain of about $\frac{1}{3}$. But, to be active, the

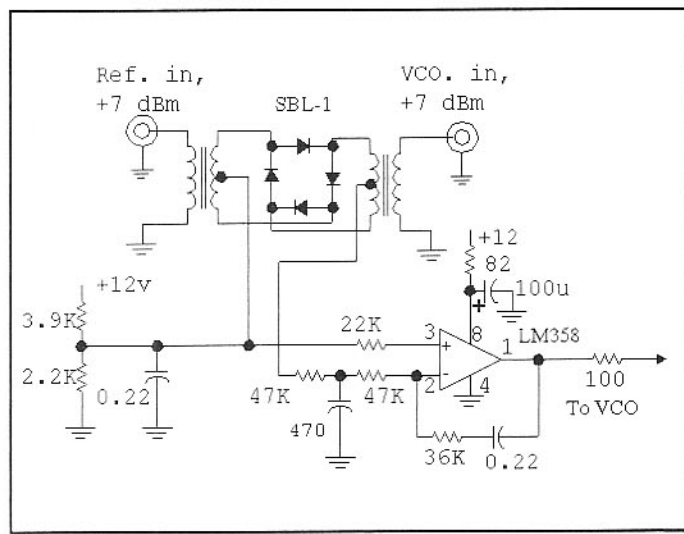


Fig 4.39—Phase locked loop using the phase detector.

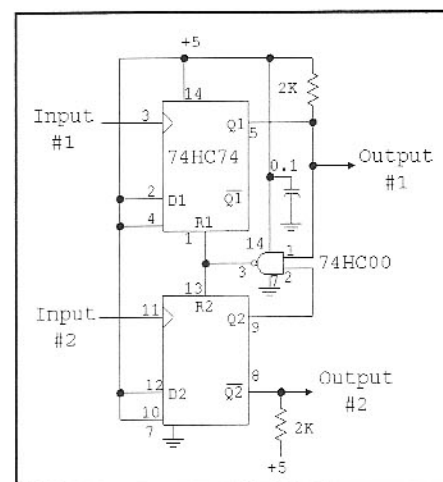


Fig 4.40—Phase frequency detector using digital integrated circuits.

A Practical Frequency Multiplying PLL LO System without a Loop Filter

The phase locked loops we have described are second order loops, ones with a capacitor in the loop filter that alters loop response. A simpler form for loops is possible, a first order circuit. This occurs when we take the dc output from a phase detector, perhaps with some amplification, and apply it directly to a VCO. This is exactly the sort of negative feedback used when we control the gain of a simple op-amp by connecting the output to the input through a resistor. The circuit is stable so long as the gain before feedback is inverting. The second order loop, with its additional capacitor, introduces the possibility of a delay between an output error and the signal reaching the amplifier input to correct that error.

An analogy may be appropriate: A rider proceeding down a hill on a bicycle controls direction with a first order feedback loop. The VCO represents the bicycle handlebars; a direction error is corrected with immediate feedback applied to the handgrips. The second order loop places springs between the rider's controlling hands and the handlebars, effecting a delay in the feedback. The system with springs might be smoother on a gentle hill, but clearly needs much more effort on the part of the designer. The consequences of failure are dramatic.

We had built a VHF transceiver (described later in the book) tuning from 52 to 53 MHz that receives most modes. While normally used with microwave transverters, we wanted to also use this for casual HF reception. We needed a stable LO that would operate in the 48 to 70-MHz area that could drive a mixer to convert HF signals to VHF. The needed LO could take on frequencies that were multiples of 1 MHz. This was done with a first order phase locked loop, shown in Fig 4A. The basis for the LO is a pair of off-the-shelf modules from Mini-Circuits: a POS-100 voltage controlled oscillator tuning from 50 to 100 MHz and a SBL-1 serving as a phase detector.

The VCO output is split with most of the energy routed to a coaxial output for mixer use. A sample is applied to a common gate amplifier, Q1, and then to the SBL-1 phase detector with a level of about +7 dBm. The RF input to the phase detector, the "reference" for the loop, is a harmonic of

a lower frequency crystal controlled oscillator. The harmonic signal should be between -40 and 0 dBm at the desired frequency.

A dual op-amp provides the rest of the control for the system. U1A is a unity gain voltage follower driven by a 10-turn 2-k Ω pot. The output signal, from 0.3 to 6 V, is applied to the diode ring in a way that this level also reaches the VCO. Note that this is not easily realized with all ring mixers. Phase detection occurs in the diode ring, creating a dc signal that is added to the applied dc bias. This is then differentially amplified with a voltage gain of +11 in U1B and routed to the VCO.

The system is generally very easy to use. The 10-turn pot is merely tuned until a lock is obtained, producing stable output signals in the receiver. A chart of the various frequencies vs the setting of the 10-turn control is kept, allowing an easy return. The capture range (how close you must tune the 10 turn control to achieve lock) is about 100 kHz if the corresponding input is at -10 dBm, but drops to 10 kHz for a -30 dBm input. The reference spurious responses in the output at plus and minus 1 MHz were at

-60 dBc when the loop was locked.

This circuit should be built over ground plane with relatively short leads in the RF areas. The U310 common gate amplifier is critical. While the gain is low, the reverse isolation is very good, needed to prevent 1-MHz energy from reaching the VCO where it can create sidebands. The amplifier is built by drilling a hole in the ground foil for the FET and soldering it in place. This is possible with the U310, for the gate is attached to the metal can. A J310 could be substituted if caution is devoted to keeping the circuit stable. Such circuits are discussed in Chapter 6.

Capacitor C1 is a VHF bypass that filters the dc coming from the phase detector. The value is small enough that it does not impact loop performance.

The greatest virtue of this circuit is its tolerance to experimental changes. Because there are no loop filter components to pick, there is little design to be done. Yet the resulting performance can be excellent.

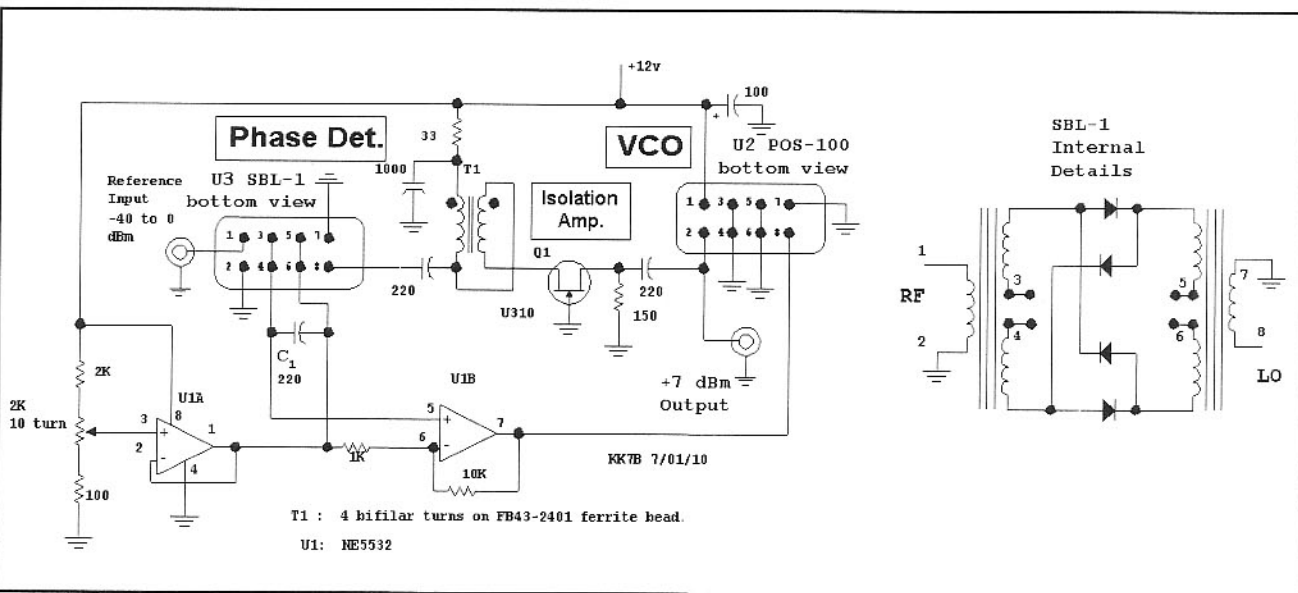


Fig 4A—A first order PLL allowing a VHF VCO to lock to harmonics of a 1-MHz input.

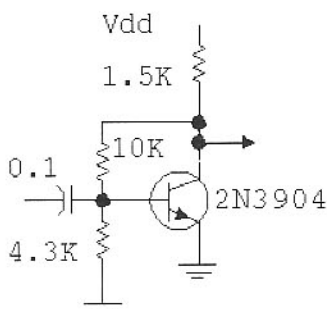


Fig 4.41—An analog signal is easily converted to digital form with the circuit shown here. The 10-k Ω and 4.3-k Ω resistors form a voltage divider with a voltage gain of about 1/3. But, to be active, the transistor base must be biased at about 0.7 V.

transistor base must be biased at about 0.7 V. Hence, the feedback loop holds the collector close to 2 V, which is between a logic 0 and 1 for TTL and for CMOS running at 5 V. This circuit will function with RF signals of -30 dBm from a 50- Ω generator, or even less, depending on frequency.

The normal phase-frequency detector outputs come from Q1 and Q2*. (Q2* = Not Q2.) Q2* is shown as Q2 with a bar above it in the schematic shown in Fig 4.40. During phase locked operation, Q1 and Q2 are both low between clock pulses. So, Q2* will be high. When Q1 and Q2* voltages are analog added with an op-amp, the result is a signal at half of the digital supply. Even when both make transitions together, the net result is the same as the resting state so long as there is no phase difference. This balance helps to suppress spurious pulses from the detector. This detector suffers from gain that drops with zero phase difference. More refined phase-frequency detectors use logic schemes that generate a gain that is constant at all phase differences.

The phase frequency detector output is sampled data. A sample occurs once per cycle and then disappears. The averaged dc component is extracted and applied to the op-amp that follows. The primary function of the loop filter is to attenuate the high frequency part of these pulses. In contrast, the output of a diode ring phase detector is continuously present, so long as there is sine wave excitation. But when clipping occurs at both inputs, which is common, the data begins to take on sampled characteristics.

A One-on-one Tracking Phase-locked Loop

The PLL scheme becomes more tractable when a mixer is added to the system, shown in Fig 4.42. The frequencies are those used in a practical VFO, a circuit designed for a two-band output. A 14-MHz VCO is mixed with a 12.5-MHz crystal oscillator and the down-converted output is selected with a low pass filter. The result is applied to a phase-frequency detector. The reference for the detector comes from a stable, free running 1.5-MHz oscillator. The detector output is filtered in the "loop filter" with the dc output controlling the VCO.

The most obvious virtue of this system is stability; the VCO has the frequency stability of the two oscillators in the system. The 12.5-MHz oscillator is crystal controlled and quite stable. The free running 1.5-MHz VFO operates at a low frequency

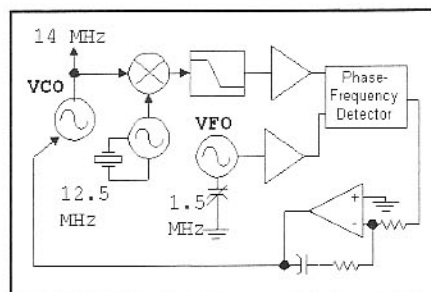


Fig 4.42—A practical one-on-one or offset tracking PLL.

and is also very stable.

Good long-term stability measured over periods of seconds to minutes is but one virtue. Another is short-term stability, the cycle-to-cycle behavior that we have characterized by phase noise content. The noise of the 1.5-MHz reference oscillator is transferred to the VCO within the bandwidth of the phase locked loop. Outside the loop bandwidth, the phase noise is dominated by the intrinsic performance of the VCO.

The astute reader is certainly posing a question at this point: Why a PLL? Why not merely mix the 1.5-MHz VFO with the 12.5-MHz crystal oscillator to directly generate the desired 14-MHz signal? The question is a good one, as is the method. A direct heterodyne approach, which will be discussed in a later chapter, is ideal. However, if the output is to be spectrally clean, the filter at 14 MHz must be a good one. The up-conversion process will generate an image at $12.5 - 1.5 = 11$ MHz. This must be well suppressed. There are other higher order mixing products that can also compromise the performance.

Another virtue is low cost. The LC filter is a relatively expensive circuit. A direct heterodyne system would be even more difficult and expensive if the frequencies were changed to, for example, a 13.5-MHz crystal oscillator and a 0.5-MHz VFO. But, the PLL for the new scheme would be virtually unchanged. Notice in Fig 4.42 that there are no bandpass filters in the system, not even simple ones. A very simple low pass filter picks the down-converted product.

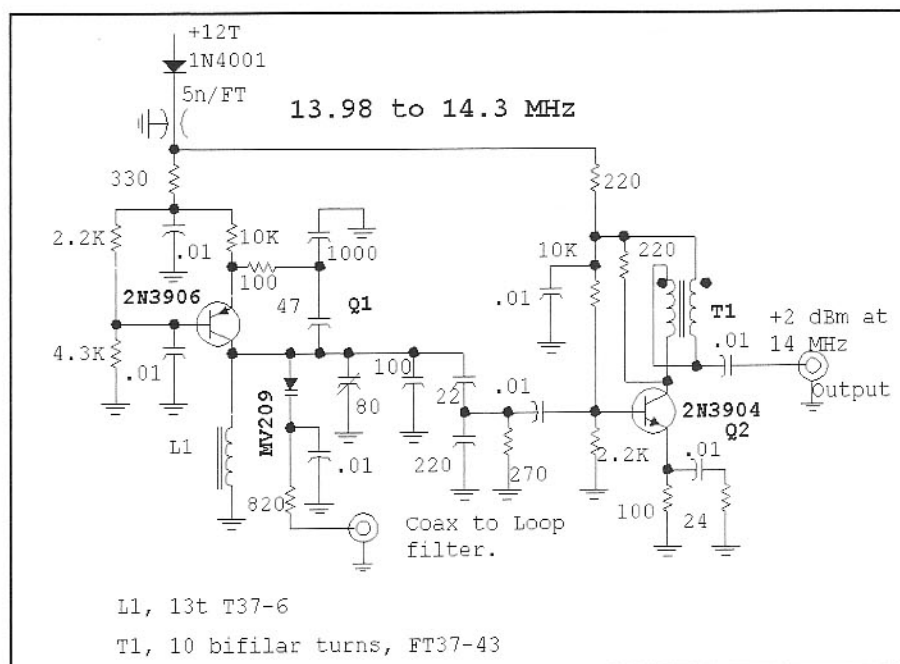


Fig 4.43—VCO for the 14-MHz tracking loop.

The PLL still has filtering properties. A detailed analysis will show that the loop behaves like a single tuned circuit at the VCO frequency with a bandwidth equaling the loop bandwidth. This *tracking filter* moves along with the output, transferring the characteristics of the reference to the VCO output. This filtering characteristic is not available to one building the more conventional heterodyne system.

Schematics are presented for a practical implementation of the system of Fig 4.42, a design we used for a 10-year period. Two output frequency bands were available: 7 to 7.1 and 14 to 14.2 MHz. The 14-MHz output was also frequency doubled to produce a 28-MHz signal. The basic circuit is a 14-MHz PLL, but the output is digitally divided to produce the 7-MHz component.

The 14-MHz VCO is shown in Fig 4.43. A 2N3906 PNP (Q1) oscillator is tuned with a MV209 abrupt junction varactor diode. The grounded collector facilitates diode biasing. The emitter current in the

PNP guarantees an operating level that never forward biases the tuning diode. A buffer increases the output to +2 dBm. There are no large bypass capacitors within the shielded VCO, for the +12-V supply is keyed.

The VCO output drives a passive power splitter where the two applications are isolated, shown in Fig 4.44. One path routes 14-MHz energy to Q3 where it is amplified to a 2.5-V pk-pk level to serve as the LO for Q4, a dual gate MOSFET mixer. The 12.5-MHz signal is generated with Q5. The level reaching the mixer is adjusted to prevent overdriving the mixer. The mixer output is filtered in a 1.7-MHz low pass filter.

The other splitter output is applied to Q6, a stage providing 14-MHz output. Some energy is "stolen" at the emitter to drive Q7 and U1, a D-flip-flop operating as a divider. The resulting square wave is further buffered in Q8 and is low pass filtered to produce a clean 7-MHz signal. The low

pass is a peaked (ultra-spherical) design, offering greater than normal harmonic attenuation. A band-switch selects the appropriate output. Even though the 7-MHz circuitry continues to operate when the 14-MHz band is in use, the 40-meter output is still 70 dB below the desired output. The 0-dBm output was used to drive a two stage, 1-W power amplifier. This was low pass filtered and used on the air for QRP activity, or applied to a FET power amplifier for more aggressive efforts.

The 1.5-MHz output from Fig 4.44 is applied to the phase frequency detector, shown in Fig 4.45. This then drives a loop filter using a LM301 op-amp. The loop was designed for a 10-kHz loop bandwidth. The reference VFO (not shown) for the phase detector was a JFET Hartley buffered with a MOSFET.

Keying and timing details, although not shown, are critical in this system. The VCO was keyed with a "+12T" voltage that started as soon as the key was pressed.

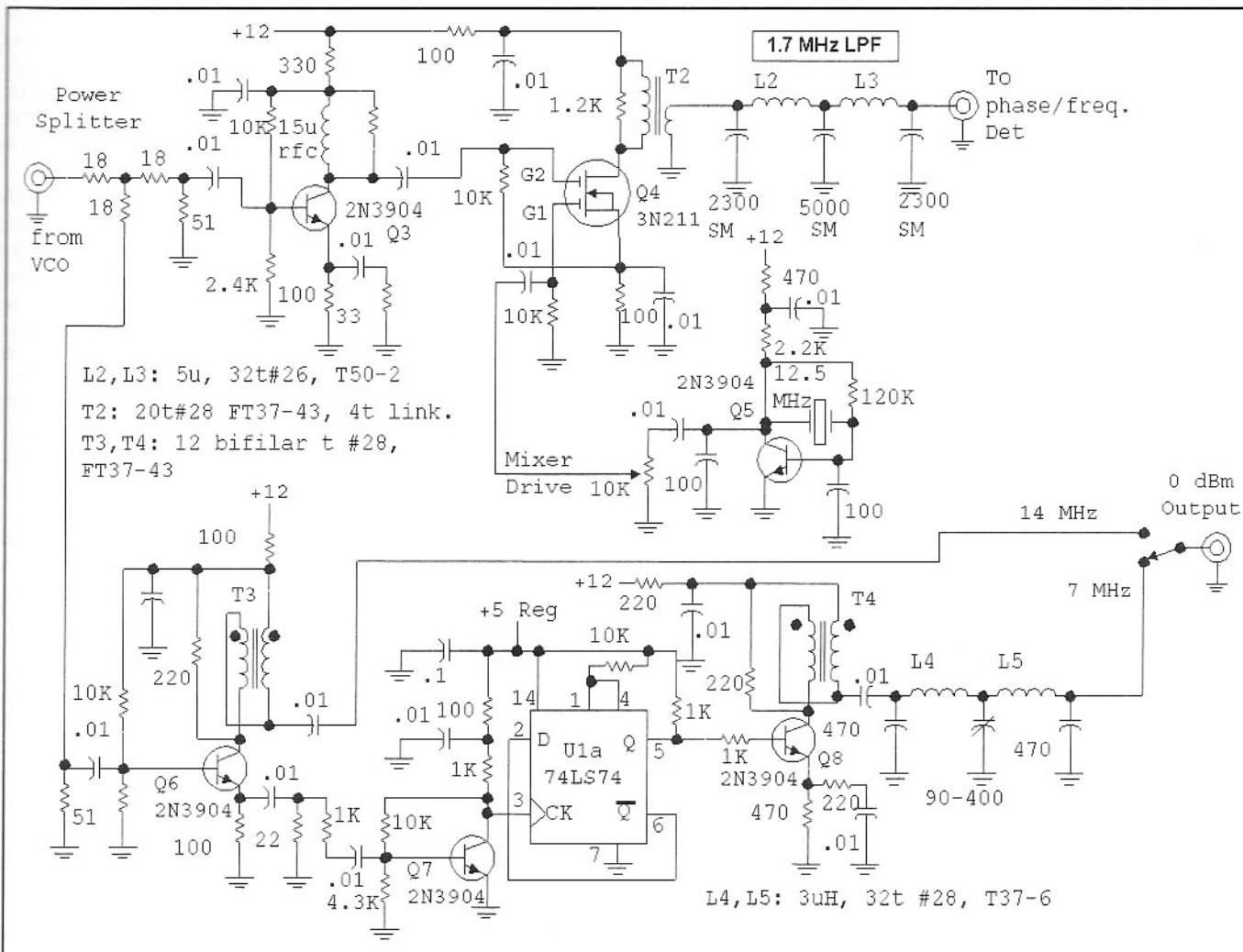


Fig 4.44—Mixer section for the tracking PLL.

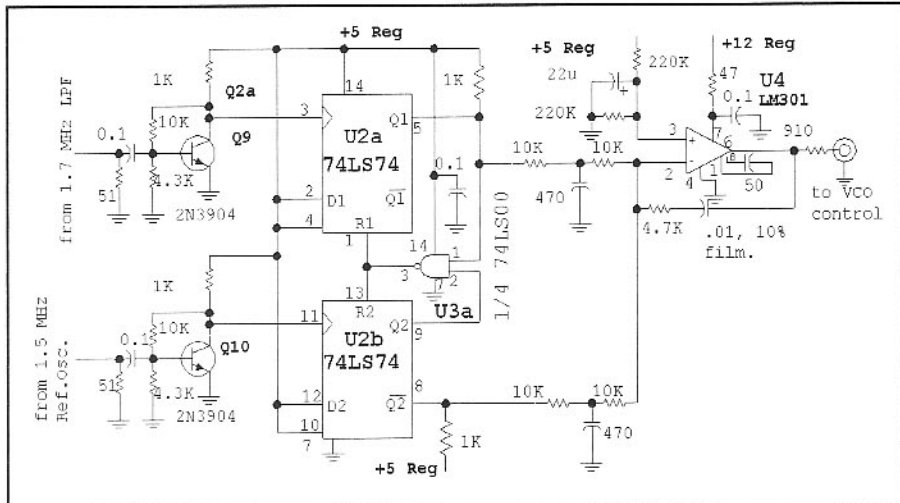
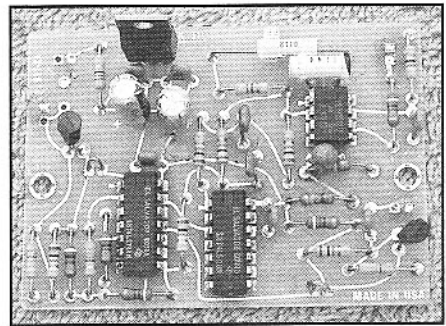


Fig 4.45—Phase-frequency detector and loop filter for the tracking PLL.



Phase-frequency detector using LS-TTL logic. This circuit is shown in Fig 4.45.

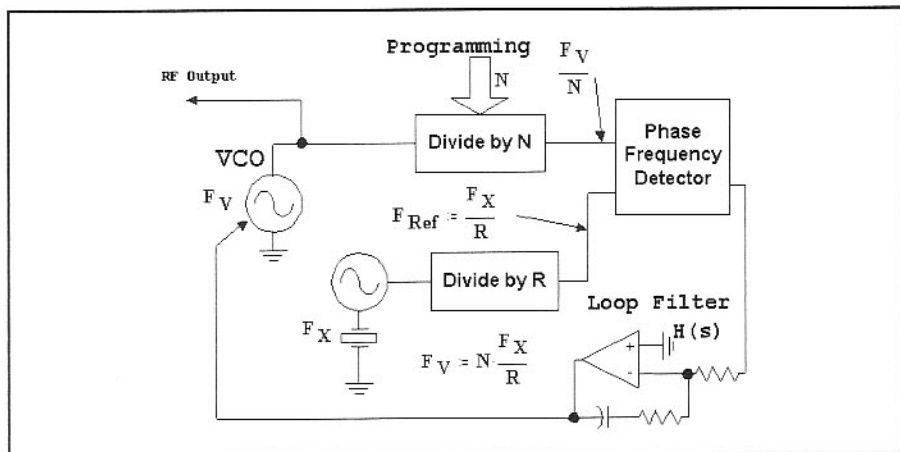


Fig 4.46—A single loop Divide-by-N PLL.

Careful listening and examination with an oscilloscope showed that phase lock was fast and always occurred before a signal was applied to the antenna. A "hold-off" circuit was included that prevented the keying voltage from reaching the power amplifier until the key had been down for 5 milliseconds. This was applied only on initial key closures. VOX-like circuitry then maintained the system in transmit mode (VCO on and T/R relay closed) for half a second or so. This system would be compromised if the VCO locking had not been quick.

A number of changes would be implemented if this system was rebuilt today. The dual-gate mixer would be replaced with a balanced circuit. The op-amp would become an up-to-date alternative, such as the OPA-27. High speed CMOS would replace the LS-TTL used. Finally, the VCO would run continuously without keying, but would operate at a different frequency. This could be 28 or 56 MHz

where direct division would produce the desired outputs.

Divide-by-N Phase Locked Synthesis

The most common scheme for frequency synthesis is the divide-by-N PLL Fig 4.46. A crystal oscillator at F_X is divided by a (usually) fixed integer R , producing a reference signal at the phase frequency detector at F_X/R . The VCO is divided by a programmable integer, N . The divided VCO must also appear at F_X/R , so $F_V = NF_X/R$. Consider an example: We wish to build a synthesizer for the 9 to 9.5-MHz range. We divide a 2-MHz crystal oscillator by $R=200$ to generate a 10-kHz reference. N must be set to 900 to produce a 9-MHz signal. Increasing N causes F_V to increase in 10-kHz steps, reaching 9.5 MHz with $N=950$.

This system would work well as a transceiver local oscillator (LO) in an environ-

ment where signals were spaced at 10-kHz intervals. It would not, as shown, be very useful as a general purpose LO.

Modifications could improve resolution. For example, increasing R to 2000 produces a 1-kHz reference. N ranging from 9000 to 9500 would then cover the desired range in 1-kHz steps. (A means of pulling the 2-MHz crystal oscillator by a mere 222 Hz would then generate all LO frequencies within the desired range.)

Generally, 100-Hz resolution produces understandable SSB while 10-Hz steps yield natural sounding voices. But dividers of 90,000 or 900,000 are impractical, even though they are easily achieved with digital logic.

Consider the 1-kHz step system with $N=9000$ to 9500. The detector reference frequency is 1-kHz, the step value. The loop filtering (plus balance effects) must produce considerable attenuation at 1 kHz. Generally, a system with a 1-kHz step would use a loop bandwidth of 100 Hz or less. The dc from the loop filter includes a small 1-kHz component that frequency modulates the VCO carrier at 1 kHz. The spectrum is a carrier with 1-kHz sidebands. These would be transmitted if the LO was part of a transmitter. If part of a receiver, the contaminated LO would cause a strong signal to be received in a couple of extra frequencies, albeit at reduced strength.

Timing problems occur when N is incremented to tune such a synthesizer. While the N change is instantaneous, the result is not. A filter with 100-Hz bandwidth is capable of change in a time commensurate with $1/B$ where B is the loop bandwidth, here 10 milliseconds. The effect can be a "chirpy" sound with tuning.

There is yet another problem, a degradation in phase noise. The PLL with a division-by-N is a frequency multiplier. Assume, for example, that 1-Hz changes the reference at the detector. With $N=9000$, that 1-Hz shift becomes a 9-kHz

shift in the VCO. If we think of the 1-Hz reference shift as a noise, the result after frequency multiplication by N is a noise increase by $20\log(N)$ dB, 79 dB for this case. Clearly, PLL synthesizers with large N should be avoided.

PLL synthesizers are still practical. With large frequency steps, perhaps 10 kHz or more, tuning seems instantaneous while keeping reference sidebands well suppressed. Gaps between steps can be filled in with schemes using additional PLLs. VCO tuning of the reference, or direct digital synthesis—a method that we will discuss later.

Numerous schemes are available for programmable frequency division, limited by the experience of the designers. One is shown in Fig 4.47. The incoming signal is digitized and applied to the down counting clock input of an Up/Down counter, a 74HC193. The state of the counter decrements by 1 with each clock pulse. When it reaches 0, the “borrow” line goes low. This is fed to the data input of a D-FF. When the Q of that part goes low, the “load” command on the ‘193 is executed, causing the data on the “jam” inputs, J_A to J_D, to be

loaded in the counter, beginning the cycle anew. This overall circuit will divide by the number loaded at J_A to J_D (0 to 15) plus 2. Several 74HC193s can be cascaded to realize large divisors. The 74HC74 forces the output to be synchronous with the input clock.

Many PLL frequency synthesizers use a prescaler, a divider that divides by a fixed amount before reaching programmable circuitry. This reduces the complexity of the programmable parts, but has the disadvantage of multiplying the synthesizer step size by the pre-scale value.

This difficulty is eliminated with a variable modulus prescaler, a chip that divides by one of two different values, depending on the status of a control pin. For example, the Motorola MC12015 is a divide by 32/33; it divides the incoming frequency by either 32 or 33. Extra circuitry is required in the programmable part of the synthesizer to accommodate prescaler programming, but the programmable circuitry is relatively slow, easing design and reducing power.

Numerous commercially manufactured LSI (large-scale integration) chips are

available for phase locked loops. One example is the Motorola MC145170, which includes programmable N and R dividers, phase-frequency detector, crystal oscillator, and digital control and memory circuits.¹⁶ This IC functions up to 160 MHz, receiving instructions as a 16-bit serial word. While the use of a this chip simplifies a synthesizer, it often means that a microprocessor or computer must be present in equipment using such a synthesizer. The MC145170 and the National LMX1501A are used in a synthesizer on the book CD, the DSP-10 transceiver.

The frequency multiplication and the resulting phase noise degradation between the reference and the VCO is a fundamental property of a divide-by-N synthesizer that cannot be avoided with “improved” design. For this reason, it is becoming common for manufacturers of PLL integrated circuits to specify the phase noise of their ICs at the phase detector. Spectral noise density in the -160 dBc/Hz region is common. The final system design is then degraded by $20\log(N)$. It will be even worse if other noise sources come into play, such as a poor VCO.

A VXO Extending Synthesizer

A simple PLL synthesizer with a single loop can be used in conjunction with a VXO for numerous special applications. This could be a divide-by-N design like that of Fig 4.46, or a modified design that includes a mixer, shown in Fig 4.48. The crystal oscillator (VXO) now serves as the LO for a mixer and as a divided programmable clock for the phase detector. The step size is no longer uniform, a consequence of the variable reference divider. However, the scheme is capable of producing very small steps with a relatively high reference frequency.

Consider an example: A 6.892-MHz oscillator is placed in the circuit of Fig 4.48 with N ranging from 32 to 64. Some (but not all) output frequencies, step sizes, and reference frequencies are given in Table 4.1.

The reference frequency varies according to the crystal frequency divided by N while the step size varies with F_X/N^2 . Con-

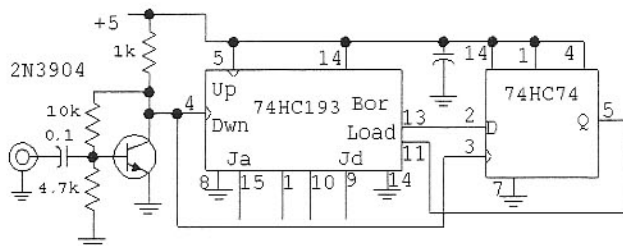


Fig 4.47—A simple programmable divider. See text.

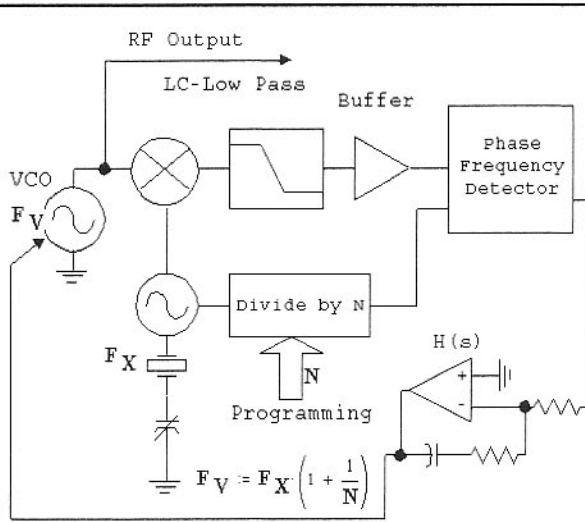


Fig 4.48—A simple PLL synthesizer featuring frequency steps much smaller than the reference frequency.

Table 4.1

N	VCO Output	Step Size	Ref. Freq.
32	7107.7 kHz	6.5 kHz	215.4 kHz
33	7101.2	6.3	208.9
63	7001.7	1.74	109.4
64	7000.0	1.68	107.7

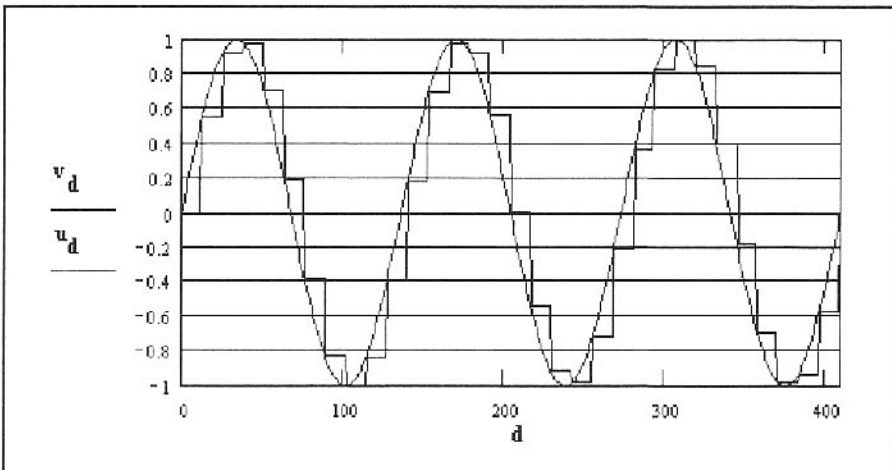


Fig 4.49—A sine wave is generated in DDS with a stepped approximation. Both the stepped, or “sampled” waveform and the desired sine wave result are shown.

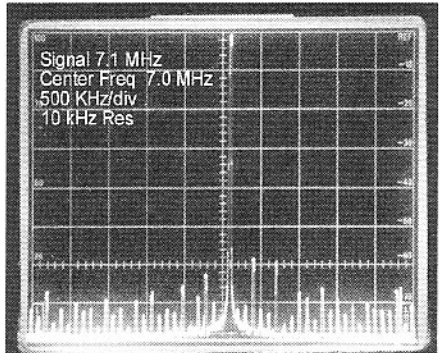


Fig 4.50—Measured output of a direct digital synthesizer using the Analog Devices 9831. Measurements were performed with a Tektronix 494A spectrum analyzer set for a center frequency of 7.0 MHz. The signal is at 7.1 MHz. This DDS device uses a 10-bit D-to-A converter and the manufacturer reports similar spurious responses.

verting the crystal oscillator to a VCO fills the gaps. When this is done, it may not be necessary to use all possible N numbers. Synthesizers of this kind are useful as a means of extending the range of a VCO to cover a larger band. However, they are best used with an independent frequency counter that provides readout. A practical project using this scheme is given elsewhere in this chapter. A practical, general-purpose counter is also presented.¹⁷

Direct Digital Synthesis

DDS, or *direct digital synthesis* is very powerful and is easily implemented with special, large-scale integrated circuits. The concept is deceptively simple: Digital approximations to values for a synthesized sine wave are calculated or looked-up from memory. These values are loaded into a digital-to-analog converter (DAC) with a new value being periodically generated after a fixed sample time.

A typical DDS IC might be clocked with a 40-MHz crystal oscillator. This signal serves as a clock for updating the output with a new sample that will persist for 25 nanoseconds (1/40 MHz) until the next update arrives. To illustrate the operation, assume we want to generate a 3-MHz sine wave with a 1 V amplitude. This is given as

$$V = \sin(2 \times \pi \times f \times t) \quad f = 3 \text{ MHz}$$

Eq 4.4

At time zero, the desired, output sine wave will have zero amplitude. But 25 nS later, it will have an amplitude calculated by inserting 25 nS into the equation, 0.454 V. At 50 nS, the signal will be 0.809 V, and so forth.

One could plot these values against n to obtain the usual sine wave. However, this is *not* what you would see when examining the DAC with a high-speed oscilloscope. Rather, you would see a line that is flat and level for 25 nS. It would then jump almost instantaneously to 454 millivolts and remain there for another 25 nS. At 50 nS it would jump to 0.809 V, and so on. This behavior is shown in Fig 4.49 where a sine wave is sampled about 10.7 times per cycle.

If we had used an even 10 samples for each cycle of the sine wave being generated, the lowest frequency in the overall signal would be that of the output. The only distortion would be harmonics. Consider a slightly different case, one where we use 10.333 samples for each cycle of the final oscillation. Three cycles of the output waveform would then be generated with 31 samples. There is a longer periodic character to the overall waveform that would create spurious outputs at one-third the output frequency. All harmonics of the low frequency are also available. The spurs become more numerous as the periods become longer.

Fig 4.50 shows the measured output of an Analog Devices AD-9831 residing on a demo-board from Analog Devices. The part used a 25-MHz clock. An output of

7.1 MHz was synthesized for this example, producing spurious outputs over a wide spectrum. Other examples produced spurs confined to limited regions. There are even some “sweet spots,” output frequencies that are virtually free of spurs!

Limited DAC accuracy is a common reason given to explain spurs in a DDS synthesizer. While this is usually dominant, it is not the only source of spurs. The analysis presented above assumed a perfect DAC and still generated spurs. The very stair-step waveform of Fig 4.49 is an approximation to a more ideal sampling waveform reconstruction.¹⁸

The wideband phase noise in the output of a DDS synthesizer is often very low, comparable with the best Divide-by-N PLL systems. However, this is of little consequence if the noise is merely replaced by a family of coherent spurious responses.

Most current commercial transceivers use a combination of PLL and DDS technology. Unfortunately, it is very difficult to gain even a basic understanding of these systems from the sketchy manuals. Rohde described an excellent example of a dual technology synthesizer.¹⁹ That design used DDS to generate a 10.7-MHz signal that was tunable in small steps. The result was bandpass filtered with a 10-kHz wide crystal filter and then frequency divided to 100 kHz where it served as the reference for a PLL controlling a 75 to 105-MHz VCO.

4.8 THE UGLY WEEKENDER, MK-II, A 7-MHZ VFO TRANSMITTER

The "Ugly Weekender" is a viable project for both the beginner and the seasoned builder. The major feature, and the source of the name, is the construction method outlined in Chapter 1. This section describes a version of that transmitter that uses frequency doubling to achieve improved oscillator isolation.

The transmitter (**Fig 4.51**) begins with a 3.5-MHz variable frequency oscillator. The familiar Hartley topology is used, although others would work as well. The oscillator, Q1, runs continuously to avoid repeated warm-up drift, oscillating a few kHz above the normal frequency, but is shifted to the desired frequency during transmit intervals. The VFO is temperature compensated with a combination of NP0 and polystyrene capacitors in the 3.5-MHz tank circuit. The combination was picked and confirmed with repeated temperature runs in a home-built environmental chamber.

The VFO is buffered with a keyed dual-gate MOSFET amplifier, Q2. A JFET source follower driving a feedback amplifier would also provide the needed 10-milliwatt output needed to drive the frequency doubler.

The 2X-frequency multiplication occurs with a pair of diodes, as discussed in greater detail in Chapter 5. The doubler output is selected with a single tuned circuit. A 10% bandwidth double tuned circuit would be a better choice in this position. The power lost in the passive frequency multiplication is regained with a buffer amplifier using Q6 and Q7.

The 7-MHz output from Q7 is applied to a $500\text{-}\Omega$ drive control with output to a keyed feedback amplifier, Q8, shown in Fig 4.52. The keying voltage is derived from Q4, an integrating waveform shaping circuit.

A feed-through capacitor in the two box version of this circuit routes the Q4 collector

tor voltage between modules. This component was eliminated in the single compartment version.

The output power amplifier, Q9, an ever-reliable 2N3866 with a small heat sink, is shown in Fig 4.52. Numerous other



Outside view of "Ugly Weekender" transmitters for 7 (left) and 3.5 MHz.

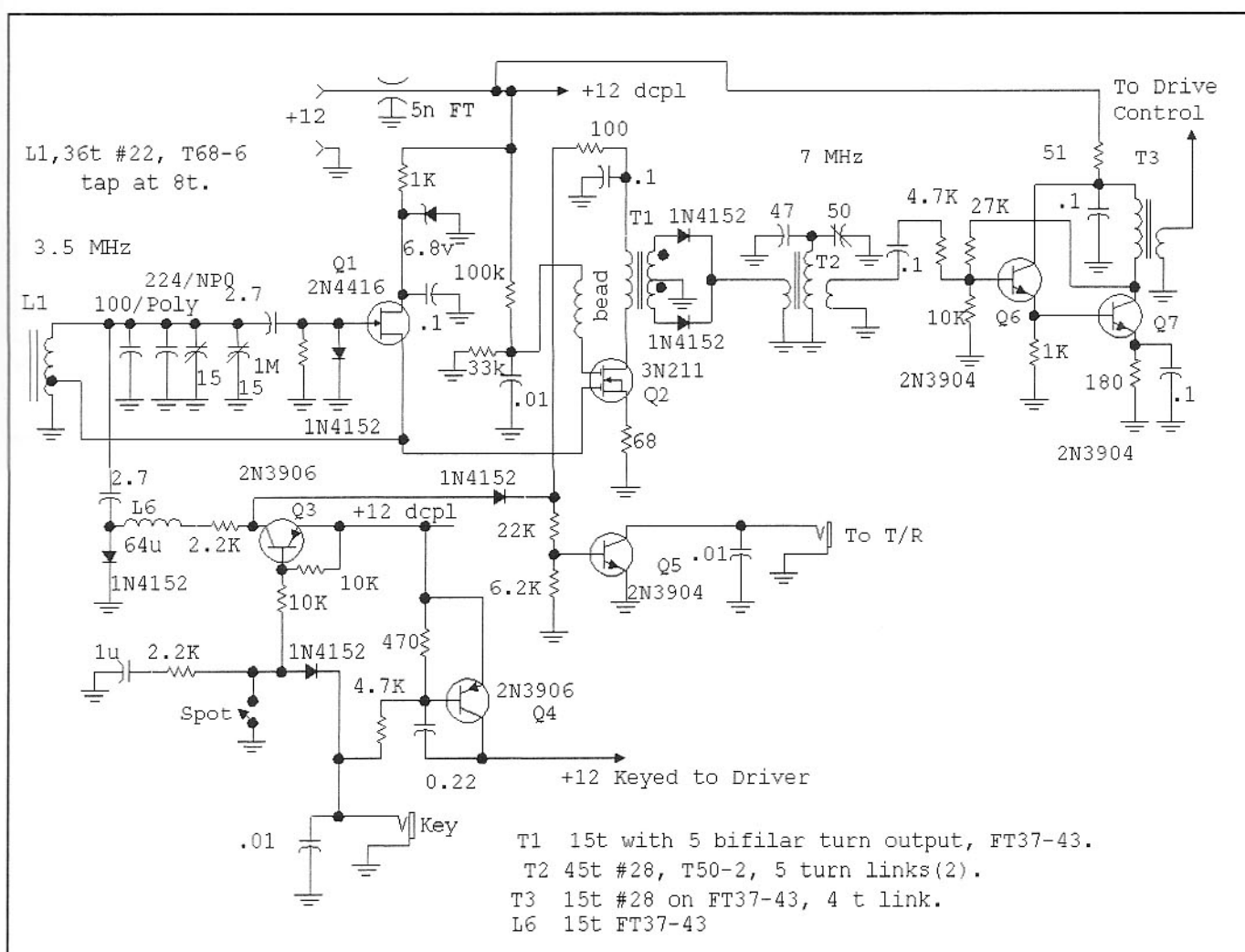
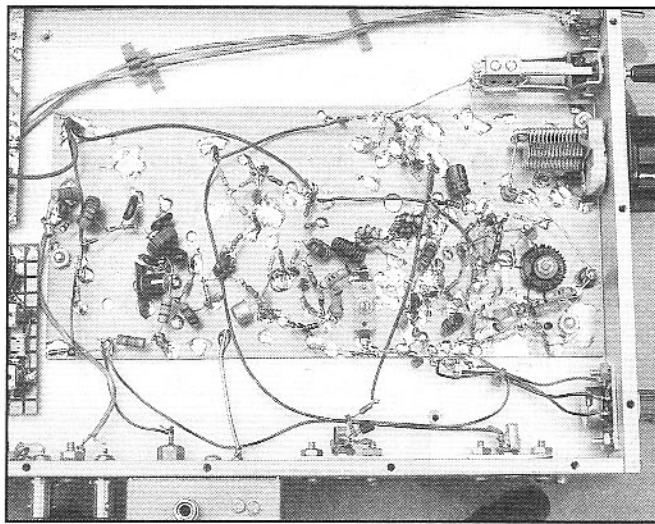
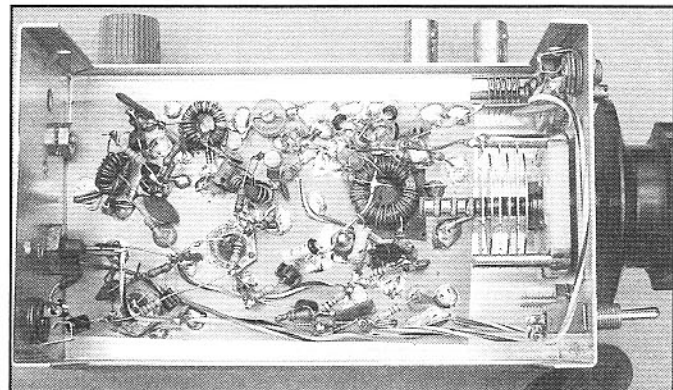


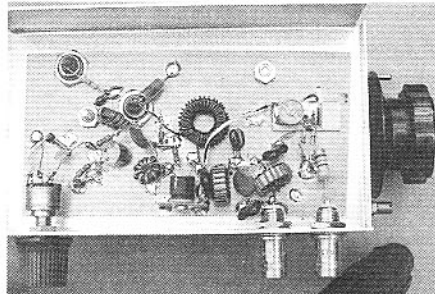
Fig 4.51—VFO and frequency multiplier for the Mk II Ugly Weekender.



Inside view of a single board version of the 7-MHz transmitter. A receiving converter is at the rear (left) of the box.



The VFO portion of the transmitter, including diode frequency doubler.



The power amplifier for the 7-MHz version.

parts will function in this position with circuit details discussed in Chapter 2. Output power is just over two watts with the drive control at maximum. A T/R system is included for QRP applications.

Q5 is a transistor switch that generates a grounded line when the key is pressed. This signal is timed to hold for a short period after the key is opened to control an electronic transmit-receive switch with a 100-W power amplifier sometimes used with this exciter.

A Digital Dial

The frequency counters we see in the amateur literature are either general-purpose test instruments or special designs, intended as a readout for a receiver or transceiver. This unit falls into the later category, but it could be expanded to serve general applications.

We wanted this design to use standard parts. Excellent special purpose counter chips are available, but they are often expensive and difficult to find. Micro-processors, such as the popular PIC and Basic Stamp Series, can be configured as counters, while serving all related display chores. But a

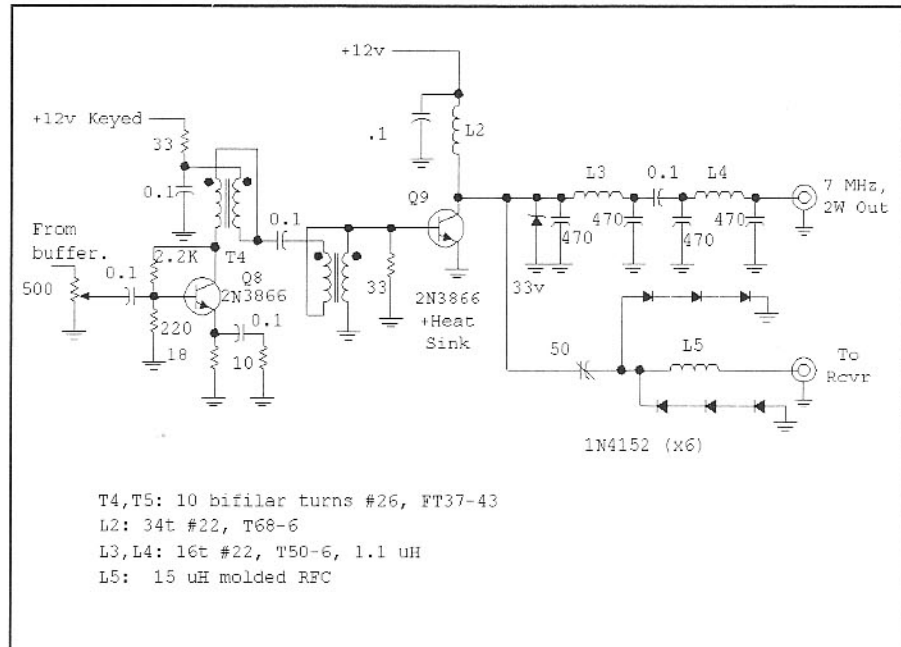


Fig 4.52—Driver and power amplifier portion of the Mk II Ugly Weekender.

simpler solution was sought, one that was usable without special programming skills.

This circuit uses a small number of readily available, inexpensive integrated circuits, including the four-LED displays. The design was intended to be cheap enough for repetitive use in a variety of projects. The approximate \$10 parts cost included the time base crystal, but did not include a PC board.²⁰

This counter avoids multiplex methods, which are prone to RF noise generation. Frequency resolution is 100 Hz.

Figure 4.53 shows a functional block diagram for the frequency counter. Signals to be counted are applied to a single

transistor conditioner that drives a gate controlled by the counter time base. For 100 Hz resolution, the gate must be “open” for 10 milliseconds. However, this design has an extra divide-by-10 to suppress last digit flicker, so a 100-mS count window is used. After the counting is finished and the gate is closed, a “strobe” signal is applied to ICs that remember the counted result and decode it to a format suitable to drive the 7-segment light emitting diode displays. This is followed by a pulse that resets the counters to zero, ready for the next cycle.

The time base, shown in **Fig 4.54**, begins with a crystal controlled bipolar tran-

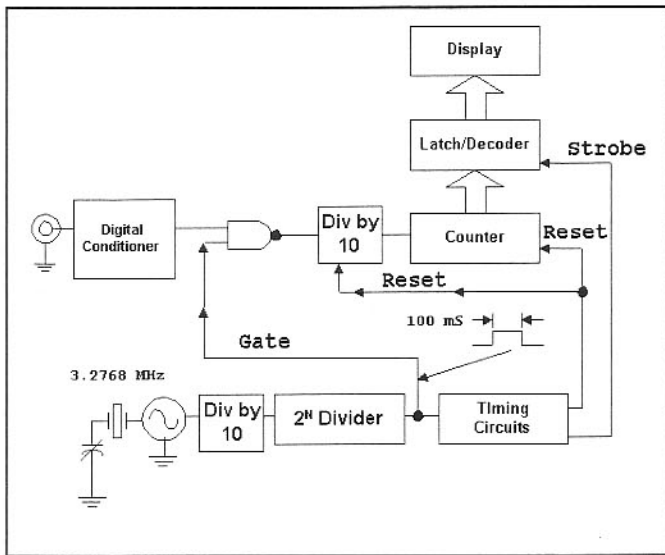
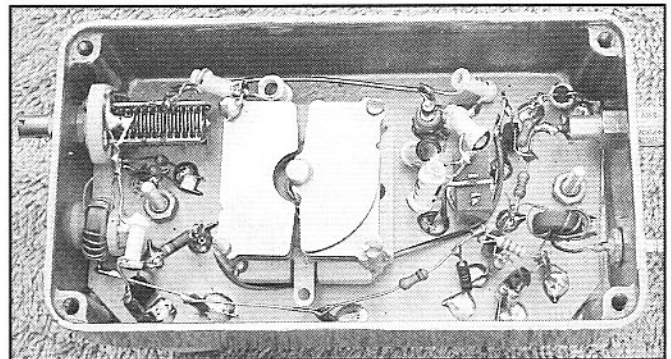


Fig 4.53—Block diagram for counter.



A clean way to fabricate an LC oscillator uses a Hammond 1590B box, offering excellent shielding. DC enters through a feedthrough capacitor and RF leaves on coaxial cable. This oscillator used a differential capacitor, but only one side is connected.

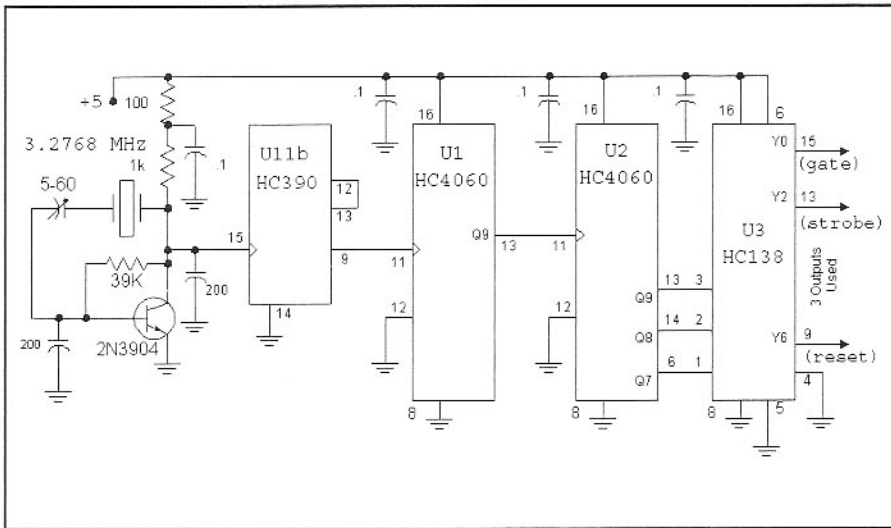


Fig 4.54—Time base portion of frequency counter.

sistor oscillator operating at 3.2768 MHz. The crystal is a readily available, off-the-shelf part. The oscillator is divided by 2^{15} in U1 and U2, a pair of 74HC4060 “timer” ICs, resulting in the desired 100-millisecond gate window. Further division in U2 provides a chain of additional 100-mS windows. These are decoded in U3 to generate strobe and reset pulses.

The rest of the counter is shown in Fig. 4.55. The signal to be counted is condi-

tioned with Q1 with the resulting logic applied to U4A, part of a quad NAND gate with other sections serving as inverters. The output is then counted by U11a, U5, and U6, 74HC390 dual decade counters. These drive the decoder drivers, U7 through U10, using 4511B decoder-driver ICs. This configuration will display kHz to the left of a decimal place and tenths of a kHz to the right of the decimal place.

We have used ICs from two families in

this design. Most of the system uses “HC” high-speed CMOS parts. This allows the circuit to function to 50 MHz or beyond. However, there is no need for high speed in the display function, so the decoder drivers use the slower standard CMOS parts. Using slower parts here should help to minimize RF noise and current consumption. We used common cathode, seven segment LEDs, type MAN4740.

Early versions of this counter used only two digits of display, showing only 0 to 99 kHz. While this worked well as a digital substitute for a mechanical dial, it became frustrating in some applications. We found ourselves wanting more resolution, including a digit to the right of the kHz decimal place. A more complete display with digits to the left allows complete elimination of mechanical dials in many systems. The lower current two-digit format is available by eliminating the related 4511 drivers and LEDs in the design presented.

Total current depends upon the digits being displayed. With 5-MHz input signals, current was about 80 mA when the display read “888.8”, dropping to 30 mA with “111.1.” The sensitivity was excellent with a 5-MHz input, counting reliably with an input of less than –40 dBm from a 50- Ω generator. The counter continues to function to over 50 MHz, but requiring higher RF drive power.

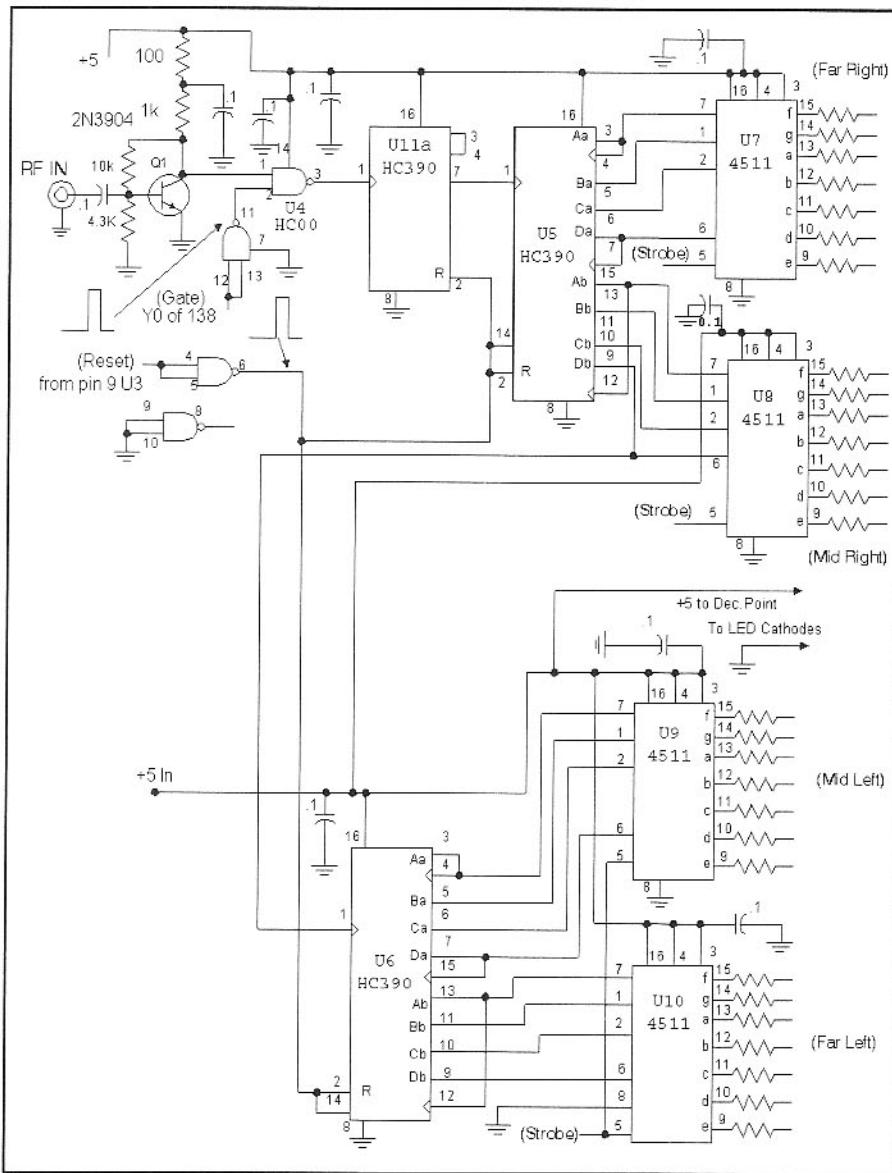
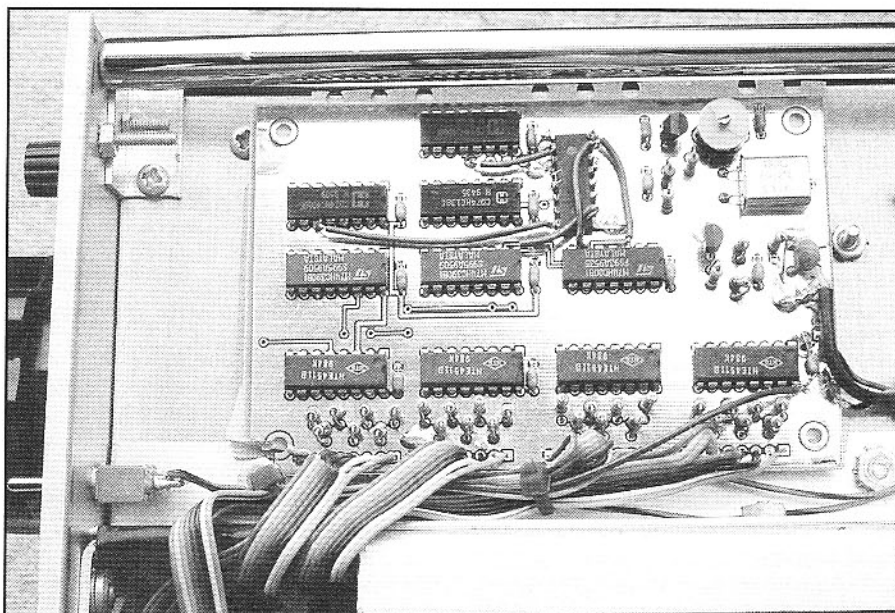


Fig 4.55—Input circuit, counter detail, and display portion of frequency counter.



Frequency counter installed in a receiver. U11 was added "dead bug style" to eliminate flicker.

4.9 REGARDING COUNTER ACCURACY

The simple counter described above is capable of good accuracy so long as the crystal and the oscillator components are stable. The capacitor in series with the crystal should be adjusted to produce the proper count when a known frequency is applied to the counter input.

The counter as shown is suitable for use with simple direct conversion transceivers or superhet systems where the intermediate frequency is an even multiple of 100 kHz. The “dial” then functions accurately when the LO alone is counted, except for the left most digit. If a “less friendly” IF is used, other schemes must be applied. The usual transceiver might have several intermediate frequencies, all of them with uneven values. The corresponding oscillators, including BFOs or carrier oscillators, could all be counted. A mixture of up and down counting might be required with the various oscillators, depending upon the way the final frequency is calculated or

measured. Clearly, this would be a good application for a microprocessor.

A simple counter that would still be accurate over a wide frequency range could be built with circuitry much like that in Fig 4.55, even if the IF is “unfriendly.” The simple up counters would be replaced with presetable up-down counters. Instead of resetting the counters to zero at the end of each cycle, the counter would be *loaded* with an appropriate digital word that causes the LO counting to produce the right readout.

It is possible in some applications to obtain reasonable results over a narrow tuning range merely by changing the crystal frequency. This counter uses a clock oscillator of 3276.8 kHz. That value is divided by a fixed value to produce a time window that drives the counting gate. The final count is the number of cycles that pass through the gate during the time interval. The display is a number that is a constant multiplied by the ratio of the two

frequencies. If the crystal frequency is changed, the “dial” can still be exactly right for one frequency. It might not be too far off at others that are close.

Consider an example, a 7-MHz transceiver using a crystal filter at 1.98 MHz. The VFO will then be tuned to 5.02 MHz when the transceiver is at 7.000 MHz. Using the counter with the standard 3.2768-MHz crystal would produce a count of “20.0” instead of the desired “00.0.” If the clock crystal was changed to 3.2899 MHz, a 13.1-kHz difference, the count would be proper at 7 MHz. The error at 7.1 MHz would be 0.4 kHz. This may be tolerable for some applications.

There are several options available to the builder wanting to use a microprocessor controlled counter. Simple units are available in kit form, ready for installation in QRP rigs and the like, with references found on the web. Some examples are also included on the book CD.²¹

4.10 A GENERAL PURPOSE VXO-EXTENDING FREQUENCY SYNTHESIZER

Fig 4.56 shows the block diagram for a unique frequency synthesizer. Although this example was built for 14 MHz using an off-the-shelf TV color-burst crystal in the VXO at 14.318 MHz, the system can be adapted for many other applications. VHF examples are given later. This example used the VXO design presented in Fig 4.30. The VCO used with the synthesizer is that of Fig 4.34, which can be scaled to other frequencies.

We only discuss the synthesizer circuits in detail here. The VCO provides the needed output. It will usually be split in a hybrid with one component used in an intended output while the other drives the synthesis circuitry. A level of -6 dBm is needed by the synthesizer at both the VCO and the VXO inputs.

The programmable frequency divider is a version of the circuit shown in Fig 4.47 using two 74HC193 chips, allowing division by up to 258. The detailed circuit is shown in Figs 4.57 and 4.57A. The division ratio is derived from two more 74HC193 chips, now operated as an up-down counter. Pulses to the “up” or the “down” inputs increment or decrement the frequency by one step. The user must establish the division range, controlled by four hard wired points below U2, marked

A, B, C, and D in Fig 4.57. The four inputs are connected to logic 0 (ground), logic 1 (+5 V), or to the outputs from U4. Some possible variations are shown in Table 4.2.

The frequency determining up-down counter, U3 and U4, may also be loaded with an often-used setting, such as a recognized calling frequency. Each line must

be hard-wired by the user to establish this frequency.

The Up/Down commands are buffered with U6. Grounding an input line (P9 or P10) will cause an up or down pulse to appear at U3. A ground command on J8 also causes the “calling frequency” to be loaded. The user may wish to add more

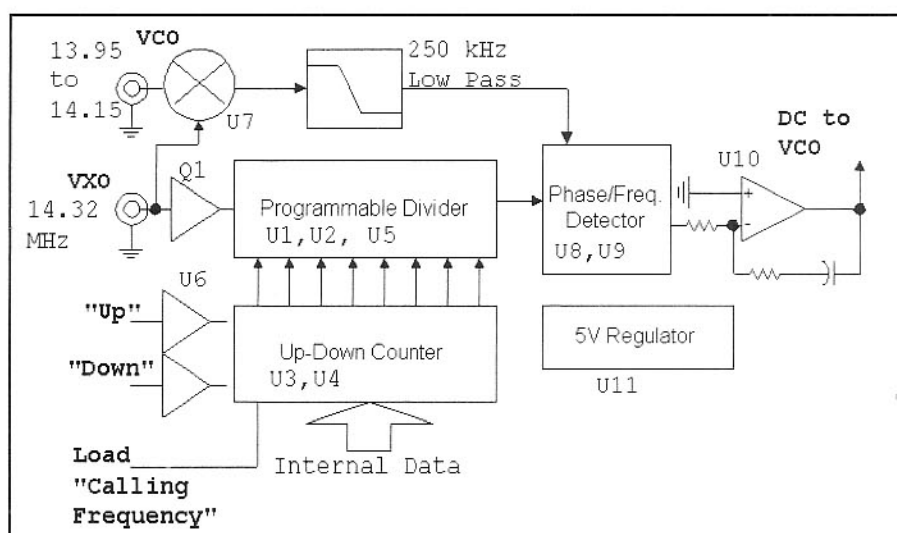


Fig 4.56—Block diagram for the VXO extending synthesizer.

Table 4.2

Available States	A	B	C	D
2 to 258	U4	U4	U4	U4
2 to 130	U4	U4	U4	0
66 to 130	U4	U4	1	0
34 to 66	U4	1	0	0

interface circuitry to the Up/Down lines; standard CW keyer circuits work well, as does a keyer paddle or an computer mouse as an input device.

The VXO and VCO are both applied to mixer U7, an NE-612. The low frequency output is low pass filtered and impedance transformed with a pi-network using L1. In the example, a 200-kHz signal is transformed from $1.5\text{ k}\Omega$ to $500\ \Omega$ with the pi network formed by L1, C18, and C19. The $600\text{-}\mu\text{H}$ inductor consists of 22 turns #26 on a FB43-6301 ferrite bead. The low pass filter components will change with other applications. The low pass filter output is amplified and conditioned for digital lev-

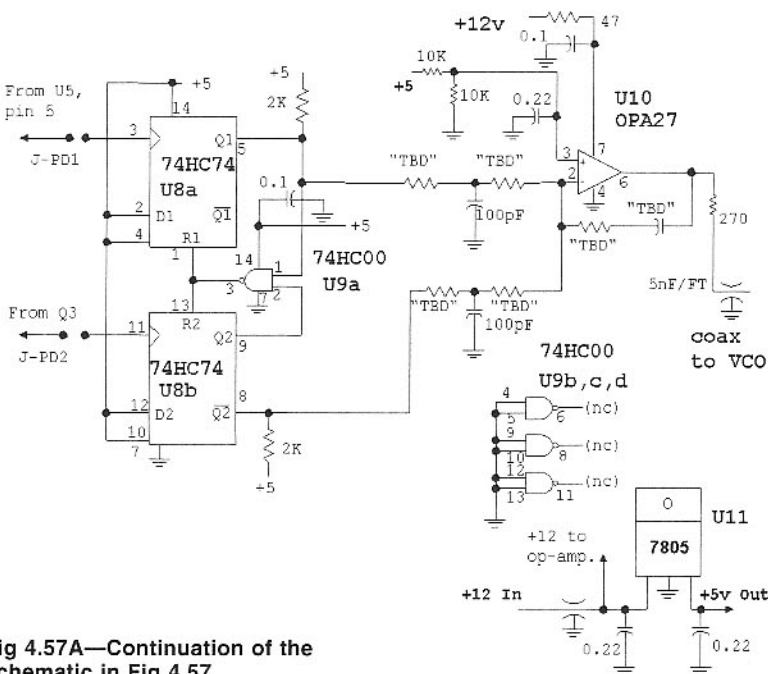


Fig 4.57A—Continuation of the schematic in Fig 4.57.

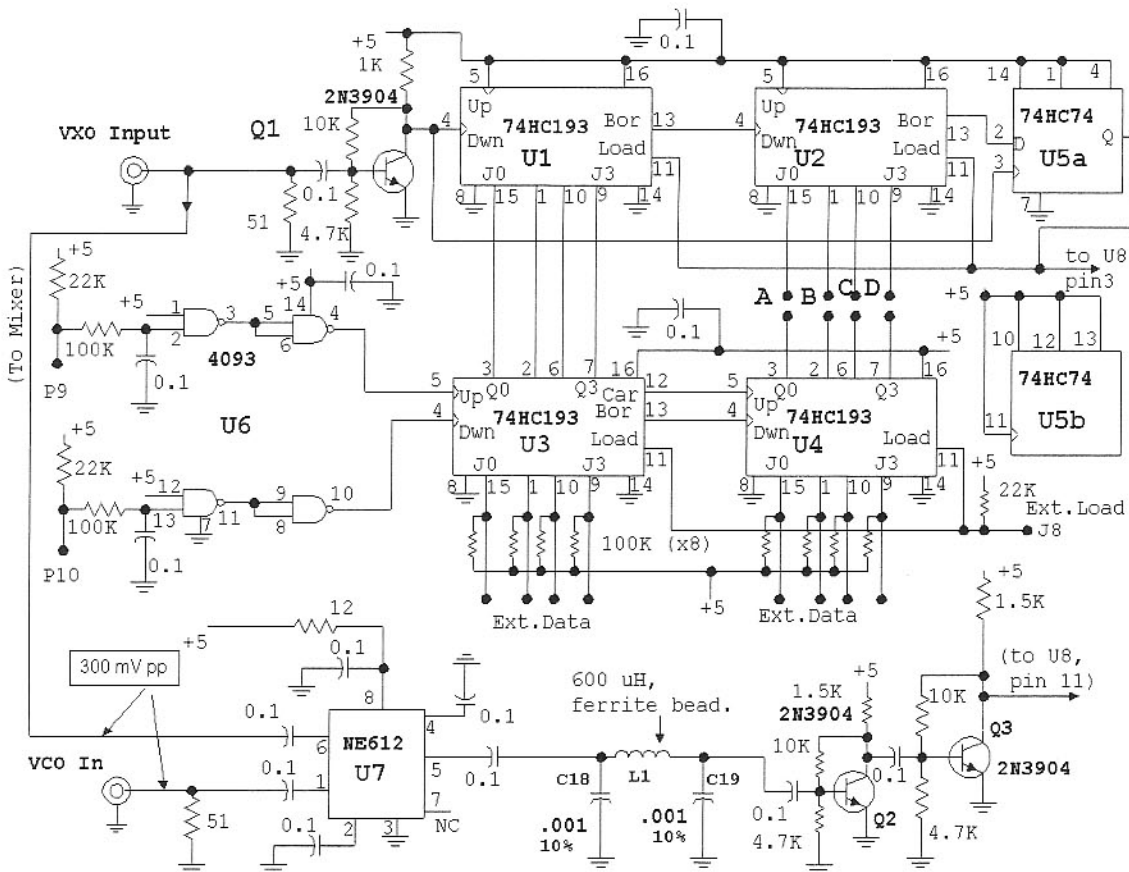


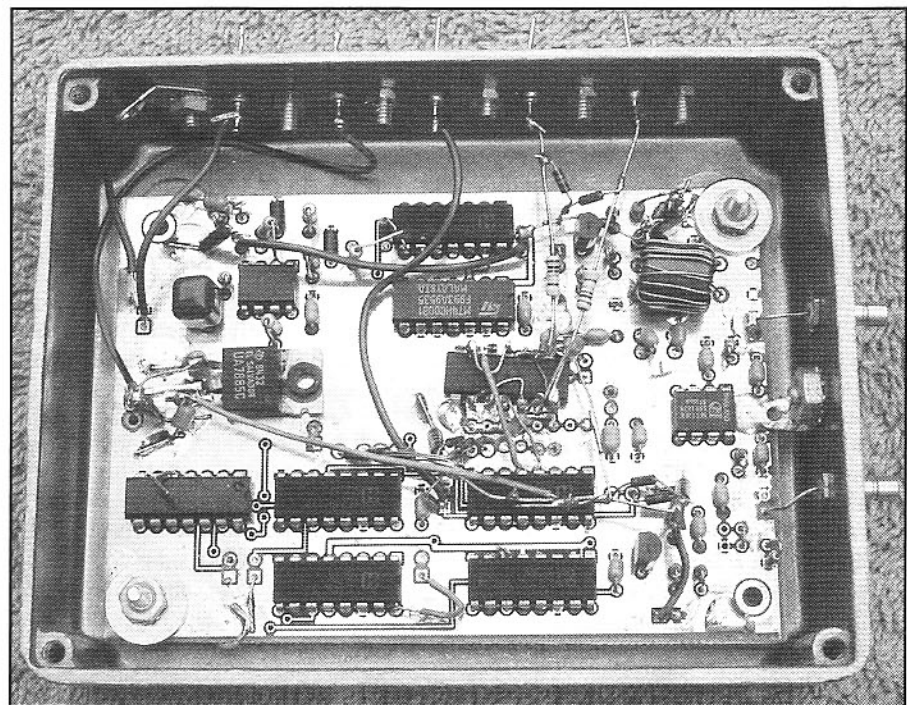
Fig 4.57—Schematic for the experimental synthesizer. See text for details.

els with Q2 and Q3.

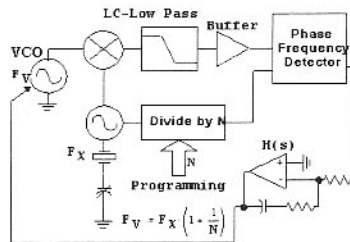
Two programmable jumpers are provided at J-PD1 and J-PD2. While pin 3 of U8 is normally driven from U5 in applications with the crystal below the VCO frequency, it may change to drive from Q3 in other systems. The frequency scheme shown has the crystal above the VCO. A VCO tuning polarity may also require a change.

The loop filter uses a premium op-amp, the OPA-27. This fast, low noise part is ideal for this application. The four input resistors are all 47 k Ω while the feedback elements are 10 k Ω and 1.0 μF for the 14-MHz example. All of these components are subject to change with other applications and are marked TBD in the schematic for "to be determined." They are picked with the PLL computer program that accompanies *Introduction to Radio Frequency Design*. Phase lock loops must be designed with some care and component values are *not* well suited to casual selection.

The 14-MHz version of this design is summarized in the equation sheet of Fig 4.58. The programming sets N for values from 34 to 66 with some frequencies listed in the table. The design equations use a



Frequency synthesizer installed in a Hammond 1590BB box. Coaxial inputs are from the VCO and reference VXO. All input/output lines are attached to feedthrough capacitors.



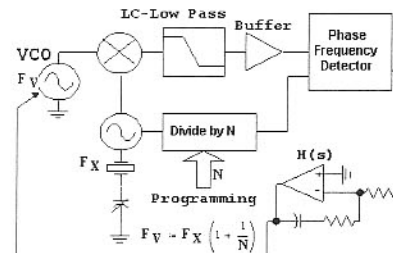
For this variation, we will start with an existing, available rock. Also, for this variation, we will use a crystal that is ABOVE the output. This changes the equation.

$$N = 40, 48, \dots, 130 \quad X = 14325 \quad (\text{VCO freq}) \quad \delta = 10 \quad (\text{VCO range})$$

$$F(N) = \left(1 - \frac{1}{N}\right) X \quad D(N) = \frac{X}{(N^2 + N)} \quad R(N) = \frac{X}{N} \quad dR(N) = \left(1 - \frac{1}{N}\right) \delta$$

Divide by N	Out Freq. F(N)	F Step	Ref. Freq.	$dR(N)$ = freq shift from VXO tuning
40	13966.875	8.735	358.125	9.75
48	14026.563	6.091	296.438	9.792
56	14059.196	4.483	255.804	9.821
64	14101.172	3.444	223.828	9.844
72	14126.042	2.725	199.958	9.861
80	14145.938	2.211	179.063	9.875
88	14162.216	1.829	162.784	9.886
96	14175.781	1.538	149.219	9.896
104	14187.26	1.312	137.74	9.904
112	14197.098	1.132	127.902	9.911
120	14205.625	0.987	119.375	9.917
128	14213.086	0.868	111.914	9.922

Fig 4.58—Summary of available frequencies and characteristics of the 14-MHz "VXO extender." This data was generated with MathCad 7.0.



L = 20000 M = 130

$$\text{Let } M=N \text{ max. and } L=\text{Low freq. Then, } X = \frac{L}{\left(1 + \frac{1}{M}\right)} \quad X = 19847.328$$

$$N = 66, 74, \dots, 130$$

$$F(N) = \left(1 + \frac{1}{N}\right) X \quad D(N) = \frac{X}{(N^2 + N)} \quad R(N) = \frac{X}{N} \quad S(N) = 2F(N) + 10000$$

$$M(N) = 2D(N)$$

Divide by N	Out Freq. F(N)	F Step	Ref. Freq.	Six M Freq.	6 M step M(N)
66	20148.045	4.488	300.717	50296.091	8.977
74	20115.533	3.576	268.207	50231.071	7.152
82	20089.369	2.916	242.041	50178.738	5.832
90	20067.834	2.423	220.526	50125.708	4.847
98	20049.852	2.046	202.524	50099.704	4.091
106	20034.567	1.75	187.239	50069.134	3.5
114	20021.428	1.514	174.094	50042.855	3.028
122	20010.011	1.323	162.683	50020.023	2.645
130	20000.000	1.165	152.672	50000.000	2.331

Fig 4.59—Summary of available frequencies and characteristics for a 20-MHz "VXO extender." The result will be frequency doubled where it then serves as the LO for a 50-MHz transceiver based upon a 10.0-MHz IF. This data was generated with MathCad 7.0.

minus sign for this case, for the crystal is above the VCO.

The synthesizer board is housed in a milled aluminum box (Hammond 1590BB) with either coaxial cables or feedthrough capacitors for all interfaces. The VXO and the VCO are each housed in individual milled boxes (Hammond 1590A.) While it is possible to include both digital and RF/analog circuitry on a single board, the isolated and shielded approach is less prone to spurious responses and is recommended.

Once the boards are functioning and checked out, the system is turned on with relative ease. An oscilloscope senses the dc on the control line while the VCO coarse tuning is adjusted.

Fig 4.59 shows a design for the 6-meter band. It is intended to be used in a mono-band super-heterodyne trans-

ceiver with a 10.0-MHz IF. The synthesizer operates in the 20-MHz range with a 19.847-MHz VXO. It is then frequency doubled and filtered to provide a 300 kHz range at 40 MHz. The circuit could also be adapted for 25-MHz operation; frequency doubling would then allow use with a 6-meter phasing transceiver.

A similar version could be built for the two-meter band where an injection frequency of $144 - 10 = 134$ MHz is needed. An especially useful scheme would use a synthesizer operating at a tenth of this frequency, 13.4 MHz. If N varies from 66 to 130, the required VXO would operate at 13.298 MHz. The synthesizer output would be multiplied by 5 with a 74HC04 and bandpass filtering, followed by a X2 diode multiplier and 134-MHz filter. The 10X scheme leads to simple frequency counting. The system can also be adapted

for direct phasing at 144 MHz. Nearly one full MHz of range is available at the 2-meter band.

The "VXO Extender" is an experimental synthesizer, something of a departure from the normal schemes in use. The method is one that provides relatively small step sizes with much higher reference frequency, but at the price of uneven step size.

Single loop synthesizers can be configured in a more traditional format with modest step size while still being used for general-purpose applications. For example, the Elecraft K2 CW/SSB transceiver uses a single loop synthesizer with 10-kHz steps. The "clock" is a voltage controlled crystal oscillator that is then driven by a DAC, allowing all gaps to be filled in with small steps. Clever firmware on the part of the designers remove tuning ambiguities.

REFERENCES

1. W. Hayward, *Introduction to Radio Frequency Design*, Chapter 7, Prentice-Hall, 1982; R. Rhea, *Oscillator Design and Computer Simulation, Second Edition*, Noble Publishing, 1995.
2. For a discussion of the squeegeing problem, see Clarke, *IEEE Transactions on Circuit Theory*, Vol CT-13, No. 1, Mar, 1966.
3. W. Hayward, "Measuring and Compensating Oscillator Frequency Drift," *QST*, Dec, 1993, pp 37-41.
4. K. Spaargaren, "Crystal Stabilized VFO," *RadCom*, Jul, 1973, pp 472-473.
5. J. Makhinson, "A Drift-Free VFO," *QST*, Dec, 1966, pp 32-36; K. Spaargaren, "Frequency Stabilization of LC Oscillators," *QEX*, Feb, 1996, pp 19-23.
6. U. Rohde, *Digital PLL Frequency Synthesizers Theory and Design*, Prentice-Hall, 1982.
7. "The RF Oscillator", *Radio Communications Handbook*, Sixth Edition, RSGB, 1994, p 6.36.
8. U. Rohde, *Digital PLL Frequency Synthesizers Theory and Design*, Prentice-Hall, 1982; U. Rohde, "Designing Low-Phase-Noise Oscillators," *QEX*, Oct, 1994, Fig 15, p 10; H. Johnson, personal correspondence with author; "Demphano - A Device for Measuring Phase Noise," *J. Makhinson, Communications Quarterly*, Spring, 1999, pp 9-17.
9. D. B. Leeson, "A Simple Model of Feedback Oscillator Noise Spectra," *Proc. IEEE*, Vol 54, Feb, 1966, pp 329-330.
10. U. Rohde, personal correspondence with author.
11. W. Hayward, "Variations in a Single-Loop Frequency Synthesizer," *QST*, Sep, 1981, pp 24-26.
12. <http://www.qsl.net/7n3wvm/supervxo.html>
13. W.S. Mortley, "Frequency-Modulated Quartz Oscillators for Broadcasting Equipment," *IEEE Proceedings, Part B*, May, 1957, pp 239-249; W.S. Mortley, "Circuit Giving Linear Frequency Modulation of Quartz Crystal Oscillator," *Wireless World*, Oct, 1951, pp 399-403; V. Manassewitsch, *Frequency Synthesizers: Theory and Design*, Third Edition, John Wiley & Sons, 1987, pp 401-405.
14. See, eg, U. Rohde, *Digital PLL Frequency Synthesizers: Theory and Design*, Prentice-Hall, 1983; U. Rohde and D. P. Newkirk, *RF/Microwave Circuit Design for Wireless Applications*, Chapter 5, John Wiley & Sons, Inc., 2000.
15. F.M. Gardner, *Phaselock Techniques*, Second Edition, Wiley, Apr, 1979; V. Manassewitsch, *Frequency Synthesizers: Theory and Design*, John Wiley & Sons, 1987, pp 401-405.
16. *CMOS Application-Specific Standard ICs*, Motorola Inc, Publication DL130/D, 1991, pp 5-101. Data sheet has a good set of references. See also design equation page.
17. W. Hayward, "Variations in a Single-Loop Synthesizer," *QST*, Sep, 1981, pp 24-26; Talbot, "N-over-M Frequency Synthesis," *RF Design*, Sep, 1997.
18. E.O. Brigham, *The Fast Fourier Transform*, Section 5.4, "Sampling Theorem," Prentice-Hall, 1974, pp 504-510.
19. U. Rohde, "A High-Performance Hybrid Frequency Synthesizer," *QST*, Mar, 1995, pp 30-38.
20. This circuit is similar to one described by G. Adcock, G4EUK, "A Simple Frequency Counter for DC Receivers," *Sprat 73*, Winter, 1992/93, p 10.
21. For the ultimate, high performance circuit, see W. Carver, "The Modular Dial," *Communications Quarterly*, Spring, 1998, pp 35-44. See also N. Heckt, "A PIC-Based Digital Frequency Display," *QST*, May, 1997, pp 36-38; and D. Benson, "Freq-Mite—A programmable Morse Code Frequency Readout," *QST*, Dec, 1998, pp 34-36.

Mixers and Frequency Multipliers

5.1 MIXER BASICS

Nearly all of the equipment we build uses at least one mixer. Even the simplest direct conversion receiver uses a product detector, which is one form of mixer. Fig 5.1 shows the block-diagram symbol for a mixer. A mixer is a three-port circuit with two input signals and one output occurring at a frequency that is the sum and/or difference of the two input frequencies. One input, the *local oscillator* (or *conversion oscillator*) is usually much stronger than the other, the *RF input*. The output in typical receiver applications is called an *intermediate frequency*, or *IF*, for it is often part way between a higher input frequency and baseband. While this historic relationship does not always apply to modern systems, the *IF* term remains.

We begin our examination of mixers with an experiment designed to analyze a simple mixer with the goal of extracted understanding. What are the device characteristics that allow mixing (difference and sum frequencies) and what are the resulting signal levels? Are there undesired output signals?

Our experimental mixer is the single JFET circuit of Fig 5.2. Both local oscillator and RF are applied at the gate. While this may not be the most common scheme, it lends itself to analysis.

Examination begins with the bias circuit of Fig 5.3. Our goal is to model the FET and to then bias it half way between pinchoff and full drain current. The Fig 5.3 circuit is built without a “test” resistor, producing a source voltage of 3.74 V. (These are actual measured results with a J310 FET.) The FET current is very low owing to the high value source resistor, so the FET pinchoff voltage will be close to -3.74 V. Test resistors from 10 k Ω down to 15 Ω were then

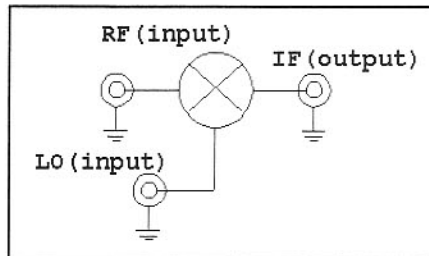


Fig 5.1—Block diagram element for a mixer.

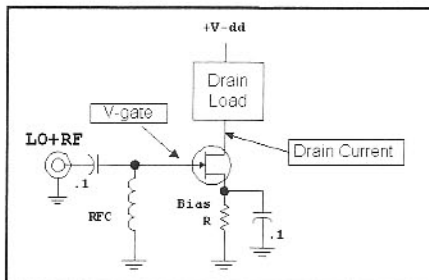


Fig 5.2—Basic JFET mixer with LO and RF applied at the gate. The drain will then have all available outputs. It can be tuned to emphasize one mixer product.

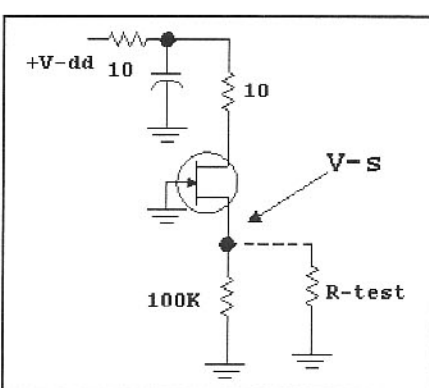


Fig 5.3—Biasing setup for FET modeling.

placed in the circuit, measuring source voltage for each. This allowed us to form a curve of drain current vs gate-source voltage, Fig 5.4. The data scatter (the bumps) resulted from thermal effects at higher current levels. The smooth curve is calculated for an ideal JFET with a -4.2 V pinchoff and $I_{DSS}=45$ mA. These parameters produced a good fit to the measured data over most of the range.

This exercise provides a mathematical model, something to use to study the mixing process. A 150- Ω resistor provides the desired bias that sets the source voltage at 2 V, about half way between full current and pinchoff.

Fig 5.5 is a modification of the smooth, modeled data. The zero voltage point has been shifted to the middle of the graph, the bias point chosen with the 150- Ω source resistor. The voltage is the actual value appearing at the gate in Fig 5.2. The total current has been split into three segments. The first is a constant, the bias current with no signals present. The second is the linear term, a straight line. The third is a parabola. The three components add to form the previous curve.

We now consider each of the three curve segments by themselves as signals are applied to the mixer input. The bias is a fixed value; the fixed current does not depend on any applied signal. This is evident in the bias curve in Fig 5.5, which is flat.

The linear term becomes more useful. If we apply a sine wave to the gate that causes the voltage to oscillate between -0.5 and 0.5 V, a 1 V peak-to-peak swing, the current will vary by about 11 mA peak-to-peak. A high impedance in the drain allows the signal current to develop an output voltage. This is the characteristic we seek when we use the JFET

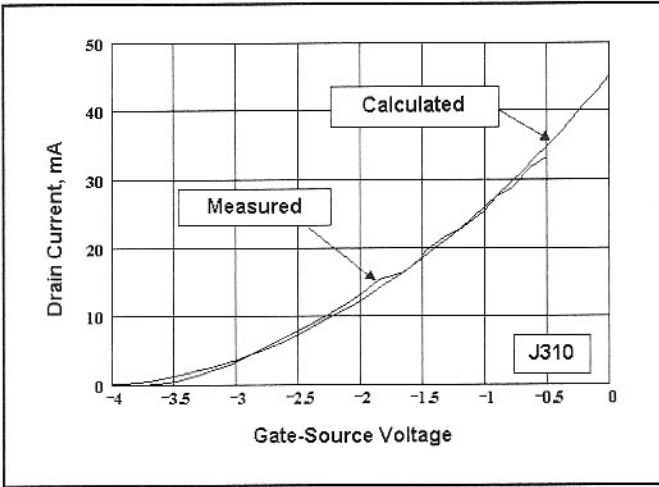


Fig 5.4—Curve fit of data for FET modeling. The bumps are the result of thermal effects in data, while the smooth curve is calculated.

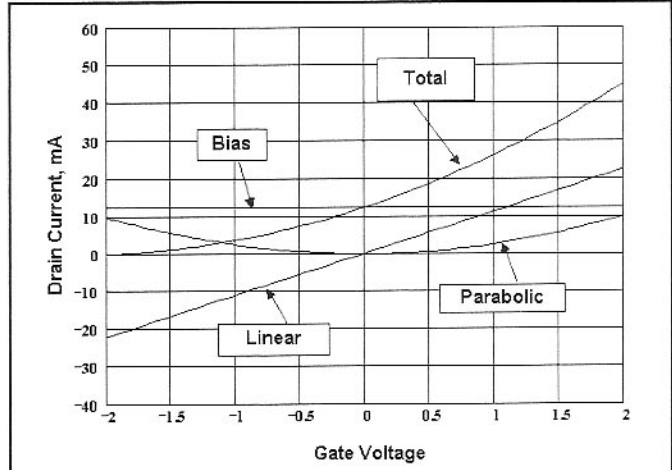


Fig 5.5—The FET current is split into three components: a fixed bias, a linear term and a parabola.

as an amplifier.

Consider the linear curve when two signals are applied to the input: Two sine wave voltages at the gate produce two sine wave currents, but nothing more; no mixing occurs as a result of the linear term. There is also no distortion. This is the behavior we intend when we speak of linearity.

It is the parabola that becomes interesting, taking us beyond amplifier behavior. A low amplitude gate signal causes no current, for the parabola is zero everywhere near 0 V. But current flows as the signal grows. Moreover, it is distorted. This is evident; for a positive excursion will produce the same positive current that is generated by a negative excursion. A large amplitude sine wave will produce two output current pulses per cycle as the signal swings both positive and negative about the bias point. We have built a frequency doubler.

We now apply the sum of two signal voltages to the gate. Again, the bias curve produces nothing. The linear curve will generate two response currents, each a replica of the input, but nothing more. No mixing occurs from the linear response. But the parabolic curve generates interesting results. Not only do we see each input frequency doubled, but we now see sum and difference products. This is not evident directly from the curves, but follows directly from the related mathematics. This is available on the book CD as a *Mathcad* file, *mixer_jfet1.mcd*. A file is also available (*mixmath.pdf*) that can be viewed even if the reader does not own *Mathcad*.

The two-component input uses one part, the “local oscillator,” at a higher level than the other, the “RF.” When this term is

applied to the parabolic curve, the result is a product of two sine waves. Multiplication is the reason our mixer symbol, Fig 5.1, uses a large multiply sign. High school trigonometry identities convert the product of two sine waves into sine waves at the sum and difference frequencies, the mixing result that we seek. The sum is often called the *upper sideband*, while the difference is the *lower sideband*, terminology left over from modulation theory. Most of the circuits that we call modulators are actually mixers. The power amplifier in a classic amplitude modulated (AM) transmitter operates as a power mixer. The circuit traditionally called a “modulator” is really just an audio power amplifier.

Fig 5.6 shows a practical version of the circuit we have designed. We use a 1-V local oscillator signal at 10 MHz with RF amplitude of 0.2 V at 14 MHz. The drain is terminated in $50\ \Omega$ by way of a wideband transformer with a 5:1 turns ratio, resulting in a drain load of $1.25\ k\Omega$. The calculated output powers for all frequencies appear in Table 5.1. These are very close to those measured when we built the circuit with the FET we had characterized. The calculations are in the *Mathcad* file mentioned earlier.

The two converted, or mixed outputs at 4 and 24 MHz have equal amplitudes, which are much less than the amplified RF output. The amplified LO is a large signal, close to the maximum possible from a J310 FET with a 12-V supply with the drain impedance used. This mixer topology is normally built with a tuned output. Tuning would eliminate the large drain voltage at the 10-MHz LO frequency. This would then allow a larger LO power to be used, which would increase conversion gain.

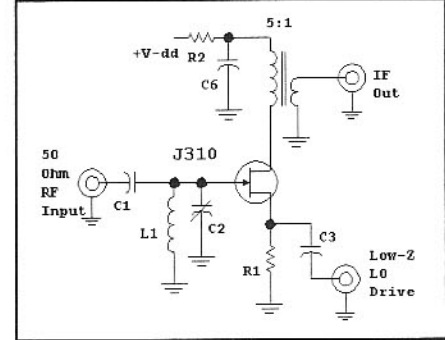


Fig 5.6—JFET mixer with a wideband output termination using a 5:1 turns ratio transformer. LO power is applied to the source, but this still results in LO between the source and drain, making this circuit the equivalent of Fig 5.2.

Table 5.1

Freq. (MHz)	Power (-dBm)	Description
4	-8 dBm	Lower Sideband mixed (down converted) output
10	+18.9	Amplified LO (feedthrough)
14	5	Amplified RF (feedthrough)
20	-0.1	Frequency doubled LO
24	-8	Upper Sideband mixed (up-converted) output
28	-28	Frequency doubled RF

Generally, FET mixers (including those using MOSFETs) will have an optimum conversion gain that is below the amplifier gain by 12 dB when the same terminating impedances are used.

The JFET example presented is but one of many devices that will produce mixing action. Mixing usually arises from *nondi*

ear device behavior. Mixing can also be produced in a system with time-dependent parameters. But, an ideal linear amplifier will never produce mixing. Even-order curvature in a device characteristic is the nonlinearity needed for mixing.

The simple single ended JFET mixer of Fig 5.6 becomes a practical circuit when the drain is tuned. But, it suffers from the wide spread in FET characteristics, making it difficult to use in a “plug-and-play” mode. A builder really needs to examine the FET to determine pinchoff and I_{DSS} , to establish bias, and to pick the right LO level. The following procedure may be used:

- (1) Build the mixer with a 100-k Ω source resistor. Measure the source voltage to approximately establish the pinchoff.
- (2) Place a small resistor or even a short circuit across the source resistor to infer I_{DSS} . (optional)
- (3) Find (mathematically or experimentally) a source resistor that sets the dc source voltage at half the magnitude of the pinchoff.
- (4) Apply LO power from a low Z source and increase LO amplitude until the peak voltage approaches the dc bias value. In the J310 example, the optimum LO signal would be nearly 2-V peak, or 4-V peak-to-peak. A high-speed oscilloscope is required.

The low impedance LO drive allows the FET to “look like” the source is grounded for RF input signals. Similarly, the RF tuned circuit should be one where the gate looks back into a low impedance at the LO frequency.

The single JFET mixer, when carefully done, is capable of excellent performance. We have measured 4 to 6-dB NF with input intercepts (third order) from 0 to +10 dBm with a 2N4416. The J310 is more difficult to drive owing to the increased I_{DSS} , but is capable of higher IIP3.

A bipolar transistor can be operated as a single-ended active mixer, shown in Fig 5.7. Lowest distortion will result from higher standing current, but this produces very low

input impedances presented to the local oscillator, making drive difficult. Emitter degeneration reduces drive power, but can compromise noise figure. We have not performed careful measurements on this mixer.

Fig 5.8 shows a mixer using a single diode. Such mixers were once very common, especially for microwave applications. They have largely disappeared in modern times.

The usual diode mixer has no bias applied, but the LO signal is large enough that it causes the diode to conduct. When the diode conducts, it looks like a small resistance, allowing current to flow as the result of the applied RF. We envision the diode as a *switch* that is controlled by the LO. The switch is “on” for half of the LO

cycle, and off for the rest. When on, virtually all of the RF power available can be delivered to a load at the IF port. But when the switch is off, none of the power can reach the load. With the RF reaching the IF load only half of the time, the voltage developed across the load from the RF generator is only half as high as it would be if present all of the time. Accordingly, the mixer has a 6-dB loss. **Fig 5.9** shows waveforms for a single diode switching mode mixer.

Switching mode mixers are extremely common, with most of the mixers we use in communications operating in this way. These mixers are typically passive and use no power supply; they offer no gain. The diode mixer of Fig 5.8 uses a series switch,

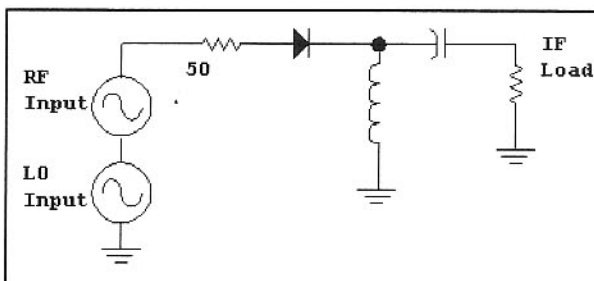


Fig 5.8—A simple diode mixer. RF and LO inputs generate an IF output, but the output is rich in signal feedthrough.

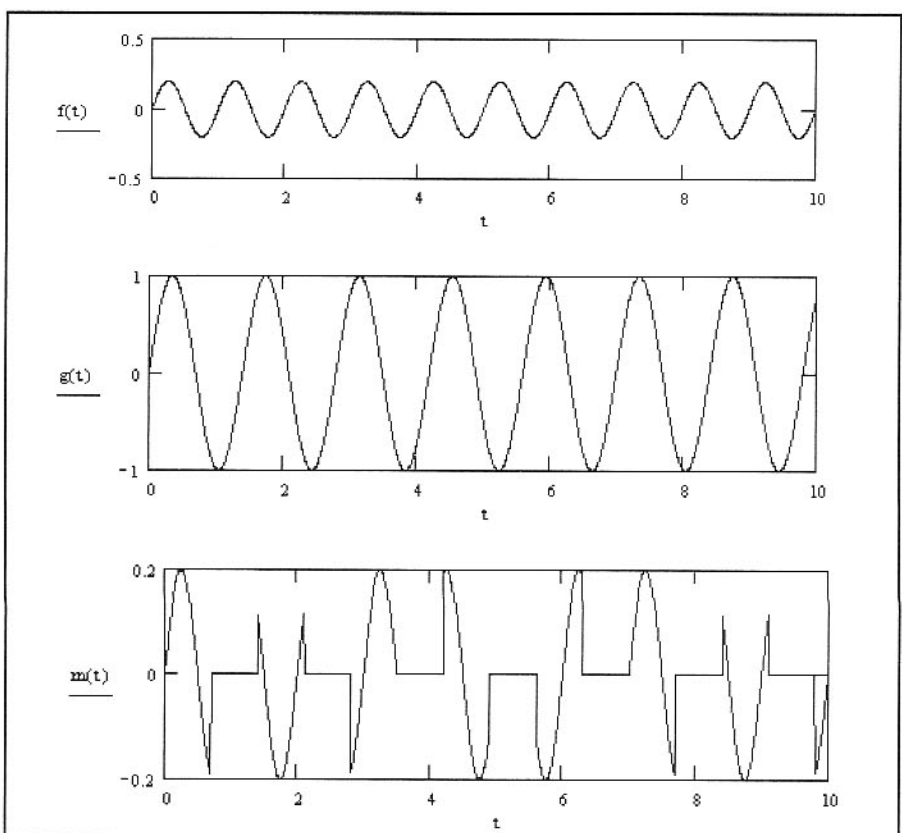
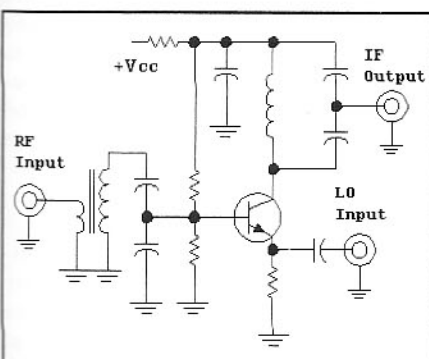


Fig 5.9—Time domain waveforms for a single diode switching mode mixer. The IF output at any instant is the RF input if the LO voltage is positive, but 0 when the LO is 0 or negative.

Fig 5.7—Simple bipolar mixer.



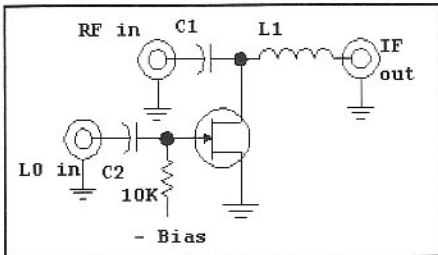


Fig 5.10—Switching mode mixer using a single FET. Although a JFET is shown, the mixer can also be implemented with a bipolar transistor, a MOSFET, or a GaAs FET. This circuit typically has a conversion loss of 6 dB. Input intercept (third order) can be from 0 to +20 dBm, depending on the FET type. LO energy at the RF port is typically reduced by 10 to 15 dB. Operating frequency will dictate the components in the diplexer filter, C1 and L1. See text.

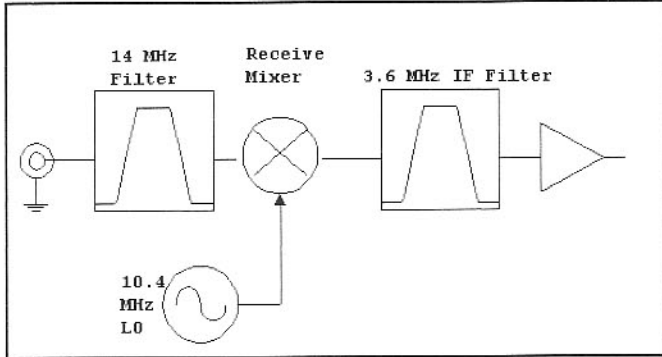


Fig 5.11—Partial block diagram of a 14-MHz receiver. The IF is 3.6 MHz, produced with a 10.4-MHz local oscillator.

but shunt switches also work well. FETs and bipolar transistors can be used in switching mode mixers.

Fig 5.10 shows a single FET as a shunt switch mixer. Steve Maas presented this circuit in detail in a 1987 paper.¹ We have used this mixer extensively in integrated form in GaAs integrated circuits.² The FET often has a bias applied to the gate, a negative voltage equaling the FET pinchoff. The LO is typically a sine wave with a peak value equal to or just over the pinchoff. All three ports are terminated in $50\ \Omega$, but the LO presents a severe mismatch. The configuration shown is a down-converter with an IF below the RF and LO. Up-converters exchange the RF and IF ports.

The diplexer filter, C1 and L1 in Fig 5.10, isolates the IF from the RF port. The capacitor is a single element high pass filter while the inductor is a low pass circuit. A common application might use an IF much lower than the RF. One can then calculate a “crossover” frequency that is the geometric average of the IF and RF. L1 and C1 are then picked to have a reactance at the crossover equal to the terminations. Higher order diplexer filters will be needed if the IF and RF are closer. A bandpass/bandstop diplexer can also be used.

Mixer Specification and Measurement

We now examine mixers in more detail, seeking the properties needed to specify and understand mixers for use in a communications system.

Chapter 2 included some vital, yet less common specifications for amplifiers including noise figure and IMD. These phenomenon, which also occur in mixer

circuits, are illustrated by the system of Fig 5.11, a CW receiver for 14 MHz with 10.4-MHz LO and 3.6-MHz IF.

IMAGES, SIDEBANDS, SUMS AND DIFFERENCES

The example receiver mixer is preceded by a 14-MHz bandpass filter that ideally passes only frequencies close to the 20-meter band. The 10.4-MHz LO drives the mixer to produce an IF output at the 3.6-MHz difference between the RF and LO frequency, 14 – 10.4.

Temporarily remove the input bandpass filter and attach a wide range signal generator at the receive mixer RF input. There is now also a response at 6.8 MHz, for $10.4 - 6.8 = 3.6$. The response to a 6.8-MHz input is called the image response. We evaluate the receiver, now with the bandpass filter reconnected, by attaching a signal generator to the input. Tune the generator to 14 MHz, deactivate receiver AGC, and measure the receiver output signal. This measurement works best with a modest input signal, perhaps -100 dBm. Note the audio output, then tune the generator to 6.8 MHz. Increase the generator level until the receiver output is identical to the original. The ratio of generator power levels is the receiver *image suppression*.

It is straightforward to build a bandpass filter at 14 MHz that will suppress 6.8-MHz signals by 100 dB or more. Early receivers, the old instruments now sought by collectors, used intermediate frequencies near 500 kHz, allowing 14 MHz to be received with a 13.5-MHz LO. The image response would then be at 13.0 MHz. It was difficult to obtain significant (by modern standards) suppression of 13 MHz in a 14-MHz filter.

The receive mixer example has two inputs: 10.4 and 14 MHz. We use the 3.6-MHz *difference* output response. But the mixer output will also contain a *sum* response, $10.4 + 14 = 24.4$ MHz. The 3.6-MHz response is terminated in the usu-

ally reasonable impedance match of the 3.6-MHz bandpass filter. But all 24.4-MHz energy is generally reflected by the IF filter. That energy can get back into the mixer “output” where it might be reconverted back to 14 MHz, but in a different phase than the original signal where it can alter conversion gain and distortion performance. These problems are especially insidious with the popular diode ring mixers. It is for this reason that we often see extra resistive pads used with such mixers. They are often used in all three ports. Active mixers such as the FET discussed earlier are much less prone to this problem.

Assume that the incoming 14-MHz signal is modulated, containing a single upper sideband at 14.002 MHz. We analyze the behavior of the sideband by considering it to be an independent signal. It will be mixed down to IF without any disturbance from the original carrier. The sideband ends up at 3.602 MHz, still above the 3.600-MHz carrier appearing at the IF; it is still a USB signal.

Our receiving mixer would function just as well if we used a 17.6-MHz LO, 3.6 MHz above the input. An upper-sideband at 14.002 MHz applied to such a receiver would produce an IF response at 3.598 MHz, now below the 3.6-MHz carrier. *Sideband inversion* has occurred. This possibility should be investigated in any SSB system. The analysis is equally valid when a carrier is suppressed. Sideband inversion is often a practical advantage to the builder/designer. For example, a popular crystal filter form is the lower sideband ladder with greater stopband attenuation on one side than the other.

ISOLATION

We are always concerned about the output at one port of a mixer as signals are applied to the others. For example, we might ask how much LO signal appears at a mixer’s RF port. This would be important in a receiver; we don’t want a large LO

signal to be radiated, for the mixer RF port may be attached to the antenna with minimal filtering. Even without radiation considerations, isolation can be important. If excessive LO was present, it could be reflected by a filter to re-appear at the mixer RF port where it would be converted to produce a dc output component. This could, in some mixers, alter the bias to change the mixer properties.

Isolation is easily measured for a mixer that is not already imbedded within a piece of equipment. If you are concerned with, for example, LO to RF port isolation, apply LO at a known level while examining the output at the RF port by attaching it to a spectrum analyzer or measurement receiver. The LO power at the RF port will be lower (we hope!) than that available from the LO source. The difference is the suppression. This will depend on mixer tuning in circuits such as the JFET described earlier. Often we hear folks talking about "mixer balance" in dB. Usually,

they are concerned with port-to-port isolation, which can be enhanced with balanced circuits, a method discussed later.

SPURIOUS RESPONSES

Consider the transmitter application shown in Fig 5.12. In this example, we want to build a 7.1-MHz transmitter that works with an existing receiver using a 5-MHz IF. This will be accomplished by mixing the signal from a 2.1-MHz LO with that from a 5-MHz crystal oscillator. The output is filtered with a bandpass filter to produce the desired output.

The ideal output response from this mixer, assuming that the output filter is removed, is that shown in Fig 5.13. The desired sum product at 7.1 MHz is accompanied by a difference response at 2.9 MHz.

The ideal is rarely realized. Fig 5.14 shows what we might actually see. This is a result of harmonic responses. Specifically, the output of a mixer excited by an LO at L MHz and RF at R MHz will be at F MHz.

$$F = n \cdot L \pm m \cdot R \quad \text{Eq 5.1}$$

where n and m are integers. This spurious response, or *spur* generation relates to harmonics *created within the mixer*, even when the inputs are free of harmonics. The upper part of Fig 5.14 presents what we would see if n and m were allowed to take on values from 0 to 7 with the bandpass filter missing. The lower display is even more extreme, allowing values of n and m up through 15. (These data were generated with *Spurtune.exe*, a program distributed with *Introduction to Radio Frequency Design*.)

These uncalibrated displays are discouraging. Undesired outputs in such abundance would discourage anyone from ever using a mixer in a transmitter! Fortunately, not all spurious responses are of equal magnitude. The spurs tend to get weaker as the total order ($n+m$) increases. Further suppression can occur with some spurs as a consequence of balance that might be used in the mixer.

Spurs are also less with some system architectures over others. For example, if the transmitter considered here used a 12.1-MHz LO instead of 2.1, the outputs of Fig 5.15 result.

A spur related to order "m" for the RF

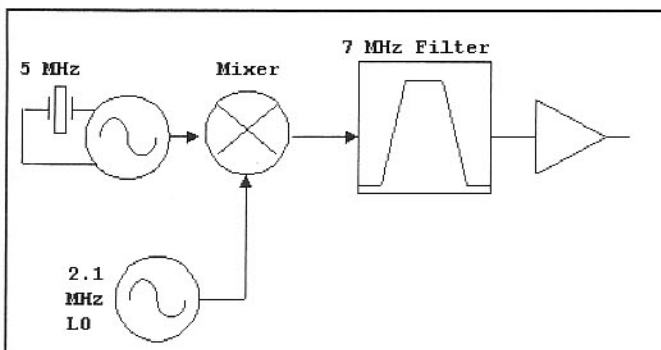


Fig 5.12—Mixer section of a 7-MHz transmitter with a 2-MHz LO and a 5-MHz crystal "carrier" oscillator.

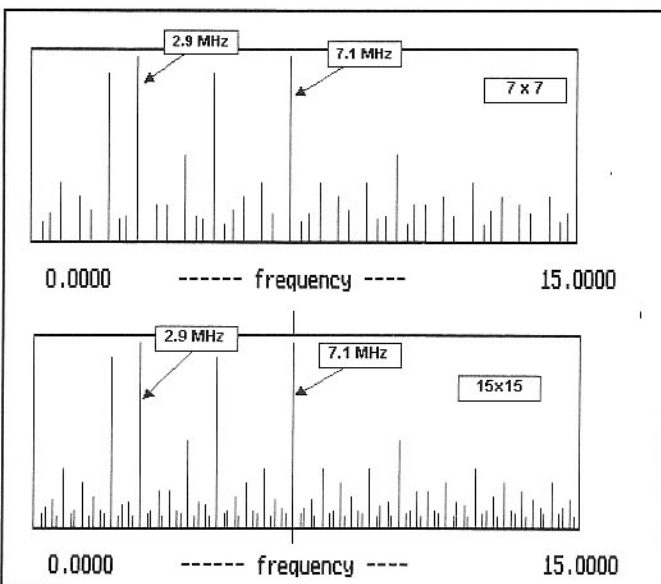


Fig 5.14—Mixer outputs with a variety of orders allowed, n and m to 7 in the upper curve and 15 in the lower.

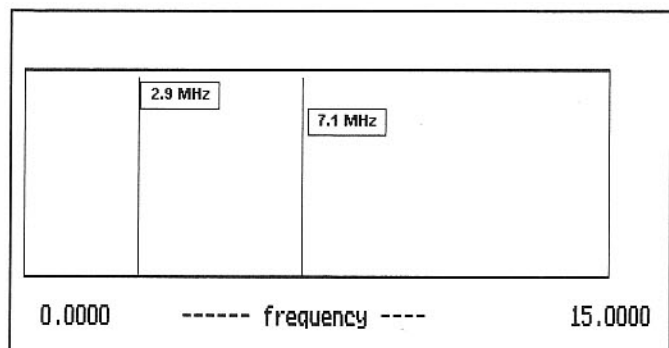


Fig 5.13—Idealized mixer output for the circuit of Fig 5.12 without the output filter.

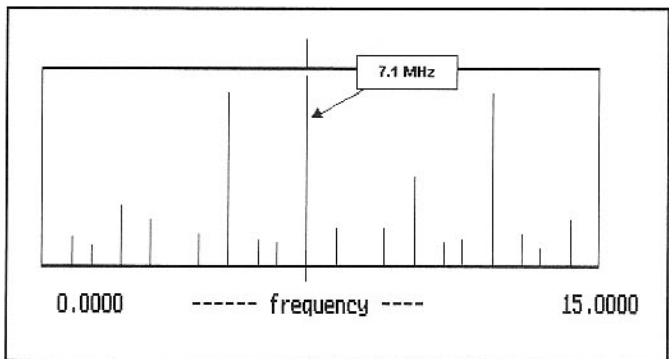


Fig 5.15—Spur spectrum for the same transmitter, but with a 12.1-MHz LO. Spur orders through 7 are shown.

will generally have a strength proportional to the "m th" power of the input at the R mixer port. Hence, decreasing the RF input by 1 dB will drop a m-order spur by m dB. Mixer overdrive should be judiciously avoided. The worst possible cases are those where the IF is related to the output by a small integer, $IF = k \times RF$, or $IF = RF/k$.

LO DRIVE LEVEL

Most commercial mixers are specified with regard to LO drive level. For example, the typical diode ring mixer is specified for +7 dBm. This is *not* the power that is actually delivered to the mixer port. Rather, it is the power available to a 50- Ω termination from the source that will eventually drive the mixer. Oscilloscope examination of the LO drive to a diode ring shows a severely distorted signal with less amplitude than the original sine wave driving a pure 50- Ω load. Many of the measurements we do with RF applications are substitutions rather than the familiar in-situ measurements of analog electronics.

Various mixers behave differently as LO power is varied. A small change in LO power makes almost no detectable difference with the typical diode ring. In contrast, the JFET studied earlier will show output decreasing almost linearly as LO drive drops.

CONVERSION GAIN (OR LOSS)

Mixers are all characterized by a conversion gain, meaning that we examine the converted output power vs that available to the RF port. The method of specifying the gain will vary slightly. A diode ring mixer, a passive circuit, might be specified with a loss, with 6 dB being a typical value. Active mixers such as the JFET considered earlier will be specified by power gain in a well-defined circuit, or perhaps by a conversion transconductance.

Terminal impedance is specified for a mixer. Most passive mixers show an RF input impedance that equals the IF termination while the JFET mixer at the beginning of this chapter shows a nearly open circuit as the input impedance at the gate, or a low impedance at the source like that of a common gate amplifier. Output (IF)

port impedances are usually high with active mixers, but related to other port terminations with switching mixers. That is, the impedance seen at the IF port equals the value presented to the RF port.

NOISE FIGURE

Mixers all exhibit noise that can be characterized by noise figure. The measurement is similar to that of an amplifier. A wideband resistive termination at 290 K is first presented to a mixer input and the noise output is noted. Then, a stronger but known noise source is applied to the input, again while observing output noise. The "noise gain" is compared with normal available power gain to infer a noise figure.

The procedures, both for definition and for measurement, are nearly identical to those used with an amplifier. Two different mixer noise figures are available during any given measurement, as shown in Fig 5.16, with the difference being the image-stripping filter. (An image-stripping filter is one that prevents an image from reaching the input of a mixer.) Single sideband noise figure is the desired parameter, for most systems use filters to eliminate the image. Care is required to guarantee that SSB NF is measured, for noise figure is defined only for a single signal case.

Passive mixers usually have a noise figure equaling the numeric value of the loss. Hence, the usual diode ring with a 6-dB conversion loss will have a noise figure of 6 dB, or just a bit more.

INTERMODULATION DISTORTION AND GAIN COMPRESSION

While noise figure limits the weakest signal a mixer can process, intermodulation distortion and gain compression usually define strong signal behavior. IMD measurement is the same as is used with an amplifier, except that the output signals are observed at the converted frequency. Two RF signals or tones are combined in a suitable hybrid circuit with the result applied to the mixer being tested. The output tones are then observed at the mixer output frequency, along with the distortion products. An intermodulation ratio is established by the measurement, allowing an

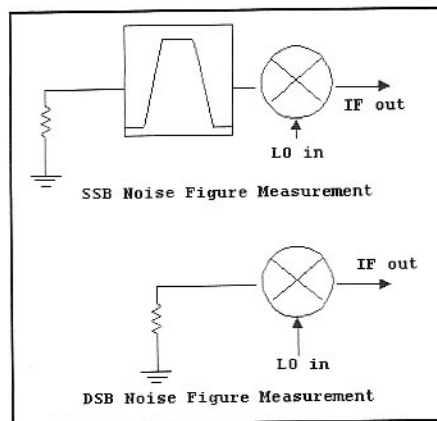


Fig 5.16—Scheme for measuring mixer noise figure. The upper circuit determines the usual single sideband NF. The lower applies noise at two frequencies and establishes what is often called double sideband noise figure. The bandpass filter eliminates any image response from the mixer input. DSB noise figure is typically 3 dB lower than the desired SSB noise figure.

input or output intercept to be calculated.

Gain is a constant for small signals, but eventually decreases as the RF level increases. A useful parameter is the available RF input power where the gain is below the small signal value by 1 dB.

Most mixer manufacturers specify their mixers by an input intercept value. This is in direct contrast to the amplifier folks who focus on the output. Both forms are fine, so long as the reader understands what is being specified.

Implicit in a mixer input intercept specification is an impedance. The usual specification uses 50- Ω terminations at all ports, and those terminations are wideband ones. This usually implies that the mixer was driving the input of a spectrum analyzer during the measurement, an instrument with a good 50- Ω input impedance at all frequencies. This occurs when the analyzer is set for at least 10 dB of input attenuation. This becomes very important with switching mode mixers where a poor output termination can destroy otherwise excellent IMD performance.

5.2 BALANCED MIXER CONCEPTS

Some intrinsic mixer problems can be reduced or eliminated when circuits are modified by adding balance. Consider Fig 5.17, part A, where we start with the familiar JFET active mixer. Local oscillator energy is applied at the source. FET gate-source capacitance couples the source voltage to the gate, degrading LO to RF isolation. Connecting a spectrum analyzer to the RF port reveals considerable LO energy at the RF port.

The term balance implies symmetry, a circuit with two sides or parts. A circuit becomes a balanced mixer through duplication, shown in Fig 5.17. The duplication presented in part B did not improve LO to RF suppression, but that in C does. The sources in C are in parallel, but the two gates are differentially driven. LO energy transferred to the gate of the first FET is exactly duplicated by that at the second FET, resulting in gate voltages that are in phase. But the transformer gate connection results in no net current, and no LO frequency signal at the transformer primary. The LO to RF port isolation is now excellent. Practically, one might expect a 30-dB improvement with balance.

The reverse, RF to LO isolation is also improved. A signal applied at the RF port results in gate voltages that are out of phase. But the sources are paralleled, resulting in reduced output at the LO port. RF to IF isolation is similarly improved, for the drains are paralleled. However, LO to IF isolation is not altered. LO is applied as an unbalanced or single-ended signal, with IF extracted from a similar single-ended connection. There are no balanced currents that can produce any cancellation.

Generally, balance improves isolation between ports that have differing termination forms, differential vs single ended.

The mixer of Fig 5.17, part C, is a singly balanced circuit because balanced circuitry is used in but one place.

The JFET balanced mixer could use other connections to obtain similar results. For example, a transformer causing differential LO energy to be applied to the sources, while keeping single ended RF at the gates improves LO to RF isolation. It would also aid LO to IF isolation, but would not improve RF to IF isolation.

A variation of the previous mixer might use a drain transformer at the IF port, shown in Fig 5.18. A basic mixer, Q1, is duplicated in Q2, with a differential output connection through the transformer. The LO is still single ended, but is now a current from the drain of Q3 applied to the sources of Q1 and Q2. Although RF is applied only to the Q1 gate, this is a differential excitation, for Q1 and Q2 are a differential pair. As such, RF at the Q1 gate causes RF signal currents in Q1 and Q2 that are equal, but out of phase. Balance in this mixer improves LO to IF suppression (single ended to differential ports), but does not help RF to IF isolation.

The active balanced mixers presented are all assumed to be built from identical transistors. Although best when the circuits are fabricated in integrated form, they can still be practical with discrete devices.

Fig 5.19 shows balanced diode mixers. Part A presents a simple, yet very useful two-diode mixer circuit. LO is applied to a transformer and causes the diodes, now

behaving as switches, to turn on during the positive half of the LO cycle. The diodes are off for the other half cycle. This mixer is configured as a down-converter; a higher frequency RF signal is applied to the diode junction through C, while lower frequency IF energy moves from the junction to the IF port.

It is instructive to examine the transformer action in greater detail. LO power causes, at one instant, a positive voltage at a dot on the transformer. But a positive voltage on one dot causes a positive signal on the other. The windings are wired to generate the polarities shown, one positive

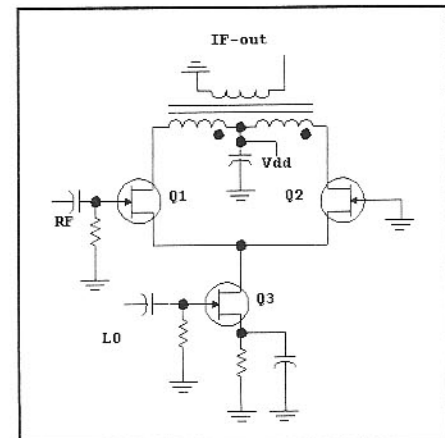


Fig 5.18—A JFET balanced mixer with single ended LO and differential IF ports. This mixer is similar to a bipolar classic, the RCA CA3028A. The RF and LO ports can be interchanged with little performance difference.

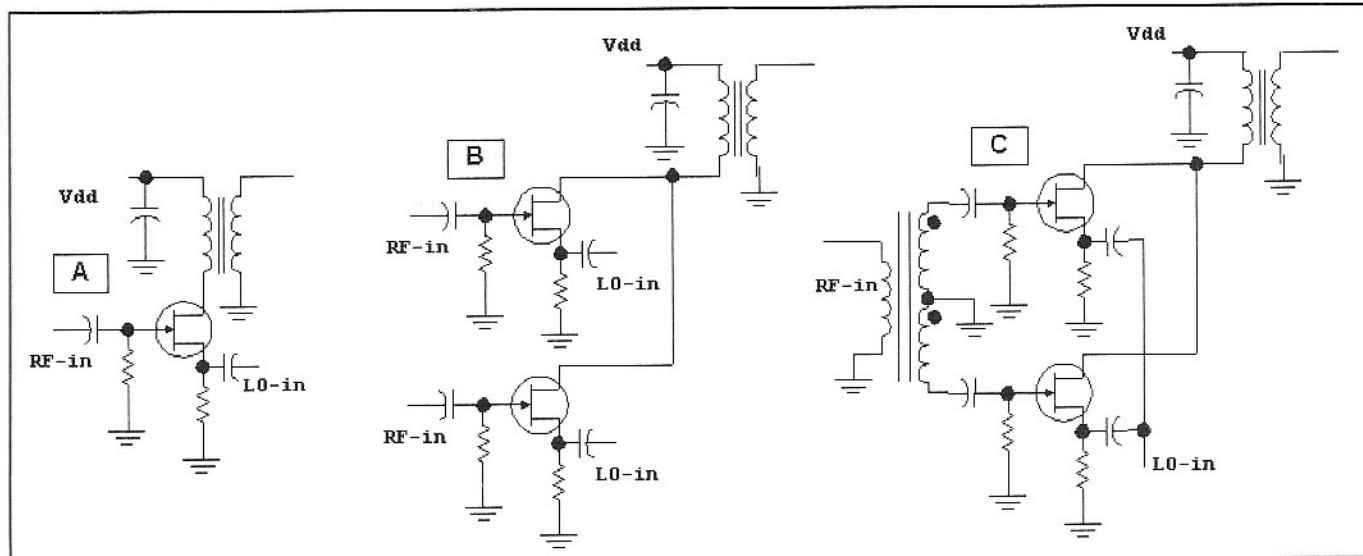


Fig 5.17—Evolution of balanced JFET mixer.

and the other negative at one instant in time. The diodes are identical, with matched on-resistance. Voltage divider action then causes the junction to be at ground, or zero LO voltage. Even when the LO polarity reverses, the identical diode reverse capacitance values generate zero LO voltage at the junction. LO to RF and LO to IF suppression are both enhanced.

The L and C values form a diplexer filter (see Chapter 3) in Fig 5.19A. The usual crossover frequency used is the geometric mean of the RF and IF, the square root of ($f_{RF} - f_{IF}$). Then, if the RF and IF impedances are 50Ω , L and C are picked to have 50Ω of reactance at the crossover frequency. More complicated diplexer filters may be needed if the IF is not small with regard to the RF.

Diode LO current is established by the diode characteristics and the source impedance provided by the LO system. The open circuit voltage must be high enough to cause the diodes to *turn on*. Greater available LO power produces higher diode current, which means that the diode on resistance is lower and conversion loss is lower. Hot carrier diodes are normally used in mixers of this sort, for they usually turn on with less voltage than a silicon junction type. The absence of a junction eliminates charge storage effects, allowing quicker diode turn-off, improving UHF performance. This mixer is still very practical at HF with silicon switching diodes such as the 1N4148. The diodes in a mixer should all be matched for voltage drop when forward biased to a few mA.

The local oscillator essentially causes the diodes to switch on and off. This combines with the transformer behavior to generate low impedance between the transformer center tap and the diode junction when the diodes are conducting. The impedance is high when the diodes are *off*. This behavior is extended to form a wideband mixer with the circuit of Fig 5.19B.

The mixers in parts A and B of Fig 5.19 present a poor load to the LO generator, for LO current only flows on half of each cycle. The addition of two more diodes, Fig 5.19C, provides a load on both halves of the LO waveform. With this connection, the LO action can be thought of as a square wave.

These three mixers (Fig 5.19, parts A, B, and C) are singly balanced with differential connections only at the LO port. But they evolve into a doubly balanced mixer in Fig 5.19D, which is labeled with LO polarity. During the polarity shown, diodes d1 and d2 conduct while diodes d3 and d4 are open circuit. The diode roles interchange when the LO polarity changes.

The switching action is further illus-

trated in Fig 5.20 showing the two LO polarities. Diodes d1 and d2 conduct with d3 and d4 off in part A. Transformer action generates a low impedance connection between the diode junction and the T1 center tap. Bold lines in Fig 5.20 emphasize the current that now flows as a result of applied RF. Part B of the figure is the same, except for an opposite LO polarity. The diode ring mixer essentially creates a direct connection between the RF input, through the RF transformer T2, to the IF load. However, the polarity of the connection changes in synchronism with the applied LO. This process is called commutation; the diode ring is the classic example of a commutation mixer.

Fig 5.20 reveals another interesting property of this circuit: The RF trans-

former, T2, communicates the IF termination through to the RF port *without* impedance transformation. The transformer used at T2 is often thought of as having a 4:1 impedance ratio, and it can certainly function this way in some applications. But this is not consistent with the figure. Rather, one half of the center-tapped secondary carries current for each polarity of the LO. The inactive side has voltage across it from transformer action, but no current other than that needed to charge stray capacitance. (Care must be exercised whenever transformers with more than two windings are used with nonlinear devices.)

Time domain waveforms for a commutation mixer are shown in Fig 5.21. The LO does no more than to commute polarity of

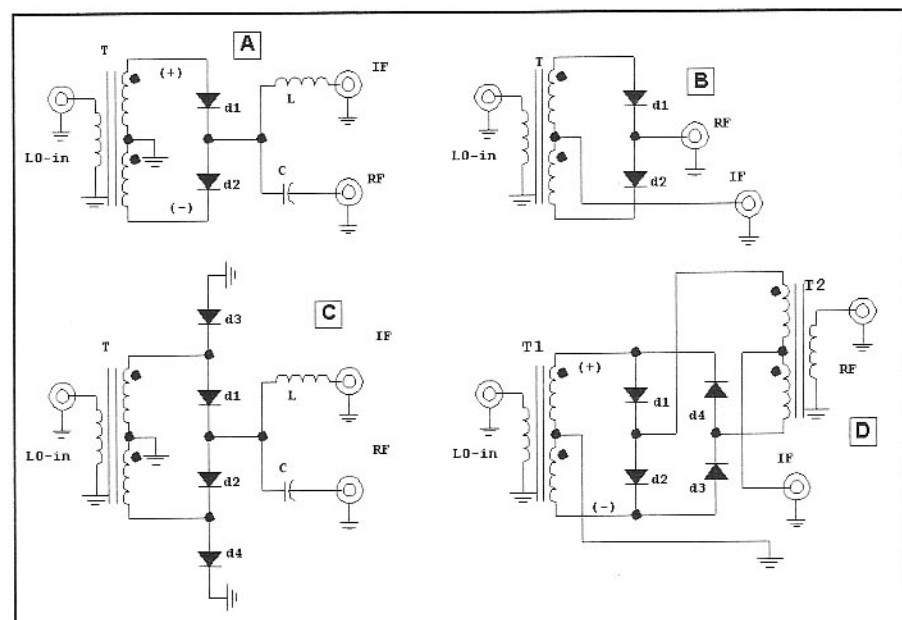


Fig 5.19—Evolution of diode mixers. Parts A and B show narrow and wideband versions of a two-diode mixer. The mixer is expanded to 4 diodes in part C, a circuit offering a better termination for the LO generator. These evolve into a diode ring, doubly balanced mixer in part D.

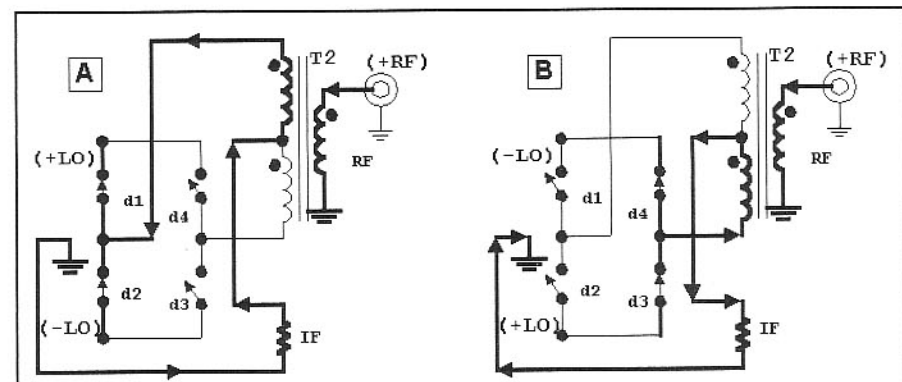


Fig 5.20—Diode ring commuting balanced mixers. See text for discussion.

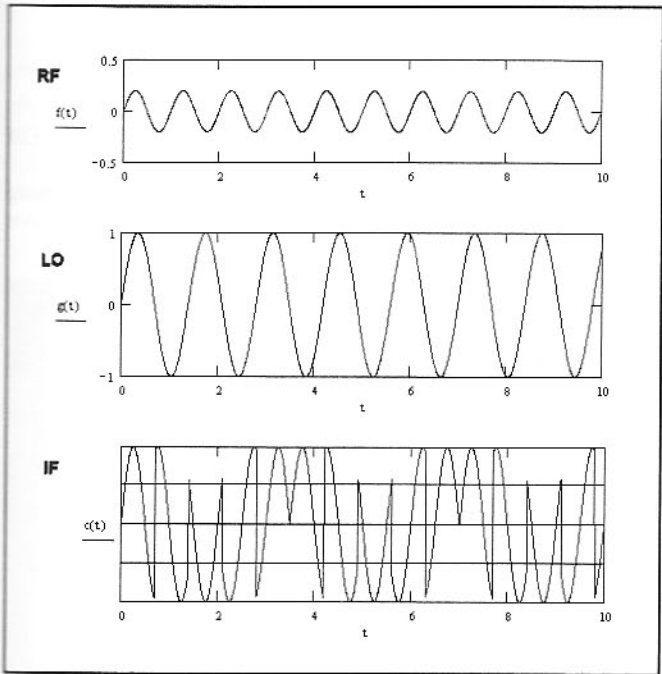


Fig 5.21—Waveforms for a diode ring commutation mixer. The RF and LO signals are those seen when the sources are examined into resistive loads. The IF signal is merely the RF waveform, except that the polarity is reversed when the LO is negative.

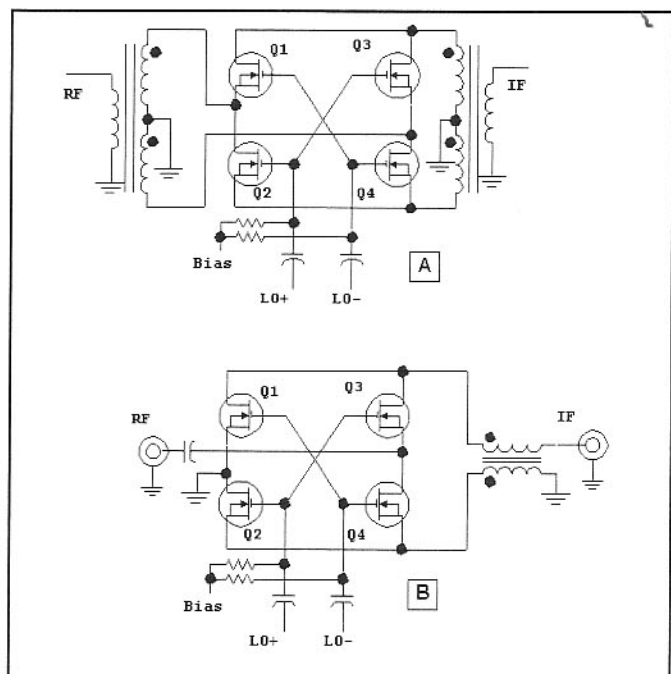


Fig 5.22—FET ring mixers using MOSFETs. The circuit at A is that originally described by Oxner while that at B is a minimum transformer topology.

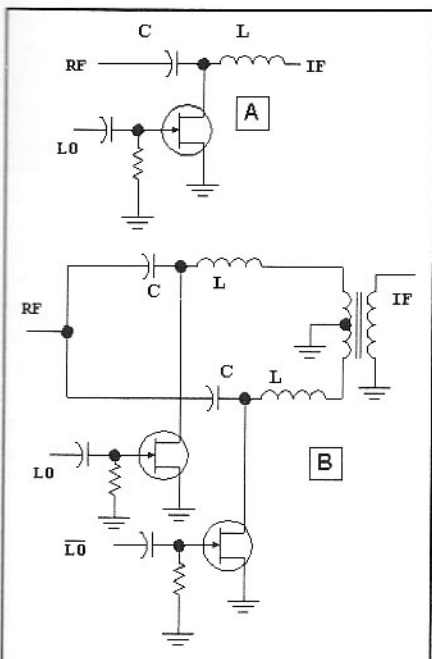


Fig 5.23—Evolution of the Maas mixer where balance improves LO to RF isolation.

the RF signal appearing at the IF port.

Field effect transistors can also be used in switching mode commutation mixers as shown in **Fig 5.22**. Part A is a doubly balanced FET ring described by Ed Oxner of Siliconix.³ Oxner's mixer originally used an integrated array of MOSFETs, the Siliconix SD8901. Many quad analog switches are also suitable in this application, although one should use those featuring low on-resistance MOSFETs. Discrete MOSFETs will also function in this circuit. A detailed analysis shows that exactly the same commutation action occurs in this mixer as we saw with the diode ring.

Oxner's mixer is an excellent performer, offering third order input intercepts in excess of +30 dBm. This low IMD occurred with a conversion loss of about 8 to 9 dB. The mixer functions well at HF, but degrades significantly at VHF. The FET ring mixer can be extended to higher frequencies with other technologies. In

some measurements we saw conversion loss under 6 dB with large area monolithic GaAsFETs, but IMD was not as low as observed with the MOSFETs.⁴

The variation in Fig 5.22 part B uses only one transformer. Performance is similar to the other ring, although the intercepts are usually not quite as high.

The passive FET mixer using shunt FETs, **Fig 5.23A**, can also be extended with balance. Duplicating the circuit with differential LO and IF, but a single ended RF results in a singly balanced mixer, **Fig 5.23B**. Typical LO to RF isolation is 40 dB, even at low microwave frequencies.

Balance is an extremely powerful and general design tool that can often be applied to enhance port-to-port isolation. If any mixer is lacking in, for example, LO-to-RF isolation, placing two of them in a balanced pair will often enhance isolation by another 30 dB, with a bonus of a 3 dB increase in IIP3.⁵

5.3 SOME PRACTICAL MIXERS

The Gilbert Cell

By far the most popular integrated mixer circuit available is the Gilbert Cell, named for Barrie Gilbert of Analog Devices. Gilbert developed a “four quadrant” multiplier circuit as an extension of a circuit presented earlier by Jones in US Patent 3,421,078 issued in 1966. The revised circuit is described in more detail in the text by Gray and Meyer.⁶

The Gilbert Cell is based upon the simpler mixer circuit shown in Fig 5.24. RF drives the base of Q1 to produce the combined dc and RF current that is then applied to the common emitters of a differential amplifier, Q2 and Q3. LO energy applied differentially to the dif-amp bases causes the RF to be toggled from one collector to the other. The IF termination is a balanced load, usually created with a transformer. This topology improves RF to IF and LO to RF isolation, for the RF input is single ended while the IF output and LO input are differential. This circuit was available from RCA in IC form as the CA3028A. This mixer suffers from poor LO to IF isolation, for differential drive at the bases of Q2 and Q3 produce directly amplified responses at the differential collectors.

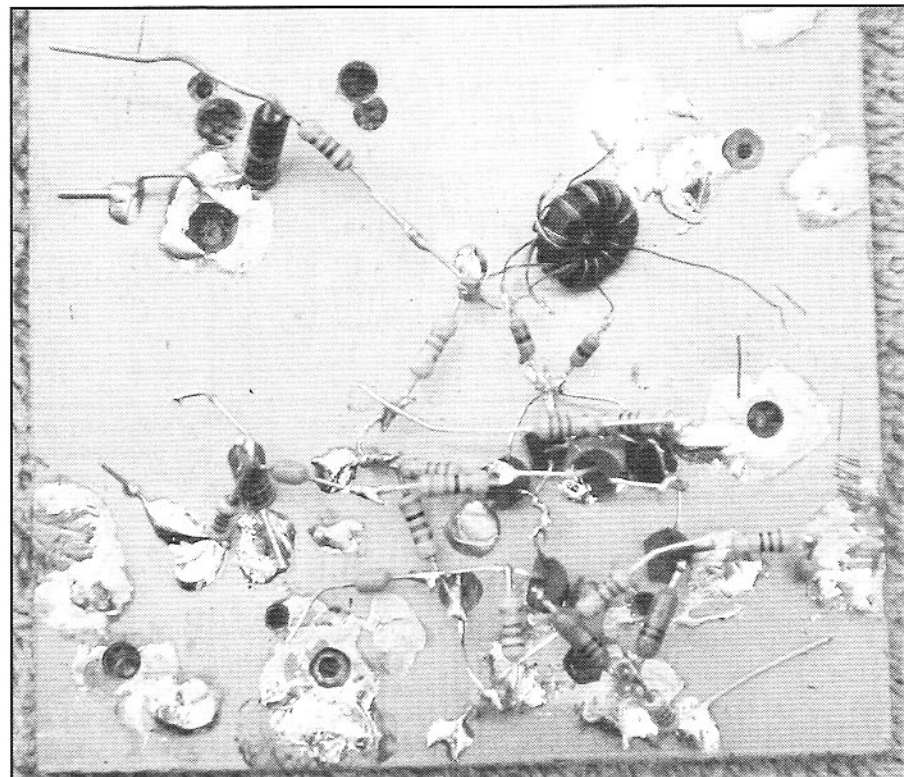
The Gilbert Cell in rudimentary form, shown in Fig 5.25, contains a pair of these differential amplifier mixers. RF is applied to the lower differential amplifier, Q1 and Q4, producing two currents containing dc bias and the RF signal. These drive the emitters of identical differential pairs that are switched by the same LO signal. The Q3 and Q5 collector currents are in phase with each other with regard to LO drive; Q2 and Q6 share the other phase. However, one of the two output collector connections is “twisted” before attachment, producing a connection that cancels LO appearing at the IF. Port to port isolation is now excellent for all combinations.

Most Gilbert Cell mixers are integrated. The popular MC1496 and similar devices have been replaced with ICs that include internal biasing resistors. The most popular of these is the NE-602 shown in Fig 5.26. This version includes load resistors as well as input biasing. One can actually measure the collector resistors with an Ohmmeter; the RF input resistors do not really appear to be there, although network analyzer measurements show the resistors to represent a good model. The test circuit of Fig 5.27 was fabricated to evaluate the NE602.

The conversion gain for this mixer was 20 dB with LO drive of 0 dBm (632 mV

pk-pk at pin 6) with the test circuit of Fig 5.27. Early Signetics data recommends a minimum LO of 200 mV peak-peak, -10 dBm in our test circuit. Conversion gain dropped to 14 dB at this level in our measurements.

Both the RF and IF ports were floating in the test circuit, allowing balanced drive



Experimental discrete transistor version of a Gilbert Cell Mixer.

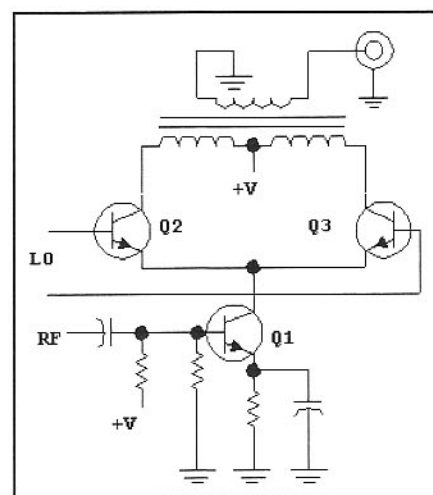


Fig 5.24—The basic bipolar differential amplifier mixer that is the basis for the Gilbert Cell. This mixer can be built with a CA3028A, or fabricated from discrete transistors. The 2N3904 would be suitable for HF applications. Biasing resistors (not shown) set the Q2 and Q3 bases at approximately mid supply.

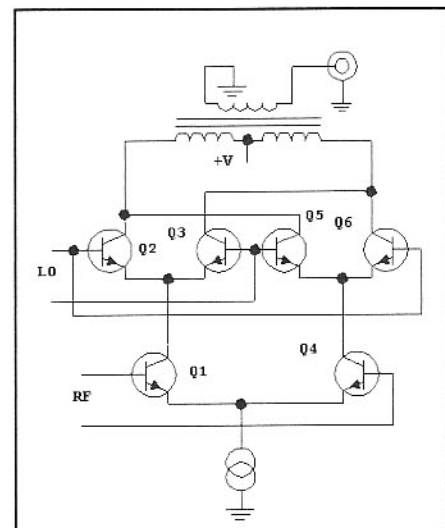


Fig 5.25—Fundamental Gilbert Cell mixer. The collector load is sometimes realized with resistors, although this will degrade intercepts, for internal load resistors absorb power that would otherwise be available to an external load.

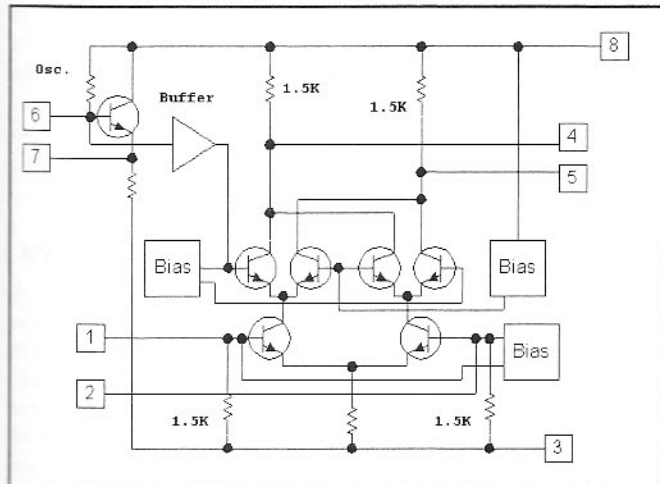


Fig 5.26—Equivalent circuit of the Phillips NE602/NE612.⁸

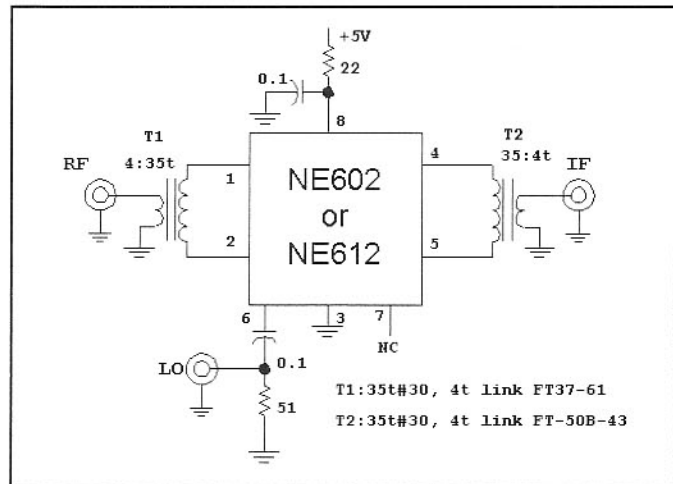


Fig 5.27—Test circuit used to evaluate the performance of the NE602. Most measurements used a 14-MHz RF, 19-MHz 0-dBm LO, and an IF of 5 MHz. The output 1 dB bandwidth extended from 0.5 to 10 MHz with the transformer shown. The RF port impedance match was a return loss of 19 dB while that at the IF was 15 dB. The internal oscillator was not used in these experiments.

to balanced loads. This balance could be altered experimentally by bypassing one end of the transformer. Bypassing pin 2 reduced gain by 2 dB and degraded the input impedance match. A similar exercise at the output (pin 5) degraded gain by 4 dB. Of greater import, unbalanced termination at either port degraded port-to-port isolation. Balanced RF drive will also alter product detector performance.

Our best IMD performance resulted with a single ended RF drive. IP_{3in} was then -17.5 dBm with conversion gain of 18 dB and 0 dBm LO drive.

Single sideband noise figure was measured at 7 dB for this test circuit. This measurement was realized with a 15-MHz low pass RF filter and a 19-MHz LO.

We usually think of the Gilbert Cell as an integrated circuit. However, there is nothing fundamental to preclude building these mixers in discrete form. A discrete Gilbert Cell mixer built from 2N3904 transistors is shown in Fig 5.28. No special transistor matching was used, although all transistors came from the same bag with identical manufacturer and date codes. The chance is reasonable that they came from the same silicon wafer.

The circuit presented some VHF oscillation difficulty when power was initially applied. Although the problems occurred at VHF, LO harmonics mixed with the VHF signal to produce a low frequency output that moved in frequency as our hand was moved close to the circuit. The frequency could also be tuned with changing supply voltage. The oscillations were suppressed with the 10- and 36-Ω resistors included in Fig 5.28.

The mixer was biased to either 5 or 15 mA with most experiments performed at the higher level. Single-ended drive is used for both RF and LO inputs, slightly compromising port-to-port isolation. Fig 5.29 shows the IF port output spectra. Conversion transducer gain for this circuit was 18 dB (15 mA, P-LO = 0 dBm, F-LO = 10.4 MHz and RF = 14.3 MHz.) Increasing LO drive by 10 dB made no difference in gain, but a drop to -10 dBm produced a 1-dB gain decrease. RF and LO signal

appear in the wideband IF output with both about 14 dB below the respective input levels. Numerous other spurious outputs are present, all expected mixer spurious responses. Most would be lower in magnitude if the circuit was actually integrated. This circuit had a third-order input intercept of +11 dBm with 15-mA bias and 0-dBm LO power.

Decreasing the standing current to 5 mA produced a IP_{3in}=-2 dBm, with 16-dB gain, still dramatically better than the

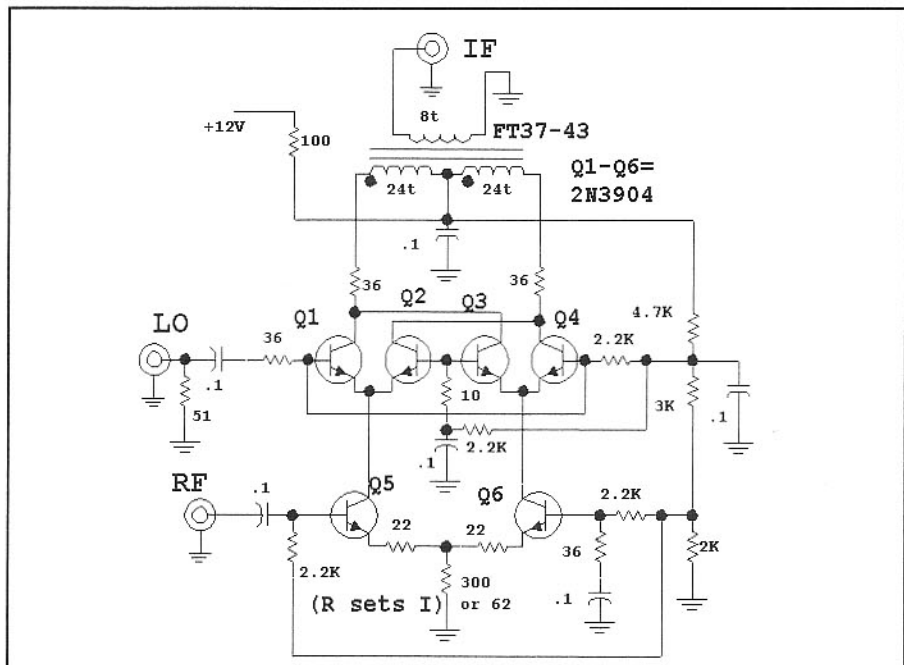


Fig 5.28—Gilbert Cell mixer built with discrete transistors. A resistor (300 or 62 Ω) at the bottom sets the bias current for the overall circuit.

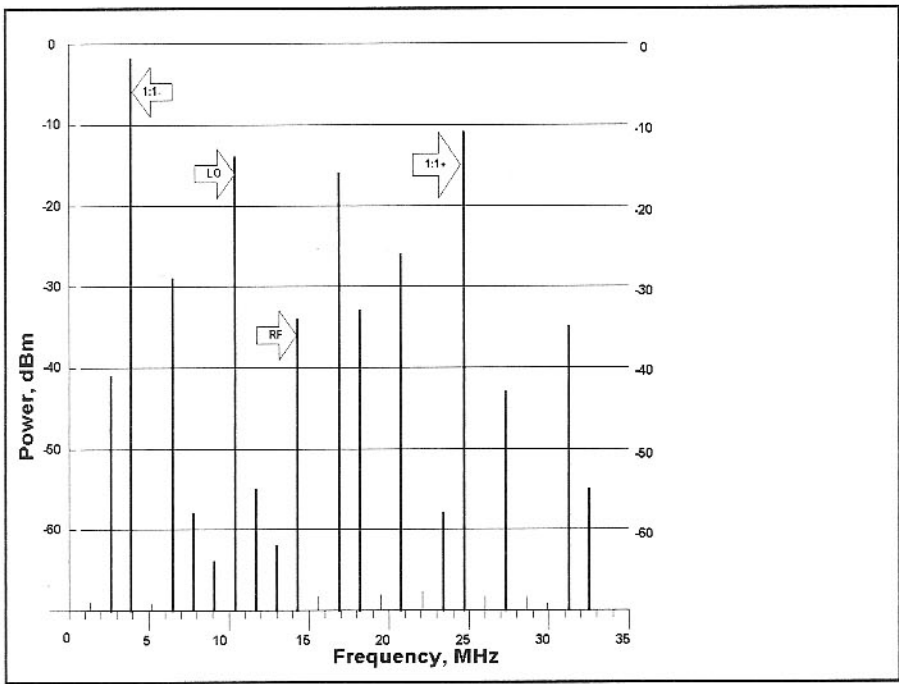


Fig 5.29—Output spectrum observed with the mixer of Fig 5.28. See text for details.

NE602. A diode noise source was used to measured DSB noise figure of 10.8 dB. This extrapolates to a SSB NF of 13.8 dB.

Degeneration (22Ω resistors in the emitters of Q5 and Q6) was needed in the RF input stage to reduce IMD. However, this degraded the noise figure.

Although the main tool used to improve IMD performance in a Gilbert Cell is to increase current, feedback can also be applied. The experimenter should exam-

ine the work of Trask.⁷

Some of the integrated Gilbert Cell mixers that were once popular (e.g., MC1496, NE602) are becoming difficult to find. The topology remains popular and is often found as part of a larger, multiple function IC. Some Gilbert Cells are available internationally, although design data is sometimes difficult to obtain. One example is the SN16913P, from Texas Instruments Japan. This device is slated for discontinuation at this writing. It

appears similar to another discontinued TI part, the TL442. The Toshiba TA7358P is still in production and could be a viable replacement in new designs. (Thanks to JG1EAD and JA3FR for information on Japanese parts.) There is ample challenge available to the experimenter.

Dual Gate MOSFET Mixers

JFET mixers were discussed earlier. A related device is the *metal oxide silicon field effect transistor*, or MOSFET. While the usual JFET is a depletion mode device, the typical MOSFET is an enhancement mode part. See the References chapter of any recent issue of *The ARRL Handbook* for definitions and further information. MOSFETs were, at one time, often built with two gates with that closest to the source termed "gate 1." When one of the gates is forward (positive) biased with respect to the source, the device behaves much like a JFET with the remaining gate as the controlling element. These devices are often modeled as a cascode connection of single gate FETs. Mixers can, of course, be built with MOSFETs, for they exhibit the same quadratic transfer characteristic seen with the JFET.

Fig 5.30A shows a mixer type that was very popular from the mid 1960s until about 1990. This circuit uses a dual gate MOSFET, an insulated gate topology with two parallel gates. A rule-of-thumb is that a dual gate FET will display a narrow band conversion transconductance of $\frac{1}{4}$ the gm expected for an amplifier biased at a similar current with similar terminating impedances. (This guideline is consistent with more refined analysis.) Traditional dual gate MOSFETs required an LO drive of about 5 V pk-pk at gate 2 to realize optimum gain.

Dual gate MOSFETs, although still available, are not as abundant as they once were. The alternative mixer of Fig 5.30B uses a cascode-connected pair of JFETs in a similar circuit. This connection was evaluated for noise figure, gain, and intercept. The 2N5454 FETs from our junk box are similar to the popular 2N4416, TIS-88, MPF-102, 2N5485, 2N5486, and many other components; any of these parts should perform well in this topology. Our initial attempt with this circuit presented a stability problem with an oscillation occurring at the resonant frequency of the input circuit. This was observed with a power meter attached to the IF output. The oscillation was eliminated when R1 was inserted across the transformer primary. A broadband IF output transformer is wound on relatively low loss type 61 ferrite core with a turns ratio to present a good output

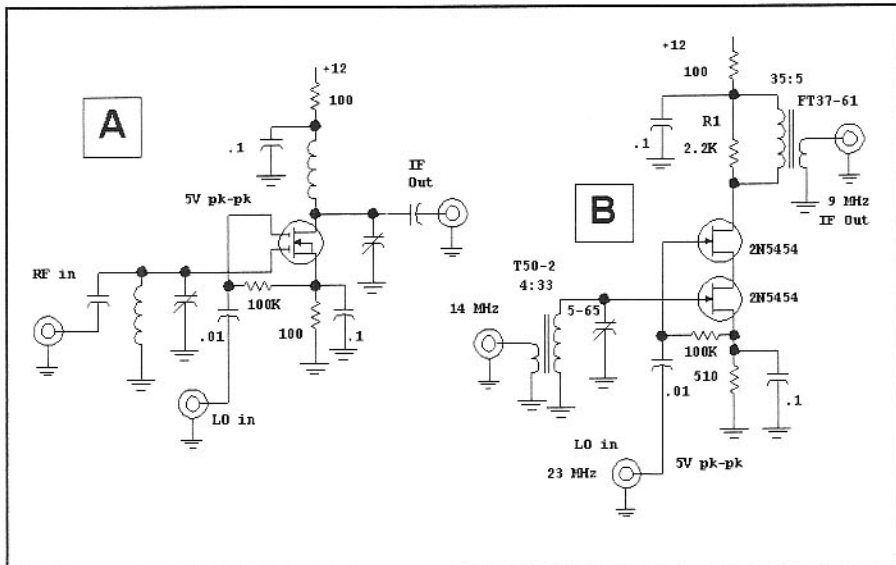
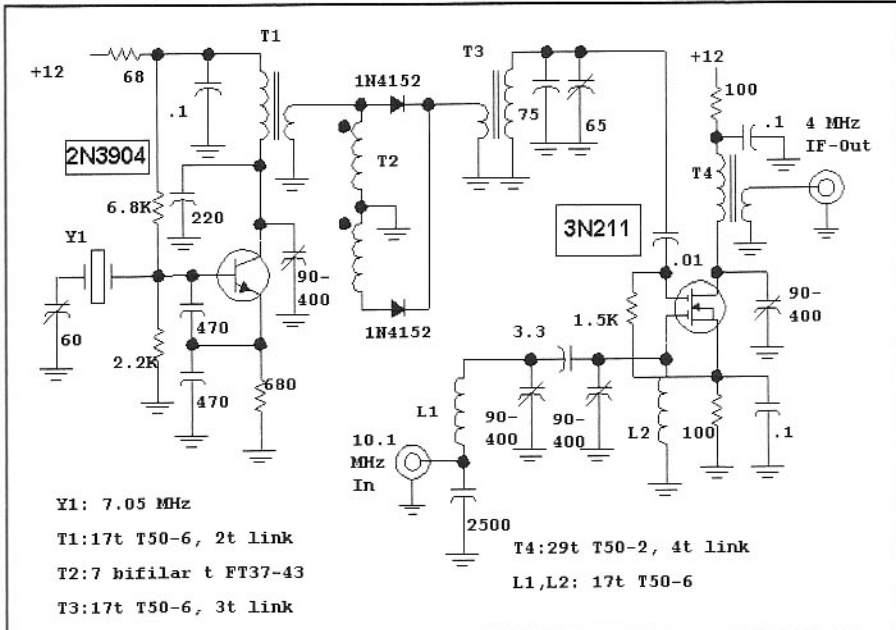


Fig 5.30—Part A shows a mixer using a dual gate MOSFET. Best gain occurs with around 5 V pk-pk at gate 2 for LO injection. The mixer at B uses a pair of JFETs in a cascode connection. This mixer is easily fabricated with nearly any available JFET type. See text.



match to $50\ \Omega$. An alternative winding would allow matching to a crystal filter. The mixer shown, biased for 3.4 mA at 12 V, has a measured conversion gain of 8 dB with a noise figure of 10 dB and IIP3 of +5 dBm. There is no balance in this circuit, so LO and RF energy is available at the IF port. This mixer is used in a simple superhet receiver appearing later in the book.

Many dual gate MOSFETs show very low *amplifier* noise figure with values of 1 dB being common. They can also function well in mixer applications. Fig 5.31 shows a receiving converter with a measured NF of 6.6 dB and a conversion gain of 22 dB. This circuit needed an LO of 14.1 MHz to convert 10.1 MHz to 4 MHz. An available 7.05-MHz junk box crystal was used with a frequency doubler. The oscillator provides 10 mW to drive the passive diode doubler. The single tuned circuit then increases the voltage to the required level. This mixer has a low noise figure because gate 2 “sees” a low impedance at all frequencies other than that of

the LO injection. Hence, noise energy within the LO system at the 4-MHz IF and at the 10.1-MHz RF does not reach the mixer output. The same mixer with a wideband LO drive circuit will usually have a noise figure closer to 10 to 12 dB. We did not measure IMD with this circuit.

The traditional dual gate MOSFET mixer biased for 5 mA at about 10 V will have OIP3 of around +20 dBm. The input intercept will be this value reduced by the conversion gain. The best dynamic range for mixers of this sort will occur when the impedance presented to gate 1 (RF input) produces lower gain. Lower impedances will also alter noise figure. The advanced experimenter (the one willing to measure and optimize results) can expect outstanding performance from either mixer in Fig 5.30.

Diode Ring Mixers and Related Circuits

The diode ring has become the workhorse for the communications industry. Although the mixer has loss, noise figure

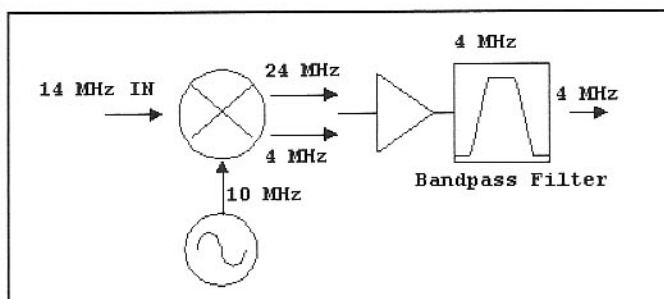
is low and intercepts are generally high, making it the best choice when dynamic range is critical. The lack of gain is not, in itself, a problem. It is important to use the ring with care if best performance is to be realized.

Probably the most critical characteristic of a diode ring, and most other switching mode mixers, is the need to carefully terminate the IF port. A proper termination (usually $50\ \Omega$) means that output energy available from the mixer is absorbed. If power is reflected from the IF, it then impinges back upon the mixer IF port where it can be reconverted back to the RF, or to image frequencies. Reconverted components can then exit the mixer RF port where they are yet again available for absorption or another reflection. With each reflection can come phase shift and distortion.

Fig 5.32 illustrates the termination problem. A diode ring is used in a 14-MHz receiver where a 10-MHz LO converts the desired signal to a 4-MHz IF. But the mixer output also contains a 24-MHz signal. The mixer is terminated in an IF amplifier with the first selectivity appearing *after* the amplifier. Typical amplifiers have an input impedance that varies with frequency. Even if the amplifier input is close to $50\ \Omega$ at 4 MHz, it probably will not be $50\ \Omega$ at 24 MHz as well. The 24-MHz component will then be scattered from the amplifier input back to the mixer output where it can participate in further conversions, all undesired.

The mixer needs to be properly terminated for any and all signals that emanate from it. Assume the receiver is tuned to 14.00 MHz, but a strong signal appears at 14.01 MHz. That signal, once translated to the IF, is probably out of the crystal filter passband. It will then be reflected by the filter and returned to the amplifier output, possibly creating excess distortion there. If the amplifier uses negative feedback, the poor output termination for the 14.01-MHz signal will be reflected back to the amplifier input, creating an improper termination for the mixer.

The obvious question that arises when a *good* impedance match is specified is “How good?” Generally, we look for an IF termination that is better than a 2:1 VSWR, or a 10-dB return loss. This match is easily measured in the home lab with a return loss bridge, signal generator, and sensitive detector. The detector could be a special receiver, a spectrum analyzer, power meter, or even an oscilloscope (see Chapter 7). The match should be examined over a wide frequency range, and with a signal level low enough to guarantee that the terminating circuitry is not overdriven.



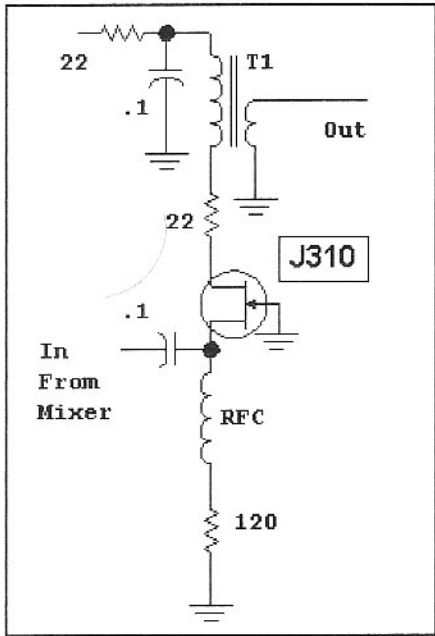


Fig 5.33—A post mixer amplifier using a junction FET. A high I_{DSS} FET is required such as the J310. See the text for transformer discussion.

In many situations the IF port termination requirements may be relaxed if the match is improved at the RF port. Generally, distortion and gain measurements will reveal the problems. The aggressive experimenter can build the instrumentation needed for these measurements.

Ideally, the best amplifier for terminating a switching mode mixer is one with excellent reverse isolation and a frequency invariant ("flat") input impedance. The amplifier must have good distortion properties, for it is often subjected to an entire band full of signals. The noise figure should be low, for it will add directly to the mixer loss to set the noise figure looking into the mixer. Finally, the gain should be high enough to compensate for mixer loss and loss in the filter that will follow, but not a lot more. Excess gain means that the signals become too large, stressing the following filter (crystal filters can be damaged by excessive signals, and can generate their own IMD) and stressing the distortion properties of the amplifier.

A grounded gate J310 JFET amplifier suitable for post mixer applications is shown in Fig 5.33. This circuit has good reverse isolation, so a crystal filter may be driven directly. The output transformer determines gain. A drain impedance of about 1200 Ω yields a gain of about 10 dB. We measured a third-order output intercept of +28 dBm for this amplifier when biased for $I_d = 14$ mA. A noise figure of less than 3 dB is possible with a slight

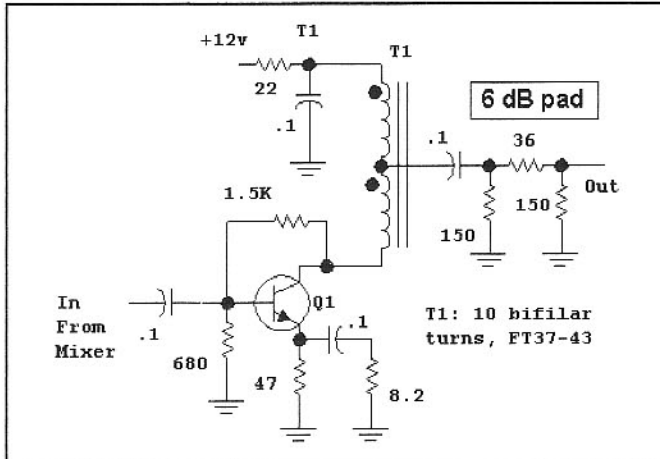


Fig 5.34—Post mixer amplifier using a medium power, high F_T bipolar transistor. See text.

input mismatch. The amplifier will normally yield an input match (return loss) better than 10 dB. Good input match and modest intercepts are found only with high current, which happens only with fairly high I_{DSS} FETs.

A favorite amplifier of ours (Fig 5.34) for terminating a switching mixer is a bipolar transistor feedback amplifier followed by a 6-dB pad. Negative feedback is used to set the gain and to stabilize the input and output impedances. This circuit was discussed in detail in the amplifier chapter. The output termination on a feedback amp will strongly influence the input impedance. As such, one should avoid driving a crystal filter directly with such an amplifier. The filter impedance changes rapidly with frequency, especially in the region at the passband edges. What may be a fine termination in the passband becomes an open or short circuit in the skirts and stop band. The resulting mixer termination may cause severe IMD problems.

These problems are largely avoided by placing a 6 dB pad in the amplifier output. This then guarantees an amplifier with a stable, frequency independent input impedance to terminate the mixer. It also guarantees a good source impedance for the crystal filter, another vital consideration.

The amplifier of Fig 5.34 uses a transistor usually specified for RF power or Community TV service. They are bipolar devices with a 1 W or better output capability and with an F_T that is at least 10 times the highest frequency IF where they will be used. The 2N3866 and 2N5109 are both available at this writing and work well in this service. Many other parts are suitable. Paralleled 2N3904s or similar plastic cased devices are also suitable and are shown later. The amplifier in the figure uses a bias emitter current of 50 mA and a collector termination of 200 Ω , provided with a bifilar transformer. The input

impedance is very close to 50 Ω and is fairly flat through the HF spectrum. Typical OIP3 is +41 dBm if the attenuator is not part of the measured circuit. The 6-dB attenuator decreases the overall output intercept to +35 dBm. The gain is 21 dB, dropping to 15 dB with the 6-dB pad.

This particular amplifier uses the feedback resistor for transistor biasing, so changing circuit elements will alter biasing as well as feedback. Altering feedback with constant bias current will maintain the output intercept while changing the gain. Input intercept will change accordingly.

Noise figure for the amplifier of Fig 5.34 will vary with transistor type and bias, but values of 5 dB are typical. Careful measurements on one version of this circuit showed lower NF with reduced current, offering some DR optimization.

An attenuator at the input of a feedback amplifier will generate stable port impedances as well as good output intercept. However, the input pad degrades noise figure.

Some receiver designs (with high level mixers) demand amplifiers with higher intercepts. This is possible with higher current. However, the output pad compromises efficiency. A better solution uses two feedback amplifier stages with attenuation between. The impedances are stable and noise figure and intercepts are maintained.

There are some situations where no amplifier is required. It is still important to maintain the proper mixer terminations. An example might be the front end of a spectrum analyzer, shown in Fig 5.35. The first mixer is preselected with a low pass filter and produces a first IF of 1.5 GHz. The pad in the mixer output stabilizes impedance in both directions, ensuring mixer and filter performance. The second mixer produces a 50-MHz IF where an amplifier with a pad is now used. This topology has

a much higher noise figure than the usual receiver, but is capable of excellent IMD performance, the parameter of greater interest for measurements.

Fig 5.36 shows a different approach to the problem. Here, a mixer is followed by a diplexer filter that then drives a post mixer amplifier using a dual gate MOSFET. (40673, or 3N211 used.) The 2.2-k Ω gate resistor is transformed to look like 50 Ω to the mixer through an L-network, L1 and C1. This only provides a termination at the IF, 1.9 MHz in this example. Sum products are terminated with a high pass filter paralleling the L-network. The preselector filter was a triple tuned circuit in this example with about 3-dB loss while the MOSFET amplifier has a noise figure of about 3 dB, for a net NF of 12 dB. Overall gain is 9 dB. Measured input intercept for the system was +15 dBm. This two-decade-old scheme is not as strong as others, but can be an efficient one for battery operation. The broadband impedance match is marginal.⁹

Perhaps the ultimate IF termination for the switching mixer is a special crystal filter that presents a proper impedance at all frequencies. This filter, and similar

amplifiers result from a now classic method described by Kurokawa, et al.¹⁰ Such a filter is discussed in the next chapter.

Parts like the MiniCircuits SBL-1, TUF-1, and ADE-1, a SMT part, represent the standard diode rings. There are, of course, many more listed in their catalogs. These mixers are specified for a LO drive power of +7 dBm. (Recall that this is *available power from the LO source*.) The mixer is usually well saturated at this +7 dBm and LO drive changes do not alter gain. The "+7-dBm" mixers will continue to function with LO drives as low as 0 to +3 dBm, with reduced gain and degraded intercepts. Some Mini-Circuits parts are available for LO power as low as 0 dBm.

Mini-Circuits +7 dBm mixers are specified for an input 1 dB compression power of +1 dBm. A rule of thumb states that the input intercept of a diode mixer is 10 to 15 dB above P_{-1dB}, placing IIP3 at +11 to +16 dBm. These values are in line with our measurements for the TUF-1 and SBL-1.

Most mixer manufacturers also build mixers specified for LO power of +17 dBm. These mixers usually use two series connected diodes in each leg of an otherwise conventional ring. One ex-

ample, the TUF-1H, has a +14 dBm value for P_{-1dB}, placing IP3in at +24 dBm or higher. Even higher power mixers are available, including some "level 27-dBm" devices with P_{-1dB} = +24 dBm.

A recent *QEX* paper examines the termination of high-level mixers to improve IMD.¹¹ That paper considers diplexer filters at both the IF and RF ports, as well as some modified LC filters. It strikes us that the Engelbrecht-Kurokawa methods may also be suitable for RF port terminations. The excellent paper by Stephensen is included on the book CD.

High Level FET Mixers

Very wide dynamic range receivers and low noise transmitters both demand high-level mixers. While some diode-based designs are suitable, they demand high LO power, a practical difficulty. Several workers have examined other devices as switches. The notable example mentioned earlier was the MOSFET ring described by Ed Oxner.

Perhaps the most exciting work published in the past decade in this area was a note appearing in Pat Hawker's ever popular and consistently informative Technical Topics column in Radio Communications.¹² Hawker presented previously unreported work on a new mixer topology by Colin Horrabin, G3SBI. This four-FET mixer, shown in **Fig 5.37**, differed from earlier circuits. Oxner's design used FETs as series switches while Horrabin used the FETs as grounded switches. This is still a commutating mixer, but transformer action now generates the needed signals. Horrabin's circuit used a monolithic quad

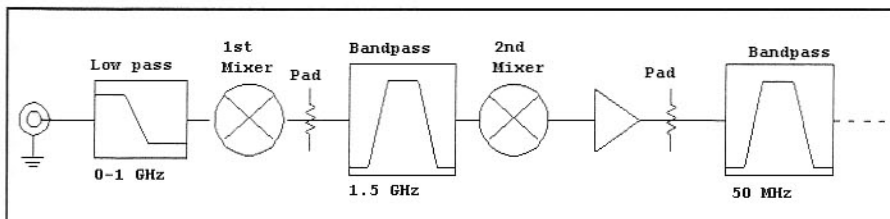


Fig 5.35—Front end of a spectrum analyzer showing ring mixers without amplifiers.

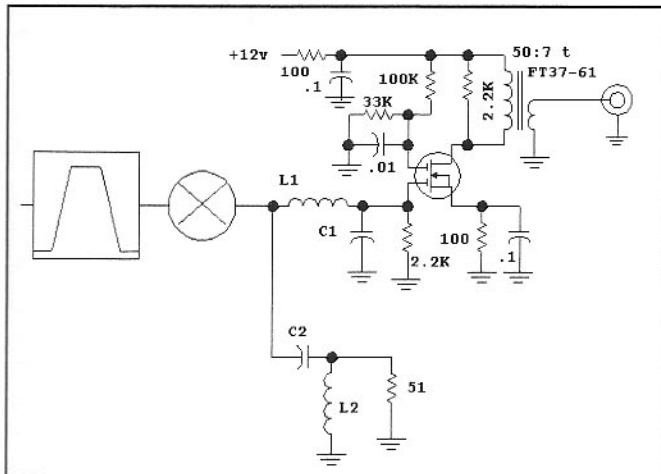


Fig 5.36—A mixer-terminating amplifier using a diplexer filter. This is a combination of a low pass and a high pass filter in this example, but could also be a bandpass and bandstop filter. This example uses a considerable impedance transformation at the amplifier input.

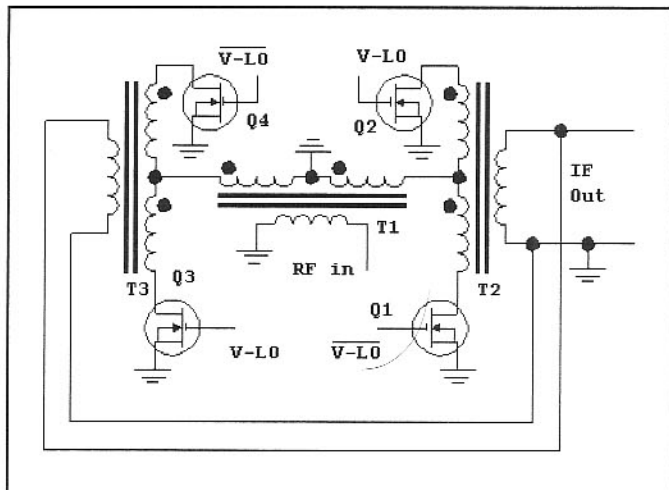


Fig 5.37—H-mode mixer using grounded FETs. This mixer, the work of Colin Horrabin, G3SBI, has produced third order input intercepts as high as +55 dBm. The circuit takes its name from the "H" shape presented by the transformers.

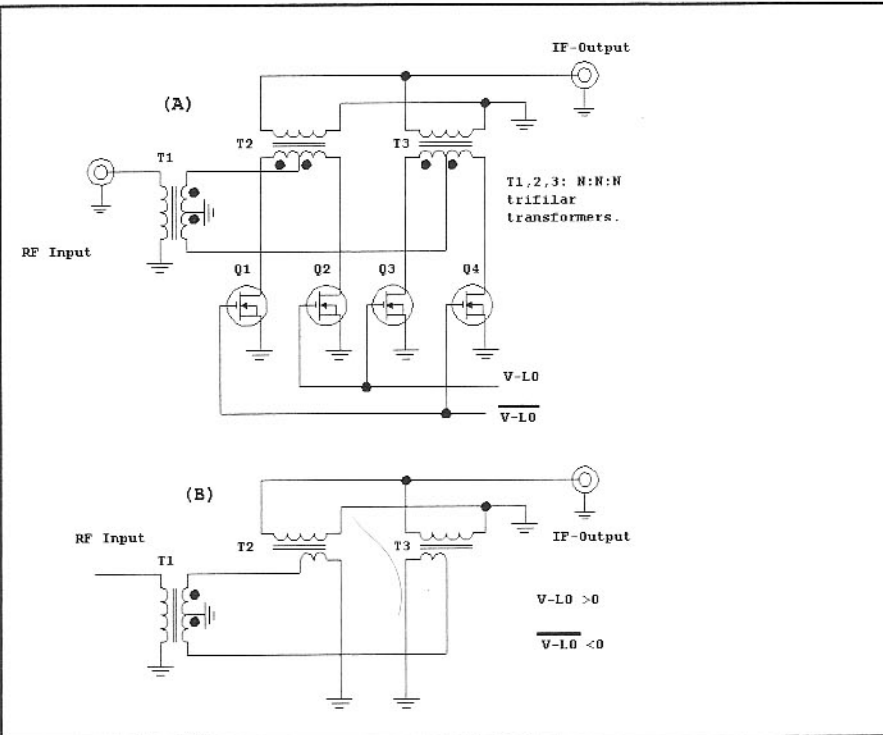


Fig 5.38—The H-mode mixer is redrawn to clarify operation. See text for explanation.

of MOSFETs, the Phillips SD5000, which is essentially the same MOSFET as used in Oxner's Si8901.

The operation of the H-mode mixer is

understood with the redrawn circuit of Fig 5.38. Part A of the figure shows the basic circuit. Assume that at one point in time V_{-LO} is positive. This causes FETs

Q_2 and Q_3 to be on, creating a low impedance to ground. The other two FET switches are off, now modeled as open circuits. The resulting circuit is shown in part B of the figure. Transformer T_1 is one with essentially three identical windings, with two configured as a larger center tapped secondary. Each secondary winding is now connected to separate output transformers T_2 and T_3 . Part of the transformers are not shown, for they are connected to open circuits at this point in time. The currents in T_2 and T_3 add at the IF output.

The polarity changes as we advance one half of a LO cycle. Q_1 and Q_4 are now on with Q_2 and Q_3 off. The other two secondary half-windings are now connected. Although not shown in the figure, detailed examination confirms commutation.

Horrabin has measured values as high as +55 dBm for IIP3. It becomes challenging to build low IMD amplifiers to accompany this robust mixer. It is difficult to measure intercepts this high, and considerable effort has been expended by Horrabin and his colleagues in this pursuit. They attribute the excellent performance to a removal of RF input signals from the gate-source switch-on path. The configuration with grounded FET sources makes it much more difficult to modulate the LO action with applied RF. Practical front-end examples using this mixer are presented in Chapter 6.

5.4 FREQUENCY MULTIPLIERS

Closely related to the mixer is a commonly used circuit, the frequency multiplier. This is a circuit with the predominant output occurring at a frequency that is an integer multiple of the input. We saw frequency multiplication when a local oscillator was first applied to a mixer; the action was a natural consequence of the circuit nonlinearity.

The simplest frequency multipliers

resemble a simple amplifier with a single device (bipolar or FET). If the output is tuned to a multiple of the input frequency and if the circuit is driven harder than it would normally be driven for amplifier service, efficient frequency multiplication can occur. Example circuits are shown in Fig 5.39.

While these circuits are simple and easy to implement, they often suffer from poor

spectral purity. If the circuit is tuned to operate as a frequency tripler, the dominant output will certainly be at 3 times the input. However, there is a good chance that

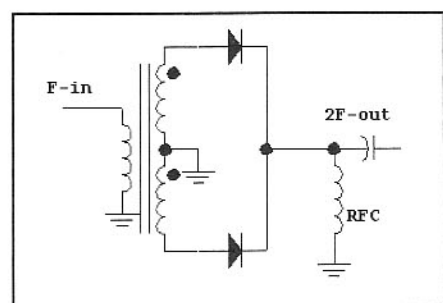


Fig 5.40—Diode frequency doubler. The diodes, ideally identical, can be silicon-switching types, such as the 1N4152 or 1N918 for use at HF and low VHF. Hot carrier diodes are recommended for UHF applications, or for critical, low phase noise HF applications. The transformer can be the familiar 10 trifilar turns on a FT37-43 core for HF applications. Often, this doubler drives a link on a single tuned circuit, eliminating the need for the RFC.

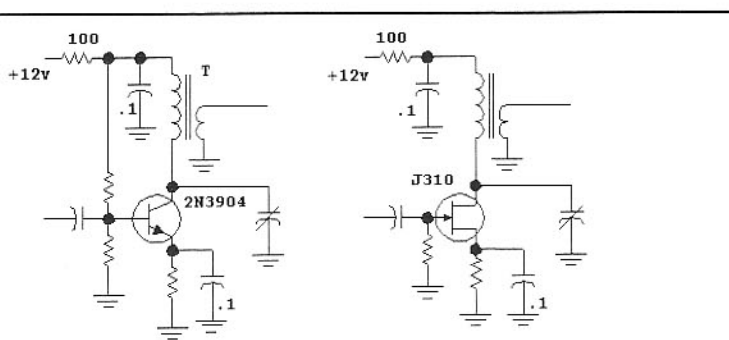


Fig 5.39—Simple, single-ended frequency multipliers using a bipolar transistor and a JFET. These classic circuits can still be useful in modern designs, but only if built with careful measurements.

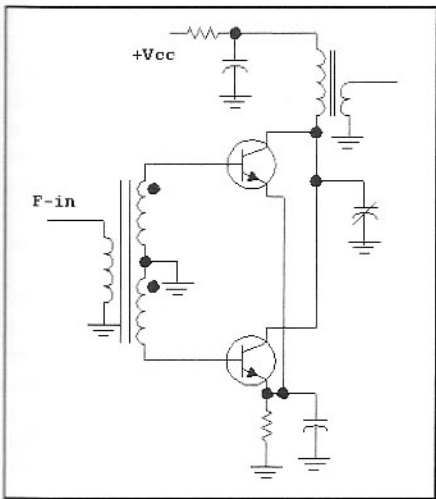


Fig 5.41—Basic push-push frequency doubler using balanced bipolar transistors.

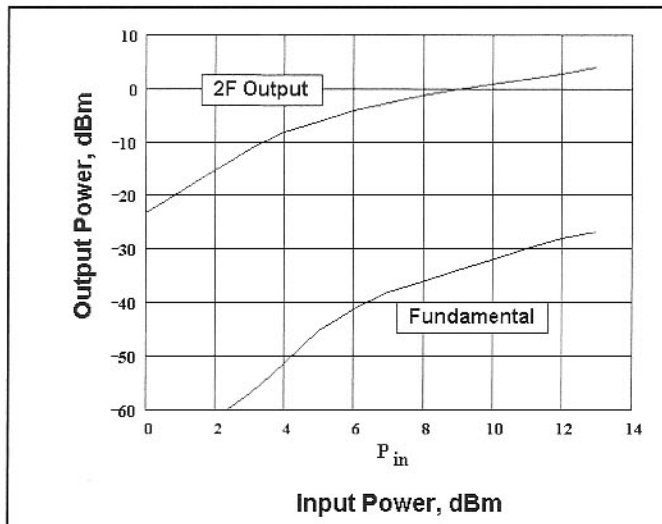


Fig 5.42—Output power and fundamental feed-through for a diode doubler using the circuit of Fig 5.40. The diodes were 1N4152 that had been matched with a DVM.

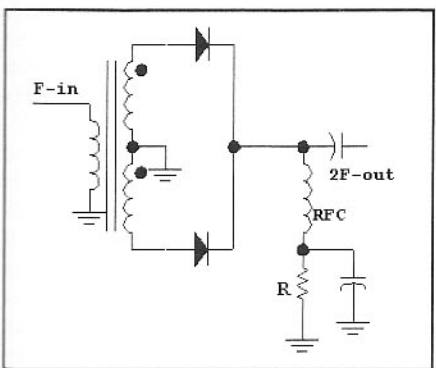


Fig 5.43—Improved balanced diode frequency doubler. Typical resistor values are from 10 to 220 Ω . See text.

there also be considerable energy at the fundamental frequency (the input), the 2nd, and the 4th harmonics of the input. The only way to improve the performance is through more filtering.

Not all output components occur at harmonics. As with Class C amplifiers, non-linear C_{cb} of a bipolar transistor can result in non-harmonic spectral components.

As with mixers, we reduce the occurrence of spurious outputs with balanced circuits. A balanced frequency doubler is shown in Fig 5.40 where two diodes operate in a circuit that is more familiar to us as a full-wave power supply rectifier. However, we now short circuit the dc output with a radio frequency choke, extracting only the 2F output. If the input transformer is well balanced and if the diodes are matched, it is common for the fundamental feedthrough for this circuit to be 30 to 40 dB below the 2F output. This circuit is passive and has no gain.

The diode frequency doubler idea is often extended to form the push-push dou-

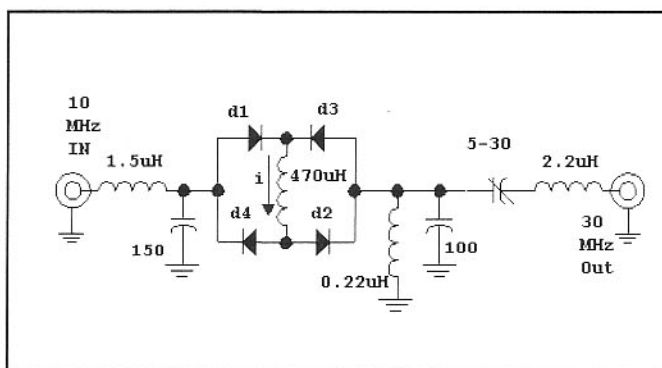


Fig 5.44—Frequency tripler using four diodes and a large inductance choke to generate a square wave. The output circuits are tuned to the 3rd harmonic of the input drive.

bler shown in Fig 5.41. This circuit is capable of gain and higher output power than is possible with the diodes. A passive doubler followed by an amplifier to regain the power lost in the diodes has similar power consumption and spectral purity.

The output power from the classic diode doubler (Fig 5.40) is typically around +2 dBm with a +10-dBm drive. A curve is shown in Fig 5.42. Although output grows with drive, gain drops. Gain tends to be more constant with the modified circuit of Fig 5.43 where a bypassed resistor is added to “terminate” the dc component. The dc signal also provides a convenient tuning indicator. The added resistor decreases multiplication gain at drive levels below +10 dBm. However, gain is higher at the highest drive levels of +20 dBm where an output of +12 dBm has been measured. At a drive of +20 dBm, the 4 \times output is -1 dBm.

The drive to a balanced frequency doubler should be relatively free of even order harmonics. A distorted drive can destroy balance, which compromises the suppression of fundamental feed-through.

Odd order frequency multiplication is also common. Although possible with the single device circuits presented earlier, it is generally done with a balanced circuit that generates a square wave. Mathematics reveals that a square wave contains no even order harmonics. Fig 5.44 shows a frequency tripler using a diode bridge tuned for a 10-MHz input with output at 30 MHz. The input circuit provides some impedance transformation from a 50- Ω source as well as some low pass filtering that helps to preserve a sine wave drive. Diodes d1 and d2 conduct on the positive drive polarity while d3/d4 conduct on the negative half of the cycle. Note that the current flowing in the intermediate inductor, shown with an arrow, is the same for both polarities. The multiplication gain for this circuit can be around -9 dB, but is level dependent. The circuit can also be tuned for $\times 5$ multiplication with reduced gain. This circuit originated from Charles Wenzel.¹³ The Web site in this reference is a wonderfully useful site with many other applications listed.

A slightly simpler odd order multiplier is presented in Fig 5.45. This circuit,

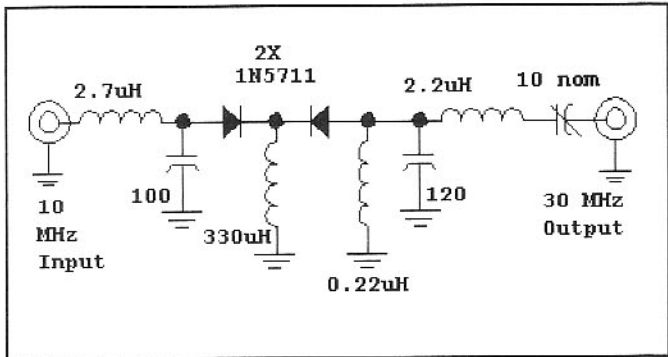


Fig 5.45—A simplified tripler circuit using only two diodes. This circuit is described in the Web site from Wenzel Associates. See text.

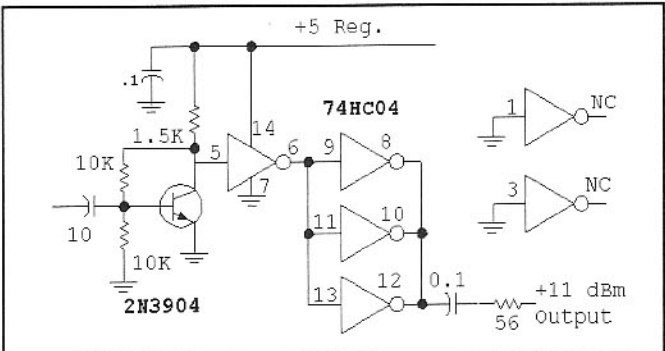


Fig 5.47—Simple limiting amplifier using a digital IC. Here, a HEX inverter generates an output with over 10 mW at the fundamental drive frequency. The inputs to unused sections should never be left floating.

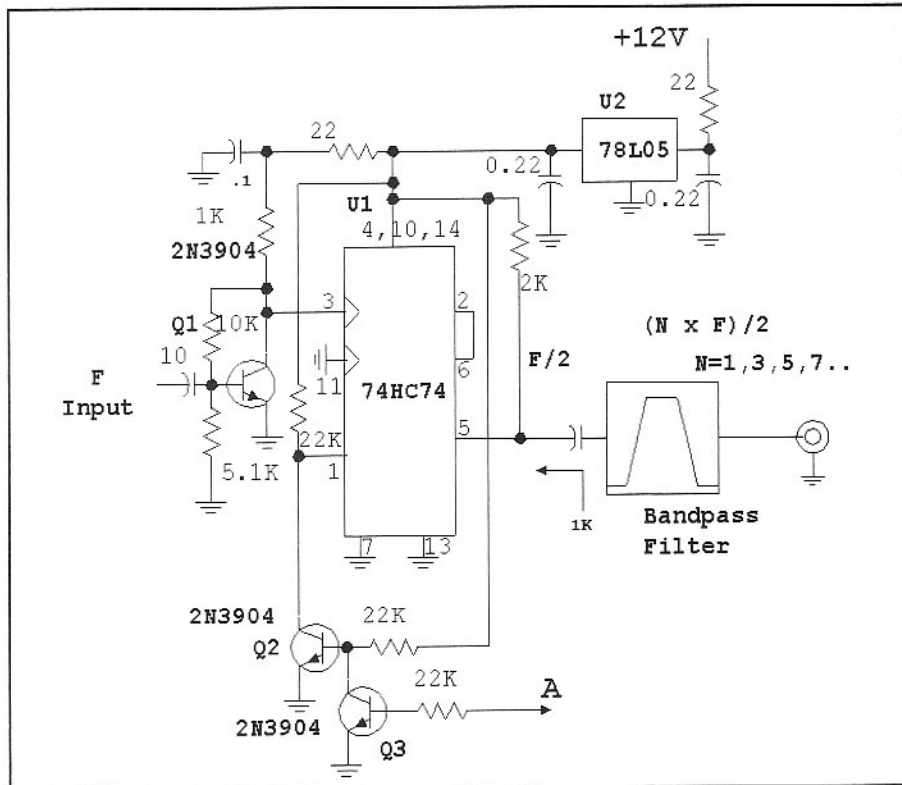


Fig 5.46—This frequency multiplier begins with a frequency division by 2 in a digital integrated circuit. The result, after division, is a very precise square wave. Odd harmonics can then be selected with a suitable bandpass filter. The output from the filter is typically -5 dBm when $n=3$. The bandpass should be designed for a termination of $1\text{ k}\Omega$ at the IC end.

which uses only two diodes, can also be tuned for $x5$ operation. While we have not yet done the experiment, it would be very interesting to examine the insertion of resistance in series with the large inductance. The tripler circuits from Wenzel work well with either junction diodes or hot carrier devices, although the hot carrier diodes are preferred for low noise applications. The Wenzel web site discusses diode selection.

Square waves are easily created and pro-

cessed with digital integrated circuits. This provides design opportunities for many interesting applications. **Fig 5.46** shows a scheme we have used for numerous VCO based transmitters. A signal is injected at the input to Q1 where it is converted to a logic friendly format. Levels from -10 to 0 dBm are suitable. The signal is then frequency divided with a 74HC74 D-flip-flop, resulting in an accurate square wave. This output is then applied to a bandpass filter where the appropriate harmonic is selected.

Transmitters using this scheme are presented later. One example might use a 14-MHz crystal in a VCO. The divider output is a 7-MHz square wave, but one rich in 21-MHz energy. A 5% bandwidth triple tuned circuit bandpass filter selects the desired 21-MHz output while providing over 60 dB suppression of 7, 14 and 28-MHz components. This scheme offers two additional advantages: First, the oscillator operates at a frequency that is well isolated from the output, so buffering is extremely effective. Second, the output is easily turned on or off with the digital input at "A", allowing keying without disturbing the operating oscillator. Shaping to remove clicks must be applied to later amplifiers.

Other digital schemes that generate square waves are useful for odd-order frequency multiplication. The buffer of **Fig 5.47** can serve this function. For example, this circuit could be driven by a VCO at 14.4 MHz and followed by a triple tuned bandpass filter at 72 MHz. The signal would then be amplified to a level of +10 dBm or so where it can be used to drive a two diode frequency doubler with a double tuned circuit at 144 MHz, resulting in 0 dBm at 2 m, ready for use with simple transmitters or transceivers.

The example of **Fig 5.47** used a Hex inverter, but other digital parts are also useful. For example, an exclusive-OR gate can be used as a digital balanced mixer, offering 40 dB or greater suppression of both "LO" and "RF" input signals before bandpass filtering.

The frequency multipliers designed by Wenzel featured low phase noise. While the multiplied output has higher noise than the driving source, that noise is worse only by the normal $20 \times \log(N)$ factor for an ideal multiplier. The multipliers using digital logic elements may well be worse than this. We have not performed the measurements needed to establish this performance.

5.5 A VXO TRANSMITTER USING A DIGITAL FREQUENCY MULTIPLIER

The original goal for this project was a transmitter that would function on the 21-MHz amateur band while using an available 14-MHz crystal. The single band transmitter described here develops an output in the 14-MHz band. 28-MHz and 50-MHz designs are presented elsewhere in the book.

The basis for the transmitter is shown in the block diagram of Fig 5.48. A crystal oscillator drives a digital divide-by-2 circuit to generate a square wave at half the oscillator frequency. This waveform is rich in odd-order harmonics while nearly devoid of even ones. A bandpass filter is fabricated to extract the harmonic of interest while suppressing the rest. The resulting signal is then amplified to the desired power.

There are several advantages to this scheme when applied to a transmitter design. First, the digital divider and related circuitry form a high gain buffer, providing excellent isolation from the output. While a common problem with a VXO is

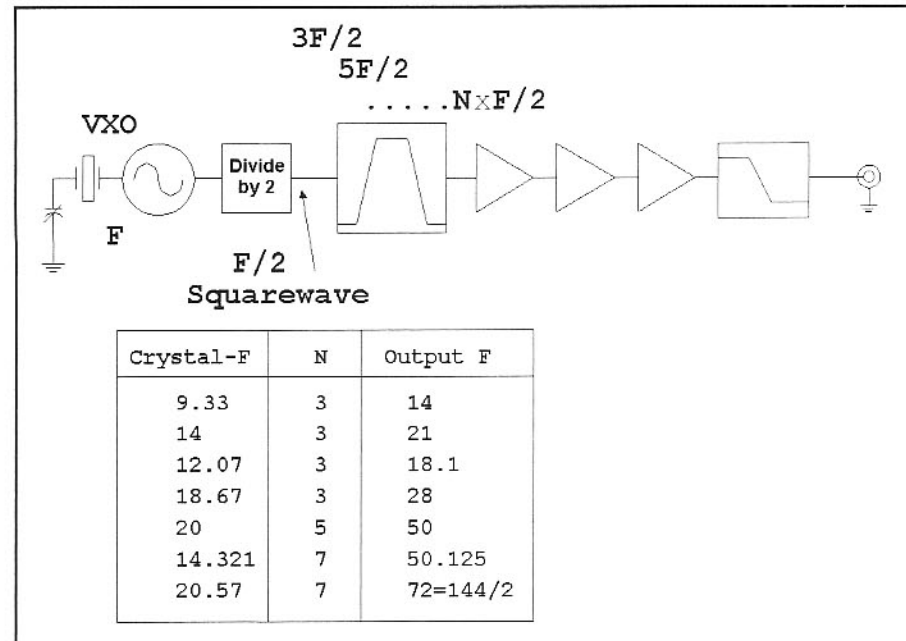


Fig 5.48—Block diagram showing the transmitter concept. The table shows some possible applications.

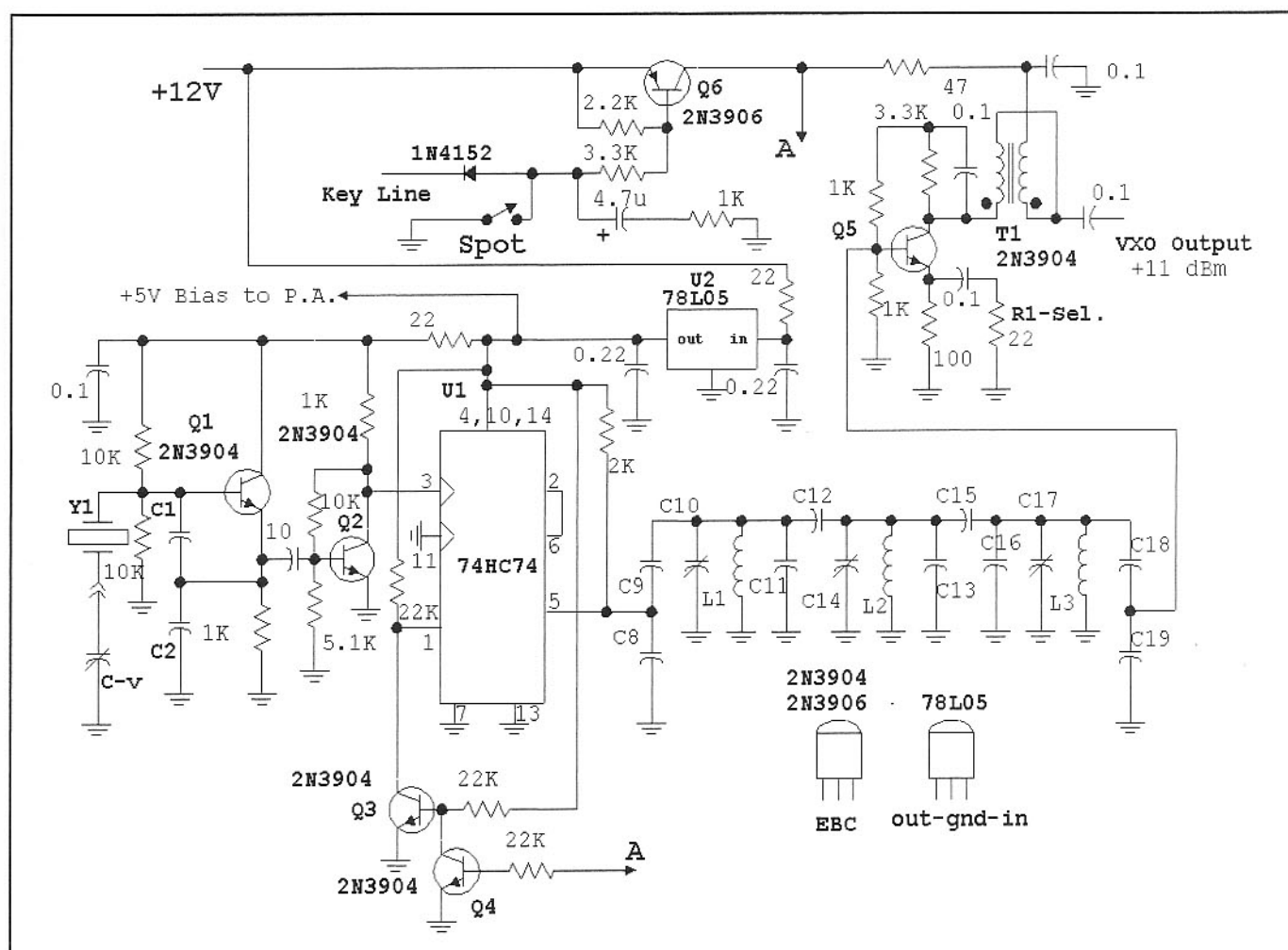


Fig 5.49—Schematic for the oscillator, divider, 14-MHz bandpass filter and buffer amplifier for the VXO transmitter.